

The Pennsylvania State University  
The Graduate School  
Department of Astronomy and Astrophysics

THE ORIGINS OF HOT SUBDWARF STARS AS  
ILLUMINATED BY COMPOSITE-SPECTRUM BINARIES

A Thesis in  
Astronomy and Astrophysics

by

Michele A. Stark

© 2005 Michele A. Stark

Submitted in Partial Fulfillment  
of the Requirements  
for the Degree of

Doctor of Philosophy

August 2005

The thesis of Michele A. Stark was read and approved<sup>1</sup> by the following:

Richard A. Wade  
Associate Professor of Astronomy and Astrophysics  
Thesis Adviser  
Chair of Committee

Robin Ciardullo  
Professor of Astronomy and Astrophysics

Lawrence W. Ramsey  
Professor of Astronomy and Astrophysics  
Head of the Department of Astronomy and Astrophysics

Mercedes T. Richards  
Professor of Astronomy and Astrophysics

Richard W. Robinett  
Professor of Physics

---

<sup>1</sup>Signatures on file in the Graduate School.

## Abstract

For this investigation I studied hot subdwarf stars listed in the *Catalogue of Spectroscopically Identified Hot Subdwarfs* (Kilkenny, Heber, & Drilling 1988, KHD). While the KHD catalog contains all varieties of hot subdwarfs, I primarily focused on the more numerous and homogeneous sdB stars.

I used improved coordinates to collect near-IR flux measurements of KHD hot subdwarfs from the Two-Micron All Sky Survey (2MASS) All-Sky Data Release Catalog. I used these 2MASS magnitudes with visual photometry from the literature to identify those hot subdwarfs whose colors indicated the presence of a late type companion. I determined that  $\sim 40\%$  of sdB stars are composite in a magnitude limited sample ( $\sim 25\%$  in a volume limited sample).

I compared the distributions of hot subdwarfs in 2MASS colors and found a bimodally distributed population. The two peaks of the bimodal distribution can be understood as single hot subdwarf stars and composite systems. Based on these distributions in 2MASS colors, *there are no (or very few) F or dM companions of the hot subdwarfs in the KHD catalog*. These observed distributions of hot subdwarfs in 2MASS colors can be reproduced equally well by assuming either main sequence or subgiant companions — photometric data alone cannot distinguish between these two possibilities.

I obtained spectroscopy of some of the 2MASS composite-colored hot subdwarfs to break the degeneracy between main sequence and subgiant companions present in photometry alone. My analysis focused on Mg I b, Na I D, and Ca II infrared triplet equivalent widths (EWs) from the late-type companion.

The observations (2MASS and visual photometry combined with EWs) for each composite hot subdwarf were compared with diluted models based on Hipparcos standard star observations, models of extended horizontal branch stars (Caloi 1972), and Kurucz (1998) spectral energy distributions, in order to determine the combination of sdB+late-type star that best explained all observations. With a few exceptions, I found that the late-type companions are best identified as main sequence (although some subgiant companions do exist). The majority of the well constrained main sequence companions have  $0.5 \lesssim (B-V)_c \lesssim 1.1$  (spectral types  $\sim$ F6–K5).

Han et al. (2002, 2003) predict that all hot subdwarfs with main sequence companions of  $\sim$ G-type or later are in short period ( $P \lesssim 40$  days), post-common envelope binaries (anything with a companion of  $\sim$ G-type or later and a long period,  $P \gtrsim 40$  days, has either a subgiant or giant companion). Yet, radial velocity studies including composite spectrum hot subdwarfs (i.e., Orosz et al. 1997; Saffer et al. 1994; Maxted et al. 2001), have said the periods for composite-spectrum binaries must be long (many months to years or more), which in the Han et al. scenario would imply that they contain the subgiant or giant companions. Yet, as I show, the majority of composite companions are consistent with main sequence stars. So, it appears something is incorrect or incomplete in the current Han et al. binary formation scenario.

## Table of Contents

List of Tables . . . . .	viii
List of Figures . . . . .	ix
Acknowledgments . . . . .	xi
Chapter 1. Introduction . . . . .	1
1.1 What is a “Hot Subdwarf”? . . . . .	1
1.1.1 Comparison with Globular Clusters . . . . .	2
1.1.2 Physical Parameters . . . . .	2
1.1.3 Kinematics and Population Membership . . . . .	3
1.1.4 Ultraviolet Excess . . . . .	4
1.2 Sidetrack: Name-ology . . . . .	5
1.3 Pulsating sdBs . . . . .	5
1.3.1 V361 Hya (EC 14026, sdBV) Stars . . . . .	5
1.3.2 PG 1716+426 Stars . . . . .	6
1.4 Formation and Evolution of Hot Subdwarf Stars . . . . .	6
1.4.1 Binary Formation Models . . . . .	6
1.4.1.1 Known Binaries . . . . .	8
1.4.1.2 Radial Velocity Studies . . . . .	9
1.4.2 Single Star Evolution . . . . .	10
1.4.2.1 Delayed Helium Flashers . . . . .	10
1.4.2.2 Hot-Flashers . . . . .	11
1.5 The Mission . . . . .	12
1.6 Outline . . . . .	12
Chapter 2. The Kilkenny, Heber, & Drilling Hot Subdwarf Catalog . . . . .	16
2.1 The Sample . . . . .	16
2.2 Coordinates . . . . .	16
2.3 Classification and Identification . . . . .	17
Chapter 3. 2MASS All-Sky Data Release . . . . .	19
3.1 Introduction . . . . .	19
3.2 Visual and IR Photometry . . . . .	19
3.2.1 Visual Photometry . . . . .	19
3.2.2 Infrared Photometry . . . . .	20
3.3 Hot Subdwarfs in Color Space . . . . .	21
3.3.1 Optical-IR Color-Color Plots . . . . .	21
3.3.2 Modelling the Distribution in Optical-IR Color-Color Space . . . . .	23
3.4 A “Volume Limited” Hot Subdwarf Sample . . . . .	25
3.5 2MASS Only Color Parameters . . . . .	26

3.6	Distribution in $J-K_S$ . . . . .	26
3.6.1	Describing the sdB $J-K_S$ Distribution . . . . .	27
3.6.2	Composites in $(J-H, J-K_S)$ Color-Color Space . . . . .	28
3.7	Summary . . . . .	28
Chapter 4.	Spectroscopic Observations of Hot Subdwarfs . . . . .	46
4.1	Introduction . . . . .	46
4.2	KPNO GoldCam . . . . .	46
4.2.1	Instrumental Set-up . . . . .	46
4.2.2	Observing Procedures . . . . .	47
4.3	McDonald LCS . . . . .	47
4.3.1	Instrumental Set-up . . . . .	47
4.3.2	Observing Procedures . . . . .	48
4.4	Target Selection and Lists . . . . .	49
4.4.1	Hot Subdwarfs . . . . .	49
4.4.2	“Standards” . . . . .	50
4.5	KPNO GoldCam Data Reduction . . . . .	50
4.6	Notes on Individual Objects in the Spectroscopic Sample . . . . .	51
4.6.1	Reddened sdBs . . . . .	51
4.6.2	Observed Subdwarf O Stars . . . . .	52
4.6.3	Visual Doubles . . . . .	53
4.6.3.1	Single in 2MASS Colors . . . . .	53
4.6.3.2	Composite in 2MASS Colors . . . . .	54
4.6.4	Objects with Emission Lines . . . . .	55
4.6.5	Other Spectral Anomalies . . . . .	56
4.6.5.1	Residual Fringing . . . . .	56
4.6.5.2	The Blue Bump . . . . .	56
4.6.5.3	Telluric Water Vapor . . . . .	57
Chapter 5.	Analysis of Spectroscopy of Hot Subdwarfs . . . . .	97
5.1	Introduction . . . . .	97
5.2	Measuring Individual Line EWs Automatically . . . . .	97
5.3	Properties of the HIP Standard Stars . . . . .	98
5.3.1	<i>Loess</i> Parameters for EW Relations . . . . .	98
5.3.2	<i>Loess</i> Parameters for Color and Magnitude Relations . . . . .	99
5.3.3	Description of the EW Fits . . . . .	100
5.4	Models of Diluted EWs based on HIP Fits . . . . .	101
5.5	Walk-through of a Model Calculation . . . . .	102
5.5.1	Choosing the Hot Subdwarf . . . . .	102
5.5.2	Choosing a Late-Type Companion . . . . .	103
5.5.3	Calculating the Diluted Parameters . . . . .	104

Chapter 6. Classification of Composite Spectrum Hot Subdwarfs . . . . .	118
6.1 Introduction . . . . .	118
6.2 Overall Comparison . . . . .	118
6.3 Matching Observations with Models . . . . .	119
6.4 Walk-through of an Individual Case . . . . .	119
6.5 Summary of Companion Classifications . . . . .	122
6.6 Interesting Cases . . . . .	123
6.6.1 Grid Edges . . . . .	123
6.6.2 Subgiant Companions . . . . .	125
6.6.3 Some Unusual Objects . . . . .	126
Chapter 7. Discussion and Summary . . . . .	158
7.1 Defining the Sample . . . . .	158
7.2 2MASS Results . . . . .	158
7.3 Spectroscopy of Composite Hot Subdwarfs . . . . .	159
7.4 Limitations and Directions for Future Work . . . . .	160
7.5 Implications . . . . .	160
Appendix A. Coordinates and Object Notes . . . . .	162
Appendix B. 2MASS All-Sky Data Release Photometry . . . . .	209
Appendix C. Tricks with Magnitudes and Colors . . . . .	246
C.1 Converting Bessel & Brett $JHK$ to 2MASS $JHK_S$ . . . . .	246
C.2 Determining Extinction Vectors . . . . .	246
C.2.1 Extinction Vectors . . . . .	246
C.2.2 Reddening Correction . . . . .	247
C.3 Creating Composite Colors and Magnitudes . . . . .	248
C.3.1 Combining Two Colors . . . . .	248
C.3.2 Combining Two Magnitudes . . . . .	251
Appendix D. Confidence Intervals for a Binomial Distribution . . . . .	255
Appendix E. HIP Standard $M_V$ Calculation . . . . .	256
Appendix F. Calculating Chi Squared Values and Errors . . . . .	261
F.1 Chi Square Goodness-of-Fit Test . . . . .	261
F.2 Confidence Intervals for a Gaussian Fit Based on Chi Squared . . . . .	261
Appendix G. Defining a “ $Q$ ” Parameter for $(J-H, J-K_S)$ Color-Color Space . . . . .	262
G.1 Finding the Least-Squares Linear Fit . . . . .	262
G.2 Defining the Color Parameter $Q$ . . . . .	263
Appendix H. All About Equivalent Widths . . . . .	265
H.1 Basics of Calculating Equivalent Widths . . . . .	265
H.1.1 EW and Poisson Error . . . . .	265
H.1.2 Continuum Fitting Errors . . . . .	266

H.2 Diluting Equivalent Widths by Combining Two Spectra . . . . .	267
H.2.1 Introduction . . . . .	267
H.2.2 Hot Subdwarf Gravity Effects . . . . .	267
H.2.3 Calculating a Diluted EW . . . . .	268
H.2.4 Predicting Diluted EWs using Stellar Flux Distributions . . .	269
Appendix I . Calculating Cubic Spline Approximations . . . . .	279
I.1 Formalism of the Cubic Spline . . . . .	279
I.2 Algorithm for Coefficient Calculation . . . . .	280
Appendix J . Second Order Lagrange Polynomial Interpolation . . . . .	281
Appendix K. Measurements of Equivalent Widths for Program Stars . . . . .	282
Appendix L. Summary of Acronyms and Abbreviations . . . . .	296
Bibliography . . . . .	300

## List of Tables

1.1	Hot Subdwarfs with dM or Brown Dwarf Companions. . . . .	15
3.1	Breakdown of the Hot Subdwarf sample discussed in §3.2. . . . .	43
3.2	Photometry of Hot Subdwarfs with dM or Brown Dwarf Companions. .	44
3.3	Binomial fractions of single and composite-color subdwarfs observed by 2MASS. . . . .	45
3.4	Parameters for the $J-K_S$ sdB Gaussian fits shown in Figure 3.8 <i>c-d</i> . .	45
4.1	Summary of Observing Runs. . . . .	80
4.2	Subdwarf Observing List . . . . .	81
4.3	Composite Subdwarf Spectroscopic Sample Parameters from Literature	86
4.4	Single Subdwarf Spectroscopic Sample Parameters from Literature . . .	91
4.5	Standard Star Observing List . . . . .	93
4.6	Parameters for the Visual Double Hot Subdwarfs. . . . .	96
5.1	<i>Loess</i> Fit to the HIP Standards' EW Measurements. . . . .	114
5.2	<i>Loess</i> Fit to the HIP Standards' $M_V$ Measurements. . . . .	115
5.3	<i>Loess</i> Fit to the HIP Main Sequence Color Measurements. . . . .	116
5.4	<i>Loess</i> Fit to the HIP Subgiant Color Measurements . . . . .	117
6.1	Best-fits to the Composite Hot Subdwarfs . . . . .	140
6.2	Adopted Parameters for the Composite Hot Subdwarfs . . . . .	145
6.3	Previous and My Companion Classifications . . . . .	149
6.4	Previous and My Hot Subdwarf Classifications . . . . .	153
6.5	Parameters for Resolved Visual Double Companions to Hot Subdwarfs	157
A.1	Hot Subdwarf Coordinates . . . . .	165
B.1	Hot Subdwarf Photometry . . . . .	211
C.1	Colors for Main Sequence Stars. . . . .	253
C.2	Colors for Main Sequence Stars Transformed into 2MASS Filters. . . .	254
C.3	Extinction Values for Various Filters. . . . .	254
E.1	HIP Standard Data . . . . .	258
H.1	Adopted Properties of Main Sequence Stars. . . . .	277
H.2	Adopted Properties for Hot Subdwarf Stars. . . . .	277
H.3	Flux Values from the Kurucz Files. . . . .	278
K.1	Blue Spectrum EW Measurements for HIP Stars . . . . .	283
K.2	Red Spectrum EW Measurements for HIP Stars . . . . .	286
K.3	Blue Spectrum EW Measurements for Hot Subdwarfs . . . . .	289
K.4	Red Spectrum EW Measurements for Hot Subdwarfs . . . . .	292



## List of Figures

1.1	Color-Magnitude Diagram of a Globular Cluster. . . . .	14
3.1	Color-color diagrams for reported single and composite hot subdwarfs .	31
3.2	Visual-IR color-color plots for hot subdwarfs. . . . .	32
3.3	Grid of theoretical composite colors by fractional contributions . . . . .	33
3.4	Grid of theoretical fractional composite colors with 2MASS subdwarfs .	34
3.5	Grid of theoretical composite colors by $M_V$ . . . . .	35
3.6	Grid of theoretical composite colors by $M_V$ with all 2MASS subdwarfs .	36
3.7	Color-magnitude diagrams of $J$ and $K_S$ vs. $(J - K_S)$ . . . . .	37
3.8	Bimodal distribution of $J - K_S$ . . . . .	38
3.9	Color-Color plot for 2MASS colors. . . . .	39
3.10	2MASS color-color plot defining the “ $Q$ ” parameter. . . . .	40
3.11	Histogram of sdB $Q$ values. . . . .	41
3.12	Histogram of sdB and sdO $Q$ values. . . . .	42
4.1	McDonald LCS Blue Flat Field. . . . .	58
4.2	The 2MASS Color-Color Plot of Spectroscopically Observed Subdwarfs.	59
4.3	2MASS CMD of Spectroscopically Observed Subdwarfs. . . . .	60
4.4	CMD of the HIP standard stars. . . . .	61
4.5	Comparison between Single, Composite, and Standard Spectra. . . . .	62
4.6	Observed Subdwarf Spectra (part 1). . . . .	63
4.7	Observed Subdwarf Spectra (part 2). . . . .	64
4.8	Observed Subdwarf Spectra (part 3). . . . .	65
4.9	Observed Subdwarf Spectra (part 4). . . . .	66
4.10	Observed Subdwarf Spectra (part 5). . . . .	67
4.11	Observed Subdwarf Spectra (part 6). . . . .	68
4.12	Observed Subdwarf Spectra (part 7). . . . .	69
4.13	Observed Subdwarf Spectra (part 8). . . . .	70
4.14	Observed Subdwarf Spectra (part 9). . . . .	71
4.15	Observed Spectra of Visual Doubles (part 1). . . . .	72
4.16	Observed Spectra of Visual Doubles (part 2). . . . .	73
4.17	Observed Spectra of Visual Doubles (part 3). . . . .	74
4.18	Observed Spectra of Visual Doubles (part 4). . . . .	75
4.19	Observed Spectra of Strong Emission Lined Stars. . . . .	76
4.20	Visual Double Finding Charts (part 1). . . . .	77
4.21	Visual Double Finding Charts (part 2). . . . .	78
4.22	Visual Double Finding Charts (part 3). . . . .	79
5.1	Demonstration of Local Continuum Fitting at Ca II 8662 Å. . . . .	106
5.2	Demonstration of Local Continuum Fitting. . . . .	107
5.3	Local Continua Fits. . . . .	108
5.4	<i>Loess</i> Fits to the HIP EW Trends. . . . .	109

5.5	<i>Loess</i> Fits to the HIP MS Color Trends. . . . .	110
5.6	<i>Loess</i> Fits to the HIP SG Color Trends. . . . .	111
5.7	Color and EW values for generated models. . . . .	112
5.8	Model EWs compared with HIP standards. . . . .	113
6.1	Comparison of Predicted Diluted EWs to Observed Composites. . . . .	128
6.2	Comparison of Predicted Diluted Colors to Observed Composites. . . . .	129
6.3	Best-fit $\chi^2$ space for #120 PHL 3802. . . . .	130
6.4	Best-fit for #120 PHL 3802 in EW and Color Space. . . . .	131
6.5	Comparison Between Two Objects with Similar Fits. . . . .	132
6.6	Comparison Between Two Objects with Different Fits. . . . .	133
6.7	Histograms of Companion $B-V$ and Spectral Types. . . . .	134
6.8	HR diagrams for the Best-fits. . . . .	135
6.9	Flux Ratios for the Best-fits. . . . .	136
6.10	Best-fits compared to Observed Colors. . . . .	137
6.11	Flux Ratios with Observed Colors. . . . .	138
6.12	Comparison Between ZAEHB and TAEHB Models. . . . .	139
H.1	SEDs for main sequence stars and hot subdwarfs with log scaling. . . . .	271
H.2	SEDs for main sequence stars and hot subdwarfs with linear scaling. . . . .	272
H.3	SEDs for proxy hot subdwarfs with log scaling. . . . .	273
H.4	SEDs for proxy hot subdwarfs with linear scaling. . . . .	274
H.5	Comparison of Hubeny SEDs. . . . .	275
H.6	SEDs for proxy hot subdwarfs extended to the UV. . . . .	276

## Acknowledgments

A great big “thank you” goes to R. Ganguly, my parents, grandparents (especially grandma O.), all of my friends, and especially my adviser R. A. Wade — I never would have made it without the support from all of you.

I would like to thank T. Bogdanovich, J. Ding, K. A. Herrmann, K. T. Lewis, and A. Narayanan for assisting with the spectroscopic observations.

Additional thanks goes to: E. M. Green for providing an annotated list of spectroscopically observed hot subdwarfs; G. B. Berriman for his help interpreting the 2MASS catalog; M. Eracleous for writing useful finding chart programs and making them available for others to use; T. C. Beers, V. Caloi, J. S. Drilling, R. F. Green, U. Heber, M. Laget, and T. Lanz for correspondence invaluable to identify KHD objects; H. A. Smith, R. Miller, I. L. Andronov, N. I. Ostrova, V. Burwitz, and J. R. Thorstensen for taking the time to observe my crazy variable emission line star.

This research has been supported in part by: NASA Grid Stars grant NAG5-9586, NASA GSRP grant NGT5-50399, Zaccheus Daniel Fund for astronomy research, Sigma Xi Grant-in-Aid of Research, NOAO Graduate Thesis Travel Support, and a NASA Space Grant Fellowship through the Pennsylvania Space Grant Consortium.

This publication has made use of: data products from the Two Micron All Sky Survey, which is a joint project of the University of Massachusetts and the Infrared Processing and Analysis Center/California Institute of Technology, funded by the National Aeronautics and Space Administration and the National Science Foundation; the USNOFS Image and Catalogue Archive operated by the United States Naval Observatory, Flagstaff Station (<http://www.nofs.navy.mil/data/fchpix/>); the SIMBAD database, operated at CDS, Strasbourg, France; the Digitized Sky Surveys, produced at the Space Telescope Science Institute under U.S. Government grant NAG W-2166; and the NASA/IPAC Extragalactic Database (NED) which is operated by the Jet Propulsion Laboratory, California Institute of Technology, under contract with the National Aeronautics and Space Administration.

*Star Guides*

Any star is enough  
if you know what star it is.

—William Stafford

From there to here, from here to there, funny  
things are everywhere.

—Dr. Seuss

Astronomy is a very dangerous occupation:  
hundreds of tons of moving metal, high volt-  
ages, total darkness, and people who haven't  
slept much — not a good combination.

—Nigel Sharp

## Chapter 1

### Introduction

#### 1.1 What is a “Hot Subdwarf”?

Hot subdwarf stars as a class have effective temperatures exceeding  $\sim 20,000$  Kelvin (K), with surface gravities higher and luminosities lower than main sequence stars of the same temperature. Spectroscopically, hot subdwarfs are divided into two major subtypes: subdwarf B (sdB) and subdwarf O (sdO). SdB stars have hydrogen-dominated atmospheres with  $T_{\text{eff}} \approx 24,000\text{--}30,000$  K and exhibit a relatively small dispersion in luminosity (and thus surface gravity,  $\log g$ , Heber 1986; Saffer et al. 1994; de Boer et al. 1997b). They often exhibit weaker lines of Helium, Carbon, and other atomic species in comparison with Population I main sequence stars. SdO stars have helium-enriched atmospheres with  $T_{\text{eff}} > 30,000$  K and exhibit a wider range of  $\log g$  and luminosity than the sdB stars (Heber 1986; Saffer et al. 1994; de Boer et al. 1997b).

There are a number of stellar objects that show up in ultraviolet (UV) excess surveys, I will take a moment to summarize those objects following the spectral descriptions of Moehler et al. (1990b):

**B** — Main sequence B-type spectra showing Balmer lines and He I absorption with He I 4388 Å being about the same strength as He I 4471 Å.

**HBB** — (horizontal branch blue) Spectra show Balmer line absorption of moderate gravity accompanied by He I (4471 Å) and/or Mg II (4481 Å) absorption.

**sdB** — Spectra show strong, broad, Balmer lines and weak (or no) He I absorption with the line at 4388 Å being much weaker than the one at 4471 Å.

**sdOB** — Spectra show strong, broad, Balmer lines accompanied by He I (4471 Å) and He II (4686 Å) absorption (both weak) — sdOBs were first introduced by Baschek & Norris (1975) and are basically hotter versions ( $T_{\text{eff}} \gtrsim 35,000$ ) of the sdBs.

**sdO** — Spectra show strong, broad, Balmer lines accompanied by He II absorption.

**He-sdB** — These (unlike “normal” sdB stars) show spectra dominated by strong He I lines accompanied by weak He II lines, and with no detectable hydrogen absorption [identical to the sdO(D) classification of Green et al. 1986].

**He-sdO** — Similar to He-sdB but are hotter stars which have spectra with strong He II absorption, sometimes weak He I, but no Balmer lines.

**DA** — Summarizes all hydrogen-dominated white dwarfs (WDs), namely stars with extremely broad Balmer lines and no helium lines at all.

I will focus mainly on the properties of the sdB and sdOB stars in this section.

### 1.1.1 Comparison with Globular Clusters

In the Hertzsprung-Russell (HR) Diagram, hot subdwarfs fall into the region occupied by the extended horizontal branch<sup>1</sup> (EHB) seen in some globular clusters. The horizontal branches (HB) seen in globular clusters extend away from the red giant branch horizontally at roughly constant brightness toward hotter temperatures (bluer colors) — see Figure 1.1 for a labelled color-magnitude diagram of a globular cluster. The EHB is the bluest extension of the HB and stretches to the hottest temperatures (bluest colors) while dropping to fainter visual magnitudes in a color magnitude diagram (thus it can be said the “horizontal” branch becomes “vertical” at the hottest temperatures — this is also called a “blue tail”). This slope change in the HB toward higher temperatures is due to increasing bolometric corrections, with a simultaneous decrease in the sensitivity of the  $B-V$  color to temperature change. Physically, the spread in temperature across the HB is due to varying envelope masses of the HB stars — the redder stars have the most massive envelopes, while the bluer stars have the least massive. In the case of EHB stars, their envelopes are so thin that they are unable to fully evolve up the asymptotic giant branch after core helium exhaustion. Thus EHB stars evolve directly to the WD cooling tracks following core helium burning as “asymptotic giant branch manqué” (AGB-manqué) stars, or leave the AGB before thermal pulsing as “post-early AGB” (Greggio & Renzini 1990; Dorman et al. 1993).

The field sdB stars, in particular, are consistent with the EHB star population defined from globular clusters (Humason & Zwicky 1947) — thus the field sdB stars are understood as core helium burning objects with very low hydrogen envelope mass ( $M_{\text{env}} \lesssim 0.01 M_{\odot}$ ) and total masses of  $M \approx 0.5 M_{\odot}$  (Saffer et al. 1994; Dorman et al. 1993; Brassard et al. 2001). This apparently homogeneous population of objects with similar formation histories forms a unique laboratory for the study of post-main sequence mass loss and binary evolution (in particular common envelope and Roche lobe overflow mechanisms). Thus, understanding the origins and properties of galactic field sdBs can lead to a better understanding of the “second parameter” (dictating the structure of globular cluster horizontal branches) and of stellar evolution theory (describing post-main sequence evolution and mass loss).

Some sdO stars have colors and luminosities that are consistent with the hottest part of the EHB (least massive H envelopes). However, there are a number of potential evolutionary paths, e.g. post-AGB evolution, that lead through the rather broad region of the HR diagram occupied by sdO stars. All hot subdwarfs, regardless of their prior evolution, are thought to be direct progenitors of WDs, although they constitute only a small fraction of all stars that evolve to become WDs.

### 1.1.2 Physical Parameters

The effective temperatures of sdBs have generally been reported in the range of  $23,000 < T_{\text{eff}} < 38,000$  K (i.e., Heber et al. 1984; Heber 1986; Moehler, Heber, &

---

<sup>1</sup>The term “extended horizontal branch” was coined by Greenstein & Sargent (1974), however references to the “blue extension of the horizontal branch” date back at least to the 1950’s (e.g., Greenstein 1952; Sandage 1953).

de Boer 1990a; Moehler et al. 1990b; Theissen et al. 1993; Saffer et al. 1994; Edelmann et al. 2003). The effective temperatures of the sdOBs are generally hotter than the sdBs, and have been reported in the range of  $26,000 < T_{\text{eff}} < 42,000$  K (i.e., Baschek et al. 1982; Heber et al. 1984; Heber 1986; Theissen et al. 1993; Saffer et al. 1994; Edelmann et al. 2003).

The surface gravities for sdB stars are generally reported in the range of  $4.5 < \log g < 6.65$  (i.e., Heber et al. 1984; Moehler et al. 1990a,b; Theissen et al. 1993; Saffer et al. 1994; Edelmann et al. 2003). The surface gravities for sdOB stars are generally higher than those of the sdBs, and have been reported in the range of  $5.25 < \log g < 6.30$  (i.e., Baschek et al. 1982; Heber et al. 1984; Theissen et al. 1993; Saffer et al. 1994; Edelmann et al. 2003).

In both sdB and sdOB stars, helium in the atmosphere is strongly depleted due to diffusion. This implies that the sdB and sdOB must have calm, stable atmospheres, or in other words, the sdB and sdOB mass loss rates must be considerably lower than expected from sdO mass loss rates (Heber 1986). Reported abundances for helium (based on number fraction) have ranged from less than  $0.0001 < n_{\text{He}}/n_{\text{H}} < 0.10$  for sdB, and  $0.0005 < n_{\text{He}}/n_{\text{H}} < 0.25$  for sdO (Baschek et al. 1982; Heber et al. 1984; Heber 1986; Moehler et al. 1990a,b; Theissen et al. 1993; Saffer et al. 1994; Edelmann et al. 2003). Initially authors found no correlations between helium abundance and any other parameters (such as  $\log g$ ,  $T_{\text{eff}}$ , or along evolutionary tracks, i.e., Moehler et al. 1990a,b; Theissen et al. 1993). However, more recently Edelmann et al. (2003) reported a separation of the sdB into two sequences in the  $(T_{\text{eff}}, \text{helium abundance})$ -plane — about 1/6th of the sdB they analyzed from the Hamburg Quasar Survey (HS; Hagen et al. 1995) have much lower helium abundances at the same temperature than the bulk of the sdBs.

### 1.1.3 Kinematics and Population Membership

There are many studies of the kinematics and space densities of hot subdwarfs, I will discuss only a few of them here.

The accepted population membership of hot subdwarfs has evolved with time. Early works (including Baschek & Norris 1970; Newell 1973; Greenstein & Sargent 1974) assumed hot subdwarfs were halo members. Later studies (including Theissen et al. 1992; Colin et al. 1994; Villeneuve et al. 1995; Thejll et al. 1997; de Boer et al. 1997a) placed the hot subdwarfs as primarily (thick or old) disk objects with a handful of possible halo objects. Finally, the most recent studies have clearly identified both disk and halo components of the hot subdwarfs (including Mitchell 1998; Altmann, de Boer, & Edelmann 2001; Altmann, Edelmann, & de Boer 2004). In particular, Mitchell (1998) claims that his results imply that high-latitude sdB stars fainter than  $B \simeq 15.5$  ( $z \gtrsim 1.5$  kpc) will predominantly come from the halo population. He further indicates that high-latitude sdB samples with  $B < 14.5$  should contain  $\sim 60\%$  disk and  $\sim 40\%$  halo stars, while samples with  $B < 13$  should contain  $\sim 80\%$  disk and  $\sim 20\%$  halo. He further suggests that these surprisingly large fractions of halo sdB stars in bright samples could account for some of the trouble previous analyses have had in arriving at consistent values of sdB disk scale heights (see following paragraph). Then, just to further muddle things, Altmann

et al. (2001, 2004) report that they additionally see some sdB stars with near-solar kinematics which are most likely associated with the thin disk (unfortunately their sample composition prevents them from unambiguously separating the two disk populations).

Similarly, reported values of scale heights for sdB stars have varied greatly, but in general they show a trend to increase with time and sample size. Early determinations started around  $150 \leq z \leq 300$  pc, such as from Theissen et al. (1992) based on a sample size of 11 objects, and increased to  $z_e = 450 \pm 150$  pc (for an exponential distribution) or  $z_0 = 600 \pm 150$  pc (for isothermal) from Villeneuve et al. (1995), and finally up to  $z_e = 1$  kpc from de Boer et al. (1997a), and Altmann et al. (2001, 2004).

Colin et al. (1994) examined the space motions of a small sample ( $N = 7$ ) of hot subdwarfs, including: proper motions, radial velocities (RVs), and distances. Among other things, they found a mean rotational velocity of  $\bar{\Theta} = +131 \pm 17$  km s<sup>-1</sup> for the sdB stars (which they note is similar to that found by Armandroff 1989, for disk globular clusters,  $+140 \pm 27$  km s<sup>-1</sup>, and very different from halo globular clusters,  $+46 \pm 23$  km s<sup>-1</sup>). Altmann et al. (2001, 2004) also determined the mean orbital velocity of the sdB stars:  $\bar{\Theta} = +175$  km s<sup>-1</sup> (which they claim is higher than other reported values due to contamination from thin disk and halo stars in their sample).

Thejll et al. (1997) analyzed the proper motions of a large sample (348) of WDs, sdB, and sdO stars. They also performed a statistical analysis to determine a value of  $M_{V,\text{sdB}} = 4.8 \pm 0.5$ . They found that the reduced proper motion distributions of the sdB and sdO imply that their absolute magnitudes are different, or their kinematics are different, or both. Assuming sdO and sdB have the same kinematics, then they infer that  $M_{V,\text{sdO}}$  is about one magnitude brighter in the mean, and one magnitude more broadly distributed, than the sdB distribution.

#### 1.1.4 Ultraviolet Excess

Hot subdwarfs (particularly sdBs) are believed to be the primary contributor to the UV excess (UVX) seen in UV observations of inactive elliptical galaxies, spiral galaxy bulges, and other old stellar populations (O’Connell 1999; Brown et al. 2000). In some cases hot horizontal branch stars have been imaged directly in elliptical galaxies (i.e., Brown et al. 2000, using the *Space Telescope Imaging Spectrograph*, STIS) — these observations demonstrate that hot subdwarfs can be the primary contributors to the integrated UVX from elliptical galaxies. It is believed from both models and observations that the lifetime UV output of hot subdwarfs is sensitive to their physical properties, in particular the helium abundance and mean envelope mass of an EHB population. Small changes in either (i.e., a change of only  $\sim 0.01 M_\odot$  in the mean envelope mass) can significantly alter the UV spectrum of an elliptical galaxy (O’Connell 1999). Thus UV observations would be a very sensitive probe of the star formation and chemical enrichment histories of galaxies *provided* we understood the basic astrophysics of hot subdwarfs and their production by their parent populations. To understand the mechanisms of UVX we must combine integrated light observations of galaxies with the stellar astrophysics derived from Galactic cluster and field hot subdwarfs. Additionally, UVX stars are important contributors to the interstellar ionizing radiation field of old populations. Characterizing the UV light of nearby elliptical galaxies and its predicted



evolution are basic to the development of realistic “K-corrections” for cosmological applications to high redshift galaxies and the interpretation of the cosmic background light (O’Connell 1999). Thus understanding field hot subdwarfs in our own Galaxy can lead to a better understanding of many other areas including: cosmology, chemical enrichment histories of galaxies, stellar mass loss, and UV background radiation.

## 1.2 Sidetrack: Name-ology

The above discussion makes the classification and identification of hot subdwarfs seem straightforward. However there is a subtle distinction that I would like to take a moment to discuss. There are in fact three ways to classify a star as a hot subdwarf: 1. EHB cluster classification (i.e., position in a cluster color-magnitude diagram), 2. sdB spectroscopic classification (i.e., the width of its spectral lines due to gravitational broadening), and 3. evolutionary classification as a core-helium burning star. Each of these methods leads to a slightly different sample (e.g., an object that is a hot core-helium burning EHB star to a theorist might not be classified sdB by a spectroscopist). This is a very subtle distinction, but one to be aware of when inter-comparing spectroscopic samples, theoretical models, and stellar cluster photometric samples. That said, I will follow the general convention of using sdB, EHB, and hot subdwarf interchangeably (with the understanding that I am coming at this issue with a spectroscopist’s point of view).

Further details of hot subdwarf spectral classification issues are discussed in Drilling et al. (2000, 2003). Theoretical discussions can be found in Caloi (1972) and Han et al. (2002, 2003). Further discussion about globular cluster EHB stars is included in Moehler (2001).

## 1.3 Pulsating sdBs

Pulsating stars have proven invaluable as probes of stellar interiors. Thus identifying pulsating stars among the sdB stars leads to the possibility of using these pulsations as probes of their interiors (Kilkenny et al. 1997).

### 1.3.1 V361 Hya (EC 14026, sdBV) Stars

The V361 Hya stars (also called EC 14026 or sdBV stars) are a class of small-amplitude, rapidly pulsating sdBs that were first identified by Kilkenny et al. (1997). These stars have periods typically  $\sim 100$ – $250$  sec (total range  $\sim 80$ – $600$  sec), with at least two oscillation frequencies (but in some cases many more), low amplitudes (less than a few hundredths of a magnitude), and surface temperatures clustering near  $33,500$  K (Kilkenny et al. 1998; Falter et al. 2003; Green et al. 2003). The variations are caused by radial and non-radial, low degree and low order acoustic pulsation modes which are driven by an opacity bump due to iron and other metals in the sdB envelope (Falter et al. 2003). The pulsation modes observed in V361 Hya stars are pressure modes with spherical harmonics (indices  $l$  and  $m$ , Falter et al. 2003).

### 1.3.2 PG 1716+426 Stars

The PG 1716 stars are a second class of multi-mode pulsating sdB that were first reported by Green et al. (2003). Stars in this second class have apparent periods that are at least a factor of ten longer than those seen in the V361 Hya stars, with peak-to-peak amplitudes  $\lesssim 0.05$  mag (Green et al. 2003). The “long” period of these pulsations implies that they must be due to gravity modes (the so called “ $g$ -modes”), unlike the pressure modes of the V361 Hya stars. Green et al. (2003) report that  $g$ -mode pulsations are only found among the cooler sdB stars with surprisingly high frequency ( $\sim 75\%$  of sdB stars with  $T_{\text{eff}} < 30,000$  K, or  $\sim 25\text{--}30\%$  of all sdB stars).

## 1.4 Formation and Evolution of Hot Subdwarf Stars

While the current evolutionary status of sdB stars is relatively well understood, how they actually arrived at the EHB with such low envelope masses is not understood. In this section I will discuss the various models that have been put forth in an attempt to describe the formation of hot subdwarfs. First I will discuss the binary formation model (§1.4.1), then I will discuss the single star formation model (§1.4.2).

### 1.4.1 Binary Formation Models

The leading theory describing the formation of field sdB stars in our Galaxy is that they lost significant envelope mass due to binary interactions during their post-main sequence evolution. The earliest references that I could find to this scenario as a possible explanation for sdB formation were Sweigart, Mengel, & Demarque (1974)<sup>2</sup> and Baschek & Norris (1975). The first attempt to theoretically describe this process was made by Mengel, Norris, & Gross (1976), while more extensive theoretical modelling was preformed only recently by Han et al. (2002, 2003).

The extensive theoretical modelling of sdB binary formation mechanisms by Han et al. (2002, 2003) aimed to distinguish among several binary formation channels, and simulate the evolution of the resulting sub-samples. They focused on three channels: 1. the common envelope (CE) ejection channel, 2. the stable Roche lobe overflow (RLOF) channel, and 3. the WD merger channel (also discussed in Iben 1990). The CE channel may account for more than 2/3 of all sdB stars. In this channel dynamically unstable mass transfer near the tip of the first giant branch causes a common envelope and spiral-in phase which then results in the ejection of the envelope and a short period binary. The CE ejection channel leads to sdB stars in binaries with typical orbital periods between 0.1–10 days, a mass distribution sharply peaked around  $\sim 0.46M_{\odot}$ , and very thin hydrogen-rich envelope. In the stable RLOF channel the progenitor system experiences stable mass transfer which strips the giant of its envelope. If this occurs near the tip of the first giant branch, then the remnant helium core can still ignite

---

<sup>2</sup>Sweigart et al. (1974) does cite a conference paper by P. Giannone presented at Frascati Study Group on Globular Clusters and Related Problems of Galactic Evolution, 1973. Unfortunately the proceedings of this meeting were never published (A. Sweigart, private communication, July 2005), so I was unable to verify this information firsthand.

core helium burning and become a sdB star in a binary with a long orbital period and fairly thick hydrogen envelope (compared to the other binary channels). This channel usually requires a fairly massive WD companion or enhanced mass loss from a stellar wind (i.e., tidally enhanced winds) before the onset of RLOF. The stable RLOF channel produces sdB stars with masses similar to the CE channel but with orbital periods of 400–1500 days ( $\sim 1$ –4 years) and relatively thick hydrogen-rich envelopes. Two helium WDs can merge due to gravitational wave radiation, if the merger product is able to ignite core helium burning, then a single sdB star is formed. The WD merger channel gives rise to single sdB stars with a fairly wide mass distribution,  $0.4$ – $0.65M_{\odot}$ , but extremely thin hydrogen-rich envelopes.

Han et al. ran multiple scenarios varying the quantities: CE ejection efficiency, fraction of CE thermal energy used for ejection, critical mass ratio above which mass transfer is stable on the red giant branch, initial mass ratio distribution of progenitor binary systems, and metallicity. Of these parameters, the two dealing with CE ejection are the least constrained due to a poor understanding of CE ejection physics. However, the value of the critical mass ratio is highly sensitive to the fraction of binaries with A-type main sequence companions. For example, the sdB+A/F binaries in the Han et al. scenario are produced from stable Roche-lobe overflow from the sdB-progenitor onto the companion star when the sdB-progenitor is on the first giant branch (or in the Hertzsprung gap for some of the earliest A-type companions). From the values for the total numbers of sdB stars reported by Han et al., it can be calculated that they predict between 10–40% of *all* sdB stars should have A-type companions (depending on the value of the critical mass ratio assumed for Roche lobe overflow on the giant branch). This is a significant difference, especially when compared to their predictions for F-type stars, 9–15% of all sdBs for the same range in critical mass ratio. Thus finding and accurately enumerating sdB+A-type binaries is of significant interest for constraining these binary formation theories.

Thus far hot subdwarfs in the Galactic field (including those I have been studying) have been identified by their blue photometric colors in the visual region of the spectrum (i.e., surveys such as the Palomar-Green, PG, and Edinburgh-Cape, EC, Surveys; Green et al. 1986; Stobie et al. 1997, respectively). Unfortunately, this technique leads to a biased sample of sdB stars. These surveys only identify sdBs that are single, or have a binary companion that does not dominate over the subdwarf at blue wavelengths (i.e., only single sdB, sdB+late-type main sequence, and sdB+WD binaries are found). These surveys have been *unable* to identify sdB stars in binaries with early-type stars (namely A and F-type main sequence stars) because in the blue region of the spectrum the A or F-type star dominates and thus masks the presence of the sdB.

One major flaw with the Han et al. scenario comes from the distribution of periods with  $T_{\text{eff}}$  for the first CE ejection and first stable RLOF channels (see Figure 15 in Han et al. 2003). According to their models, all hot subdwarfs with MS star companions later than  $\sim$ mid-F should exist in binaries that went through the first CE ejection phase, and thus will have periods *shorter than  $\sim 40$  days*. The binaries with periods longer than 40 days (with types later than  $\sim$ mid-F) were formed through the first stable RLOF channel but contain a subgiant or giant companion to the hot subdwarf. These predictions can be tested by radial velocity studies (see §1.4.1.2).

#### 1.4.1.1 Known Binaries

Surveys have identified field binary (sdB+WD or sdB+dM) and composite sdB+late-type companion (usually G or K type) systems. Most of these studies have been done in the visual and blue region of the spectrum where the subdwarf dominates the light, and there are indeed few identifications of dM companions — thus far there are seven known:

1. HS 0705+6700<sup>3</sup> (Drechsel et al. 2001),
2. PG 1017–086 (KHD sequence number #407; Maxted et al. 2002),
3. PG 1241–084/HW Vir (#605; Menzies & Marang 1986),
4. PG 1329+159 (#687; Green et al. 2004; Morales-Rueda, Maxted, & Marsh 2004; Morales-Rueda et al. 2003),
5. PG 1336–018 (#695; Kilkenney et al. 1998),
6. PG 1438–029 (#816; Green et al. 2004), and
7. HS 2333+3927<sup>3</sup> (Heber et al. 2004).

Additionally, the sdOB star HD 269696 (AA Dor, LB 3459, KHD sequence #218) is an eclipsing, single-lined spectroscopic binary ( $P = 0.2615$ d) showing a reflection effect, in which the companion is believed to be a brown dwarf (BD;  $M \approx 0.066 M_{\odot}$ ; see Paczyński 1980; Rauch 2000, and references therein). All of these dM and BD binaries are very short period (see Table 1.1) and the nature of the companion was studied in part by eclipses or reflection effects in the light curve.

The usual technique that has been employed when studying the individual properties of the two components of a composite spectrum sdB (sdB+late-type) is to assume “typical” properties for the sdB itself (in particular the luminosity), then attempt to deduce the properties of the late-type companion; or conversely, to assume a luminosity for the companion and attempt to deduce the properties of the sdB. Some authors have favored less luminous sdBs ( $M_V > 5.0$ ) and main sequence companions (Bixler, Bowyer, & Laget 1991; Ferguson, Green, & Liebert 1984), whereas others favor more luminous sdB ( $M_V < 5.0$ ) and subgiant companions (Allard et al. 1994; Jeffery & Pollacco 1998). However, current observations do not distinguish between the two possibilities.

Total binary fractions extrapolated from the observed composite spectrum systems by previous studies lie in the range 50–100%, depending on assumptions made about the physical parameters of the companion and/or sdB itself. For example, uncertainties in the luminosity of field sdBs (usually quoted in the range  $M_V \approx 4.0$ –5.5) make the determination of the luminosity of the unresolved late-type companion uncertain (i.e., main sequence or subgiant), which impacts the extrapolation to even cooler companions such as M dwarfs (dM). Additionally, the evolutionary models of Han et al. (2002, 2003) predict field hot subdwarfs will have a much larger spread in masses and luminosities than what has been observed in clusters (i.e., Han et al. 2002 discuss sdBs with a mass range of 0.4–0.8  $M_{\odot}$ ).

---

<sup>3</sup>Not in KHD.

Past surveys have generally concluded that  $\gtrsim 50\%$  of hot subdwarfs have late type companions (e.g., Allard et al. 1994; Bixler et al. 1991; Ferguson et al. 1984). However, these percentages depend greatly on the corrections made to account for late type companions that were undetectable by the survey (i.e., M-dwarfs) and the assumed luminosity of the subdwarfs or observed companions (i.e., main sequence or subgiant). Based on their observations of composite spectrum sdB stars from the PG survey (Green et al. 1986), Ferguson et al. (1984) extrapolated that about 50% of the sdB stars in the PG catalog had main sequence companions of G8 or later (and a few had companions earlier than G8). Allard et al. (1994) identified 31 composite candidates out of 100 sdB stars observed photometrically, and deduced a fraction of sdB stars with cool main sequence companions of 54–66%, when allowance was made for perceived selection effects. From intermediate resolution spectroscopy of the Ca II IR triplet region of 40 sdB stars, and an assumed “typical” luminosity of a sdB star, Jeffery & Pollacco (1998) claim that the seven composite systems they observed contained subgiant companions. Therefore they conclude that the binary fraction must be much higher than what Allard et al. (1994) concluded based on assuming main sequence companions. From a sample of 40 UV selected hot subdwarfs, Bixler et al. (1991) found that eight showed composite spectra, and calculated that 65–100% of hot subdwarfs had a late type main sequence companion. Unfortunately, comparisons between these surveys is difficult due to the unknown selection effects involved in each. Additionally, as I will discuss in Chapter 3, magnitude limited samples will overestimate the fraction of composite-spectrum binaries present among currently known sdB stars.

If field sdB stars truly are the same objects as globular cluster EHB stars, then one would expect that both field sdB and cluster EHB stars would have been formed through similar processes. Observations of globular clusters show a wide range of HB morphologies: some contain only red HB stars, others only blue, and some a mixture of both. Invoking *only* binary processes to produce cluster and field hot subdwarfs would imply that the binary fraction varies dramatically from cluster to cluster, which seems highly unlikely (although stellar encounters in the dense globular cluster environment may have an affect too). Thus there must be some other process, or a combination of other processes, through which field and cluster hot subdwarfs can form, implying that the presence of field sdB stars in binary systems is largely coincidental and that in most cases the two stars exist in *wide* binaries which never interacted, or as single stars. (Or if the composite spectrum binaries did interact, then it was through a Roche-lobe overflow mechanism, and the late-type star would have had enough time to adjust to the increase in mass.) In fact, if sdB stars descend from F or G main sequence stars, one would expect a large fraction of them to be in binary systems with *any* separation up to  $\sim 10^4$  AU (Duquennoy & Mayor 1991). In that case, some of the binaries should be resolvable with high angular resolution imaging (Heber et al. 2002; Wade & Stark 2004).

#### 1.4.1.2 Radial Velocity Studies

Lending support to the idea of a large range in binary separations, spectroscopic radial velocity studies of sdB stars (Saffer, Green, & Bowers 2001; Maxted et al. 2001) have found three distinct groups based on their spectral features. Group I ( $\sim 35\%$  of

all sdB stars) exhibit no detectable features from a companion in the visible and insignificant velocity variations. Group II ( $\sim 45\text{--}60\%$ ) comprises single-lined spectroscopic binaries with periods of  $\sim 1\text{--}30$  days (sdB+WD and sdB+dM). Group III ( $\sim 13\text{--}20\%$ ) are composite spectrum binaries (with FGK-type companions) showing slowly varying or nearly constant velocities indicating widely separated binaries (periods of at least many months to many years; see also Orosz, Wade, & Harlow 1997). Group I might be an analog of Group III binaries with undetectably faint companions.

This seems to indicate that, in the case of Groups I and III at least, binary interaction did not play a significant role in the formation of the sdB, apparently contradicting the current binary formation theory. In this case however, the FGK companions of Group III are then also unaffected by binary interactions and may be used to better characterize the subdwarfs' luminosities independent of any uncertainties in modelling the sdB's spectrum. If on the other hand, Groups I and III, are in fact sdB+MS binaries with periods on the order of a few years, then they could have interacted through a Roche-lobe overflow mechanism. However in this case the late-type star would have had time to adjust to the increase in mass so it should still look like a normal MS star (just one that is more massive than it initially formed as), and can still be used to better characterize the subdwarfs' luminosities.

At this point it would be good to review the predictions made by Han et al. (2002, 2003, see introduction to §1.4.1) for composite hot subdwarf binaries with companions of  $\sim G$ -type or later: those with periods shorter than  $\sim 40$  days will have MS companions and formed through CE ejection, while those with periods longer than  $\sim 40$  days will have subgiant or giant companions and formed through RLOF. Combining this theory with radial velocity observations would predict that all late-type companions observed in the composite spectrum binaries are subgiants or giants (since all observed have periods longer than 40 days). This itself is contradictory to what the majority of the hot subdwarf community (including Han et al. 2003) have assumed for the nature of the late-type companions: they are MS. Thus understanding the evolutionary state of the late-type companions is of particular interest in respect to verifying binary evolution theory.

## 1.4.2 Single Star Evolution

### 1.4.2.1 Delayed Helium Flashers

Castellani & Castellani (1993) suggests that the EHB stars in globular clusters can be explained by a “delayed helium-flash.” In this scenario a star that experiences massive amounts of mass-loss (due to high mass-loss efficiency from enhanced stellar wind and/or dynamical interactions with other stars in dense stellar cores) on the red giant branch (RGB) can fail to ignite the helium flash at the tip of the RGB. This star then evolves to the WD cooling sequence with an electron-degenerate helium core. Then depending on the amount of residual hydrogen-rich envelope mass, the star can either ignite helium-burning at the bright end of the WD cooling sequence (“early hot flasher”) or later along the WD cooling sequence (“late hot flasher”). After the helium flash, these stars settle on the zero-age EHB (ZAEHB).

Cassisi et al. (2003) investigates core helium-flash after the tip of the RGB in low-mass stars that experienced extreme mass loss and have very thin hydrogen-rich

envelopes. When the helium-flash occurs a convective zone is driven up to penetrate the hydrogen-rich layers and triggers a thermonuclear runaway which results in surface enrichment of helium and carbon. From their modelling, the stars that experienced this dredge-up event are significantly hotter than their counterparts with hydrogen-rich envelopes. Thus, Cassisi et al. (2003) suggest that these stars are a possible source of stars observed in some clusters (i.e., NGC 6752) beyond the canonical blue end of the EHB and are fainter than the bluest end of the EHB by up to  $\sim 0.7$  mag in the UV (A.K.A., “blue hook stars”).

#### 1.4.2.2 Hot-Flashers

D’Cruz et al. (1996) investigated the effects of metallicity and a large range of mass loss efficiency (described by Reimers’ formula and the mass-loss efficiency parameter,  $\eta_R$ ) in an attempt to understand how EHB stars can be produced over a large range of metallicities without fine-tuning the mass loss process. They discovered that sufficiently rapid mass loss on the RGB causes stars to “peel-off” the RGB, evolve to high temperatures, and settle on the WD cooling curve. Some of these stars had sufficient core mass to then undergo a helium flash later and at high temperatures (D’Cruz et al. 1996, called these objects “hot He-flashers”). These stars would then settle at the very blue end of the EHB forming a “blue hook.” These “hot-flashers” are a part of the EHB and follow AGB-manqué evolution.

The four major results of the D’Cruz et al. (1996) investigation are:

1. “Producing EHB stars requires no more fine-tuning than producing ordinary HB stars in globular clusters.” They found that the values of  $\eta_R$  that produces EHB stars is comparable to that producing normal HB.
2. Even though high-metallicity stars must lose more mass to reach the EHB than low-metallicity stars, they can still achieve this mass loss with  $\eta_R$ -values that are comparable to those needed for low metallicity star. Therefore “it is no more difficult to produce EHB stars at high metallicity than at low.” However they admit they do not know the physical interpretation of this result.
3. “It becomes more difficult to make ordinary blue HB (IBHB<sup>4</sup>) stars at higher metallicity... [thus] the ZAHB<sup>5</sup> becomes increasingly *bimodal* for metal-rich populations.” They note that this is consistent with the models of Yi et al. (1995) and observations of NGC 6791 which shows a lack of IBHB stars but up to ten EHB stars.
4. “The range of values of  $\eta_R$  producing EHB stars is almost constant for all metallicities. To make EHB stars at high metallicity,  $\eta_R$  does not have to increase, and its distribution does not have to be more finely tuned.”

In summary, assuming red giants lose mass following something like the Reimers mass-loss formula, and provided there is a broad enough distribution in  $\eta_R$ , then HB morphology (and EHB stars) in clusters can be explained at both low and high metallicities by differing mass-loss rates without any fine tuning. So, while this theory has

---

<sup>4</sup>IBHB = intermediate blue horizontal branch: stars that lie blueward of the instability strip but can still reach the AGB after core-helium depletion (Dorman, O’Connell, & Rood 1995).

<sup>5</sup>ZAHB = zero-age horizontal branch

some promise of producing EHB stars through single star evolution, there is no true predictive power in this theory, since there is no physical reason for RGB stars to lose mass according to Reimers' mass-loss formula.

## 1.5 The Mission

In this work, I will determine the physical properties of the late-type companion in unresolved composite spectrum sdBs. The radial velocity studies of these composite spectrum systems seem to indicate that they are in wide binaries which therefore did not interact (see §1.4.1.2), or interacted only through stable RLOF. So, the FGK companions of the radial velocity Group III are then also unaffected by binary interactions and may be used to better characterize the subdwarfs' luminosities independent of any uncertainties in modelling the sdB's spectrum. Current observations do not clearly distinguish between main sequence and subgiant companions in the composite spectrum sdBs (see §1.4.1.1). However, binary evolution theory by Han et al. (2002, 2003) predict that among companions of  $\sim$ G-type or later, the MS stars will exist in short period binaries ( $P \lesssim 40$  days), while the subgiant and giant companions will exist in long period binaries ( $P \gtrsim 40$  days). So, determining the evolutionary state of the late-type companions is of great interest for refining binary population synthesis models.

Combining spectroscopy with photometry, I directly determine the companion's spectral type and luminosity class (main sequence or subgiant), along with the fraction of light contributed by each component. Using this information I will resolve the current degeneracy between MS and subgiant, while providing an independent measure of the luminosity, and constraints on the age and progenitor mass of the sdB. Additionally, these classifications will help refine binary population synthesis models (such as those of Han et al. 2002, 2003).

## 1.6 Outline

I will briefly outline the major information presented in each of the following chapters and appendices. In Chapter 2, I will discuss the source of object coordinates and adopted object classifications. In Chapter 3, I will discuss the results of the study of all hot subdwarfs using the *Two Micron All Sky Survey*. In Chapter 4, I will discuss the observation procedures, target selection procedures, and data reduction procedures for my spectroscopic observations. In Chapter 5, I will discuss the extraction of equivalent width values from my spectra, and the processing of these values. In Chapter 6, I will discuss the results of my spectroscopic study of the late-type companions in composite spectrum sdBs. In Chapter 7, I will summarize the major aspects of this study and suggest directions for follow-up work.

Appendix A includes the list of all hot subdwarf coordinates, names, classifications, and notes. Appendix B includes the *Two Micron All Sky Survey* photometry of all hot subdwarfs. Appendix C includes descriptions of color conversions, reddening/extinction corrections, creating composite colors, and combining magnitudes. Appendix D describes the process of calculating confidence intervals for a binomial distribution. Appendix E describes the calculation of  $M_V$  (and its associated error) for the



Hipparcos standard stars. Appendix F deals with the chi-square goodness-of-fit test, and using chi-square to calculate errors on a Gaussian fit to a binomial distribution. Appendix G discusses the calculation of the *Two Micron All Sky Survey* “*Q*” parameter. Appendix H deals with many aspects of measuring equivalent widths and their errors, and diluting equivalent widths by combining two spectra. Appendix I discusses the calculation of a cubic spline approximation through a set of points. Appendix J describes how to calculate a second order Lagrange polynomial to interpolate between points. Appendix K gives the measured EWs for all of my spectroscopic measurements. Appendix L provides a list with definitions of acronyms and abbreviations I use throughout this work, along with the first page where they occur.

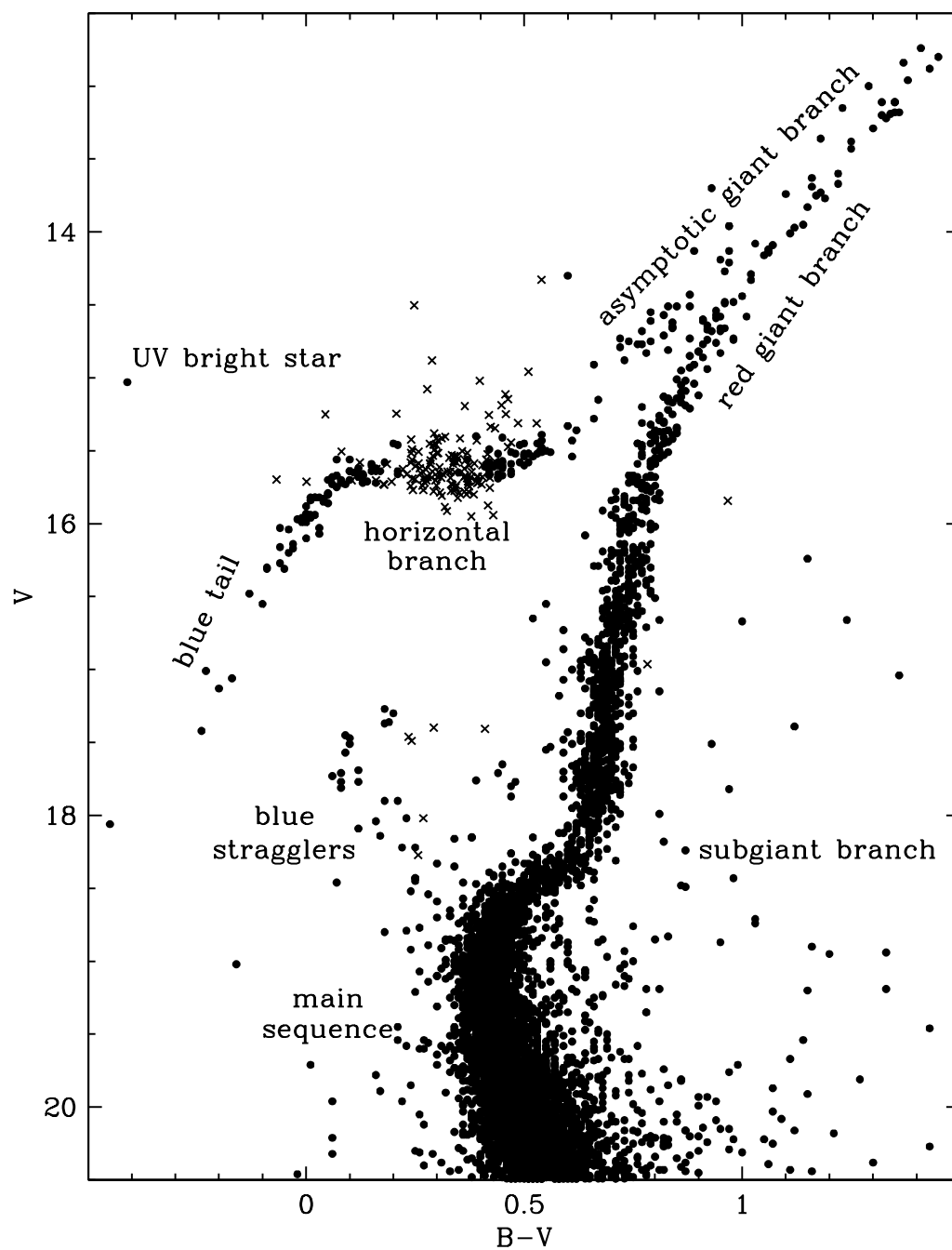


Fig. 1.1 Color-Magnitude Diagram of the globular cluster M3 labelled after Moehler (2001), using M3 photometry from Buonanno et al. (1994), circles, and variable star photometry from Hartman et al. (2005), crosses (“×”).

Table 1.1. Hot Subdwarfs with dM or Brown Dwarf Companions.

No. <sup>a</sup>	Name	Period (d)	K (km/s)	$f(m)$ ( $M_{\odot}$ )	$M_{2,\min}$ ( $M_{\odot}$ )	Mag / Band	References <sup>b</sup>
218	HD 269696 <sup>c</sup>	0.262	40.8 <sup>d</sup>	0.0018 <sup>e</sup>	0.066 <sup>d</sup>	11.13 / V	Paczynski (1980)
...	HS 0705+6700	0.906	85.8	0.00626	0.13	14.2 / B	Drechsel et al. (2001)
407	PG 1017-086	0.073	51.0	0.0010 <sup>e</sup>	0.0687	14.43 / y	Maxted et al. (2002)
605	PG 1241-084	0.117	87.9	0.0082 <sup>e</sup>	0.12	10.58 / y	Menzies & Marang (1986)
687	PG 1329+159	0.250	40.2	0.002	0.083	13.48 / V	Morales-Rueda et al. (2003)
695	PG 1336-018	0.101	78.0	0.0050 <sup>e</sup>	0.16	13.45 / y	Kilkenny et al. (1998)
816	PG 1438-029	...	...	...	...	13.82 / P	Green et al. (2004)
...	HS 2333+3927	0.172	89.6	0.0128	0.32	14.6 / B	Heber et al. (2004)

<sup>a</sup>Sequence number if the star is in the KHD sample (if no number is given then the star is not in KHD).

<sup>b</sup>Reference for the initial identification of the subdwarf companion as dM or BD.

<sup>c</sup>HD 269696 = LB 3459 = AA Dor. Companion is believed to be a brown dwarf (all the rest are dM).

<sup>d</sup>Values from Rauch (2000).

<sup>e</sup>Value calculated by me based on the reported period and velocity amplitude:  $f(m) = \frac{PK^3}{2\pi G}$ .

NOTE: Please refer to §1.4.1.1 and Table 3.2 for more information.

## Chapter 2

# The Kilkenny, Heber, & Drilling Hot Subdwarf Catalog

## 2.1 The Sample

For this investigation I studied hot subdwarf stars listed in the *Catalogue of Spectroscopically Identified Hot Subdwarfs* (Kilkenny, Heber, & Drilling 1988) as updated and expanded in an electronic version c. 1992, kindly made available to us by D. Kilkenny. This catalog (hereinafter referred to as KHD) contains 1527 entries, of which 302 entries were added since the 1988 publication (about half of these additions are from the Carnegie Southern Observatory H&K survey, Beers et al. 1992). Hot subdwarfs from the PG survey of UV-excess objects (Green, Schmidt, & Liebert 1986) are an important component of the catalog (1017 objects with PG designations, or >65% of all KHD entries, were either discovered or recovered by the PG survey), so the characteristics of the entire KHD catalog closely mirror those of the PG-only sample. More recent or ongoing surveys, including the Hamburg Quasar Survey (HS; Hagen et al. 1995) and Edinburgh-Cape (EC; Stobie et al. 1997) surveys are not included. However, KHD is the most complete single compilation of field hot subdwarfs available, especially for the northern sky and for relatively bright objects.

While the KHD catalog contains all varieties of hot subdwarfs, I am primarily interested in the more numerous sdB stars. As mentioned in Ch. 1, sdB stars are understood to be relatively homogeneous and probably have a common evolution history from the zero age extended horizontal branch (ZAEHB) and beyond, while sdO stars likely follow multiple evolutionary pathways and might be expected to be less homogeneous and to have less simply explained properties. In the following discussions, while I focus on the sdB stars, I will take the sdO stars “along for the ride” and comment on the two groups either separately (sdB or sdO), or combined as “hot subdwarfs” in general (both sdB and sdO). I further discuss the adopted classifications of objects from KHD and my treatment of them in §2.3.

## 2.2 Coordinates

To make a comparison of the KHD data with existing databases or to obtain new observations of the correct star, accurate coordinates on a consistent system are required. For each entry the object’s position was verified by referring whenever possible to original published finding charts or by contacting knowledgeable observers, then locating the object on a chart prepared from the U.S. Naval Observatory (USNO) A2.0 Catalog<sup>1</sup> (Monet et al. 1998). Coordinates were adopted from USNO A2.0, except for bright

---

<sup>1</sup><http://www.nofs.navy.mil/data/fchpix/>

objects missing from that source, in which case coordinates from the Tycho-2 (TYC, Høg et al. 2000) or Hipparcos (HIP, Perryman et al. 1997; ESA 1997) catalogs were used. These updated ICRS<sup>2</sup> 2000.0 coordinates are accurate to a few arcseconds ( $\sim 2''$  or better) at the epoch of observation; in many cases this represents a very substantial improvement over the coordinates reported by KHD. During the time of this study, there were confirmed and improved coordinates for 1486 objects (not counting 15 duplicate entries), while for 26 objects the correct star had not yet been positively identified. These remaining 26 unrecovered objects are not included in the present study.

Improved coordinates based on the *Two Micron All Sky Survey* (2MASS, when available, see Chapter 3), USNO A2.0, or the original unverified coordinates for all KHD objects along with other notes (including those from KHD) are given in Appendix A starting on page 162.

### 2.3 Classification and Identification

During my analysis, I divided the total sample of hot subdwarfs into two sub-samples: “sdB” and “sdO” based on their classifications in KHD. For definiteness, I took the first classification given, even if there were additional conflicting classifications. My “sdB” group comprises those objects classified as sdB, sdB–O, sd, and sdOB (as I discussed in §1.1, the sdOB are just hotter versions of the sdBs). My “sdO” group comprises sdO, sdO(A), sdO(B), sdO(C), and sdO(D). There is ongoing discussion in the community regarding appropriate multi-dimensional classification schemes for hot subdwarf stars, which likely will depend on the spectral resolution used (Jeffery et al. 1997; Drilling et al. 2000, 2003). Meanwhile, I have made no attempt to improve upon, regularize, or rationalize the various classifications summarized in KHD.

A total of 44 objects were excluded from my complete 2MASS sample (discussed in Chapter 3) because they are not subdwarfs or had unusual properties. These objects are classified: HBB (six objects; Tables A.1 and B.1 sequence #<sup>3</sup>: 184, 350, 642, 662, 1185, and 1298), DA (three; #163, 265, and 588), non-sd (twelve; #264, 287, 553, 572, 574, 635, 734, 794, 1138, 1396, 1443, and 1501), only as “bin” or “bin?” (five; #732, 905, 1069, 1076, and 1095), or had no classification (five; #398, 702, 849, 884, and 967) in KHD. Additionally, #276 KUV 08388+4029 is listed as “sdB” in KHD, however, SIMBAD<sup>4</sup> lists this object as a Seyfert 1 galaxy at  $z \approx 0.15$ . I verified its AGN nature with a low-resolution spectrum obtained from the Hobby-Eberly Telescope<sup>5</sup> (HET), which clearly showed the  $H\alpha$  and  $H\beta$  broad emission lines at wavelengths consistent with a

<sup>2</sup>ICRS = International Celestial Reference System

<sup>3</sup>These sequence numbers are not intended to be used as a new designator in the literature, but are useful in navigating the KHD catalog and Tables A.1 and B.1.

<sup>4</sup>SIMBAD = Set of Identifications, Measurements and Bibliography for Astronomical Data, <http://simbad.u-strasbg.fr/Simbad>, operated at Centre de Données astronomiques de Strasbourg, France

<sup>5</sup>The Hobby-Eberly Telescope is operated by McDonald Observatory on behalf of The University of Texas at Austin, the Pennsylvania State University, Stanford University, Ludwig-Maximilians-Universität München, and Georg-August-Universität Göttingen. The Marcario Low Resolution Spectrograph is a joint project of the Hobby-Eberly Telescope partnership and the Instituto de Astronomía de la Universidad Nacional Autónoma de México.

redshift  $z \approx 0.15$ . Also, #1273 KUV 20432+7457, which is listed as “sd?” is in fact listed as a Seyfert 1 galaxy at  $z \approx 0.10$  in SIMBAD. One object, #200 BD−13°842, which is classified as “sd”, is clearly seen in both images as the central star of a bright planetary nebula. Finally, there are five objects classified “sdB”, “sd”, “sdO”, or “sdOB” whose spectra show emission lines, PG 1444+232 (entry #835 in Tables A.1 and B.1; Herbig 1992), LS IV−08°03 (#1108; this work), BD+28°4211 (#1347; Reid & Wegner 1988), PB 5333 (#1461; this work), and PG 2337+300 (#1493; Koen & Orosz 1997). Specifically, BD+28°4211 and PB 5333 are hot sdOs exhibiting NLTE<sup>6</sup> processes in their atmospheres; PG 1444+232 is dominated by Fe II emission formed in the outer layers of the star (in high density gas) or in a strong stellar wind; PG2337+300 is a cataclysmic variable (CV); and LS IV−08°03 is a (currently) unclassified variable emission line star (§4.6.4). Because of their peculiar natures, these five objects with emission lines have been included with the “non-subdwarfs” (see also §4.4 and §4.6.4).

Hereafter, when I refer to “sdB stars” I mean the group consisting of sdB, sdB−O, sd, and sdOB; when I refer to “sdO stars” I mean the group consisting of sdO, sdO(A), sdO(B), sdO(C), and sdO(D); and when I refer to “hot subdwarfs” I mean the entire sample (both sdB and sdO) excluding the “non-subdwarfs” and other unusual objects just mentioned.

---

<sup>6</sup>NLTE = non-LTE, non-local thermodynamic equilibrium.

## Chapter 3

# 2MASS All-Sky Data Release<sup>1</sup>

### 3.1 Introduction

The systematic survey of the entire sky that was carried out by the *Two Micron All Sky Survey*<sup>2</sup> (2MASS) provided the opportunity to further explore the question of whether all sdB stars (and sdO stars, to the extent that they represent the EHB) are in composite binary systems. The source of targets (the KHD<sup>3</sup> catalog), their improved coordinates, and classifications were already discussed in Chapter 2. I collected readily available visible and near-infrared (near-IR) flux measurements of hot subdwarfs from the 2MASS All-Sky Data Release (ASDR) Catalog<sup>4</sup> and identified those whose colors indicated the presence of a late type companion. I thus determined the fraction of subdwarfs that exist in composite spectrum binaries. (Note that not all classes of companion star will be identified this way, in particular WD companions.) This method is similar to that used by Thejll, Ulla, & MacDonald (1995) and Ulla & Thejll (1998), but my sample is much larger and the IR photometry is more precise. When this study was nearly completed, a similar study using the 2MASS ASDR was published by Reed & Stiening (2004). Their study was independent of ours, uses a slightly different source list, and slightly different analysis techniques, but arrives at similar conclusions.

### 3.2 Visual and IR Photometry

#### 3.2.1 Visual Photometry

Visual photometry ( $BV$  or  $uvby$ ) for the hot subdwarfs was taken from KHD, Al-lard et al. (1994), Landolt (1992), Mooney et al. (2000), Williams, McGraw, & Grashuis (2001), and/or the Tycho-1 Catalog (Høg et al. 1998). For the photometry taken from KHD, when more than one set of photoelectric measurements was given, I favored Johnson  $BV$  over Strömgren  $uvby$ , unless the only  $BV$  measurement was reported as “uncertain” (then  $uvby$  was used). If only a single “uncertain”  $BV$  measurement was available for an object (and no Strömgren data were found), then that uncertain measurement was nevertheless used and treated as exact. For consistency, I took the first of these

---

<sup>1</sup>Results for the 2MASS Second Incremental Data Release can be found in Stark & Wade (2003), while preliminary results for the All-Sky Data Release can be found in Stark, Wade, & Berriman (2004).

<sup>2</sup><http://www.ipac.caltech.edu/2mass/>

<sup>3</sup>Kilkenny, Heber, & Drilling (1988) as updated and expanded in an electronic version by Kilkenny, c. 1992, kindly made available by D. Kilkenny.

<sup>4</sup><http://www.ipac.caltech.edu/2mass/releases/allsky/index.html>

measurements listed in KHD, unless it was uncertain, and even if additional measurements differed significantly from the first. Those hot subdwarfs with only photographic visual photometry were not included in the optical-infrared color space examination of hot subdwarfs discussed in §3.3.1–3.3.2 (however, those with 2MASS detections are included in the objects discussed in §3.6). For stars listed in Allard et al. (1994), Landolt (1992), or Williams et al. (2001) the magnitudes from those sources were used in place of any reported in KHD. Strömgren *uvby* was taken from Mooney et al. (2000) for two objects: #320 PG 09146+0004 and #1327 PG 21325+1235 in preference to uncertain  $V$  and no  $BV$  (respectively) in KHD. Tycho-1  $BV$  magnitudes (Høg et al. 1998; ESA 1997) were taken for #234 BD +34°1543, which had only a single  $V$  magnitude listed in KHD. No further literature search was undertaken to locate additional visual photometry. No errors are reported for the photometry given in KHD and I did not refer to original references to locate errors for each individual observation. However typical errors are  $\lesssim 0.02$  mag for those surveys comprising the majority of the visual photometry (i.e., Allard et al. 1994; Green et al. 1986; Mooney et al. 2000; Wesemael et al. 1992; Williams et al. 2001)—thus, for simplicity, all measurements of visual photometry were treated as exact.

When only Strömgren photometry was available (or was taken in place of uncertain  $BV$ ), I assumed that  $y = V$ , and  $b - y$  was converted to  $B - V$  using:

$$(B - V) = 1.584 \times (b - y) + 0.681 \times m_1 - 0.116$$

where:  $m_1 \equiv (v - b) - (b - y)$  (Turner 1990). Two objects have only synthetic  $b$  and  $y$  reported: #1076 Balloon 083500007 and #1095 Balloon 083600004. For these two objects,  $B - V$  was estimated by setting  $m_1 = 0$  in this equation.

Tycho-1  $B$  and  $V$  magnitudes for one object, #234 BD +34°1543, were converted to Johnson  $B$  and  $V$  magnitudes using:

$$\begin{aligned} V_J &= V_T - 0.090 \times (B_T - V_T) \\ (B - V)_J &= 0.850 \times (B_T - V_T) \end{aligned}$$

This conversion is valid over  $-0.2 < (B_T - V_T) < 1.8$ , and generally gives errors  $< 0.015$  in  $V_J$  and  $< 0.05$  in  $(B - V)_J$  (ESA 1997).

### 3.2.2 Infrared Photometry

Infrared photometry ( $J$ ,  $H$ , and  $K_S$ ) from the 2MASS All-Sky Data Release (ASDR) was collected by performing searches within  $\sim 10''$  of the updated coordinates. Visual verification was performed for crowded fields by comparing images from the Digitized Sky Survey<sup>5</sup> (DSS) with images from 2MASS (most hot subdwarfs are uncrowded, with no other comparably bright field stars within  $\sim 30''$ ). Objects are included in the 2MASS ASDR if they have signal-to-noise ratio,  $S/N \geq 7$  in at least one band ( $J$ ,  $H$ , or  $K_S$ ), or if they have  $S/N \geq 5$  in all three bands. This results in nominal completeness

---

<sup>5</sup><http://archive.stsci.edu/dss/index.html>



limits (for  $S/N \geq 10$ ) of  $J = 15.8$ ,  $H = 15.1$ , and  $K_S = 14.3$ <sup>6</sup>.  $J-K_S$  errors (which are generally worse than  $J-H$  errors) for my objects are typically less than  $\sim 0.2$  mag, with an average  $J-K_S$  error of  $\sim 0.12$  mag for our sample. Of the initial sample (1486 objects), I was able to retrieve 2MASS photometry for 1193 hot subdwarfs (1237 before removing objects classified as non-subdwarfs). Of the 1193 hot subdwarfs, only 817 had  $J$ ,  $H$ , and  $K_S$  magnitudes listed, while 826 had both  $J$  and  $K_S$  (with only an upper limit on  $H$ ).  $J$  measurements exist for 1190 objects. A small fraction (few percent) of subdwarfs have two possible identifications within  $\sim 10-20''$  of the input coordinates. The hot subdwarf members of these visual doubles were included in the present study since both finding charts and 2MASS images were available to identify the correct member of the pair.

Photometry for all KHD objects can be found in Appendix B starting on page 209 (the color parameter  $Q$  listed in this table will be discussed in §3.6.2). A summary of the numbers and types of subdwarfs at each stage in the data gathering process is presented in Table 3.1.

### 3.3 Hot Subdwarfs in Color Space

#### 3.3.1 Optical-IR Color-Color Plots

After examining various combinations of color indices, I chose to focus on  $(J-K_S)$  vs.  $(B-V)$  and  $(J-K_S)$  vs.  $(V-K_S)$ . These two combinations allow me to extract most of the information from the available photometry. Substituting  $J-H$  in place of  $J-K_S$  shows the same features and trends. Likewise, substituting  $V-J$  for  $V-K_S$  shows the same features and trends. Using  $H-K_S$  did not provide any additional information.

The locations of single and composite hot subdwarfs in color space were determined by selecting samples of hot subdwarfs reported as single and composite from the literature. A total of 69 reportedly single stars and 37 reported composites with 2MASS detections were taken from the literature (KHD; Ferguson et al. 1984; Beers et al. 1992; Allard et al. 1994; Thejll et al. 1995; Ulla & Thejll 1998) or a list of hot subdwarfs spectroscopically observed and kindly provided to us by E. M. Green. After removing from this list stars with incomplete photometry and stars classified as “non-sd” by KHD, 32 (28 sdB, 4 sdO) of the reported composites and 58 (48 sdB, 10 sdO) of the reported singles remained and are used here to determine the composite and single loci (these stars are flagged in Table B.1 with “SGL” or “COM” in the last column).

When plotted in  $(J-K_S, B-V)$  or  $(J-K_S, V-K_S)$  color spaces relative to the location of the Pop I main sequence<sup>7</sup> (Figure 3.1), the reported single hot subdwarfs (both sdB and sdO) occupy the same area in color space as other O and B stars, with the sdOs in general having slightly bluer colors than the sdBs (in agreement with the higher  $T_{\text{eff}}$  of sdOs compared to sdBs). Most of the single hot subdwarfs occupy the

<sup>6</sup>However, according to the *Explanatory Supplement to the 2MASS All Sky Data Release* (located at: <http://www.ipac.caltech.edu/2mass/releases/allsky/doc/explsup.html>), at high Galactic latitude, the 2MASS Point Source Catalog contains accurate detections 0.5–1.0 magnitudes fainter than these limits.

<sup>7</sup>A discussion of Pop I main sequence colors in 2MASS filters is given in Appendix C.1 starting on page 246.

region:  $(B-V) \lesssim +0.1$ ,  $(V-K_S) \lesssim +0.2$ , and  $(J-K_S) \lesssim +0.05$ . This region is marked by a box on Figure 3.1. On the other hand, reported composite hot subdwarfs (both sdB and sdO) occupy a separate and distinct region of color space; they have redder colors than single subdwarf stars. Composite subdwarfs show a consistent and quite large color difference from the “typical” single subdwarf in  $J-K_S$ . The difference in  $V-K_S$  is also large in the mean, but the distributions of single and composite systems overlap slightly. The least average difference is in  $B-V$  (Figure 3.1).

These patterns can be understood if the hot subdwarf’s companion star in the composite systems is cool and relatively faint at visible wavelengths. The bluest color index,  $B-V$ , will be relatively unaffected by the additional light from the companion. The visual-infrared index,  $V-K_S$ , will betray a large infrared “excess” compared to a single hot subdwarf, but there will be a large spread because the index depends on the competing light from the two stars at  $V$ . The pure infrared index,  $J-K_S$ , will be dominated by the cool companion, whose color is very different from that of the hot star.

Three reported composite sdOBs have distinctly different colors in Figure 3.1 compared with all of the other reported composites. The first (labelled “1” in Figure 3.1) is #1355 BD  $-3^\circ 5357$  (or FF Aqr, with  $B-V = +0.895$ ,  $J-K_S = +0.752$ , and  $V-K_S = +2.838$ ), an eclipsing binary (orbital period  $\sim 9.2$  days) classified sdOB+G8III (Dworetzky et al. 1977; Etzel et al. 1977). The second (“2”) is #1457 BD  $-7^\circ 5977$  (with  $B-V = +0.541$ ,  $J-K_S = +0.569$ , and  $V-K_S = +2.129$ ), classified sdOB+K0IV–III by Viton et al. (1991). The third (“3”) is #127 PG 0205+134 (with  $B-V = +0.006$ ,  $J-K_S = +0.847$ , and  $V-K_S = +2.771$ ), classified “sdOB comp” by Green et al. (1986), and further refined to sdOB+M3.5(IV?) by Allard et al. (1994) and Williams et al. (2001). All of these cool companions are atypically luminous for sdB-type composites, which otherwise have main sequence or subgiant companions reported, so it is not unreasonable for these three objects to have exceptionally red colors.

The two sdB stars labelled “4” (#964 PG 1548+166) and “5” (#744 TON 183) in Figure 3.1, have anomalously blue  $J-K_S$  colors,  $J-K_S = -0.472 \pm 0.232$  and  $-0.457 \pm 0.093$  respectively ( $1\sigma$  errors). These colors could be due to photometric errors, or they could be intrinsic to the objects themselves. The color index  $J-H$  generally shows the same trend as  $J-K_S$ , and these two stars have similar  $J-H$  colors as all other single sdBs ( $J-H = +0.011 \pm 0.121$  and  $-0.197 \pm 0.068$ ).

One reported single sdB star, #483 TON 64 (labelled “6” in the right plot of Figure 3.1), has a rather red value for  $V-K_S$  (+0.580), yet appears “normal” in the other colors ( $B-V = -0.220$ ,  $J-K_S = -0.021$ ). Its unusual position may be due to an error in the standardization of the  $V$  magnitude. The two measurements for the visual magnitude of this star in KHD are discrepant:  $V = 15.86$  and  $y = 14.59$ . My adopted procedure is to favor  $V$  over  $y$ ; if however I were to use  $y = 14.59$  in place of  $V = 15.86$ , I would have  $V-K_S = -0.690$  (again assuming  $y-K_S = V-K_S$ ), which places this star near the center of the single subdwarf locus. Nevertheless for consistency, I continue to use the value of  $V$  for this object.

Now placing all of the hot subdwarfs with  $V$  (or  $B-V$ ),  $J$ , and  $K_S$  measurements in color space (Figure 3.2), I observe that they occupy the same areas in color space as defined by the smaller sample of known composites and singles. (Objects with only upper limits on  $K_S$  from 2MASS are not plotted in Figure 3.2.) There is some additional scatter,

which is most likely due to errors in the photometry. This scatter could, in principle, also be due in part to differences in interstellar extinction and reddening from object to object. Additionally, some hot subdwarfs are known to pulsate, such as the V361 Hya stars<sup>8</sup> (O’Donoghue et al. 1999) and the “PG 1716” stars (Green et al. 2003). In the case of the V361 Hya stars, the pulsation amplitudes are generally less than 0.01 mag and typically only a few milli-mags with typical periods of 100–250 seconds (i.e., Kilkenny et al. 1997; Østensen et al. 2001; Green et al. 2003). The “PG 1716” stars have peak-to-peak amplitudes  $\lesssim 0.05$  magnitudes over timescales of about an hour (Green et al. 2003). Light variations due to both of these pulsations are typically less than other sources of error.

Figure 3.2 suggests that candidates for composite systems (hot subdwarf+late type star) can be identified and targeted for future study using  $B - V$  or  $V - K_S$  in combination with  $J - K_S$ . Unfortunately, in order to use this technique, accurate visual photometry is needed in addition to IR photometry.

### 3.3.2 Modelling the Distribution in Optical-IR Color-Color Space

To test the interpretation offered above, that the colors of single and composite hot subdwarfs may be understood if the companions are cool stars, I attempted to reproduce the location of composite subdwarfs in color space by combining the colors of a typical sdB with those of late type Pop I main sequence stars (a discussion of Pop I main sequence colors in 2MASS filters is given in Appendix C.1 starting on page 246). The “typical” colors for sdBs were taken from the center of the clump of reported single stars in Figure 3.1. I used  $(B - V)_{\text{sdB}} \approx -0.25$ ,  $(V - K_S)_{\text{sdB}} \approx -0.75$ ,  $(J - K_S)_{\text{sdB}} \approx -0.15$ . Based on the spread seen in Figure 3.1, however, it is likely that single sdB stars in fact have spreads in color index on the order of  $\Delta(B - V) \sim \pm 0.1$ ,  $\Delta(V - K_S) \sim \pm 0.2$ , and  $\Delta(J - K_S) \sim \pm 0.15$ , as might be expected from variations in the physical properties of the sdBs (most notably the effective temperature); some of the spread in  $V - K_S$  and  $J - K_S$  is however due to limited IR photometric precision.

The colors were combined, varying the fraction of the light at  $V$  that arises from the companion (for more details see Appendix C.3 starting on page 248). The resultant locus passes among the known composite sdBs with contributions from the companion of  $\sim 10$ –60% at  $V$ , and spectral types G–K (Figure 3.3). These fractional contributions and companion types agree with those reported by Allard et al. (1994) for sdBs, and Ferguson et al. (1984) and Orosz, Wade, & Harlow (1997) for hot sdBs and sdOs. While this general analysis also fits the sdOs, the unreddened colors of a “typical” sdO should be somewhat bluer than those of a sdB, since sdOs are hotter than sdBs.

The loci are plotted with the entire subdwarf sample in Figure 3.4.

By introducing assumed absolute magnitudes along with colors, we can synthesize composite colors specifically for sdB+late type main sequence stars. The sdB colors used in the previous calculation were again adopted. The absolute magnitudes of sdB stars are poorly constrained, with reported values spanning the range from  $M_{V,\text{sdB}} \approx 3.5$ –6.2 (Allard et al. 1994; Bixler et al. 1991; Ferguson et al. 1984; Liebert et al. 1994; Moehler

---

<sup>8</sup>also known unofficially as “EC 14026” stars

et al. 1990a; Orosz et al. 1997; Thejll et al. 1997). I therefore treated  $M_{V,\text{sdb}}$  as a parameter, and varied it (choosing  $M_{V,\text{sdb}} = 3.5, 4.0, 4.5, 5.0$ , and  $5.5$ ) to see its effect on the location of the synthesized composites in color space (Figure 3.5). I found that the locus of synthetic composites passes among the observed composite systems and best characterizes the observed companions as having Pop I spectral types G–K when  $M_{V,\text{sdb}} \approx 4.5–5.0$  mag (if the companions lie on the main sequence). It should be noted, however, that the same pattern of color loci can be created by fixing  $M_{V,\text{sdb}}$  and instead varying the absolute magnitudes of the companions from their main sequence values. If G–K type companions were subgiants, they would be more luminous by perhaps  $\sim 2$  magnitudes, and would therefore give the same pattern with a more luminous sdb,  $M_{V,\text{sdb}} \approx 2.5–3.0$  mag (but we would not expect to see evolved M–type companions). In nature, there is likely to be some range in absolute magnitude for both the sdb stars and their companions. (In addition to the variations of luminosity and bolometric correction along the zero-age EHB, sdb stars should evolve to higher luminosity on timescales of  $10^8$  years.)

The (main-sequence) loci are plotted with the entire hot subdwarf sample in Figure 3.6.

These simple models give results consistent with previous studies concerning the companion spectral types and their light contributions. I cannot, however, assume an  $M_V$  for the companion and invert the calculation case-by-case to give reliable individual values for  $M_{V,\text{sdb}}$ , nor *vice versa*, because of the uncertainties in the measured magnitudes, colors, and reddening. Additionally there is the expected intrinsic spread in  $M_{V,\text{sdb}}$  referred to above (for further discussion see Saffer et al. 1994). For similar reasons, neither can I infer exact companion spectral types for individual objects.

Of the 33 reported composite hot subdwarf systems, essentially all of the cool companion stars for which a spectral class is known are of spectral types G or K. My models show that composite systems with G, K, and early M-type companions show the most significant differences in color from a single sdb (particularly in  $J-K_S$ ) and from main sequence stars. This could explain why most *known* composite systems have GK-type companions: for companions earlier than  $\sim G$ , the combined system looks more like a main sequence star (or a cool, Pop II subdwarf) than a sdb star. Such systems would likely be excluded from catalogs of hot subdwarfs. For main-sequence companions much later than  $\sim M0$ , the effect on the combined system light is so small that the companion would not easily be detected in the visual. Most of the spectroscopic studies of composite sdbBs have been done in the visual and blue region of the spectrum where very little color difference between a composite sdb+dM and a single sdb exists, and there are indeed few identifications of dM companions: thus far only seven are known (see list in §1.4.1.1, and Table 1.1). Of the known dM and brown dwarf (BD) binaries, the five sd+dM binaries and the one sdOB+BD binary that are in KHD are included in the 2MASS sample. Colors for such close binary stars, constructed from non-simultaneous measurements of visible and infrared magnitudes, may be unusual. The color indices for these stars are nevertheless consistent with single hot subdwarfs (see Table 3.2). A few other objects can be noted in the region of color space that, based on my simple models, would be occupied by sd+dM composites (Figures 3.4 and 3.6). Owing to uncertainties in the measured magnitudes and colors, however, I cannot clearly distinguish early M

companions from late K companions — near-IR or IR spectroscopy will be needed to distinguish clearly between late K and early M-type companions. Yet it seems clear, based on my color plots, that there are not great numbers of “hidden” early M-type ( $\sim M0$ ) companions to hot subdwarfs. For main sequence companions substantially later than  $\sim M0$ , the  $J-K_S$  color is rapidly returning to that of a single subdwarf.

Identifying and characterizing further M-type companions to sdB stars would help settle some of the questions about the nature of earlier-type (G–K) companions, in particular whether they are predominately main sequence or subgiant stars. Late M-type companions can safely be assumed to be on the main sequence. If many of these are found among the sdB stars with “composite” colors, the relatively faint  $M_{V,\text{sdB}}$  inferred from such systems would imply that the G–K type companions in other composite-color systems are also close to the main sequence. If late-M companions are not found in great numbers, it could be inferred that the G–K companions are mostly subgiants, since the corresponding bright  $M_{V,\text{sdB}}$  inferred from this assumption would explain the absence of sd+dM systems detectable from photometry. The existence of many subgiant companions, with their short lifetimes as subgiants, would be interesting, since the evolutionary timescale of sdB stars is also short.

### 3.4 A “Volume Limited” Hot Subdwarf Sample

A strong selection bias in these data exists, because 2MASS itself is an approximately *magnitude* limited survey (albeit with different magnitude limits in each of three passbands). The entire sample of hot subdwarfs I have been discussing (common to both KHD and 2MASS) is thus a *magnitude* limited sample (MLS) in some sense. The *volume* sampled for single subdwarfs is therefore smaller than that sampled for composites, since the presence of the late type companion increases the distance at which a composite system remains brighter than the limiting 2MASS magnitude.

To further explore this selection bias, I constructed  $(J, J-K_S)$  and  $(K_S, J-K_S)$  color-magnitude diagrams for the 2MASS sample (Figure 3.7). Several interesting patterns are noted. First, the two populations (single and composite) can be seen, and both are observed to cover the entire magnitude range (i.e., composites and/or singles are not “clumped” at a specific apparent magnitude). Second, a majority of the objects with extreme  $J-K_S$  colors (either blue or red) are found at the faintest magnitudes, an effect largely explained by photometric errors. Third, it can be seen that the sample is limited by detections in the  $K_S$  band. There is a clear cut-off at  $K_S \approx 15.75$ , while in  $J$  the cut-off magnitude varies by color (redder objects that are detected in *both*  $J$  and  $K_S$  run to a fainter  $J$  magnitude than the bluer objects).

The interpretation of this third feature is that a blue (single) object detected near  $J = 15.5$  or fainter is missing at  $K_S$  and thus is not part of the plotted sample; a red (composite) object at the same  $J$  will also have a  $K_S$  detection and thus will appear in Figure 3.7. (This effect is distinct from the fact that composites appear brighter at  $J$  due to the combined light from two stars.)

Recognizing this selection bias, I can attempt to define an approximately *volume* limited sample (VLS) of hot subdwarfs<sup>9</sup>. To define my volume limited sample, I try to remove those subdwarfs that I observe to be composite, but which would *not* have been detected by 2MASS had they been single. With only a single color index to work with, and with uncertainties in both the photometry and the relative luminosities of the hot subdwarfs and their companions, I cannot rely on such a technique to say whether any given individual system lies within the defined volume. The sample so constructed can be used in a statistical sense, however, to reflect the general nature of the true distribution, and at least to indicate the size of the selection effect.

The observed cut-off magnitude from Figure 3.7 for a single hot subdwarf is  $K_S \approx 15.75$ . Taking this limit as the apparent magnitude of the hot subdwarf component in a composite system, I can compute the corresponding apparent magnitude for the total light from the system, using the models discussed in §3.3.2 and shown in Figures 3.3 and 3.4. This total magnitude will vary as the spectral type and/or relative luminosity of the late type companion is varied. The locus of thus-computed magnitudes is shown in the lower panel of Figure 3.7 for a hot subdwarf with the “typical” color  $J-K_S = -0.15$  adopted in §3.3.2, for companions with colors of the Pop I main sequence spectral types G0, K0, K5, and M0. Along each of these lines, the color and total magnitude vary as the relative brightnesses of the two component stars are varied. Note that *no assumption has been made about the absolute magnitude of either the hot subdwarf or the cool companion*.

I now replace the family of lines (corresponding to different spectral types of the cool star) with a single representative line. (This is because based on  $J-K_S$  alone I cannot know the true spectral types of the late type companions without making assumptions about the relative luminosities of the component stars.) I use this line to approximate the appropriate magnitude limit for a volume limited sample, again in a *statistical* sense. The line is chosen to pass through the middle of the known composite sdBs shown in Figure 3.3; it thus represents a  $\sim 5\%$  contribution (at  $V$ ) by a K5 star, or a contribution of 40–80% at K0 in Figure 3.7. The change in the volume-limiting  $K_S$  magnitude is thus most rapid near  $J-K_S \approx +0.3$  (see Figure 3.3). All hot subdwarf stars in the  $(K_S, J-K_S)$  color-magnitude diagram that fall above and to the left of this line are included in our statistical volume limited sample. The average error in  $J-K_S$  for this new sample is 0.10 mag (slightly reduced from 0.12 mag, which applies to the full  $J-K_S$  sample).

### 3.5 2MASS Only Color Parameters

### 3.6 Distribution in $J-K_S$

Since visual photometry is not available for all of the hot subdwarfs contained in 2MASS, and since there is a more distinct separation between composites and single

---

<sup>9</sup>To our knowledge, the first time that this bias has been discussed in the context of hot subdwarf composites was in Stark & Wade (2003). Theissen et al. (1992) discussed a “statistically complete” sample containing 11 hot subdwarfs, however they did not address the composite vs. single bias. Reed & Stiening (2004) made a magnitude cut in USNO photographic  $B$  magnitude which will roughly approximate our VLS for companions that are faint enough that they do not affect the  $B$  magnitude.

subdwarfs stars in  $J-K_S$  than in the other colors, I examined the distribution of subdwarfs based on their  $J-K_S$  colors alone. A histogram of  $J-K_S$  (and also of  $J-H$ ) for subdwarfs with  $J$  and  $K_S$  measurements, reveals a bimodal distribution (Figure 3.8, panel *a* for the MLS, panel *b* for the VLS). In both sub-samples, one peak is centered near  $J-K_S \approx -0.15$  ( $\sim$ B2–B3 spectral type), and the other is centered near  $J-K_S \approx +0.30$  ( $\sim$ G5 spectral type if interpreted as a single star). There are also wings stretching to both redder and bluer colors. This distribution cannot be explained by reddening, because no significant trends were observed with galactic latitude. I would also expect reddening to produce a tail to the red from a single peak, but not a pronounced second peak. Finally, the amount of extinction that would be required is excessive.

I sorted the sdB and sdO samples into three groups by  $J$  magnitude. The bimodal peaks are very pronounced in the brightest third of each sample, less distinct in the middle third, and practically non-discernible in the faintest third. This pattern can be fully explained by the increase in photometric uncertainty at fainter magnitudes.

In keeping with the results found from my modelling of color-color distributions, I postulate that the stars within the blue peak of the  $J-K_S$  distribution ( $J-K_S < +0.05$ ) are single stars (or sd+WD pairs, with colors indistinguishable from single hot subdwarfs), and that stars in the red peak ( $J-K_S > +0.05$ ) are composite (sd+late type) systems. The color index separating these two groups of stars was adopted from the box defining the region of single subdwarfs in Figure 3.1. With this definition, I find that for the MLS,  $59 \pm 3\%$  of all the subdwarf stars in our 2MASS sample are apparently single, and  $41 \pm 3\%$  are composite (with  $76 \pm 3\%$  and  $24 \pm 3\%$  respectively for the VLS, see Table 3.3). The quoted 95% confidence errors are sampling errors computed from the binomial distribution, taking the size of the sample into account (see also Appendix D starting on page 255). If the color index of the boundary separating single and composites in the MLS is increased (decreased) by 0.05 mag, the fraction of subdwarfs that are “blue” (i.e., single) is increased (decreased) by 3% (4%).

### 3.6.1 Describing the sdB $J-K_S$ Distribution

I have fitted the bimodal  $J-K_S$  distribution of the sdB stars (alone) to the sum of two Gaussians, centered on the blue and red peaks for both the MLS and the VLS. An initial “fit-by-eye” to the binned data was improved by minimizing  $\chi^2$  on all non-zero bins (see also Appendix F starting on page 261). The  $\chi^2$  minimization was done using a systematic gridded search in the neighborhood of the initial fit. There are six fitting parameters: two mean values (or centers), two dispersions (or widths), and two normalizations (or amplitudes). The parameters for the fits are listed in Table 3.4 and the fits are shown in Figure 3.8 panels *c* and *d*.

While the  $\chi^2$  statistic provides a useful criterion for improving the fit, its final numerical value should be used with caution, since some of the data bins are zero and others contain only a few members. In particular, the 95% confidence intervals shown in Table 3.4 are indicative rather than definitive. The small value of  $\chi^2_R$  nevertheless demonstrates the plausibility of a two-Gaussian fit, which is confirmed by visual inspection.

I find that the Gaussian areas are consistent with the binomial fractions from a cut at  $J-K_S = +0.05$  (compare the percentages in Table 3.3 with the area proportions from Table 3.4). The dispersions of both blue Gaussians, and the VLS red Gaussian, are consistent with the average 2MASS photometric error [ $\sigma(J-K_S) \approx 0.1$ ], implying there is little intrinsic spread in  $J-K_S$  of single sdBs or the VLS late type companions.

### 3.6.2 Composites in $(J-H, J-K_S)$ Color-Color Space

The distribution of hot subdwarfs in 2MASS  $(J-H, J-K_S)$  color-color space shows two distinct loci of sdB stars (Figure 3.9a). I calculated the linear least-squares fit to the sdBs that had  $\sigma(J-K_S)$  and  $\sigma(J-H) \leq 0.1$ . The coefficients of the linear fit ( $y = a + bx$ , taking  $x = J-H$  and  $y = J-K_S$ ) are  $a = -0.0197$  and  $b = 1.329$ .

I then defined a parameter that increases along this linear fit (and has lines of constant value perpendicular to the line). This parameter (which I will call “ $Q$ ”) can be defined as:

$$\begin{aligned} Q &= \frac{1}{b}(J-H) + (J-K_S) \\ Q &= 0.752(J-H) + (J-K_S) \end{aligned}$$

The linear fit and orientation of  $Q$  is shown in Figure 3.10. A more detailed description about the least-square fit and definition of  $Q$  can be found in Appendix G starting on page 262.

Binning the data points in  $Q$  (along the linear fit line, Figures 3.11 and 3.12) will show a greater separation between composite and single sdBs than using only a single color. As in  $J-K_S$  and  $J-H$  alone, the distribution of sdBs in  $Q$  is strongly bimodal (Figure 3.11), with the split between single and composite colors occurring at  $Q \approx +0.15$  (singles have  $Q \lesssim +0.15$ , and composites  $Q \gtrsim +0.15$ ). The peaks are at  $Q \approx -0.275$  and  $+0.500$ . The sdOs, unlike the sdBs, show only a single blue peak (at  $Q \approx -0.35$ ) with a long tail stretching to redder colors (Figure 3.12). The binomial fractions of single and composite-colored subdwarfs are given in Table 3.3; these values are comparable to those based on  $J-K_S$  alone.

The strongly *bimodal* distribution in  $J-K_S$ ,  $J-H$ , and  $Q$  all indicate *there are no (or few) companions that are dM, or  $\sim F0$  and earlier in KHD*. In Figure 3.11 (and for  $J-K_S$  alone in Figure 3.8a), the  $Q$  values of sdB+MS composites are indicated assuming  $M_{V,\text{sdB}} = 4.5$ ,  $(J-H)_{\text{sdB}} = +0.10$ , and  $(J-K_S)_{\text{sdB}} = -0.15$ . Companions of type F0 and earlier or M0 and later would fall in the gap between the two loci. If a significant population of such companions existed, the area between the loci should have been filled with their composites.

## 3.7 Summary

Using updated and improved coordinates for hot subdwarfs cataloged by KHD, I have retrieved 2MASS ASDR photometry for more than 1000 hot subdwarfs. This is the largest sample of hot subdwarfs, and in particular composite systems, ever examined. I divided the sample into two sub-samples, sdB/sd/sdOB/sdB-O (“sdB” group), and sdO,



based on their classifications in KHD, and examined these sub-samples both independently and combined as a whole. I defined an approximately volume limited sample of hot subdwarfs for statistical purposes. I examined the distribution of hot subdwarfs in optical-IR color-color plots, by combining 2MASS with visual photometry ( $BV$  or  $uvby$ ) from KHD (or a few selected other sources). The most revealing combinations of color indices we found were:  $(J-K_S, B-V)$  and  $(J-K_S, V-K_S)$ . I defined the color parameter  $Q = 0.752(J-H) + (J-K_S)$ , which gives the clearest separation between composite and single hot subdwarfs based on 2MASS photometry alone. I compared the distributions in  $J-K_S$ ,  $J-H$ , and  $Q$ , and found them all to show a bimodally distributed population.

In keeping with the exploratory nature of this work and the large sample size, I have favored a statistical approach, in contrast to the attempt to find a best characterization of individual binaries. (The relatively large mean errors of the 2MASS photometry also figured in the decision to use this approach.) In the same spirit, I have contented myself with “naive” modelling of the colors, e.g., adopting single values for the colors and magnitudes of the subdwarfs rather than a distribution of these quantities — my goal in the modelling is to support the overall division of the sample of stars into single and composite groups, by demonstrating the plausibility of such modelling.

I found that the locations of hot subdwarfs in visual-IR color-color diagrams can be modelled (very simply and without assuming luminosities for either the hot subdwarf or the companion) as either a single B-type star or as a combination of two stars (spectral type B representing the hot subdwarf, and spectral type G–K for a companion) with contributions from the late type companion of  $\sim 10-60\%$  at  $V$ . To a first approximation sdO stars can be described in the same manner as sdB stars. If main sequence companions are adopted, then the sdB stars are best described with  $M_{V,\text{sdB}} \approx 4.5 - 5.0$  mag, and they typically have G–K type companions. However, the observed distribution can be reproduced equally well by assuming subgiant companions with more luminous sdB stars ( $M_{V,\text{sdB}} \approx 2.5 - 3.0$  mag) — my current data cannot distinguish between these two possibilities. In a histogram of the IR color indices  $J-K_S$  and  $Q$ , the two peaks of the bimodal distribution can be understood as single stars (blue peak at  $J-K_S = -0.170$ ,  $Q \approx -0.275$ ) and composite systems (red peak at  $J-K_S = +0.289$ ,  $Q \approx +0.500$ ). This bimodal distribution is also present in the approximately volume limited sample, again with the two peaks at  $J-K_S = -0.167$  and  $+0.248$ , and  $Q \approx -0.275$  and  $+0.475$ . Making a cut at  $J-K_S = +0.05$ , I found the ratio between single and composite sdB stars is 56:44 (favoring singles) in the magnitude limited sample, while in the volume limited sample it is 73:27 (favoring singles). Similarly, making a cut at  $Q = +0.15$  results in a ratio between single and composite sdBs of 60:40 in the MLS and 75:25 in the VLS (both favoring singles). Note that these ratios *do not include any extrapolation to companions that do not affect the photometry* (i.e., WD or late M dwarfs), since such extrapolation depends on the assumptions made about the absolute magnitude of the subdwarfs or their companions. The  $J-K_S$  distribution for both the magnitude limited and volume limited samples can be described as the sum of two Gaussians with very little overlap and with fractions of single vs. composite in agreement with a sharp cut at  $J-K_S = +0.05$ . An interpretation of these ratios is difficult due to biases in the initial subdwarf catalog.

*There are no (or very few) F or dM companions of the hot subdwarfs in the KHD catalog.* This is evident from the bimodal distribution in 2MASS colors ( $Q$ ,  $J-K_S$ , and  $J-H$ ). Were there a large population of F or dM companions, their composite colors would have filled in the gap between the two bimodal peaks. However, the distribution in 2MASS colors can be described by only a very small (or no) spread in the colors of the late-type companions.

Comparison to other surveys of composite systems is difficult due to the unknown selection effects involved. Other surveys have generally concluded that  $\gtrsim 50\%$  of hot subdwarfs have late type companions (e.g., Allard et al. 1994; Bixler et al. 1991; Ferguson et al. 1984). However, these percentages depend greatly on the corrections made to account for late type companions that were undetectable by the survey (i.e., M-dwarfs) and the assumed luminosity of the subdwarfs or observed companions (i.e., main sequence or subgiant). Based on their observations of composite spectrum sdB stars from the PG survey (Green et al. 1986), Ferguson et al. (1984) extrapolated that about 50% of the sdB stars in the PG catalog had main sequence companions of G8 or later (and a few had companions earlier than G8). Allard et al. (1994) identified 31 composite candidates out of 100 sdB stars observed photometrically, and deduced a fraction of sdB stars with cool main sequence companions of 54–66%, when allowance was made for perceived selection effects. From intermediate resolution spectroscopy of the Ca II IR triplet region of 40 sdB stars, and an assumed “typical” luminosity of a sdB star, Jeffery & Pollacco (1998) claim that the seven composite systems they observed contained subgiant companions. Therefore they conclude that the binary fraction must be much higher than what Allard et al. (1994) concluded based on assuming main sequence companions. From a sample of 40 UV selected hot subdwarfs, Bixler et al. (1991) found that eight showed composite spectra, and calculated that 65–100% of hot subdwarfs had a late type main sequence companion. However, our volume limited sample shows significantly fewer composites than our magnitude limited sample. Thus, by studying only magnitude limited samples (or even less well-defined samples) of hot subdwarfs, it is conceivable that the total number of composite systems could have been significantly over-estimated by these previous surveys (all other factors being equal).

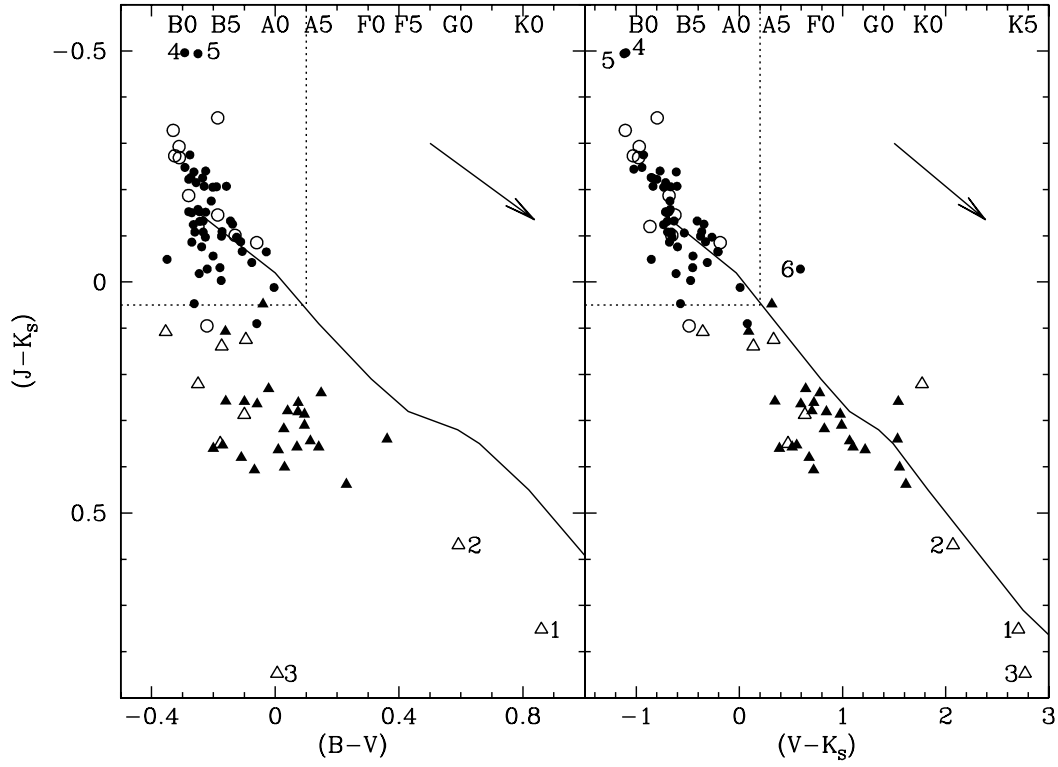


Fig. 3.1 Color-color diagrams for reported single (circles) and composite (triangles) hot subdwarfs. Filled points represent hot subdwarfs in the sdB group (48 single, 28 composite), open points represent stars in the sdO group (10 single, 4 composite) — these stars are flagged “SGL” or “COM” in Table B.1. The left panel shows  $(J-K_S)$  vs.  $(B-V)$ , while the right panel shows  $(J-K_S)$  vs.  $(V-K_S)$ . The diagonal solid line in each panel indicates the location of the Population I main sequence (with the approximate Pop I spectral types indicated along the  $B-V$  and  $V-K_S$  axes). The single hot subdwarfs are mostly contained within the box defined by:  $B-V \lesssim +0.1$ ,  $V-K_S \lesssim +0.2$ , and  $J-K_S \lesssim +0.05$ , which is shown in each panel with a dotted line. Objects labelled 1–5 in both panels, and 6 in the right panel, are discussed further in the text (§3.3.1). The arrows indicate color shift due to one magnitude of extinction at  $V$  ( $A_V = 1$ , see §C.2).

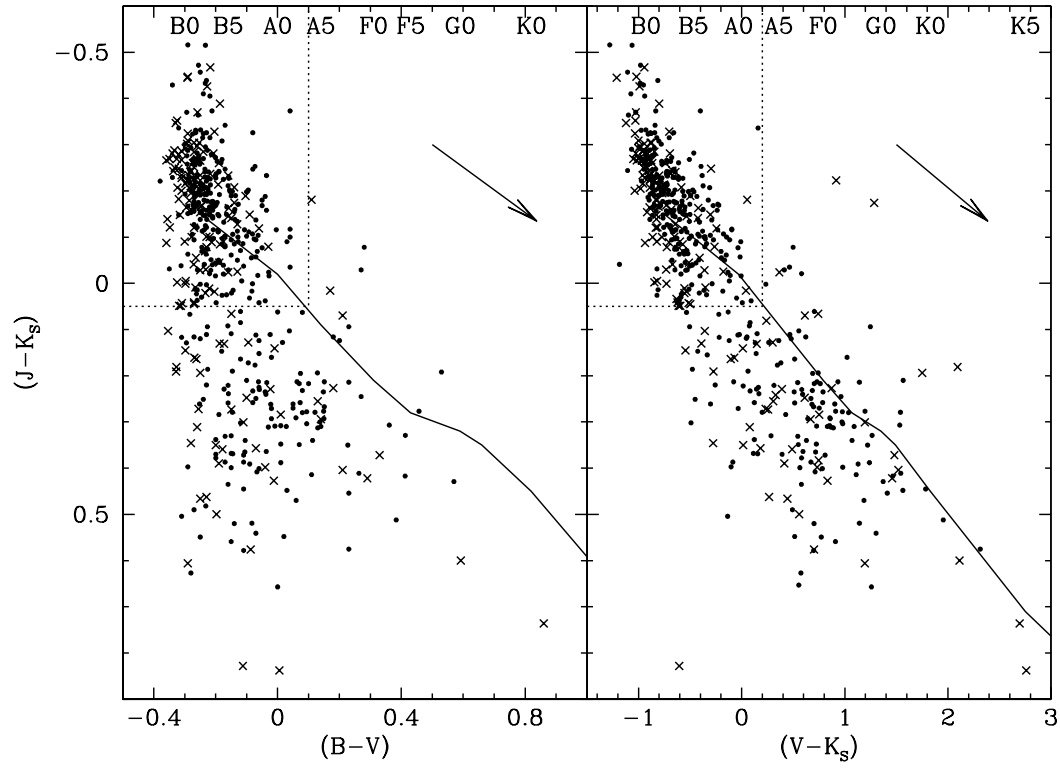


Fig. 3.2 Same as Figure 3.1 but for all hot subdwarfs with photoelectric visual, and 2MASS IR magnitudes. However, in both panels, solid dots represent the sdB group, crosses ( $\times$ ) are the sdO group.

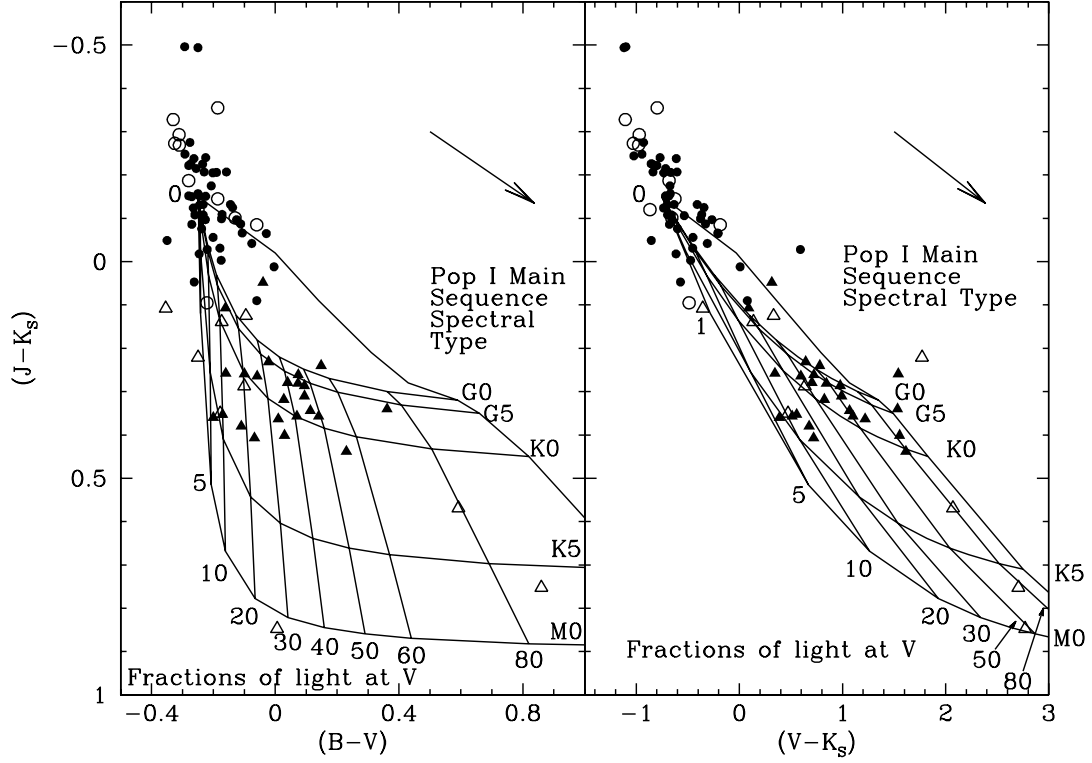


Fig. 3.3 Grid of composite colors computed by combining the light from a hot subdwarf ( $B-V \approx -0.25$ ,  $V-K_S \approx -0.75$ ,  $J-K_S \approx -0.15$ ) with that of “typical” Pop I main sequence stars (G0, G5, K0, K5, and M0; Johnson 1966) assuming varying fractional contributions to the total light in the  $V$  band by the late type star (fractions contributed by the companion: 0, 1, 5, 10, 20, 30, 40, 50, 60, 80, and 100%). Circles are the reported single subdwarfs (solid: sdB, open: sdO) and triangles are the reported composite subdwarfs (solid: sdB, open: sdO) from Figure 3.1. The large arrows indicate the color change due to one magnitude of extinction at  $V$  ( $A_V = 1$ , see §C.2).

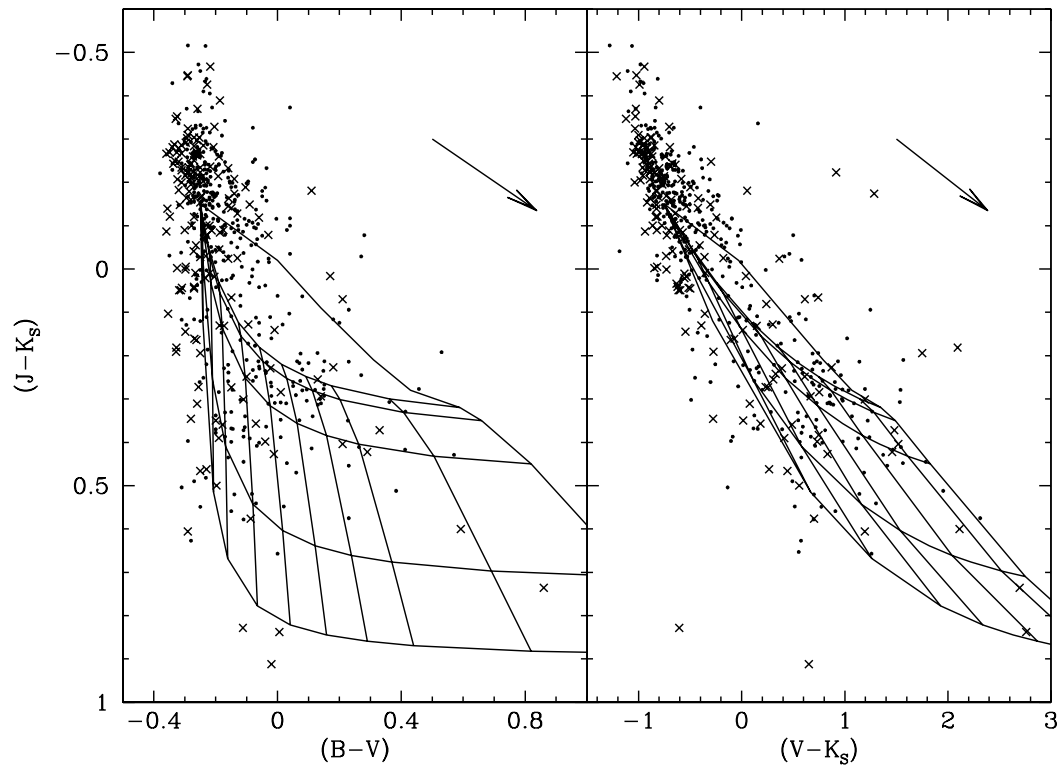


Fig. 3.4 Same as Figure 3.3, except all sdBs (circles) and sdOs (crosses,  $\times$ ) with 2MASS photometry are shown, as in Figure 3.2.

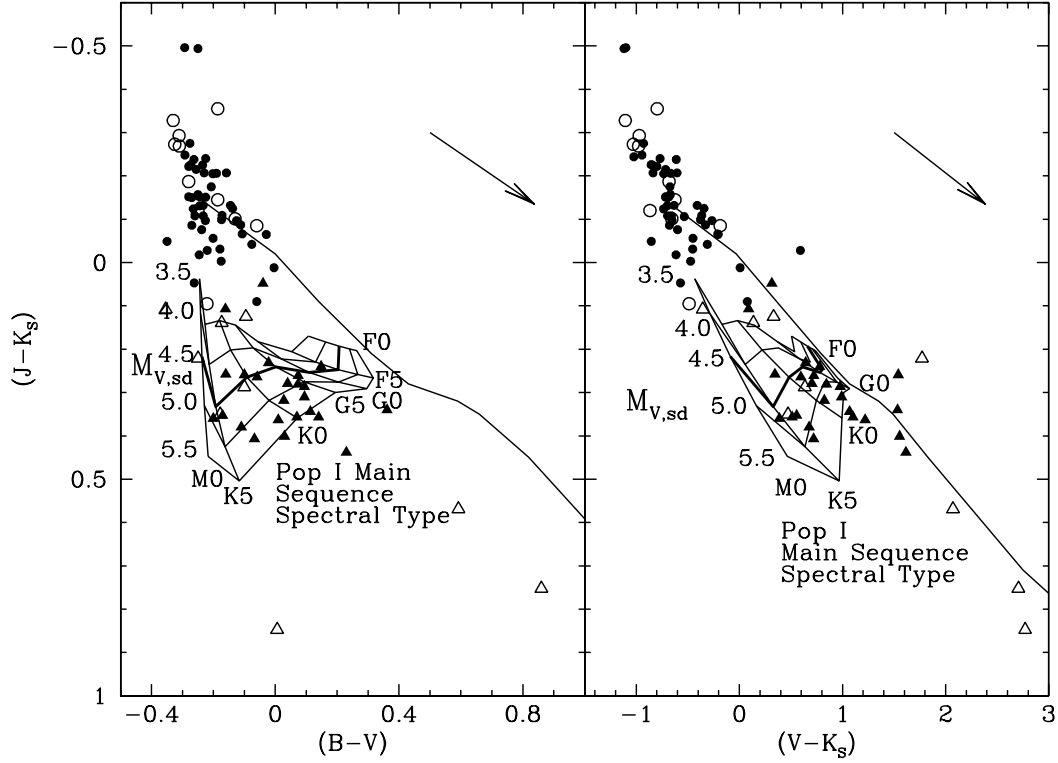


Fig. 3.5 Grid of composite colors computed by combining the light from a hot subdwarf ( $B-V \approx -0.25$ ,  $V-K_S \approx -0.75$ ,  $J-K_S \approx -0.15$ ) with that of “typical” Pop I main sequence stars (F0, F5, G0, G5, K0, K5, and M0; Johnson 1966) and assuming values of  $M_V$  for the subdwarf ( $M_{V,\text{sdB}} = 3.5, 4.0, 4.5, 5.0$ , and  $5.5$ ) — the line for  $M_{V,\text{sdB}} = 4.5$  has been thickened to help guide the eye. The lines for G5 and F5 have been left off the right plot for clarity. Circles are the reported single subdwarfs (solid: sdB, open: sdO) and triangles are the reported composite subdwarfs (solid: sdB, open: sdO) from Figure 3.1. The large arrows indicate the color change due to one magnitude of extinction at  $V$  ( $A_V = 1$ , see §C.2).

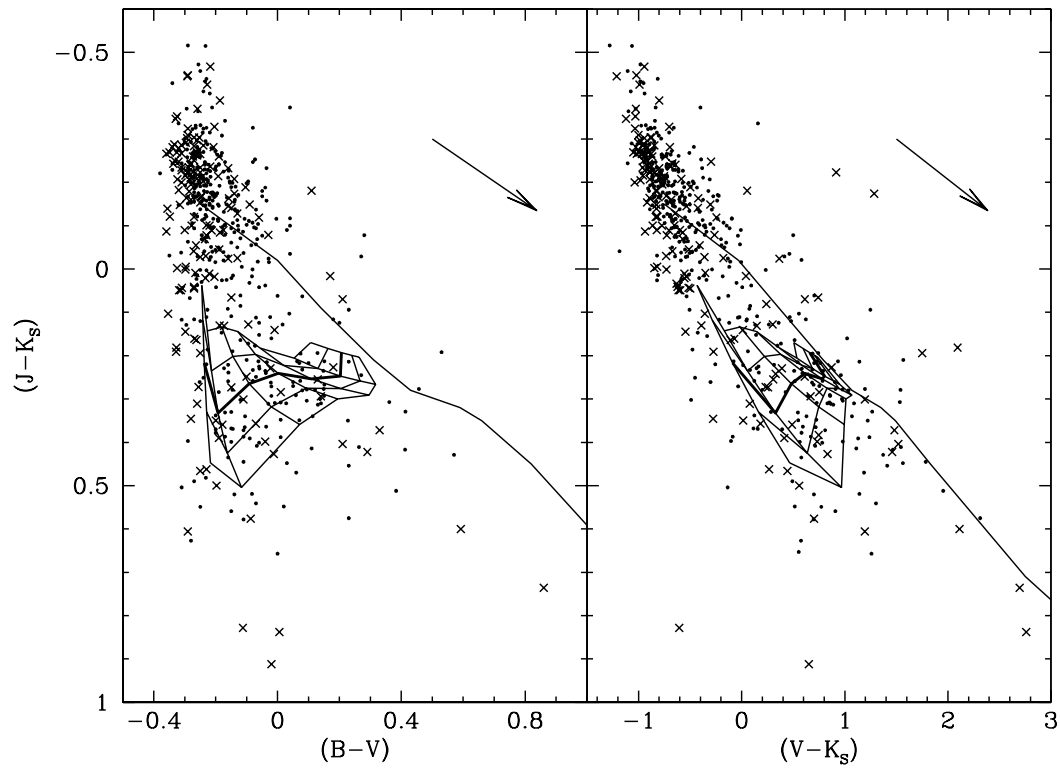


Fig. 3.6 Same as Figure 3.5, except all sdBs (circles) and sdOs (crosses,  $\times$ ) with 2MASS photometry are shown as in Figure 3.2.



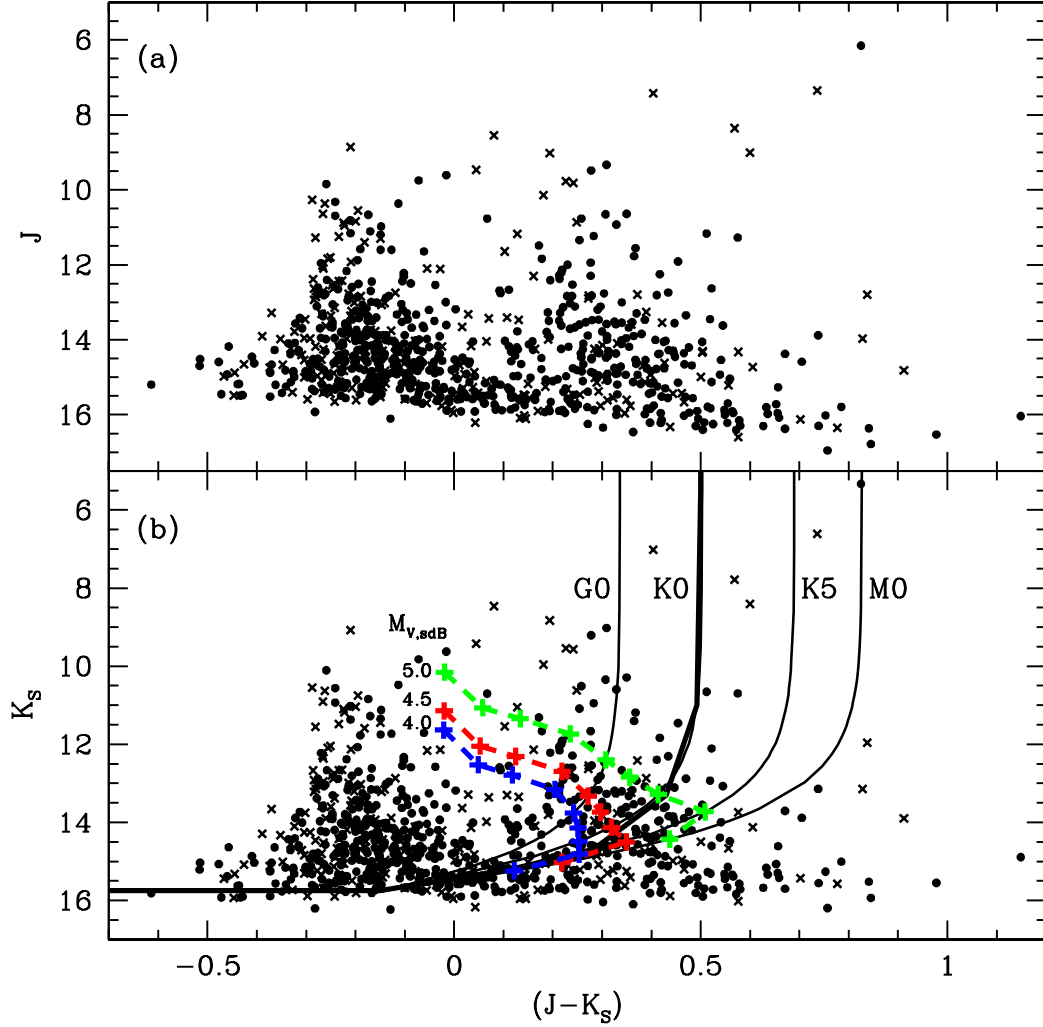


Fig. 3.7 Color-magnitude diagrams of  $J$  (panel *a*) and  $K_S$  (panel *b*) vs.  $(J - K_S)$ . In both panels the sdBs are plotted as circles and the sdOs as crosses ("x"). Panel *b* shows the cut made to get an approximately volume limited sample (thick line), as well as the limits (thin lines) for companions with colors corresponding to the Pop I main sequence spectral types: G0, K0, K5, and M0 assuming an apparent magnitude for the subdwarf of  $K_S = 15.75$ . In panel *b*, thick dotted lines show the composite colors assuming main sequence companions (marks from top to bottom: A0, A5, F0, F5, G0, G6, K0, K5, and M0) and values of  $M_{V,sdB} = 4.0, 4.5, \text{ and } 5.0$ .

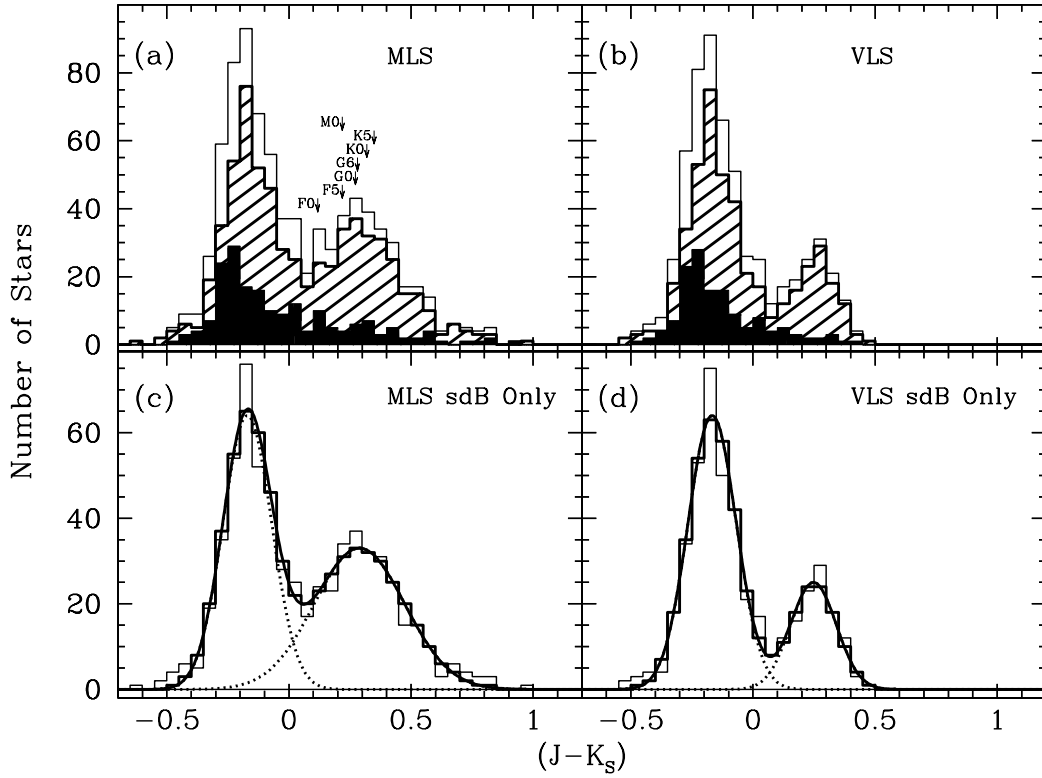


Fig. 3.8 Bimodal distribution of  $J-K_S$ , panels *a* and *c* represent the Magnitude Limited Sample (MLS), and panels *b* and *d* represent the approximately Volume Limited Sample (VLS). In panels *a* and *b*, the white histogram is all hot subdwarfs, the diagonally hashed histogram is sdBs only, and the solid black histogram is sdOs only. Panel *a* also shows the composite  $J-K_S$  colors of sdB+MS stars assuming  $M_V = 4.5$  and  $J-K_S = -0.15$  for the sdB. Panels *c* and *d* show the Gaussian fits to the sdB only distributions (parameters are given in Table 3.4).

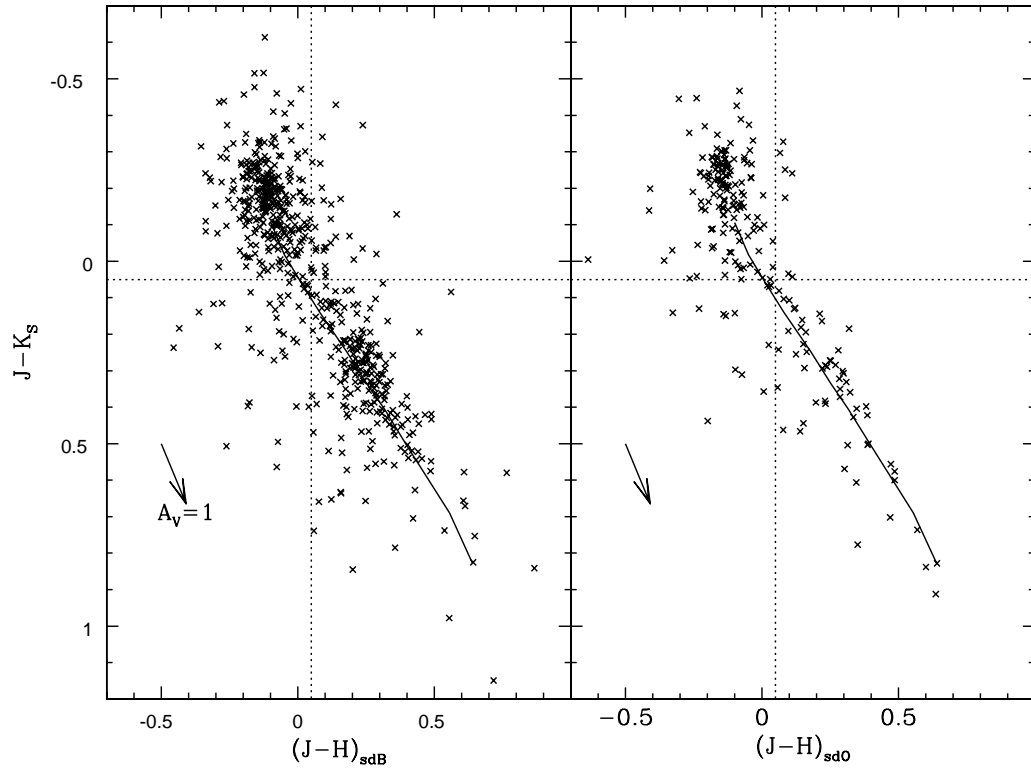


Fig. 3.9 Color-Color plot for 2MASS colors. Left panel shows sdB only; right panel shows sdO only. Solid line is the Pop I main sequence from B8 (upper left) to M0 (lower right). Dotted lines represent the cuts made in a single color to define single and composite objects [ $J-K_S=+0.5$ ,  $J-H=+0.5$ ]. An arrow indicates the shift in  $(J-K_S, J-H)$  due to one magnitude of extinction at  $V$  ( $A_V = 1$ , see §C.2).

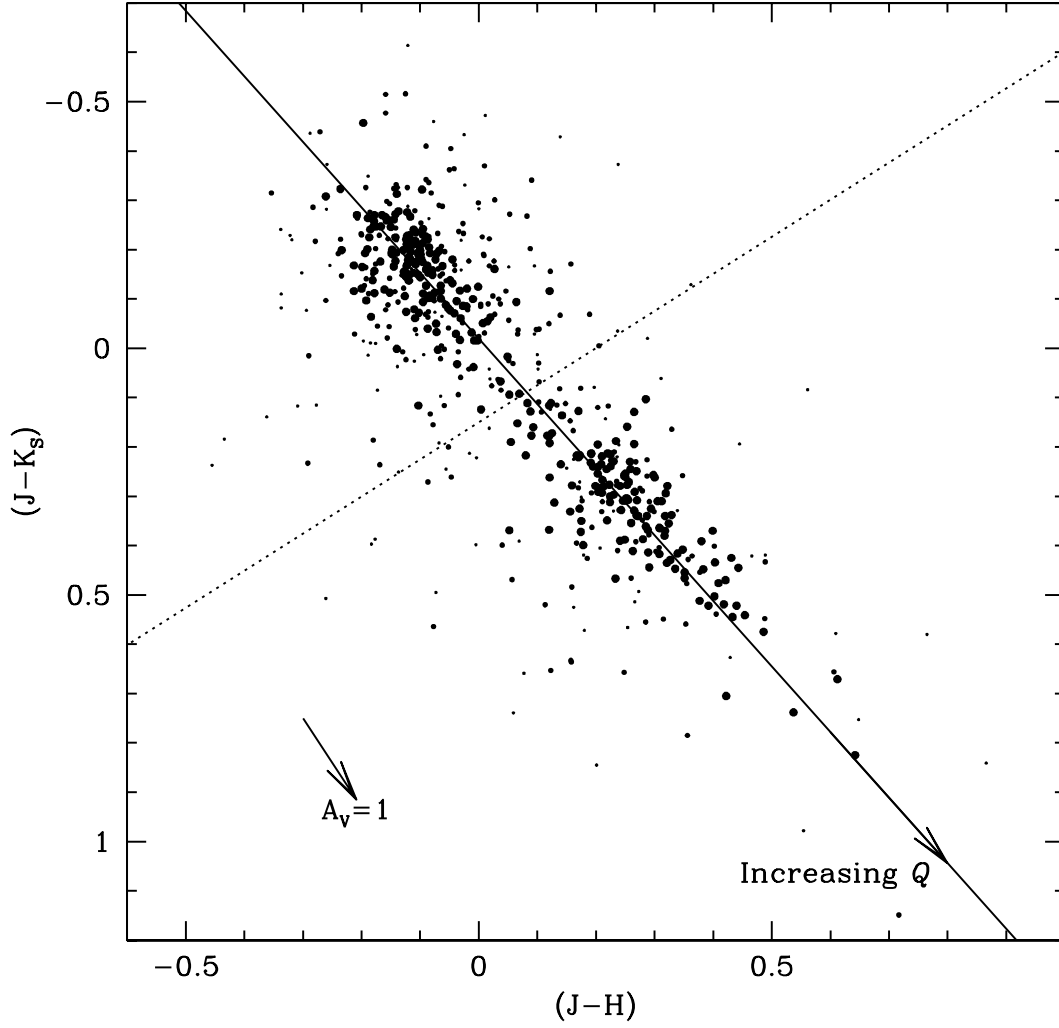


Fig. 3.10 Color-Color plot for 2MASS colors of sdBs only with the linear fit shown as the solid line, the parameter  $Q$  increases along this line as indicated. The dashed line is mathematically perpendicular to the linear fit line, and demonstrates a contour of constant  $Q$  (the two lines cross at  $Q = +0.15$ ). The point diameters indicate the size of the  $J-K_S$  and  $J-H$  errors: the largest points are for sdB with both  $\sigma(J-K_S)$  and  $\sigma(J-H) < 0.1$ , the middle sized points are for sdB with both  $\sigma(J-K_S)$  and  $\sigma(J-H) < 0.2$ , and the smallest points are for sdB with  $\sigma(J-K_S)$  and/or  $\sigma(J-H) \geq 0.2$ . An arrow indicates the shift in  $(J-K_S, J-H)$  due to one magnitude of extinction at  $V$  ( $A_V = 1$ , see §C.2).

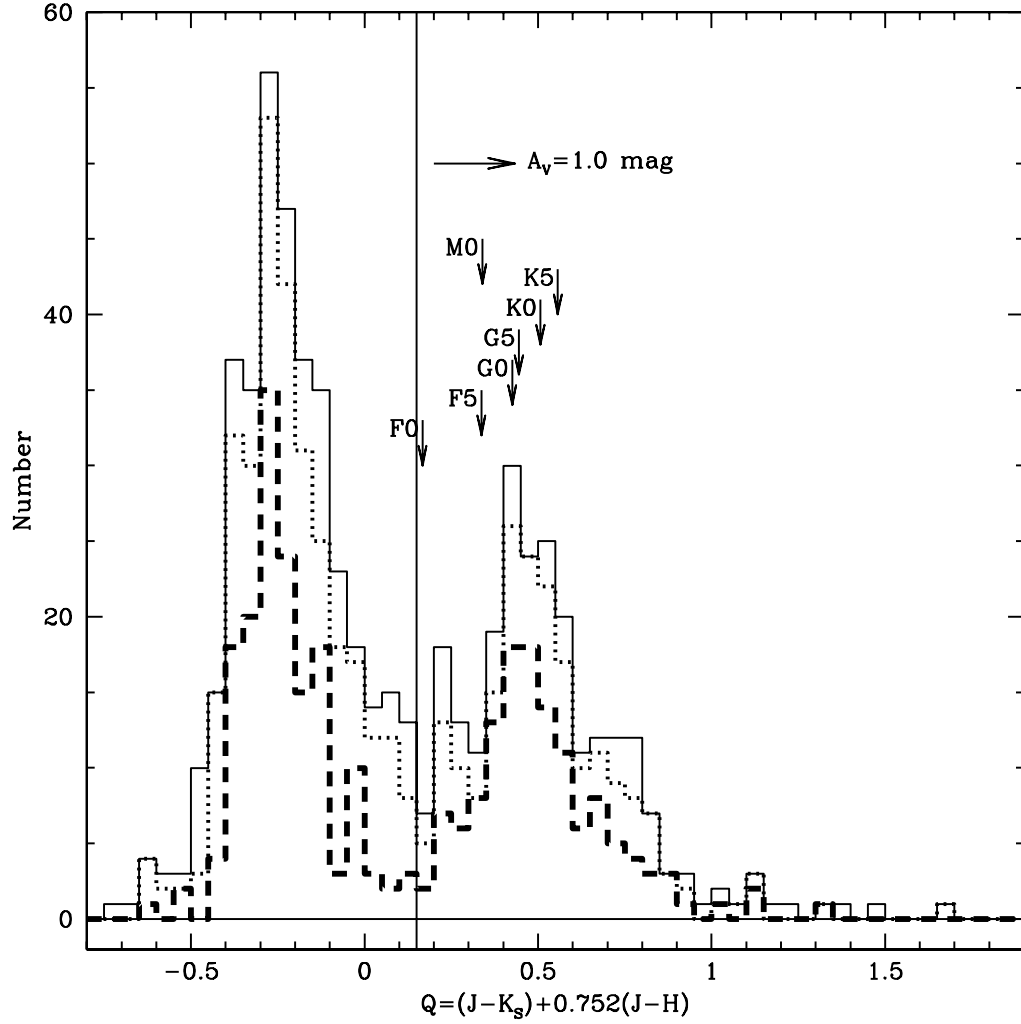


Fig. 3.11 Histogram of sdB  $Q$  values (bin size is 0.05 in  $Q$ ), the solid line is for all sdB, the dotted line is for sdB with both  $\sigma(J - K_S)$  and  $\sigma(J - H) < 0.2$  the dashed line is for sdB with both  $\sigma(J - K_S)$  and  $\sigma(J - H) < 0.1$ . Single sdBs fall in the left peak ( $Q < 0.15$ ), composites fall in the right peak ( $Q \geq 0.15$ ). The  $Q$  values of sdB+main sequence composites (assuming  $M_{V,\text{sdB}} = 4.5$  mag) are indicated by downward pointing arrows and labelled with the corresponding Pop I main sequence type. An arrow indicates the shift in  $Q$  due to one magnitude of extinction at  $V$  ( $A_V = 1$ , see §C.2).

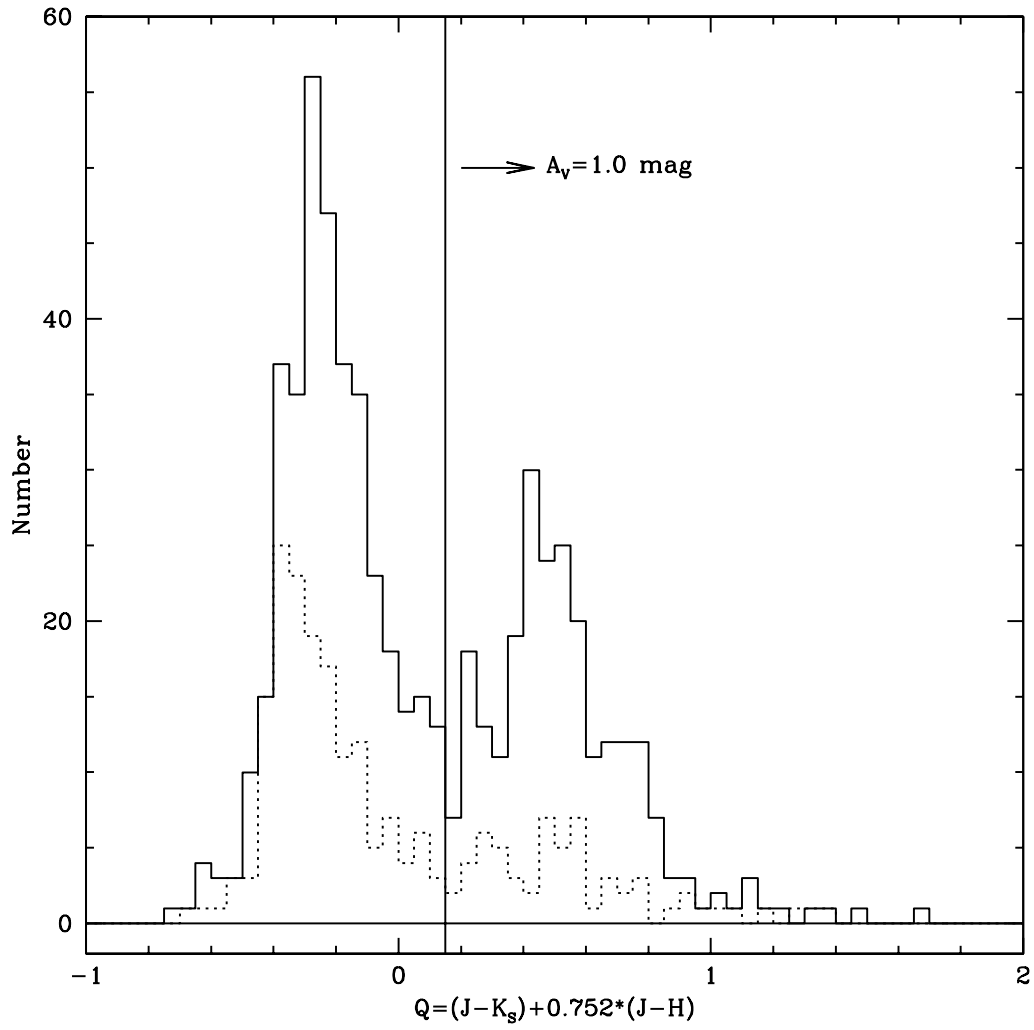


Fig. 3.12 Same as Figure 3.11, except comparing all sdB and sdO  $Q$  values (bin size is 0.05 in  $Q$ ), the solid line is for all sdB, the dotted line is for all sdO.

Table 3.1. Breakdown of the Hot Subdwarf sample discussed in §3.2.

Sub-Sample	Number of Objects
1527 Objects in KHD	
Unrecovered	26
Duplicate	15
Input to 2MASS ASDR	1486
1237 IDs from 1486 input to 2MASS ASDR	
Subdwarfs	1193
Non-subdwarfs	44
1193 Hot Subdwarfs from 2MASS ASDR	
With 2MASS $J$ , $H$ , and $K_S$	817
With 2MASS $J$ and $K_S$	826
With 2MASS $J$	1190
With $V$ (or $y$ )	720
With $BV$ (or $uvby$ )	704
817 with $J$ , $H$ , and $K_S$	
sdB/sdB–O/sd/sdOB	630
sdO/sdO(A)/sdO(B)/sdO(C)/sdO(D)	187
826 with $J$ and $K_S$	
sdB/sdB–O/sd/sdOB	636
sdO/sdO(A)/sdO(B)/sdO(C)/sdO(D)	190
With $V$ (or $y$ )	562
With $BV$ (or $uvby$ )	550
562 with $V$ (or $y$ ), $J$ , and $K_S$	
sdB/sdB–O/sd/sdOB	423
sdO/sdO(A)/sdO(B)/sdO(C)/sdO(D)	139
550 with $BV$ (or $uvby$ ), $J$ , and $K_S$	
sdB/sdB–O/sd/sdOB	414
sdO/sdO(A)/sdO(B)/sdO(C)/sdO(D)	136

Table 3.2. Photometry of Hot Subdwarfs with dM or Brown Dwarf Companions.

No. <sup>a</sup>	Name	$B-V$	$J-K_S$	$V-K_S$
218	HD 269696 <sup>b</sup>	-0.270	-0.251	-0.916
...	HS 0705+6700	...	-0.202	...
407	PG 1017-086	-0.225	-0.176	-0.417
605	PG 1241-084	-0.332	-0.149	-0.110
687	PG 1329+159	-0.225	-0.200	-0.755
695	PG 1336-018	-0.237	-0.041	-1.185
816	PG 1438-029	...	-0.033	...
...	HS 2333+3927	...	+0.061 <sup>c</sup>	...

<sup>a</sup>Sequence number if the star is in the KHD sample (if no number is given then the star is not in KHD).

<sup>b</sup>Companion is believed to be a brown dwarf (all the rest are dM).

<sup>c</sup>Large error on  $K_S$ ,  $J-K_S = +0.061 \pm 0.133$ .

NOTE: Please refer to §3.3.2, §1.4.1.1, and Table 1.1 for more information.



Table 3.3. Binomial fractions of single and composite-color subdwarfs observed by 2MASS.

Group	Magnitude Limited Sample (MLS)		Volume Limited Sample (VLS)	
	Single <sup>a</sup> (#)	Composite <sup>a</sup> (#)	Single <sup>a</sup> (#)	Composite <sup>a</sup> (#)
Based on $J-K_S$ <sup>b</sup>				
sdB	$56 \pm 4\%$ (353)	$44 \pm 4\%$ (283)	$73 \pm 4\%$ (323)	$27 \pm 4\%$ (122)
sdO <sup>c</sup>	$69 \pm 7\%$ (132)	$31 \pm 7\%$ (58)	$85 \pm 6\%$ (119)	$15 \pm 6\%$ (21)
Both	$59 \pm 3\%$ (485)	$41 \pm 3\%$ (341)	$76 \pm 3\%$ (442)	$24 \pm 3\%$ (143)
Based on $Q$ <sup>d</sup>				
sdB	$60 \pm 4\%$ (380)	$40 \pm 4\%$ (250)	$75 \pm 4\%$ (333)	$25 \pm 4\%$ (112)
sdO <sup>c</sup>	$75 \pm 6\%$ (140)	$25 \pm 6\%$ (47)	$89 \pm 5\%$ (124)	$11 \pm 5\%$ (16)
Both	$64 \pm 3\%$ (520)	$36 \pm 3\%$ (297)	$78 \pm 3\%$ (457)	$22 \pm 3\%$ (128)

<sup>a</sup>Errors reported are the 95% marginal confidence intervals.

<sup>b</sup>Single are those with  $J-K_S < +0.05$ , composite with  $J-K_S \geq +0.05$ .

<sup>c</sup>Since the sdOs have a broader distribution in  $M_V$  and higher  $T_{\text{eff}}$  than the sdBs, the same color cut in  $J-K_S$  or  $Q$  is likely biased, so interpret these percentages with caution.

<sup>d</sup>Single are those with  $Q < +0.15$ , composite with  $Q \geq +0.15$ .

Table 3.4. Parameters for the  $J-K_S$  sdB Gaussian fits shown in Figure 3.8c-d.

Parameter	MLS		VLS	
	Blue <sup>a</sup>	Red <sup>a</sup>	Blue <sup>a</sup>	Red <sup>a</sup>
Center	$-0.170^{+0.010}_{-0.008}$	$+0.289^{+0.015}_{-0.012}$	$-0.167^{+0.012}_{-0.008}$	$+0.248^{+0.014}_{-0.015}$
Amplitude	$64^{+5}_{-9}$	$33^{+2}_{-3}$	$64^{+5}_{-7}$	$25 \pm 4$
Dispersion	$0.100^{+0.005}_{-0.009}$	$0.185^{+0.006}_{-0.017}$	$0.099^{+0.004}_{-0.008}$	$0.093^{+0.009}_{-0.012}$
Area Proportion	51 : 49		73 : 27	
Integral of Fit	627		434	
$\chi^2$ , $\chi_R^2$ (DOF)	24.06, 1.00 (24)		13.40, 0.89 (15)	

<sup>a</sup>Errors reported are the 95% marginal confidence intervals.

## Chapter 4

# Spectroscopic Observations of Hot Subdwarfs

## 4.1 Introduction

For the spectroscopic portion of my study, I chose to focus on the wavelength region 4500–7000 Å. This wavelength region was chosen in the “red” for several reasons: (1) the late-type companion starts to dominate the blended light in the red so its features become more prominent, (2) this region contains several features that are strong in late-type stars (specifically late-F to K spectral type), (3) these prominent spectral features (namely Mg I b, Na I D, and the Ca II IR triplet) behave differently from each other as temperature and surface gravity are varied, (4) there are additionally a number of Hydrogen and Helium lines present in this wavelength region from the hot subdwarf. While there are many features from both the late-type companion and the hot subdwarfs in this wavelength region, I have chosen to focus on only the strongest: Mg I b, Na I D, and the Ca II IR triplet. The Ca II triplet ( $\lambda = 8498, 8542, 8662$  Å) has a nearly constant equivalent width for main sequence stars of spectral types late-F to K, making it an excellent indicator of the amount of dilution present from the hot subdwarf (and is thus an indicator of the relative contributions from the two stars). The Na I D doublet is sensitive to temperature changes in late-type stars (equivalent width increases with decreasing temperature), while the Mg I b triplet is sensitive to surface gravity changes (see also §5.3). Thus combining the equivalent widths of these three features from the late-type companion with the 2MASS and visual colors I will be able to determine the temperature and surface gravity of the late-type companion.

In this chapter I will discuss the spectroscopic observations I made of 2MASS composite-colored hot subdwarfs. In §4.2 and 4.3 I will discuss the observations and observing procedure used at the Kitt Peak National Observatory (KPNO) 2.1m telescope and the McDonald 2.7m telescope respectively. Then, in §4.4, I will describe the target selection criteria (for both hot subdwarfs and standard stars), and the objects observed. In §4.5 I will discuss the data reduction procedure for the KPNO data. Finally, in §4.6 I will discuss features of individual objects.

## 4.2 KPNO GoldCam

This section will summarize the procedures for the observations I took at the KPNO 2.1m telescope.

### 4.2.1 Instrumental Set-up

I took the majority of my observations using the Gold Camera (GoldCam) on the KPNO 2.1m. GoldCam is the CCD spectrometer on the Gold Spectrograph at the

KPNO 2.1m telescope. The GoldCam Spectrograph (originally called the Image-Tube Spectrograph) is a cassegrain-mounted spectrograph that was built in the early 1970s. With the exception of the shutter and CCD, the entire spectrograph is operated manually (i.e., gratings, tilts, filters, slits, focus, etc. are all set manually).

With GoldCam and the F3Ka CCD I needed to use two different set-ups which I will refer to as the “red” and “blue” settings to cover the wavelength regions of interest. The red setting used grating #35 in first order, with the OG570 filter to prevent second order contamination, and a  $1''.5$  ( $115\mu$ ) slit resulting in a wavelength coverage of roughly  $6500\text{--}9000\text{\AA}$  with  $\sim 3.3\text{\AA}$  resolution ( $\sim 1.3\text{\AA}/\text{pix}$ ). This wavelength range covers  $\text{H}\alpha$  at the blue, out to the Ca II IR Triplet (CaT) on the red. The blue setting used grating #26new in the first order, with a GG385 second order blocking filter, and a  $1''.3$  ( $100\mu$ ) slit resulting in a wavelength coverage of roughly  $4500\text{--}7000\text{\AA}$  with  $\sim 3.3\text{\AA}$  resolution ( $\sim 1.3\text{\AA}/\text{pix}$ ). This wavelength range covers  $\text{H}\beta$  at the blue to  $\text{H}\alpha$  at the red, and includes the Na I D doublet and the Mg I b triplet. I attempted to observe all target objects with both settings of GoldCam.

#### 4.2.2 Observing Procedures

A list of all KPNO observing runs is included in Table 4.1. For a typical observing run of five nights, I would start by using the red setting for the first three nights, and then would switch to the blue setting for the last two nights. Both settings included all the normal calibration images: biases (evening and morning), flat fields (see following paragraphs), and comparison lamps (one at each pointing).

When using the red GoldCam setting, flat fields needed to be taken at each pointing since the F3KA CCD has significant fringing at wavelengths longer than  $\sim 7500\text{\AA}$ . Comparison lamps were taken at each pointing to insure proper wavelength calibration. A typical sequence of events for observing with the red setting are as follows: observe the target, then take three quartz flat field exposures followed by a HeNeAr comparison lamp spectrum.

When using the blue GoldCam setting series of flat fields were taken only at the beginning and ending of each night. HeNeAr comparison lamps were taken at each pointing.

### 4.3 McDonald LCS

This section will summarize the procedures for the observations I took at the McDonald Observatory Harlan Smith 2.7m telescope.

#### 4.3.1 Instrumental Set-up

I attempted to take observations with the Large Cassegrain Spectrograph (LCS) on the McDonald Observatory 2.7m. LCS is attached to the Automated Telescope Offset Guider (ATOG) module at the 2.7m’s  $f/18$  Cassegrain focus. The ATOG provides acquisition and guiding capabilities, as well as calibration lamp illumination. The LCS itself is capable of auto-guiding on-axis from reflected light off the slit jaws or off-axis using other field stars. Unfortunately, during the first two out of my three runs on the

2.7m, auto-guiding was unavailable (the first time because auto-guiding had not been “fixed” after a massive ATOG failure and rebuild, the second because the appropriate guide camera was being used to replace a broken guide camera at the HET). In both of these cases I was required to guide “by hand”: watching light from the slit viewer display and manually making adjustments to the telescope to keep the object centered on the slit.

With LCS and the CC1-CCD I needed to use two different set-ups as with Gold-Cam, however LCS could only cover smaller, non-overlapping wavelength regions. I will again refer to these two settings as the “red” and “blue” settings. For both settings I used grating #44 in first order, but with a different grating tilt for each setting. The red setting used the RG610 filter to prevent second order contamination, and a 1" slit resulting in a wavelength coverage of roughly 7500–8900Å with  $\sim 2.8\text{\AA}$  resolution (full width at half-maximum, FWHM). This wavelength range covers the A-Band to just redward of the CaT. The blue setting used the OG515 second order blocking filter, and a 1" slit resulting in a wavelength coverage of roughly 5400–6800Å with  $\sim 2.8\text{\AA}$  resolution (FWHM). This wavelength range includes H $\alpha$  at the red end and the Na I D doublet toward the blue. (Unfortunately, I was unable to obtain the Mg I b triplet with LCS.) I attempted to observe all target objects with both settings of LCS.

#### 4.3.2 Observing Procedures

A list of all McDonald observing runs is included in Table 4.1. My runs using LCS followed the same format as I described for GoldCam: begin with the red setting for the first  $\sim$ half of the run, then switch to the blue setting for the second  $\sim$ half of the run. Both settings included all the normal calibration images: biases (evening and morning), dome flat fields (evening and morning), and comparison lamps (one each of Argon and Neon at each pointing).

Only dome flats were available with the 2.7m, since the LCS did not have an internal flat field lamp, so it was only possible to take flats at the beginning and ending of each night. Fortunately, LCS’s CC1-CCD does not have the red fringing problems that GoldCam’s F3KA CCD has. Unfortunately, grating #44 turned out to have a pronounced Wood’s Anomaly<sup>1</sup> (see Wood 1935) which fell in the middle of the blue setting. Additional flat fielding complications arose in the blue setting because the flat field lamp had emission lines from Na I and Li I. Figure 4.1 shows a cut along the dispersion direction through a LCS blue flat field with the various anomalies marked and labelled.

Comparison lamps were taken at each pointing with both the red and blue settings. There were two separate comparison lamps available, Argon and Neon, neither of

---

<sup>1</sup>A Wood’s Anomaly is an enhancement in the efficiency of the grating at a given critical wavelength (which is dependent on grating tilt). In a grating, light in successive orders is diffracted over a range in angles from the normal of the grating. At some order, and critical wavelength value, the diffracted light lies in the plane of the grating. After this point (since it is not possible for the light to be diffracted into/through the grating) the power from these “forbidden regions” is redistributed back to the allowed orders causing a (highly polarized) enhancement of efficiency in those orders. The enhancement appears as a sharp cut at the critical wavelength with a steep decline to the red. For more information see Wood (1935) and Murdin (1990).

which alone was suitable for the wavelength regions I was covering. So, at each pointing an exposure of each lamp was taken, then during processing the two images were added together to provide better wavelength calibration than either could provide alone.

## 4.4 Target Selection and Lists

### 4.4.1 Hot Subdwarfs

Hot subdwarf targets were selected from KHD<sup>2</sup> based on their  $V$  and  $J$  magnitudes and  $J-K_S$  color from 2MASS (see Chapter 3 starting on page 19). Targets for the 2002 observing runs were selected based on the 2MASS Second Incremental Data Release (2IDR) photometry, while targets for the 2003 observing runs were selected based on the 2MASS ASDR. (It is worthwhile to note that all targets selected based on 2IDR photometry still satisfied the selection criteria when their ASDR photometry became available.) Targets for each run consisted of composite-colored ( $J-K_S > +0.05$ ) hot subdwarfs (focusing mainly on sdB types, but not excluding those of other classifications to fill observing time) that had  $V < 14$  (although a few extra objects with  $V > 14$  were also done to fill gaps during observing). Some single-colored hot subdwarfs ( $J-K_S < +0.05$ ) were also observed; these generally had  $V < 12$ .

I was able to observe (both red and blue) 54 composite-colored hot subdwarfs at KPNO. This includes both sdB, a few sdO, several visual doubles, and several objects that showed emission lines. For two other objects I was only able to obtain GoldCam blue spectra. Table 4.2 contains a listing of all hot subdwarf stars observed using the KPNO 2.1m telescope with GoldCam. Figure 4.2 shows the distribution of all KPNO spectroscopically observed hot subdwarfs in 2MASS ( $J-H$ ,  $J-K_S$ ) color space, and Figure 4.3 shows the distribution in 2MASS ( $J$ ,  $J-K_S$ ) space. A (non-exhaustive) listing of physical parameters (including  $T_{\text{eff}}$  and  $\log g$  for the subdwarf, and classification or  $T_{\text{eff}}$  for the companion) reported in the literature for the observed composite-colored hot subdwarfs (from Table 4.2) is given in Table 4.3. A similar table of literature values for the single-colored hot subdwarfs (from Table 4.2) is given in Table 4.4.

Due to a combination of: smaller LCS wavelength coverage, LCS flat field anomalies, lower LCS sensitivity, shorter and fewer LCS runs, increased targets with the release of 2MASS-ASDR for later KPNO runs, and generally crummy weather when at McDonald, I ended up with unique composite-colored subdwarf observations totalling: three objects for which I have *only* LCS red and blue observations (#460 PG 1104+243, #476 PG 1111+339, and #583 LB 2392), two for which I have *only* LCS blue observations (#408 PG 1018-047 and #435 TON 1281), and two for which I have LCS red and blue observations but also GoldCam blue observations (#234 BD+34°1543 and #294 PG 0900+400). All other objects that I observed at McDonald I was able to reobserve at KPNO. Thus, my analysis will focus almost exclusively on the observations made at KPNO.

---

<sup>2</sup>Kilkenny, Heber, & Drilling (1988) as updated and expanded in an electronic version by Kilkenny, c. 1992, kindly made available by D. Kilkenny.

#### 4.4.2 “Standards”

KPNO spectral standard stars were chosen to cover the range of spectral types from  $\sim$ mid-F to  $\sim$ early-M ( $+0.4 \lesssim B-V \lesssim +1.5$ ) and a range of absolute magnitudes ( $1 \lesssim M_V \lesssim 9$ , computed from *Hipparcos* parallaxes, see Appendix E on pg. 256 for the calculation of absolute magnitude from parallax). Tycho-1  $B_T$  and  $V_T$  magnitudes for these stars were converted to Johnson  $B_J$  and  $V_J$  magnitudes using:

$$\begin{aligned} V_J &= V_T - 0.090 \times (B_T - V_T) \\ (B-V)_J &= 0.850 \times (B_T - V_T) \end{aligned}$$

This conversion is valid over  $-0.2 < (B_T - V_T) < 1.8$ , and generally gives errors  $< 0.015$  in  $V_J$  and  $< 0.05$  in  $(B-V)_J$  (ESA 1997).

Effort was concentrated in the range of  $+0.4 \lesssim B-V \lesssim +1$  and  $2 \lesssim M_V \lesssim 6$  which covers both main sequence and post-main sequence (early subgiant) mid-F to mid-K spectral types with a noticeable “turn-off” and clear split between the main sequence and subgiants for  $B-V \gtrsim +0.7$  (Figure 4.4) — the appearance of the color magnitude diagram (CMD) for my standards closely resembles that of Sandage, Lubin, & Vandenberg (2003) for the Galactic disk (including the deficit of subgiants with  $B-V > 1.0$ ).

Table 4.5 contains a listing of all stars observed as standards using the KPNO 2.1m telescope with GoldCam.

### 4.5 KPNO GoldCam Data Reduction

Data reduction for the KPNO GoldCam observations was done using the usual IRAF<sup>3</sup> `noao/twodspect` and `onedspect` routines. For each night biases frames were combined and subtracted from each image. Flat fields for each object were averaged together, then each object (and comparison lamp) image was divided by the corresponding flat field. Only one averaged flat field was created each night for the blue GoldCam setup, but for the red GoldCam setup each pointing had its own flat field.

There are several bad columns in the F3Ka CCD. I took care to assure during instrument set-up that these columns did not fall at any vital wavelengths. Since these bad columns caused wildly deviant values in the extracted spectrum, and for ease in plotting and characterizing the spectrum, the worst of these columns were corrected using the `fixpix` routine in IRAF after bias subtraction and flat fielding were performed.

Apertures were traced and extracted for each object, then the object’s apertures were applied to its corresponding HeNeAr comparison lamp to extract the comparison lamp spectrum for wavelength calibration. HeNeAr lines were **identified** or **reidentified** in each comparison lamp and a dispersion solution was determined for each object.

All spectra were linearly dispersion-corrected to a wavelength interval of:  $\Delta\lambda = 1.272 \text{ \AA/pix}$ . For ease in comparing spectra from all observing runs, all spectra were

---

<sup>3</sup>IRAF (Image Reduction and Analysis Facility) is distributed by the National Optical Astronomy Observatories (NOAO), which are operated by the Association of Universities for Research in Astronomy, Inc., under cooperative agreement with the National Science Foundation.

trimmed to cover the following wavelengths: 6392.0–8927.096 Å (red set-up) or 4600.0–6734.168 Å (blue set-up). This dispersion and wavelength coverage were chosen so the region around H $\alpha$  overlapped perfectly (bin-to-bin) between the blue and red spectra.

The wavelength calibrated spectra were initially continuum fitted in IRAF, but these “rough” fits were improved upon, externally to IRAF. Extracted and wavelength calibrated spectra, error spectra, and rough continuum fits were written to text files for further processing outside of IRAF. These text files were read into a program I wrote to improve the continuum fit. My program calculated a spline fit (see Appendix I, page 279) through points in the spectrum that I predefined and was able to change interactively. This continuum fit has only been used to display the full spectra in Figures 4.5–4.19, it was not used to calculate equivalent widths (EWs). Further processing, including measurements of line EWs was accomplished through programs I wrote and which will be discussed in more detail in Chapter 5 (starting on page 97).

Figure 4.5 compares the appearance of a “typical” single hot subdwarf (#1263 LS IV+00°21), a “typical” composite hot subdwarf (#59 PB 6107), and a single HIP standard star (HIP 13081). Figures 4.6–4.14 contain the complete spectra, ordered by increasing  $J-K_S$  color, for all hot subdwarfs observed (except for #91 and #1027, which are not plotted in these figures because they turned out to be very close visual doubles where the spectrum from each component was still contaminated by its companion). Figures 4.15–4.18 contain the complete spectra from both components of resolved visual doubles (see §4.6.3), including the two very close pairs (#91 and #1027). Finding charts identifying the components observed are provided in Figures 4.20–4.22. Figure 4.19 contains the spectra of three objects, classified as hot subdwarfs, but which contain strong emission lines (#835, 1108, and 1493 — see §4.6.4).

## 4.6 Notes on Individual Objects in the Spectroscopic Sample

### 4.6.1 Reddened sdBs

Of the objects previously classified as “sdB”, seven objects (five composite-colored, two single-colored) lie along sightlines which show significant ( $> 0.2$ ) values of  $E(B-V)$  as estimated following Schlegel et al. (1998, see Tables 4.3 and 4.4). These objects are:

1. #172 PG 0314+103 [ $E(B-V) \lesssim 0.53$ ] — Fig 4.13
2. #199 KUV 04110+1434 [ $E(B-V) \lesssim 0.61$ ] — Fig 4.8
3. #203 KUV 04237+1649 [ $E(B-V) \lesssim 0.41$ ] — Fig 4.13
4. #216 KUV 05109+1739 [ $E(B-V) \lesssim 0.34$ ] — Fig 4.8
5. #1108 LS IV–08°03 [ $E(B-V) \lesssim 0.47$ ] — Fig 4.19
6. #1194 BD+48°2721 [ $E(B-V) \lesssim 0.29$ ] — Fig 4.7
7. #1223 HD 185510 [ $E(B-V) \lesssim 0.26$ ] — Fig 4.14

Of these seven objects, at least #172, 199, 203, and 1108 clearly show diffuse interstellar bands (DIBs) at  $\sim 5780$  Å and  $5794/5797$  Å (Herbig 1975) — these DIBs are labelled in Figures 4.8, 4.13, and 4.14. It is difficult to tell if DIBs are present in #1223 due to the

large number of spectral features present in its spectrum, and in #216 due to low S/N. #1194 does not show noticeable DIBs in its spectrum.

#### 4.6.2 Observed Subdwarf O Stars

There are six objects that have been classified “sdO” in my composite sample (see also Tables 4.2 and 4.3). I will treat them as sdB during the analysis, and I will report the results of my analysis. However, these results should be taken with extreme caution due to the large dispersion in luminosity inherent to the sdOs and the fact that their temperatures fall outside my model grid, which was created specifically for sdBs. The six sdOs are:

1. #71 BD−11°162 [sdO+G?]<sup>4</sup> — Fig 4.11
2. #87A PG 0105+276 [sdO(B), sdB+K7]<sup>4</sup> — Fig 4.14 and 4.15
3. #533 BD+10°2357 [sdO+A]<sup>4</sup> — Fig 4.8
4. #1304 PG 2116+008 [sdO(B)]<sup>4</sup> — Fig 4.13
5. #1356 PG 2158+082 [sdO He]<sup>4</sup> — Fig 4.8
6. #1519 CD−17 16503 [sdO?, sdOB]<sup>4</sup> — Fig 4.8

Of the six, five show He II lines either strongly (#87A, 1304, and 1356) or weakly (#71 and very weakly in 533), while the sixth (#1519) shows no He features at all. He I is additionally seen in #1304 and 1356 (but none of the others). Stars #71 and 1519 show features indicative of a cool star (CaT, Na I, Mg I, etc.). Star #533 shows a strong Paschen series overlapped by the CaT, and additionally weak Na I and weak Mg I. Star #87 is a close visual double where the two components have blended colors in 2MASS, but I was able to get individual spectra of the two components, see §4.6.3. Star #1304 shows strong Na I, but no obvious CaT (however, the spectrum at CaT is of low quality). Star #1356 shows strong Na I, possibly a very weak CaT, and no apparent Mg I — however this object additionally seems to show a DIB just blueward of Na I, so it is possible the Na I could be nearly or entirely interstellar. Unfortunately, this might be contradicted by a relatively low value of  $E(B-V)$  from Schlegel et al. (1998):  $E(B-V) \sim 0.08$  (see Table 4.3).

There are four hot subdwarfs classified as “sdO” in my single-colored spectroscopic sample (one of which has conflicting classifications of both sdB and sdO; see also Tables 4.2 and 4.4). The four objects are:

1. #130A Feige 19 [sdO He, sdO]<sup>4</sup> — Fig 4.6 and 4.16
2. #1181 [CW83] 1735+22 [sdB, sdO]<sup>4</sup> — Fig 4.7
3. #1187 BD+39°3226 [sdOp, sd]<sup>4</sup> — Fig 4.6
4. #1347 BD+28°4211 [sdO7p]<sup>4</sup> — Fig 4.6

---

<sup>4</sup>Classification(s) from KHD, also listed in Table 4.3.

<sup>4</sup>Classification(s) from KHD, also listed in Table 4.3.



Subdwarf #1181 is dominated by Balmer lines, but also shows very weak He II lines. The other three all show strong He II lines, with #1187 and 130A also showing strong He I lines (including He I at  $\lambda 4921.9$ ,  $\lambda 5015.7$ , and  $\lambda 5047.7$ ). #1347 additionally shows NLTE emission cores in both  $H\alpha/\text{He II}$  and  $H\beta/\text{He II}$  (see §4.6.4 for more information).

### 4.6.3 Visual Doubles

There are eleven visual doubles in my complete subdwarf sample. I will discuss them in two groups based on their 2MASS colors: (1) those where the subdwarf looks single-colored, and (2) those where the subdwarf looks composite-colored. Please note that in all the visual doubles in my sample I have always called the hot subdwarf member component “A” and the companion to the hot subdwarf component “B” — **these designations do not imply a relationship between the apparent magnitudes of the two stars**. In some pairs the hot subdwarf is in fact the visually brighter star, however in others pairs it is not (see Figures 4.20 to 4.22). The parameters of the visual doubles (including separations, magnitude differences, and colors) are listed in Table 4.6.

#### 4.6.3.1 Single in 2MASS Colors

The five visual double subdwarfs that are single based on 2MASS colors are:

1. #50 PG 0027+222 — Fig 4.15
2. #130 Feige 19 — Fig 4.16
3. #157 PB 9286 — Fig 4.16
4. #550 HZ 18 — Fig 4.17
5. #700 PG 1340+607 — Fig 4.17

In all cases these pairs clearly have two detections in 2MASS (one for the subdwarf, and one for the companion). The subdwarfs themselves are single spectroscopically. With the exception of #130A, all of the subdwarfs in these visual doubles are dominated by Balmer lines. Star #130A, Feige 19, on the other hand, is dominated by He I and He II lines (in line with its classification as “He-sdO”).

With the exception of #550B, the companions all show late-type stellar features. Star #550B (companion to HZ 18) shows only Balmer lines which appear nearly as strong as the subdwarf itself (although there is a lot of noise in the spectrum, and only the blue observation was taken). Based on the appearance of their spectra, coupled with the fact that both stars appear blue in 2MASS [ $(J-K_S)_A < -1.137$ ,  $(J-K_S)_B = -0.042$ ], make it possible that this is a *resolved* pair of sdB (or sdB+HBB) stars. To my knowledge there are only two other reported sdB+sdB binaries: HE 0301–3039, which is a double-lined spectroscopic binary consisting of two very similar hot subdwarfs (Lisker et al. 2004), and PG 1544+488 (#959 in KHD), which is a double-lined spectroscopic binary consisting of two different, helium-rich, hot subdwarfs (Ahmad, Jeffery, & Fullerton 2004). Assuming the two stars of #550 HZ 18 are associated, given  $V_A = 15.15$  (Table 4.2), a separation of  $\sim 7''$ , and assuming  $M_{V,A} \sim 5.0-4.5$  (following §3.3.2), then their projected physical

separation would be  $\sim 7500\text{--}9500\text{ AU}$ <sup>5</sup>. I attempted to cross-correlate the spectra I took of these two stars using `fxcor` in IRAF. When I did this using 550A as the template, and 550B as the object, I got a velocity difference of  $\sim -130 \pm 50\text{ km s}^{-1}$ . This could imply: (1) that these two stars are not associated, (2) that at least one of the two stars is in a close binary, or (3) that my spectra are not good enough to accurately determine radial velocity differences (although cross-correlating the sky spectra from the two observations yielded  $\sim 13 \pm 2\text{ km s}^{-1}$ ). More time-series observations are needed of these two stars to choose among the possibilities.

#### 4.6.3.2 Composite in 2MASS Colors

The six subdwarfs in visual doubles that are composite based on 2MASS colors are:

1. #87 PG 0105+276 — Fig 4.15
2. #91 PB 8555 — Fig 4.15
3. #187 HDE 283048 — Fig 4.16
4. #1027 PG 1618+562 — Fig 4.17
5. #1348 PG 2151+100 — Fig 4.18
6. #1461 PB 5333 — Fig 4.18

Of these six objects, three (#87, 91, and 1027) are obviously blended in 2MASS (only one object was found in 2MASS, and/or the one object looks elongated). Stars #91 and 1027 were barely resolved at the telescope. I attempted to get individual spectra of each component, however, there is still significant contamination from the neighbor in both cases, so I am unable to determine whether the composite is truly resolved (I cannot verify that the hot subdwarfs have no further contamination by any additional unresolved late-type companions). The spectra are nevertheless good enough to allow me to identify which component is the “hotter” star (and thus the subdwarf). Silvotti et al. (2000) noted #1027 is a visual double, classified the companion as F3, and determined that the two stars show the same radial velocity (strongly suggesting these two stars are a wide binary — see the notes in Table 4.3). Incidentally this would seem to rule out the presence of a close companion to the subdwarf (i.e., rule out a hierarchical triple in this system) since any close binary companion to the hot subdwarf would cause a significant RV offset in the hot subdwarf from the system velocity (the two resolved stars would not have shown the same RV in this case).

The other three visual double pairs (#187, 1348, and 1461) are clearly resolved in 2MASS. Star #187A shows composite colors and composite features in its spectrum. On the other hand, while #1461A is still composite-colored, it shows no features from

---

<sup>5</sup>If instead the B component were a background MS star, assuming  $V \sim 15$  (since the two stars are about the same magnitude in  $R$ ), and say it is an A0 star with  $M_V \sim 0$  for simplicity, then then it would lie at  $d \sim 10\text{ kpc}$ . However, since this star is at  $\alpha \sim 12\text{h}$ ,  $\delta \sim +37^\circ$ , it lies nearly at the North Galactic Pole. It would be extremely unlikely to find an AB-type MS star at a distance of  $\sim 10\text{ kpc}$  in the direction of the North Galactic Pole.

a late-type star in its spectrum. This star does show NLTE emission in the core of  $H\alpha$ , so it is possible that there are additional factors contributing to its red color in 2MASS. Star #1348A is particularly interesting: in the DSS images (Figure 4.22) the two components observed spectroscopically are labelled as “A” and “B”. However, in 2MASS the “A” component itself resolves into two components: the West star is the much brighter subdwarf (I’ve labelled this as “A” in Table 4.2 and Figure 4.22), and the East star is a very faint star that was not seen at the telescope (I’ve labelled this as “Ab” in Table 4.2 and Figure 4.22). The 2MASS  $J$ -band image is shown in Figure 4.22; in it all three components (A, B, and Ab) are visible. In the DSS (red) image in the same figure there is a slight E–W elongation to component A which resolves into the two components, A and Ab, in 2MASS. Regardless, the subdwarf component still has a composite color in 2MASS. In its spectrum (which may be a blend of A and Ab) the CaT and Mg I is extremely weak, while the Na I lines are proportionally a lot stronger.

#### 4.6.4 Objects with Emission Lines

Five objects observed as part of my 2MASS color-selected composite sample show emission lines in their spectra:

1. #835 PG 1444+232 (called “Haro’s Star” by G. H. Herbig 1992) — Fig 4.19
2. #1108 LS IV–08°03 (this work) — Fig 4.19
3. #1347 BD+28°4211 (Reid & Wegner 1988) — Fig 4.6
4. #1461 PB 5333 (this work) — Fig 4.11 and 4.18
5. #1493 PG 2337+300 (Koen & Orosz 1997) — Fig 4.19

Stars #1347 BD+28°4211 and #1461 PB 5333 are hot sdOs exhibiting NLTE processes in their atmospheres (specifically emission in the core of  $H\alpha$ , and additionally  $H\beta$  in the case of #1347). Star #835 PG 1444+232 is dominated by Fe II emission formed in the outer layers of the star (in high density gas) or in a strong stellar wind (Arkhipova et al. 2002). Star #1491 PG2337+300 is reported to be a CV based on flickering and the presence of emission lines (Koen & Orosz 1997).

Star #1108 LS IV–08°03 shows very broad absorption lines with core emission in  $H\alpha$ ,  $H\beta$ , and He I, as well as emission from C III/N III — all of which are significantly time-variable in as little as  $\sim 30$  min (in both the emission strength and profile shape). Additionally, #1108 coincides with a Rosat X-ray source, 1RXS J165630.2–083442 or 1WGA J1656.4–0834 (Voges et al. 1999; White et al. 2000, both of whom list the star LS IV–08°03 as a possible optical counterpart). Photometry<sup>6</sup> of this object shows it to

---

<sup>6</sup>Photometry taken by H. A. Smith and R. Miller at the Michigan State University 24” telescope (July–September 2004), and I. L. Andronov, N. I. Ostrova, and V. Burwitz at the Observatori Astronòmic de Mallorca using one of their 30-cm MEADE UHTC Schmidt-Cassegrain telescopes (July 2004) — private communications. Similar behavior for this star is seen in the Northern Sky Variability Survey (NSVS, Woźniak et al. 2004, <http://skydot.lanl.gov/> — where LS IV–08°03 corresponds to NSVS 16408817). NSVS reports a median unfiltered optical magnitude of 11.855, with a maximum observed magnitude of 11.698, and a minimum of 11.977 for this object.

be photometrically time variable (both rapid flickering and more gradual changes over timescales of  $\sim$ days). Recent radial velocity observations by J. R. Thorstensen (private communications, July 2005), indicate a  $\sim 5$  cycle per day periodicity ( $P = 0.1953^{\text{d}}$ ) — it is not yet clear whether this period is present in the photometry. The presence of the X-rays, emission lines, and the rapid variability all seem to indicate that this object is likely a “short” period interacting binary of some type. If the identification of this star with the Rosat X-ray source is correct, and this star is in fact a binary, then LS IV–08°03 is a rather (optically) bright, although highly reddened (see §4.6.1), X-ray binary ( $V \approx 11.5$ ).

#### 4.6.5 Other Spectral Anomalies

In this subsection I discuss a few “anomalies” that are apparent in the spectra. These are: residual fringing effects, an unidentified “bump” in the spectra just blueward of Na I D, and strong telluric water vapor absorption.

##### 4.6.5.1 Residual Fringing

The first effect I will discuss (which is the worst by far) is residual fringing. During the June 2003 run I had a lot of difficulty with thermal changes in the spectrograph and telescope. I did not learn the severity of the problem until after the run during data reduction. The thermal changes I experienced resulted in significant residual fringing, which I was unable to remove from the spectra. In particular most of the spectra from the night of 2003 June 11 show significant residual fringing effects (two excellent example of this are #849, PG 1451+472, in Figure 4.12, and #850, PG 1452+198, in Figure 4.7). I attempted to reobserve the objects affected by fringing from the June 2003 run on the following run in September, but I was unable to reobserve them all.

There were eleven observations that had significant residual fringing in the region of the CaT. The objects affected are: #533 (BD+10°2357), 551 (PB 3854), 630 (TON 139), 638 (PG 1257–026), 849 (PG 1451+472), 937 (PG 1536+278), 1051 (PG 1629+081), 1096<sup>7</sup> (PG 1648+080), 1182<sup>7</sup> (BD+29°3070), 1297<sup>7</sup> (PG 2110+127), 1306<sup>7</sup> (PG 2118+126), and 1346<sup>7</sup> (PG 2148+095). For these observations, an additional systematic error was included to account for the approximate magnitude (in EW) of the fringing. This additional systematic error was added to the value of  $\sigma_W(C)$  listed in Table K.4 and ranged from 0.3–0.7 Å.

##### 4.6.5.2 The Blue Bump

The next anomaly I will mention is more a curiosity rather than a true problem. In a significant number of my GoldCam blue spectra, there was a noticeable “bump” just blueward of Na I D. I cannot explain the presence of this bump, other than to assume it was a feature of the spectrograph. In most spectra shown in Figures 4.6 to 4.19, this bump was normalized out. There are a few cases however, where it still shows prominently (for example, #95, PG 0110+262, and #912, PG 1524+611, in Figure 4.9). Since this “bump” did not directly affect any lines (other than to be near Na I D and

---

<sup>7</sup>Also has repeat observations on other runs.

He I 5875), I have not worried about its origin or effects (other than cosmetic) on the spectra.

#### 4.6.5.3 Telluric Water Vapor

The final annoyance I will mention is telluric water vapor. In the red spectra plotted in Figures 4.6 to 4.19, I removed the regions of strong telluric water vapor (and oxygen) absorption leaving gaps. There is also a weaker band of water vapor just redward of Na I D ( $\sim 5875\text{--}6000$ ) which shows up in some of my blue spectra (particularly those taken during less desirable weather conditions). This water vapor band primarily affects the single hot subdwarfs (in my sample, these tend to be brighter, and I observed them under poorer weather conditions). There are seven cases where this water vapor band showed strongly (six are single-colored systems). In these cases, the water vapor band has been marked above the spectra in Figures 4.6 to 4.8.

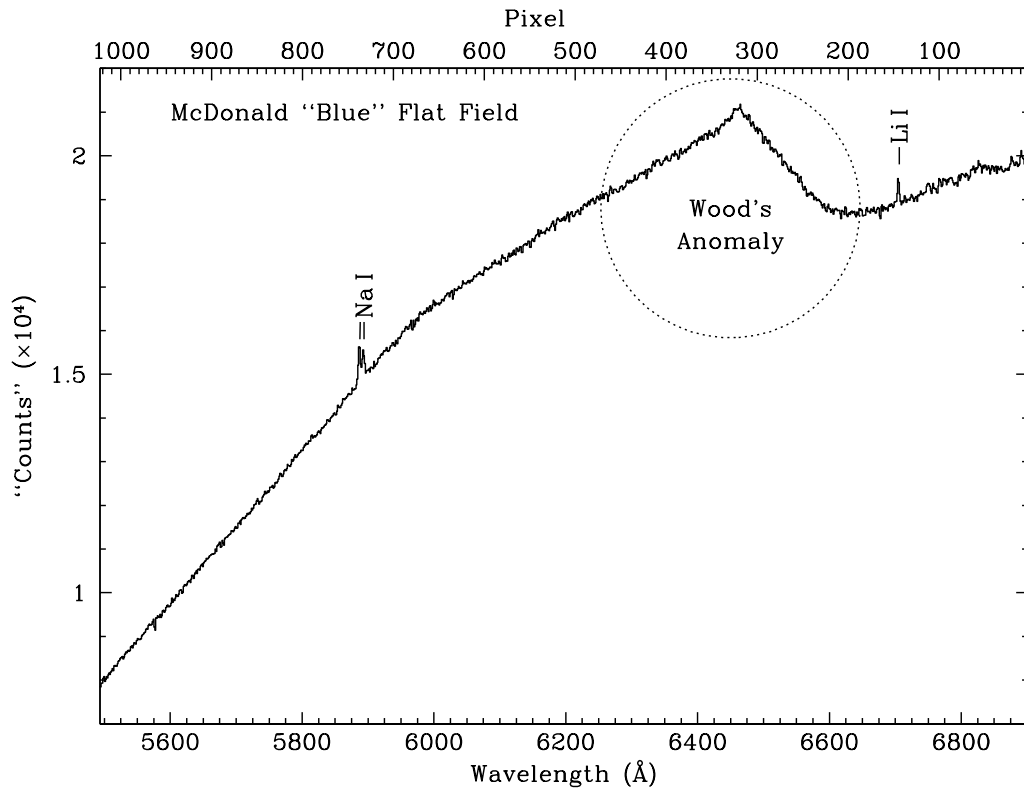


Fig. 4.1 Extracted flat field from the “blue” setting of the McDonald LCS showing the Na I and Li I emission lines (marked with ticks and labels), and the Wood’s Anomaly (roughly circled with a dotted line). The pixel coordinates are given across the top, while the wavelength scale (in  $\text{\AA}$ ) is given across the bottom. The exact location of the peak in the Wood’s Anomaly depended on grating tilt and shifted slightly in both pixel number and wavelength from run to run.

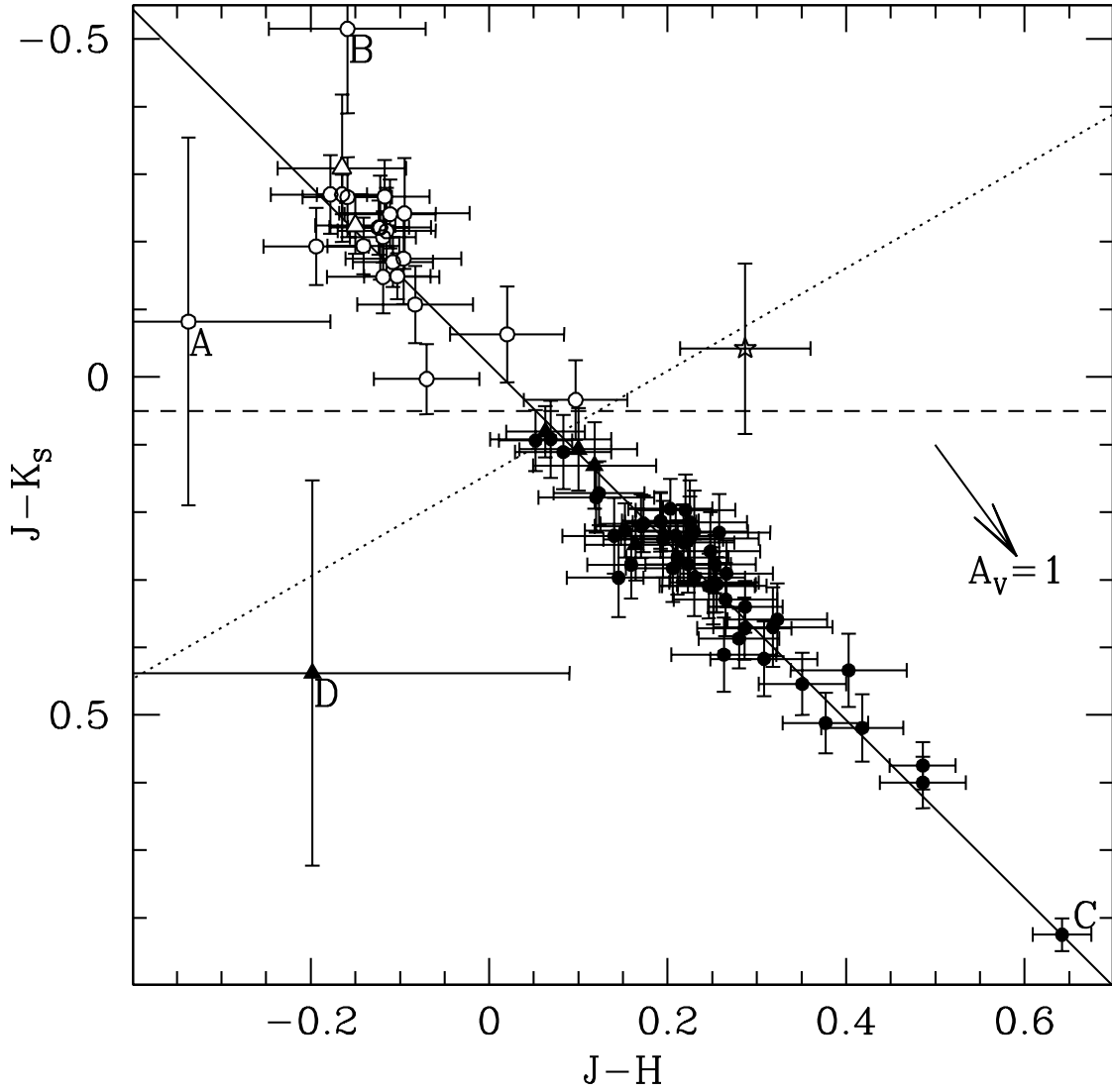


Fig. 4.2 The 2MASS Color-Color Plot of hot subdwarfs observed spectroscopically (the stars are listed in Table 4.2). Solid symbols are composite-colored hot subdwarfs and the open symbols are single-colored hot subdwarfs. Circles are for stars classified sdB, and triangles for sdO. The starred point represents the resolved companion of #550 HZ 18 (see §4.6.3 and the notes to Table 4.2). In this plot, the solid line is a best-fit to the distribution of all hot subdwarfs, the dotted line is the perpendicular indicating  $Q = +0.15$  (see §3.6.2), and the dashed line indicates  $J - K_S = +0.05$ . (Compare this figure with Figure 3.10, which shows all hot subdwarfs found in 2MASS.) Labelled objects are as follows: A = #50A PG 0027+222, B = #1158 PG 1716+426, C = #1223 HD 185510, and D = #1304 PG 2116+008.

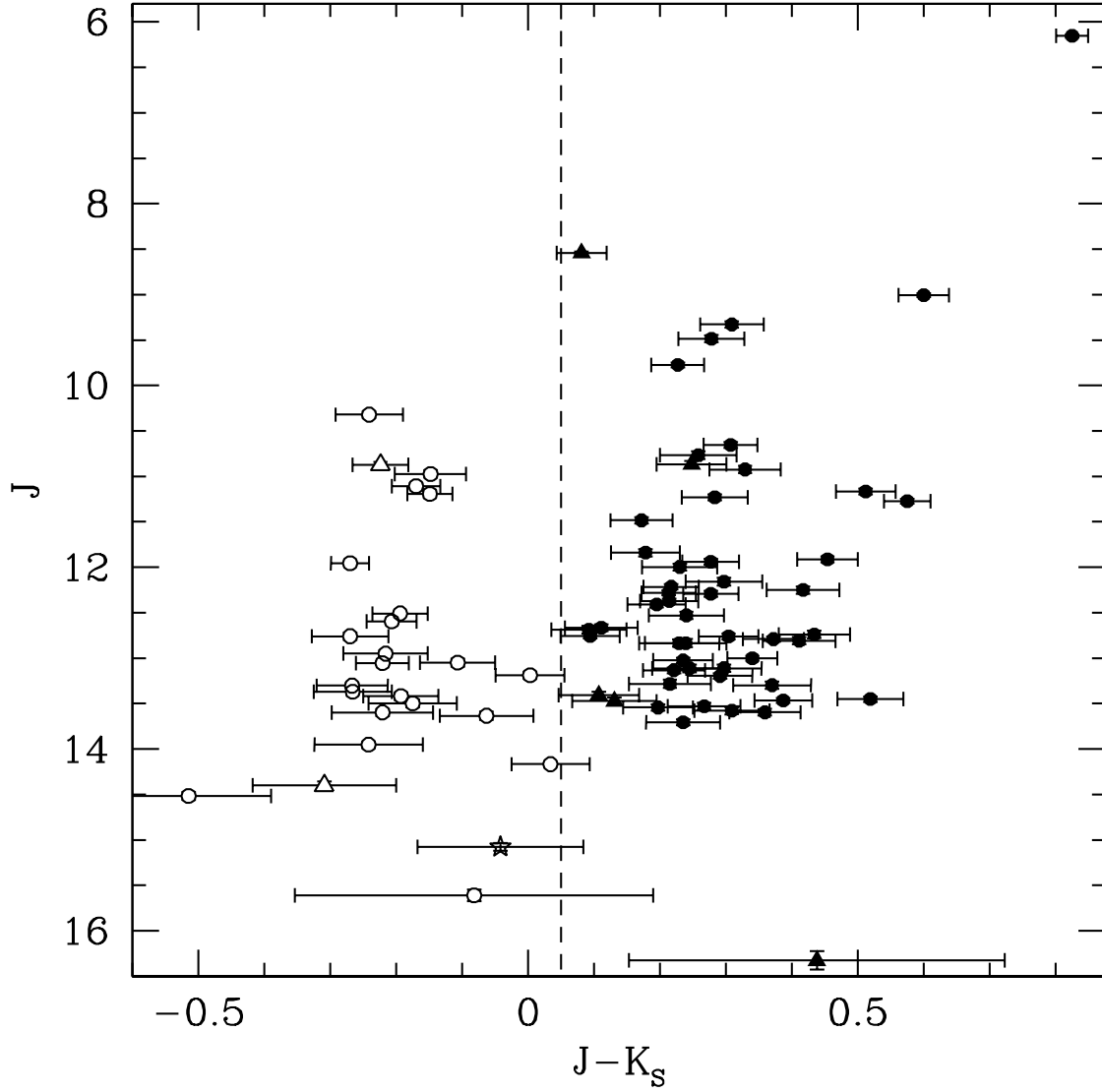


Fig. 4.3 The 2MASS CMD of hot subdwarfs observed spectroscopically (also listed in Table 4.2 and shown in Figure 4.2). Solid symbols are composite-colored hot subdwarfs and the open symbols are single-colored hot subdwarfs. Circles denote sdB stars, and triangles denote sdO stars. Note that in most cases the error bar on the  $J$  magnitude is smaller than the point size. The starred point represents the resolved companion of #550 HZ 18 (see §4.6.3 and the notes to Table 4.2). In this plot, the dashed line indicates  $J - K_S = +0.05$ .



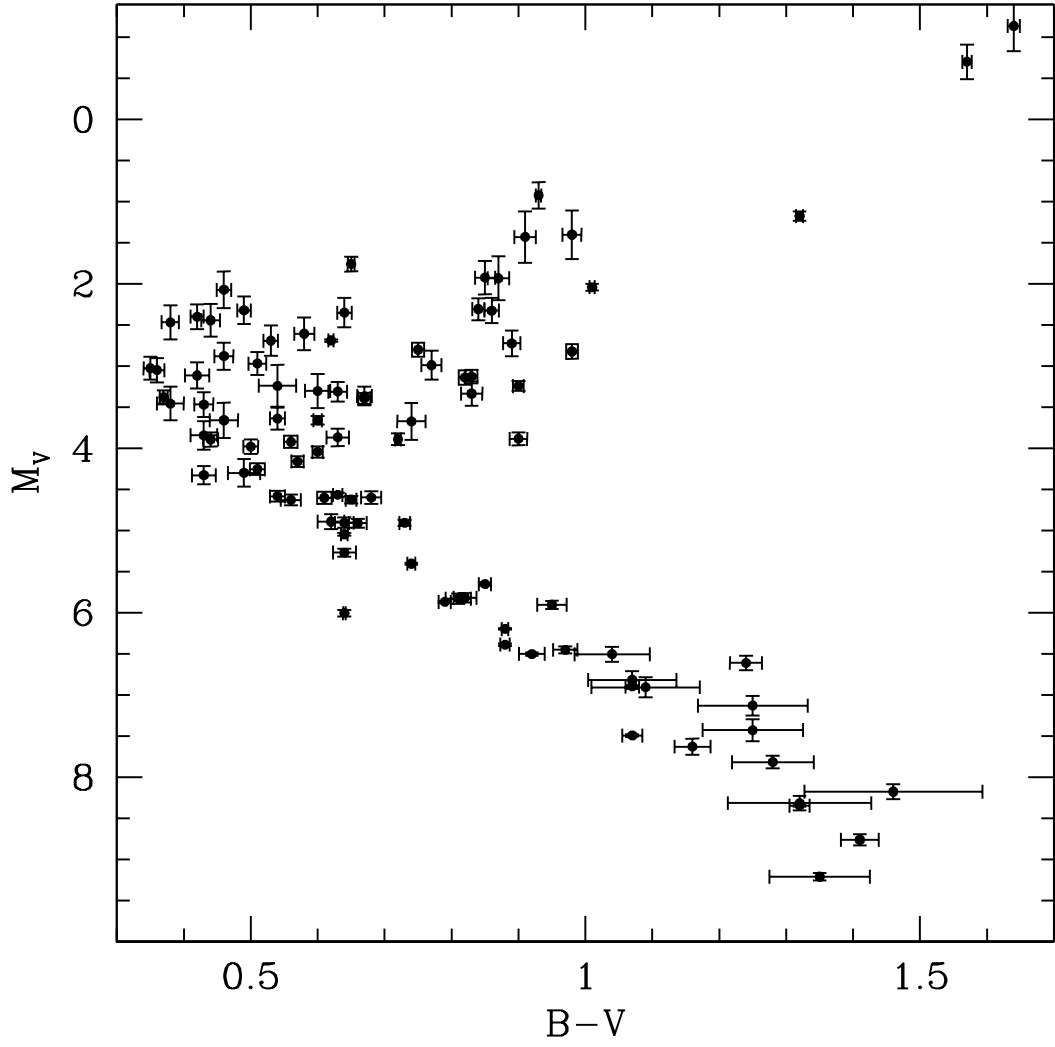


Fig. 4.4 CMD of the HIP stars used as standards and listed in Table 4.5. The appearance of this CMD closely resembles that of Sandage, Lubin, & Vandenberg (2003) for the Galactic disk (including the deficit of subgiants with  $B-V > 1.0$ ).

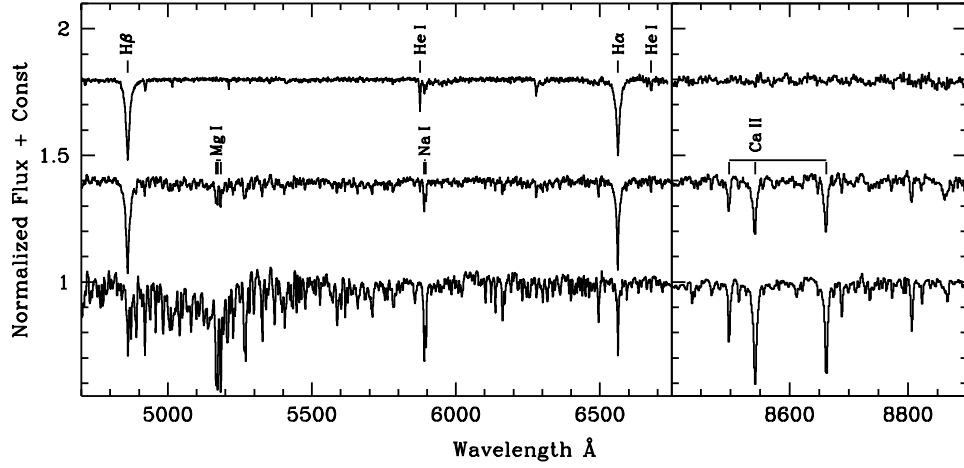


Fig. 4.5 Normalized spectra for a “typical” single hot subdwarf (top, #1263 LS IV+00°21), a composite hot subdwarf (middle, #59 PB 6107), and a single HIP standard star (bottom, HIP 13081). Left panel shows the “blue” region from  $H\beta$  to  $H\alpha$ , right panel shows the CaT from the “red” setting. Prominent spectral lines are labelled.

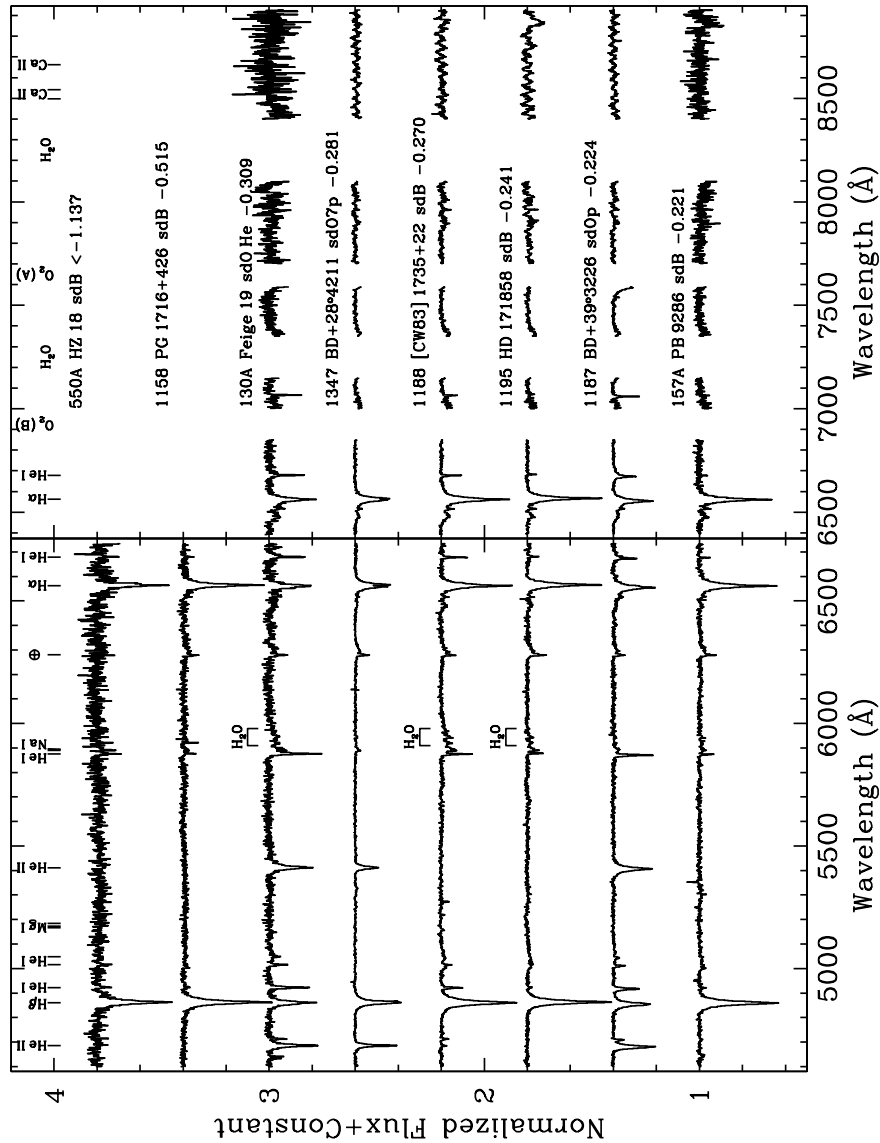


Fig. 4.6 Normalized spectra for all hot subdwarfs, ordered by increasing  $J - K'_S$  color. For each spectrum the normalized flux runs from zero to one, and vertical offsets of +0.4 have been applied to adjacent spectra. The left panel shows the “blue” spectral region for an object, the right panel shows the “red” spectral region for the same object. Above each spectrum is a label corresponding to the ID#, object name, KHD classification, and  $J - K'_S$  color (as: “NNNN Name type  $\pm$ N.NNN”). Prominent spectral features are marked at the top of each panel. In the left panel, telluric  $\text{H}_2\text{O}$  and a strong Diffuse Interstellar Band (DIB) are marked above an individual spectrum if visible. In the right panel, gaps in the spectra mark regions of strong telluric absorption which were removed for clarity in the plot. Spectra were taken at KPNO unless noted in the figure caption.



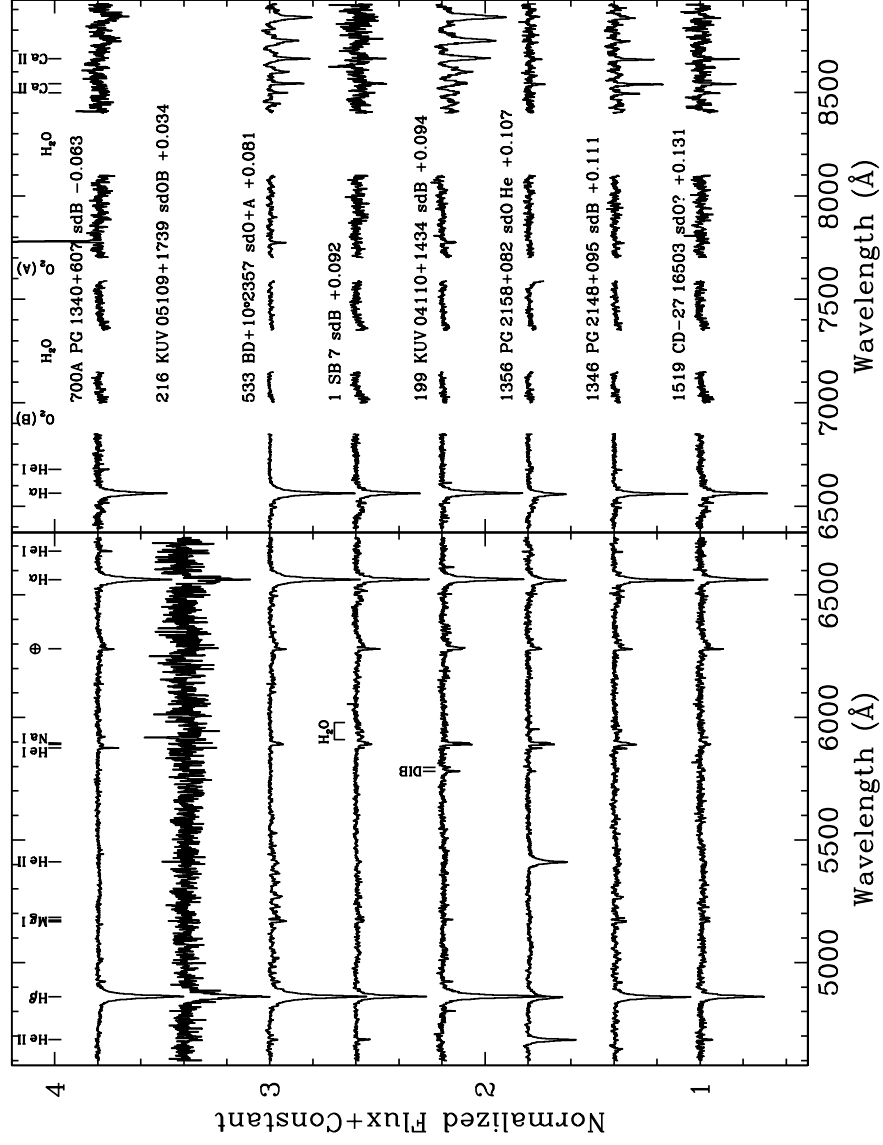


Fig. 4.8 Same as Figure 4.6.





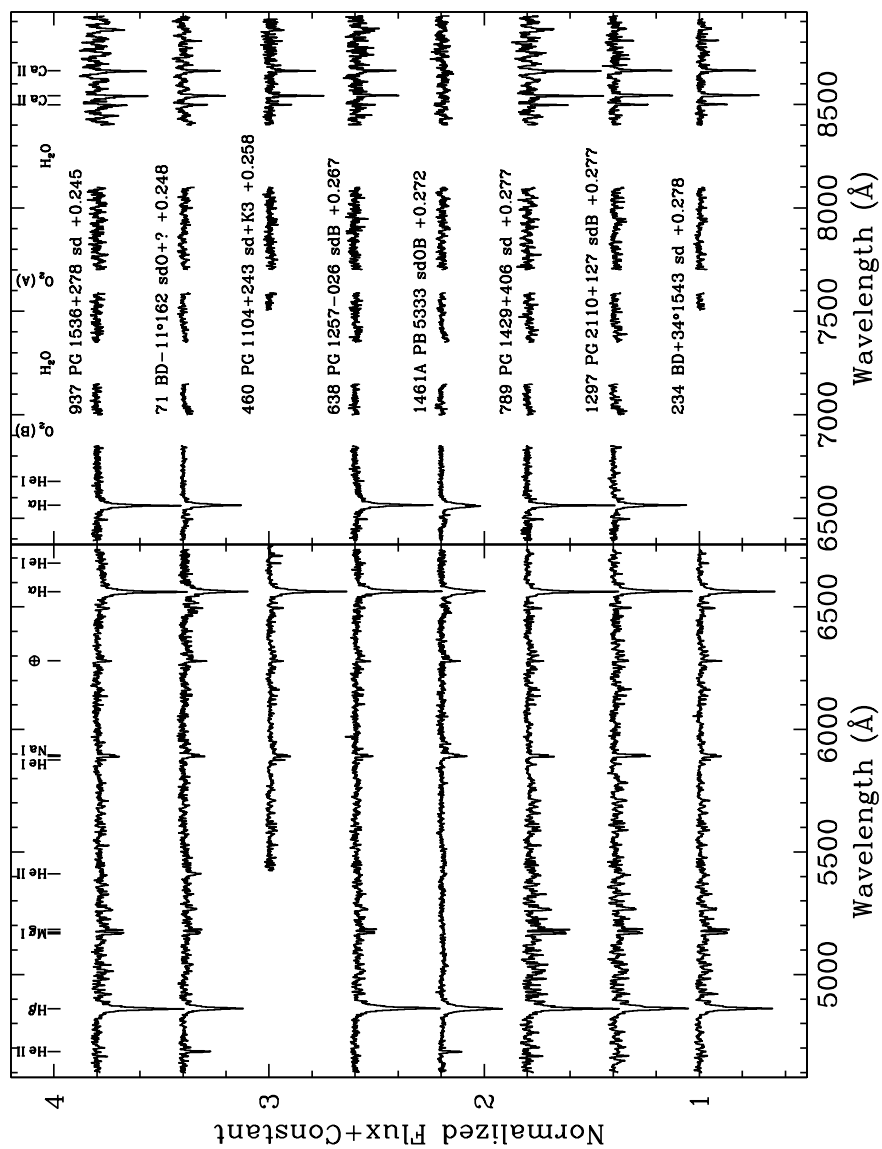


Fig. 4.11 Same as Figure 4.6. Both of the spectra for #460 PG 1104+243 and the red spectrum for #234 BD+34° 1543 were taken at McDonald (no spectra were taken at KPNO for those regions).



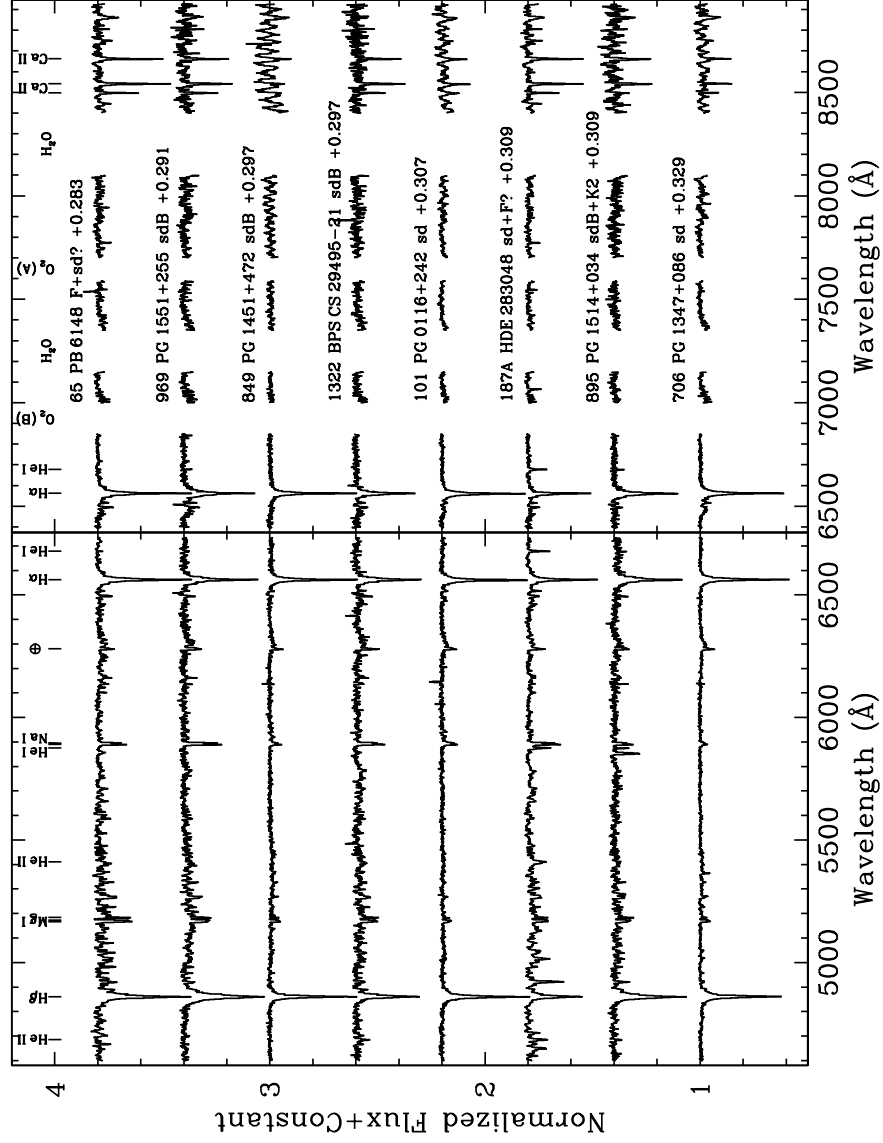


Fig. 4.12 Same as Figure 4.6.



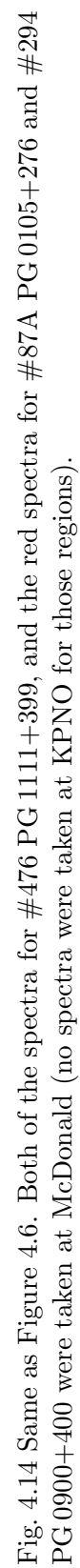


Fig. 4.15 Observed spectra of both members of resolved visual doubles. Notation and layout are the same as in Figure 4.6, except the spectra of both members of visual doubles are plotted one after the other, and are ordered by the sequence number of the subdwarf. For each spectra the normalized flux runs from zero to one, and vertical offsets of  $+0.5$  have been applied to adjacent spectra. Finding charts for the visual doubles are in Figures 4.20–4.22. The red spectra for both components of #87 PG0105+276 were taken at McDonald (no red spectra were taken at KPNO for these objects). The two stars of #91 PB8555 are extremely close (see Figure 4.20), so the spectra presented here are contaminated by light from the other star.

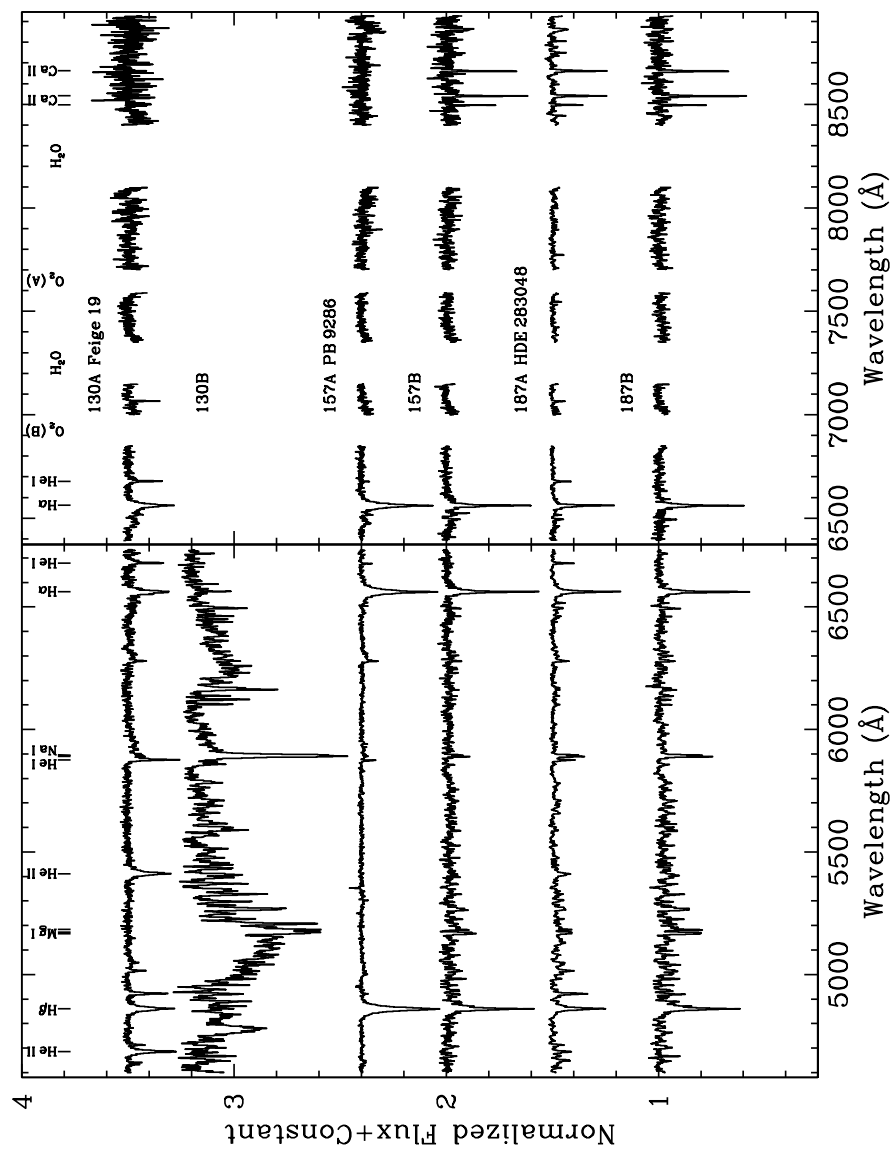


Fig. 4.16 Same as Figure 4.15.

Fig. 4.17 Same as Figure 4.15. The two stars of #1027 PG 1618+562 are extremely close (see Figure 4.22), so the spectra presented here are each contaminated by light from the other star.

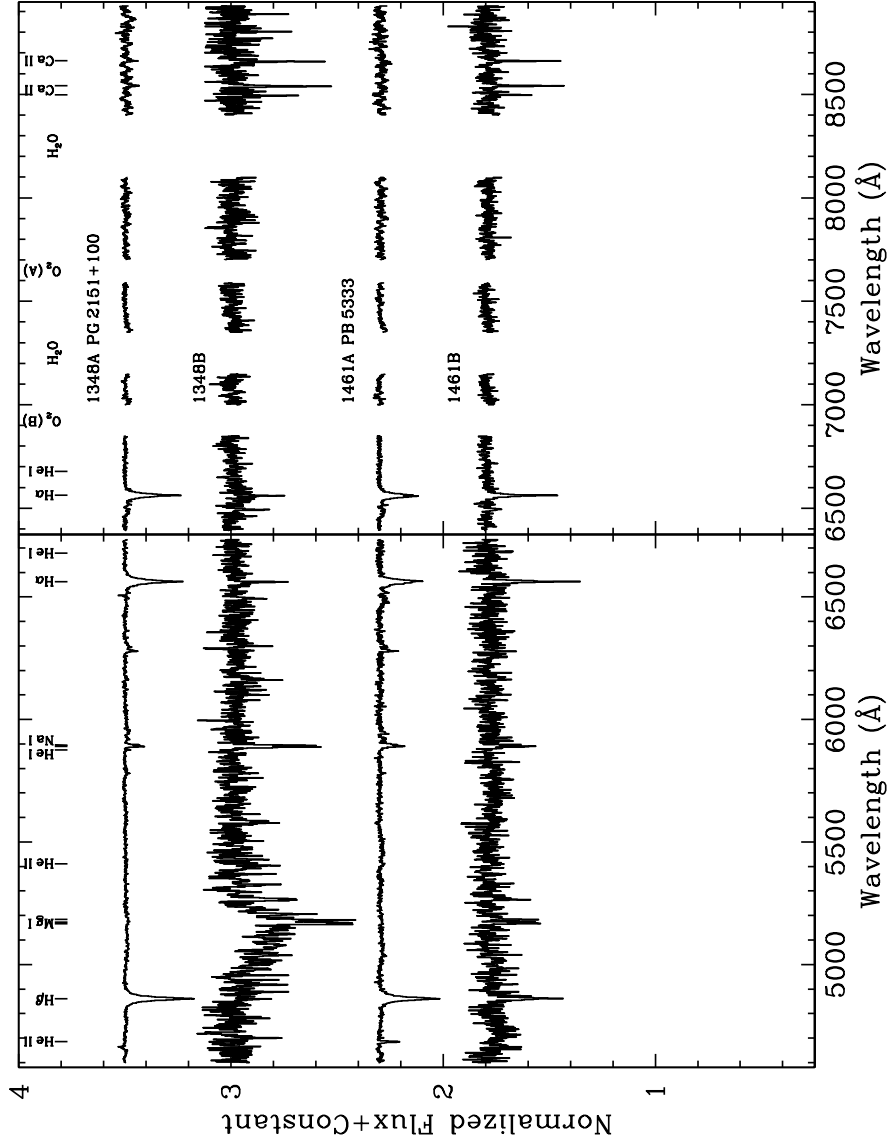


Fig. 4.18 Same as Figure 4.15. Component A of #1348 PG 2151+100 is actually two stars blended together, but they are resolved in 2MASS: the West star is the subdwarf, and the East star is a very faint companion (see also Figure 4.22, the notes for Table 4.2, and §4.6.3).

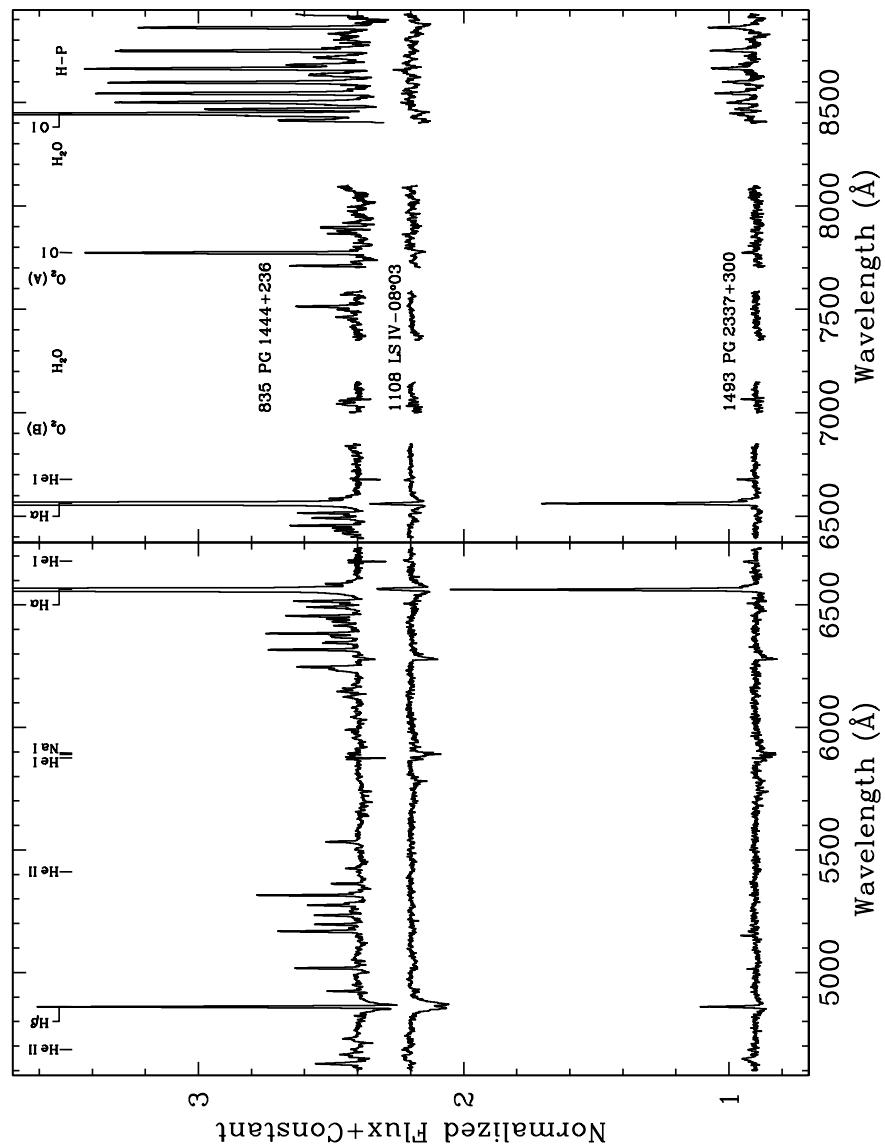


Fig. 4.19 Observed spectra of strong emission lined objects. Layout and labelling are the same as Figure 4.6, except the spectra are ordered by the sequence number of the object. For each spectra the normalized flux runs from zero to one, vertical offsets of  $-0.1$ ,  $+1.2$ , and  $+1.4$  have been applied to #1493, 1108, and 835 respectively. The strongest emission lines of #835 PG 1444+236 have been decapitated so the weak features in the other two stars can be seen.



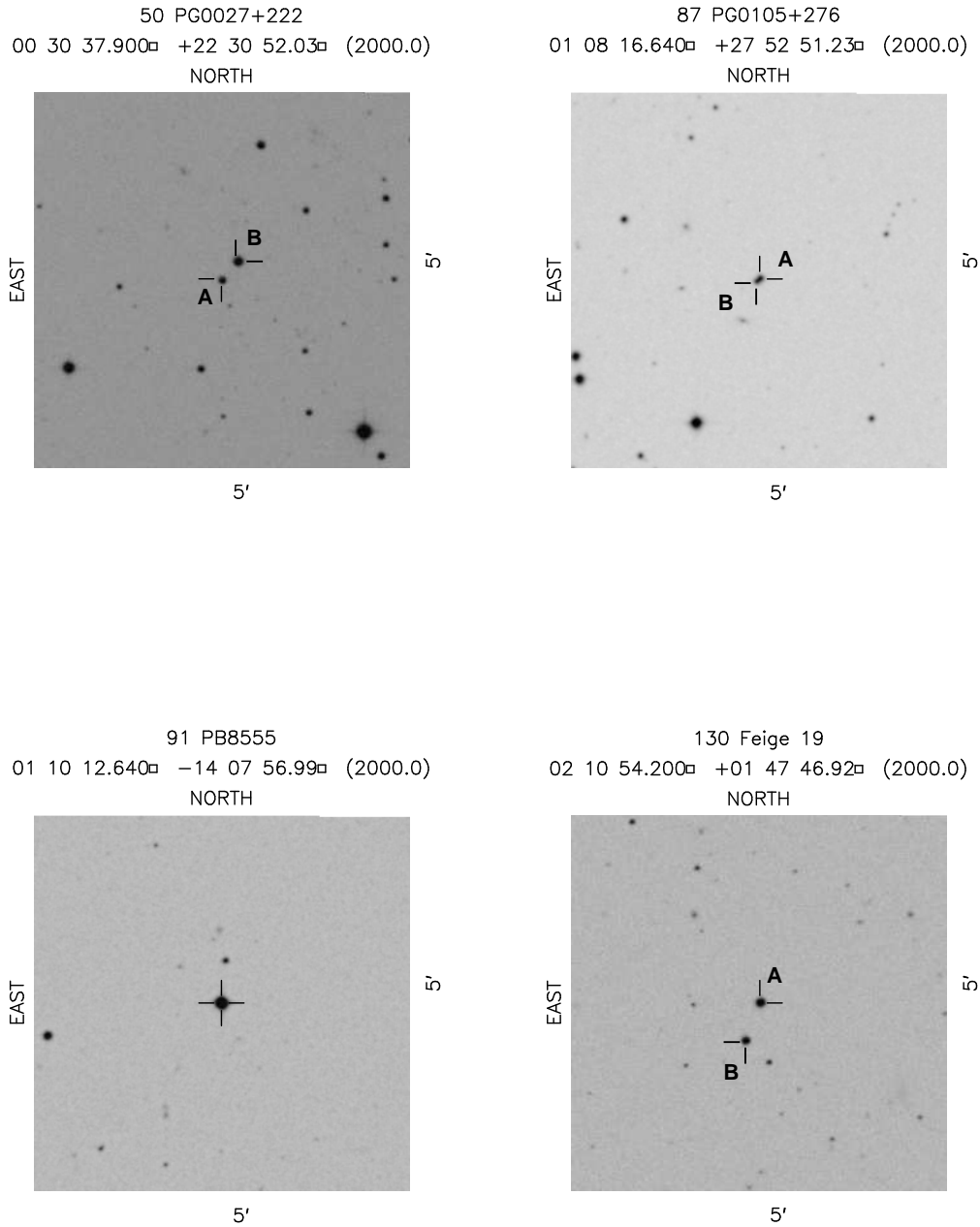


Fig. 4.20 Finding charts for the visual double subdwarfs listed in Table 4.2 for which separate spectra were obtained for both objects (see Figures 4.15–4.18). For each image, the sequence number, name, and coordinates are given above the image. If the two stars are resolved (or nearly resolved) in the DSS2-red images, then both are marked and the subdwarf is labelled “A”, while the companion is labelled “B”. If the two stars are not resolved in the DSS2-red images (namely star #91, in which the sd=NE\*, companion=SW\*), then the blended “single” object is marked.

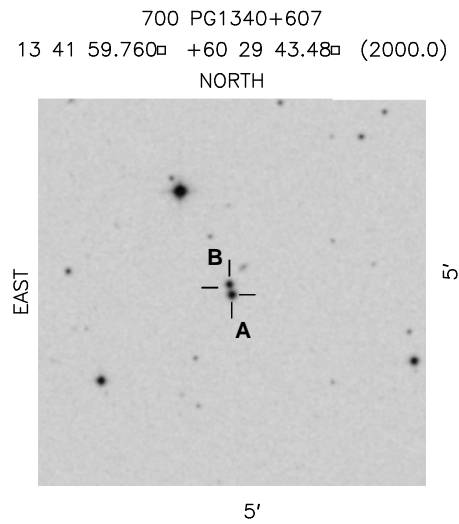
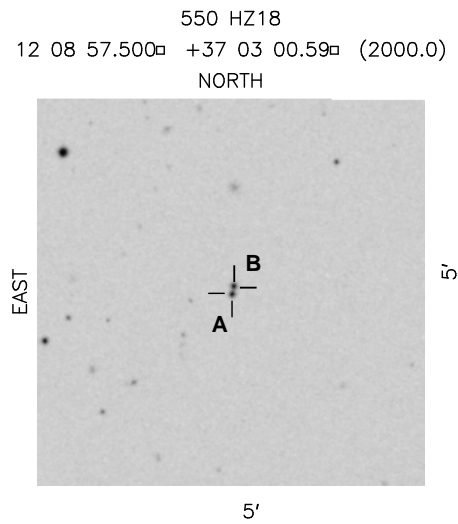
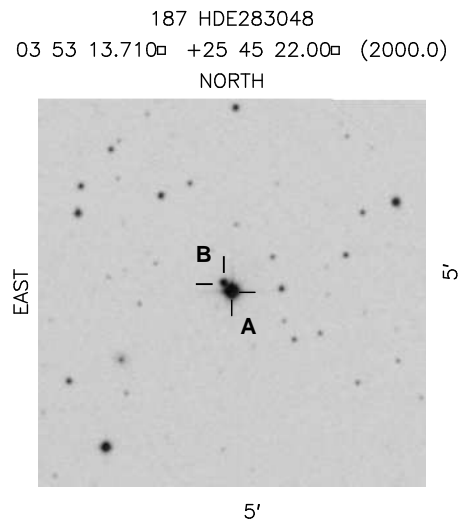
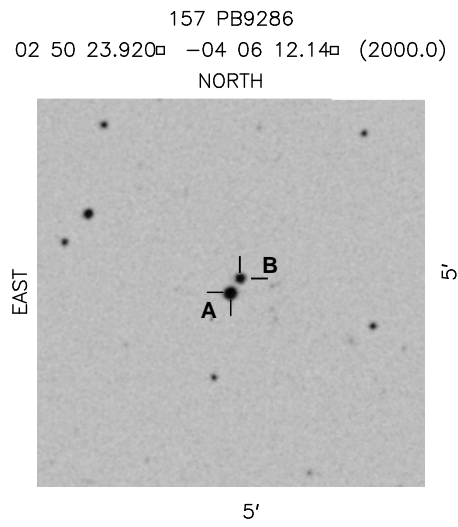


Fig. 4.21 Same as Figure 4.20.

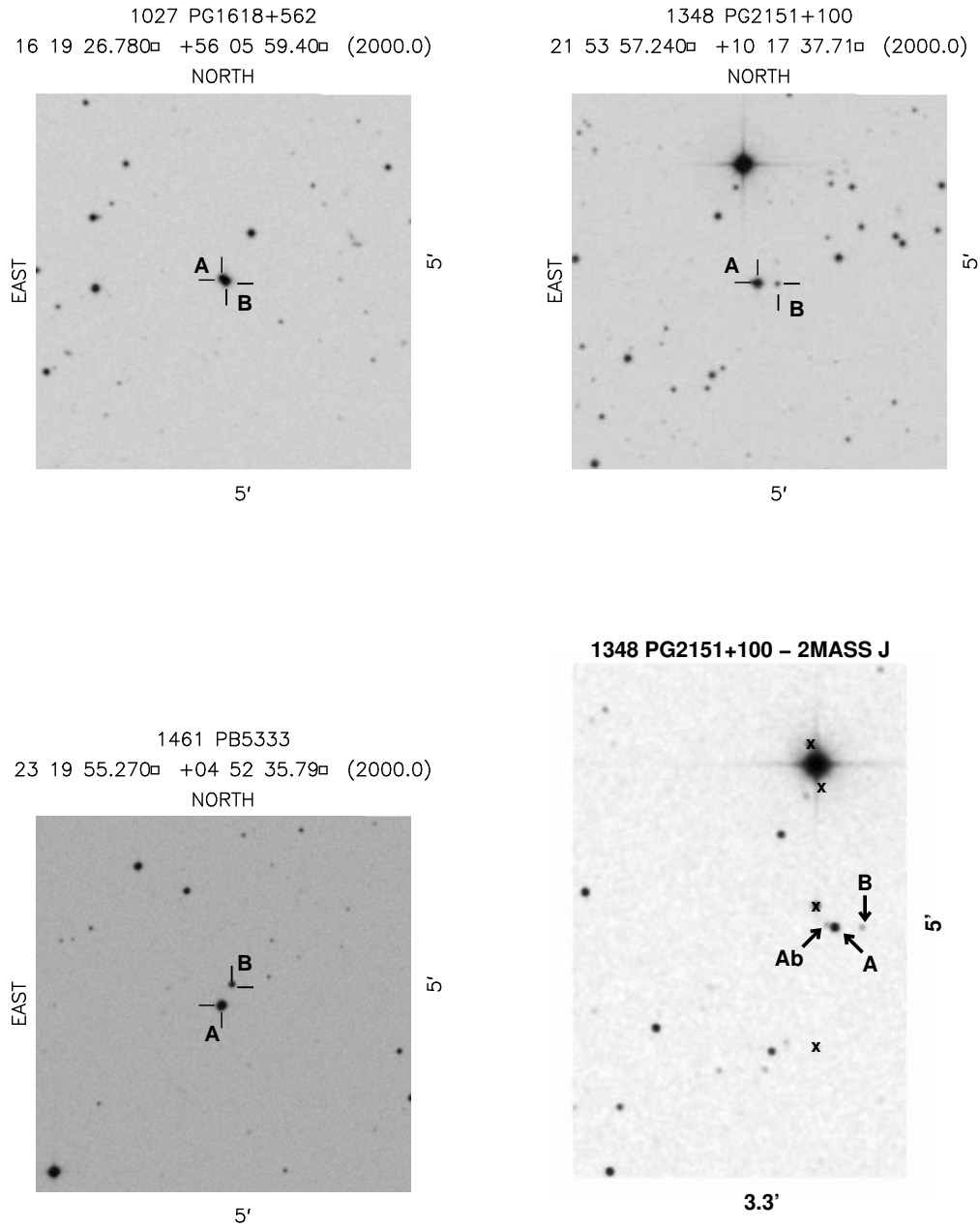


Fig. 4.22 Same as Figure 4.20. However, in the bottom right has been added the 2MASS *J*-band image of #1348 PG 2151+100 (shown at the top right). In the 2MASS image the hot subdwarf is labelled “A”, the companion observed spectroscopically is labelled “B”, and the faint close companion to the hot subdwarf (discussed in §4.6.3) is labelled “Ab”. Some persistent artifacts in the 2MASS image have been marked with crosses (“x”).

Table 4.1. Summary of Observing Runs.

Dates	Telescope	Instrument	Objects Observed <sup>a</sup>		Weather	Features Covered <sup>c</sup>
			Comp. <sup>b</sup>	Sing.		
Mar 9–11, 2002	McD. 2.7m	LCS	12	5	☺	CaT, H $\alpha$ , Na
Jun 14–17, 2002	McD. 2.7m	LCS	9	3	☺	CaT, H $\alpha$ , Na
Jun 28–Jul 1, 2002	KPNO 2.1m	GoldCam	7	1	☺	CaT, H $\alpha$ , Na, Mg, H $\beta$
Oct 11–15, 2002	KPNO 2.1m	GoldCam	10	2	☺	CaT, H $\alpha$ , Na, Mg, H $\beta$
Nov 7–10, 2002	McD. 2.7m	LCS	5	4	☺	CaT, H $\alpha$ , Na
Jun 8–13, 2003 <sup>d</sup>	KPNO 2.1m	GoldCam	21	4	☺	CaT, H $\alpha$ , Na, Mg, H $\beta$
Sep 12–18, 2003 <sup>d</sup>	KPNO 2.1m	GoldCam	26	6	☺	CaT, H $\alpha$ , Na, Mg, H $\beta$
Total Number of Unique Objects:			61	21		96

<sup>a</sup>Number of composite (“Comp.”) and single (“Sing.”) colored hot subdwarfs observed during the run (some objects were observed repeatedly). “Stand.” is the number of spectral classification standards observed.

<sup>b</sup>“Composites” includes objects with emission lines, and those in resolved visual doubles (each visual double counts as one observation).

<sup>c</sup>CaT = Ca II IR Triplet (CaT), Na = Na I D, Mg = Mg I b.

<sup>d</sup>Hot subdwarf targets for these runs were selected based on the 2MASS All-Sky Data Release, all other runs were based on the 2MASS Second Incremental Data Release.

Table 4.2: Observing list for sdBs ordered by RA.

ID# <sup>1</sup>	Name	RA (J2000)	Dec	V/y	J	J - K <sub>S</sub>	Type	Obs. Year <sup>3</sup>	Red UT <sup>4</sup> Date	Blue UT <sup>4</sup> Date	Notes <sup>2</sup>
<b>Composite-Colored Hot Subdwarfs (<math>J - K_S \gtrsim +0.05</math>)</b>											
1525	BPCS 22957-23	00 01 32.285	-05 19 16.76	13.7	B	12.740	+0.434 sdB	2002B	Oct 12	Oct 15	
1	SB 7	00 03 24.371	-16 21 06.34	12.67	y	12.688	+0.092 sdB	2002B	Oct 14	Oct 15,16	
59	PB 6107	00 42 06.085	+05 09 24.37	12.881		12.530	+0.240 sdB	2003B	Sep 13	Sep 18	
65	PB 6148	00 45 21.431	+07 06 12.02	12.00	P	11.232	+0.283 F+sd?	2003B	Sep 15	Sep 18	
71	BD-11°162	00 52 15.07	-10 39 46.0	11.23		10.868	+0.248 sdO+?	2002B	Oct 12	Oct 15	NW*
87A	PG 0105+276	01 08 16.645	+27 52 51.23	14.448		14.323	+0.576 sdO(B)	2002B	...	Oct 16	
								2002-3	Nov 8	...	
91A	PB 8555	01 10 12.640	-14 07 56.99	13.00	P	11.556	+0.368 sd+F?	2002B	Oct 12	Oct 15	NE* <sup>a</sup>
95	PG 0110+262	01 13 14.875	+26 27 31.15	12.903		12.410	+0.195 sdB-O	2002B	Oct 12	Oct 15	
101	PG 0116+242	01 19 29.015	+24 25 35.79	11.88	y	10.654	+0.307 sd	2002B	Oct 12	Oct 16	
102	PB 8783	01 23 43.223	-05 05 45.28	12.50	P	11.840	+0.178 sdB?HB	2002B	Oct 14	Oct 15	
120	PHL 3802	01 48 43.923	-26 36 12.18	12.35	y	11.997	+0.230 sdB	2002B	Oct 14	Oct 16	
150	PG 0232+095	02 35 11.957	+09 45 37.73	12.61	y	11.167	+0.512 sd	2003B	Sep 13	Sep 17	
172	PG 0314+103	03 17 42.240	+10 30 55.27	13.30	y	12.251	+0.417 sdB	2003B	Sep 13	Sep 17	
187A	HDE 283048	03 53 13.71	+25 45 22.0	10.30	P	9.329	+0.309 sd+F?	2003B	Sep 13	Sep 19	SW*
199	KUV 04110+1434	04 13 49.517	+14 41 26.07	13.91		12.756	+0.094 sdB	2003B	Sep 14	Sep 18	
203	KUV 04237+1649	04 26 34.530	+16 55 27.43	13.90		12.791	+0.372 sdOB	2003B	Sep 14	Sep 19	
234	BD+34°1543	07 10 07.68	+34 24 54.3	10.184		9.485	+0.278 sd	2002B	...	Oct 16	
								2002-1	Mar 9,10	Mar 11	
294	PG 0900+400	09 03 19.450	+39 51 00.43	12.87		11.912	+0.454 sdB+K3	2002-3	Nov 8	...	
								2002B	...	Oct 16	
								2002-1	Mar 10	Mar 11,12	
460	PG 1104+243	11 07 26.224	+24 03 11.17	11.295		10.768	+0.258 sd+K3	2002-3	Nov 9	...	
476	PG 1111+339	11 14 36.505	+33 40 26.97	13.01		11.272	+0.575 sd	2002-1	Mar 9	Mar 11	
533	BD+10°2357	11 55 56.65	+09 50 49.1	8.70		8.542	+0.081 sdO+A	2002-2	Jun 16	Jun 17	
								2003A	Jun 11	Jun 12	

Continued on Next Page...

Table 4.2 – Continued

ID# <sup>1</sup>	Name	RA (J2000)	Dec	V/y	J	J−K <sub>s</sub>	Type	Obs. Year <sup>3</sup>	Red UT <sup>4</sup> Date	Blue UT <sup>4</sup> Date	Notes <sup>2</sup>
551	PB 3854	12 09 16.783	+16 11 56.01	13.75	13.466	+0.387	sdB+?	2003A	Jun 11	Jun 12	
583	LB 2392	12 34 50.867	+49 47 20.94	13.98	13.706	+0.235	sd	2002-1	Mar 10	Mar 12	
630	TON 139	12 56 04.932	+28 07 19.69	12.76	12.215	+0.217	sdB	2003A	Jun 11	Jun 12	
638	PG 1257−026	13 00 13.827	−02 49 52.28	13.96	13.530	+0.267	sdB	2003A	Jun 11	Jun 14	
697	Feige 87	13 40 14.581	+60 52 50.36	11.693	11.484	+0.172	sdB	2003A	Jun 10	Jun 12	
702	PG 1343+578	13 45 01.440	+57 30 13.09	13.78	13.543	+0.197	...	2002A	Jun 29	Jul 01	
706	PG 1347+086	13 50 15.794	+08 19 22.63	11.86	10.924	+0.329	sd	2003A	Jun 09	Jun 14	
789	PG 1429+406	14 31 11.177	+40 22 09.99	12.86	11.941	+0.277	sd	2003A	Jun 10	Jun 12	
835	PG 1444+236	14 47 08.183	+23 21 37.99	13.14	13.269	+0.190	sd	2003A	Jun 10	Jun 13,14	em
844	PG 1449+653	14 50 36.230	+65 05 51.38	13.611	13.283	+0.215	sdB	2003A	Jun 10	Jun 12	
849	PG 1451+472	14 53 13.967	+47 02 46.94	13.12	12.158	+0.297	sdB	2003A	Jun 11	Jun 12	d
895	PG 1514+034	15 17 14.258	+03 10 28.29	13.997	13.579	+0.309	sdB+K2	2003A	Jun 10	Jun 13	
912	PG 1524+611	15 25 13.443	+60 53 23.57	12.80	12.283	+0.213	sdB-O	2002A	Jun 30	Jul 02	
937	PG 1536+278	15 38 07.405	+27 41 43.59	13.83	13.112	+0.245	sd	2003A	Jun 11	Jun 12	
969	PG 1551+255	15 53 21.715	+25 24 13.12	13.76	13.196	+0.291	sdB	2003A	Jun 10	...	
1010	PG 1610+519	16 12 00.577	+51 49 44.21	13.726	13.596	+0.359	sdOB	2003B	Sep 15,16	Sep 17	
1027A	PG 1618+562	16 19 26.777	+56 05 59.40	12.55	y	>+0.171	sdOB	2002A	Jun 29	Jul 01	NE* <sup>a</sup>
1051	PG 1629+081	16 32 01.316	+07 59 39.91	12.764	12.836	+0.239	sdB-O	2003B	Sep 16	Sep 18	
1092	TON 264	16 49 08.969	+25 10 05.98	14.074	13.451	+0.519	sdB+?	2002A	Jun 30	...	
1096	PG 1648+080	16 51 10.106	+08 03 32.98	13.94	12.808	+0.411	sd	2003A	Jun 11	Jun 12	b
1108	LS IV −08°03	16 56 29.684	−08 34 39.03	11.51	y		sdB	2003B	Sep 15	Sep 19	low SN
1133	PG 1701+359	17 03 21.671	+35 48 48.45	13.226	13.133	+0.221	sdB	2003A	Jun 10	Jun 13	
1164	PG 1718+519	17 19 45.407	+51 52 10.16	13.733	13.003	+0.340	sdB-O	2003B	Sep 14	Sep 17	
								2003A	Jun 09,11	Jun 14	em
								2003B	Sep 14,15	Sep 17,19	
								2003A	Jun 09,10	Jun 12,13	
								2003B	Sep 13	Sep 17	
								2002A	Jun 29	Jul 01	HST res
								2003B	Sep 13	Sep 17	

Continued on Next Page...

Table 4.2 – Continued

ID# <sup>1</sup>	Name	RA (J2000)	Dec	V/y	J	$J-K_S$	Type	Obs. Year <sup>3</sup>	Red UT <sup>4</sup> Date	Blue UT <sup>4</sup> Date	Notes <sup>2</sup>
1182	BD+29°3070	17 38 21.20	+29 08 47.1	10.42	9.773	+0.227	sdOB+F	2003A Jun 10	Jun 10	Jun 12	
								2003B Sep 13	Sep 13	Sep 19	
1223	HD 185510	19 39 38.80	−06 03 49.2	8.341	6.153	+0.825	sdB+ K0III-IV	2003A Jun 09,10	Jun 09,10	Jun 12	
								2003B Sep 13	Sep 13	Sep 19	
1297	PG 2110+127	21 13 21.049	+12 57 09.80	12.927	12.293	+0.277	sdB	2003A Jun 10	Jun 10	Jun 13	
								2003B Sep 13	Sep 13	Sep 17	
1304	PG 2116+008	21 19 21.381	+00 57 50.15	15.41	P 16.327	+0.438	sdO(B)	2003B Sep 15	Sep 15	Sep 19	faint
1306	PG 2118+126	21 21 02.291	+12 50 50.53	13.579	13.025	+0.235	sdB	2002A Jun 29	Jun 29	Jul 01	
								2003A Jun 11	Jun 11	Jun 13	
								2003B Sep 16	Sep 16	Sep 17	
1322	BPS CS 29495−21	21 32 55.435	−23 59 22.36	13.5	B 13.112	+0.297	sdB	2002B Oct 12	Oct 12	...	
								2003B Sep 13	Sep 13	Sep 17	
1346	PG 2148+095	21 51 16.877	+09 46 59.71	13.021	12.665	+0.111	sdB	2003A Jun 11	Jun 11	Jun 12	
								2003B Sep 14	Sep 14	Sep 17	
1348A	PG 2151+100	21 53 57.30	+10 17 34.9	12.75	y 12.835	+0.229	sd	2002A Jun 29	Jun 29	Jul 01	E <sup>*e</sup>
								2003B Sep 14	Sep 14	Sep 19	
1355	BD−3°5357	22 00 36.40	−02 44 26.8	9.31	7.351	+0.736	sdOB+G8III	2002A Jun 30	Jun 30	Jul 01	e.bin, em
1356	PG 2158+082	22 01 02.367	+08 30 49.66	12.66	P 13.407	+0.107	sdO He	2003B Sep 14	Sep 14	Sep 19	
1424	Balloon 090900007	22 53 18.439	+21 53 55.42	13.30	12.372	+0.214	sdB+G2	2003B Sep 13	Sep 13	...	
								2003B Sep 15	Sep 15	Sep 17	
1457	BD−7°5977	23 17 46.78	−06 28 31.0	10.52	y 9.006	+0.600	sdOB	2002B Oct 12	Oct 12	Oct 15	
1461A	PB 5333	23 19 55.34	+04 52 34.5	12.856	12.896	+0.272	sdOB	2002B Oct 12	Oct 12	Oct 15	SE*
								2003B Sep 16	Sep 16	...	
1493	PG 2337+300	23 40 04.327	+30 17 47.72	13.91	y 13.775	+0.128	sd	2003B Sep 14,15,16	Sep 14,15,16	Sep 17,19	em
1519	CD−27 16503	23 59 07.112	−26 38 40.23	13.49	y 13.474	+0.131	sdO?	2003B Sep 13	Sep 13	Sep 18	

Continued on Next Page...

Table 4.2 – Continued

ID# <sup>1</sup>	Name	RA (J2000)	Dec	V/y	J	$J-K_S$	Type	Obs. Year <sup>3</sup>	Red UT <sup>4</sup> Date	Blue UT <sup>4</sup> Date	Notes <sup>2</sup>
<b>Single-Colored Hot Subdwarfs (<math>J-K_S \lesssim +0.05</math>)</b>											
50A	PG 0027+222	00 30 37.99	+22 30 51.6	14.77	P	15.611	-0.082 sdB	2002B	Oct 14	Oct 16	SE*
130A	Feige 19	02 10 54.22	+01 47 47.1	13.709		14.401	-0.309 sdO He	2002B	Oct 14	Oct 15	NW*
157A	PB 9286	02 50 23.94	-04 06 13.9	12.50	P	13.597	-0.221 sdB	2003B	Sep 16	Sep 18, 19	SE*
216	KUV 05109+1739	05 13 49.733	+17 42 03.39	13.50	P	14.167	+0.034 sdOB	2002B	...	Oct 16	
550A	HZ 18	12 08 57.45	+37 02 57.8	15.15		16.178	<-1.137 sdB	2003A	...	Jun 13	S*
700A	PG 1340+607	13 41 59.77	+60 29 40.5	13.14	y	13.634	-0.063 sdB	2002A	Jun 29	Jul 01	S*
								2003A	...	Jun 14	
850	PG 1452+198	14 54 40.459	+19 36 53.03	12.48	y	13.276	-0.221 sdB	2003A	Jun 11	Jun 13	
1152	PG 1710+490	17 12 18.709	+48 58 36.07	12.90	y	13.419	-0.193 sdB	2003A	Jun 11	Jun 12	
1158	PG 1716+426	17 18 03.825	+42 34 13.63	13.97	y	14.518	-0.515 sdB	2003A	...	Jun 14	
1181	[CW83]1735+22	17 37 26.494	+22 08 57.68	11.80	B	12.509	-0.194 sdB	2003A	Jun 11	Jun 13	also LSE 161
1187	BD+39°3226	17 46 31.90	+39 19 09.1	10.21		10.873	-0.224 sdOp	2003B	Sep 16	Sep 17	
1188	[CW83]1758+36	18 00 18.974	+36 28 55.88	11.36		11.956	-0.270 sdB	2002A	Jun 30	Jul 02	
1194	BD+48°2721	18 34 09.116	+48 27 36.60	10.70		11.107	-0.170 sdB	2002A	Jun 29,30	Jul 01	
								2003B	Sep 14	Sep 18	
1195	HD 171858	18 37 56.68	-23 11 35.2	9.86	y	10.321	-0.241 sdB	2003B	Sep 14	Sep 17	
1263	LS IV+00°21	20 31 18.209	+01 05 26.44	12.44	y	12.950	-0.216 sdB	2003A	...	Jun 14	
1347	BD+28°4211	21 51 11.05	+28 51 50.9	10.53		11.275	-0.281 sdO7p	2003B	Sep 16	Sep 18	
								2003A	Jun 10,11	Jun 12,13,14 flux, em	
1357	PG 2159+051	22 01 58.655	+05 24 28.56	12.98	y	13.049	-0.107 sd	2003B	Sep 14,16	Sep 17,18,19	
								2002A	Jun 29	...	c
1459	PHL 457	23 19 24.483	-08 52 37.37	12.95	y	13.499	-0.175 sdB	2002B	Oct 12	Oct 15	
								2002B	Oct 14	Oct 16	
<b>Visual Double and Nearby Companions of Hot Subdwarfs</b>											
50B	(PG 0027+222)	00 30 37.07	+22 31 06.5	...		12.848	+0.394 ...	2002B	Oct 14	Oct 16	NW*

Continued on Next Page...



Table 4.2 – Continued

ID# <sup>1</sup>	Name	RA (J2000)	Dec	V/y	J	J−K <sub>S</sub>	Type	Obs. Year <sup>3</sup>	Red UT <sup>4</sup> Date	Blue UT <sup>4</sup> Date	Notes <sup>2</sup>
87B	(PG 0105+276)	01 08 16.645	+27 52 51.23	...	...	...	...	2002B ...	Oct 16	SE*	
								2002-3 Nov 8	...		
91B	(PB 8555)	01 10 12.640	−14 07 56.99	...	...	...	...	2002B Oct 12	Oct 15	SW* <sup>a</sup>	
130B	(Feige 19)	02 10 54.97	+01 47 16.1	...	12.872	+0.814	...	2002B ...	Oct 15	SE*	
157B	(PB 9286)	02 50 23.45	−04 06 02.5	...	13.844	+0.311	...	2003B Sep 16	Sep 18,19	NW*	
187B	(HDE 283048)	03 53 14.19	+25 45 28.6	...	12.755	+0.453	...	2003B Sep 13	Sep 19	NE*	
550B	(HZ 18)	12 08 57.35	+37 03 04.6	...	15.078	−0.042	...	2003A ...	Jun 13	N*	
700B	(PG 1340+607)	13 41 59.94	+60 29 48.7	...	12.868	+0.568	...	2002A Jun 29	Jul 01	N*	
								2003A ...	Jun 14		
1027B	(PG 1618+562)	16 19 26.777	+56 05 59.40	...	...	...	...	2002A Jun 30	...	SW* <sup>a</sup>	
1348B	(PG 2151+100)	21 53 56.23	+10 17 34.8	...	15.222	+0.606	...	2002A Jun 29	Jul 01	W* <sup>e</sup>	
								2003B Sep 14	Sep 19		
1348Ab	(PG 2151+100)	21 53 57.62	+10 17 36.2	...	15.363	+0.688	...	...	...	E* <sup>e</sup>	
1461B	(PB 5333)	23 19 54.76	+04 52 51.4	...	14.702	+0.295	...	2002B Oct 12	Oct 15	NW*	
								2003B Sep 16	...		

<sup>1</sup>An “A” or “B” following the ID number indicates that this star is part of a visual double. “A” is the hot subdwarf component and will be listed either under the “Composite Color” list or the “Single Color” list of hot subdwarfs. The “B” indicates the cooler component and is listed under “Visual Double and Nearby Companions”. At this time it is unclear whether these pairs are true common proper motion pairs, or line-of-sight doubles (however, the members of #1027 PG 1618+562 are probably a true binary, Silvotti et al. 2000). The spectrum of both stars in these systems was obtained when possible.

<sup>2</sup>*a* = Visual double barely resolved, individual spectra contaminated by light from the other star. *b* = Star #1051, PG 1629+081, was barely resolved in the KPNO 2m slit camera (however, the spectrum obtained with the KPNO 2m is a blend of both stars, it is also elongated in 2MASS); the components are: sd=NE\*, companion=SW\*. *c* = A close, faint companion can be seen to star #1357, PG 2159+051, in DSS images, however this companion was not seen in the slit view camera at the KPNO 2m (most likely because it was too faint in comparison to PG 2159+051 itself), *d* = The classification listed for star #849, PG 1451+472, in this table is the second classification from KHD, the first classification given in KHD is “???”. *e* = In 2MASS component A (the E\* of the wider visual double) of #1348 PG 2151+100 resolves into two stars: the W\*, “A”, is the subdwarf; and the E\*, “Ab”, is a faint companion (which was not visible at the telescope) — component B is to the west of the blended components of A (see Figure 4.22 and §4.6.3).

<sup>3</sup>Observing Semester/Trimester the observations were taken in: 2002A, 2002B, 2003A, 2003B = KPNO semesters; 2002-1, 2002-2, 2002-3 = McDonald trimesters (Note: McDonald observations are only listed if no KPNO observations are available, or if KPNO coverage was not complete).

<sup>4</sup>UT = Universal Time.

Table 4.3: Composite-Colored Hot Subdwarf Spectroscopic Sample  
Physical Parameters from Literature.

ID# <sup>1</sup>	Name	Class <sup>2</sup>	$E(B-V)^3$	$T_{\text{eff}} \text{ (kK)}^4$	$\log g$	Companion <sup>5</sup>	Other Notes <sup>6</sup>	Ref <sup>7</sup>
1	SB 7	sdB,	0.02319	$55 \pm 10$	...	$\approx 7000$	...	H86
59	PB 6107	sdB, sdB+K4	0.03287	26.7	5.9	5750(G2)	...	U98
					4.7	...	...	M90b
					...	K4	...	A94
65	PB 6148	late F + sdOB?		23	...	unresolved w/ HST	...	H02
71	BD-11°162	sdO+?, sdO+G?	0.03914	...	...	late F + sdOB?	...	B80
87A	PG 0105+276	sdO(B), sdB+K7	0.03648	35	5.9	F4-G0	...	U98
			0.05776	32	...	K7.5	...	A94
				$35.85 \pm 0.98$	$6.0 \pm 0.2$	$5450 \pm 200$	...	A01
91A	PB 8555	sd+F?	0.02330	32	...	HST res 3 comp	sdO	H02
95	PG 0110+262	sdB-O, sdB+K2	0.06657	...	...	F8-G1	...	U98
				22	...	K2.5	...	A94
				22	5.5	6000-5000(F9-K1)	...	T95
				21	5.9	5000(K1)	...	U98
				$21.05 \pm 0.575$	$6.0 \pm 0.2$	$5485 \pm 200$	...	A01
				$21.0 \pm 0.75$	$5.17 \pm 0.17$	$5250 \pm 800$	...	A02
101	PG 0116+242	sd	0.07410	14	...	G5-G6	...	U98
102	PB 8783	sdB?HB	0.03406	33	5.7	7000	pulsating	K97
120	PHL 3802	sdB, sdOB	0.01564	$30 \pm 0.3$	...	$\approx 5500$	...	H86
150	PG 0232+095	sd, sd+K	0.11208	25-50	...	comp?	...	M90
				18-30(21:)	$6.9 \pm 0.3$	4600-5000(K1-K6)	...	T95
				21	6.6	4750(K2)	...	U98
				$21.5 \pm 0.5$	$6.0 \pm 0.2$	$4575 \pm 50$	...	A01
172	PG 0314+103	sdB	0.53473	18	...	later than K6	...	U98
187A	HDE 283048	sd+F?	0.19801	40-80	$6.4 \pm 0.3$	4000-4600(K3-K8)	...	T95
199	KUV 04110+1434	sdB		40	6.2	7500(A8)	...	U98
203	KUV 04237+1649	sdOB	0.60795	...	...	...	no CaT	J98
			0.40769	...	...	...	...	...

Continued on Next Page...

Table 4.3 – Continued

ID# <sup>1</sup>	Name	Class <sup>2</sup>	$E(B-V)^3$	$T_{\text{eff}} \text{ (kK)}^4$	$\log g$	Companion <sup>5</sup>	Other Notes <sup>6</sup>	Ref <sup>7</sup>
234	BD+34°1543	sd, sdB+F	0.06884	25	5.9	6010 ± 70(F8-G0)	...	T95
				26	6.0	5500(G8)	...	U98
294	PG 0900+400	sdB+K3	0.02194	31	...	K3	...	F84
				...	5.9	K3V	...	O97
				25 ± 0.925	5.0 ± 0.2	5150 ± 130	...	A01
				28.6 ± 1.0	3.6 ± 0.1	5.84 ± 0.96	H-deficient, low $\log g$ , non-sd	J01
460	PG 1104+243	sd+K3	0.01484	28	...	K2	...	F84
				27.5	...	K3.5	...	A94
				...	5.2	G8V	...	O97
				...	...	4000–6000	CaT seen	J98
				28 ± 0.875	5.0 ± 0.2	5735 ± 150	...	A01
				32.85 ± 1.55	5.40 ± 0.12	6400 ± 1000	...	A02
476	PG 1111+339	sd	0.02514	...	...	...	...	...
533	BD+10°2357	sdO+A	0.02783	25–35	5.6	7300–7900(A8–A9)	...	T95
				27	5.9	5750(G2)	...	U98
551	PB 3854	sdB+?, sdB	0.03797	...	...	...	...	...
583	LB 2392	sd, sdB+K5	0.01688	28	6.1	K5	...	B91
				...	...	...	no CaT	J98
630	TON 139	sdB, sd	0.00925	18	...	4750(K2)	sd shows $\Delta V \rightarrow$ triple	U98
				20	...	HST res 2 comp	...	H02
638	PG 1257–026	sdB	0.03302	...	...	...	...	...
697	Feige 87	sdB, sd+K4	0.01857	23.5	...	K4.5	...	A94
				...	...	4000–6000	CaT seen	J98
702	PG 1343+578	...	0.00491	...	...	...	HBB	M90
706	PG 1347+086	sd	0.02533	...	...	...	...	...
789	PG 1429+406	sd	0.01167	...	...	...	...	...
835	PG 1444+236	sd	0.03210	...	...	...	Haro's Star, em	H92

Continued on Next Page...

Table 4.3 – Continued

88

ID# <sup>1</sup>	Name	Class <sup>2</sup>	$E(B-V)^3$	$T_{\text{eff}}$ (kK) <sup>4</sup>	log $g$	Companion <sup>5</sup>	Other Notes <sup>6</sup>	Ref <sup>7</sup>
844	PG 1449+653	sdB, sd+K4	0.01667	...	...	G-band	...	M90
			28	28	...	K4	...	A94
			...	...	...	...	no CaT	J98
			28.15 ± 9	5.5 ± 0.2	...	4700 ± 1475	...	A01
			28	...	...	unresolved w/ HST	...	H02
849	PG 1451+472	sdB v.cool	0.01863	...	...	...	...	...
895	PG 1514+034	sdB+K2, sdB+K4	0.03926	31	...	K2	...	F84
			...	...	5.0	G8V	...	O97
912	PG 1524+611	sdB-O	0.01770	...	...	...	...	...
937	PG 1536+278	sd	0.02897	...	...	...	...	...
969	PG 1551+255	sdB	0.06080	...	...	...	...	...
1010	PG 1610+519	sdOB, sdB	0.02589	32.5	...	K8	...	A94
1027A	PG 1618+562	sdOB, sdB	0.00410	33.9 ± 1.5	5.8 ± 0.2	vis bin F3	pulsating	S00
1051	PG 1629+081	sdB-O, sd+K7	0.07627	32.5	...	K7.5	...	A94
			26.4 ± 1.15	5.5 ± 0.2	...	3825 ± 575	...	A01
1092	TON 264	sdB+?, sdB, sdB?, sdOB bin, sd+K7	0.08290	36.5 ± 1.5	6.00	composite	...	T93
			28.5	...	...	K7	...	A94
			26	...	...	HST unusual PSF	...	H02
1096	PG 1648+080	sd	0.12005	...	...	...	...	...
1108	LS IV-08°03	sdB	0.46602	...	...	...	(em)	...
1133	PG 1701+359	sdB, sdB bin, sd+K6	0.02496	26.25 ± 1.25	5.8	composite	...	T93
			28.5	...	...	K6.5	...	A94
			30	5.0	...	composite	...	Th95
			31.4	> 5.50	...	composite	no $\Delta RV$	M01
			36.075 ± 0.7	6.0 ± 0.2	...	6450 ± 230	...	A01
			32.5 ± 1.325	5.75 ± 0.12	...	6000 ± 1000	...	A02

Continued on Next Page...

Table 4.3 – Continued

ID# <sup>1</sup>	Name	Class <sup>2</sup>	$E(B-V)^3$	$T_{\text{eff}} \text{ (kK)}^4$	$\log g$	Companion <sup>5</sup>	Other Notes <sup>6</sup>	Ref <sup>7</sup>
1164	PG 1718+519	sdB-O, sdB bin, sd+K3	0.02717	23.5 ± 1.0: 25	4.25: ...	composite K3.5	...	T93 A94
				30	5.0	composite	...	Th95
				29.95 ± 1.1	6.0 ± 0.2	5925 ± 70	...	A01
				29 ± 1.55	6.0 ± 0.14	5200 ± 400	...	A02
1182	BD+29°3070	sdOB+F, G+B	0.05255	18	...	HST res 2 comp	2 comp =RV (1 spect)	H02
				32.85 ± 2.75	6.0 ± 0.2	5250(K0)	...	U98
1223	HD 185510	sdB+K0III-IV	0.25653	~20–30	~6	K0III-IV	...	A01
1297	PG 2110+127	sdB, sdB bin, sd+K2	0.08117	25.4 ± 1.6:	4.20:	composite	(RSCVn type var)	F85
				26	...	K2.5	...	T93
				33.7	5.33	composite	...	A94
				30	5.0	composite	...	S94
				34	5.9	5750(G2)	...	Th95
				24.9 ± 6.5	7.0 ± 0.2	5500 ± 575	...	U98
				26.5 ± 1.7	5.2 ± 0.18	5400 ± 400	...	A01
1304	PG 2116+008	sdO(B) high g	0.08142	...	...	...	...	A02
1306	PG 2118+126	sdB, sd+K2	0.08945	26.5	...	K2	...	...
				25	6.0	5250(K0)	...	A94
1322	BPS CS 29495–21	sdB	0.04820	...	...	...	...	U98
1346	PG 2148+095	sdB, sd+K3	0.06337	26	...	K3.5	...	...
				25	5.8	5000(K1)	...	A94
				22.95 ± 0.825	6.0 ± 0.2	4375 ± 200	...	U98
				30 ± 0.86	4.9 ± 0.16	5700 ± 400	...	A01
				26	...	HST unusual PSF	...	A02
1348A	PG 2151+100	sd	0.06636	27	6.7	3500(M2)	...	H02
1355	BD –3°5357	sdOB+G8III	0.13662	35–40 40	...	4600	(em)	U98
				...	8.1	4500(K4)	...	M95
				...	...	G8III	...	U98
				...	...	K0IV-III	...	K88
				...	...	...	...	B93

Continued on Next Page...

Table 4.3 – Continued

ID# <sup>1</sup>	Name	Class <sup>2</sup>	$E(B-V)$ <sup>3</sup>	$T_{\text{eff}}$ (kK) <sup>4</sup>	$\log g$	Companion <sup>5</sup>	Other Notes <sup>6</sup>	Ref <sup>7</sup>
1356	PG 2158+082	sdO He, sdO	0.08374	67	5.5	...	...	D90
							He-sdO	M90
1424	Balloon 0909000007	sdB+G2	0.09090	24	...	(no companion noted)	...	U98
1457	BD-7° 5977	sdOB bin	0.03457	31 ± 0.5	5.9	G2	...	B91
					5.0	K0IV-III	...	V91
					7.1	4750(K2)	...	U98
1461A	PB 5333	sdOB, sdB	0.06225	...	...	unresolved w/ HST	...	H02
					...	unusual colors	sdOB	M90
					...	...	...	A94
1493	PG 2337+300	sd	0.09625	37.9	5.81	...	...	S94
1519	CD-27 16503	sdO?, bin?, sdOB	0.01598	75 ± 15	...	...	CV	K97b
1525	BPS CS 22957-23	sdB	0.03403	...	...	≈ 7000	...	H86
					...	...	...	...

<sup>1</sup>An “A” following the ID number indicates that this star is part of a visual double. “A” refers to the hot subdwarf component, the companions are listed in Table 4.2. At this time it is unclear whether these pairs are true common proper motion pairs, or line-of-sight doubles.

<sup>2</sup>List of classifications given in KHD, omitting duplicates (these have no relation to the citations given in the last column).

<sup>3</sup> $E(B-V)$  for the line-of-sight from Schlegel et al. (1998).

<sup>4</sup>Temperatures listed in kilo-Kelvins (kK, 1000 Kelvin).

<sup>5</sup>Information about the late-type companion is listed here, it can include:  $T_{\text{eff}}$  (K), spectral type, whether the companion was resolved by HST, notes regarding whether the object was observed to be composite.

<sup>6</sup>Other notes related to the citation, can include for example: spectral classification of the hot subdwarf, “puls” to indicate a V361 Hya-type pulsating variable star (see §1.3.1), notes about radial velocities, or whether late-type spectral features were seen.

<sup>7</sup>References given are as follows: A94 = Allard et al. (1994), A01 = Aznar Cuadrado & Jeffery (2001), A02 = Aznar Cuadrado & Jeffery (2002), B80 = Berger & Fringant (1980), B91 = Bixler, Bowyer, & Laget (1991), B93 = Boffin, Cerf, & Paulus (1993), B02 = Billères et al. (2002), D90 = Dreizler et al. (1990), F84 = Ferguson et al. (1984), F85 = Fekel & Simon (1985), H86 = Heber (1986), H92 = Herbig (1992), H02 = Heber et al. (2002), J98 = Jeffery & Pollacco (1998), J01 = Jeffery & Aznar Cuadrado (2001), K88 = Kilkenny et al. (1988), K97 = Koen et al. (1997), K97b = Koen & Orosz (1997), M90 = Moehler et al. (1990b), M90b = Moehler et al. (1990a), M95 = Marilli et al. (1995), M01 = Maxted et al. (2001), O97 = Orosz, Wade, & Harlow (1997), S94 = Saffer et al. (1994), S00 = Silvotti et al. (2000), T93 = Theissen et al. (1993), T95 = Theissen et al. (1995), Th95 = Theissen et al. (1995), U98 = Ulla & Thejll (1998), V91 = Viton et al. (1991).

Table 4.4: Single-Colored Hot Subdwarf Spectroscopic Sample  
Physical Parameters from Literature.

ID# <sup>1</sup>	Name	Class <sup>2</sup>	$E(B-V)^3$	$T_{\text{eff}}$ (kK)	$\log g$	Other Notes <sup>4</sup>	Ref <sup>5</sup>
50A PG 0027+222		sdB	0.03243	...	...	...	...
130A Feige 19		sdO He, sdO	0.02712	40.0	5.0	...	D90
				45.0	6.0	...	T94
157A PB 9286		sdB	0.03711	...	...	...	...
216 KUV 05109+1739		sdOB	0.33659	...	...	...	...
550A HZ 18		sdB	0.02131	...	...	...	...
700A PG 1340+607		sdB	0.00991	25.01	5.04	non-var	B02
850 PG 1452+198		sdB	0.02699	26.4	5.0	...	M90b
				28.025 $\pm$ 7.475	6.0 $\pm$ 0.2	...	A01
1152 PG 1710+490		sdB	0.02133	28.3	5.3	...	M90b
				28.6 $\pm$ 3	5.45	...	T93
				29.9	5.74	...	S94
				...	...	unseen companion, short P bin	M01
				...	...	non-var	B02
1158 PG 1716+426		sdB	0.07757	25.2	5.3	...	M90b
				25.6 $\pm$ 0.9	5.2	...	T93
				27.4	5.47	...	S94
				...	...	unseen companion, RV var	S98
				...	...	unseen companion, short P bin	M01
				26.1	5.33	$M_{\text{comp}} > 0.366M_{\odot}$ , P=1.77732d	M03
				...	...	gravity mode puls	G03
1181 [CW83] 1735+22		sdB, sdO		27.527 $\pm$ 0.119	5.40 $\pm$ 0.02	multi-mode puls	R04
1187 BD+39°3226		sdOp, sd	0.03838	...	...	$M_{\text{comp}} > 0.54M_{\odot}$ , RV var P=1.284d	E01
1188 [CW83] 1758+36		sdB	0.04407	45	5.5	no IR companion	U98
			0.07005	32.1	5.91	...	S94
				...	...	unusual metal abund	E01
1194 BD+48°2721		sdB, sd	0.28724	...	...	<sup>3</sup> He enriched	E01
1195 HD 171858		sdB	0.10851	27.7	5.25	$M_{\text{comp}} > 0.51M_{\odot}$ , RV var P=1.529d	M03

Continued on Next Page...

Table 4.4 – Continued

ID# <sup>1</sup>	Name	Class <sup>2</sup>	$E(B-V)^3$	$T_{\text{eff}}$ (kK)	$\log g$	Other Notes <sup>4</sup>	Ref <sup>5</sup>
1263	LS IV+00°21	sdB	0.09344	34	...	no IR companion	U98
1347	BD+28°4211	sdO7p	0.06729	...	...	H $\alpha$ , H $\beta$ core em	R89
				...	...	H $\alpha$ core em	M90c
				82	6.2	...	N99
1357	PG 2159+051	sd	0.06729	15	...	no IR companion	U98
1459	PHL 457	sdB	0.03061	25	5.3	...	H86

<sup>1</sup>An “A” following the ID number indicates that this star is part of a visual double. “A” refers to the hot subdwarf component, the companions are listed in Table 4.2. At this time it is unclear whether these pairs are true common proper motion pairs, or line-of-sight doubles.

<sup>2</sup>List of classifications given in KHD, omitting duplicates (these have no relation to the citations given in the last column).

<sup>3</sup> $E(B-V)$  for the line-of-sight from Schlegel et al. (1998).

<sup>4</sup>Other notes related to the citation, can include for example: “puls” to indicate a V361 Hya-type pulsating variable star (see §1.3.1), notes about radial velocities, or unseen companions detected by radial velocities.

<sup>5</sup>References given are as follows: A01 = Aznar Cuadrado & Jeffery (2001), B02 = Billères et al. (2002), D90 = Dreizler et al. (1990), E01 = Edelmann, Heber, & Napiwotzki (2001), G03 = Green et al. (2003), H86 = Heber (1986), M90b = Moehler et al. (1990a), M90c = Massey & Gronwall (1990), M01 = Maxted et al. (2001), M03 = Morales-Rueda et al. (2003), N99 = Napiwotzki (1993, 1999), R89 = Reid & Wegner (1988, 1989), R04 = Reed et al. (2004), S94 = Saffer et al. (1994), S98 = Saffer, Livio, & Yungelson (1998), T93 = Theissen et al. (1993), T94 = Thejll et al. (1994), U98 = Ulla & Thejll (1998).



Table 4.5: Observing list for Standard Stars.

HIP#	HD#	RA (J1991.25)	Dec	$V^a$	$M_V^a$	$B - V^a$	NOAO Sem.	Ca II UT Date	Na I & Mg I UT Date	Notes
954	745	00 11 47.55	+09 08 24.0	7.45	1.91	+0.891	2003B	Sep 15	Sep 18	
1078	...	00 13 24.36	+19 04 17.9	9.86	7.12	+1.190	2003B	Sep 13	Sep 18	BD+18°15
1169	1031	00 14 36.56	+01 17 48.7	7.03	2.39	+0.461	2003B	Sep 15	Sep 18	
1427	1352	00 17 49.85	+16 19 51.9	7.21	3.89	+0.477	2003B	Sep 13	Sep 18	
1495	1449	00 18 39.63	+22 52 46.7	7.14	1.91	+0.885	2003B	Sep 13	Sep 18	
1499	1461	00 18 41.62	-08 03 09.5	6.47	4.62	+0.674	2002B	Oct 12	Oct 15	
1532	...	00 19 05.58	-09 57 50.8	9.90	8.31	+1.318	2003B	Sep 13	Sep 18	BD-10°47
1691	1689	00 21 13.11	-03 18 43.1	7.36	2.86	+0.529	2003B	Sep 13	Sep 18	
2050	2173	00 25 58.65	+21 01 27.4	7.50	1.43	+0.929	2003B	Sep 15	Sep 18	
2498	2816	00 31 41.51	+12 54 50.0	7.25	2.69	+0.906	2003B	Sep 15	Sep 18	
2512	2827	00 31 51.06	+18 06 20.0	7.22	2.32	+0.535	2003B	Sep 15	Sep 18	
3093	3651	00 39 22.09	+21 15 04.9	5.88	5.65	+0.850	2003B	Sep 13	Sep 18	
3203	3821	00 40 47.48	-07 13 56.6	7.02	4.96	+0.620	2002B	Oct 12	Oct 15	
3765	4628	00 48 22.53	+05 17 00.2	5.74	6.38	+0.890	2002B	Oct 12	Oct 15	
3979	4915	00 51 10.69	-05 02 20.4	6.98	5.26	+0.663	2002B	Oct 12	Oct 15	
4087	5036	00 52 28.14	+21 24 36.3	7.28	2.43	+0.493	2003B	Sep 13	Sep 18	
4893	6133	01 02 50.29	+26 17 57.6	7.21	3.02	+0.406	2003B	Sep 15	Sep 18	
5291	6720	01 07 42.98	-19 18 43.3	7.93	3.68	+0.775	2003B	Sep 14	Sep 18	
5315	6734	01 07 59.58	+01 59 38.7	6.44	3.11	+0.847	2002B	Oct 14	Oct 16	
5741	7377	01 13 44.88	-08 18 56.9	9.10	6.43	+1.035	2003B	Sep 14	Sep 18	
5806	7449	01 14 29.42	-05 02 49.4	7.50	4.57	+0.575	2003B	Sep 14	Sep 18	
6308	8117	01 21 03.60	+25 09 31.1	7.86	4.31	+0.534	2003B	Sep 14	Sep 18	
6442	8331	01 22 43.51	+10 22 11.2	7.47	3.86	+0.681	2003B	Sep 14	Sep 17	BD+12°172
6558	...	01 24 16.37	+12 54 27.9	9.52	6.88	+1.020	2003B	Sep 14	Sep 17	
6917	8997	01 29 04.61	+21 43 25.0	7.74	5.92	+0.966	2003B	Sep 14	Sep 17	
7117	9307	01 31 42.65	+10 53 21.8	7.03	1.40	+0.988	2003B	Sep 15	Sep 18	
7549	9958	01 37 16.16	-00 21 00.5	7.08	2.35	+0.671	2003B	Sep 14	Sep 18	
7564	9939	01 37 25.23	+25 10 05.8	6.99	3.87	+0.900	2003B	Sep 15	Sep 18	
8524	11170	01 49 55.99	+07 13 25.3	7.43	2.63	+0.621	2003B	Sep 15	Sep 17	
8872	11616	01 54 11.94	+09 57 02.9	7.78	3.27	+0.653	2003B	Sep 15	Sep 17	
9035	11833	01 56 22.43	+08 30 34.7	7.95	3.25	+0.590	2003B	Sep 15	Sep 17	
9911	13043	02 07 34.42	-00 36 59.7	6.88	4.04	+0.624	2002B	Oct 14	Oct 15	
10781	14290	02 18 46.03	+07 42 20.9	7.97	3.44	+0.436	2003B	Sep 15	Sep 18	
10915	14516	02 20 30.80	-06 22 43.9	7.91	3.83	+0.470	2003B	Sep 15	Sep 18	
12114	16160	02 36 03.83	+06 53 00.1	5.79	6.50	+0.918	2003B	Sep 13	Sep 18	

Continued on Next Page...

Table 4.5 – Continued

HIP #	HD #	RA (J1991.25)	Dec	$V^a$	$M_V^a$	$B - V^a$	NOAO Sem.	Ca II UT Date	Na I & Mg I UT Date	Notes
12350	16548	02 39 00.65	-08 55 39.9	6.98	3.36	+0.702	2002B	Oct 14	Oct 15	
12493	...	02 40 42.71	+01 11 53.2	9.51	7.77	+1.185	2003B	Sep 13	Sep 17	
12926	17190	02 46 15.05	+25 39 00.9	7.89	5.84	+0.840	2003B	Sep 15	Sep 17	
13026	17397	02 47 26.98	+01 03 33.4	7.93	4.30	+0.502	2003B	Sep 14	Sep 18	
13081	17382	02 48 08.97	+27 04 08.2	7.56	5.81	+0.820	2003B	Sep 13	Sep 17	
13345	...	02 51 44.43	-08 16 09.5	9.82	7.41	+1.216	2003B	Sep 14	Sep 18	
15457	20630	03 19 21.54	+03 22 11.9	4.84	5.03	+0.681	2002B	Oct 12	Oct 15	
15776	21019	03 23 17.70	-07 47 36.8	6.20	3.36	+0.702	2002B	Oct 12	Oct 15	
16537	22049	03 32 56.42	-09 27 29.9	3.72	6.18	+0.881	2002B	Oct 12	Oct 15	
17027	22713	03 39 01.13	-05 37 32.5	5.97	3.24	+0.921	2002B	Oct 12	Oct 15	
19431	26337	04 09 40.87	-07 53 35.2	7.03	3.28	+0.712	2002B	Oct 12	Oct 15	
20373	27642	04 21 46.30	+02 23 25.6	6.92	2.96	+0.571	2002B	...	Oct 16	
22319	30508	04 48 27.65	+02 42 54.5	6.51	3.12	+0.846	2002B	Oct 12	Oct 15	
22336	30562	04 48 36.20	-05 40 24.4	5.77	3.65	+0.631	2002B	Oct 14	Oct 15	
22919	31412	04 55 55.80	+04 40 15.1	7.02	4.24	+0.561	2002B	Oct 12	Oct 15	
23105	31738	04 58 17.08	+00 27 14.4	7.20	4.57	+0.705	2002B	Oct 14	Oct 15	
24130	33555	05 10 57.97	-02 15 13.5	6.24	2.82	+0.984	2002B	Oct 14	Oct 15	
27058	38277	05 44 17.56	-10 00 59.0	7.11	4.14	+0.637	2002B	Oct 14	Oct 15	
27253	38529	05 46 34.96	+01 10 06.7	5.95	2.81	+0.773	2002B	Oct 12	Oct 15	
27435	38858	05 48 34.90	-04 05 38.7	5.97	5.01	+0.639	2002B	Oct 12	Oct 15	
31083	46090	06 31 21.55	+02 54 40.6	7.14	4.90	+0.710	2002B	Oct 14	Oct 16	
32984	50281	06 52 18.37	-05 10 25.3	6.58	6.88	+1.071	2002B	Oct 12	Oct 16	
61946	110463	12 41 44.40	+55 43 28.9	8.28	6.45	+0.955	2002A	Jun 29	Jul 01	
65420	116568	13 24 33.14	-05 09 50.1	5.76	3.37	+0.415	2003A	Jun 09	Jun 12	
68619	122603	14 02 47.73	+03 32 44.7	7.54	3.62	+0.594	2003A	Jun 09	Jun 13	
69881	125184	14 18 00.57	-07 32 30.5	6.47	3.89	+0.723	2003A	Jun 09	Jun 13	
70755	126868	14 28 12.22	-02 13 40.6	4.84	1.75	+0.693	2002A	...	Jul 01	
70782	126961	14 28 31.25	+02 47 19.3	7.02	3.98	+0.549	2003A	...	Jun 14	
72659A	131156A	14 51 23.28	+19 06 02.3	4.67	5.54	+0.725	2002A	...	Jul 01	<i>b</i>
72659B	131156B	14 51 23.00	+19 06 08.0	6.82	7.69	+1.156	2002A	...	Jul 01	<i>b</i>
79119	145328	16 08 58.33	+36 29 24.4	4.76	2.06	+1.015	2002A	Jun 30	Jul 01	
80021	147266	16 20 04.29	+21 07 57.9	6.04	0.92	+0.938	2002A	Jun 30	Jul 01	
80214	147767	16 22 29.22	+33 42 12.1	5.41	-0.71	+1.523	2002A	Jun 30	Jul 01	
81693	150680	16 41 17.48	+31 36 06.8	2.89	2.72	+0.650	2002A	Jun 30	Jul 02	
95962	183658	19 30 52.80	-06 30 50.7	7.27	4.60	+0.640	2002B	...	Oct 16	
96100	185144	19 32 20.59	+69 39 55.4	4.70	5.90	+0.786	2002A	Jun 29	Jul 01	

Continued on Next Page...

Table 4.5 – Continued

HIP #	HD #	RA (J1991.25)	Dec	$V^a$	$M_V^a$	$B - V^a$	NOAO Sem.	Ca II UT Date	Na I & Mg I UT Date	Notes
96901	186427	19 41 52.10	+50 31 04.5	6.20	4.55	+0.661	2002A	Jun 29	Jul 01	
97255	186704	19 45 57.30	+04 14 54.6	7.02	4.62	+0.612	2002B	...	Oct 16	
97635	188056	19 50 37.73	+52 59 17.4	5.02	1.17	+1.286	2002A	Jun 29	Jul 01	
98416	189340	19 59 47.49	-09 57 26.2	5.87	3.92	+0.598	2002B	Oct 12	Oct 15	
99894	192699	20 16 06.03	+04 34 51.3	6.44	2.30	+0.867	2002B	Oct 12	Oct 15	
100501	194193	20 22 45.29	+41 01 34.1	5.93	-1.17	+1.632	2002A	Jun 30	Jul 01	
101622	196203	20 35 47.09	-00 00 04.1	7.09	2.05	+0.512	2003A	Jun 09	Jun 13, Jun 14	
101955	196795	20 39 37.20	+04 58 18.7	7.88	6.53	+1.241	2002A	Jun 29	Jul 02	
104202	200964	21 06 39.79	+03 48 10.8	6.48	2.31	+0.880	2003A	Jun 10	Jun 13	
104214	201091	21 06 50.84	+38 44 29.4	5.21	7.50	+1.069	2002A	Jun 30	Jul 01	
104217	201092	21 06 52.19	+38 44 03.9	5.21	7.49	+1.309	2002A	Jun 30	Jul 01	
107857	207687	21 51 05.60	-10 02 17.0	7.49	2.97	+0.801	2002B	Oct 14	Oct 15	
108782	209290	22 02 10.54	+01 24 03.3	9.17	9.10	+1.453	2003B	Sep 13	Sep 17	
109378	210277	22 09 29.82	-07 32 51.2	6.54	4.90	+0.773	2002B	Oct 14	Oct 15	
							2003A	Jun 10	Jun 13	
109820	211022	22 14 37.20	-15 06 05.4	7.23	2.46	+0.436	2003B	Sep 13	Sep 18	
110205	211786	22 19 25.06	+12 27 36.1	7.98	4.87	+0.666	2003B	Sep 14	Sep 17	
111312	213612	22 33 01.49	-17 30 05.0	7.57	3.34	+0.827	2003B	Sep 13	Sep 18	
111571	214100	22 36 09.65	-00 50 24.5	9.98	8.76	+1.411	2003B	Sep 13	Sep 17	
114854	219452	23 15 52.57	-13 11 02.0	7.28	3.04	+0.433	2003B	Sep 13	Sep 17	
114906	219516	23 16 28.07	-10 12 41.2	7.98	3.64	+0.529	2003B	Sep 13	Sep 17	
115004	...	23 17 32.23	+09 41 36.8	9.72	6.87	+1.130	2003B	Sep 14	Sep 17	BD+08°5036
116384	...	23 35 00.08	+01 36 19.2	9.59	8.16	+1.329	2003B	Sep 14	Sep 17	BD+00°5017
116600	222111	23 37 49.09	+03 22 13.1	7.30	3.12	+0.461	2003B	Sep 14	Sep 17	
117112	222878	23 44 32.50	-03 10 31.3	7.26	2.68	+0.561	2003B	Sep 14	Sep 18	
117980	224173	23 55 48.72	-13 57 59.9	7.30	3.45	+0.498	2003B	Sep 15	Sep 18	

<sup>a</sup>Johnson  $V$ ,  $M_V$ , and  $B - V$  derived from Tycho photometry and Hipparcos parallax (see §4.4.2 and Appendix E).

<sup>b</sup>These two stars comprise a resolved binary (separation  $\sim 7''$ ), they have only one entry in both HIP and HD, however, they have separate identifiers in Tycho, they are (A and B respectively): TYC1481-722-1 and TYC1481-722-2.

Table 4.6. Parameters for the Visual Double Hot Subdwarfs.

No.	Name	Sep.	Comp. <sup>a</sup>	$J_A^b$	$J_B - J_A^c$	$(J - K_S)_A^d$	$(J - K_S)_B^d$
50	PG 0027+222	19'6	A→B	15.611 ± 0.064	-2.763 ± 0.063	-0.082 ± 0.272	+0.394 ± 0.032
87	PG 0105+276	2'9	A→B	14.323 ± 0.051	...	+0.576 ± 0.075	...
91	PB 8555	~1-3''	A→B	11.556 ± 0.046	...	+0.368 ± 0.062	...
130	Feige 19	33'0	A→B	14.401 ± 0.044	-1.529 ± 0.043	-0.309 ± 0.109	+0.814 ± 0.040
157	PB 9286	13'6	A→B	13.591 ± 0.037	+0.253 ± 0.045	-0.221 ± 0.077	+0.311 ± 0.052
187	HDE 283048	9'3	A→B	9.329 ± 0.034	+3.426 ± 0.055	+0.309 ± 0.048	+0.453 ± 0.058
550	HZ 18	7'0	A→B	16.178 ± 0.091	-1.100 ± 0.098	<-1.137	-0.042 ± 0.126
700	PG 1340+607	8'3	A→B	13.634 ± 0.044	-0.766 ± 0.040	-0.063 ± 0.071	+0.568 ± 0.036
1027	PG 1618+562	3'6	A→B	>11.719	...	>+0.171	...
1348	PG 2151+100	15'8	A→B	12.835 ± 0.041	+2.387 ± 0.055	+0.229 ± 0.061	+0.606 ± 0.109
		4'9	A→Ab		+2.528 ± 0.082 <sup>e</sup>		+0.688 ± 0.138 <sup>e</sup>
1461	PB 5333	19'0	A→B	12.806 ± 0.037	+1.896 ± 0.047	+0.272 ± 0.055	+0.295 ± 0.075

<sup>a</sup>Visual double components are identified in Figures 4.20–4.22 and discussed in §4.6.3.<sup>b</sup> $J$  magnitude of the hot subdwarf.<sup>c</sup>Difference between the  $J$  magnitudes of the two visual double components ( $A$  = subdwarf,  $B$  = companion).<sup>d</sup> $J - K_S$  colors for the hot subdwarf (“A”) and the visual companion (“B”).<sup>e</sup>Values of  $J_{Ab} - J_A$  and  $(J - K_S)_{Ab}$ .

## Chapter 5

# Analysis of Spectroscopy of Hot Subdwarfs

### 5.1 Introduction

In this chapter I will discuss the measurement and extraction techniques I used to measure the EWs in my spectra (§5.2). I will also discuss the properties of the HIP standard stars (§5.3). Then I will discuss how I predicted diluted EWs, based on the properties of the HIP standard stars, that I can use to compare with the observed composite systems (§5.3).

### 5.2 Measuring Individual Line EWs Automatically

I read my reduced spectra into a program that I wrote, which fitted local continua and measured the equivalent widths (EWs) of each line of the CaT, Na I D, Mg I b, He I 6678 Å, He I 5875 Å, H $\alpha$ , H $\beta$ , and Paschen-14 8598 Å.

The program, written to measure the EWs of all lines of interest automatically, starts by taking a small piece of spectrum around a feature of interest. It then finds the actual center of the absorption/emission line. To do this, it first fits a parabola to the “predicted” line wavelength and two points to either side of the approximate line center (these points are roughly in the continuum at  $\pm 10$  pixels, or  $\sim 12.7$  Å, to either side of the predicted center). The purpose of “fitting” the parabola is to determine if the line is in absorption or emission so the actual center of the line can be correctly identified automatically by the program. The equation for a parabola is  $y = Ax^2 + Bx + C$ . The value of  $A$  is of primary interest in this context, since  $A > 0$  implies that the parabola opens upward while  $A < 0$  implies the parabola opens downward. Given three points  $(x_1, y_1)$ ,  $(x_2, y_2)$ , and  $(x_3, y_3)$ , where  $x_1 < x_2 < x_3$ , the equation for the coefficient  $A$  is:

$$A = \frac{y_3 - y_2}{(x_3 - x_2)(x_3 - x_1)} - \frac{y_1 - y_2}{(x_1 - x_2)(x_3 - x_1)} \quad (5.1)$$

Knowing whether the line is in absorption or emission, it is possible to find the exact center by looking for the minimum or maximum of the line.

The local continua were fitted with first order Legendre polynomials (straight lines) following the technique described in Sembach & Savage (1992) and briefly outlined in §H.1.2. Regions containing strong absorption lines were excluded from the continuum fits; these regions are shown in Figures 5.1 and 5.2. Example continua fits are shown in Figure 5.3.

Once the local continuum is fitted, the EW of the feature is extracted. The EW is taken from  $\pm 13.0$  Å of the feature minimum (or over  $-13.0$  to  $+19.0$  Å from the minimum of the Na I D<sub>2</sub> feature, or over  $-13.0$  to  $+27.0$  Å from the minimum of the

Mg I b<sub>2</sub> feature) using the equations for EW given in Appendix H.1. As long as the normalized flux at feature center was either  $>1.01$  for emission or  $<0.99$  for absorption, the EW of the feature was calculated, regardless of whether the feature truly existed in the spectrum. The EW measurement error is calculated in two parts. The first,  $\sigma_W(F)$ , takes the combined Poisson statistical error calculated from the equations given in §H.1.1. The second,  $\sigma_W(C)$ , takes the error from the continuum fit into account following §H.1.2. The total EW error is the quadrature sum of these two values [ $\sigma_W^2 = \sigma_W^2(F) + \sigma_W^2(C)$ ].

The output from this program resulted not in a true EW, but rather in an EW-like index for each line or set of lines. These measured EWs for all HIP standards and hot subdwarfs are presented in Appendix K (page 282).

### 5.3 Properties of the HIP Standard Stars

In order to use the observations of the HIP Standards as an effective template from which to infer the properties of the composite hot subdwarfs, I first needed to characterize the properties of the standards. Thus I fitted smooth curves through all parameters I had for the standards against their value of  $M_V$  or  $B-V$ .

To fit the parameters of the HIP standard stars I used a *robust locally weighted regression* technique otherwise known as *lowess* (locally-weighted scatterplot smoother; for example, see description in Cleveland 1985). The idea of *lowess* is to pass a smooth curve through the points on a scatterplot which describes the middle of the distribution in  $y$  for each value of  $x$ . I decided to use the *lowess* routine (called “loess”) contained in the statistical program “R”<sup>1</sup>.

In R’s *loess* routine, the fitting of a curve to the scatter plot is done locally at each point. For a given point  $x$ , the fit at that location is made using points in the region around  $x$ , weighted by their distances from  $x$ . The size of this region is controlled by a “smoothness parameter”,  $\alpha$  (where  $\alpha \leq 1$ ). The region around  $x$  then includes the  $\alpha N$  nearest points to  $x$  (where  $N$  is the total number of points in the scatter plot), and these points have weighting proportional to:

$$w = \left[ 1 - \left( \frac{d}{d_{\max}} \right)^3 \right]^3 \quad (5.2)$$

where  $d$  is the distance of the point from  $x$  and  $d_{\max}$  is the distance of the  $\alpha N$ -th closest point from  $x$ . The actual local fitting is done using a weighted least squares technique.

#### 5.3.1 Loess Parameters for EW Relations

The fits were done by least-squares (in R terminology ‘family = “gaussian” ’), with  $B-V$  acting as the abscissa and the EW acting as the ordinate. Additional control values were set to the following: surface = “direct” (fit surface directly instead of using interpolation from a kd tree), statistics = “exact” (compute the statistics exactly), trace.hat = “exact” (compute the trace of the smoother matrix exactly), iterations = 4

---

<sup>1</sup>See: “The R Project for Statistical Computing” website at “<http://www.r-project.org/>”.

(number of iterations to reject outliers in robust fitting). The smoothness parameter,  $\alpha$ , had the following values for the main sequence:

$$\begin{aligned}\alpha_{\text{Ca},B-V} &= 0.99 \\ \alpha_{\text{Na},B-V} &= 0.65 \\ \alpha_{\text{Mg},B-V} &= 0.50\end{aligned}$$

and subgiants:

$$\begin{aligned}\alpha_{\text{Ca},B-V} &= 0.99 \\ \alpha_{\text{Na},B-V} &= 0.85 \\ \alpha_{\text{Mg},B-V} &= 0.95\end{aligned}$$

These values of  $\alpha$  were chosen to be the smallest values which resulted in no trends in the residuals (observed points minus fit).

The output from  $R$  was the value of the smoothed fit at eleven points evenly spaced throughout the range in  $B-V$ , along with the standard errors at each point. The corresponding range and step in  $B-V$  color for the main sequence is:

$$+0.350 \leq (B-V)_{\text{MS}} \leq +1.460, \text{ step} = 0.111$$

and for the subgiants is:

$$+0.350 \leq (B-V)_{\text{SG}} \leq +1.640, \text{ step} = 0.129$$

The resulting fits to the EWs of the HIP standards are shown in Figure 5.4, and the actual values are given in Table 5.1.

### 5.3.2 *Loess* Parameters for Color and Magnitude Relations

I performed two different fits for the HIP colors. The first was a fit with  $M_V$  as the ordinate and  $B-V$  as the abscissa (color-magnitude). Then the rest of the colors were fitted with  $B-V$  again as the abscissa and each color as the ordinate (color-color).

In all cases the fits for the color relations used all the same *loess* parameters as the EW relations. The fits were done by least-squares, the surface was fit directly, exact statistics were computed, the trace of the smoother matrix was computed exactly, and there were four rejection iterations for robustness. However, it was easier to fit the main sequence ( $M_V \gtrsim 4.0$ ) and subgiant stars ( $M_V \lesssim 4.0$ ) separately. Additionally, the smoothness parameters,  $\alpha$ , were as follows for the main sequence fits:

$$\begin{aligned}\alpha_{M_V,B-V} &= 0.95 \\ \alpha_{V-J,B-V} &= 0.95 \\ \alpha_{V-K_S,B-V} &= 0.95 \\ \alpha_{J-H,B-V} &= 0.95 \\ \alpha_{J-K_S,B-V} &= 0.95\end{aligned}$$

and for the subgiants:

$$\begin{aligned}
 \alpha_{M_V, B-V} &= 0.90 \\
 \alpha_{V-J, B-V} &= 0.99 \\
 \alpha_{V-K_S, B-V} &= 0.99 \\
 \alpha_{J-H, B-V} &= 0.95 \\
 \alpha_{J-K_S, B-V} &= 0.95
 \end{aligned}$$

Again, the output was the value of the smoothed fit and the standard errors, at the same eleven evenly spaced points covering the corresponding range in color for both the main sequence and the subgiants that was used for the EW fits.

The resulting color-magnitude and color-color fits to the HIP standards are shown in Figures 5.5 and 5.6, and the fit values are given in Tables 5.2–5.4.

### 5.3.3 Description of the EW Fits

From Figure 5.4 it is obvious that each of the three features I am focusing on shows distinctly different behaviors with temperature and surface gravity. These differing behaviors will allow me to uniquely identify the dilution of the late-type star by the subdwarf, the temperature of the late type star, and the surface gravity (MS or subgiant) of the late-type star.

The EW of the combined CaT remains roughly constant through the range in  $B-V$  covered by the MS HIP stars. The fit does droop at both the red and blue end for two reasons: at the blue (hot) end, the atoms are being further ionized so the amount of Ca II is decreasing so the lines are becoming weaker; at the red (cool) end, the atoms are becoming more neutral as the star’s atmosphere cools, and additional opacity from molecules depresses the continuum. On the other hand, the EW of the combined CaT continues to increase toward lower temperatures in the subgiant HIP stars, due to the decrease in the surface gravity.

The EW of the combined Na I D doublet lines increases with decreasing temperature for both MS and subgiants, however the rate of increase is different for the two groups. The EW in the MS stars increases more dramatically with decreasing temperature than the subgiants due to the higher pressure (higher surface gravity) in the MS stars.

The EW of the combined Mg I b triplet in MS stars initially increases with decreasing temperature, but then turns over at  $B-V \sim 1.1$  and the EW begins decreasing again as temperature continues to decrease. There are two factors causing this turn-over: (1) the Mg I b lines grow in strength as the star cools but then level-off and become more constant when the line saturates, (2) the opacity of other “metal” lines depresses the surrounding continuum forming a pseudo-continuum which is much lower than the real continuum thus makes the Mg I b lines appear weaker than they really are. In the subgiants, the EW of Mg I b does not increase as rapidly as in MS stars. Thus the EW in the subgiants simply rises slowly with decreasing temperature.



## 5.4 Models of Diluted EWs based on HIP Fits

Using the fits to the parameters of the HIP standard stars, and combining them with Kurucz (1998, hereafter referred to as just “Kurucz”) spectral energy distributions (SEDs), I can predict the values of the diluted EWs and colors for various combinations of sdBs and late-type companions. The exact details of these calculations can be found in Appendix H.2 (page 267). The basic steps of this process are first to choose a value of  $B-V$  color for the late-type companion, then to use the various HIP fits to interpolate the other colors and EWs for that particular companion. The late-type models generated based on the fits to the HIP standard parameters are shown in Figure 5.7. The next step is to choose a hot subdwarf by interpolating (using Lagrange interpolation, discussed in Appendix J) through the adopted hot subdwarf parameters (listed in Table H.2). The late-type and hot subdwarf “models” are then matched to a Kurucz flux distribution by  $B-V$  color. Once the two stars are chosen, their values of  $M_V$  are used to calculate the dilution of the companion by the sdB at  $V$ , then using the Kurucz flux ratios the dilution at  $V$  is extrapolated to the wavelengths for the features of interest.

From Appendix H.2 (see Eqn. H.17), the diluted EW of a line is:

$$W_d = D W_u \quad (5.3)$$

where “ $W_u$ ” refers to the undiluted EW, “ $W_d$ ” to the diluted EW, and “ $D$ ” refers to the fraction of the combined light contributed by the star with the intrinsic spectral feature (the late-type star in the specific case of a sd+late-type composite).

From §C.3.1 (see Eqn. C.19–C.22), the composite colors are:

$$(J-K_S)_{\text{blend}} = 2.5 \log \left( 10^{[(J-K_S)_{\text{sd}} + (V-J)_{\text{sd}}]/2.5} + \nu 10^{[(J-K_S)_{\text{comp}} + (V-J)_{\text{comp}}]/2.5} \right) - 2.5 \log \left( 10^{(V-J)_{\text{sd}}/2.5} + \nu 10^{(V-J)_{\text{comp}}/2.5} \right) \quad (5.4)$$

$$(H-K_S)_{\text{blend}} = 2.5 \log \left( 10^{[(H-K_S)_{\text{sd}} + (V-H)_{\text{sd}}]/2.5} + \nu 10^{[(H-K_S)_{\text{comp}} + (V-H)_{\text{comp}}]/2.5} \right) - 2.5 \log \left( 10^{(V-H)_{\text{sd}}/2.5} + \nu 10^{(V-H)_{\text{comp}}/2.5} \right) \quad (5.5)$$

$$(V-K_S)_{\text{blend}} = 2.5 \log \left( 10^{(V-K_S)_{\text{sd}}/2.5} + \nu 10^{(V-K_S)_{\text{comp}}/2.5} \right) - 2.5 \log (1 + \nu) \quad (5.6)$$

$$(B-K_S)_{\text{blend}} = 2.5 \log \left( 10^{[(B-K_S)_{\text{sd}} + (V-B)_{\text{sd}}]/2.5} + \nu 10^{[(B-K_S)_{\text{comp}} + (V-B)_{\text{comp}}]/2.5} \right) - 2.5 \log \left( 10^{(V-B)_{\text{sd}}/2.5} + \nu 10^{(V-B)_{\text{comp}}/2.5} \right) \quad (5.7)$$

In all cases  $\nu = \frac{F_{V,\text{comp}}}{F_{V,\text{sd}}}$ . All other colors can be calculated as combinations of these colors [i.e.,  $B-V = (B-K_S) - (V-K_S)$ ].

The blended magnitude in a single band from §C.3.2 (see Eqn. C.24) is:

$$m_{\text{tot}} = -2.5 \log \left[ 10^{-m_{\text{sd}}/2.5} + 10^{(2.5 \log F_{\text{rat}} - m_{\text{sd}})/2.5} \right] \quad (5.8)$$

where  $F_{\text{rat}} = \nu \equiv \frac{F_{V,\text{comp}}}{F_{V,\text{sd}}}$  when the magnitudes are  $V$ , and  $F_{\text{rat}} = \kappa \equiv \frac{F_{K_S,\text{comp}}}{F_{K_S,\text{sd}}}$  for  $K_S$  magnitudes. The values  $\nu$  and  $\kappa$  are related by:

$$\log \kappa = \log \nu + \frac{(V-K_S)_{\text{comp}}}{2.5} - \frac{(V-K_S)_{\text{sd}}}{2.5} \quad (5.9)$$

(see also Eqn. C.25).

## 5.5 Walk-through of a Model Calculation

In this section I will walk through a complete calculation of a diluted model. I will begin with choosing the hot subdwarf, then the late-type companion, and finally calculating the diluted colors and EWs.

### 5.5.1 Choosing the Hot Subdwarf

The first step in creating a model is to choose a hot subdwarf based on  $B-V$  color. For this example I will use:  $(B-V)_{\text{sd}} = -0.2375$ . Then, Lagrange interpolation on the  $(B-V)_{\text{sd}}$  color is used in order to find the other parameters for this hot subdwarf.

The relevant parameters (from Tables H.2 and H.3) used in the Lagrange interpolation for hot subdwarfs (assumed to be ZAEHB) are:

$(B-V)_{\text{sd}}$	$R_{\text{sd, Na/Ca}}$	$R_{\text{sd, Mg/Ca}}$	$F_{\text{sd, Ca}}$	$\log L_{\text{sd}}$	
-0.2790	1.8769	2.2550	1.3181 E-6	1.169	
-0.2420	1.9503	2.4062	4.8873 E-6	1.193	
-0.1960	2.0090	2.5209	2.0615 E-5	1.262	
$(B-V)_{\text{sd}}$	$\text{BC}_{B,\text{sd}}$	$\text{BC}_{V,\text{sd}}$	$\text{BC}_{J,\text{sd}}$	$\text{BC}_{H,\text{sd}}$	$\text{BC}_{K,\text{sd}}$
-0.2790	-2.781	-3.053	-3.748	-3.868	-3.977
-0.2420	-2.355	-2.588	-3.193	-3.297	-3.389
-0.1960	-1.750	-1.933	-2.413	-2.493	-2.562

Where  $R_{\text{Na/Ca}}$  and  $R_{\text{Mg/Ca}}$  are the ratios of flux at the wavelengths of the lines (see §H.2.4), and “BC” stands for Bolometric Correction.

I will walk through the interpolation of  $\log L$ . First the calculation of the three 2nd order Lagrange coefficients (from Eqn. J.3–J.5):

$$\begin{aligned} L_{2,0}(-0.2375) &= \frac{[-0.2375 - (-0.2420)][-0.2375 - (-0.1960)]}{[-0.2790 - (-0.2420)][-0.2790 - (-0.1960)]} = -0.060811 \\ L_{2,1}(-0.2375) &= \frac{[-0.2375 - (-0.2790)][-0.2375 - (-0.1960)]}{[-0.2420 - (-0.2790)][-0.2420 - (-0.1960)]} = 1.011898 \\ L_{2,2}(-0.2375) &= \frac{[-0.2375 - (-0.2790)][-0.2375 - (-0.2420)]}{[-0.1960 - (-0.2790)][-0.1960 - (-0.2420)]} = 0.048913 \end{aligned}$$

These coefficients result in a final interpolated value (from Eqn J.6) for  $\log L$  of:

$$P(-0.2375) = 1.169 \times -0.060811 + 1.193 \times 1.011898 + 1.262 \times 0.048913 = 1.1978$$

Similarly the final interpolated values for the hot subdwarf with  $B-V = -0.2375$  are:

$$\begin{aligned}
\log L_{\text{sd}} &= 1.1978 \\
R_{\text{sd, Na/Ca}} &= 1.9576 \\
R_{\text{sd, Mg/Ca}} &= 2.4210 \\
F_{\text{sd, Ca}} &= 5.8736 E-6 \\
\text{BC}_{B, \text{sd}} &= -2.2995 \\
\text{BC}_{V, \text{sd}} &= -2.5277 \\
\text{BC}_{J, \text{sd}} &= -3.1211 \\
\text{BC}_{H, \text{sd}} &= -3.2230 \\
\text{BC}_{K, \text{sd}} &= -3.3128
\end{aligned}$$

From these values, the values of  $J-H$ ,  $J-K_S$ ,  $V-K_S$ ,  $V-J$ , and  $M_V$  can be calculated:

$$\begin{aligned}
(J-H)_{\text{sd}} &= 0.990(\text{BC}_{H, \text{sd}} - \text{BC}_{J, \text{sd}}) - 0.049 &= -0.1498 \\
(J-K_S)_{\text{sd}} &= 0.983(\text{BC}_{K, \text{sd}} - \text{BC}_{J, \text{sd}}) - 0.018 &= -0.2064 \\
(V-K_S)_{\text{sd}} &= \text{BC}_{K, \text{sd}} - \text{BC}_{V, \text{sd}} - 0.039 + 0.001(\text{BC}_{K, \text{sd}} - \text{BC}_{J, \text{sd}}) &= -0.8243 \\
(V-J)_{\text{sd}} &= (V-K_S)_{\text{sd}} - (J-K_S)_{\text{sd}} &= -0.6179 \\
M_{V, \text{sd}} &= 4.76 - 2.5 \log L_{\text{sd}} - \text{BC}_{V, \text{sd}} &= 4.2931
\end{aligned}$$

Note that these equations include conversions to the 2MASS filters from Johnson filters.

### 5.5.2 Choosing a Late-Type Companion

The next step is to similarly choose a companion based on  $B-V$ . In this case I will take  $(B-V)_c = +0.9200$ . The error on the companion's  $B-V$  color was taken as half the difference between its  $B-V$  and the next successive model in  $B-V$  [for the set of models I used,  $\Delta(B-V)_c = 0.02375$ , so  $\sigma(B-V)_c = 0.0119$ ]. The first group of values to be determined by interpolation is the flux ratios. The relevant values (from Table H.3) for the chosen  $B-V$  are:

$(B-V)_c$	$R_{c, \text{Na/Ca}}$	$R_{c, \text{Mg/Ca}}$	$F_{c, \text{Ca}}$
+0.9330	0.7282	0.4648	3.0529 $E-6$
+0.8510	0.7772	0.5495	4.2601 $E-6$
+0.7690	0.8232	0.6222	6.3187 $E-6$

The second group is from the fits to the observed parameters and includes the EWs<sup>2</sup> and colors of the companion, the relevant terms (from Tables 5.1–5.3) to be interpolated over are:

---

<sup>2</sup>All EWs listed are measured in Å.

$(B-V)_c$	$W_{c,Ca}$	$\sigma W_{c,Ca}$	$W_{c,Na}$	$\sigma W_{c,Na}$	$W_{c,Mg}$	$\sigma W_{c,Mg}$	$M_{V,c}$	$\sigma M_{V,c}$
+0.7940	6.7772	0.1365	2.8473	0.1479	7.0134	0.2183	5.5068	0.1108
+0.9050	6.6567	0.1621	4.1766	0.1465	9.0122	0.2095	6.1781	0.1286
+1.0160	6.5767	0.1630	5.8122	0.1415	10.0467	0.1949	6.6858	0.1300

$(B-V)_c$	$(J-H)_c$	$\sigma(J-H)_c$	$(J-K_S)_c$	$\sigma(J-K_S)_c$	$(V-J)_c$	$\sigma(V-J)_c$
+0.7940	+0.4208	0.0180	+0.5396	0.0227	+1.4473	0.0723
+0.9050	+0.4737	0.0214	+0.5944	0.0270	+1.6582	0.0859
+1.0160	+0.5165	0.0214	+0.6487	0.0269	+1.9221	0.0857

The resultant values from Lagrange interpolation are:

$$\begin{aligned}
R_{c,Na/Ca} &= 0.7361 \\
R_{c,Mg/Ca} &= 0.4791 \\
F_{c,Ca} &= 3.1875 E-6 \\
W_{c,Ca} &= 6.6435 \pm 0.1636 \\
W_{c,Na} &= 4.3797 \pm 0.1460 \\
W_{c,Mg} &= 9.2084 \pm 0.2079 \\
M_{V,c} &= 6.2563 \pm 0.1297 \\
(J-H)_c &= +0.4800 \pm 0.0216 \\
(J-K_S)_c &= +0.6018 \pm 0.0272 \\
(V-J)_c &= +1.6907 \pm 0.0867
\end{aligned}$$

### 5.5.3 Calculating the Diluted Parameters

Now that the parameters for the two star have been determined, they need to be combined and diluted appropriately. First the dilution at each measured spectral line from Eqns. H.18–H.20:

$$\begin{aligned}
D_{c,Ca} &= \frac{F_{c,Ca}}{F_{c,Ca} + F_{sd,Ca}} \\
D_{c,Na} &= \frac{D_{c,Ca}}{D_{c,Ca} + (1 - D_{c,Ca}) \left( \frac{R_{sd,Na/Ca}}{R_{c,Na/Ca}} \right)} \\
D_{c,Mg} &= \frac{D_{c,Ca}}{D_{c,Ca} + (1 - D_{c,Ca}) \left( \frac{R_{sd,Mg/Ca}}{R_{c,Mg/Ca}} \right)}
\end{aligned}$$

Then the diluted EWs and errors are simply:

$$\begin{aligned}
W_{i,D} &= D_i \times W_i \\
\sigma W_{i,D} &= D_i \times \sigma W_i
\end{aligned}$$

This results in diluted EWs of:

$$\begin{aligned} W_{\text{Ca},\text{D}} &= 2.3370 \pm 0.0576 \\ W_{\text{Na},\text{D}} &= 0.7423 \pm 0.0247 \\ W_{\text{Mg},\text{D}} &= 0.8929 \pm 0.0202 \end{aligned}$$

Then the diluted colors need to be calculated. First the value of  $\nu$  from:

$$\log \nu = \frac{M_{V,\text{sd}} - M_{V,\text{c}}}{2.5}$$

The values of the diluted colors are calculated using the equations given in §5.4 (see Eqn. 5.4–5.7). The final diluted colors are:

$$\begin{aligned} (J-K_S)_{\text{D}} &= +0.3305 \\ (V-K_S)_{\text{D}} &= +0.4868 \\ (H-K_S)_{\text{D}} &= +0.0731 \\ (B-K_S)_{\text{D}} &= +0.3545 \end{aligned}$$

The errors on the colors proved difficult to calculate analytically. So the errors were calculated by alternately adding, then subtracting each error from each value, and re-calculating the value of  $\nu$  and the diluted color (the values for the hot subdwarf were taken as exact, the errors only enter from the companion values). The final error on the diluted color was then taken as half the difference between the two extreme values. The final errors on these colors become:

$$\begin{aligned} \sigma(J-K_S)_{\text{D}} &= 0.0131 \\ \sigma(V-K_S)_{\text{D}} &= 0.0106 \\ \sigma(H-K_S)_{\text{D}} &= 0.0245 \\ \sigma(B-K_S)_{\text{D}} &= 0.0132 \end{aligned}$$

From these colors and errors it is possible to calculate all other colors and their associated errors. In particular the colors of interest for the actual fitting procedure (see §6.3) are:

$$\begin{aligned} (B-V)_{\text{D}} &= -0.1323 \pm 0.0169 \\ (J-K_S)_{\text{D}} &= +0.3305 \pm 0.0131 \\ (J-H)_{\text{D}} &= +0.2574 \pm 0.0278 \\ (V-K_S)_{\text{D}} &= +0.4868 \pm 0.0106 \end{aligned}$$

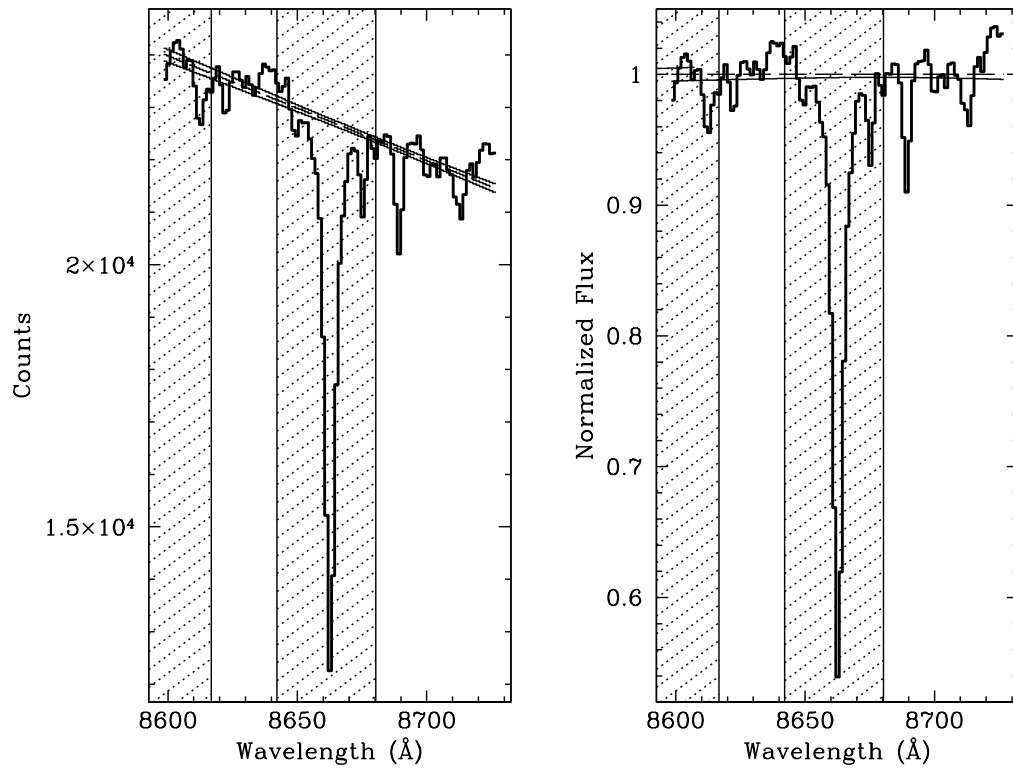


Fig. 5.1 Both panels show the Ca II 8662 Å line from the standard HIP 7117, along with its local continuum fit (dashed line), three times the continuum fit errors (thin solid lines), and the regions excluded from the continuum fit (shaded regions). The left panel shows the line and fit in detector counts, while the right shows the line and fit normalized.

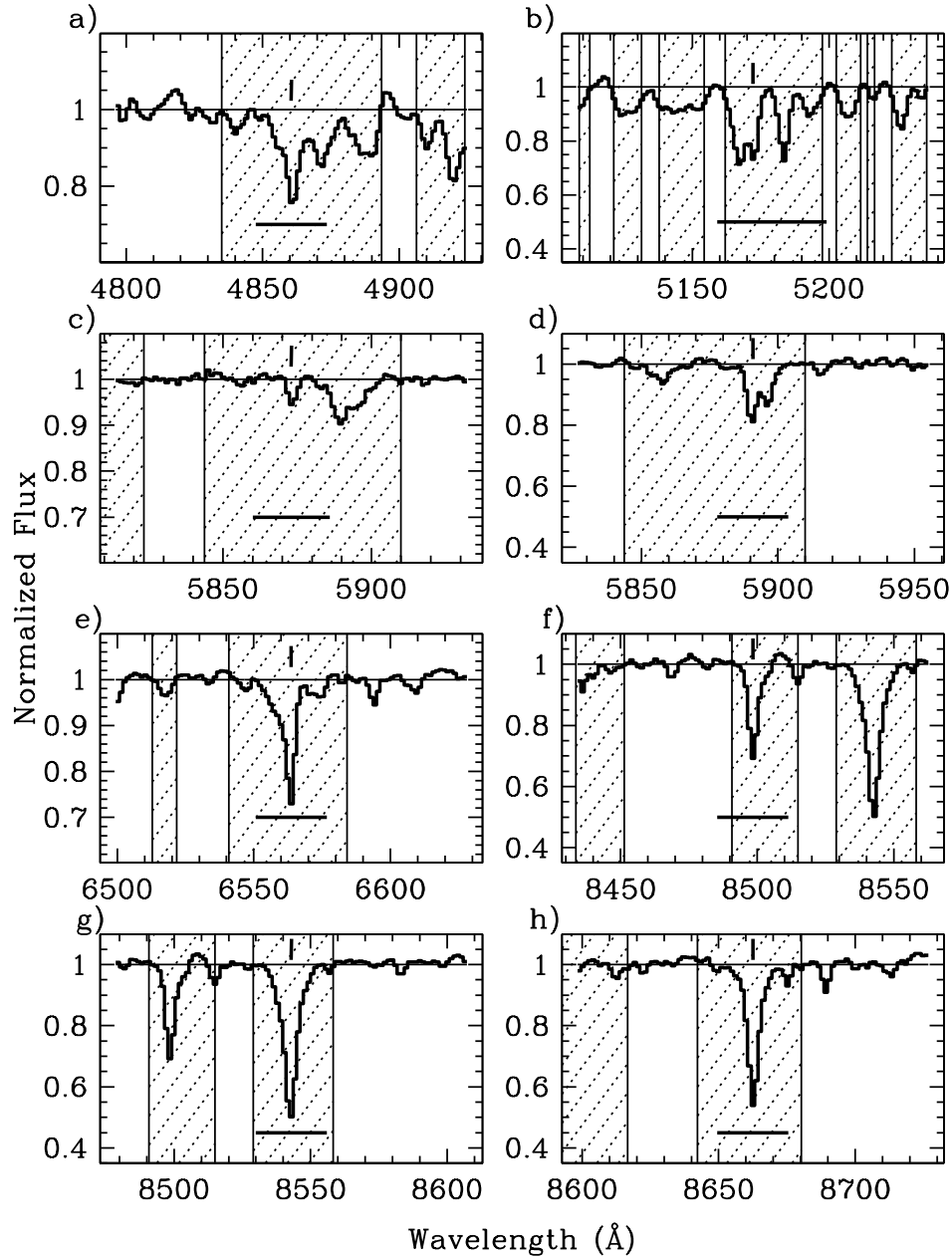


Fig. 5.2 Local continua fits for the lines: H $\beta$  (panel a), MgI b (panel b), HeI 5875 Å (panel c), Na I D (panel d), H $\alpha$  (panel e), Ca II triplet (panels f, g, and h). The shaded regions indicate wavelengths that were excluded when fitting the local continuum. The solid horizontal bar below the spectrum indicates the region EWs for the line were extracted over. (All lines are from the standard HIP 7117, except the He I line which is from the composite hot subdwarf #1346 PG 2148+095.)

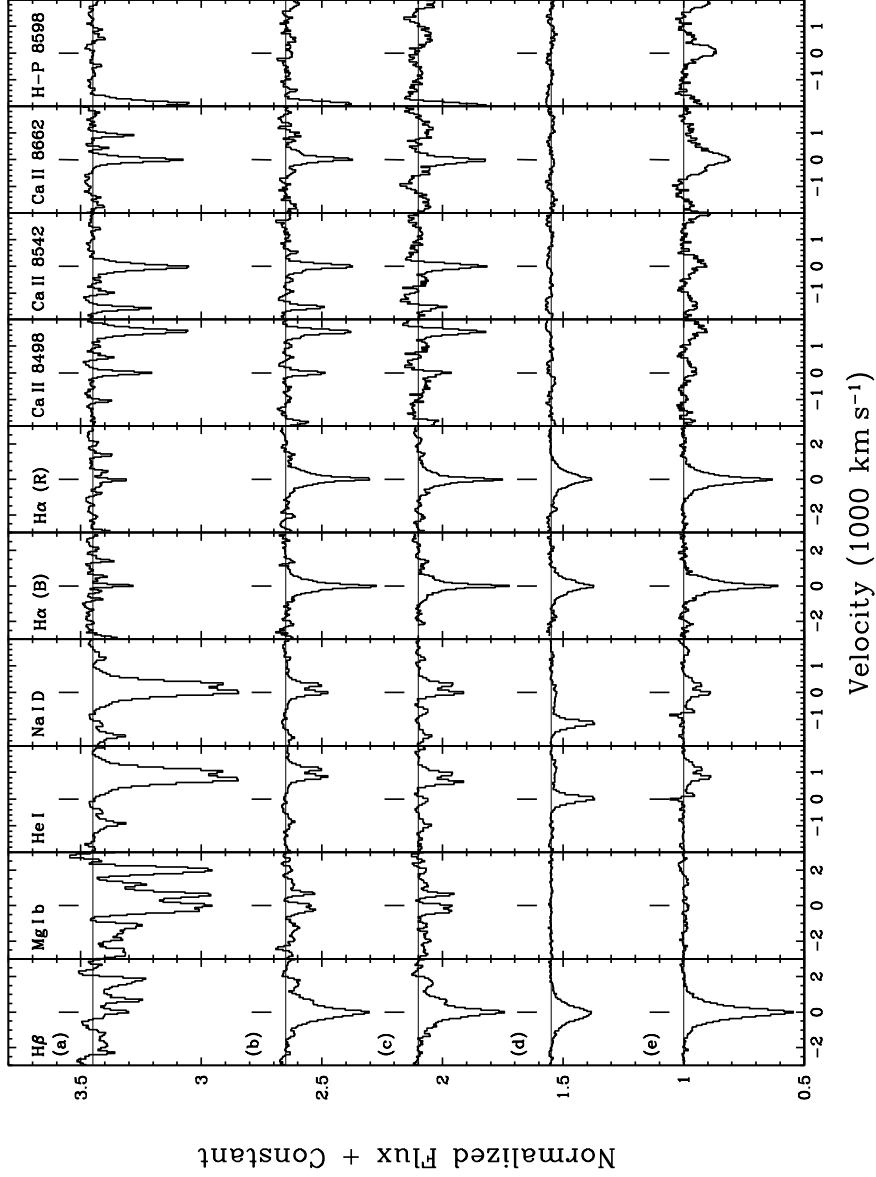


Fig. 5.3 Examples of local continua fits of the lines of interest for five objects (top to bottom): a. HIP 13345 (standard), b. #1306 PG 2118+126 (composite without He I 5875), c. #1096 PG 1648+080 (composite with He I 5875), d. #1187 BD+39°3226 (single without H-Paschen lines), e. #1357 PG 2159+051 (single with H-Paschen lines). The five left panels come from the blue spectrograph setup [H $\beta$ , Mg I b, He I 5875Å, Na I D, H $\alpha$  (B)], while the five right panels come from the red spectrograph setup [H $\alpha$  (R), Ca II 8498Å, Ca II 8542Å, Ca II 8662Å, Paschen-14 8598Å — H $\alpha$  is shown twice, once from each setup]. Each line is plotted in velocity coordinates, with zero corresponding to line center.



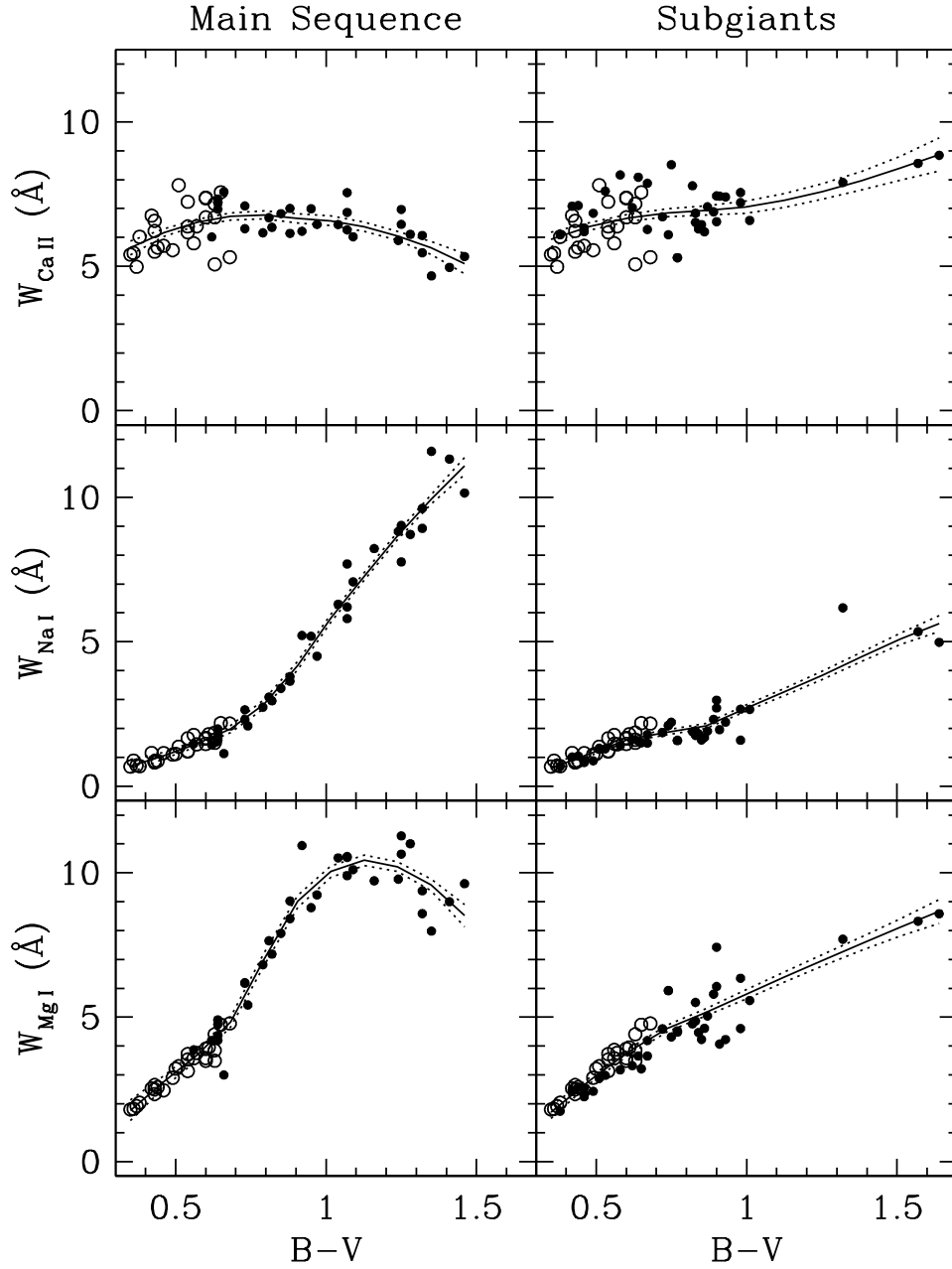


Fig. 5.4 *Loess* Fits to the HIP standard EW trends. All panels show EW (in Å) as the ordinate and  $B-V$  color as the abscissa, the solid line represents the *loess* fit, the dotted lines indicate  $\pm 1$  standard error on the fit (in the EW direction), and open circles represent objects that were used in both the main sequence and subgiant fits. Left panels are for main sequence stars, right are for subgiants. Top panels are for the total Ca II triplet, middle for Na I D, and bottom for Mg I b. *Loess* fit values are given in Table 5.1.

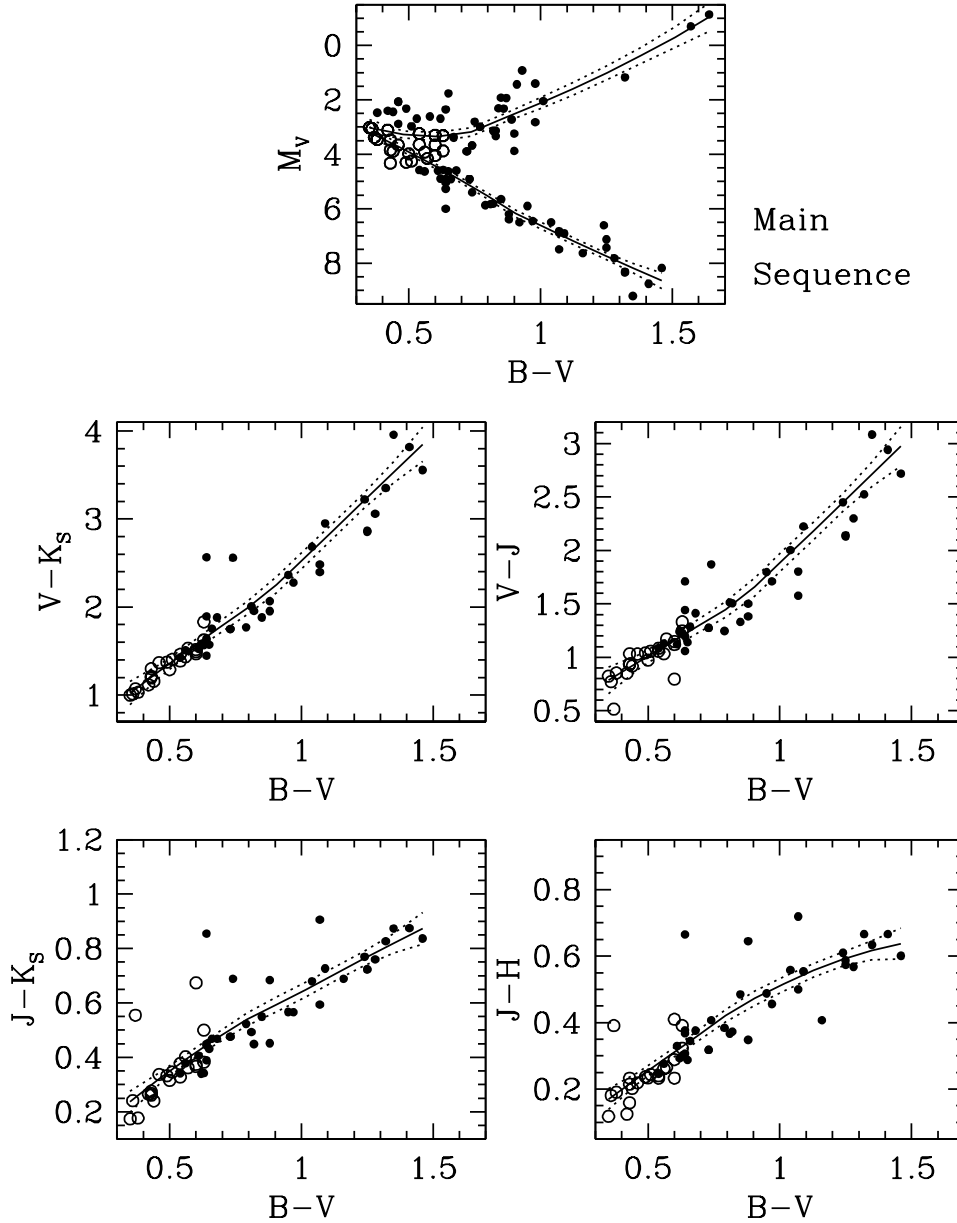


Fig. 5.5 *Loess* Fits to the HIP standard main sequence color trends. Top panel is the fit for all of the HIP stars'  $B-V$  color against  $M_V$ . The remaining panels all show the color-color fits for the HIP MS stars alone using  $B-V$  color as the abscissa and all other colors as the ordinate. Middle left panel is for  $V-K_S$ , middle right is for  $V-J$ , bottom left is for  $J-K_S$ , and bottom right is for  $J-H$ . In all panels, the open symbols were used in both the main sequence and subgiant fits, the solid line represents the best fit line, and the dashed lines indicate  $\pm 1$  standard error (in the  $M_V$  direction for the top panel, and in the ordinate color for all other panels). *Loess* fit values are given in Tables 5.2–5.4.

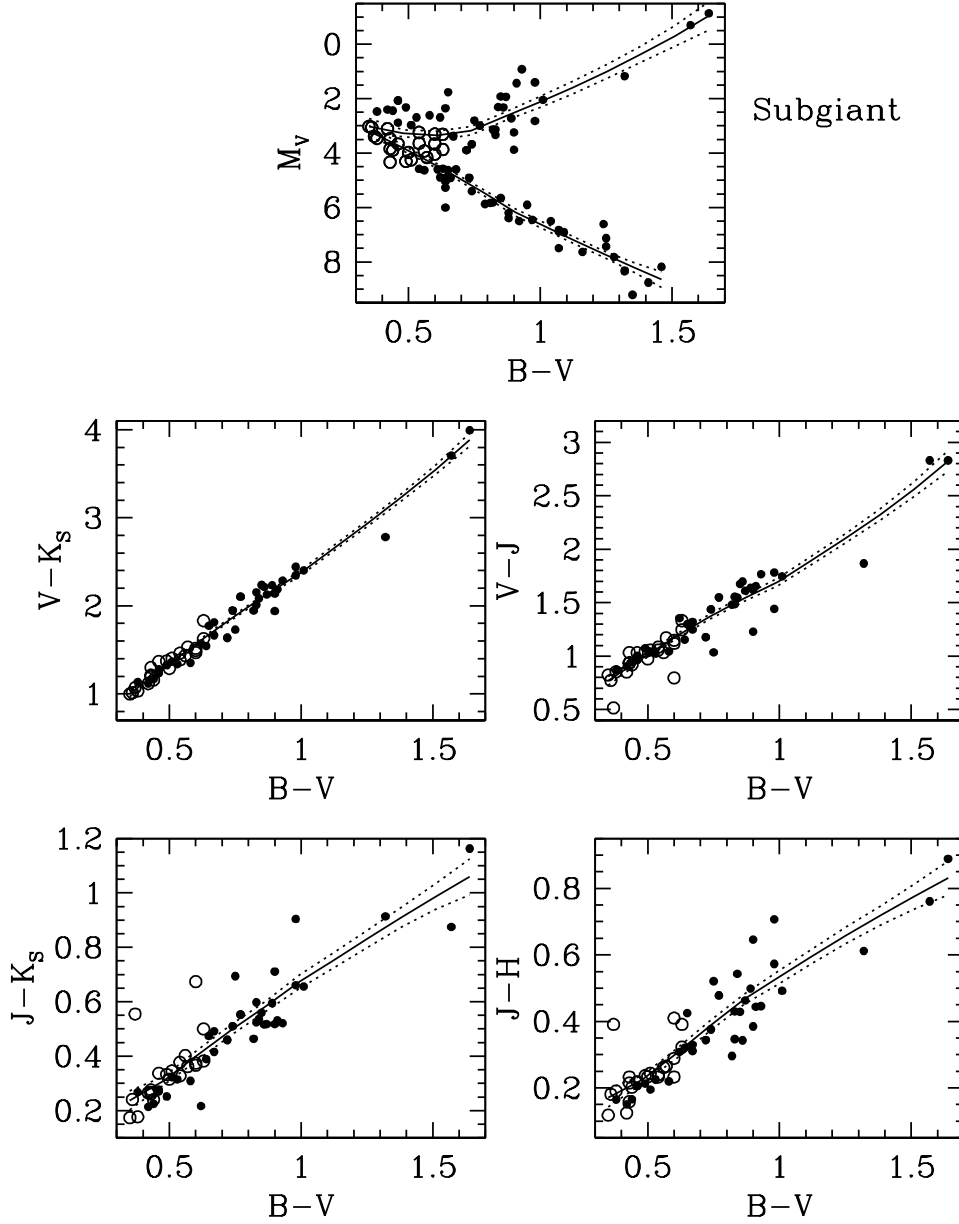


Fig. 5.6 Same as Figure 5.5 except showing the color-color *loess* fits for the HIP subgiants only, the  $(B-V, M_V)$  *loess* fit for all HIP stars is repeated in the top panel. *Loess* fit values are given in Tables 5.2–5.4.

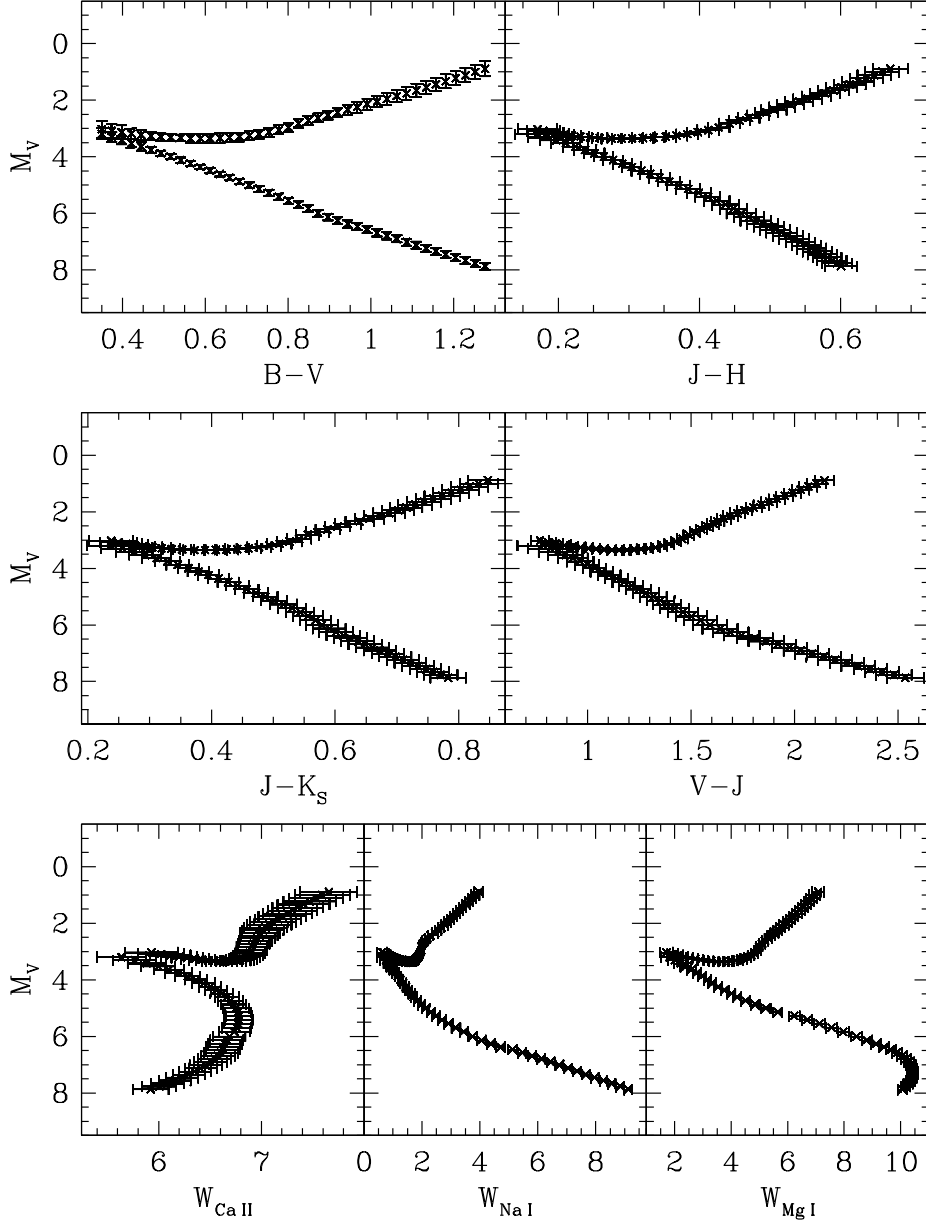


Fig. 5.7 Color and EW values of the models generated from the fits to the HIP standard parameters. Color-magnitude diagrams (all using  $M_V$  as the ordinate) are for:  $B-V$  (upper left),  $J-H$  (upper right),  $J-K_S$  (middle left),  $V-J$  (middle right). Diagrams of EW (in Å) and  $M_V$  are: Ca II (lower left), Na I (lower center), Mg I (lower right).

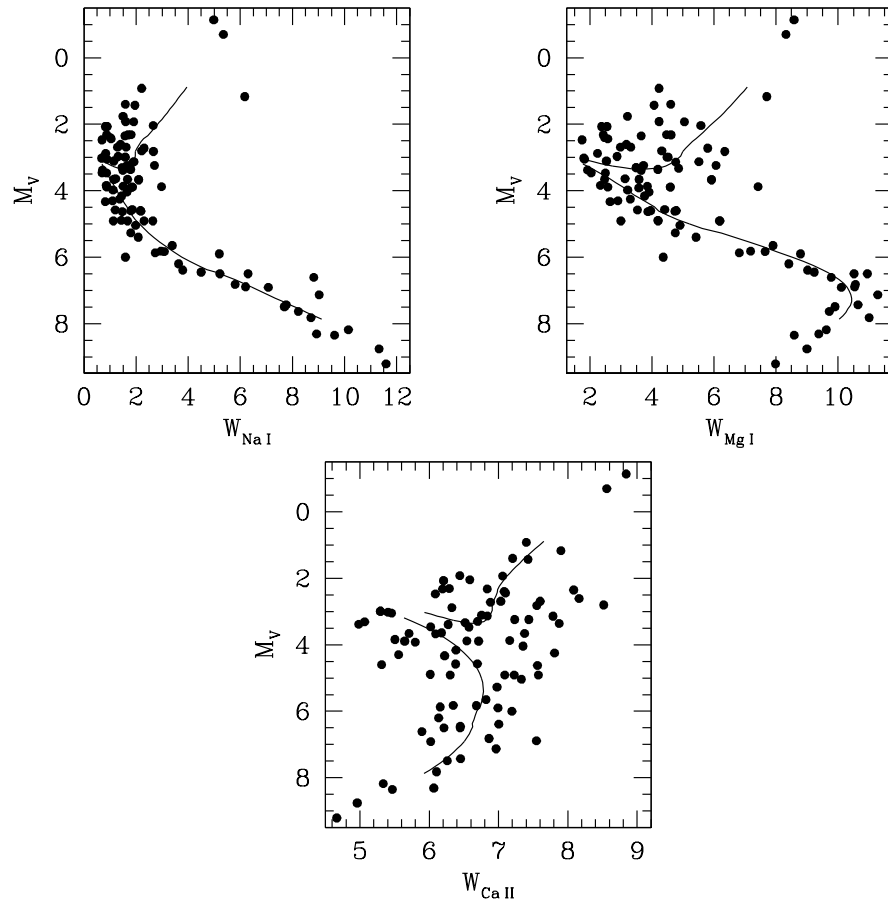


Fig. 5.8 Model EW compared with the observed EW values for the HIP standards. Diagrams of EW (in  $\text{\AA}$ ) and  $M_V$  are: Na I (upper left), Mg I (upper right), Ca II (lower center).

Table 5.1. *Loess* Fit to the HIP Standards' EW Measurements.

$B-V^a$	Ca II		Na I		Mg I	
	EW (Å)	Std. Err.	EW (Å)	Std. Err.	EW (Å)	Std. Err.
Main Sequence						
+0.350	5.63775	0.24098	0.68936	0.23470	1.77434	0.35661
+0.461	6.16397	0.13586	1.05957	0.11291	2.77094	0.19786
+0.572	6.52335	0.10832	1.47921	0.10933	3.70305	0.18254
+0.683	6.73024	0.12265	1.98127	0.12058	4.83446	0.17989
+0.794	6.77720	0.13645	2.84731	0.14793	7.01337	0.21831
+0.905	6.65665	0.16206	4.17660	0.14646	9.01223	0.20949
+1.016	6.57671	0.16297	5.81220	0.14153	10.04668	0.19488
+1.127	6.36834	0.15561	7.26904	0.13495	10.43262	0.18231
+1.238	6.05542	0.15932	8.66564	0.12575	10.21294	0.16806
+1.349	5.63489	0.21901	9.93036	0.15782	9.58594	0.20430
+1.460	5.09368	0.35057	11.08427	0.29371	8.51517	0.39030
Subgiants						
+0.350	5.92951	0.25547	0.62288	0.16318	1.71221	0.22149
+0.479	6.38168	0.13214	1.12793	0.06930	2.81497	0.09547
+0.608	6.67800	0.12755	1.62903	0.08013	3.80047	0.10712
+0.737	6.85415	0.14150	1.86735	0.08751	4.61928	0.11641
+0.866	6.93761	0.15846	2.08576	0.08363	5.17032	0.12085
+0.995	7.04656	0.21339	2.68859	0.10819	5.77673	0.15758
+1.124	7.28170	0.24002	3.25837	0.12626	6.38760	0.17611
+1.253	7.59375	0.26842	3.84317	0.13910	6.96988	0.19660
+1.382	7.96680	0.31788	4.47984	0.15827	7.54505	0.23180
+1.511	8.39404	0.41382	5.09849	0.20007	8.11181	0.30101
+1.640	8.87071	0.57291	5.63057	0.27958	8.66281	0.41741

<sup>a</sup>Independent variable.

Table 5.2. *Loess* Fit to the HIP Standards'  $M_V$  Measurements.

Main Sequence			Subgiant		
$B-V^a$	$M_V$	Std. Err.	$B-V^a$	$M_V$	Std. Err.
+0.350	+3.19357	0.19550	+0.350	+3.02372	0.29545
+0.461	+3.71794	0.10474	+0.479	+3.27244	0.12992
+0.572	+4.28210	0.08420	+0.608	+3.35374	0.15803
+0.683	+4.87272	0.09712	+0.737	+3.18000	0.15832
+0.794	+5.50676	0.11083	+0.866	+2.64820	0.15550
+0.905	+6.17813	0.12859	+0.995	+2.13141	0.20150
+1.016	+6.68578	0.12995	+1.124	+1.59104	0.23628
+1.127	+7.20338	0.12270	+1.253	+0.99775	0.26149
+1.238	+7.70173	0.12396	+1.382	+0.36820	0.29675
+1.349	+8.17886	0.17235	+1.511	-0.30751	0.37336
+1.460	+8.64874	0.28259	+1.640	-1.04461	0.52168

<sup>a</sup>Independent variable.

Table 5.3. *Loess* Fit to the HIP Main Sequence Color Measurements.

$B-V^a$	$V-K_S$		$V-J$		$J-H$		$J-K_S$	
	Color	Std. Err.	Color	Std. Err.	Color	Std. Err.	Color	Std. Err.
+0.350	+1.02198	0.13155	+0.78468	0.12486	+0.17007	0.03116	+0.23730	0.03919
+0.461	+1.27424	0.07029	+0.95139	0.06672	+0.23342	0.01665	+0.32285	0.02094
+0.572	+1.51658	0.05669	+1.11587	0.05381	+0.29564	0.01343	+0.40072	0.01689
+0.683	+1.75496	0.06577	+1.28265	0.06243	+0.35730	0.01558	+0.47231	0.01960
+0.794	+1.98689	0.07618	+1.44732	0.07231	+0.42080	0.01805	+0.53957	0.02270
+0.905	+2.25259	0.09047	+1.65816	0.08588	+0.47365	0.02143	+0.59443	0.02696
+1.016	+2.57079	0.09027	+1.92206	0.08568	+0.51651	0.02139	+0.64873	0.02690
+1.127	+2.88670	0.08631	+2.18068	0.08193	+0.55678	0.02045	+0.70602	0.02572
+1.238	+3.20828	0.08820	+2.44515	0.08372	+0.59042	0.02090	+0.76312	0.02628
+1.349	+3.53062	0.12131	+2.71160	0.11515	+0.61715	0.02874	+0.81902	0.03614
+1.460	+3.84751	0.19507	+2.97378	0.18516	+0.63755	0.04621	+0.87373	0.05812

<sup>a</sup>Independent variable.



Table 5.4. *Loess* Fit to the HIP Subgiant Color Measurements

$B-V^a$	$V-K_S$		$V-J$		$J-H$		$J-K_S$	
	Color	Std. Err.	Color	Std. Err.	Color	Std. Err.	Color	Std. Err.
+0.350	+0.99911	0.03288	+0.76914	0.04275	+0.17064	0.02753	+0.23755	0.03531
+0.479	+1.29437	0.01700	+0.98180	0.02211	+0.22472	0.01225	+0.31027	0.01571
+0.608	+1.58265	0.01651	+1.18376	0.02147	+0.30274	0.01462	+0.40467	0.01876
+0.737	+1.86037	0.01827	+1.37102	0.02376	+0.38720	0.01531	+0.49837	0.01963
+0.866	+2.12433	0.02040	+1.54077	0.02652	+0.46658	0.01497	+0.58314	0.01920
+0.995	+2.36942	0.02749	+1.69549	0.03574	+0.53114	0.01936	+0.67416	0.02483
+1.124	+2.65265	0.03091	+1.90002	0.04020	+0.59663	0.02176	+0.75243	0.02791
+1.253	+2.93901	0.03476	+2.10633	0.04520	+0.65926	0.02433	+0.83244	0.03121
+1.382	+3.23535	0.04131	+2.32420	0.05372	+0.71830	0.02856	+0.91101	0.03663
+1.511	+3.54848	0.05380	+2.56159	0.06996	+0.77504	0.03690	+0.98688	0.04733
+1.640	+3.88600	0.07442	+2.82691	0.09678	+0.83134	0.05120	+1.05913	0.06567

<sup>a</sup>Independent variable.

## Chapter 6

# Classification of Composite Spectrum Hot Subdwarfs

## 6.1 Introduction

This chapter will describe the identification of the best fit models for the observed composite hot subdwarfs. First I will discuss briefly the overall classification that appears to be most consistent with the majority of the composite hot subdwarfs. Then I will demonstrate choosing the best fit for an individual composite hot subdwarf, and I will walk through the fitting process in detail for one of the objects. Finally, I will discuss the results of the individual fits and point out a few interesting and unusual cases.

## 6.2 Overall Comparison

A general comparison between all observed composite hot subdwarfs and the diluted composite models is illuminated in Figures 6.1 and 6.2. Figure 6.1 shows a projection of the three dimensional space formed by the three values of EW, and compares the distribution of the observed composite hot subdwarfs with main sequence and subgiant models separately. Figure 6.2 shows the 2MASS color-color spaces of  $(J-K_S, B-V)$  and  $(J-K_S, H-K_S)$ , again comparing the distributions of observed composites with main sequence and subgiant models separately. In both of these figures, the locus of observed composite points is overall more consistent with the main sequence models than with the subgiant models (with the exception of a few extreme outliers).

Four outliers are labelled with the numbers 1–4 in Figures 6.1 and 6.2. These four objects are as follows:

1. #1223 HD 185510
2. #150 PG 0232+095
3. #1457 BD–7°5977
4. #551 PB 3854

Stars #1223 and #1457 were both previously classified to have subgiant or giant companions (see Table 4.3, and also §6.6.2). Star #150 has been called “sd+K”; previous temperature determinations of the subdwarf have placed it at  $\sim 21$  kK, but with  $\log g \sim 6.0 - 6.9$ , which is rather high for a “cool” hot subdwarf (see Table 4.3, and also §6.6.3). Star #551 has very little prior published information (no determination of  $T_{\text{eff}}$  or  $\log g$ , and no classification of the late-type companion; see Table 4.3).

The next step is to identify the best fit for each hot subdwarf individually.

### 6.3 Matching Observations with Models

Using the collection of diluted (sdB+late-type star) models discussed in §5.4, I found the model that best matches each observed hot subdwarf. I did this by comparing the parameters for the observed composite hot subdwarfs with those of the models using a minimum  $\chi^2$  technique (see also §F.1). To calculate  $\chi^2$  I considered the following measurements: EWs of CaT, Na I D, and Mg I b, along with the colors  $J-K_S$ ,  $J-H$ ,  $V-K_S$ , and  $B-V$  (or the available subset of these seven). I considered the errors on both the observed quantities and the fitted models when calculating  $\chi^2$  (see §6.4 for an example).

For the  $V-K_S$  and  $B-V$  colors, an error of 0.02 mag was assumed on the observed  $V$  magnitude. This error was used in the calculation of the  $V-K_S$  error, and directly as the error for  $B-V$ . For the several objects that had visible DIBs in their spectra (§4.6.1), a reddening correction (following §C.2.2) was made to their colors to account for the values of  $E(B-V)$  for their lines of sight (given in Table 4.3) before calculating  $\chi^2$ . Reddening corrections (of the amount given in Table 4.3) were applied to the colors of: #172 PG 0314+103, #199 KUV 04110+1434, and #203 KUV 04237+1649, before calculating the value of  $\chi^2$ . No corrections were made to the EWs to account for interstellar absorption.

The best fit model was taken to be that which produced the minimum value of  $\chi^2$ . Errors on the best fit were taken as the “ $3\sigma$  range” in  $\chi^2$  around the best fit, defined by:  $\chi_i^2 - \chi_{\min}^2 \leq 3$ . The resulting fits to individual observations are given in Table 6.1.

The adopted fits are given in Table 6.2. In cases where more than one observation exists, then the adopted values of  $B-V$  and  $M_V$  are the average of the individual observations (ignoring any observations that were significantly affected by fringing at the CaT). Temperature for both the late-type companion and the hot subdwarf (based on the  $B-V$  color), and the approximate spectral type of the late type companion (based on  $T_{\text{eff}}$ ), are also listed in Table 6.2.

### 6.4 Walk-through of an Individual Case

In this section I will walk through the calculation of  $\chi^2$  for the case of #120, PHL 3802, as an example of the procedure.

The observed properties of the composite subdwarf are as follows:

$$\begin{aligned}
 V_{\text{obs}} &= 12.35 \pm 0.02 \\
 (B-V)_{\text{obs}} &= -0.059 \pm 0.02 \\
 J_{\text{obs}} &= 11.997 \pm 0.038 \\
 (J-H)_{\text{obs}} &= +0.258 \pm 0.057 \\
 (J-K_S)_{\text{obs}} &= +0.230 \pm 0.057 \\
 (V-K_S)_{\text{obs}} &= +0.583 \pm 0.071 \\
 W_{\text{Ca, obs}} &= 1.9347 \pm 0.1958 \\
 W_{\text{Na, obs}} &= 0.8093 \pm 0.0693 \\
 W_{\text{Mg, obs}} &= 1.0615 \pm 0.0912
 \end{aligned}$$

The error on the  $V$  magnitude is assumed to be 0.02, while the  $B-V$  error is set equal to the  $V$  error. The errors listed for the EWs are the total errors [ $\sigma_W^2 = \sigma_W^2(F) + \sigma_W^2(C)$ ]. For this object, no reddening correction was made [ $E(B-V)$  was assumed to be zero].

The best-fit model (the one with the lowest value of  $\chi_R^2$  is comprised of the following two stars:

$$M_{V,c} = 5.8332^{+0.4231}_{-0.1427} \quad (6.1)$$

$$(B-V)_c = +0.8487^{+0.0713}_{-0.0238} \quad (6.2)$$

$$M_{V,sd} = 4.2247^{+0.0684}_{-0.0700} \quad (6.3)$$

$$(B-V)_{sd} = -0.2333^{+0.0041}_{-0.0042} \quad (6.4)$$

The ratio of the flux at  $V$  between these two stars ( $F_{V, \text{rat}} = \frac{F_{V, \text{comp}}}{F_{V, \text{sd}}}$ , drawn from Equ. C.23) is:

$$\log F_{V, \text{rat}} = \frac{M_{V, \text{sd}} - M_{V, \text{comp}}}{2.5} = \frac{4.2247 - 5.8332}{2.5} = -0.6434$$

which results in  $F_{V, \text{rat}} = 0.2273$ .

The values of the diluted colors calculated for this best-fit model are:

$$(B-V)_D = -0.0985 \pm 0.0120$$

$$(J-K_S)_D = +0.3370 \pm 0.0130$$

$$(J-H)_D = +0.2597 \pm 0.0265$$

$$(V-K_S)_D = +0.5660 \pm 0.0194$$

and the diluted EWs:

$$W_{\text{Ca}, D} = 2.5916 \pm 0.0568$$

$$W_{\text{Na}, D} = 0.6839 \pm 0.0299$$

$$W_{\text{Mg}, D} = 0.9952 \pm 0.0273$$

The value of  $\chi^2$  for this fit was calculated using:

$$\chi^2 = \sum_{k=0}^n \frac{(O_k - D_k)^2}{\sigma_{k,O}^2 + \sigma_{k,D}^2} \quad (6.5)$$

where  $n$  is the number of measurements,  $O_k$  are the observed values,  $D_k$  are the model values,  $\sigma_{k,O}^2$  is the error on the measured values, and  $\sigma_{k,D}^2$  is the error on the model values.

For this object the individual terms of  $\chi^2$  are:

$$\begin{aligned}
\frac{[(B-V)_{\text{obs}} - (B-V)_{\text{D}}]^2}{\sigma_{B-V, \text{obs}}^2 + \sigma_{B-V, \text{D}}^2} &= \frac{[(-0.059) - (-0.0985)]^2}{0.02^2 + 0.0120^2} = 2.864656 \\
\frac{[(V-K_S)_{\text{obs}} - (V-K_S)_{\text{D}}]^2}{\sigma_{V-K_S, \text{obs}}^2 + \sigma_{V-K_S, \text{D}}^2} &= \frac{(0.583 - 0.5660)^2}{0.071^2 + 0.0194^2} = 0.053647 \\
\frac{[(J-K_S)_{\text{obs}} - (J-K_S)_{\text{D}}]^2}{\sigma_{J-K_S, \text{obs}}^2 + \sigma_{J-K_S, \text{D}}^2} &= \frac{(0.230 - 0.3370)^2}{0.057^2 + 0.0130^2} = 3.350858 \\
\frac{[(J-H)_{\text{obs}} - (J-H)_{\text{D}}]^2}{\sigma_{J-H, \text{obs}}^2 + \sigma_{J-H, \text{D}}^2} &= \frac{(0.258 - 0.2597)^2}{0.057^2 + 0.0265^2} = 0.000716 \\
\frac{(W_{\text{Ca, obs}} - W_{\text{Ca, D}})^2}{\sigma_{\text{Ca, obs}}^2 + \sigma_{\text{Ca, D}}^2} &= \frac{(1.9347 - 2.5916)^2}{0.1958^2 + 0.0568^2} = 10.381867 \\
\frac{(W_{\text{Na, obs}} - W_{\text{Na, D}})^2}{\sigma_{\text{Na, obs}}^2 + \sigma_{\text{Na, D}}^2} &= \frac{(0.8093 - 0.6839)^2}{0.0693^2 + 0.0299^2} = 2.759438 \\
\frac{(W_{\text{Mg, obs}} - W_{\text{Mg, D}})^2}{\sigma_{\text{Mg, obs}}^2 + \sigma_{\text{Mg, D}}^2} &= \frac{(1.0615 - 0.9952)^2}{0.0912^2 + 0.0273^2} = 0.485187
\end{aligned}$$

This results in a total  $\chi^2 = 19.896$ ; my program gives a value of 19.903 (this slight difference can be accounted for by rounding errors I made in this example calculation). Given that there are seven degrees of freedom (DOF),  $\chi_R^2 = \chi^2/\text{DOF} = 19.903/7 = 2.84$ , for the best-fit. In this example, the value of  $\chi^2$  was dominated by the CaT EW, followed by the  $J-K_S$  and  $B-V$  colors, then the Na I D EW and the Mg I b EW, and finally the  $V-K_S$  and  $J-H$  colors contributed very little.

The  $3\sigma$  spread is listed as the error on each parameter of the two stars in this fit [specifically as errors on  $(B-V)_c$ ,  $M_{V,c}$ ,  $(B-V)_{\text{sd}}$ , and  $M_{V,\text{sd}}$ ]. For each model, the difference in its value of  $\chi^2$  from the minimum  $\chi^2$  was taken. For those models that had  $\chi_i^2 - \chi_{\text{min}}^2 \leq 3$ , the difference between those most deviant from the best-fit and the values of the best-fit were used as errors. In this example, the  $3\sigma$  ( $\Delta\chi^2 \leq 3$ ) range in the parameters is:

$$\begin{aligned}
5.6905 &\leq M_{V,c} \leq 6.2563 \\
+0.8249 &\leq (B-V)_c \leq +0.9200 \\
4.1547 &\leq M_{V,\text{sd}} \leq 4.2931 \\
-0.2375 &\leq (B-V)_{\text{sd}} \leq -0.2292
\end{aligned}$$

The difference between the values for the best fit and these values resulted in the errors shown in Eqn. 6.1–6.4. These values are somewhat correlated (see Figure 6.3) and actually form a tilted ellipse.

A graphical representation of the  $\chi^2$  space for #120 PHL 3802 in terms of  $(B-V)_c$ ,  $(B-V)_{\text{sd}}$ , and  $M_{V,\text{sd}}$  is shown in Figure 6.3. Figure 6.4 compares the  $1-3\sigma$  intervals for the best-fit models to the observed parameters of #120 PHL 3802.

The temperature corresponding to this best-fit model was determined using the  $B-V$  color and interpolating (see Appendix J) the values given in Table H.1. For this object,  $(B-V)_c = 0.8487$ , the corresponding three values from Table H.1 to interpolate among are:

Type	$B-V$	$T_{\text{eff}}$
K2	0.933	5000
K0	0.851	5250
G7	0.769	5500

The three 2nd order Lagrange coefficients (from Eqn. J.3–J.5) become:

$$\begin{aligned}
L_{2,0}(0.8487) &= \frac{(0.8487-0.851)(0.8487-0.769)}{(0.933-0.851)(0.933-0.769)} = -0.01363 \\
L_{2,1}(0.8487) &= \frac{(0.8487-0.933)(0.8487-0.769)}{(0.851-0.933)(0.851-0.769)} = 0.999213 \\
L_{2,2}(0.8487) &= \frac{(0.8487-0.933)(0.8487-0.851)}{(0.769-0.933)(0.769-0.851)} = 0.014418
\end{aligned}$$

These coefficients result in a final interpolated temperature value (from Eqn J.6) of:

$$P(0.8487) = 5000 \times -0.01363 + 5250 \times 0.999213 + 5500 \times 0.014418 = 5257$$

The actual value (without the rounding errors of this example calculation) has been rounded to 5250 K, and identified with an appropriate spectral type of K0V in Table 6.2.

## 6.5 Summary of Companion Classifications

Aside from some objects that I will discuss in §6.6, the majority of composite-colored hot subdwarfs are well modelled as the combination of sdB+MS. Comparisons of fits are shown in Figures 6.5–6.6. Figure 6.5 compares the spectra of two composites that were both fitted with similar hot subdwarfs and companions, while Figure 6.6 compares the spectra of two composites that were fitted with similar companions (in this case G0IV and G0-IIIV companions) but different hot subdwarfs (one a cool, bright hot subdwarf and the other a hot, faint hot subdwarf).

Values for the best fits ( $B-V$ ,  $M_V$ ,  $\chi^2$ , DOF, etc.) for all observations are given in Table 6.1. The corresponding  $T_{\text{eff}}$ , spectral type, and the final adopted values for each object are given in Table 6.2. Plots of various parameters (including the best-fit models and the observed composite colors) are given in Figures 6.7–6.11. In general, from Figure 6.7, the majority of MS companions cluster in the range of  $0.5 \lesssim (B-V)_c \lesssim 1.1$ . There are outliers at both low and high  $(B-V)_c$ .

A comparison of my classifications for the late-type companions with previous classifications from the literature is given in Table 6.3. A similar table comparing my temperature for the hot subdwarf with previous determinations from the literature is given in Table 6.4. In some cases, where multiple previous determinations for the companion were available, the best-fit parameters could differ significantly from each other (for example, #1 SB 7:  $\approx 7000$  vs. 5750 (G2); and #1182 BD+29°3070: 5250 (K0) vs.  $8550 \pm 400$ ). However, most of the time my fit for the late-type companion is reasonably close to at least one of the previous determinations (within one spectral type, or within the temperature errors). The cases where my determinations differ significantly from previous determinations are marked with a star (“\*”) in the notes column of Table 6.3. Note that in some of these cases the previous determination is very uncertain, such as #120 PHL 3802 where the previous determination is:  $\approx 5500$  K.

Since I am assuming ZAEHB hot subdwarf stars in my models, I attempted to determine the effect evolution of the subdwarf would have on the my classifications by refitting the composites with approximate terminal-age EHB (TAEHB) models. To approximate a TAEHB model, I increased the model luminosity of the EHB stars by 0.3 dex (which corresponds to 0.75 mag, based on the models of Dorman, Rood, & O’Connell 1993), then recalculated the diluted EWs, colors, and  $\chi^2$ . Figure 6.12 displays the comparisons of  $(B-V)_{\text{ZAEHB}}$  with  $(B-V)_{\text{TAEHB}}$  and  $M_V^{\text{ZAEHB}}$  with  $M_V^{\text{TAEHB}}$  for both the late-type companion and the hot subdwarf from the best-fit for each object. In this figure, the diagonal lines indicate no variation between the ZAEHB and TAEHB. There is significant scatter around the line of no variation, however there are no distinct trends (i.e., the companions are not obviously all uniformly earlier-type — there may be a slight trend of selecting slightly earlier and more luminous companions with TAEHB subdwarfs than with ZAEHB). Regardless, I am simply reporting the results for the ZAEHB models.

I attempted to classify the late-type companions in resolved visual doubles (see §4.6.3) using the undiluted late-type companion models. I only attempted to classify those companions whose spectra were not contaminated by light from the neighboring hot subdwarf and which had reliable measurements of Mg I b, Na I D, and CaT (if available). Thus I excluded the companion to #550 (HZ 18) which appears to be another sdB or HBB-type star, as well as #91 (PB 8555) and #1027 (PG 1618+562) which have partially blended spectra. The final adopted fits are listed in Table 6.5. Based on a comparison by eye of absolute magnitude of the best model, the apparent magnitude difference from Figures 4.20–4.22, and the average  $M_V$  of a hot subdwarf, it seems possible that #50, 87, 700, and 1348 may be associated, while #157, 187, 1461, and #130 are likely not associated.

## 6.6 Interesting Cases

Some objects posed unique difficulties in fitting, I will discuss these objects here. All of these objects are marked with a symbol (\*, †, §) in the “Notes” column of Table 6.2. These “interesting” cases can be broken into three groups: (1) off the grid (†), (2) fit with subgiant companion (§), and (3) a couple of strange objects (\*).

### 6.6.1 Grid Edges

Eighteen objects have late-type companion best-fits right at or very near the edge of the grid (these objects are marked with a “†” in the notes column of Table 6.2). These are:

1. #95 PG 0110+262,  $(B-V)_c \lesssim +0.35$
2. #102 PB 8783,  $(B-V)_c \lesssim +0.35$
3. #172 PG 0314+103,  $(B-V)_c \lesssim +0.35$  [ $E(B-V) \approx 0.53$ , with DIBs visible in the spectrum]
4. #187A HDE 283048,  $(B-V)_c \lesssim +0.35$

5. #199 KUV 04110+1434,  $(B-V)_c \lesssim +0.35$  [ $E(B-V) \approx 0.61$ , with DIBs visible in the spectrum, and Paschen lines]
6. #203 KUV 04237+1649,  $(B-V)_c \lesssim +0.35$  [ $E(B-V) \approx 0.41$ , with DIBs visible in the spectrum]
7. #533 BD+10°2357,  $(B-V)_c \lesssim +0.35$  (Paschen lines, fringing, sdO)
8. #638 PG 1257-0233,  $(B-V)_c \lesssim +0.40$  (fringing)
9. #937 PG 1536+278,  $(B-V)_c \lesssim +0.37$  (fringing)
10. #1182 BD+29°3070,  $(B-V)_c \lesssim +0.39$
11. #1297 PG 2110+127,  $(B-V)_c \lesssim +0.35$
12. #1304 PG 2116+008,  $(B-V)_c \gtrsim +1.28$  (sdO)
13. #1306 PG 2118+126,  $(B-V)_c \lesssim +0.35$
14. #1346 PG 2148+095,  $(B-V)_c \lesssim +0.35$
15. #1348 PG 2151+100,  $(B-V)_c \gtrsim +1.28$
16. #1356 PG 2158+082,  $(B-V)_c \lesssim +0.35$  (sdO)
17. #1424 Balloon 090900007,  $(B-V)_c \lesssim +0.35$
18. #1461A PB 5333,  $(B-V)_c \gtrsim +1.28$

The following objects are those where the 3-sigma range about the best-fit hot subdwarf model extends beyond the grid of models (and is therefore poorly defined):

1. #533 BD+10°2357,  $(B-V)_{sd} \gtrsim -0.200$  (Paschen lines, fringing, sdO)
2. #583 LB 2392,  $(B-V)_{sd} \gtrsim -0.200$  (McDonald spectrum, very low S/N)
3. #702 PG 1343+578,  $(B-V)_{sd} \gtrsim -0.200$  (some Paschen lines)
4. #706 PG 1347+086,  $(B-V)_{sd} \gtrsim -0.200$
5. #789 PG 1429+406,  $(B-V)_{sd} \lesssim -0.279$
6. #937 PG 1536+278,  $(B-V)_{sd} \lesssim -0.279$  (fringing)
7. #1182 BD+29°3070,  $(B-V)_{sd} \lesssim -0.267$
8. #1297 PG 2110+127,  $(B-V)_{sd} \lesssim -0.267$
9. #1346 PG 2148+095,  $(B-V)_{sd} \gtrsim -0.200$
10. #1356 PG 2158+082,  $(B-V)_{sd} \lesssim -0.275$  (sdO)
11. #1424 Balloon 090900007,  $(B-V)_{sd} \lesssim -0.279$

The values for the companions or hot subdwarfs should be taken as limits (either upper or lower as appropriate). It is also possible that some the objects are not in fact sdB+late-type composites (they could be metal poor early-type stars), or that the hot members are not truly sdB stars (i.e., they could be HBB, or sdO stars with either higher or lower luminosities than normal sdB stars and are therefore not covered by my modelling). A few of these are affected by fringing at the CaT, and it is possible this has adversely affected the classification of those objects.



Objects #199 and 533 both show strong Paschen lines (#702 shows weak Paschen lines). Additionally, #199 is highly reddened,  $E(B-V) \approx 0.61$ , so with a  $(J-K_S)_{\text{obs}} = +0.094$ , it is most likely a single star which slipped into the composite sample due to reddening (its “fit” is still listed in Tables 6.1–6.4 for completeness). Star #533 has been previously classified as sdO+A, so it is not surprising that there are strong Paschen lines, or that my models have difficulty fitting it.

Objects #102, 187A, 1304, 1356, 1461A, all show He II, which could indicate they are actually sdO (#1304 and 1356 have been previously classified sdO). Object #187A shows incredibly strong He I lines, as well as weaker He II (in fact it has some of the strongest He I lines of any of the hot subdwarfs observed). Object #1356 shows strong He II lines, and also He I, in fact it has been previously classified as He-sdO, so it no surprise that I was unable to fit it.

### 6.6.2 Subgiant Companions

Nine objects were best fitted with subgiant companions (marked with “§” in the notes column of Table 6.2):

1. #101 PG 0116+242 (G0IV)
2. #150 PG 0232+095 (G2IV) – see also §6.6.3
3. #294 PG 0900+400 (G1IV) – see also §6.6.3
4. #706 PG 1347+086 (G0IV)
5. #789 PG 1429+406 (F8IV)
6. #849 PG 1451+472 (G0IV)
7. #1096 PG 1648+080 (G0-1IV)
8. #1223 HD 185510 (K3IV)
9. #1457 BD–7°5977 (G7IV)

Objects #101, 294, 706, 789, and 937 are best modelled with late-F or early-G subgiants companions (even if the hot subdwarf is TAEHB). Objects #150, 849, and 1096 had more significant changes when TAEHB was assumed: #150 became K0IV, #849 became <A9V, and #1096 became G4IV. Additionally, #1457 was best modelled with a later-type companion of K0IV when assuming TAEHB. Object #1223 showed no change between ZAEHB and TAEHB.

Both #1223 and 1457 have been previously classified as sdB+K0III-IV (see Table 4.3). My classifications are close, but not entirely consistent with these previous classifications. There was one other previously classified subgiant companion in my initial sample, #1355 BD–3°5357 (which is classified as sdOB+G8III), however, this object also shows emission lines in its spectrum (Figure 4.14) so I did not attempt to classify it using my technique.

Six objects in addition to the ten above were classified with subgiant companions when TAEHB hot subdwarfs were assumed. These additional objects are:

1. #234 BD+34°1543 (F8IV)

2. #460 PG 1104+243 (G0-1IV)
3. #630 TON 139 (F7-8IV)
4. #895 PG 1514+034 (F8-9IV)
5. #937 PG 1536+278 (G0IV)
6. #1164 PG 1718+519 (G0-1IV)

### 6.6.3 Some Unusual Objects

There is the case of #150 PG 0232+095 (there is a “\*” in the notes column of Table 6.2, spectrum is shown in Figure 4.14). This object shows many spectral features in common with #1223 HD 185510, #1457 BD−7°5977, and #1355 BD−3°5357, in particular they all show a dip in their spectra around  $\sim 7900\text{--}8000\text{ \AA}$  that is likely due to a CN-red molecular band system. (*These four objects are the only composite spectrum hot subdwarfs in my sample to show this feature.*) However, the CaT in #150 is exceptionally weak compared to other composite subdwarfs. Including the CaT in the ZAEHB classification of this object leads to a rather poor upper limit fit with a very hot main sequence companion [ $(B-V)_c \lesssim +0.35$ ,  $\chi_R^2 \approx 41$ , Table 6.1), whereas excluding CaT from the fit leads to a fit (also poor) with a subgiant companion ( $\chi_R^2 \approx 36$ , Table 6.1). (However, when fitting this object with TAEHB, both with and without the CaT, this degeneracy disappears and it is best fit with a subgiant of K0IV — the fit  $\chi_R^2 \approx 25$  and 16, for CaT and without CaT respectively.) Based on the spectral features evident in #150, and the poor quality of fit that I can achieve with my ZAEHB models (but better fit with TAEHB), I am inclined to believe that the hot member of this system is in fact *not* a true sdB star, and that this composite is a subgiant (III-IV luminosity class) with a hot companion that is more luminous than a typical sdB. Another possibility is that this is just a freak chance superposition of a sdB star with a distant background giant star.

My two possible ZAEHB fits for the late-type companion in #150 are:  $<7120\text{ K}$ , and  $5550 \pm 60\text{ K}$ ; with subdwarfs of:  $>32.0\text{ kK}$ , and  $28.5^{+2.1}_{-0.6}\text{ kK}$  respectively. The TAEHB fit is  $4760 \pm 50\text{ K}$  and  $<20.5\text{ kK}$  for the companion and hot subdwarf respectively. Previous classifications (see Table 4.3) of the late-type companion are:  $4600\text{--}5000\text{ K}$  (K1–K6),  $4750\text{ K}$  (K2), and  $4575 \pm 50\text{ K}$ . The previous temperature determinations (see Table 4.3) include:  $25\text{--}50\text{ kK}$ ,  $18\text{--}30\text{ kK}$  (with a best estimate of  $\sim 21\text{ kK}$ ),  $21\text{ kK}$ , and  $21.5 \pm 0.5\text{ kK}$ ; and  $\log g$  have tended to be on the high side:  $6.9 \pm 0.3$ ,  $6.6$ , and  $6.0 \pm 0.2$ . It is interesting to note that the previous determinations have tended to favor a cooler hot subdwarf ( $\sim 21\text{ kK}$ ), which in my case would favor the TAEHB with subgiant companion. The previous temperature determinations of the late-type companion ( $4750$  and  $4575\text{ K}$  particularly) are consistent with the temperature I found for the subgiant ( $4760\text{ K}$ ) with a TAEHB star. This object deserves more careful scrutiny in further studies.

Another unusual object is #1092 TON 264 (marked with a “\*” in the notes column of Table 6.2, spectrum is shown in Figure 4.14). This object shows very broad and shallow hydrogen lines (much broader and shallower than the other hot subdwarfs in my sample), with some weak He I, yet hints of a strong (diluted) complex of lines around Mg I b, Na I D and CaT (Figure 4.14). This object has something unusual going on,

which requires more observations to understand. I propose one of two scenarios: (1) this object is actually under-luminous for hot subdwarfs, and with higher surface gravity (it could possibly be WD+dM or late-K); or (2) the  $H\alpha$  line is filled in with NLTE emission (which would be evident with higher spectral resolution), so it is actually a very hot sdO (similar to objects #1347, BD+28°4211, and #1461, PB 5333, described in §4.6.4).

Star #294 PG 0900+400 (also BL Lyn, is marked with a “\*” in the notes column of Table 6.2, spectrum is shown in Figure 4.14), was reclassified by Jeffery & Aznar Cuadrado (2001) as a hydrogen-deficient, low-mass, early-B spectral type giant with an unresolved G-type giant companion (see also Table 4.3). Jeffery & Aznar Cuadrado (2001) report  $T_{\text{eff}} = 28.6 \pm 1.0$  kK,  $\log g = 3.6 \pm 0.1$  for the hot member, and  $T_{\text{eff}} = 5840 \pm 960$  K,  $\log g = 3.2 \pm 0.3$  for the cool member. This reclassification was discovered late in the analysis, so this star remains included in the sample.

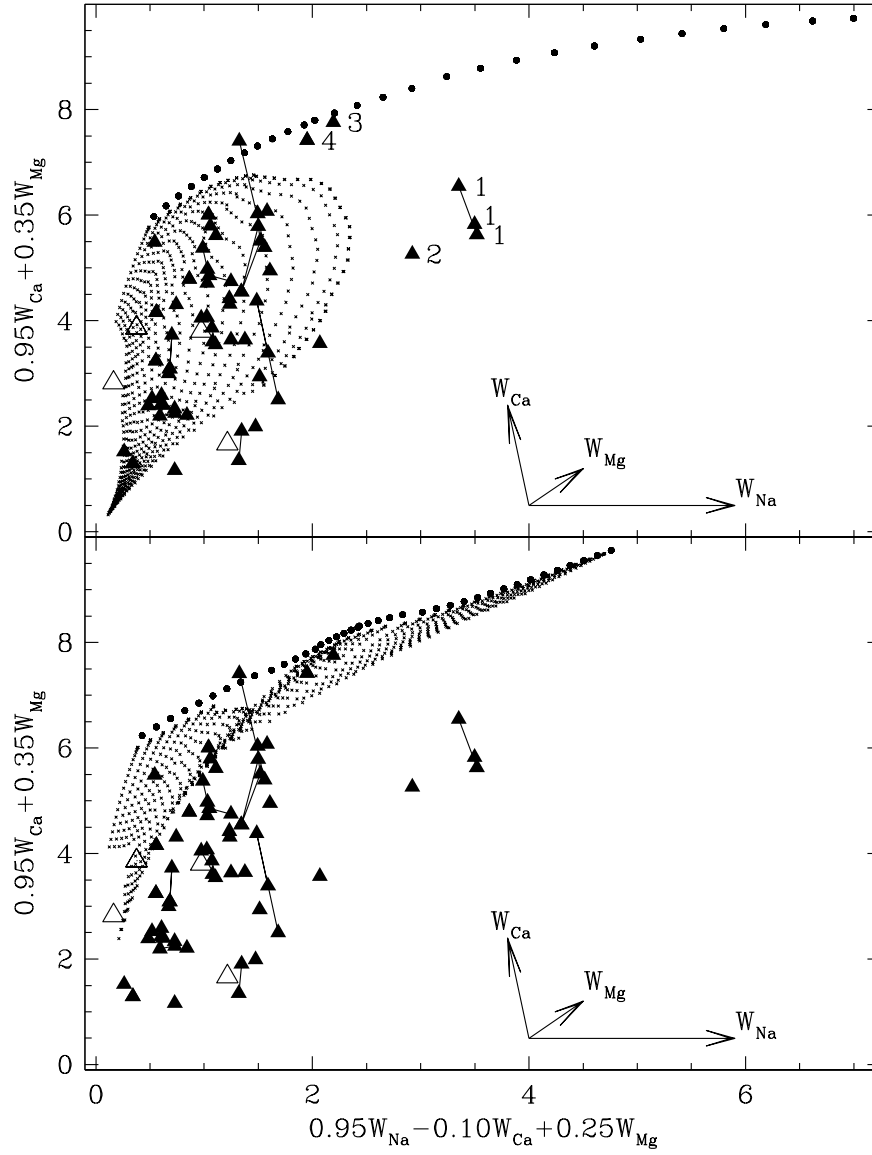


Fig. 6.1 Comparison of the observed EWs of composite hot subdwarfs with predicted diluted EWs based on the fits to the HIP standard stars. In both panels, circles represent the models chosen from the fits to the HIP stars, small crosses represent predicted diluted values when blended with hot subdwarfs of varying temperatures, and triangles represent observed values for composite hot subdwarfs (solid = sdB, open = sdO). Multiple observations of the same object are connected by lines. The top panel shows only main sequence models, while the bottom panel shows only subgiant models. Both panels are projections of the three dimensional space defined by  $(W_{\text{Ca}}, W_{\text{Na}}, W_{\text{Mg}})$ , where  $x = 0.95W_{\text{Na}} - 0.10W_{\text{Ca}} + 0.25W_{\text{Mg}}$  and  $y = 0.95W_{\text{Ca}} + 0.25W_{\text{Mg}}$ ; a set of arrows indicates the directions and magnitudes of a  $2 \text{ \AA}$  shift in EW for each line. Numbered objects are discussed in §6.2 (“1” = #1223 HD 185510; “2” = #150 PG 0232+095; “3” = #1457 BD-7°5977; “4” = #551 PB 3854).

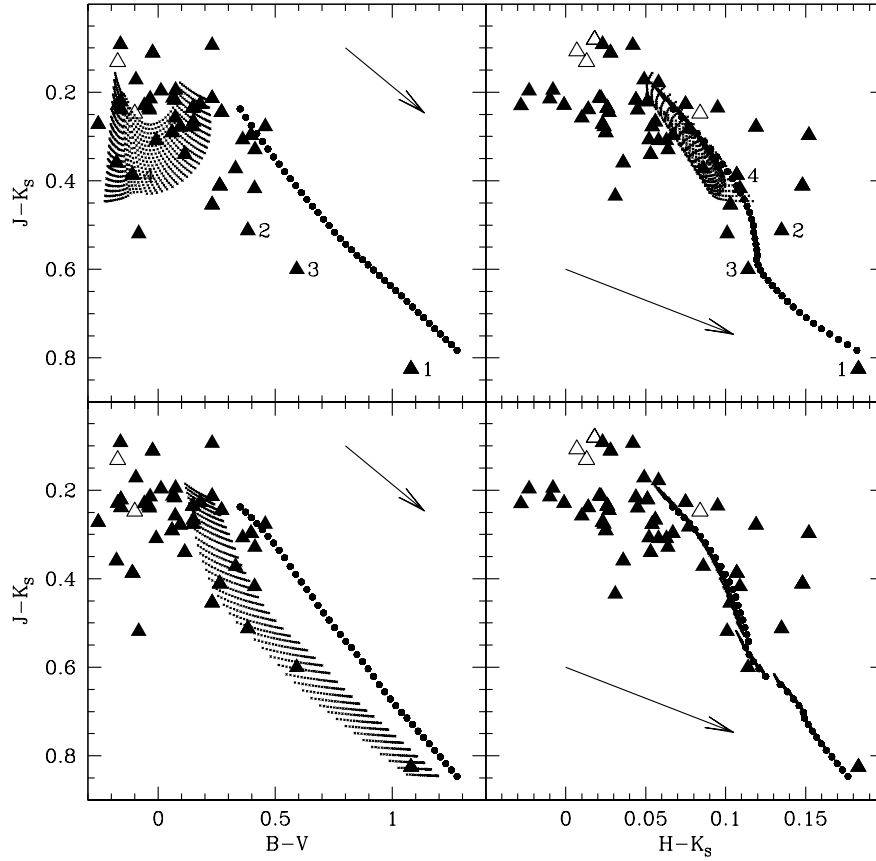


Fig. 6.2 Comparison of the observed colors of composite hot subdwarfs with predicted diluted colors based on the fits to the HIP standard stars. In all panels, circles represent the models chosen from the fits to the HIP stars, small crosses represent predicted diluted values when blended with hot subdwarfs of varying temperatures, and triangles represent observed values for composite hot subdwarfs (solid = sdB, open = sdO). The top panels shows only main sequence models, while the bottom panels shows only subgiant models. Left panels are the color-color plots of  $(J-K_S, B-V)$ . Right panels are the color-color plots of  $(J-K_S, H-K_S)$ . Arrows indicate  $A_V = 1$ . Numbered objects are discussed in §6.2 (“1” = #1223 HD 185510; “2” = #150 PG 0232+095; “3” = #1457 BD-7°5977; “4” = #551 PB 3854).

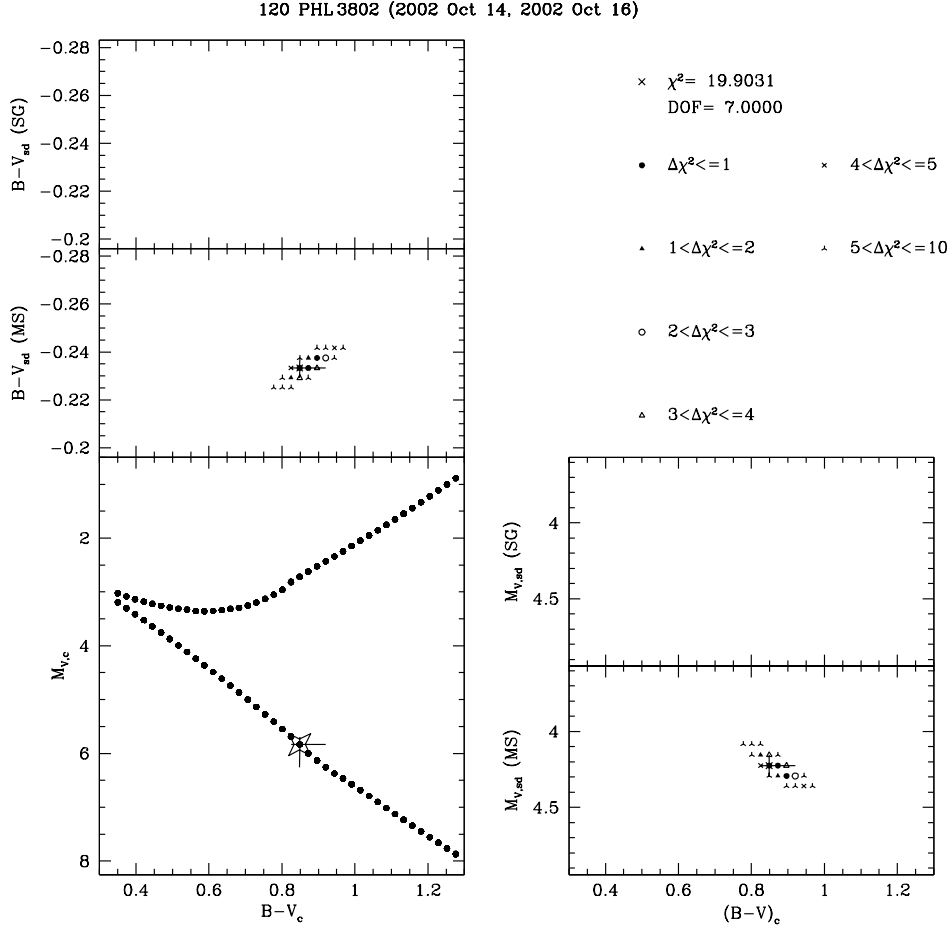


Fig. 6.3 Representation of the  $\chi^2$  space for #120 PHL 3802. Bottom left panel shows a HR Diagram for the modelled companions (circles) with the best-fit companion labelled with a star and bars representing the range of the “ $3\sigma$  errors” ( $\chi^2 - \chi_{\min}^2 = \Delta\chi^2 = 3$ ) on the companion’s  $M_V$  and  $B - V$ . Top left panels show the  $\chi^2$  range in the color-color space of the companion  $[(B - V)_c]$  and subdwarf  $[(B - V)_{sd}]$  colors, with the top panel showing only subgiant (SG), and the bottom showing only main sequence (MS) companions. Bottom right panels show the  $\chi^2$  range in  $M_{V,sd}$  vs.  $(B - V)_c$ , again with only SG companions in the top panel and MS in the bottom. The key to symbols in both the upper left and lower right panels, is given at the upper right of the figure, along with the minimum value of  $\chi^2$  and the number of DOF. The best fit is marked with a large cross (and bars representing the “ $3\sigma$ ”, or  $\Delta\chi^2 = 3$  range in parameters), solid circles mark  $\Delta\chi^2 = 1$ , solid triangles  $\Delta\chi^2 = 2$ , open circles  $\Delta\chi^2 = 3$ , open triangles  $\Delta\chi^2 = 4$ , small crosses  $\Delta\chi^2 = 5$ , and three-pointed stars  $\Delta\chi^2 \leq 10$ .

120 PHL 3802 (2002 Oct 14, 2002 Oct 16)

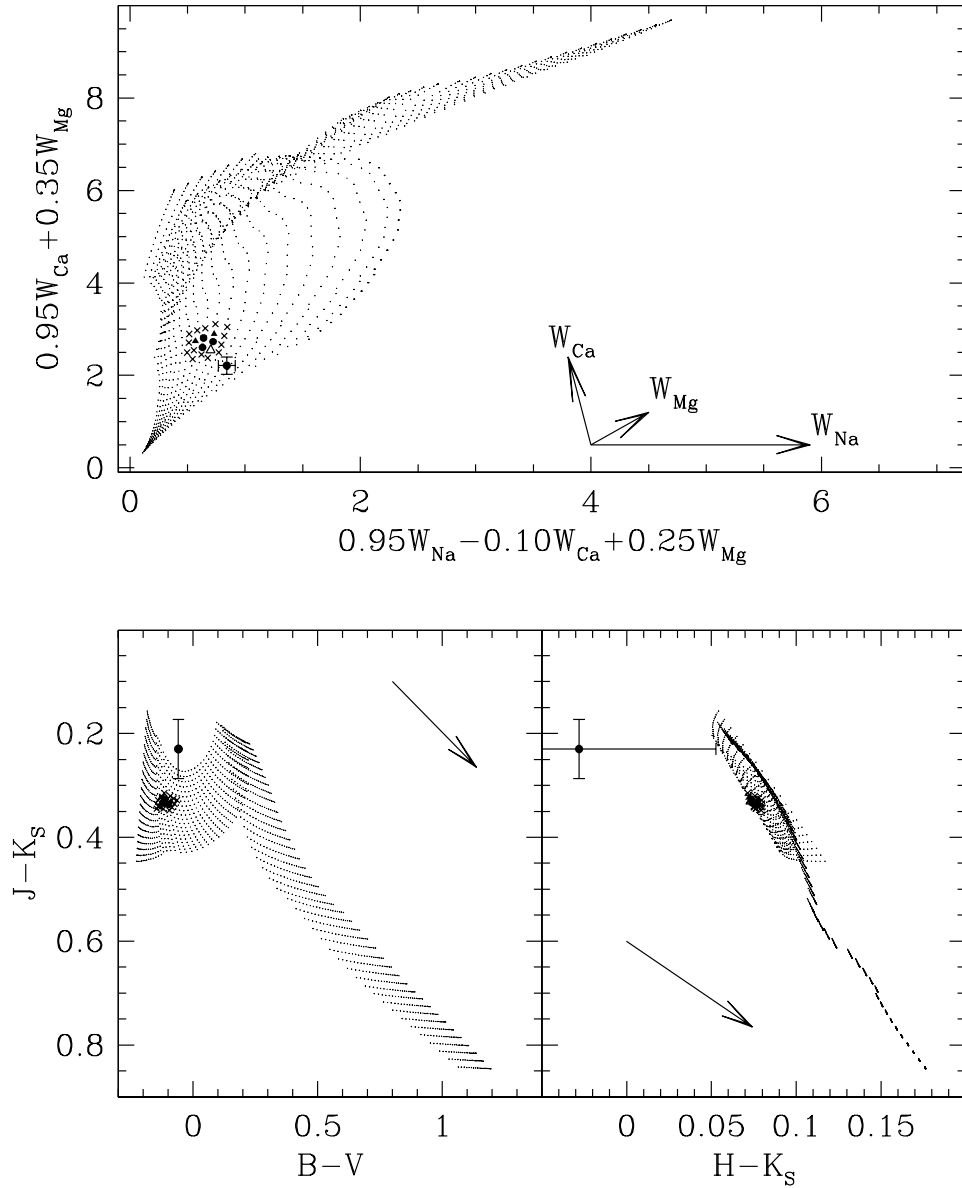


Fig. 6.4 The observed properties of #120 PHL 3802 compared to the diluted models in both EW space (top panel, compare to Figure 6.1) and color-color space (bottom panel, compare to Figure 6.2). The observed values are indicated with a large solid circle with error bars, the models within  $\chi^2 - \chi_{\text{min}}^2 = \Delta\chi^2 = 1$  of the best fit are solid circles,  $\Delta\chi^2 = 2$  are solid triangles,  $\Delta\chi^2 = 3$  are open triangles, models  $\Delta\chi^2 < 10$  are very small crosses, and all other models are specks. Arrows in the top panel indicate the direction and magnitude of a  $2 \text{ \AA}$  shift in EW for each of the three lines measured. Arrows in the bottom panels indicate the shift in colors due to  $A_V = 1$ .

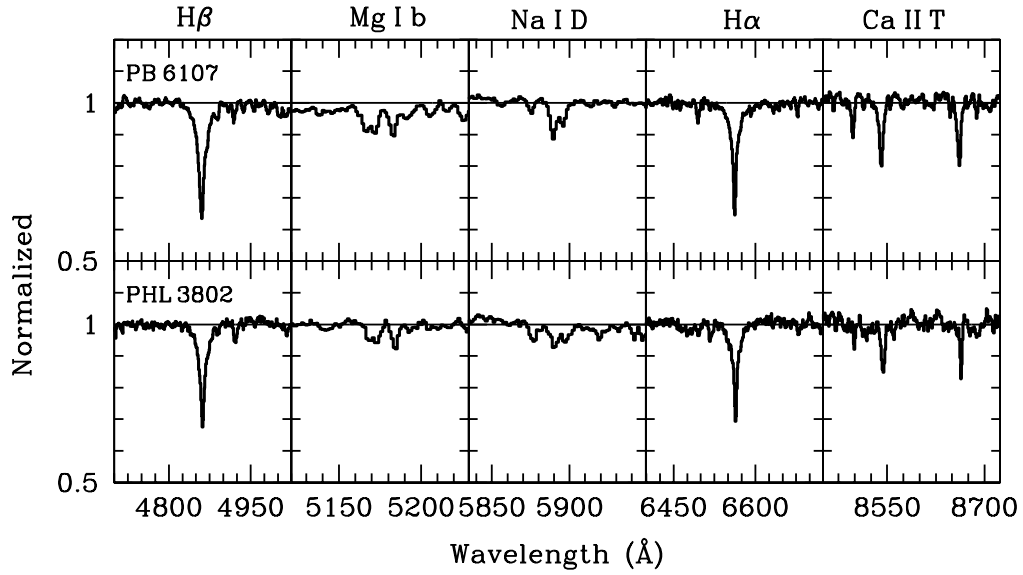


Fig. 6.5 Comparison of the major spectral features in the spectra of #59 PB 6107 and #120 PHL 3802. Panels from left to right show:  $H\beta$ , Mg I b, Na I D,  $H\alpha$ , and CaT. These two stars were both fit with similar hot subdwarfs ( $B-V = -0.246$  &  $-0.233$  and  $M_V = 4.43$  &  $4.22$  for PB 6107 and PHL 3802 respectively) and companions (G9V–K0V), so their spectra look similar.



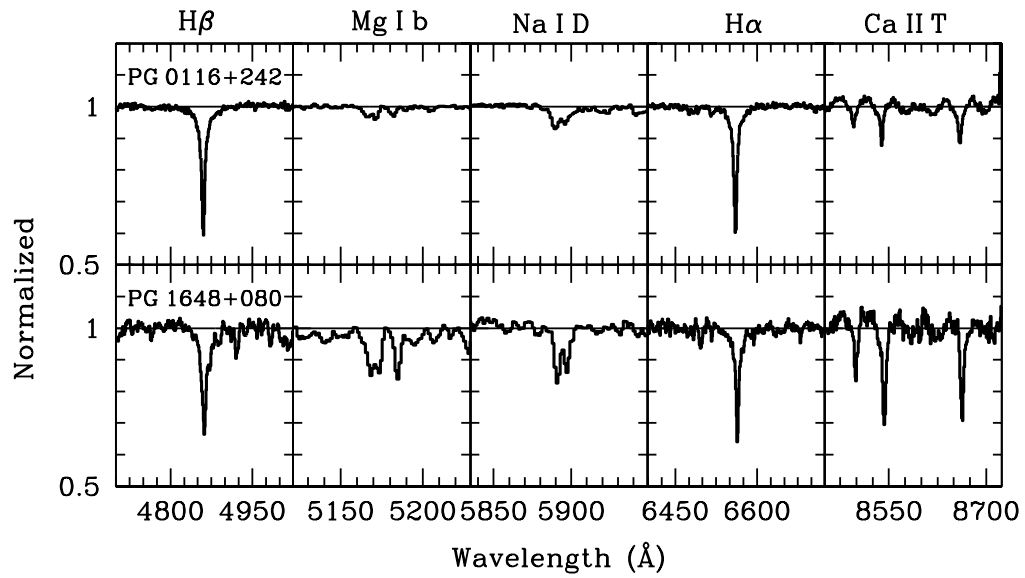


Fig. 6.6 Comparison of the major spectral features in the spectra of #101 PG 0116+242 and #1096 PG 1648+080. Panels from left to right show:  $H\beta$ , Mg I b, Na I D,  $H\alpha$ , and CaT. These two stars were fit with similar companions (G0IV) but different hot subdwarfs (PG 1648+080 was fit with a hotter, fainter hot subdwarf, while PG 0116+242 was fit with a cooler, brighter hot subdwarf). In PG 1648+080, the late-type companion dominates over the hot subdwarf so its lines appear much stronger in the combined spectra, while in PG 0116+242, the brighter hot subdwarf washes out the features from the late-type star making them appear much weaker.

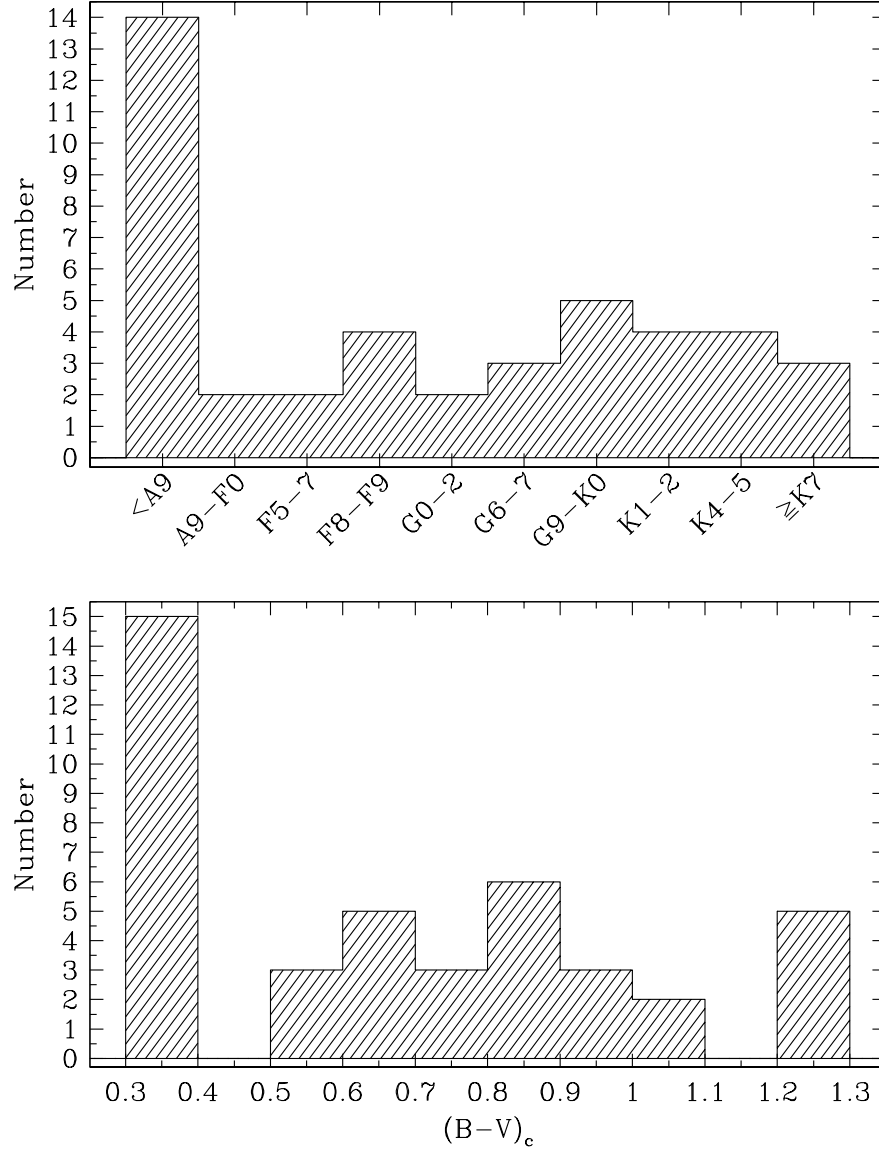


Fig. 6.7 Histogram showing the distribution of late-type companions in  $B-V$  (bottom) and approximate Spectral Type (top). Objects in the last bins on either end of the histograms are upper or lower limits and either (1) have problems with their fits or (2) belong outside the range of parameters examined (see §6.6.1). Star #150, and those stars fitted with subgiant companions (assuming ZAEHB hot subdwarfs, §6.6.2) have been excluded from this plot.

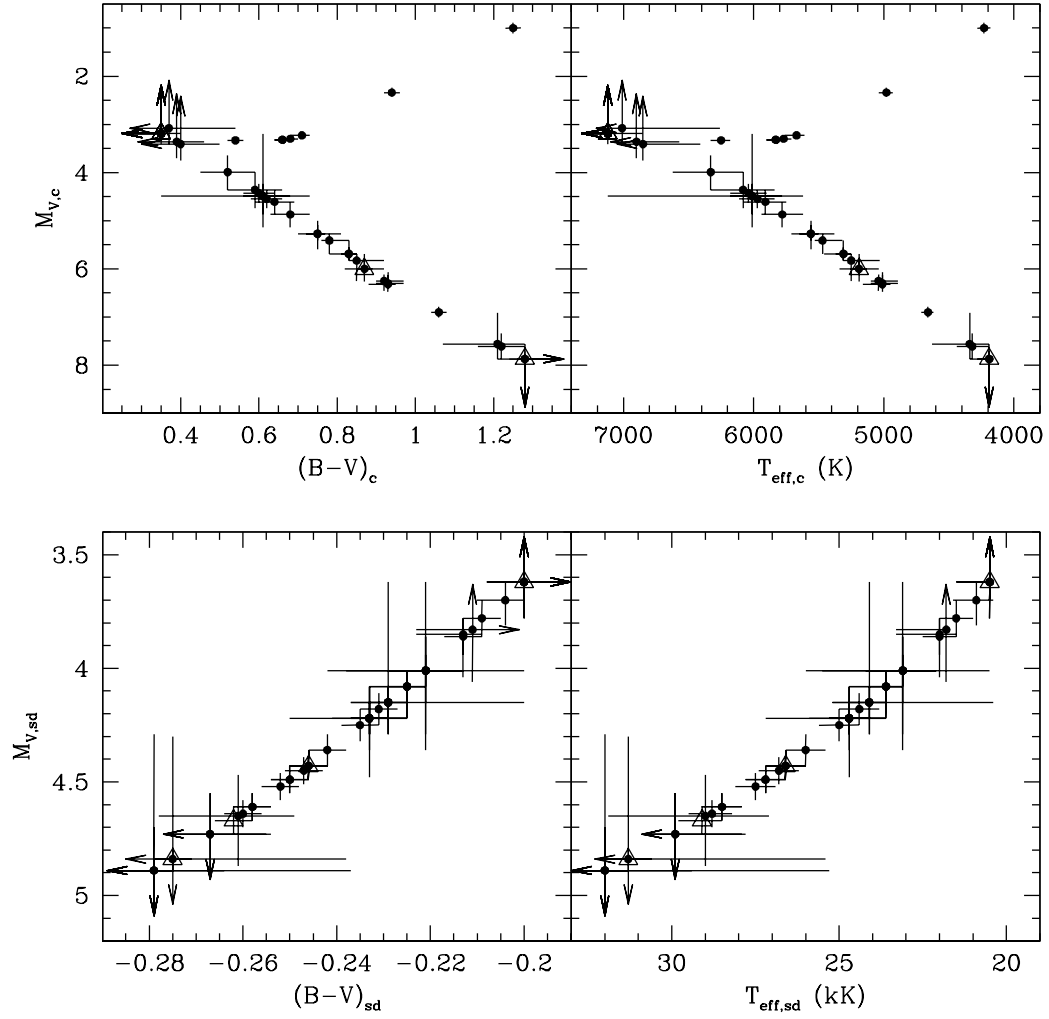


Fig. 6.8 HR diagrams for the best-fit models. Left panels show  $M_V$  vs.  $B-V$ , right panels show  $M_V$  vs.  $T_{\text{eff}}$ . Top panels are for the late-type companion, bottom for the hot subdwarf. In all plots, solid circles represent objects previously classified as sdB, while large open triangles represent those previously classified as sdO. Star #150 has been excluded from this plot. Arrows represent either upper or lower limits on the best fit.

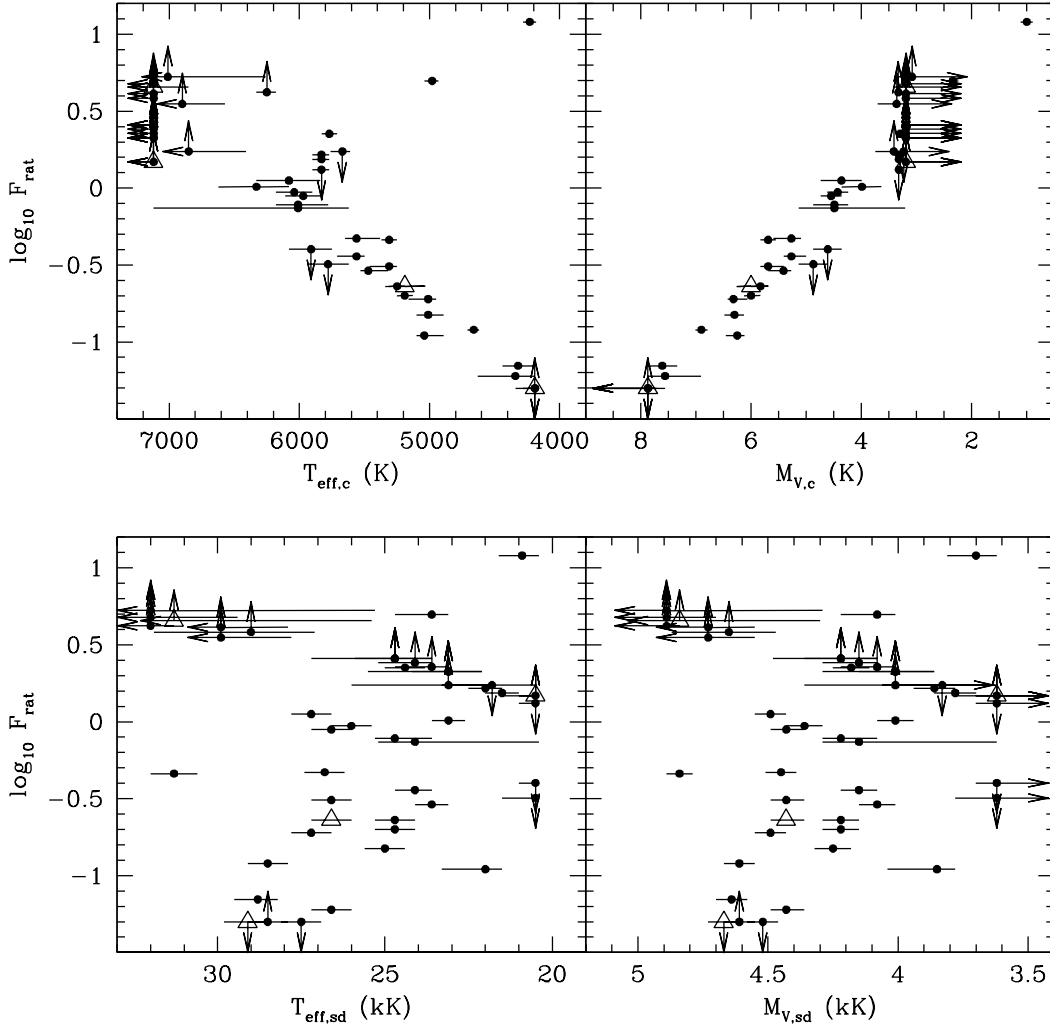


Fig. 6.9 Flux ratios ( $F_{\text{rat}} = F_{\text{comp}}/F_{\text{sd}}$ ) for the best-fit models vs.  $M_V$  and  $T_{\text{eff}}$ . Left panels show  $F_{\text{rat}}$  vs.  $T_{\text{eff}}$ , right panels show  $F_{\text{rat}}$  vs.  $M_V$ . Top panels are for the late-type companion, bottom for the hot subdwarf. In all plots, solid circles represent objects previously classified as sdB, while large open triangles represent those previously classified as sdO. Star #150 has been excluded from this plot. Arrows represent either upper or lower limits on the best fit.

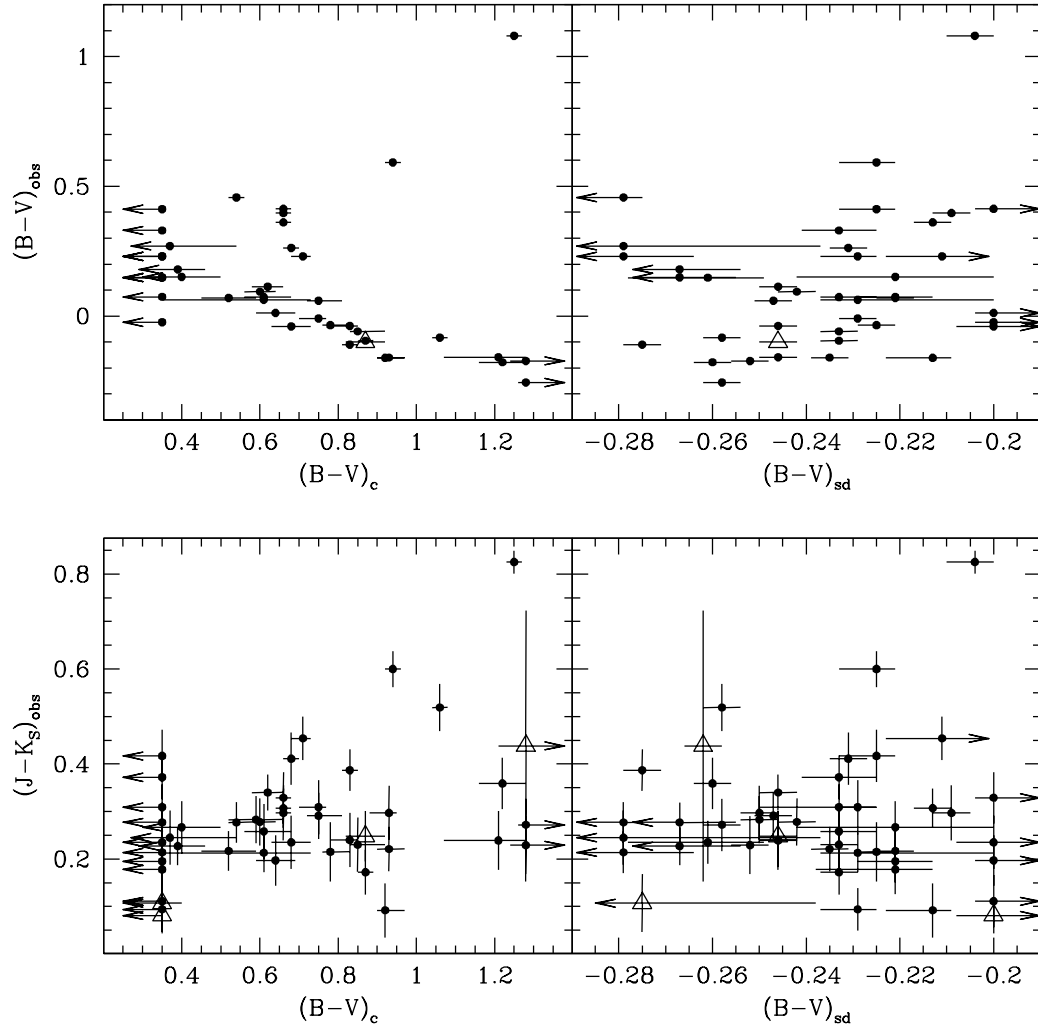


Fig. 6.10 Observed colors compared to the best-fit  $(B-V)_c$  and  $(B-V)_{\text{sd}}$ . Left panels show  $B-V$  for the best-fit companion, while right show  $B-V$  for the best-fit hot subdwarf. Top panels show  $(B-V)_{\text{obs}}$ , bottom panels show  $(J-K_S)_{\text{obs}}$ . In all plots, solid circles represent objects previously classified as sdB, while large open triangles represent those previously classified as sdO. Star #150 has been excluded from this plot. Arrows represent either upper or lower limits on the best fit.

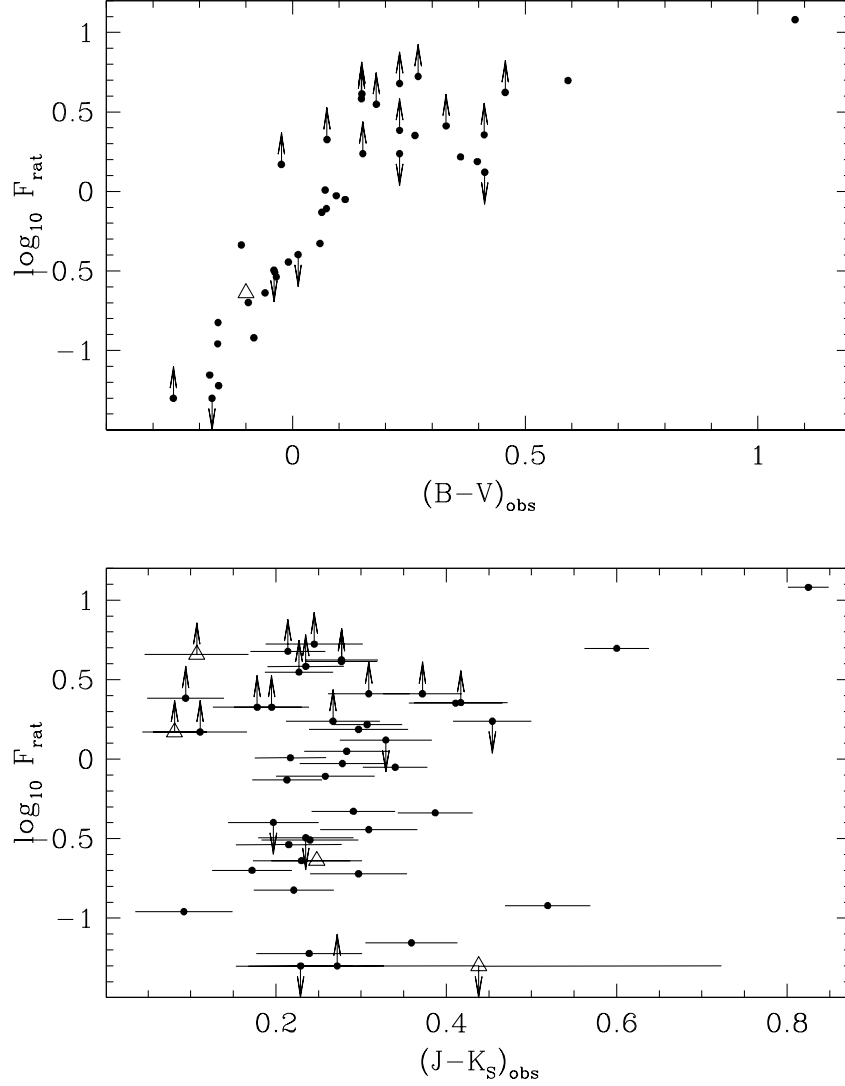


Fig. 6.11 Flux ratios ( $F_{\text{rat}} = F_{\text{comp}}/F_{\text{sd}}$ ) for the best-fit models vs. observed composite colors. Top panel shows  $F_{\text{rat}}$  vs.  $(B-V)_{\text{obs}}$ , bottom shows  $F_{\text{rat}}$  vs.  $(J-K_S)_{\text{obs}}$ . In both plots, solid circles represent objects previously classified as sdB, while large open triangles represent those previously classified as sdO. Star #150 has been excluded from this plot. Arrows represent either upper or lower limits on the best fit.

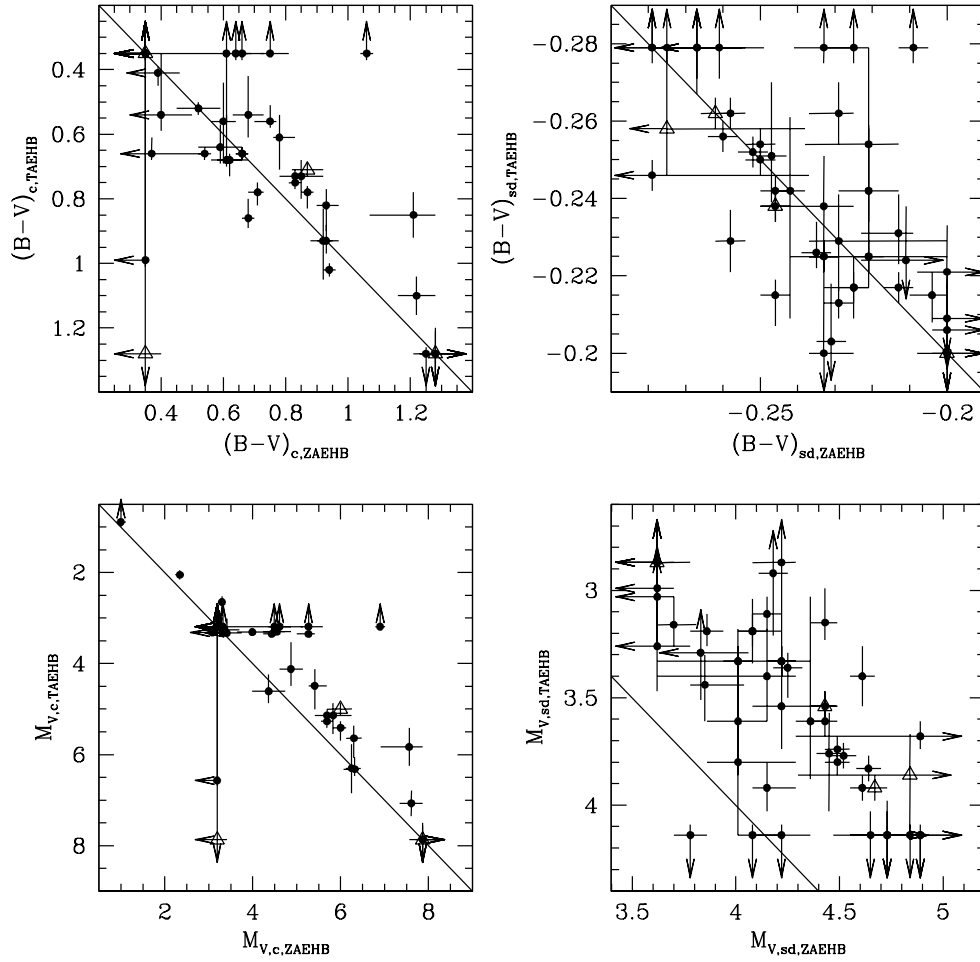


Fig. 6.12 Comparison between the best-fit models based on ZAEHB and TAEHB hot subdwarfs. In all panels the values for the best-fit model based on the ZAEHB are plotted as the abscissa, while the TAEHB are plotted as the ordinate, a diagonal straight line indicates no variation. The left panels are for the late-type companion, the right panels are for the hot subdwarf. The top show  $B-V$  color, the bottom show  $M_V$ . In all plots, solid circles represent objects previously classified as sdB, while large open triangles represent those previously classified as sdO. All points in the bottom right panel are offset from the diagonal line by design — the  $M_V$  at each temperature was increased in order to simulate TAEHB. Star #150 has been excluded from this plot. Arrows represent either upper or lower limits on the best fit.

Table 6.1: Best-fit Models for Composite-Colored Hot Subdwarfs.

ID#	Name	UT Date <sup>a</sup>		$\chi^2_{\min}$	DOF	Late-type	Companion <sup>b</sup>	Hot Subdwarf <sup>b</sup>	$F_{V,\text{rat}}^c$	$E(B-V)^d$
		Red	Blue			$M_{V,c}$	$(B-V)_c$	$M_{V,\text{sd}}$	$(B-V)_{\text{sd}}$	
1	SB 7	021014	021015	32.4751	7	$6.1311^{+0.3316}_{-0.1326}$	$0.8963^{+0.0712}_{-0.0238}$	$3.6206^{+0.3147}_{-0.0166}$	0.0990	0.0000
		021014	021016	38.5593	7	$6.3740^{+0.0888}_{-0.1177}$	$0.9438^{+0.0237}_{-0.0238}$	$4.0831^{+0.0716}_{-0.0731}$	0.1212	0.0000
59	PB 6107	030913	030918	11.5630	7	$5.6905^{+0.1427}_{-0.2804}$	$0.8250^{+0.0238}_{-0.0475}$	$4.4252^{+0.0637}_{-0.0653}$	0.3118	0.0000
65	PB 6148	030915	030918	3.3497	5	$4.3630^{+0.3770}_{-0.3692}$	$0.5875^{+0.0713}_{-0.0712}$	$4.4889^{+0.0621}_{-0.0637}$	1.1229	0.0000
71	BD-11°162	021012	021015	15.4550	7	$5.9985^{+0.2578}_{-0.3080}$	$0.8725^{+0.0475}_{-0.0475}$	$4.4252^{+0.0637}_{-0.0653}$	0.2348	0.0000
95	PG 0110+262	021012	021015	29.9006	7	$<3.1936$	$<0.3500$	$4.0100^{+0.1447}_{-0.1510}$	2.1211	0.0000
101	PG 0116+242	021012	021016	90.3897	7	$3.3158^{+0.0159}_{-0.0027}$	$0.6587^{+0.0238}_{-0.0238}$	$3.8590^{+0.0763}_{-0.0779}$	1.6492	0.0000
102	PB 8783	021014	021015	20.6493	5	$<3.1936$	$<0.3500$	$4.0100^{+0.2831}_{-0.1510}$	2.1211	0.0000
120	PHL 3802	021014	021016	19.9031	7	$5.8332^{+0.4231}_{-0.1427}$	$0.8487^{+0.0713}_{-0.0238}$	$4.2247^{+0.0684}_{-0.0700}$	0.2273	0.0000
150	PG 0232+095	030913	030917	286.7452	7	$<3.1936$	$<0.3500$	$>4.8905$	4.7727	0.0000
		...	030917	216.3873	6	$3.1312^{+0.0674}_{-0.0796}$	$0.7538^{+0.0237}_{-0.0238}$	$4.6115^{+0.1721}_{-0.0605}$	3.9095	0.0000
172	PG 0314+103	030913	030917	405.5848	7	$<3.1936$	$<0.3500$	$4.0831^{+0.1416}_{-0.0731}$	2.2688	0.5347
187A	HDE 283048	030913	030919	39.7494	5	$<3.1936$	$<0.3500$	$4.2247^{+0.2642}_{-0.1416}$	2.5849	0.0000
199	KUV 04110+1434	030914	030918	767.2206	7	$<3.1936$	$<0.3500$	$4.1547^{+0.1384}_{-0.0716}$	2.4235	0.6079
203	KUV 04237+1649	030914	030919	290.2349	7	$<3.1936$	$<0.3500$	$4.2247^{+0.1352}_{-0.1416}$	2.5849	0.4077
234	BD+34d1543	020310	021016	14.5972	7	$4.4879^{+0.1241}_{-0.1249}$	$0.6112^{+0.0238}_{-0.0238}$	$4.4252^{+0.0637}_{-0.0653}$	0.9439	0.0000
		020310	020311	10.2099	6	$4.3630^{+0.2490}_{-0.2462}$	$0.5875^{+0.0475}_{-0.0475}$	$4.2931^{+0.0668}_{-0.0684}$	0.9376	0.0000

Continued on Next Page...



Table 6.1 – Continued

ID#	Name	UT Date <sup>a</sup>		$\chi^2_{\min}$	DOF	Late-type Companion <sup>b</sup>		Hot Subdwarf <sup>b</sup>		$F_{V,\text{rat}}^c$	$E(B-V)^d$
		Red	Blue			$M_{V,c}$	$(B-V)_c$	$M_{V,\text{sd}}$	$(B-V)_{\text{sd}}$		
294	PG 0900+400	020310	021016	13.0333	7	3.1986 <sup>+0.0553</sup> -0.0674	0.7300 <sup>+0.0238</sup> -0.0238	3.6206 <sup>+0.1605</sup> ----	-0.2001 <sup>+</sup> -0.0083	1.4750	0.0000
		020310	020312	36.6203	6	3.2971 <sup>+0.0053</sup> -0.0432	0.6825 <sup>+0.0238</sup> -0.0238	4.1547 <sup>+0.1384</sup> -0.1447	-0.2292 <sup>+0.0083</sup> -0.0083	2.2031	0.0000
		020310	020311	17.9826	6	3.1986 <sup>+0.0985</sup> -0.0674	0.7300 <sup>+0.0238</sup> -0.0475	3.7016 <sup>+0.3815</sup> ----	-0.2043 <sup>+</sup> -0.0208	1.5893	0.0000
460	PG 1104+243	020309	020311	7.7176	6	4.4879 <sup>+0.3820</sup> -0.2487	0.6112 <sup>+0.0713</sup> -0.0475	4.2247 <sup>+0.0684</sup> -0.1416	-0.2333 <sup>+0.0083</sup> -0.0042	0.7847	0.0000
533	BD+10°2357	030611*	030612	24.1591	6	<3.1936	<0.3500	3.6206 <sup>+0.1605</sup> ----	-0.2001 <sup>+</sup> -0.0083	1.4818	0.0000
551	PB 3854	030611*	030612	56.3409	7	5.6905 <sup>+0.1427</sup> -0.1410	0.8250 <sup>+0.0238</sup> -0.0238	4.8379 <sup>+0.0526</sup> -0.0542	-0.2749 <sup>+0.0042</sup> -0.0042	0.4560	0.0000
583	LB 2392	020310	020312	1.7437	5	4.8700 <sup>+0.2659</sup> -0.2580	0.6825 <sup>+0.0475</sup> -0.0475	3.6206 <sup>+0.1605</sup> ----	-0.2001 <sup>+</sup> -0.0083	0.3164	0.0000
630	TON 139	030611*	030612	4.8672	7	3.9938 <sup>+0.3692</sup> -0.3539	0.5163 <sup>+0.0712</sup> -0.0713	4.0100 <sup>+0.0731</sup> -0.0747	-0.2209 <sup>+0.0042</sup> -0.0042	1.0150	0.0000
638	PG 1257-026	030611*	030614	5.1673	7	3.4131 <sup>+0.3429</sup> ----	0.3975 <sup>+0.0950</sup> ----	4.0100 <sup>+0.3500</sup> -0.3894	-0.2209 <sup>+0.0208</sup> -0.0041	1.7328	0.0000
697	Feige 87	030610	030612	24.4664	7	5.9985 <sup>+0.1326</sup> -0.1653	0.8725 <sup>+0.0238</sup> -0.0238	4.2247 <sup>+0.0684</sup> -0.0700	-0.2333 <sup>+0.0041</sup> -0.0042	0.1952	0.0000
702	PG 1343+578	020629	020701	15.9842	6	4.6120 <sup>+0.2580</sup> -0.2490	0.6350 <sup>+0.0475</sup> -0.0475	3.6206 <sup>+0.0810</sup> ----	-0.2001 <sup>+</sup> -0.0042	0.4013	0.0000
706	PG 1347+086	030609	030614	151.3228	7	3.3158 <sup>+0.0159</sup> -0.0027	0.6587 <sup>+0.0238</sup> -0.0238	3.6206 <sup>+0.0810</sup> ----	-0.2001 <sup>+</sup> -0.0042	1.3241	0.0000
789	PG 1429+406	030610	030612	61.4256	7	3.3317 <sup>+0.0228</sup> -0.0186	0.5400 <sup>+0.0238</sup> -0.0238	4.8905 <sup>+</sup> -0.0526	-0.2790 <sup>+0.0042</sup> ----	4.2026	0.0000
844	PG 1449+653	030610	030612	10.0684	7	5.4101 <sup>+0.2804</sup> -0.1376	0.7775 <sup>+0.0475</sup> -0.0237	4.0831 <sup>+0.0716</sup> -0.0731	-0.2251 <sup>+0.0042</sup> -0.0042	0.2946	0.0000
849	PG 1451+472	030611*	030612	69.8031	7	3.3158 <sup>+0.0159</sup> -0.0027	0.6587 <sup>+0.0238</sup> -0.0238	3.7811 <sup>+0.0779</sup> -0.0795	-0.2085 <sup>+0.0042</sup> -0.0041	1.5350	0.0000
895	PG 1514+034	030610	030613	8.1177	7	5.2725 <sup>+0.1376</sup> -0.2706	0.7538 <sup>+0.0237</sup> -0.0475	4.1547 <sup>+0.0700</sup> -0.0716	-0.2292 <sup>+0.0042</sup> -0.0041	0.3572	0.0000
912	PG 1524+611	020630	020702	34.6436	7	4.4879 <sup>+0.6480</sup> -1.2943	0.6112 <sup>+0.1188</sup> -0.2612	4.1547 <sup>+0.1384</sup> -0.5341	-0.2292 <sup>+0.0291</sup> -0.0083	0.7357	0.0000

Continued on Next Page...

Table 6.1 – Continued

ID#	Name	UT Date <sup>a</sup>		$\chi^2_{\min}$	DOF	Late-type Companion <sup>b</sup>		$M_{V,c}$	Hot Subdwarf <sup>b</sup>		$F_{V,\text{rat}}^c$	$E(B-V)^d$
		Red	Blue			$(B-V)_c$	$M_{V,\text{sd}}$		$(B-V)_{\text{sd}}$			
937	PG 1536+278	030611*	030612	8.3520	7	3.0821 <sup>+0.3310</sup> ....	0.3738 <sup>+0.1663</sup> ....	4.8905 <sup>+</sup> -0.5974	-0.2790 <sup>+0.0415</sup> ....	5.2888	0.0000	
969	PG 1551+255	030610	030917	60.9858	7	5.2725 <sup>+0.4180</sup> -0.1366	0.7538 <sup>+0.0712</sup> -0.0238	4.4252 <sup>+0.0637</sup> -0.0653	-0.2458 <sup>+0.0042</sup> -0.0042	0.4582	0.0000	
		030915	030917	36.7528	7	5.1359 <sup>+0.2743</sup> -0.1340	0.7300 <sup>+0.0475</sup> -0.0238	4.4889 <sup>+0.0621</sup> -0.0637	-0.2500 <sup>+0.0042</sup> -0.0041	0.5511	0.0000	
		030916	030917	83.5489	7	5.4101 <sup>+0.2804</sup> -0.2743	0.7775 <sup>+0.0475</sup> -0.0475	4.4252 <sup>+0.0637</sup> -0.0653	-0.2458 <sup>+0.0042</sup> -0.0042	0.4037	0.0000	
1010	PG 1610+519	020629	020701	5.5464	7	7.6610 <sup>+0.2075</sup> -0.4268	1.2287 <sup>+0.0475</sup> -0.0950	4.6705 <sup>+0.0574</sup> -0.0590	-0.2624 <sup>+0.0042</sup> -0.0042	0.0637	0.0000	
		030916	030918	19.5914	7	7.5558 <sup>+0.3128</sup> -0.1064	1.2050 <sup>+0.0712</sup> -0.0238	4.6115 <sup>+0.0590</sup> -0.0605	-0.2582 <sup>+0.0042</sup> -0.0042	0.0664	0.0000	
1051	PG 1629+081	030611*	030612	10.6619	5	7.5558 <sup>+0.3128</sup> -0.6544	1.2050 <sup>+0.0712</sup> -0.1425	4.4252 <sup>+0.0637</sup> -0.0653	-0.2458 <sup>+0.0042</sup> -0.0042	0.0559	0.0000	
1092	TON 264	030915	030919	136.5813	7	6.9014 <sup>+0.1142</sup> -0.1103	1.0625 <sup>+0.0237</sup> -0.0237	4.6115 <sup>+0.0590</sup> -0.0605	-0.2582 <sup>+0.0042</sup> -0.0042	0.1214	0.0000	
1096	PG 1648+080	030610*	030613	35.6075	7	3.2971 <sup>+0.0053</sup> -0.0432	0.6825 <sup>+0.0238</sup> -0.0238	4.1547 <sup>+0.0700</sup> -0.0716	-0.2292 <sup>+0.0042</sup> -0.0041	2.2031	0.0000	
		030914	030613	35.0040	7	3.2971 <sup>+0.0053</sup> -0.0432	0.6825 <sup>+0.0238</sup> -0.0238	4.1547 <sup>+0.0700</sup> -0.0716	-0.2292 <sup>+0.0042</sup> -0.0041	2.2031	0.0000	
		030914	030917	34.4853	7	3.2971 <sup>+0.0053</sup> -0.0432	0.6825 <sup>+0.0238</sup> -0.0238	4.2247 <sup>+0.0684</sup> -0.0700	-0.2333 <sup>+0.0041</sup> -0.0042	2.3498	0.0000	
1133	PG 1701+359	030609	030612	16.0074	7	6.2563 <sup>+0.1177</sup> -0.2578	0.9200 <sup>+0.0238</sup> -0.0475	4.2247 <sup>+0.0684</sup> -0.0700	-0.2333 <sup>+0.0041</sup> -0.0042	0.1539	0.0000	
		030610	030613	12.4533	7	6.2563 <sup>+0.1177</sup> -0.1251	0.9200 <sup>+0.0238</sup> -0.0238	4.2247 <sup>+0.0684</sup> -0.0700	-0.2333 <sup>+0.0041</sup> -0.0042	0.1539	0.0000	
		030913	030917	14.2595	7	6.3740 <sup>+0.3072</sup> -0.1177	0.9438 <sup>+0.0712</sup> -0.0238	4.2931 <sup>+0.0668</sup> -0.0684	-0.2375 <sup>+0.0042</sup> -0.0042	0.1471	0.0000	
1164	PG 1718+519	020629	020701	26.0806	7	4.4879 <sup>+0.2521</sup> -0.1249	0.6112 <sup>+0.0475</sup> -0.0238	4.4252 <sup>+0.0637</sup> -0.0653	-0.2458 <sup>+0.0042</sup> -0.0042	0.9439	0.0000	
		030913	030917	16.0237	7	4.6120 <sup>+0.1280</sup> -0.2490	0.6350 <sup>+0.0238</sup> -0.0475	4.4252 <sup>+0.0637</sup> -0.0653	-0.2458 <sup>+0.0042</sup> -0.0042	0.8419	0.0000	

Continued on Next Page...

Table 6.1 – Continued

ID#	Name	UT Date <sup>a</sup>		$\chi^2_{\min}$	DOF	Late-type Companion <sup>b</sup>		$M_{V,c}$	$(B-V)_c$	$M_{V,sd}$	Hot Subdwarf <sup>b</sup>		$F_{V, \text{rat}}^c$	$E(B-V)^d$
		Red	Blue											
1182	BD+29°3070	030610*	030612	7.7553	7	3.4131 <sup>+0.3429</sup> —	—	3.4131 <sup>+0.3429</sup> —	0.3975 <sup>+0.0712</sup> —	4.7278 <sup>+</sup> —	—0.1769 —	—0.2666 <sup>+0.0125</sup> —	3.3564	0.0000
		030913	030919	7.1493	7	3.3024 <sup>+0.3375</sup> —	—	3.3024 <sup>+0.3375</sup> —	0.3738 <sup>+0.0712</sup> —	4.7278 <sup>+</sup> —	—0.1769 —	—0.2666 <sup>+0.0125</sup> —	3.7167	0.0000
1223	HD 185510	030609	030612	195.8414	7	1.0001 <sup>+</sup> —0.1132	—	1.0001 <sup>+</sup> —0.1132	1.2525 <sup>+0.0237</sup> —	3.7016 <sup>+</sup> —	—0.0795 —	—0.2043 <sup>+</sup> —0.0042	12.0393	0.0000
		030610	030612	211.4795	7	1.0001 <sup>+</sup> —0.1132	—	1.0001 <sup>+</sup> —0.1132	1.2525 <sup>+0.0237</sup> —	3.7016 <sup>+</sup> —	—0.0795 —	—0.2043 <sup>+</sup> —0.0042	12.0393	0.0000
		030913	030919	132.4674	7	1.0001 <sup>+</sup> —0.1132	—	1.0001 <sup>+</sup> —0.1132	1.2525 <sup>+0.0237</sup> —	3.7016 <sup>+</sup> —	—0.1573 —	—0.2043 <sup>+</sup> —0.0083	12.0393	0.0000
1297	PG 2110+127	030610*	030613	29.7705	7	<3.1936	—	<3.1936	<0.3500	4.7836 <sup>+</sup> —0.1721	—	—0.2707 <sup>+0.0125</sup> —	4.3251	0.0000
		030913	030917	31.0550	7	<3.1936	—	<3.1936	<0.3500	4.6705 <sup>+</sup> —0.1816	—	—0.2624 <sup>+0.0124</sup> —	3.8973	0.0000
1304	PG 2116+008	030915	030919	5.9211	5	7.8685 <sup>+</sup> —0.3128	—	7.8685 <sup>+</sup> —0.3128	1.2763 <sup>+</sup> —0.0712	4.6705 <sup>+</sup> —0.0574	—0.0590 —	—0.2624 <sup>+0.0042</sup> —0.0042	0.0526	0.0000
1306	PG 2118+126	030611*	030613	17.8880	7	3.1936 <sup>+0.2195</sup> —	—	3.1936 <sup>+0.2195</sup> —	0.3500 <sup>+0.0475</sup> —	4.6115 <sup>+</sup> —0.1863	—0.2263 —	—0.2582 <sup>+0.0124</sup> —0.0166	3.6911	0.0000
		020629	020701	25.0914	7	<3.1936	—	<3.1936	<0.3500	4.6705 <sup>+</sup> —0.1816	—0.2200 —	—0.2624 <sup>+0.0124</sup> —0.0166	3.8973	0.0000
		030916	030917	25.6171	7	<3.1936	—	<3.1936	<0.3500	4.6705 <sup>+</sup> —0.1816	—0.2200 —	—0.2624 <sup>+0.0124</sup> —0.0166	3.8973	0.0000
1322	BPS CS 29495–21	021012	030917	2.2972	5	6.3740 <sup>+0.0888</sup> —0.2428	—	6.3740 <sup>+0.0888</sup> —0.2428	0.9438 <sup>+0.0237</sup> —0.0475	4.4889 <sup>+</sup> —0.0621	—0.0637 —	—0.2500 <sup>+0.0042</sup> —0.0041	0.1762	0.0000
		030913	030917	5.4521	5	6.2563 <sup>+0.1177</sup> —0.2578	—	6.2563 <sup>+0.1177</sup> —0.2578	0.9200 <sup>+0.0238</sup> —0.0475	4.4889 <sup>+</sup> —0.0637	—0.0621 —	—0.2500 <sup>+0.0042</sup> —0.0041	0.1964	0.0000
1346	PG 2148+095	030611*	030612	44.0473	7	<3.1936	—	<3.1936	<0.3500	<3.6206	>	>–0.2001	1.4818	0.0000
		030914	030917	46.5590	7	<3.1936	—	<3.1936	<0.3500	<3.6206	>	>–0.2001	1.4818	0.0000
1348	PG 2151+100	020629	020701	34.8787	6	7.8685 <sup>+</sup> —0.2075	—	7.8685 <sup>+</sup> —0.2075	1.2763 <sup>+</sup> —0.0475	4.5510 <sup>+</sup> —0.0621	—0.0605 —	—0.2541 <sup>+0.0041</sup> —0.0042	0.0471	0.0000
		030914	030919	21.1947	7	7.8685 <sup>+</sup> —0.1033	—	7.8685 <sup>+</sup> —0.1033	1.2763 <sup>+</sup> —0.0237	4.4889 <sup>+</sup> —0.0637	—0.0621 —	—0.2500 <sup>+0.0042</sup> —0.0041	0.0445	0.0000

Continued on Next Page...

Table 6.1 – Continued

ID#	Name	UT Date <sup>a</sup>		$\chi^2_{\min}$	DOF	Late-type Companion <sup>b</sup> $M_{V,c}$	$(B-V)_c$	Hot Subdwarf <sup>b</sup> $M_{V,sd}$	$(B-V)_{sd}$	$F_{V, \text{rat}}^c$	$E(B-V)^d$
		Red	Blue								
1356	PG 2158+082	030914	030919	5.7150	3	3.1936 <sup>+0.2195</sup> —	0.3500 <sup>+0.0475</sup> —	4.8379 <sup>+...</sup> -0.5448	-0.2749 <sup>+0.0374</sup> —	4.5469	0.0000
1424	Balloon 090900007	030913	030917	14.2989	7	<3.1936	<0.3500	4.8905 <sup>+...</sup> -0.1627	-0.2790 <sup>+0.0125</sup> —	4.7727	0.0000
		030915	030917	21.0780	7	<3.1936	<0.3500	4.8905 <sup>+...</sup> -0.2200	-0.2790 <sup>+0.0166</sup> —	4.7727	0.0000
1457	BD-7° 5977	021012	021015	10.7057	7	2.3395 <sup>+0.0905</sup> -0.0960	0.9438 <sup>+0.0237</sup> -0.0238	4.0831 <sup>+0.1416</sup> -0.0731	-0.2251 <sup>+0.0042</sup> -0.0083	4.9824	0.0000
1461A	PB 5333	021012	021015	33.1962	7	7.8685 <sup>+...</sup> -0.1033	1.2763 <sup>+...</sup> -0.0237	4.6115 <sup>+0.0590</sup> -0.0605	-0.2582 <sup>+0.0042</sup> -0.0042	0.0498	0.0000
		030916	021015	25.3474	6	7.8685 <sup>+...</sup> -0.1033	1.2763 <sup>+...</sup> -0.0237	4.6115 <sup>+0.0590</sup> -0.0605	-0.2582 <sup>+0.0042</sup> -0.0042	0.0498	0.0000
1519	CD-27 16503	030913	030918	35.0986	7	6.1311 <sup>+0.2428</sup> -0.1326	0.8963 <sup>+0.0475</sup> -0.0238	3.9353 <sup>+0.1479</sup> -0.1542	-0.2167 <sup>+0.0083</sup> -0.0083	0.1323	0.0000
1525	BPS CS 22957-23	021012	021015	6.6915	5	6.6812 <sup>+0.2202</sup> -0.2184	1.0150 <sup>+0.0475</sup> -0.0475	4.7278 <sup>+0.1627</sup> -0.0574	-0.2666 <sup>+0.0042</sup> -0.0125	0.1654	0.0000

<sup>a</sup>The UT dates are given for the two exposures used for the fit in two digit year, month, day, as in: YYMMDD. If there is a star (\*) following the Red exposure date, then the EW of CaT from that observation were significantly affected by fringing.

<sup>b</sup>If an error is missing (given as “±...”), it means that there is no constraint in that direction (the acceptable values reach the edge of the grid and likely pass beyond the edge of the grid), so the value of the best-fit should be taken as a limit.

<sup>c</sup>Flux ratio at  $V$  between the best-fit companion and hot subdwarf:  $F_{V, \text{rat}} = F_{V, \text{comp}}/F_{V, \text{sd}}$ .

<sup>d</sup>Value of  $E(B-V)$  used for reddening correction of the colors before  $\chi^2_2$  was calculated.

<sup>e</sup>Star #199 is highly reddened, so appeared composite-colored due to reddening. The fit presented here is therefore bogus, but presented for completeness.

Table 6.2: Adopted Parameters from the Best-fit Models for the Composite-Colored Hot Subdwarfs.

ID#	Name		Late-type Companion <sup>a</sup>			Hot Subdwarf <sup>a</sup>			$F_{V,\text{rat}}$ <sup>b</sup>	Notes <sup>c</sup>
	Red	Blue	$M_{V,c}$	$(B-V)_c$	$T_{\text{eff},c}$	Type	$M_{V,\text{sd}}$	$(B-V)_{\text{sd}}$		
1	SB 7		$6.25^{+0.21}_{-0.13}$	$+0.92^{+0.05}_{-0.02}$	$5040^{+60}_{-150}$	K1V	$3.85^{+0.19}_{-0.07}$	$-0.213^{+0.004}_{-0.010}$	$22.0^{+1.3}_{-0.5}$	0.11
59	PB 6107		$5.69^{+0.14}_{-0.28}$	$+0.83^{+0.02}_{-0.05}$	$5310^{+150}_{-60}$	G9V	$4.43^{+0.06}_{-0.07}$	$-0.246^{+0.004}_{-0.004}$	$26.6^{+0.6}_{-0.6}$	0.31
65	PB 6148		$4.36^{+0.38}_{-0.37}$	$+0.59^{+0.07}_{-0.07}$	$6080^{+250}_{-240}$	F7V	$4.49^{+0.06}_{-0.06}$	$-0.250^{+0.004}_{-0.004}$	$27.2^{+0.6}_{-0.6}$	1.12
71	BD-11°162		$6.00^{+0.26}_{-0.31}$	$+0.87^{+0.05}_{-0.05}$	$5190^{+150}_{-150}$	K0V	$4.43^{+0.06}_{-0.07}$	$-0.246^{+0.004}_{-0.004}$	$26.6^{+0.6}_{-0.6}$	0.23 sdO
95	PG 0110+262		$<3.19$	$<+0.35$	$<7120$	<A9V	$4.01^{+0.14}_{-0.15}$	$-0.221^{+0.008}_{-0.008}$	$23.1^{+1.1}_{-1.0}$	2.12 †
101	PG 0116+242		$3.32^{+0.02}_{-0.01}$	$+0.66^{+0.02}_{-0.02}$	$5830^{+70}_{-60}$	G0IV	$3.86^{+0.08}_{-0.08}$	$-0.213^{+0.004}_{-0.004}$	$22.0^{+0.5}_{-0.5}$	1.65 §
102	PB 8783		$<3.19$	$<+0.35$	$<7120$	<A9V	$4.01^{+0.28}_{-0.15}$	$-0.221^{+0.008}_{-0.017}$	$23.1^{+2.4}_{-1.0}$	2.12 †
120	PHL 3802		$5.83^{+0.42}_{-0.14}$	$+0.85^{+0.07}_{-0.02}$	$5250^{+60}_{-220}$	K0V	$4.22^{+0.07}_{-0.07}$	$-0.233^{+0.004}_{-0.004}$	$24.7^{+0.6}_{-0.6}$	0.23
150	PG 0232+095		$<3.19$	$<+0.35$	$<7120$	<A9V	$>4.89$	$<-0.279$	$>32.0$	~4.77 *
172	PG 0314+103		$3.13^{+0.07}_{-0.08}$	$+0.75^{+0.02}_{-0.02}$	$5550^{+60}_{-60}$	G2IV	$4.61^{+0.17}_{-0.06}$	$-0.258^{+0.004}_{-0.013}$	$28.5^{+2.1}_{-0.6}$	3.91 *, §
187A	HDE 283048		$<3.19$	$<+0.35$	$<7120$	<A9V	$4.08^{+0.14}_{-0.07}$	$-0.225^{+0.004}_{-0.008}$	$23.6^{+1.1}_{-0.5}$	2.27 †
199	KUV 04110+1434		$<3.19$	$<+0.35$	$<7120$	<A9V	$4.22^{+0.26}_{-0.14}$	$-0.233^{+0.008}_{-0.017}$	$24.7^{+2.5}_{-1.1}$	2.58 †
203	KUV 04237+1649		$<3.19$	$<+0.35$	$<7120$	<A9V	$4.15^{+0.14}_{-0.07}$	$-0.229^{+0.004}_{-0.008}$	$24.1^{+1.1}_{-0.5}$	2.42 RED, †
234	BD+34d1543		$4.43^{+0.19}_{-0.19}$	$+0.60^{+0.04}_{-0.04}$	$6040^{+140}_{-140}$	F8V	$4.36^{+0.07}_{-0.07}$	$-0.242^{+0.004}_{-0.004}$	$26.0^{+0.6}_{-0.6}$	2.58 †
294	PG 0900+400		$3.23^{+0.05}_{-0.06}$	$+0.71^{+0.02}_{-0.03}$	$5670^{+90}_{-60}$	G1IV	$3.83^{+0.23}_{-0.00}$	$-0.211^{+0.004}_{-0.012}$	$21.8^{+1.5}_{-0.00}$	0.94
										1.73 *, §

Continued on Next Page...

Table 6.2 – Continued

ID#	Name		Late-type Companion <sup>a</sup>				Hot Subdwarf <sup>a</sup>			$F_{V,\text{rat}}$ <sup>b</sup>	Notes <sup>c</sup>
	Red	Blue	$M_{V,c}$	$(B-V)_c$	$T_{\text{eff},c}$	Type	$M_{V,\text{sd}}$	$(B-V)_{\text{sd}}$	$T_{\text{eff},\text{sd}}$		
460	PG 1104+243		4.49 <sup>+0.38</sup> <sub>-0.25</sub>	+0.61 <sup>+0.07</sup> <sub>-0.05</sub>	6010 <sup>+170</sup> <sub>-230</sub>	F8V	4.22 <sup>+0.07</sup> <sub>-0.14</sub>	-0.233 <sup>+0.008</sup> <sub>-0.004</sub>	24.7 <sup>+0.6</sup> <sub>-1.1</sub>	0.78	
533	BD+10°2357		<3.19	<+0.35	<7120	<A9V	3.62 <sup>+0.16</sup> <sub>-...</sub>	-0.200 <sup>+...</sup> <sub>-0.008</sub>	20.5 <sup>+1.0</sup> <sub>-...</sub>	1.48 F, sdO, †	
551	PB 3854		5.69 <sup>+0.14</sup> <sub>-0.14</sub>	+0.83 <sup>+0.02</sup> <sub>-0.02</sub>	5310 <sup>+60</sup> <sub>-60</sub>	G9V	4.84 <sup>+0.05</sup> <sub>-0.05</sub>	-0.275 <sup>+0.004</sup> <sub>-0.004</sub>	31.3 <sup>+0.7</sup> <sub>-0.7</sub>	0.46	F
583	LB 2392		4.87 <sup>+0.27</sup> <sub>-0.26</sub>	+0.68 <sup>+0.05</sup> <sub>-0.05</sub>	5780 <sup>+160</sup> <sub>-160</sub>	G2V	3.62 <sup>+0.16</sup> <sub>-...</sub>	-0.200 <sup>+...</sup> <sub>-0.008</sub>	20.5 <sup>+1.0</sup> <sub>-...</sub>	0.32	†
630	TON 139		3.99 <sup>+0.37</sup> <sub>-0.35</sub>	+0.52 <sup>+0.07</sup> <sub>-0.07</sub>	6330 <sup>+290</sup> <sub>-250</sub>	F5V	4.01 <sup>+0.07</sup> <sub>-0.07</sub>	-0.221 <sup>+0.004</sup> <sub>-0.004</sub>	23.1 <sup>+0.5</sup> <sub>-0.5</sub>	1.02	F
638	PG 1257-026		3.41 <sup>+0.34</sup> <sub>-...</sub>	+0.40 <sup>+0.10</sup> <sub>-...</sub>	6850 <sup>+...</sup> <sub>-440</sub>	F0V	4.01 <sup>+0.35</sup> <sub>-0.39</sub>	-0.221 <sup>+0.021</sup> <sub>-0.021</sub>	23.1 <sup>+2.9</sup> <sub>-2.6</sub>	1.73	F, †
697	Feige 87		6.00 <sup>+0.13</sup> <sub>-0.17</sub>	+0.87 <sup>+0.02</sup> <sub>-0.02</sub>	5190 <sup>+60</sup> <sub>-60</sub>	K0V	4.22 <sup>+0.07</sup> <sub>-0.07</sub>	-0.233 <sup>+0.004</sup> <sub>-0.004</sub>	24.7 <sup>+0.6</sup> <sub>-0.6</sub>	0.20	
702	PG 1343+578		4.61 <sup>+0.26</sup> <sub>-0.25</sub>	+0.64 <sup>+0.05</sup> <sub>-0.05</sub>	5910 <sup>+170</sup> <sub>-160</sub>	G0V	3.62 <sup>+0.08</sup> <sub>-...</sub>	-0.200 <sup>+...</sup> <sub>-0.004</sub>	20.5 <sup>+0.5</sup> <sub>-...</sub>	0.40	†
706	PG 1347+086		3.32 <sup>+0.02</sup> <sub>-0.01</sub>	+0.66 <sup>+0.02</sup> <sub>-0.02</sub>	5830 <sup>+70</sup> <sub>-60</sub>	G0IV	3.62 <sup>+0.08</sup> <sub>-...</sub>	-0.200 <sup>+...</sup> <sub>-0.004</sub>	20.5 <sup>+0.5</sup> <sub>-...</sub>	1.32	†, §
789	PG 1429+406		3.33 <sup>+0.02</sup> <sub>-0.02</sub>	+0.54 <sup>+0.02</sup> <sub>-0.02</sub>	6250 <sup>+80</sup> <sub>-70</sub>	F8IV	4.89 <sup>+...</sup> <sub>-0.05</sub>	-0.279 <sup>+0.004</sup> <sub>-...</sub>	32.0 <sup>+...</sup> <sub>-0.7</sub>	4.20	†, §
844	PG 1449+653		5.41 <sup>+0.28</sup> <sub>-0.14</sub>	+0.78 <sup>+0.05</sup> <sub>-0.02</sub>	5470 <sup>+60</sup> <sub>-150</sub>	G7V	4.08 <sup>+0.07</sup> <sub>-0.07</sub>	-0.225 <sup>+0.004</sup> <sub>-0.004</sub>	23.6 <sup>+0.5</sup> <sub>-0.5</sub>	0.29	
849	PG 1451+472		3.32 <sup>+0.02</sup> <sub>-0.01</sub>	+0.66 <sup>+0.02</sup> <sub>-0.02</sub>	5830 <sup>+70</sup> <sub>-60</sub>	G0IV	3.78 <sup>+0.08</sup> <sub>-0.08</sub>	-0.209 <sup>+0.004</sup> <sub>-0.004</sub>	21.5 <sup>+0.5</sup> <sub>-0.5</sub>	1.54	F, §
895	PG 1514+034		5.27 <sup>+0.14</sup> <sub>-0.27</sub>	+0.75 <sup>+0.02</sup> <sub>-0.05</sub>	5560 <sup>+150</sup> <sub>-60</sub>	G6V	4.15 <sup>+0.07</sup> <sub>-0.07</sub>	-0.229 <sup>+0.004</sup> <sub>-0.004</sub>	24.1 <sup>+0.6</sup> <sub>-0.5</sub>	0.36	
912	PG 1524+611		4.49 <sup>+0.65</sup> <sub>-1.29</sub>	+0.61 <sup>+0.12</sup> <sub>-0.26</sub>	6010 <sup>+1110</sup> <sub>-390</sub>	F8V	4.15 <sup>+0.14</sup> <sub>-0.53</sub>	-0.229 <sup>+0.029</sup> <sub>-0.008</sub>	24.1 <sup>+1.1</sup> <sub>-3.7</sub>	0.74	
937	PG 1536+278		3.08 <sup>+0.33</sup> <sub>-...</sub>	+0.37 <sup>+0.17</sup> <sub>-...</sub>	7010 <sup>+...</sup> <sub>-750</sub>	<A9V	4.89 <sup>+...</sup> <sub>-0.60</sub>	-0.279 <sup>+0.042</sup> <sub>-...</sub>	32.0 <sup>+...</sup> <sub>-6.7</sub>	5.29	F, †
969	PG 1551+255		5.27 <sup>+0.32</sup> <sub>-0.18</sub>	+0.75 <sup>+0.06</sup> <sub>-0.03</sub>	5560 <sup>+90</sup> <sub>-180</sub>	G6V	4.45 <sup>+0.06</sup> <sub>-0.06</sub>	-0.247 <sup>+0.004</sup> <sub>-0.004</sub>	26.8 <sup>+0.6</sup> <sub>-0.6</sub>	0.47	
1010	PG 1610+519		7.61 <sup>+0.26</sup> <sub>-0.27</sub>	+1.22 <sup>+0.06</sup> <sub>-0.06</sub>	4320 <sup>+120</sup> <sub>-130</sub>	K5V	4.64 <sup>+0.06</sup> <sub>-0.06</sub>	-0.260 <sup>+0.004</sup> <sub>-0.004</sub>	28.8 <sup>+0.7</sup> <sub>-0.6</sub>	0.07	

Continued on Next Page...

Table 6.2 – Continued

ID#	Name	Late-type Companion <sup>a</sup>				Hot Subdwarf <sup>a</sup>			$F_{V,\text{rat}}$ <sup>b</sup>	Notes <sup>c</sup>
		$M_{V,c}$	$(B-V)_c$	$T_{\text{eff},c}$	Type	$M_{V,\text{sd}}$	$(B-V)_{\text{sd}}$	$T_{\text{eff},\text{sd}}$		
1051	PG 1629+081	$7.56^{+0.31}_{-0.65}$	$+1.21^{+0.07}_{-0.14}$	$4340^{+290}_{-150}$	K5V	$4.43^{+0.06}_{-0.07}$	$-0.246^{+0.004}_{-0.004}$	$26.6^{+0.6}_{-0.6}$	0.06	F
1092	TON 264	$6.90^{+0.11}_{-0.11}$	$+1.06^{+0.02}_{-0.02}$	$4660^{+50}_{-40}$	K4V	$4.61^{+0.06}_{-0.06}$	$-0.258^{+0.004}_{-0.004}$	$28.5^{+0.6}_{-0.6}$	0.12	
1096	PG 1648+080	$3.30^{+0.01}_{-0.04}$	$+0.68^{+0.02}_{-0.02}$	$5770^{+60}_{-60}$	G0-1IV	$4.18^{+0.07}_{-0.07}$	$-0.231^{+0.004}_{-0.004}$	$24.4^{+0.6}_{-0.6}$	2.25	§
1133	PG 1701+359	$6.30^{+0.18}_{-0.17}$	$+0.93^{+0.04}_{-0.03}$	$5010^{+90}_{-120}$	K2V	$4.25^{+0.07}_{-0.07}$	$-0.235^{+0.004}_{-0.004}$	$25.0^{+0.6}_{-0.6}$	0.15	
1164	PG 1718+519	$4.55^{+0.19}_{-0.19}$	$+0.62^{+0.04}_{-0.04}$	$5970^{+140}_{-130}$	F9V	$4.43^{+0.06}_{-0.07}$	$-0.246^{+0.004}_{-0.004}$	$26.6^{+0.6}_{-0.6}$	0.89	
1182	BD+29°3070	$3.36^{+0.34}_{-...}$	$+0.39^{+0.07}_{-...}$	$6900^{+...}_{-330}$	A9V	$4.73^{+...}_{-0.18}$	$-0.267^{+0.013}_{-...}$	$29.9^{+...}_{-2.1}$	3.53	†
1223	HD 185510	$1.00^{+0.11}_{-0.11}$	$+1.25^{+0.02}_{-0.02}$	$4230^{+50}_{-50}$	K3IV	$3.70^{+0.11}_{-0.08}$	$-0.204^{+0.004}_{-0.006}$	$20.9^{+0.7}_{-0.5}$	12.04	§
1297	PG 2110+127	$<3.19$	$<+0.35$	$<7120$	<A9V	$4.73^{+...}_{-0.18}$	$-0.267^{+0.012}_{-...}$	$29.9^{+...}_{-2.0}$	4.11	†, *
1304	PG 2116+008	$7.87^{+...}_{-0.31}$	$+1.28^{+...}_{-0.07}$	$4190^{+150}_{-...}$	K7V	$4.67^{+0.06}_{-0.06}$	$-0.262^{+0.004}_{-0.004}$	$29.1^{+0.7}_{-0.6}$	0.05	sdO, †
1306	PG 2118+126	$<3.19$	$<+0.35$	$<7120$	<A9V	$4.65^{+0.22}_{-0.18}$	$-0.261^{+0.012}_{-0.017}$	$29.0^{+2.9}_{-1.9}$	3.83	†
1322	BPS CS 29495-21	$6.32^{+0.10}_{-0.25}$	$+0.93^{+0.02}_{-0.05}$	$5010^{+150}_{-60}$	K2V	$4.49^{+0.06}_{-0.06}$	$-0.250^{+0.004}_{-0.004}$	$27.2^{+0.6}_{-0.6}$	0.19	
1346	PG 2148+095	$<3.19$	$<+0.35$	$<7120$	<A9V	$3.62^{+0.08}_{-...}$	$-0.200^{+...}_{-0.004}$	$20.5^{+0.5}_{-...}$	1.48	†
1348	PG 2151+100	$7.87^{+...}_{-0.16}$	$+1.28^{+...}_{-0.04}$	$4190^{+90}_{-...}$	K7V	$4.52^{+0.06}_{-0.06}$	$-0.252^{+0.004}_{-0.004}$	$27.5^{+0.6}_{-0.6}$	0.05	†
1356	PG 2158+082	$3.19^{+0.22}_{-...}$	$+0.35^{+0.05}_{-...}$	$7120^{+...}_{-270}$	<A9V	$4.84^{+...}_{-0.54}$	$-0.275^{+0.037}_{-...}$	$31.3^{+...}_{-5.9}$	4.55	sdO, †
1424	Balloon 090900007	$<3.19$	$<+0.35$	$<7120$	<A9V	$4.89^{+...}_{-0.19}$	$-0.279^{+0.015}_{-...}$	$32.0^{+...}_{-2.6}$	4.77	†
1457	BD-7°5977	$2.34^{+0.09}_{-0.10}$	$+0.94^{+0.02}_{-0.02}$	$4980^{+60}_{-50}$	G7IV	$4.08^{+0.14}_{-0.07}$	$-0.225^{+0.004}_{-0.008}$	$23.6^{+1.1}_{-0.5}$	4.98	§
1461A	PB 5333	$7.87^{+...}_{-0.10}$	$+1.28^{+...}_{-0.02}$	$4190^{+50}_{-...}$	K7V	$4.61^{+0.06}_{-0.06}$	$-0.258^{+0.004}_{-0.004}$	$28.5^{+0.6}_{-0.6}$	0.05	†

Continued on Next Page...

Table 6.2 – Continued

ID#	Name		Late-type Companion <sup>a</sup>			Hot Subdwarf <sup>a</sup>		$F_{V,\text{rat}}$ <sup>b</sup>	Notes <sup>c</sup>
	Red	Blue	$M_{V,c}$	$(B-V)_c$	$T_{\text{eff},c}$	Type	$M_{V,\text{sd}}$ $(B-V)_{\text{sd}}$		
1519	CD-27 16503		$6.13^{+0.24}_{-0.13}$	$+0.90^{+0.05}_{-0.02}$	$5100^{+60}_{-150}$	K1V	$3.94^{+0.15}_{-0.15}$ $-0.217^{+0.008}_{-0.008}$	$22.5^{+1.1}_{-1.0}$	sdO
1525	BPS CS 22957-23		$6.68^{+0.22}_{-0.22}$	$+1.02^{+0.05}_{-0.05}$	$4760^{+140}_{-120}$	K4V	$4.73^{+0.16}_{-0.06}$ $-0.267^{+0.004}_{-0.013}$	$29.9^{+2.2}_{-0.7}$	0.17

<sup>a</sup> $T_{\text{eff}}$  for the companions is given in K, and kK for the hot subdwarfs. If an error is missing (given as “ $\pm \dots$ ”), it means that there is no constraint in that direction (the acceptable values reach the edge of the grid and likely pass beyond the edge of the grid), so the value of the best-fit should be taken as a limit.

<sup>b</sup>Flux ratio at  $V$  between the companion and hot subdwarf:  $F_{V,\text{rat}} = F_{V,\text{comp}}/F_{V,\text{sd}}$

<sup>c</sup>A symbol (\*, †, or §) in this column indicates the object is discussed in the text in §6.6. Those objects that were previously classified as “sdO” (see §4.6.2) are labelled with that designation in this column. If the letter “F” appears in the notes, it means that the observation(s) used for the fit was affected by residual fringing at the CaT. “RED” = star #199 is highly reddened, so appeared composite-colored due to reddening; the fit presented here is therefore bogus, but presented for consistency. For star #1096 adopted value is the average of 3rd and 4th measurements listed in Table 6.1.



Table 6.3: Previous and My Classifications of the Companions in Composite-Colored Hot Subdwarfs.

ID#	Name	My Classification		Previous Classifications <sup>a</sup>	Notes <sup>b</sup>
		$(B-V)_c$	$T_{\text{eff},c}$	Type	
1	SB 7	$+0.92^{+0.05}_{-0.02}$	$5040^{+60}_{-150}$	K1V	$\approx 7000, 5750(\text{G2})$ *
59	PB 6107	$+0.83^{+0.02}_{-0.05}$	$5310^{+150}_{-60}$	G9V	K4 *
65	PB 6148	$+0.59^{+0.07}_{-0.07}$	$6080^{+250}_{-240}$	F7V	late F+sdOB?
71	BD-11°162	$+0.87^{+0.05}_{-0.05}$	$5190^{+150}_{-150}$	K0V	F4-G0 sdO, *
95	PG 0110+262	$<+0.35$	$<7120$	$<\text{A9V}$	K2.5, 6000-5000(F9-K1), 5000(K1), 5485 $\pm$ 200, 5250 $\pm$ 800 *
101	PG 0116+242	$+0.66^{+0.02}_{-0.02}$	$5830^{+70}_{-60}$	G0IV	G5-G6 *
102	PB 8783	$<+0.35$	$<7120$	$<\text{A9V}$	7000
120	PHL 3802	$+0.85^{+0.07}_{-0.02}$	$5250^{+60}_{-220}$	K0V	$\approx 5500$ *
150	PG 0232+095	$<+0.35$	$<7120$	$<\text{A9V}$	4600-5000(K1-K6), 4750(K2), 4575 $\pm$ 50 †
		$+0.75^{+0.02}_{-0.02}$	$5550^{+60}_{-60}$	G2IV	
172	PG 0314+103	$<+0.35$	$<7120$	$<\text{A9V}$	later than K6 *
187A	HDE 283048	$<+0.35$	$<7120$	$<\text{A9V}$	4000-4600(K3-K8), 7500(A8)
199	KUV 04110+1434	$<+0.35$	$<7120$	$<\text{A9V}$	...
203	KUV 04237+1649	$<+0.35$	$<7120$	$<\text{A9V}$	...

Continued on Next Page...

Table 6.3 – Continued

ID#	Name	My Classification		Type	Previous Classifications <sup>a</sup>		Notes <sup>b</sup>
		$(B-V)_c$	$T_{\text{eff},c}$				
234	BD+34°1543	+0.60 <sup>+0.04</sup> <sub>-0.04</sub>	6040 <sup>+140</sup> <sub>-140</sub>	F8V	6010 ± 70(F8-G0), 5500(G8)		
294	PG 0900+400	+0.71 <sup>+0.02</sup> <sub>-0.03</sub>	5670 <sup>+90</sup> <sub>-60</sub>	G1IV	K3V, 5150 ± 130		*
460	PG 1104+243	+0.61 <sup>+0.07</sup> <sub>-0.05</sub>	6010 <sup>+170</sup> <sub>-230</sub>	F8V	K2, K3.5, G8V, 4000–6000, 5735 ± 150, 6400 ± 1000		
533	BD+10°2357	<+0.35	<7120	<A9V	7300–7900(A8–A9), 5750(G2)		sdO
551	PB 3854	+0.83 <sup>+0.02</sup> <sub>-0.02</sub>	5310 <sup>+60</sup> <sub>-60</sub>	G9V	...		
583	LB 2392	+0.68 <sup>+0.05</sup> <sub>-0.05</sub>	5780 <sup>+160</sup> <sub>-160</sub>	G2V	K5		*
630	TON 139	+0.52 <sup>+0.07</sup> <sub>-0.07</sub>	6330 <sup>+290</sup> <sub>-250</sub>	F5V	4750(K2)		*
638	PG 1257–026	+0.40 <sup>+0.10</sup> <sub>-...</sub>	6850 <sup>+...</sup> <sub>-440</sub>	F0V	...		
697	Feige 87	+0.87 <sup>+0.02</sup> <sub>-0.02</sub>	5190 <sup>+60</sup> <sub>-60</sub>	K0V	K4.5, 4000–6000		*
702	PG 1343+578	+0.64 <sup>+0.05</sup> <sub>-0.05</sub>	5910 <sup>+170</sup> <sub>-160</sub>	G0V	...		
706	PG 1347+086	+0.66 <sup>+0.02</sup> <sub>-0.02</sub>	5830 <sup>+70</sup> <sub>-60</sub>	G0IV	...		
789	PG 1429+406	+0.54 <sup>+0.02</sup> <sub>-0.02</sub>	6250 <sup>+80</sup> <sub>-70</sub>	F8IV	...		
844	PG 1449+653	+0.78 <sup>+0.05</sup> <sub>-0.02</sub>	5470 <sup>+60</sup> <sub>-150</sub>	G7V	K4, 4700 ± 1475		*
849	PG 1451+472	+0.66 <sup>+0.02</sup> <sub>-0.02</sub>	5830 <sup>+70</sup> <sub>-60</sub>	G0IV	...		
895	PG 1514+034	+0.75 <sup>+0.02</sup> <sub>-0.05</sub>	5560 <sup>+150</sup> <sub>-60</sub>	G6V	K2, G8V		

Continued on Next Page...

Table 6.3 – Continued

ID#	Name	My Classification		Type	Previous Classifications <sup>a</sup>	Notes <sup>b</sup>
		$(B-V)_c$	$T_{\text{eff},c}$			
912	PG 1524+611	+0.61 <sup>+0.12</sup> <sub>-0.26</sub>	6010 <sup>+1110</sup> <sub>-390</sub>	F8V	...	
937	PG 1536+278	+0.37 <sup>+0.17</sup> <sub>...</sub>	7010 <sup>+</sup> <sub>-750</sub>	<A9V	...	
969	PG 1551+255	+0.75 <sup>+0.06</sup> <sub>-0.03</sub>	5560 <sup>+90</sup> <sub>-180</sub>	G6V	...	
1010	PG 1610+519	+1.22 <sup>+0.06</sup> <sub>-0.06</sub>	4320 <sup>+120</sup> <sub>-130</sub>	K5V	K8	*
1051	PG 1629+081	+1.21 <sup>+0.07</sup> <sub>-0.14</sub>	4340 <sup>+290</sup> <sub>-150</sub>	K5V	K7.5, 3825 ± 575	
1092	TON 264	+1.06 <sup>+0.02</sup> <sub>-0.02</sub>	4660 <sup>+50</sup> <sub>-40</sub>	K4V	K7	*
1096	PG 1648+080	+0.68 <sup>+0.02</sup> <sub>-0.02</sub>	5770 <sup>+60</sup> <sub>-60</sub>	G0-1IV	...	
1133	PG 1701+359	+0.93 <sup>+0.04</sup> <sub>-0.03</sub>	5010 <sup>+90</sup> <sub>-120</sub>	K2V	K6.5, 6450 ± 230, 6000 ± 1000	
1164	PG 1718+519	+0.62 <sup>+0.04</sup> <sub>-0.04</sub>	5970 <sup>+140</sup> <sub>-130</sub>	F9V	K3.5, 5925 ± 70, 5200 ± 400	
1182	BD+29°3070	+0.39 <sup>+0.07</sup> <sub>...</sub>	6900 <sup>+</sup> <sub>-330</sub>	A9V	5250(K0), 8050 ± 400	
1223	HD 185510	+1.25 <sup>+0.02</sup> <sub>-0.02</sub>	4230 <sup>+50</sup> <sub>-50</sub>	K3IV	K0III-IV	
1297	PG 2110+127	<+0.35	<7120	<A9V	K2.5, 5750(G2), 5500 ± 575, 5400 ± 400	*, †
1304	PG 2116+008	+1.28 <sup>+</sup> <sub>-0.07</sub>	4190 <sup>+150</sup> <sub>...</sub>	K7V	...	sdO
1306	PG 2118+126	<+0.35	<7120	<A9V	K2, 5250(K0)	*
1322	BPS CS 29495-21	+0.93 <sup>+0.02</sup> <sub>-0.05</sub>	5010 <sup>+150</sup> <sub>-60</sub>	K2V	...	

Continued on Next Page...

Table 6.3 – Continued

ID#	Name	My Classification		Type	Previous Classifications <sup>a</sup>	Notes <sup>b</sup>
		$(B-V)_c$	$T_{\text{eff},c}$			
1346	PG 2148+095	$<+0.35$	$<7120$	$<\text{A9V}$	K3.5, 5000(K1), $4375 \pm 200$ , $5700 \pm 400$	*
1348	PG 2151+100	$+1.28^{+...}_{-0.04}$	$4190^{+90}_{-...}$	K7V	3500(M2)	
1356	PG 2158+082	$+0.35^{+0.05}_{-...}$	$7120^{+...}_{-270}$	$<\text{A9V}$	...	
1424	Balloon 090900007	$<+0.35$	$<7120$	$<\text{A9V}$	G2	*
1457	BD-7°5977	$+0.94^{+0.02}_{-0.02}$	$4980^{+60}_{-50}$	G7IV	K0IV-III, 4750(K2)	
1461A	PB 5333	$+1.28^{+...}_{-0.02}$	$4190^{+50}_{-...}$	K7V	...	
1519	CD-27 16503	$+0.90^{+0.05}_{-0.02}$	$5100^{+60}_{-150}$	K1V	$\approx 7000$	sdO, *
1525	BPS CS 22957-23	$+1.02^{+0.05}_{-0.05}$	$4760^{+140}_{-120}$	K4V	...	

<sup>a</sup>Previous classifications listed with references in Table 4.3.<sup>b</sup>Hot subdwarfs previously classified as sdOs are indicated. A star (“\*”) indicates an inconsistency between my best fit and previous fits reported in the literature (see §6.5). Objects marked with a “+” in the notes column are discussed in §6.6.3. “RED” = star #199 is highly reddened, so appeared composite-colored due to reddening, the fit presented here is therefore bogus, but presented for consistency.

Table 6.4: Previous and My Classifications of the Hot Subdwarfs in Composite-Colored Systems.

ID#	Name	My Classifications		Previous Classifications <sup>a</sup>	Notes <sup>b</sup>
		$(B-V)_{sd}$	$T_{eff, sd}$		
1	SB 7	$-0.213^{+0.004}_{-0.010}$	$22.0^{+1.3}_{-0.5}$	55 ± 10, 50	*
59	PB 6107	$-0.246^{+0.004}_{-0.004}$	$26.6^{+0.6}_{-0.6}$	26.7, 25, 23	
65	PB 6148	$-0.250^{+0.004}_{-0.004}$	$27.2^{+0.6}_{-0.6}$	...	
71	BD-11°162	$-0.246^{+0.004}_{-0.004}$	$26.6^{+0.6}_{-0.6}$	35, sdO	*
95	PG 0110+262	$-0.221^{+0.008}_{-0.008}$	$23.1^{+1.1}_{-1.0}$	22, 22, 21, 21.05 ± 0.575, 21.0 ± 0.75	
101	PG 0116+242	$-0.213^{+0.004}_{-0.004}$	$22.0^{+0.5}_{-0.5}$	14	*
102	PB 8783	$-0.221^{+0.008}_{-0.017}$	$23.1^{+2.4}_{-1.0}$	33	*
120	PHL 3802	$-0.233^{+0.004}_{-0.004}$	$24.7^{+0.6}_{-0.6}$	30 ± 0.3	*
150	PG 0232+095	$< -0.279$	$> 32.0$	25-50, 18-30(21:), 21, 21.5 ± 0.5	†
172	PG 0314+103	$-0.258^{+0.004}_{-0.013}$	$28.5^{+2.1}_{-0.6}$	18	*
187A	HDE 283048	$-0.225^{+0.004}_{-0.008}$	$23.6^{+1.1}_{-0.5}$	40-80, 40	*
199	KUV 04110+1434	$-0.233^{+0.008}_{-0.017}$	$24.7^{+2.5}_{-1.1}$	...	RED
203	KUV 04237+1649	$-0.229^{+0.004}_{-0.008}$	$24.1^{+1.1}_{-0.5}$	...	
234	BD+34°1543	$-0.233^{+0.008}_{-0.008}$	$24.7^{+1.2}_{-1.1}$	25, 26	
294	PG 0900+400	$-0.242^{+0.004}_{-0.004}$	$26.0^{+0.6}_{-0.6}$	31, 25 ± 0.925	*
		$-0.211^{+...}_{-0.012}$	$21.8^{+1.5}_{-...}$		

Continued on Next Page...

Table 6.4 – Continued

ID#	Name	My Classifications ( $B-V$ ) <sub>sd</sub>	$T_{\text{eff, sd}}$	Previous Classifications <sup>a</sup>	Notes <sup>b</sup>
460	PG 1104+243	-0.233 <sup>+0.008</sup> <sub>-0.004</sub>	24.7 <sup>+0.6</sup> <sub>-1.1</sub>	28, 27.5, 28 ± 0.875, 32.85 ± 1.55	*
533	BD+10°2357	-0.200 <sup>+</sup> <sub>-0.008</sub>	20.5 <sup>+1.0</sup> <sub>-...</sub>	25–35, 27, sdO	*
551	PB 3854	-0.275 <sup>+0.004</sup> <sub>-0.004</sub>	31.3 <sup>+0.7</sup> <sub>-0.7</sub>	...	
583	LB 2392	-0.200 <sup>+</sup> <sub>-0.008</sub>	20.5 <sup>+1.0</sup> <sub>-...</sub>	28	*
630	TON 139	-0.221 <sup>+0.004</sup> <sub>-0.004</sub>	23.1 <sup>+0.5</sup> <sub>-0.5</sub>	18, 20	*
638	PG 1257–026	-0.221 <sup>+0.021</sup> <sub>-0.021</sub>	23.1 <sup>+2.9</sup> <sub>-2.6</sub>	...	
697	Feige 87	-0.233 <sup>+0.004</sup> <sub>-0.004</sub>	24.7 <sup>+0.6</sup> <sub>-0.6</sub>	23.5	
702	PG 1343+578	-0.200 <sup>+</sup> <sub>-0.004</sub>	20.5 <sup>+0.5</sup> <sub>-...</sub>	HBB	
706	PG 1347+086	-0.200 <sup>+</sup> <sub>-0.004</sub>	20.5 <sup>+0.5</sup> <sub>-...</sub>	...	
789	PG 1429+406	-0.279 <sup>+0.004</sup> <sub>-...</sub>	32.0 <sup>+</sup> <sub>-0.7</sub>	...	
844	PG 1449+653	-0.225 <sup>+0.004</sup> <sub>-0.004</sub>	23.6 <sup>+0.5</sup> <sub>-0.5</sub>	28, 28.15 ± 9	*
849	PG 1451+472	-0.209 <sup>+0.004</sup> <sub>-0.004</sub>	21.5 <sup>+0.5</sup> <sub>-0.5</sub>	...	
895	PG 1514+034	-0.229 <sup>+0.004</sup> <sub>-0.004</sub>	24.1 <sup>+0.6</sup> <sub>-0.5</sub>	31	*
912	PG 1524+611	-0.229 <sup>+0.029</sup> <sub>-0.008</sub>	24.1 <sup>+1.1</sup> <sub>-3.7</sub>	...	
937	PG 1536+278	-0.279 <sup>+0.042</sup> <sub>-...</sub>	32.0 <sup>+</sup> <sub>-6.7</sub>	...	
969	PG 1551+255	-0.247 <sup>+0.004</sup> <sub>-0.004</sub>	26.8 <sup>+0.6</sup> <sub>-0.6</sub>	...	
1010	PG 1610+519	-0.260 <sup>+0.004</sup> <sub>-0.004</sub>	28.8 <sup>+0.7</sup> <sub>-0.6</sub>	32.5	*

Continued on Next Page...

Table 6.4 – Continued

ID#	Name	My Classifications ( $B-V$ ) <sub>sd</sub>	$T_{\text{eff, sd}}$	Previous Classifications <sup>a</sup>	Notes <sup>b</sup>
1051	PG 1629+081	-0.246 <sup>+0.004</sup> <sub>-0.004</sub>	26.6 <sup>+0.6</sup> <sub>-0.6</sub>	32.5, 26.4 ± 1.15	
1092	TON 264	-0.258 <sup>+0.004</sup> <sub>-0.004</sub>	28.5 <sup>+0.6</sup> <sub>-0.6</sub>	36.5 ± 1.5, 28.5, 26	
1096	PG 1648+080	-0.231 <sup>+0.004</sup> <sub>-0.004</sub>	24.4 <sup>+0.6</sup> <sub>-0.6</sub>	...	
1133	PG 1701+359	-0.235 <sup>+0.004</sup> <sub>-0.004</sub>	25.0 <sup>+0.6</sup> <sub>-0.6</sub>	26.25 ± 1.25, 28.5, 30, 31.4, 36.075 ± 0.7, 32.5 ± 1.325	
1164	PG 1718+519	-0.246 <sup>+0.004</sup> <sub>-0.004</sub>	26.6 <sup>+0.6</sup> <sub>-0.6</sub>	23.5 ± 1.0, 25, 30, 29.95 ± 1.1, 29 ± 1.55, 27	
1182	BD+29°3070	-0.267 <sup>+0.013</sup> <sub>-0.013</sub>	29.9 <sup>+...</sup> <sub>-2.1</sub>	18, 32.85 ± 2.75	
1223	HD 185510	-0.204 <sup>+0.004</sup> <sub>-0.006</sub>	20.9 <sup>+0.7</sup> <sub>-0.5</sub>	~20–30	
1297	PG 2110+127	-0.267 <sup>+0.012</sup> <sub>-0.012</sub>	29.9 <sup>+...</sup> <sub>-2.0</sub>	25.4 ± 1.6, 26, 33.7, 30, 34, 24.9 ± 6.5, 26.5 ± 1.7	†
1304	PG 2116+008	-0.262 <sup>+0.004</sup> <sub>-0.004</sub>	29.1 <sup>+0.7</sup> <sub>-0.6</sub>	sdO	
1306	PG 2118+126	-0.261 <sup>+0.012</sup> <sub>-0.017</sub>	29.0 <sup>+2.9</sup> <sub>-1.9</sub>	26.5, 25	*
1322	BPS CS 29495–21	-0.250 <sup>+0.004</sup> <sub>-0.004</sub>	27.2 <sup>+0.6</sup> <sub>-0.6</sub>	...	
1346	PG 2148+095	-0.200 <sup>+...</sup> <sub>-0.004</sub>	20.5 <sup>+0.5</sup> <sub>-...</sub>	26, 25, 22.95 ± 0.825, 30 ± 0.86, 26	*
1348	PG 2151+100	-0.252 <sup>+0.004</sup> <sub>-0.004</sub>	27.5 <sup>+0.6</sup> <sub>-0.6</sub>	27	
1356	PG 2158+082	-0.275 <sup>+0.037</sup> <sub>-0.037</sub>	31.3 <sup>+...</sup> <sub>-5.9</sub>	67, He-sdO	*
1424	Balloon 090900007	-0.279 <sup>+0.015</sup> <sub>-0.015</sub>	32.0 <sup>+...</sup> <sub>-2.6</sub>	24	*
1457	BD–7°5977	-0.225 <sup>+0.004</sup> <sub>-0.008</sub>	23.6 <sup>+1.1</sup> <sub>-0.5</sub>	31 ± 0.5, 31, 29	*
1461A	PB 5333	-0.258 <sup>+0.004</sup> <sub>-0.004</sub>	28.5 <sup>+0.6</sup> <sub>-0.6</sub>	37.9, sdOB	*

Continued on Next Page...

Table 6.4 – Continued

ID #	Name	My Classifications $(B - V)_{\text{sd}}$	$T_{\text{eff, sd}}$	Previous Classifications <sup>a</sup>	Notes <sup>b</sup>
1519	CD-27 16503	$-0.217^{+0.008}_{-0.008}$	$22.5^{+1.1}_{-1.0}$	$75 \pm 15$ , sdO	*
1525	BPS CS 22957-23	$-0.267^{+0.004}_{-0.013}$	$29.9^{+2.2}_{-0.7}$	...	

<sup>a</sup>Previous classifications listed with references in Table 4.3.

<sup>b</sup>A star (“\*”) indicates an inconsistency between my best fit and previous fits reported in the literature (see §6.5). Objects marked with a “+” in the notes column are discussed in §6.6.3. “RED” = star #199 is highly reddened, so appeared composite-colored due to reddening, the fit presented here is therefore bogus, but presented for consistency.



Table 6.5. Parameters for Resolved Visual Double Companions to Hot Subdwarfs

ID#	Name <sup>a</sup>	$M_{V,c}$	$(B-V)_c$	$T_{\text{eff},c}$ <sup>b</sup>	Type	Pair? <sup>c</sup>
50B	PG 0027+222B	$3.6399^{+0.2341}_{-0.3375}$	$0.4450^{+0.0475}_{-0.0712}$	$6640^{+350}_{-200}$	F2V	y
87B	PG 0105+276B	$5.4101^{+0.1393}_{-0.1376}$	$0.7775^{+0.0238}_{-0.0237}$	$5470^{+70}_{-70}$	G7V	y
130B	Feige 19B	$7.8685^{+...}_{-0.1033}$	$1.2763^{+...}_{-0.0237}$	$4200^{+50}_{-...}$	>K7V	n
157B	PB 9286B	$3.1936^{+0.1088}_{-0.0118}$	$0.3500^{+0.0238}_{-...}$	$7120^{+...}_{-130}$	<A9V	n
187B	HDE 283048B	$4.3630^{+0.1249}_{-0.1237}$	$0.5875^{+0.0238}_{-0.0237}$	$6080^{+80}_{-80}$	F7V	n
700B	PG 1340+607B	$5.2725^{+0.1376}_{-0.1366}$	$0.7538^{+0.0237}_{-0.0238}$	$5550^{+70}_{-70}$	G6V	y
1348B	PG 2151+100B	$6.3740^{+0.1978}_{-0.1177}$	$0.9438^{+0.0475}_{-0.0238}$	$4970^{+70}_{-140}$	K2V	y
1461B	PB 5333B	$3.7560^{+0.4832}_{-0.5625}$	$0.4688^{+0.0950}_{-0.1188}$	$6530^{+580}_{-370}$	F3V	n

<sup>a</sup>Resolved visual companions for which the spectra were not contaminated. See also §4.6.3, Figures 4.15–4.17 and 4.20–4.22, and Table 4.2.

<sup>b</sup> $T_{\text{eff}}$  for the companions is given in K. If an error is missing (given as “ $\pm \dots$ ”), it means that there is no constraint in that direction (the acceptable values reach the edge of the grid and likely pass beyond the edge of the grid), so the value of the best-fit should be taken as a limit.

<sup>c</sup>Estimate by eye of the possibility that this star is associated with the hot subdwarf based on the apparent magnitude differences, the fitted absolute magnitude of the resolved companion, and the average absolute magnitude of a hot subdwarf: “y” = likely associated, “n” = likely unassociated.

## Chapter 7

### Discussion and Summary

#### 7.1 Defining the Sample

For this investigation I studied hot subdwarf stars listed in the *Catalogue of Spectroscopically Identified Hot Subdwarfs* (Kilkenny, Heber, & Drilling 1988, KHD) as updated and expanded in an electronic version by Kilkenny, c. 1992, kindly made available to me by D. Kilkenny (§2.1). While the KHD catalog contains all varieties of hot subdwarfs, I primarily focused on the more numerous sdB stars. The sdB are understood to be relatively homogeneous and probably have a common evolution history from the ZAEHB, while sdO stars likely follow multiple evolutionary pathways and might be expected to be less homogeneous and to have less simply explained properties (§1.1).

To make a comparison of the KHD data with existing databases (such as 2MASS) or to obtain new observations of the correct star, accurate coordinates on a consistent system are required. For each entry the object's position was verified by referring whenever possible to original published finding charts or by contacting knowledgeable observers, then locating the object on a chart prepared from the USNO A2.0 Catalog (§2.2).

#### 7.2 2MASS Results

I collected readily available visible and near-IR flux measurements of hot subdwarfs from the 2MASS ASDR Catalog and identified those whose colors indicate the presence of a late type companion (Ch. 3). I thus determined the fraction of hot subdwarfs that exist in composite spectrum binaries ( $\sim 40\%$  of sdBs from KHD are composite in a MLS). I defined an approximately volume limited sample of hot subdwarfs from KHD for statistical purposes, and found that  $\sim 25\%$  of sdBs are composite in a VLS (§3.4).

I defined the color parameter  $Q = 0.752(J-H) + (J-K_S)$ , which gives the clearest separation between composite and single hot subdwarfs based on 2MASS photometry alone (§3.6.2, §G.2). I compared the distributions in  $J-K_S$ ,  $J-H$ , and  $Q$ , and found them all to show a bimodally distributed population. In a histogram of the IR color indices  $J-K_S$  and  $Q$ , the two peaks of the bimodal distribution can be understood as single stars (blue peak at  $J-K_S = -0.170$ ,  $Q \approx -0.275$ ) and composite systems (red peak at  $J-K_S = +0.289$ ,  $Q \approx +0.500$ ). This bimodal distribution is also present in the approximately VLS, again with the two peaks at  $J-K_S = -0.167$  and  $+0.248$ , and  $Q \approx -0.275$  and  $+0.475$ .

*There are no (or very few) F or dM companions of the hot subdwarfs in the KHD catalog.* This is evident from the bimodal distribution in 2MASS colors ( $Q$ ,  $J-K_S$ , and  $J-H$ ). Were there a large population of F or dM companions, their composite colors would have filled in the gap between the two bimodal peaks. However, the distribution

in 2MASS colors can be described by only a very small (or no) spread in the colors of the late-type companions. In the case of F-type and earlier companions, should they actually exist, it is likely that most of them were never identified as containing a hot subdwarf. The F-type star would dominate the light at visual wavelengths, and the combined light would look spectroscopically like a metal-poor Pop II star (the metal lines of the Pop I star being diluted by the hot subdwarf so they look like a Pop II star). So, it is understandable that there are very few of these objects in the current KHD catalog. The dM stars on the other hand, have no obvious reason to be selected against in surveys that have identified hot subdwarfs. The dM is significantly fainter than the hot subdwarf, so that it should be basically undiscernible in the visible (both photometrically and spectroscopically). So, the fact that there are no (or very few) dM companions in the KHD sample represents a true trend in the hot subdwarf population (as opposed to a possible selection bias as in the case of the F-type and earlier stars).

The observed distribution of hot subdwarfs in 2MASS colors can be reproduced equally well by either assuming main sequence companions with a  $M_{V,\text{sdb}} \approx 4.5\text{--}5.0$  mag, or by assuming subgiant companions with more luminous sdb stars ( $M_{V,\text{sdb}} \approx 2.5\text{--}3.0$  mag) — photometric data alone cannot distinguish between these two possibilities.

### 7.3 Spectroscopy of Composite Hot Subdwarfs

Spectroscopy of a sub-sample of the 2MASS composite-colored hot subdwarfs was obtained to break the degeneracy between MS and subgiant companions present in the 2MASS and visual photometry alone. Observations were made primarily at the KPNO 2.1m telescope using the GoldCam spectrograph, but some additional observations came from the McDonald 2.7m telescope with LCS (Ch. 4). Both sets of observations cover roughly 4500–9000 Å with  $\sim 3.3$  Å resolution ( $\sim 1.3$  Å/pix). This wavelength region covers H $\beta$ , Mg I b, He I 5875 Å, Na I D, H $\alpha$ , He I 6678 Å, and CaT. My analysis focused on Mg I b, Na I D, and CaT EWs. Each of these lines has a very different behavior with  $T_{\text{eff}}$  and  $\log g$  (see Fig. 5.4), so they are useful for constraining the dilution by the hot subdwarf, as well as  $T_{\text{eff}}$  and  $M_V$  of the late-type companion, thus breaking the MS-subgiant degeneracy present in the 2MASS and visual photometry alone.

The observations (2MASS and visual photometry combined with EWs) for each composite hot subdwarf were compared with diluted models based on HIP standard star observations, models of EHB stars (Caloi 1972), and Kurucz (1998) SEDs, in order to determine the combination of sdb+late-type star that best explained all observations. In most cases the actual fit was driven primarily by the measured EWs, and secondarily by  $J - K_S$  color (this agrees with the previous determination that photometry alone cannot distinguish between MS and subgiant companions in these cases). With a few exceptions, it was found that the late-type companions in composite-spectrum systems are best identified as MS (§6.5). The majority of the well constrained MS companions have  $0.5 \lesssim (B - V)_c \lesssim 1.1$  (spectral types  $\sim \text{F6--K5}$ ).

There are some interesting objects identified through my spectroscopy. These include:

- Two new emission line objects, #1108 LS IV–08°03 and #1461 PB 5333 (one may be an X-ray binary, the other shows NLTE emission in the core of H $\alpha$ ) — §4.6.4

- One possible new NLTE core emission object, #1092, TON 264 — §6.6.3
- Nine objects best fit with subgiant companions (assuming ZAEHB or TAEHB hot subdwarfs), with an additional six best fit with subgiants assuming TAEHB hot subdwarfs — §6.6.2
- A possible *resolved* visual double sdB+sdB (or sdB+HBB), #550 HZ 18, which may also contain an inner short-period binary (based on the velocity difference between the spectra for the two stars) — §4.6.3

There were 18 cases in which the late-type companion was poorly fitted by my models (namely the best-fit parameters fell right at or near the edge of my model grid — §6.6.1). Additional refinement of the models, or extension of the models to include a larger temperature range in both the late-type stars (by obtaining more observations of standards) and the hot subdwarfs (more models over a larger temperature range) are needed to accurately fit these objects.

## 7.4 Limitations and Directions for Future Work

My modelling procedure is limited in the range of both hot subdwarf and late-type stars included. These models could be greatly improved by including a greater range in temperatures for both the companion and particularly for the hot subdwarf. Specifically I have trouble identifying and coping with the hottest sdBs, and the sdOs. I am also using the assumption that the hot member is in fact a true sdB-type star; if it is in fact a HBB or post-EHB star, then my modelling breaks down, giving bogus fits. Adding additional information to help constrain and tie down the properties of hot subdwarf would be of value (including whether it is sdB, sdO, post-EHB, or HBB). This additional information could include: UV observations or spectra with coverage farther to the blue. Also, including additional late-type spectral features from my spectra would help better constrain the fits.

Future work related to, or stemming from, this project includes:

1. Classification of more composite hot subdwarfs.
2. Long-term RV studies of composite spectrum systems to determine periods (or at least set lower limits on the periods).
3. Follow-up observations of “unusual” objects identified, including (for example): #150 PG 0232+095 (§6.6.3), #1092 TON 264 (§6.6.3), #550 HZ 18 (§4.6.3), and the emission lined objects (§4.6.4).
4. Further observations of the resolved visual doubles §4.6.3, including proper motions, and better classifications of the companions (particularly #550, HZ 18, which may be a resolved binary sdB+sdB or sdB+HBB system).

## 7.5 Implications

Understanding the current state of hot subdwarf binaries will place useful limits on all binary formation processes and models (e.g., the Han et al. 2002, 2003 models).

These models have broad reaching implications affecting all fields that involve interacting binaries, including areas such as supernova Ia progenitors and gravitational wave sources.

Han et al. (2002, 2003) predict that all MS companions later than  $\sim G$  are in short period ( $P \lesssim 40$  days), post-CE binaries. Additionally, any companion later than  $\sim G$  and in a long period ( $P \gtrsim 40$  days), post-RLOF binary is either a subgiant or giant companion. This is interesting because Han et al. assume that the hot subdwarfs with subgiant and giant companions were excluded from surveys for hot subdwarfs (however, I have identified some subgiant companions, so they were not all excluded). Yet, RV studies which have looked at composite spectrum hot subdwarfs (i.e., Orosz et al. 1997; Maxted et al. 2001; Saffer et al. 2001), have said the periods for FGK-composite binaries must be long (many months to years or more), which in the Han et al. scenario would imply that they contain the subgiant or giant companions. Yet, as I have shown, the majority of composite companions are consistent with MS stars, so it appears something is incorrect or incomplete in the current Han et al. binary formation scenario.

## Appendix A

### Coordinates and Object Notes

Table A.1 contains a listing of all hot subdwarfs (ordered by sequence number) from the KHD<sup>1</sup> catalog with updated coordinates (from 2MASS or other sources as noted) and other notes from KHD and our studies. The table notes are as follows:

1. The identifiers listed in the first column are consistent with SIMBAD nomenclature.
2. Coordinates are from the 2MASS All-Sky Data Release, unless they are immediately followed by a single letter (U, O, or D) after the declination, in that case they are from the sources as follows: U = coordinates listed originated from the USNO-A2.0 catalog; O = coordinates originated from a source other than 2MASS or USNO-A2.0 (i.e., from the Tycho catalog, or other source); D = coordinates listed are the original, and *unverified*, coordinates given in KHD precessed to J2000. The 2MASS coordinates listed here can be truncated and used to form the 2MASS identifier as: “2MASS Jhhmmss[.]s±ddmmss[.]s”. For example, the first object in the table, #1 SB 7, has the 2MASS identifier: “2MASS J00032442–1621062”.
3. Beers = T. C. Beers private communication; Caloi = V. Caloi private communication(?); CBS = Pesch & Sanduleak (1983); CS = Beers et al. (1992); Drill = J. S. Drilling private communication; Feige = Feige (1958); GD = Giclas, Burnham, & Thomas (1965); Heber = U. Heber private communication; HD = Henry Draper Catalog; HIP = Perryman et al. (1997); HZ = Humason & Zwicky (1947); JL = Jaidee & Lyngå (1974); KPD = Downes (1986); KUV = Noguchi, Maehara, & Kondo (1980); LBQS = Hewett, Foltz, & Chaffee (1995); LOB = Giclas, Burnham, & Thomas (1961); LSE = Drilling & Bergeron (1995); LSN = Stock, Nassau, & Stephenson (1960); LSS = Stephenson & Sanduleak (1971); MCT = Demers et al. (1990); ML = M. Laget private communication; PB = Berger & Fringant (1977, 1980, 1984); PG = Green et al. (1986); PGWD = Green et al. (1986) mis-classified as a white dwarf; pl = plausible identification based on colors and magnitudes; pre = precessed coordinates; RFG = R. F. Green private communication; RL = Rubin & Losee (1971); RWT = Rubin, Westpfahl, & Tuve (1974); SM = Schweizer & Middleditch (1980); SB = Slettebak & Brundage (1971); SIM = SIMBAD database, operated at CDS, Strasbourg, France; TL = T. Lanz private communication; TON = Iriarte & Chavira (1957); Chavira (1959); TOND = TON(?); TONS = Chavira (1958); TYC = Høg et al. (1998); *a* = KHD Declination very wrong, PHL=BPS? (1 mag err); *b* = SIMBAD ID with Tycho star likely in

---

<sup>1</sup>Kilkenny, Heber, & Drilling (1988) as updated and expanded in an electronic version by Kilkenny, c. 1992, kindly made available by D. Kilkenny.

error, probably=EC star;  $c$  = PG, no published chart, pending confirmation by R. F. Green;  $d$  = U. Heber: NOT the Tycho star;  $e$  = not a subdwarf (Dufton et al);  $f$  = Also EC;  $g$  = precessed from Berg et al. (1992), USNO screwy.

4. P, B, J = photographic magnitude is listed;  $y$  = Strömgren  $y$  magnitude given instead of Johnson  $V$ , and the value of  $B-V$  listed was converted from Strömgren photometry; (B) = photoelectric  $B$  given instead of Johnson  $V$ ;  $v$  = magnitude variable; colon (:) = magnitude or color is uncertain.
5. The first identifier that appears in KHD for a given entry. For example, the designator CSHK 30339–8 used by KHD for star #25 in this table is equivalent to the SIMBAD designator BPS CS 30339–8, and the designator KPD 00330+5229 used by KHD for star #55 in this table is equivalent to the SIMBAD designator KPD 0033+5229. If no other ID is given in this column, then the SIMBAD identifier (given in column 2) is consistent with the notation used in KHD. For duplicate entries in KHD (see note 6), if the duplicate’s name in KHD does not conform to the SIMBAD standards then the duplicate’s KHD identifier is listed in parentheses in the line below the main entry. Objects that had dual identities in both PG and KUV have been abbreviated as ‘K/P’ (i.e., #169, PG 0313+005 is listed as “KUV/PG 03137+0031” in KHD).
6. #NNNN = indicates a duplicate entry sequence number, the duplicate’s name from KHD is listed in the following line in parentheses (the duplicate entry is not otherwise listed in this table);  $a$  = #87, Heber et al. (2002) report that this pair is resolved into three components with HST: the sdO is the NW star of the “pair,” while the SE “companion” star resolves into two components separated from the sdO by  $3''.37$  and  $4''.48$ .  $b$  = #284, variable double M (KHD);  $c$  = #293, Ulla et al. (2001) report two close companions (“B” located  $\leq 2''.4$  E, and “C” located  $\sim 3''.5$  NW);  $d$  = #1337 and 1322 were listed with the same name (CSHK 29495–21) by KHD when in fact they are two different objects: #1322 is named correctly, while #1337 is not — #1337 should read CSHK 29495–63 (BPS CS 29495–63) in KHD;  $e$  = #1273 is listed as a Seyfert 1 galaxy in SIMBAD;  $f$  = our note, not from KHD;  $g$  = objects #233 and #873 which are listed with “UVO” designations (SIMBAD usage: “[CW83]”) in KHD, do not appear in the final published lists from Carnochan & Wilson (1983) and thus do not appear in SIMBAD with a “[CW83]” designation, we have supplied an alternative SIMBAD designator;  $h$  = object #423, listed as “UVO 1032+40” in KHD, has two distinct entries in SIMBAD: the first entry as “[CW83] 1032+40” and the second entry including the designator “PG 1032+406”;  $i$  = object #1320, PHL 25 is incorrectly identified with TYC 6365–74–1 by SIMBAD, PHL 25 is NOT this Tycho star;  $j$  = object #277, PG 0839+399 has two distinct entries in SIMBAD: the first including the “PG 0839+399” designation and the second under the designation “KUV 08399+3956”;  $k$  = objects #938 and 940 have the same PG names: “PG 1536+097” following the naming criteria given in Green, Schmidt, & Liebert (1986) — to distinguish them we have included #1 (for 938) and #2 (940) following the names, object #940 has an entry in SIMBAD

under the name “PG 1536+097”, object #938 has no entry in SIMBAD; em = emission lines seen in spectrum; AEA =  $V$  and  $B-V$  from Allard et al. (1994); LAN =  $V$  and  $B-V$  from Landolt (1992); MEA = #1327, Strömgren *uvby* from Mooney et al. (2000); TYC =  $V$  and  $B-V$  for #234 and #1223 are converted from Tycho magnitudes:  $V_T = 10.194$ ,  $(B_T - V_T) = +0.111$  and  $V_T = 8.455$ ,  $(B_T - V_T) = +1.271$  respectively (ESA 1997); WMG =  $V$  and  $B-V$  from Williams et al. (2001);



Table A.1: Updated Coordinates and Notes for All Subwarfs.

No.	ID <sup>1</sup>	Coordinates <sup>2</sup> (J2000.0)	Chart Source <sup>3</sup>	Type	$V$	$V / y^4$	$B - V^4$	KHD ID <sup>5</sup>	Notes <sup>6</sup>
1 SB 7		00 03 24.426 -16 21 06.27	SB,CS	sdB	12.67	$y$	-0.161	... (CSHK 29517-41)	#3 (BPS CS 29517-41) AEA
2 TON S 135		00 03 22.063 -23 38 57.93	SB	sdB	13.302		-0.235	...	...
4 BPS CS 29517-49		00 03 30.799 -16 43 58.19	U CS	He-sdB	14.3	B	...	CSHK 29517-49	...
6 TON S 137		00 04 31.005 -24 26 21.31	SB,CS	sdO	13.87	$y$	-0.273	...	#5 (BPS CS 29503-9)
7 LBQS 0002-0200		00 04 42.887 -01 44 09.22	U LBQS	sdBp	17.6	J	...	...	...
8 BPS CS 22876-35		00 05 56.713 -34 53 06.65	CS	sdB	15.4	B	...	CSHK 22876-35	...
9 LBQS 0003+0053		00 06 22.637 +01 09 58.94	U LBQS	sdBp	18.7	J	...	...	...
10 TON S 140		00 06 46.273 -27 20 53.31	SB,CS	sdOB	13.97	$y$	-0.253	...	#11 (BPS CS 29503-2) AEA
12 PHL 678		00 07 33.775 +13 35 57.65	PGWD	sdB	13.032		-0.076	...	...
13 LBQS 0005+0023		00 07 37.948 +00 40 04.69	U LBQS	sdB	18.4	J	...	...	...
14 PHL 687		00 08 17.773 +18 07 58.50	PG	sdB	14.390		-0.291	...	AEA
15 LBQS 0006+0151		00 08 43.205 +02 07 53.30	U LBQS	sdO	18.3	J	...	...	...
16 PG 0006+120		00 08 45.360 +12 17 19.37	PG	sdB	14.69	$y$	-0.127	PG 00061+1200	...
18 PB 5775		00 10 08.778 +02 52 32.48	PG	sd	15.63	P	...	...	...
19 TON S 144		00 10 06.922 -26 12 56.48	SB,CS	sdO	12.8		-0.15	...	#17 (BPS CS 29503-25)
20 JL 163		00 10 33.227 -50 15 24.32	JL	sdB:	12.88		-0.17	...	...
21 PHL 717		00 11 25.133 -12 28 44.13	MCT	sdB	14.51	$y$	-0.209	...	...
22 PHL 2726		00 12 27.764 +03 54 31.69	PG	B	13.16	$y$	-0.125	...	...
23 JL 166		00 12 43.022 -45 51 15.33	JL	sdOB	15.23		-0.23	...	...
24 LBQS 0010+0231		00 13 23.863 +02 48 15.23	U LBQS	sdB	18.2	J	...	...	...
25 BPS CS 30339-8		00 13 42.192 -35 27 01.55	CS	sdB	14.7	B	...	CSHK 30339-8	...
26 PG 0011+221		00 14 19.320 +22 24 17.65	PG	sd	13.55	$y$	-0.229	PG 00117+2207	...
27 PG 0011+283		00 14 22.236 +28 36 55.77	PG	sd	12.76	$y$	-0.228	PG 00117+2820	...
28 BPS CS 30339-3		00 16 22.491 -36 28 23.88	CS	sdB	15.2	B	...	CSHK 30339-3	...
29 PHL 766		00 16 54.260 +07 04 29.90	PG	sd	15.55	P	...	...	...
30 LBQS 0015-0206		00 17 40.522 -01 50 18.94	U LBQS	sdOB	18.2	J	...	...	...
31 LBQS 0015+0216		00 17 57.081 +02 33 31.51	LBQS	sdOB	17.6	J	...	...	...
32 PHL 780		00 18 37.159 +15 21 51.08	U PG	sdO(D)	16.21	P	...	...	...
33 PG 0016+285		00 19 28.974 +28 44 46.46	PG	sdB	15.89	P	...	PG 00168+2828	...
35 TON S 154		00 21 58.721 -24 25 21.04	SB,CS	sdO	14.48	$y$	-0.356	...	#34 (BPS CS 29503-51)

Continued on Next Page...

Table A.1 – Continued

No.	ID <sup>1</sup>	Coordinates <sup>2</sup> (J2000)	Chart Source <sup>3</sup>	Type	$V / y^4$	$B - V^4$	KHD ID <sup>5</sup>	Notes <sup>6</sup>
36PG 0020+240		00 23 03.487 +24 19 08.16	PG	sdB	15.60 P	...	PG 00204+2402	...
37PB 5943		00 25 27.755 +08 57 54.34	PGWD	sdB	15.62	-0.18	...	...
38PG 0023+298		00 25 53.665 +30 05 12.45	PG	sdO(A)	15.44 P	...	PG 00232+2948	CV?
39PG 0023+299		00 25 58.959 +30 15 11.62	PG	sdB	15.72 P	...	PG 00233+2958	NW* <sup>f</sup>
40LB 7736		00 25 58.372 -20 57 30.40	SB	sdOB	13.98 <i>y</i>	-0.262	...	...
41LBQS 0024-0042		00 26 45.512 -00 25 31.77	LBQS	sdB	17.6 J	...	...	...
42BPS CS 30339-49		00 26 52.788 -35 34 01.74	CS	sdB	15.5 B	...	CSHK 30339-49	...
43PHL 809		00 27 02.359 +13 33 23.55	PG	sdB	15.64 P	...	...	...
44PB 8240		00 27 02.783 -07 51 11.94	PB	sdB/DA	13.50 P	...	...	...
45LBQS 0025+0203		00 28 06.714 +02 20 18.00	U LBQS	sdB	18.8 J	...	...	E* of close vd <sup>f</sup>
46KPD 0025+5402		00 28 28.977 +54 19 15.03	KPD	sdB	13.89	-0.15	KPD 00256+5402	...
47LBQS 0025-0210		00 28 29.300 -01 53 43.74	U LBQS	sdB	18.3 J	...	...	...
48PB 5984		00 29 09.017 +04 56 23.43	PG	sd	14.72 P	...	...	...
49LBQS 0026-0043		00 29 11.50 -00 27 16.01	O LBQS-B	sdB	18.8 J	...	...	extend. on DSS2 <sup>f</sup>
50PG 0027+222		00 30 37.991 +22 30 51.60	PG	sdB	14.77 P	...	PG 00279+2214	...
51CD-48 106		00 31 41.659 -47 25 20.08	SIM	sdB	12.36	-0.26	...	...
52LBQS 0030+0103		00 33 10.442 +01 19 33.44	U LBQSHe	sdB	18.6 J	...	...	...
53TON S 163		00 33 53.893 -27 08 23.73	GD	sdOB	14.22 <i>y</i>	-0.266	...	...
54PG 0032+247		00 35 32.046 +24 59 15.88	PG	sdB	14.080	-0.280	PG 00328+2442	AEA
55KPD 0033+5229		00 35 52.386 +52 45 49.52	KPD	sdO	16.00	-0.11	KPD 00330+5229	...
56PG 0033+266		00 35 46.542 +26 54 54.30	PG	sdB	14.279	-0.231	PG 00331+2638	AEA
57LB 1566		00 40 13.297 -55 01 52.06	JL	sdO	13.07	-0.29	...	...
58PG 0038+199		00 41 35.327 +20 09 17.08	PG	sdO(C)	14.544	-0.352	PG 00389+1952	WMG
59PB 6107		00 42 06.118 +05 09 23.35	PGWD	sdB	12.881	-0.038	...	AEA
60PG 0039+103		00 42 13.465 +10 39 10.69	PGWD	sdB-O	15.16 <i>y</i>	-0.20	PG 00396+1022	...
61PG 0039+134		00 42 16.570 +13 45 40.61	PG	sdO He	13.683	-0.186	PG 00396+1329	AEA
62CD-38 222		00 42 58.311 -38 07 37.31	SIM	sdB	10.48 <i>y</i>	-0.284	...	...
63PHL 818		00 44 46.646 +09 43 50.90	PG	sdB	15.69 P	...	...	...
64PG 0042+211		00 45 11.127 +21 21 08.02	PG	sdO(A)	15.13 P	...	PG 00425+2104	...
65PB 6148		00 45 21.488 +07 06 10.93	PB	pec	...	...	...	...
66HD 4539		00 47 29.215 +09 58 55.68	SIM	F+sd?	12.00 P	...	...	...
67PG 0045+251		00 47 55.285 +25 20 27.63	U PG	sdB	10.272	-0.240	...	AEA
68PG 0046+247		00 48 48.532 +24 58 05.53	U PG	sd	15.94 P	...	PG 00452+2504	...
69PG 0046+207		00 49 17.147 +20 56 40.41	PG	sdB	16.15 P	...	PG 00461+2441	...
					14.559	-0.221	PG 00466+2040	AEA

Continued on Next Page...

Table A.1 – Continued

No.	ID <sup>1</sup>	Coordinates <sup>2</sup> (J2000)	Chart <sup>3</sup> Source	Type	$V / y^4$	$B - V^4$	KHD ID <sup>5</sup>	Notes <sup>6</sup>
70	PHL 860	00 51 07.028 +00 42 32.24	PGWD	sdO(B)	15.91 $y$	-0.30	...	...
71	BD-11° 162	00 52 15.075 -10 39 46.03	SIM	sdO+?	11.23	-0.10	...	...
72	PG 0050+222	00 53 16.907 +22 29 38.94	PG	sd	15.89 $P$	...	PG 00506+2213	...
73	PG 0050+201	00 53 41.495 +20 21 20.26	PG	sd	16.18 $P$	...	PG 00509+2004	...
74	LBQS 0052-0105	00 54 36.041 -00 49 39.58	U LBQS	sdB	18.5 $J$	...	...	...
75	PB 6208	00 54 48.277 +06 05 24.68	PG	sd	16.08 $P$	...	...	...
76	PG 0053+239	00 56 20.670 +24 09 08.94	PG	sd	15.85 $P$	...	PG 00536+2352	...
77	BPS CS 22942-17	00 56 19.579 -26 37 12.59	CS	sdB	15.94	-0.02	CSHK 22942-17	...
78	KPD 0054+5406	00 57 38.994 +54 22 54.67	KPD	sdB	14.12	-0.07	KPD 00547+5406	...
79	PG 0055+016	00 58 24.661 +01 54 35.06	PGWD	sdB-O	15.21 $P$	...	PG 00558+0137	...
80	SB 395	00 59 11.646 -18 18 00.30	SB	sdB	12.55 $y$	-0.174	...	...
81	PHL 932	00 59 56.675 +15 44 13.68	PG	sdB	12.076	-0.273	...	AEA
82	TON S 183	01 01 17.577 -33 42 45.43	SB	sdB	12.65 $y$	-0.252	...	...
83	BPS CS 22942-30	01 03 43.730 -26 51 53.41	CS	sdB	15.7 $B$	...	CSHK 22942-30	...
84	Feige 11	01 04 21.673 +04 13 36.90	Feige	sdB	12.06	-0.26	...	...
85	PG 0102+261	01 05 22.422 +26 22 54.14	PG	sdB-O	14.50 $y$	-0.091	PG 01026+2606	...
86	TON S 191	01 06 51.066 -33 20 31.30	SB	sdB	13.54 $y$	-0.257	...	...
87	PG 0105+276	01 08 16.796 +27 52 49.17	PG	sdO(B)	14.448	-0.087	PG 01056+2736	NW* <sup>f</sup> , $a$ , AEA
88	KPD 0106+5227	01 09 03.287 +52 43 49.37	KPD	sdB	15.46	+0.15	KPD 01060+5227	...
89	CD-33 417	01 08 26.779 -32 43 11.63	SB	sdB	12.30 $y$	-0.255	...	...
90	CD-27 372	01 08 37.333 -26 53 09.59	TONS	sdB	12.59 $y$	-0.138	...	...
91	PB 8555	01 10 12.696 -14 07 57.79	PB	sd+F?	13.00 $P$	...	...	NE* <sup>f</sup> (v.close)
92	PG 0108+195	01 11 03.732 +19 47 42.38	PG	sd	14.61	-0.27	PG 01083+1931	...
93	PG 0108+209	01 11 27.415 +21 11 15.86	U PG	sdB	15.85 $P$	...	PG 01087+2055	...
94	TON S 201	01 12 11.675 -26 13 27.74	TONS	sdO	13.17 $y$	-0.245	...	...
95	PG 0110+262	01 13 14.876 +26 27 31.20	PG	sdB-O	12.903	+0.074	PG 01105+2611	AEA
96	PG 0111+177	01 13 45.515 +17 58 50.05	PG	sdB	15.85 $P$	...	...	NE* <sup>f</sup>
97	PG 0112+142	01 15 17.378 +14 28 18.44	PG	sdB	14.70 $P$	...	PG 01126+1412	...
98	JL 236	01 14 06.699 -52 44 02.14	JL	sdB	13.45 ;	-0.28	...	...
99	PG 0113+259	01 15 54.269 +26 14 00.20	PG	sdO(B)	14.50 $y$	-0.218	PG 01131+2558	...
100	KPD 0114+5402	01 17 13.906 +50 58 58.45	U KPD	sdB	16.51	-0.14	KPD 01141+5402	...
101	PG 0116+242	01 19 29.042 +24 25 31.50	PG	sd	11.88 $y$	+0.361	PG 01167+2409	...
102	PB 8783	01 23 43.244 -05 05 45.72	PB	sdB? hb	12.50 $P$	...	...	...
103	PB 6419	01 24 30.293 +06 48 57.55	U PG	sdB	16.02 $P$	...	...	...
104	PG 0122+214	01 25 29.597 +21 36 30.72	PG	sd	12.84 $y$	-0.215	PG 01227+2121	...

Continued on Next Page...

Table A.1 – Continued

No.	ID <sup>1</sup>	Coordinates <sup>2</sup> (J2000)	Chart Source <sup>3</sup>	Type	$V / y^4$	$B - V^4$	KHD ID <sup>5</sup>	Notes <sup>6</sup>
105BPS	CS 29504-11	01 25 22.285 -33 15 09.64	CS	sdB	15.6	B	CSHK 29504-11	...
106PG	0123+159	01 26 37.079 +16 08 11.60	PG	sd	14.34	y	PG 01239+1552	...
107BPS	CS 22953-35	01 27 45.562 -59 53 37.53	CS	sdB	12.8	B	CSHK 22953-35	...
108PG	0132+151	01 35 08.117 +15 24 03.57	PG	sd	15.13	P	PG 01324+1508	...
109PG	0133+114	01 36 26.186 +11 39 32.11	PG	sdB	12.31	y	PG 01337+1124	...
110PG	0135+242	01 38 08.708 +24 30 13.40	PG	sdO(D)	15.05	...	PG 01353+2415	...
111PHL	1079	01 38 23.41 +03 38 13.65D	...	sdB	13.38	y	...	...
112BPS	CS 29504-37	01 42 20.051 -35 40 25.60	CS	sdB	15.7	B	CSHK 29504-37	...
113SB	705	01 43 07.502 -38 33 16.25	SB	sdO	13.03	y	...	...
114PG	0142+183	01 45 37.435 +18 32 08.45	PG	sdB	15.45	P	PG 01429+1817	...
115PG	0142+148	01 45 39.524 +15 04 42.13	PGWD	sdB	13.694	...	PG 01429+1449	AEA
116CD	-24 731	01 43 48.539 -24 05 10.17	SB	sdB	11.720	...	...	AEA
117LB	3229	01 47 17.478 -51 33 39.15	JL	sdO He	13.55	...	...	...
118PHL	1164	01 48 03.688 -05 55 45.66	Feige	sdO	12.79	y	...	...
119BPS	CS 29504-46	01 48 37.715 -34 11 47.67	CS	sdO	14.8	B	CSHK 29504-46	...
120PHL	3802	01 48 44.033 -26 36 12.72	SB	sdB	12.35	y	...	...
121PHL	1210	01 52 34.76 -19 14 13.81D	...	sdB	14.01	y	...	...
122PHL	1212	01 52 50.791 -16 35 30.88	GD1099	sdB	12.8	B	...	...
123PG	0154+204	01 57 11.143 +20 39 17.88	PG	sdB-O	15.24	P	PG 01544+2024	...
124PG	0154+182	01 57 27.889 +18 27 39.79	PG	sdB-O	15.27	P	PG 01547+1813	...
125BD	+37° 442	01 58 33.433 +38 34 23.89	SIM	sdO	9.98	...	...	...
126PG	0200+131	02 02 42.563 +13 20 40.93	PG	sdB	15.12	P	PG 02000+1306	...
127PG	0205+134	02 08 03.509 +13 36 25.61	PG	sdO(B)	14.721	...	PG 02053+1322	AEA
128PG	0206+225	02 09 13.807 +22 44 32.08	PG	sdB	14.071	...	PG 02064+2230	AEA
129PB	6710	02 10 14.987 +00 45 02.28	PG	sdB	14.77	P	...	...
130Feige	19	02 10 54.222 +01 47 47.14	Feige	sdO He	13.709	...	...	WMG
131PB	6727	02 11 38.701 -01 13 45.00	PG	sdB	14.020	...	...	AEA
132PB	6740	02 12 26.597 +01 55 17.43	PG	sdBp?	15.39	P	...	...
133JL	286	02 13 12.412 -50 04 39.95	JL	sdB	14.31	...	...	...
134LB	3241	02 13 11.931 -49 44 53.75	JL	sdOB	12.81	y	...	...
135PG	0212+230	02 14 49.973 +23 19 53.13	PG	sdB-O	15.36	P	PG 02120+2305	...
136PG	0212+148	02 15 11.106 +15 00 04.11	PG	sdB	14.452	...	PG 02124+1446	AEA
137PG	0212+143	02 15 41.665 +14 29 18.04	PG	sdB	14.541	...	PG 02129+1415	AEA
138PG	0215+183	02 18 15.735 +18 31 38.36	PG	sdB	13.423	...	PG 02154+1818	AEA
139PHL	1256	02 19 18.909 +03 26 51.48	PG	sdO(C)	14.599	...	...	WMG
140PG	0216+246	02 19 44.601 +24 47 23.72	PG	sdO(D)	15.86	P	PG 02168+2433	...

Continued on Next Page...

Table A.1 – Continued

No.	ID <sup>1</sup>	Coordinates <sup>2</sup> (J2000)	Chart <sup>3</sup> Source	Type	$V / y^4$	$B - V^4$	KHD ID <sup>5</sup>	Notes <sup>6</sup>
141 PG	0217+241	02 20 26.750 +24 19 28.30	U PG	sdB	16.14	P	PG 02175+2405	...
142 PG	0217+155	02 20 35.602 +15 44 06.69	PG	sdO(B)	15.099		PG 02178+1530	AEA
143 PG	0219+241	02 22 33.648 +24 20 58.79	PG	sdB	16.07	P	PG 02197+2407	...
144 PG	0220+132	02 23 38.420 +13 27 34.94	PG	sdB	14.775		PG 02209+1314	AEA
145 PG	0221+217	02 24 01.296 +21 56 50.03	PG	sdB	15.62	P	...	...
146 PG	0226+151	02 28 49.727 +15 20 34.01	PG	sdO(C)	16.143		PG 02260+1507	WMG
147 PG	0229+064	02 32 36.329 +06 38 52.23	PG	B	11.919		PG 02299+0625	AEA
148 PG	0231+051	02 33 41.358 +05 18 44.35	PG	sdO:	16.105		PG 02310+0505	LAN
149 PHL	1359	02 34 00.31 -12 43 52.38	D ...	sdOB	14.05	y	...	...
150 PG	0232+095	02 35 11.981 +09 45 37.62	PG	sd	12.61	y	PG 02325+0932	...
151 Feige	26	02 40 04.390 +03 55 42.25	Feige	sdO	14.10	y	...	...
152 PHL	1434	02 41 06.83 -19 01 12.10	D ...	sdB	12.58	y	...	...
153 BPS	CS 22954-6	02 41 58.850 -06 28 35.79	CS	sdB	15.0	B	CSHK 22954-6	...
154 PG	0240+046	02 43 22.759 +04 50 36.24	RFG	sdO(B)	14.14	y	PG 02407+0437	...
155 PG	0242+132	02 45 38.881 +13 25 55.66	PG	sdB	13.205		PG 02429+1313	AEA
156 PG	0245+182	02 48 07.492 +18 26 15.11	PG	sdO(D)	15.79	P	PG 02453+1813	...
157 PB	9286	02 50 23.947 -04 06 13.96	PB	sdB	12.50	P	...	SE*f
158 CPD	-56 464	02 50 21.633 -56 12 52.43	SIM	sdB	12.01	y	...	...
159 PG	0250+189	02 53 48.782 +19 09 59.02	PG	sdB	14.112		PG 02509+1857	AEA
160 CPD	-71 172	02 53 30.688 -71 22 31.75	SIM	sdOB+	12.05		...	Comp A [vd]
161 PB	6958	02 58 34.787 +03 10 52.44	PG	F3-4IV	15.81	P	...	...
162 BPS	CS 22963-36	03 01 15.817 -02 40 13.41	CS	sdB	13.84		CSHK 22963-36	...
163 PG	0302+028	03 04 37.335 +02 56 57.86	Feige	DA 2	15.05	y	...	...
164 PG	0305+152	03 07 54.307 +15 25 14.47	PG	sd	14.51	y	PG 03051+1513	...
165 PG	0306+141	03 09 09.472 +14 14 36.67	PG	sd	15.47	P	PG 03064+1403	...
166 BPS	CS 22968-19	03 09 47.908 -56 23 49.45	CS	He-sdB	13.9	B	CSHK 22968-19	...
167 PG	0310+149	03 13 37.247 +15 06 21.97	PG	sdO	15.477		PG 03108+1455	WMG
168 KPD	0311+4801	03 14 45.911 +48 12 05.78	KPD	sdB	14.32		KPD 03112+4801	...
169 PG	0313+005	03 16 20.122 +00 42 22.89	PG	sd	16.01	P	K/P 03137+0031	...
170 PG	0314+146	03 17 38.023 +14 46 24.04	PG	sdO(B)	12.53	y	PG 03140+1437	...
171 PG	0314+180	03 17 46.337 +18 13 18.18	PG	sd	14.31	y	PG 03149+1802	...
172 PG	0314+103	03 17 42.265 +10 30 54.78	PG	sdB	13.30	y	PG 03149+1019	...
173 KUV	03163+0031	03 18 54.123 +00 41 35.10	U KUV	sdB	16.30	P	...	...
174 KPD	0319+4553	03 22 38.968 +46 04 33.75	KPD	sdO	13.68		KPD 03192+4553	...

Continued on Next Page...

Table A.1 – Continued

No.	ID <sup>1</sup>	Coordinates <sup>2</sup> (J2000)	Chart Source <sup>3</sup>	Type	$V / y^4$	$B - V^4$	KHD ID <sup>5</sup>	Notes <sup>6</sup>
175PG 0319+054		03 21 38.670+05 38 40.26	PG	sdB	15.04	-0.05	...	...
176PG 0322+114		03 25 11.212+11 40 09.45	PG	sdB	15.26	P	PG 032224+1129	...
177PG 0322+078		03 25 34.159+07 59 52.17	PG	sd	16.01	P	PG 032228+0749	CV?
178PHL 1534		03 26 14.970-25 18 37.78	CS <sup>a</sup>	sdB?	14.7	B	...	...
179BPS CS 22185-3		03 26 32.885-16 05 21.46	CS	sdB	15.10	-0.28	CSHK 22185-3	...
180PHL 1548		03 29 04.75 -11 41 42.57	D ...	sdOB	13.32	y	...	...
181LS I+63°198		03 29 05.669+64 04 42.02	pre	sdO	12.0	B	...	...
182BPS CS 22190-34		03 43 09.613-13 06 00.57	CS	sdB	13.64	-0.25	CSHK 22190-34	...
183BPS CS 22190-3		03 44 58.830-16 52 42.09	CS	sdB He	14.90	-0.27	CSHK 22190-3	...
184PG 0342+026		03 45 34.563+02 47 52.68	PG	HBB	10.957	-0.140	PG 03429+0238	AEA
185KUV 03439-0048		03 46 25.171-00 38 38.65	KUV	sdO	14.91	-0.29	...	...
186PG 0349+094		03 51 59.163+09 38 24.63	PG	sdB	15.69	P	PG 03492+0929	...
187HDE 283048		03 53 13.715+25 45 21.83	SIM	sd+F?	10.30	P	...	SE*/brighter* <sup>f</sup>
188BPS CS 22190-4		03 52 46.882-17 10 50.57	CS	sdB	14.0	B	CSHK 22190-4	...
189HZ 3		03 53 31.323+10 45 04.12	HZ	sdO6	12.86	-0.14	...	...
190BPS CS 22169-1		03 56 23.319-15 09 19.30	CS	sdB	12.87	-0.27	CSHK 22169-1 (CSHK 22190-9)	#191 (BPS CS 22190-9)
192KPD 0402+4232		04 06 05.286+42 41 20.09	KPD	sdB	15.49	+0.04	KPD 04026+4232	...
193RL 92		04 08 34.983+51 14 48.18	RWT	sdB	14.03	+0.15	RWT 92	...
194TONS 401		04 08 46.499-29 49 11.42	plaus <sup>b</sup>	sdB p?	12.28	y	...	...
195BPS CS 22182-8		04 09 49.712-28 20 03.25	CS	sdB	12.2	B	CSHK 22182-8	...
197TONS 403		04 10 01.719-28 22 57.86	U TONS(:	sdO	12.97	y	...	...
198BPS CS 22173-33		04 10 11.175-19 48 53.61	CS	sdB	13.61	-0.27	CSHK 22173-33 (CSHK 30494-50)	#196 (BPS CS 30494-50)
199KUV 04110+1434		04 13 49.508+14 41 25.88	KUV	sdB	13.91	+0.23	...	...
200BD-13°842		04 14 15.764-12 44 21.90	SIM	sd	11.99	y	...	CSPN <sup>f</sup>
201KPD 0422+5421		04 26 06.870+54 28 16.98	KPD	sdB	14.66	+0.20	KPD 04222+5421	...
202KUV 04233+1502		04 26 08.021+15 08 28.42	KUV	sdO	14.72	-0.15	...	...
203KUV 04237+1649		04 26 34.594+16 55 26.53	KUV	sdOB	13.90	+0.33	...	...
204BPS CS 22182-37		04 29 10.722-29 02 48.19	CS	sdO He	14.10	-0.31	CSHK 22182-37	...
205RL 105		04 31 12.274+42 59 10.35	RWT	sdB	14.60	+0.04	RWT 105	...
206LB 1735		04 31 09.76 -53 35 38.80	D ...	sdB?	13.63	y	...	...
207LB 1741		04 36 14.49 -53 45 59.48	D ...	sdO He	12.58	y	...	...
208KUV 04402+1455		04 43 03.340+15 00 24.13	KUV	sdO	13.97	+0.21	...	...
209KUV 04421+1416		04 44 56.897+14 21 50.23	KUV	sdB	15.08	+0.18	...	...

Continued on Next Page...

Table A.1 – Continued

No.	ID <sup>1</sup>	Coordinates <sup>2</sup> (J2000)	Chart Source <sup>3</sup>	Type	$V / y^4$	$B - V^4$	KHD ID <sup>5</sup>	Notes <sup>6</sup>
210 KUV	04456+1502	04 48 29.793 +15 07 39.67	KUV	sdO	15.80 P	...	...	...
211 HZ	1	04 50 13.524 +17 42 06.14	HZ	sdOp	12.62	-0.06	...	...
212 LB	1766	04 59 18.789 -53 52 54.77	TL	sdB He	12.34 $y$	-0.269	...	...
213 KUV	05053+1628	05 08 12.879 +16 32 16.33	KUV	sdOB	15.50 P	...	...	...
214 KUV	05072+1249	05 10 02.761 +12 52 46.21	KUV	sdB	16.2	...	...	...
215 RL	114	05 11 51.344 +41 41 29.26	RWT	sdOB	15.59	-0.07	RWT 114	...
216 KUV	05109+1739	05 13 49.787 +17 42 02.92	KUV	sdOB	13.50 P	...	...	...
217 [CW83]	0512-08	05 14 43.930 -08 48 06.45	pl	sdO	11.32 $y$	-0.258	UVO 0512-08	...
218 HD	269696	05 31 40.355 -69 53 02.19	SIM	sdOB+	11.13	-0.270	...	e.bin
219 CPD	-64 481	05 47 59.301 -64 23 03.04	TYC	degen	11.31 $y$	-0.258	...	...
220 KPD	0549+1642	05 52 31.027 +16 42 50.45	KPD	sdB	15.28	-0.07	KPD 05495+1642	...
221 KPD	0549+1948	05 52 40.124 +19 49 13.55	KPD	sdO	14.87	-0.16	KPD 05496+1948	...
222 KPD	0550+1922	05 53 12.487 +19 23 50.21	KPD	sdB	14.55	-0.13	KPD 05502+1922	...
223 CD	-61 1208	05 52 08.051 -61 07 13.98	SIM	sdB	11.19 $y$	-0.193	...	...
224 KPD	0552+1903	05 55 40.401 +19 04 25.88	KPD	sdO	14.68	+0.11	KPD 05527+1903	...
225 KPD	0553+1755	05 56 02.308 +17 56 13.41	KPD	sdO	15.13	+0.07	KPD 05531+1755	...
226 HS	0600+6602	06 05 25.912 +66 02 17.57	Heber	sdB	16.4	...	...	...
227 LS	V+22° 38	06 16 13.331 +22 45 48.75	pre	sdO	12.00 B	...	...	nebula in field <sup>f</sup>
228 RL	54	06 18 42.838 +21 35 34.67	RL	sdB	14.69	-0.11	...	...
229 HD	45166	06 26 19.153 +07 58 28.06	TYC	B8V+	9.90	...	...	...
230 KPD	0629-0016	06 31 53.811 -00 19 12.96	KPD	sdO?	14.92	-0.01	KPD 06293+0016	...
231 KPD	0640+1412	06 43 31.919 +14 09 26.13	KPD	sdB	14.85	+0.04	KPD 06407+1412	...
232 HD	49798	06 48 04.696 -44 18 58.45	HIP	sdO	8.27	-0.28	...	s.bin
233 HD	51155	06 55 18.213 -23 32 16.47	HDstar	sdB	9.53 $y$	-0.133	UVO 0653-23	$g$
234 BD	+34° 1543	07 10 07.693 +34 24 53.81	HIP	sd	10.184	+0.094	...	TYC
235 KUV	07088+3232	07 12 02.28 +32 26 39.87D	...	sdO	15.00 P	...	...	...
236 [CW83]	0711+22	07 14 29.875 +22 16 59.37	pl	sdOp	11.70 P	...	UVO 0711+22	...
237 KUV	07116+3209	07 14 51.160 +32 04 09.20	U KUV	sdB	17.00 P	...	...	...
238 KPD	0716+0258	07 18 57.837 +02 53 14.78	KPD	sdB	14.892	-0.164	KPD 07163+0258	AEA
239 KPD	0720-0003	07 22 56.263 -00 09 37.77	KPD	sdO	15.78	-0.28	KPD 07203-0003	...
240 KPD	0721-0026	07 24 14.372 -00 33 04.09	RWT	sdB	13.83	-0.17	KPD 07216-0026	...
241 KPD	0732+0057	07 35 26.135 +00 51 30.68	KPD	sdB	15.35	-0.23	KPD 07327+0057	...
242 CD	-31 4800	07 36 30.195 -32 12 43.74	LSS	sdO8	10.52	-0.31	...	...

Continued on Next Page...

Table A.1 – Continued

No.	ID <sup>1</sup>	Coordinates <sup>2</sup> (J2000)	Chart Source <sup>3</sup>	Type	$V / y^4$	$B - V^4$	KHD ID <sup>5</sup>	Notes <sup>6</sup>
243	LSS 630	07 39 41.739 - 27 27 22.08	LSS	sdO	13.30 B	...	...	...
244	PG 0749+658	07 54 24.404 + 65 42 07.37	PG	sdB-O	12.121	-0.106	PG 07496+6550	AEA
245	EGGR 55	07 51 34.80 - 38 28 45.47 D	...	sdOB	13.66	-0.13	EG 55	...
246	PG 0752+770	07 59 24.329 + 76 46 22.26	PG	sdB	16.11	-0.15	PG 07520+7700	...
247	KUV 07571+4233	08 00 35.333 + 42 24 30.02	KUV	sdB	14.97	+0.57	...	...
248	KUV 07592+3931	08 02 31.531 + 39 22 28.65	KUV	sdB	15.26	-0.29	...	...
249	KUV 07596+4123	08 02 59.809 + 41 14 38.09	KUV	sdO	15.380	-0.26	...	...
250	BD-3° 2179	08 02 14.887 - 03 58 16.26	HIP	sdO	10.33	-0.29	...	...
251	TON 299	08 06 28.094 + 32 30 59.23	TOND	sdB	15.2	-0.30	...	...
252	BD+75° 325	08 10 49.475 + 74 57 57.91	HIP	sdO	9.60 y	-0.334	...	...
253	PG 0806+516	08 10 07.646 + 51 29 56.05	PG	sdB	15.21	-0.19	PG 08063+5138	...
254	PG 0806+682	08 11 56.254 + 68 03 43.48	PG	sdB	15.69 P	...	PG 08069+6812	...
255	LSS 982	08 10 31.713 - 40 32 46.99	LSS	sdO	12.60 B	...	...	...
256	PG 0812+478	08 15 48.946 + 47 40 39.14	PG	sd	15.42 P	...	PG 08122+4750	...
257	PG 0812+482	08 16 07.925 + 48 03 49.57	PG	sdB	15.45 P	...	PG 08126+4814	...
258	TON 313	08 19 35.878 + 31 14 16.41	TON	sdB	15.64 P	...	...	...
259	KUV 08191+3951	08 22 26.267 + 39 41 19.59 U	KUV	sdO	16.5	...	...	...
260	TON 317	08 24 34.050 + 30 28 54.80	TON	sd	15.94 P	...	...	...
261	PG 0822+645	08 27 16.549 + 64 22 25.24	PG	sdB	15.59	-0.37	PG 08227+6432	...
262	PG 0823+546	08 26 49.615 + 54 28 00.33	PG	sdO(C)	14.255	-0.282	PG 08230+5437	WMG
263	PG 0823+465	08 26 33.236 + 46 23 36.78	PG	sdB	14.54	-0.18	PG 08230+4633	...
264	PG 0823+499	08 27 36.770 + 49 45 33.93	PG	non-sd	12.01 y	-0.142	PG 08239+4955	...
265	PG 0824+288	08 27 05.085 + 28 44 02.41	PG	dC+ DA	14.73 P	...	PG 08240+2853	NW* <sup>f</sup> (close)
266	[CW83] 0825+15	08 28 32.875 + 14 52 02.49	pl	sdO	11.70 P	...	UVO 0825+15	...
267	PG 0826+480	08 30 06.200 + 47 51 50.49	PG	sdB	16.08 :	-0.20	PG 08265+4802	...
268	[CW83] 0832-01	08 35 23.869 - 01 55 52.62	pl	sdOp	11.46 y	-0.288	UVO 0832-01	...
269	PG 0832+675	08 37 34.737 + 67 24 13.62	PG	BIV	14.146	-0.208	PG 08329+6734	AEA
270	PG 0833+699	08 38 15.029 + 69 42 48.16	PG	sdO(A)	13.492	-0.186	PG 08333+6953	AEA
271	LB 1814	08 36 19.701 + 20 57 47.93 U	PG	sdB	15.90 P	...	...	...
272	PG 0836+619	08 40 44.002 + 61 47 52.05	PG	sdO	14.407	-0.175	PG 08369+6156	WMG
273	PG 0837+401	08 41 01.296 + 39 56 18.13	PG	sdB	14.90 P	...	K/P 08377+4007	...
274	PG 0838+164	08 41 22.717 + 16 17 34.44	PG	sdB	14.90 P	...	PG 08385+1628	...
275	PG 0838+132	08 41 43.861 + 13 04 30.12	PG	sdO He	13.655	-0.286	PG 08389+1315	WMG
276	KUV 08388+4029	08 42 03.741 + 40 18 31.24	KUV	sdB	16.40	...	...	Seyfert 1 <sup>f</sup>

Continued on Next Page...



Table A.1 – Continued

No.	ID <sup>1</sup>	Coordinates <sup>2</sup> (J2000)	Chart Source <sup>3</sup>	Type	$V / y^4$	$B - V^4$	KHD ID <sup>5</sup>	Notes <sup>6</sup>
277 PG 0839+399		08 43 12.710+39 44 49.88	PG	sdB	14.29	-0.27	...	<i>j</i>
278 TON 943		08 43 05.009+33 27 45.14	TON	sdB	14.92	-0.19	...	...
279 TON 202		08 44 08.229+31 02 11.14	TON <sup>342</sup>	sdB	14.65	...	...	...
280 TON 345		08 45 39.172+22 57 28.20	TON	sdO	15.79	...	...	...
281 TON 346		08 46 11.992+24 25 10.88	RFG	sdB-O	15.47	...	...	...
282 TON 349		08 47 18.919+23 00 30.08	TON	sdO(B)	15.34	-0.28	...	...
283 CD -34 5246		08 46 53.204 -35 23 58.27	LSS	sdO	12.90	...	...	...
284 PG 0845+129		08 48 44.772+12 41 49.14	U PG	sdO(B)	16.48	...	PG 08459+1253	v.dbl.
285 PG 0848+416		08 51 19.102+41 23 31.17	PG	sdB+ K1	16.13	+0.04	PG 08480+4134	...
286 TON 357		08 51 37.819+24 41 50.40	TON	sdB	14.25	-0.27	...	...
287 PG 0848+186		08 51 44.469+18 27 22.60	PG	non-sd	13.25	-0.171	PG 08489+1838	...
288 TON 358		08 52 54.618+31 43 36.76	TON	sdO(A)	14.53	-0.23	...	...
289 PG 0850+170		08 53 23.669+16 49 35.31	PG	sdB	13.98	-0.233	PG 08505+1700	...
290 LB 8827		08 53 41.359+19 01 41.97	PG	sdO(A)	16.38	-0.31	...	...
291 HD 76431		08 56 11.168+01 40 37.60	HIP	BO/sd?	9.22	-0.273	...	...
292 PG 0854+385		08 57 54.627+38 18 52.09	PG	sdB	15.71	-0.29	K/P 08547+3830	...
293 PG 0856+121		08 59 02.642+11 56 27.89	PG	sdB	13.47	-0.19	PG 08563+1208	<i>c</i>
294 PG 0900+400		09 03 19.427+39 51 00.42	PG	sdB+ K3	12.87	+0.23	PG 09001+4003	...
295 KUV 09008+3752		09 03 59.697+37 40 18.82	U KUV	sdO?	17.20	...	...	...
296 PG 0901+309		09 04 47.695+31 32 51.01	PG,CBS	sdB-O	14.84	...	PG 09013+3057	#297 (CBS 2)
298 PG 0902+057		09 05 05.355+05 33 01.06	PG	sdO(D)	14.06	...	PG 09024+0545	...
299 PG 0902+124		09 05 40.921+12 12 28.24	PG	sdB	14.96	...	PG 09029+1224	...
300 PG 0903-032		09 06 11.879 -03 21 02.86	PG	sdB	15.56	...	PG 09036-0309	...
301 [CW83] 0904-02		09 07 08.123 -03 06 13.93	pl	sdOp	12.00	...	UVO 0904-02	...
302 PG 0904+735		09 09 55.461+73 18 46.04	PG	sdB	15.13	...	PG 09046+7331	...
303 PG 0905+627		09 09 57.810+62 29 26.94	U PG	sd	15.97	...	PG 09059+6241	...
304 PG 0906+190		09 08 53.198+18 53 09.92	PG	sd	16.32	...	PG 09061+1905	...
305 PG 0906+597		09 10 21.540+59 30 33.76	RFG	sdB	15.37	-0.35	PG 09065+5942	...
306 PG 0907+123		09 10 25.449+12 08 27.05	PG	sdB	13.94	-0.207	PG 09077+1220	...
307 CBS 95		09 11 37.596+35 30 35.66	U CBS	sdB	17.00	...	...	...
308 TON 390		09 11 36.864+27 52 40.40	U TON	sdB	16.04	...	...	...
309 PG 0909+169		09 11 55.381+16 42 57.62	PG	sd	16.28	...	PG 09091+1655	...
310 PG 0909+164		09 12 07.293+16 13 20.49	PG	sdB	13.85	-0.260	PG 09093+1625	...
311 PG 0909+275		09 12 51.660+27 20 31.40	PG	sdO(A)	10.74	...	PG 09099+2733	...

Continued on Next Page...

Table A.1 – Continued

No.	ID <sup>1</sup>	Coordinates <sup>2</sup> (J2000)	Chart Source <sup>3</sup>	Type	$V / y^4$	$B - V^4$	KHD ID <sup>5</sup>	Notes <sup>6</sup>
312PG	0911+042	09 14 08.663+03 58 04.38	PG	sdB	15.48	-0.17	PG 09115+0410	...
313PG	0910+621	09 14 12.953+61 57 34.52	PG	sdB	15.54 P	...	...	...
314PG	0911+456	09 14 55.369+45 23 41.45	PG	sdB-O	14.92 P	...	PG 09116+4536	...
315CBS	98	09 23 54.766+36 23 36.93	CBS	sdB-O	16.00 B	...	...	...
316PG	0912+189	09 15 07.094+18 47 16.13	PG	sd	16.05 P	...	PG 09123+1859	...
317PG	0912+119	09 15 28.409+11 41 54.16	PG	sdO	15.95 P	...	PG 09127+1154	...
318AG	+81 266	09 21 18.66+81 43 19.24	...	sdO	11.85	-0.34	AGK2+81 266	...
319PG	0914+201	09 17 19.177+19 54 37.30	PG	sdB	16.33 P	...	PG 09144+2007	...
320PG	0914+001	09 17 12.244+00 08 38.41	PG	sdB	14.583 $y$	-0.150	PG 09146+0004	MEA
321PG	0914-037	09 17 15.582-03 53 56.16	PG	sdO(D)	16.37 P	...	PG 09147-0341	...
322PG	0914+120	09 17 38.394+11 49 55.51	PG	sdB	16.420	...	PG 09149+1202	CV?
323LSS	1274	09 18 56.017-57 04 25.42	LSS	sdO	12.40 B	...	...	...
324PG	0917+037	09 20 19.112+03 32 26.99	PG	sd	16.86	-0.20	PG 09177+0344	...
325CD	-45 5058	09 20 10.134-45 31 54.91	LSS	sdO	11.33	-0.31	...	...
326HD	80836	09 20 34.006-45 35 20.34	TYC	sdB	9.62 $y$	-0.028	...	...
327PG	0918+029	09 21 28.214+02 46 02.30	PG	sdB	13.327	-0.271	PG 09188+0258	LAN
328TON	13	09 22 39.833+27 02 25.49	TON	sdB	12.645	-0.276	...	AEA
329TON	14	09 23 13.375+29 26 58.39	TON	sdO(A)	14.80 $y$	-0.265	...	...
330PG	0920+029	09 23 08.307+02 42 09.90	PG	sdB	14.40 $y$	-0.226	PG 09205+0255	...
331TON	1055	09 24 05.256+20 35 46.40	TON	sd	14.69 P	...	...	...
332BD	+37° 1977	09 24 26.371+36 42 53.27	HIP	sdO	10.00	-0.31	...	...
333CBS	7	09 24 40.066+30 50 12.49	TON	sdO(B)	14.60 $y$	-0.232	...	...
334PG	0921+161	09 24 38.092+15 53 19.15	PG	sd	14.58 $y$	-0.246	PG 09218+1606	...
335PG	0922+259	09 25 51.357+25 38 57.76	TON	sdB+ K4	16.41	-0.10	PG 09229+2551	...
336TON	1059	09 26 38.592+32 45 11.49	TON	sdB	14.94	-0.26	...	...
337PG	0924+565	09 28 30.521+56 18 11.60	PG	sd	16.05 P	...	PG 09248+5631	...
338PG	0926+065	09 28 56.048+06 16 35.00	PG	sdB	15.34 P	...	PG 09264+0629	...
339PG	0926+526	09 30 06.763+52 28 03.72	PG	sdB	16.09 P	...	PG 09266+5241	...
340TON	427	09 30 15.464+30 50 34.64	CBS	sdB	15.08 ;	-0.31	...	...
341BD	+48° 1777	09 30 46.776+48 16 23.94	GD	sdOp	10.76	-0.32	...	...
342PG	0928+031	09 30 59.633+02 50 32.51	PG	sdB	15.06 P	...	PG 09284+0303	...
343PG	0930+085	09 32 45.816+08 16 17.86	PG	sdB	15.97 P	...	PG 09300+0829	...
344PG	0931+691	09 35 59.793+68 52 02.04	PG	sdO(C)	15.92 P	...	PG 09317+6905	...
345TON	438	09 35 12.131+31 10 00.30	TON	sdB	15.00 B	...	...	...
346LB	10889	09 35 16.794+22 49 40.08	RFG	sd	16.13 P	...	...	...

Continued on Next Page...

Table A.1 – Continued

No.	ID <sup>1</sup>	Coordinates <sup>2</sup> (J2000)	Chart <sup>3</sup> Source	Type	$V / y^4$	$B - V^4$	KHD ID <sup>5</sup>	Notes <sup>6</sup>
347PG	0932+166	09 35 41.311+16 21 09.73	PG	sd	15.68	-0.11	PG 09329+1634	...
348PG	0933+004	09 36 09.720+00 13 13.82	PG	sdB	14.39 $y$	-0.252	PG 09335+0026	...
349PG	0933+383	09 36 59.765+38 07 21.93	PGWD	sdB	15.47 $y$	-0.14	...	...
350PG	0934+145	09 37 03.903+14 18 21.63	PG	HBB	13.51 $y$	-0.136	...	...
351PG	0934+163	09 36 52.277+16 05 15.60	U PG	sdB	16.28 P	...	PG 09341+1618	...
352PG	0934+186	09 37 16.277+18 25 11.29	PG	sdB	13.14 $y$	-0.265	PG 09344+1838	...
353GD	299	09 38 20.338+55 05 50.05	GD	sdO	12.071	-0.269	...	WMG
354PG	0935+084	09 37 40.935+08 13 20.95	PGWD	sdB	15.35 P	...	PG 09350+0826	...
355PG	0935-038	09 38 10.341-03 59 58.55	PG	sdB	14.97 $y$	-0.295	PG 09356-0346	...
356PG	0936+037	09 39 20.602+03 26 31.91	PG	sdB	15.98 P	...	PG 09367+0340	...
357PG	0940+171	09 43 15.829+16 55 56.96	PG	sdB	16.13 P	...	...	...
358PG	0941+280	09 43 54.551+27 46 59.27	TON	sdB	12.46 P	...	...	...
359HS	0941+4649	09 44 45.339+46 35 32.52	U Heber	sdO	16.8 (B)	...	...	only $B$ mag given <sup>f</sup>
360PG	0942+461	09 45 14.973+45 54 44.71	PG	sd	14.93 P	...	PG 09420+4608	...
361PG	0942-029	09 45 11.847-03 09 21.01	PG	sdB	14.004	-0.294	PG 09426-0255	LAN
362PG	0943+043	09 46 22.990+04 04 56.10	PG	sd	15.87 P	...	PG 09437+0419	...
363GD	104	09 47 03.360-09 19 49.27	GD	sdB	15.91 $y$	-0.340	...	...
364TON	24	09 47 29.337+27 16 27.98	U TON	sdB	16.25 P	...	...	...
365LSS	1349	09 46 57.109-50 12 16.04	LSS	sdO	13.80 B	...	...	...
366CBS	109	09 48 56.991+33 41 51.66	U CBS	sdO(B)	17.00 B	...	...	...
367TON	456	09 49 43.679+30 15 10.84	U CBS	sdO(C)	16.08 P	...	...	...
368PG	0947+639	09 51 38.079+63 45 36.87	PG	sdB	14.78 P	...	...	...
369PG	0948+533	09 51 25.901+53 09 30.72	PGWD	sd	15.33 P	...	PG 09480+5323	...
370PG	0948+187	09 50 58.065+18 26 18.59	PG	sdB	16.25 :	-0.28	PG 09481+1840	...
371PG	0948+041	09 51 01.290+03 47 56.93	PG	sdB-O	15.77 P	...	PG 09484+0403	...
372PG	0948+632	09 52 38.929+62 58 18.77	PG	sdB	14.95 P	...	PG 09488+6311	...
373PG	0949-101	09 51 55.809-10 21 37.26	PG	sdO(B)	14.86 P	...	PG 09494-1007	...
374PG	0950+158	09 53 16.927+15 33 41.91	PG	sdO(D)	15.86 P	...	PG 09505+1547	...
375PG	0950+120	09 53 31.964+11 45 00.09	PG	sdO(A)	15.15 :	-0.27	PG 09507+1200	...
376GD	300	09 55 19.458+51 36 59.00	GD	sdO	12.651	-0.333	...	WMG
377PG	0953+024	09 55 34.597+02 12 48.84	PG	sdO(C)	14.994	-0.292	PG 09530+0226	WMG
378PG	0954+049	09 57 01.488+04 38 58.20	PG	sd	12.90 $y$	-0.064	PG 09544+0453	...
379TON	468	09 57 29.550+24 29 44.23	TON	sdO(A)	15.49 P	...	...	...
380CBS	115	09 59 32.273+36 18 25.81	CBS	sdB	12.00 B	...	...	...
381PG	0956-117	09 59 06.664-11 59 13.90	PG	sdB	15.32 P	...	PG 09566-1144	...

Continued on Next Page...

Table A.1 – Continued

No.	ID <sup>1</sup>	Coordinates <sup>2</sup> (J2000)	Chart Source <sup>3</sup>	Type	$V / y^4$	$B - V^4$	KHD ID <sup>5</sup>	Notes <sup>6</sup>
382	TON 1137	09 59 56.029 +35 39 59.22	TON	sdO(B)	15.15 P	...	...	...
383	PG 0957+037	09 59 52.025 +03 30 32.74	PGWD	sd	15.65 P	...	PG 09572+0344	...
384	PG 0958-116	10 00 41.825 -11 51 34.53	PG	sdB	15.33 P	...	PG 09582-1137	...
385	PG 0958-119	10 00 42.587 -12 05 59.16	PG	sdO(B)	14.09 y	-0.228	PG 09582-1151	...
386	GD 108	10 00 47.253 -07 33 31.01	GD	sdB	13.60	-0.21	...	...
387	CBS 17	10 01 54.971 +30 18 05.94	U CBS	sdB-O	15.00 B	...	...	...
388	PG 0959-085	10 01 33.252 -08 42 50.62	PG	sdO(D)	16.12 P	...	PG 09590-0828	...
389	TON 27	10 02 22.581 +29 27 55.14	U TON	sd	15.91 P	...	...	...
390	HS 1000+4704	10 03 24.083 +46 49 46.28	U Heber	sdO	18.2 (B)	...	...	only $B$ mag given <sup>f</sup>
391	KUV 10003+3732	10 03 19.668 +37 16 34.85	PG	sdB	15.46 P	...	...	...
392	CBS 123	10 03 29.968 +35 56 21.56	U CBS	sdO(A)	16.00 B	...	...	...
393	KUV 10009+4049	10 03 54.284 +40 34 18.22	PG	sdO	13.299	-0.325	...	AEA
394	CBS 19	10 05 43.346 +30 47 55.88	CBS	sdB	16.00 B	...	...	...
395	LB 567	10 06 45.727 +00 32 05.08	RFG	sd	16.01 P	...	...	...
396	PG 1006-145	10 09 23.001 -14 43 02.92	PG	sdB	15.84 P	...	PG 10069-1428	...
397	CBS 20	10 10 18.836 +30 20 28.25	U CBS	sdB	15.00 B	...	...	...
398	PG 1008+689	10 12 00.922 +68 43 20.49	PG	...	12.87 y	-0.109	...	...
399	PG 1008+756	10 12 42.609 +75 19 38.97	PG	sdB	15.94 P	...	PG 10083+7534	...
400	PG 1009+491	10 12 42.234 +48 49 37.66	U PG	sdB	16.23 P	...	PG 10095+4904	...
401	PG 1009+069	10 12 13.236 +06 40 31.29	PG	sdO(B)	16.41 P	...	PG 10095+0655	...
402	LBQS 1009+0059	10 12 18.969 +00 44 13.82	U LBQS	sdOB	17.9 J	...	...	...
403	PG 1011+649	10 15 17.587 +64 43 56.88	PG	sdO(B)	14.90	-0.26	PG 10116+6458	...
404	PG 1012+007	10 15 09.296 +00 33 00.60	PG	sdB	14.90 y	-0.18	PG 10125+0047	...
405	PG 1017-113	10 19 28.720 -11 32 38.48	PG	sdB	16.17 P	...	PG 10170-1117	...
406	PG 1017+430	10 20 29.791 +42 50 21.80	PG	sdOB	15.28 P	...	PG 10174+4305	...
407	PG 1017-086	10 20 14.477 -08 53 46.46	PG	sdB	14.43 y	-0.225	PG 10177-0838	...
408	PG 1018-047	10 21 10.586 -04 56 19.55	PG	sdB	13.32 y	-0.200	PG 10186-0441	...
409	PG 1020+694	10 23 58.668 +69 11 45.15	PG	sdO(B)	14.63 y	-0.249	PG 10201+6927	...
410	LB 10383	10 23 27.679 +13 59 26.44	PG	sdB	15.19	-0.07	...	...
411	PG 1021-029	10 24 18.015 -03 10 37.45	PG	sdB-O	15.43 P	...	PG 10217-0255	...
412	PG 1022+459	10 25 41.247 +45 43 33.51	PG	sdB	15.76 P	...	PG 10226+4558	...
413	LBQS 1023+0044	10 25 47.057 +00 28 59.58	U LBQS	sdB	18.2 J	...	...	...
414	CD-24 9052	10 25 50.895 -24 53 19.99	SIM	sdO	11.77 y	-0.287	...	...
415	PG 1024+238	10 27 04.697 +23 33 50.92	PG	sd	15.71 P	...	PG 10243+2349	...
416	TON 516	10 27 51.149 +24 09 17.00	PG	sdB	15.99 P	...	...	...

Continued on Next Page...

Table A.1 – Continued

No.	ID <sup>1</sup>	Coordinates <sup>2</sup> (J2000)	Chart Source <sup>3</sup>	Type	$V / y^4$	$B - V^4$	KHD ID <sup>5</sup>	Notes <sup>6</sup>
417PG	1026–037	10 28 50.021 – 03 59 59.84	PG	sdB-O	15.94 ;	–0.24	PG 10262–0344	...
418 TON	519	10 29 07.246 + 25 40 09.09	TON	sdO(C)	16.01 P	...	...	...
419PG	1027–077	10 30 22.733 – 07 59 00.57	PG	sdB	16.19 ;	–0.20	PG 10278–0743	...
420PG	1029–048	10 32 17.814 – 05 04 58.21	U PG	sd	15.95 P	...	PG 10297–0449	...
421PG	1030–104	10 32 34.762 – 10 38 25.58	U PG	sdO(B)	16.08 P	...	PG 10301–1023	...
422PG	1030+665	10 33 44.321 + 66 16 12.48	PG	sdO(B)	15.48 P	...	PG 10301+6632	...
423PG	1032+406	10 35 16.587 + 40 21 14.61	PG	sdB	11.52 $y$	–0.283	UVO 1032+40	$h$
424PG	1032+007	10 35 12.766 + 00 27 28.84	PG	sd	16.42 P	...	PG 10326+0043	...
425PG	1033+097	10 35 49.718 + 09 25 52.12	U PG	sdO:	15.95 P	...	PG 10332+0941	...
426PG	1033+201	10 36 38.933 + 19 52 02.22	PG	sdB	15.671	–0.170	PG 10339+2007	AEA
427 CBS	129	10 39 07.679 + 36 45 32.09	CBS	sdB	13.00 B	...	...	...
428 Feige	34	10 39 36.741 + 43 06 09.23	Feige	sdO	11.183	–0.354	...	WMG
429 LB	10694	10 40 25.669 + 14 05 06.89	PG	sdB	15.42 P	...	...	...
430PG	1038+143	10 41 23.129 + 50 44 20.21	PG	sdO(B)	14.82 P	...	PG 10383+1420	...
431PG	1038+139	10 41 30.373 + 13 41 14.37	PG	sdB-O	15.71 P	...	PG 10388+1356	...
432PG	1039–118	10 42 00.781 – 12 06 11.27	U PG	sd	15.95 P	...	PG 10390–1151	...
433 TON	1273	10 41 52.709 + 21 40 32.89	TON	sdB	13.15 $y$	–0.285	...	...
434PG	1040+451	10 43 32.714 + 44 53 30.18	U PG	sdB	16.94	–0.31	PG 10406+4509	...
435 TON	1281	10 43 39.353 + 23 09 06.42	TON	sdB	13.439	+0.094	...	AEA
436PG	1043+760	10 47 04.978 + 75 44 22.94	PG	sdB	13.77 $y$	–0.219	PG 10430+7600	...
437 TON	1285	10 46 16.014 + 20 21 27.74	TON	sdB	15.81 P	...	...	...
438PG	1045+100	10 47 39.163 + 09 44 25.12	U PG	sdO(B)	16.16 P	...	PG 10450+1000	...
439PG	1045+096	10 47 51.003 – 09 50 48.47	PG	sd	15.89 P	...	PG 10453+0934	elongated? <sup>f</sup>
440PG	1046+189	10 49 33.565 + 18 42 40.60	PG	sdB	15.29 P	...	PG 10468+1858	...
441PG	1047+003	10 50 02.813 – 00 00 36.91	PG	sdB	13.474	–0.290	PG 10474+0015	LAN
442PG	1047–046	10 50 26.899 – 04 52 35.87	PG	sdB	14.68 ;	–0.18	PG 10479–0436	...
443PG	1047–066	10 50 28.787 – 06 53 25.95	PG	sdO(B)	14.77	–0.35	PG 10479–0637	...
444PG	1049+013	10 52 28.179 + 01 03 45.75	PG	sdB	14.397	–0.132	PG 10498+0119	AEA
445PG	1050–065	10 53 26.461 – 06 46 14.69	PG	sd	14.21 $y$	–0.245	PG 10509–0630	...
446PG	1051+501	10 54 18.520 + 49 49 59.73	PG	sdB	14.59	–0.32	PG 10513+5006	...
447PG	1052–081	10 55 25.385 – 08 20 45.81	PGWD	sd	15.39 $y$	–0.05	PG 10529–0804	...
448 CBS	32	10 59 05.246 + 32 06 20.73	CBS	sdB	15.13 ;	–0.020	...	...
449PG	1100+526	11 02 55.985 + 52 18 58.63	U PG	sdO(B)	16.22 P	...	PG 11000+5235	...
450PG	1100–008	11 03 02.341 – 01 03 38.67	PG	sdB	16.10 P	...	PG 11004–0047	...
451PG	1100–141	11 03 03.970 – 14 25 27.43	PGWD	sd	15.58 $y$	–0.22	PG 11005–1409	...

Continued on Next Page...

Table A.1 – Continued

No.	ID <sup>1</sup>	Coordinates <sup>2</sup> (J2000)	Chart Source <sup>3</sup>	Type	$V / y^4$	$B - V^4$	KHD ID <sup>5</sup>	Notes <sup>6</sup>
452LB 1938		11 03 43.201 +58 50 32.84	PG	sd	13.64	-0.16	...	...
453LB 1941		11 04 03.038 +52 37 12.82	PG	sdB	14.88	+0.13	...	...
454PG 1101+113		11 03 53.545 +11 00 05.61	PG	sdO(A)	15.17	-0.28	PG 11012+1116	...
455Feige 36		11 04 31.652 +24 39 42.61	Feige	sdB	12.70	-0.23	...	...
456PG 1102+097		11 04 45.011 +09 25 31.44	U PG	sd	15.87	P	PG 11021+0941	...
457PG 1102+499		11 05 23.167 +49 34 59.84	PG	sdO(B)	14.32	y	PG 11025+4951	...
458CBS 135		11 05 51.691 +36 20 32.27	U CBS	sdO(A)	17.00	B	...	...
459PG 1104+022		11 06 40.219 +01 54 51.34	PG	sdB+K2	11.82	+0.04	PG 11041+0211	...
460PG 1104+243		11 07 26.224 +24 03 11.17	PG	sd+K3	11.295	+0.073	...	AEA
461TON 54		11 06 50.481 +29 35 32.30	TON	sdB	15.77	;	...	...
462TON 56		11 08 21.528 +29 36 49.07	CBS	sdB	16.13	;	...	...
463PG 1106-085		11 08 32.200 -08 43 25.94	U PG	sdB	16.80	-0.32	PG 11060-0827	...
464G 56-17		11 08 44.117 +08 01 39.90	LOB	sdB	16.08	+0.31	...	high prop. motion <sup>f</sup>
465LB 254		11 09 32.005 +60 35 02.68	PG	sdB	15.32	P	...	...
466PG 1106-097		11 09 08.235 -09 58 47.34	U PG	sdO	16.06	P	PG 11066-0942	...
467TON 59		11 09 20.381 +26 47 25.48	TON	sdB	15.06	P	...	...
468CBS 36		11 10 21.048 +30 47 38.49	CBS	sdB	17.00	B	...	...
469PG 1108-018		11 11 12.561 -02 06 29.97	PG	sdO(A)	16.61	-0.27	PG 11086-0150	...
470PG 1109-070		11 11 36.302 -07 18 32.34	PG	sdB+K2	14.16	;	PG 11091-0702	...
471PG 1109-016		11 12 23.134 -01 55 05.64	PG	sdB	15.36	P	PG 11098-0138	...
472PG 1109-114		11 12 28.481 -11 40 03.19	U PG	sdB	16.01	P	PG 11099-1123	...
473TON 62		11 13 04.491 +29 07 46.34	CBS	sdB	14.09	y	...	...
474PG 1110+045		11 13 17.318 +04 13 14.36	PG	sdO(A)	15.12	P	PG 11107+0429	...
475PG 1111-077		11 13 48.413 -08 00 20.61	PG	sdB-O	13.666	-0.202	PG 11112-0744	AEA
476PG 1111+339		11 14 36.505 +33 40 26.97	PG	sd	13.01	+0.23	PG 11118+3356	...
477TON 1371		11 14 53.315 +33 39 01.88	TON	sdB	15.21	P	...	...
478Feige 38		11 16 49.354 +06 59 32.99	Feige	sdB	13.00	-0.23	...	...
479PG 1115-065		11 18 11.657 -06 47 32.06	PG	sdB-O	15.03	-0.26	PG 11156-0631	...
480TON 577		11 18 29.783 +27 17 01.99	TON	sdB	15.41	P	...	...
481TON 1384		11 18 34.786 +19 49 47.12	TON	sd	13.20	y	...	...
482TON 63		11 19 04.829 +29 51 52.79	TON	sdB	14.34	y	...	...
483TON 64		11 20 00.367 +30 56 59.89	TON	sdB	15.86	-0.22	...	...
484PG 1118+099		11 20 56.258 +09 36 42.11	U PG	sdB	15.97	P	PG 11183+0953	...
485PG 1118+061		11 21 02.678 +05 49 01.50	PG	sdB	14.28	-0.15	PG 11184+0605	...
486PG 1119+377		11 22 17.892 +37 26 52.51	PG	sdB	15.72	P	PG 11195+3743	...

Continued on Next Page...

Table A.1 – Continued

No.	ID <sup>1</sup>	Coordinates <sup>2</sup> (J2000)	Chart Source <sup>3</sup>	Type	$V / y^4$	$B - V^4$	KHD ID <sup>5</sup>	Notes <sup>6</sup>
487LB 256		11 22 42.725 +61 37 58.22	PG	sdB	15.60	P	...	...
488LB 2009		11 24 54.370 +51 28 33.40	U PG	sdB-O	16.01	P	...	...
489PG 1124+123		11 26 37.080 +11 59 59.94	PG	sd	15.71		-0.22 PG 11240+1216	...
490PG 1125+175		11 28 15.636 +17 14 09.15	U PG	sdO(B)	15.95	P	PG 11256+1730	...
491PG 1125-055		11 28 12.291 -05 46 14.49	U PG	sdO(C)	16.28	P	PG 11257-0529	...
492 TON 67		11 28 29.309 +29 15 04.32	TON	sdB	14.72	P	...	...
493PG 1127-088		11 29 47.439 -09 04 32.92	U PG	sd	16.27	P	PG 11272-0848	...
494PG 1127+019		11 30 03.708 +01 37 37.25	PG	sdO(D)	13.01	P	PG 11274+0154	...
495PG 1127+746		11 31 01.162 +74 20 52.49	U PG	sdO(B)	15.91	P	PG 11275+7437	...
496PG 1128+199		11 31 11.527 +19 36 40.68	PG	sdB	15.15	P	PG 11285+1953	...
497CBS 141		11 31 49.346 +34 41 01.11	CBS	sdB	16.00	B	...	...
498PG 1129-081		11 32 21.280 -08 21 25.82	PG	sdB-O	16.06	P	PG 11298-0805	...
499PG 1130-063		11 32 41.588 -06 36 52.84	PG	sdB	16.09		-0.33 PG 11302-0620	...
500PG 1130+054		11 32 57.487 +05 06 48.58	PG	sdB	14.92		-0.19 PG 11303+0523	...
501LB 239		11 33 40.606 +56 06 24.97	PG	sdB	15.26		-0.21	...
502LBQS 1131+0209		11 34 18.011 +01 53 22.11	U LBQS	sdB	17.9	J	...	...
503LB 2045		11 34 44.657 +61 08 26.73	PG	sdB	15.71	P	...	...
504PG 1133+103		11 35 47.514 +10 03 14.97	PG	sdB-O	15.42	P	PG 11332+1019	...
505CBS 143		11 36 59.827 +35 09 12.38	U CBS	sdB	17.00	B	...	...
506PG 1134+463		11 37 30.868 +46 00 06.38	PG	sdO(B)	15.107		-0.325 PG 11348+4616	WMG
507LBQS 1134-0006		11 37 25.150 -00 22 57.74	U LBQS	sdB	18.1	J	...	...
508Feige 46		11 37 26.365 +14 10 14.18	Feige	sdO	13.260		-0.297	WMG
509PG 1135-116		11 38 10.554 -11 51 03.55	PG	sdO(B)	15.70	P	PG 11356-1134	...
510PG 1136-003		11 38 40.695 -00 35 31.75	PG	sdB	14.52	y	-0.276 PG 11361-0018	...
511PG 1137+470		11 39 42.040 +46 43 50.01	PG	sdB	15.46	P	PG 11379+4700	...
512LBQS 1137-0023		11 39 41.265 -00 40 08.58	U LBQS	sdO	17.8	J	...	...
513KUV 11386+4229		11 41 14.834 +42 12 22.60	PG	sdB-O	15.90		-0.22	...
514PG 1138-101		11 41 09.880 -10 20 09.52	PG	sdB	14.54	y	-0.252 PG 11386-1003	...
515PG 1140-050		11 42 57.832 -05 17 14.13	PG	sdB-O	15.33	:	-0.15 PG 11404-0500	...
516LBQS 1140+0026		11 43 12.579 +00 09 26.73	LBQS	sdB	18.3	J	...	...
517PG 1140-078		11 43 11.239 -08 01 34.17	U PG	sdB	16.89		-0.26 PG 11406-0745	...
518PG 1141-116		11 44 18.036 -11 50 39.06	PG	sd	14.77	P	PG 11417-1133	...
519PG 1141+000		11 44 29.346 -00 17 18.03	PG	sdB	15.97		-0.22 PG 11419+0000	...
520PG 1142-037		11 44 57.230 -03 56 53.35	PG	sdB-O	15.88		-0.21 PG 11424-0340	...
521PG 1144+005		11 46 35.169 +00 12 33.60	PG	sdO(B)	15.04	P	PG 11440+0029	...
522Feige 48		11 47 14.491 +61 15 31.77	Feige	sd	13.48		-0.25	...

Continued on Next Page...

Table A.1 – Continued

No.	ID <sup>1</sup>	Coordinates <sup>2</sup> (J2000)	Chart Source <sup>3</sup>	Type	$V / y^4$	$B - V^4$	KHD ID <sup>5</sup>	Notes <sup>6</sup>
523LBQS 1144-0007		11 47 20.485 -00 24 04.80 U LBQS	sdOB	sdOB	18.4 J	...	...	...
524PG 1145-135		11 48 11.886 -13 46 18.44 PG	PG	sd	14.27 y	-0.187	PG 11456-1329	...
525PG 1147-085		11 49 45.041 -08 48 54.56 U PG	PG	sdB	16.15 P	...	PG 11471-0832	...
526LBQS 1147-0038		11 49 46.700 -00 54 56.75 U LBQS	LBQS	sdB	18.2 J	...	...	...
527CBS 146		11 50 06.573 +36 00 18.19 CBS	CBS	sdB	16.00 B	...	...	...
528KUV 11495+3925		11 52 04.031 +39 08 27.19 PG	PG	sdB	15.35	+0.03	...	...
529PG 1150-105		11 53 28.594 -10 46 41.97 PG	PG	sdB	15.06 y	-0.267	PG 11509-1029	...
530TON 1460		11 53 58.855 +35 39 30.37 U TON	TON	sdB	16.56	-0.29	...	...
531PG 1152-119		11 55 09.919 -12 11 54.98 PG	PG	sdB	16.08 P	...	PG 11526-1155	...
532PG 1153-119		11 55 34.123 -12 12 24.90 U PG	PG	sdB	16.09 P	...	PG 11530-1155	...
533BD+10°2357		11 55 56.641 +09 50 49.27 HIP	HIP	sdO + A	8.70	...	...	...
534TON 1462		11 56 00.316 +34 07 25.08 TON	TON	sdB	14.91 P	...	...	...
535PG 1153-080		11 56 02.715 -08 17 31.88 U PG	PG	sdO	16.04 P	...	PG 11534-0800	...
536PG 1154-031		11 56 54.077 -03 25 10.37 PG	PG	sdB-O	16.29 P	...	PG 11543-0308	...
537PG 1154-070		11 57 03.655 -07 17 30.05 PGWD	PGWD	sd	14.33 y	-0.08	PG 11545-0701	...
538LB 2063		11 37 54.157 +58 15 24.54 U PG	PG	sdB	15.91 P	...	...	...
539PG 1155+741		11 58 40.544 +73 50 26.04 PG	PG	sdB	15.39	-0.15	PG 11559+7406	...
540PG 1200+094		12 03 19.373 +09 09 51.52 PG	PG	sdB-O	14.96 P	...	PG 12007+0926	...
541TON 74		12 03 41.202 +25 31 11.55 TON	TON	sdB-O	15.31 P	...	...	...
542LB 2197		12 04 38.561 +60 32 08.27 Feige	Feige	sdB	13.61	-0.38	...	...
543HZ 17		12 05 12.552 +40 07 48.52 HZ	HZ	sdB	15.50	-0.22	...	...
544PG 1203+093		12 05 34.590 +09 03 15.80 PG	PG	sdB	15.26 P	...	PG 12030+0919	...
545PG 1203-108		12 05 56.570 -11 05 28.21 PG	PG	sdO(C)	15.56 P	...	PG 12033-1048	...
546PG 1203+084		12 06 06.002 +08 09 44.23 U PG	PG	sdO(B)	16.17	-0.27	PG 12035+0826	...
547LB 2211		12 06 24.413 +57 09 36.08 PG	PG	sdB	14.92 P	...	...	...
548LBQS 1204+1110		12 07 15.365 +10 53 36.44 U LBQS	LBQS	sdB	18.4 J	...	...	...
549LB 2216		12 07 28.485 +54 01 29.60 U PG	PG	sdO(C)	15.75 P	...	...	...
550HZ 18		12 08 57.451 +37 02 57.82 HZ	HZ	sdB	15.15	-0.17	...	S*f
551PB 3854		12 09 16.693 +16 11 55.15 PG	PG	sdB + ?	13.75	-0.11	...	...
552PG 1206-028		12 09 27.965 -03 02 05.72 U PG	PG	sdO(B)	16.24 P	...	PG 12069-0245	...
553PG 1208+224		12 11 16.092 +22 06 36.86 PG	PG	non-sd	15.10 y	-0.199	PG 12087+2223	...
554LBQS 1209+1650		12 11 48.871 +16 33 45.58 U LBQS	LBQS	sdB	16.4 J	...	...	...
555PG 1210+141		12 12 33.876 +13 46 24.72 PG	PG	sd	14.71 y	-0.227	PG 12100+1403	...
556HZ 20		12 12 38.588 +42 40 01.83 HZ	HZ	sdBp+	15.02	+0.01	...	...
557CBS 158		12 12 52.561 +33 54 02.35 HZ	HZ	sdB	14.00 B	...	...	...

Continued on Next Page...



Table A.1 – Continued

No.	ID <sup>1</sup>	Coordinates <sup>2</sup> (J2000)	Chart Source <sup>3</sup>	Type	$V / y^4$	$B - V^4$	KHD ID <sup>5</sup>	Notes <sup>6</sup>
558	HZ 22	12 14 48.537 +36 38 49.32	HZ	sdB-O	13.11 $y$	-0.238 ...	...	s.bin
559	LBQS 1212+1407	12 15 23.753 +13 51 02.90	U LBQS	sdB	18.6 J	...	...	...
560	PG 1214+031	12 16 49.041 +02 47 25.68	PG	sd	13.94 $y$	-0.242 PG	12142+0304	...
561	PG 1215+025	12 17 56.293 +02 10 47.23	U PG	sdB	16.15 P	...	PG 12154+0227	...
562	LBQS 1216+1719	12 18 51.633 +17 03 19.88	U LBQS	sdOB	18.6 J	...	...	...
563	CBS 58	12 19 55.064 +31 39 44.44	U CBS	sdO(A)	17.00 B	...	...	...
564	LBQS 1217+1405	12 20 15.172 +13 49 11.02	U LBQS	sdB	17.9 J	...	...	...
565	LBQS 1218+1606	12 21 08.339 +15 50 05.52	LBQS	sdB	18.7 J	...	...	...
566	PG 1219+533	12 21 29.084 +53 04 36.71	PG	sd	13.23 $y$	-0.299 PG	12190+5321	...
567	LBQS 1219+1732	12 22 22.057 +17 15 38.46	U LBQS	sdB	17.9 J	...	...	...
568	PG 1220-056	12 22 58.945 -05 53 04.85	PG	sdO(C)	14.754	-0.318 PG	12204-0536	WMG
569	LBQS 1220+1055	12 23 03.652 +10 38 39.62	U LBQS	sdO	18.3 J	...	...	...
570	Balloon 110607002	12 23 45.56 +01 18 22.56	D ...	sdB+ K0	12.8 $y$	...	BBL110607002	...
571	LBQS 1221+1028	12 24 10.630 +10 12 17.19	U LBQS	sdB	18.7 J	...	...	...
572	PG 1223+059	12 25 35.239 +05 35 59.91	PG	non-sd	15.99 P	...	PG 12230+0552	...
573	PG 1223+617	12 25 55.357 +61 24 29.16	U PG	sdB-O	16.23 P	...	PG 12235+6141	...
574	PG 1224+672	12 26 17.090 +66 53 15.37	PG	non-sd	11.86 $y$	-0.213 PG	12240+6709	...
575	LB 242	12 26 37.179 +57 59 28.30	U PG	sd	16.39 P	...	...	...
576	PG 1225-122	12 28 07.412 -12 30 29.79	PG	sdB	14.604	-0.205 PG	12255-1213	AEA
577	PG 1226-107	12 29 12.022 -10 56 35.11	U PG	sd	16.47	-0.08 PG	12266-1039	...
578	LBQS 1227+0923	12 30 22.199 +09 06 36.10	U LBQS	sdB	18.4 J	...	...	...
579	PG 1230+226	12 32 55.272 +22 21 23.72	PG	sd	15.19 P	...	PG 12304+2237	...
580	PG 1230+052	12 33 12.565 +04 57 37.65	PG	sdB	13.26	-0.20 PG	12306+0514	...
581	PG 1230+067	12 33 23.200 +06 25 17.70	PG	sdO(B)	13.20 $y$	-0.248 PG	12308+0641	...
582	LBQS 1231+1316	12 33 32.303 +13 00 26.06	U LBQS	sdB	18.6 J	...	...	...
583	LB 2392	12 34 50.867 +49 47 20.94	PG	sd	13.98	-0.04	...	...
584	LBQS 1232+1046	12 35 13.005 +10 29 59.11	LBQS	sdB	16.6 J	...	...	...
585	PG 1232-136	12 35 18.737 -13 55 08.88	PG	sdO(A)	13.24	-0.13 PG	12327-1338	...
586	PG 1232+228	12 35 14.102 +22 35 19.11	PG	sd	15.62 P	...	PG 12327+2251	...
587	Feige 65	12 35 51.151 +42 22 39.73	Feige	sdB	12.0	-0.23	...	...
588	PG 1234+481	12 36 45.183 +47 55 22.33	PGWD	DA	14.545	-0.350 PG	12343+4811	AEA
589	TON 90	12 36 52.667 +50 15 13.56	TON	sdB	14.73 $y$	-0.24	...	...
590	LBQS 1234+1437	12 37 17.916 +14 20 50.17	U LBQS	sdB	18.7 J	...	...	...
591	BD+25° 2534	12 37 23.521 +25 03 59.83	Feige	sdB	10.5	-0.27	...	...
592	CS 1235	12 38 23.232 -62 42 05.34	pre	sdB	16.22	+0.14	...	...
593	PG 1236+479	12 39 05.055 +47 37 50.94	TON	sdB	15.60	-0.21	...	...

Continued on Next Page...

Table A.1 – Continued

No.	ID <sup>1</sup>	Coordinates <sup>2</sup> (J2000)	Chart Source <sup>3</sup>	Type	$V / y^4$	$B - V^4$	KHD ID <sup>5</sup>	Notes <sup>6</sup>
594	TON 97	12 39 39.424 +12 57 37.90	TON	sdB	14.65 $y$	-0.235	...	...
595	PG 1237-141	12 39 56.535 -14 24 47.74	PG	sdB	15.72 P	...	PG 12373-1408	...
596	TON 98	12 40 06.246 +11 32 19.05	TON	sdB-O	15.99	-0.13	...	...
597	TON 101	12 40 25.059 +23 03 48.39	TON	sd	14.95	-0.18	...	...
598	TON 102	12 40 38.278 +51 16 00.14	TON	sdO He	13.54	-0.25	...	...
599	CS 1238	12 41 37.476 -62 39 07.17	pre	sdO	16.34	+0.06	...	...
600	BD+18°2647	12 41 51.790 +17 31 19.78	Feige	sdO	11.846	-0.337	...	WMG
601	TON 107	12 42 01.790 +43 40 24.38	TON	sdO(D)	16.25 P	...	...	...
602	TON 108	12 42 31.043 +04 06 43.73	TON	sdB	15.50 ;	-0.25	...	...
603	TON 109	12 42 31.395 +11 44 01.28	TON	sdO(B)	15.733	-0.296	...	WMG
604	CS 1240	12 42 59.868 -64 07 50.76	pre	sdB	16.12	+0.17	...	...
605	PG 1241-084	12 44 20.241 -08 40 16.80	PG	sdB	10.58 $y$	-0.219	...	e.bin, #609 (BD-7°3477)
606	LBQS 1241+0852	12 43 52.293 +08 35 47.29	U LBQS	sdB	18.3 J	...	...	...
607	PG 1241-101	12 43 56.509 -10 21 39.39	PG	sdB	15.57 P	...	PG 12413-1005	...
608	LBQS 1241+1628	12 43 59.891 +16 12 03.81	U LBQS	sdBp	18.3 J	...	...	...
610	LP736-4	12 44 53.665 -10 51 05.45	U PG	sdB	15.05 P	...	...	...
611	TON 123	12 44 51.207 +43 52 52.97	U TON	sd	16.13 P	...	...	...
612	TON 640	12 45 05.963 +23 52 24.26	TON	sdB	15.32	-0.34	...	...
613	LB 651	12 45 06.915 +60 10 19.75	U PG	sdB-O	15.69 P	...	...	...
614	TON 126	12 47 06.777 -00 39 25.59	U TON	sdB-O	16.48	-0.21	...	...
615	PG 1244+113	12 47 06.620 +11 03 13.56	PG	sdB	14.17	-0.23	PG 12445+1119	...
616	CS 1244	12 47 58.639 -63 05 10.99	pre	sdO	14.57	-0.16	...	...
617	LBQS 1245+1208	12 47 38.703 +11 52 34.60	U LBQS	sdOB	18.2 J	...	...	...
618	PG 1245-042	12 48 13.892 -04 30 47.10	PG	sd	13.61 $y$	-0.128	PG 12456-0414	...
619	TON 129	12 48 19.057 +03 50 04.50	U TON	sdO(B)	16.05 P	...	...	...
620	CS 1246	12 49 37.629 -63 32 09.88	pre	sdB	14.59	+0.28	...	...
621	PG 1246-122	12 49 21.661 -12 29 31.92	PG	sdO	14.55	-0.16	PG 12467-1213	...
622	PG 1247-115	12 49 54.169 -11 46 59.54	PG	sd	15.21 P	...	PG 12470-1128	...
623	G 60-38B	12 49 59.741 +03 57 26.53	LOB	sdO(B)	14.55	-0.02	...	...
624	PB 4288	12 51 29.175 +06 21 52.29	PG	sdO(B)	15.94 P	...	...	...
625	PG 1249+761	12 50 39.920 +75 53 00.37	PG	sdO He	15.423	-0.323	PG 12490+7609	WMG
626	GD 150	12 52 17.134 +15 44 43.59	GD	sdB	14.63	-0.27	...	...
627	PG 1249+028	12 52 29.609 -03 01 29.69	PG	sdB	15.61 P	...	PG 12499-0245	...
628	HZ 35	12 53 18.513 +30 06 29.06	HZ	sdB	15.85	-0.32	...	...

Continued on Next Page...

Table A.1 – Continued

No.	ID <sup>1</sup>	Coordinates <sup>2</sup> (J2000)	Chart Source <sup>3</sup>	Type	$V / y^4$	$B - V^4$	KHD ID <sup>5</sup>	Notes <sup>6</sup>
629 PG	1251+019	12 54 08.331 +01 43 24.40	PG	sdO(B)	15.571	-0.328	PG 12515+0159	WMG
630 TON	139	12 56 04.892 +28 07 19.43	TON	sdB	12.76	+0.07	...	...
631 TON	140	12 56 27.401 +27 42 31.98	TON	sdB	15.43	P	...	...
632 PG	1255+089	12 57 40.825 +08 37 51.19	PG	sdB	16.17	P	PG 12551+0854	...
633 PG	1255+546	12 57 49.315 +54 25 35.42	PG	sdO(A)	13.53	y	PG 12556+5441	...
634 HZ	38	12 59 21.247 +27 34 06.03	HZ	sdO	14.46	-0.28	...	...
635 HZ	47	12 59 26.030 +27 21 22.82	HZ	non-sd	15.51	-0.22	...	...
636 PG	1257+171	12 59 41.465 +16 48 27.24	PG	sdB	14.319	-0.265	PG 12572+1704	AEA
637 KUV	12572+2811	12 59 34.713 +27 54 55.03	U KUV	sdO	16.70	...	...	...
638 PG	1257-026	13 00 13.829 -02 49 52.52	PG	sdB	13.96	y	PG 12576-0233	...
639 PG	1257+010	13 00 25.542 +00 45 30.09	PG	sdB-0	15.79	-0.06	PG 12578+0101	...
640 HD	113001	13 00 26.182 +35 45 20.63	HIP	sdO+F	10.58	-0.25	...	v.bin
641 PG	1258+012	13 00 59.159 +00 57 11.52	PG	sdO(B)	15.89	P	PG 12584+0113	...
642 PG	1258-030	13 01 09.884 -03 16 48.11	PG	HBB	13.10	y	PG 12585-0300	...
643 LB	27	13 02 41.767 +27 40 41.94	PG	sdO	15.97	-0.25	...	...
644 TON	143	13 03 46.616 +26 46 31.42	TON	sdO He	15.658	-0.309	...	WMG
645 KUV	13023+3145	13 04 39.567 +31 29 05.22	U KUV	sdB	16.00	...	...	...
646 HZ	39	13 04 48.628 +28 07 29.29	HZ	sdB	15.40	-0.24	...	...
647 CS	1303	13 06 09.490 -62 38 32.41	pre	sd/DA	15.99	+0.72	...	...
648 PG	1303+122	13 05 44.092 +11 58 41.24	U PG	sdB	15.66	P	PG 13032+1214	...
649 PG	1303+097	13 06 03.872 +09 24 31.10	PG	sdB	14.50	y	PG 13035+0940	...
650 PG	1303-114	13 06 23.123 -11 41 33.43	PG	sdB	13.96	y	PG 13037-1125	...
651 PG	1304+491	13 06 15.572 +48 50 20.95	Feige	sdB-O	13.78	y	...	#653 (Feige 73)
652 KUV	13096+3008	13 11 59.946 +29 51 59.68	U KUV	sdOB	17.5	...	...	...
654 PG	1310+179	13 12 48.783 +17 41 01.15	PG	sdB-O	15.38	-0.20	PG 13103+1756	...
655 Balloon	081300002	13 13 03.89 +15 40 06.57	D ...	sdB+K1	14.3	y	BBL081300002	...
656 LB	249	13 12 49.542 +54 32 44.72	PG	sdB-O	15.98	-0.21	...	...
657 HZ	40	13 13 33.009 +36 56 49.08	HZ	sdB	14.81	-0.23	...	...
658 PG	1313+165	13 15 46.077 +16 13 26.15	PG	sdB-O	15.93	-0.23	PG 13133+1629	...
659 Feige	75	13 15 58.132 +12 57 40.02	Feige	sdB	14.57	-0.218	...	...
660 PG	1314+442	13 16 33.102 +43 59 05.46	PG	sdO(A)	15.16	P	PG 13143+4414	...
661 PG	1314+003	13 17 24.748 +00 02 37.32	PG	sdO(C)	16.063	-0.357	PG 13148+0018	WMG
662 PG	1315-077	13 17 36.987 -07 57 49.16	PG	HBB	12.25	y	...	...
663 PG	1315-123	13 17 39.268 -12 32 52.37	PG	sdB	15.39	+0.01	PG 13150-1217	CV?
664 PG	1315+013	13 17 45.817 +01 04 50.82	U PG	sdB-O	16.87	-0.12	PG 13152+0120	...

Continued on Next Page...

Table A.1 – Continued

No.	ID <sup>1</sup>	Coordinates <sup>2</sup> (J2000)	Chart Source <sup>3</sup>	Type	$V / y^4$	$B - V^4$	KHD ID <sup>5</sup>	Notes <sup>6</sup>
665 PG	1316–125	13 18 52.316 – 12 45 29.81	PG	sd	15.15	–0.11	PG 13162–1229	...
666 PB	146	13 18 47.091 + 44 35 42.12	PG	sdO(B)	14.77 P	...	...	...
667 PG	1316+212	13 19 17.401 + 20 57 16.03	PG	sdO	14.72 P	...	PG 13168+2113	...
668 Feige	80	13 19 53.609 + 12 03 58.28	Feige	sdO+?	11.350	–0.095	...	WMG
669 PG	1318+062	13 20 44.379 + 05 59 01.38	PG	sdO(C)	14.771	–0.289	PG 13182+0614	WMG
670 PG	1319+405	13 22 09.905 + 40 15 58.04	U PG	sdB	16.87 ;	–0.24	PG 13199+4031	...
671 TON	158	13 23 23.523 + 26 16 32.31	TON	sdB-O	16.18	–0.25	...	...
672 LBQS	1321+0103	13 24 01.793 + 00 47 45.68	U LBQS	sdB	18.2 J	...	...	...
673 HZ	44	13 23 35.269 + 36 07 59.58	HZ	sdO	11.712	–0.311	...	WMG
674 TON	708	13 24 34.864 + 28 18 02.74	TON	sdB	15.09	–0.26	...	...
675 PG	1323+391	13 25 15.246 + 38 53 00.99	PG	sdB	16.30 P	...	PG 13230+3908	...
676 PG	1323–085	13 25 39.469 – 08 49 19.05	PG	B?	13.481	–0.140	PG 13230–0833	LAN
677 PG	1323+125	13 25 57.232 + 12 12 21.25	PG	sdO	15.37 P	...	PG 13234+1227	...
678 PG	1323+042	13 26 19.957 + 03 57 54.60	PG	sdO(A)	15.26	–0.04	PG 13238+0413	...
679 PG	1325+101	13 27 48.577 + 09 54 51.05	PG	sdB-O	13.76	–0.31	PG 13253+1010	...
680 PG	1325+054	13 28 21.373 + 05 08 55.95	PG	sdO He	14.409	–0.300	PG 13258+0524	WMG
681 PG	1326–132	13 29 12.200 – 13 28 43.77	PG	sd	15.85 ;	–0.31	PG 13265–1312	...
682 LBQS	1326–0222	13 29 18.455 – 02 38 16.80	U LBQS	sdB	18.0 J	...	...	...
683 PG	1327–119	13 29 39.757 – 12 13 06.27	PG	sdB	15.72 P	...	PG 13270–1157	...
684 PG	1327+546	13 29 17.493 + 54 20 27.80	PG	sdB	15.17 P	...	PG 13273+5436	...
685 PG	1328+000	13 30 40.949 – 00 17 10.73	PG	sdB	16.17 ;	–0.27	PG 13281+0001	...
686 LBQS	1329+0121	13 31 37.104 + 01 06 33.78	U LBQS	sdB	17.5 J	...	...	...
687 Feige	81	13 31 53.559 + 15 41 17.79	Feige	sdB	13.48	–0.225	...	...
688 PG	1330–074	13 33 16.623 – 07 41 37.92	PG	sdB-O	14.89 P	...	PG 13306–0726	...
689 LB	270	13 33 38.044 + 58 49 34.19	PG	sdB	15.01 P	...	...	...
690 PG	1332–091	13 34 43.707 – 09 21 45.00	PG	sd	15.88 P	...	PG 13321–0906	...
691 Feige	84	13 35 11.980 + 13 27 44.17	Feige	sd	11.84	–0.17	...	...
692 TON	165	13 35 16.552 + 27 52 42.05	PG=TON <sup>c</sup>	sdB	15.5	–0.43	...	...
693 PG	1334+629	13 35 51.656 + 62 41 09.53	PG	sdB	15.41 P	...	PG 13341+6256	...
694 PG	1334+117	13 36 53.983 + 11 26 05.40	PG	sdB-O	16.37	–0.19	PG 13344+1141	...
695 PG	1336–018	13 38 48.149 – 02 01 49.13	PG	sdB	13.45 $y$	–0.237	PG 13362–0146	...
696 PG	1338+481	13 40 08.840 + 47 51 51.89	PG	sdB	13.605	–0.244	PG 13380+4807	AEA
697 Feige	87	13 40 14.702 + 60 52 47.55	Feige	sdB	11.693	–0.095	...	AEA
698 PG	1339+052	13 41 31.470 + 04 54 46.60	PG	sdO	15.76 P	...	PG 13390+0509	...
699 NGC	5272 1128	13 42 18.19 + 28 25 53.79	D ...	sdO	14.93	–0.27	vZ 1128 in M3	...

Continued on Next Page...

Table A.1 – Continued

No.	ID <sup>1</sup>	Coordinates <sup>2</sup> (J2000)	Chart <sup>3</sup> Source	Type	$V / y^4$	$B - V^4$	KHD ID <sup>5</sup>	Notes <sup>6</sup>
700 PG	1340+607	13 41 59.773 +60 29 40.58	PG	sdB	13.14 $y$	-0.231	PG 13402+6044	S* <sup>f</sup>
701 PG	1343-101	13 46 07.982 -10 26 48.44	PG	sdB-O	13.76 $y$	-0.214	PG 13434-1011	...
702 PG	1343+577	13 45 01.421 +57 30 12.84	PG	...	13.78 $y$	+0.012	...	...
703 TON	168	13 46 32.666 +28 17 22.66	TON	sdB	14.68 P	...	...	...
704 PG	1344+114	13 47 00.459 +11 11 23.56	PG	sdB	14.76 P	...	PG 13445+1126	...
705 LBQS	1345-0057	13 48 20.403 -01 12 24.50	U LBQS	sdB	18.4 J	...	...	...
706 PG	1347+086	13 50 15.550 +08 19 16.29	PG	sd	11.86 $y$	+0.413	PG 13477+0834	...
707 PG	1348+745	13 48 43.558 +74 15 45.70	PG	sdB	15.75 P	...	PG 13480+7430	...
708 PG	1348+083	13 50 56.867 +08 01 10.01	PG	sdB	15.65 P	...	PG 13484+0815	...
709 PG	1348+606	13 50 16.067 +60 24 38.05	U PG	sdO He	15.78 P	...	PG 13486+6039	...
710 PG	1348+369	13 50 52.783 +36 42 02.00	PG	sdO(B)	13.525	-0.328	PG 13487+3656	WMG
711 PG	1349-012	13 51 53.192 -01 29 45.52	PG	sdB	15.40 P	...	PG 13493-0114	...
712 PG	1349+659	13 50 45.135 +65 42 08.22	PG	sdO(A)	15.72 P	...	PG 13493+6556	...
713 LSE	44	13 52 40.781 -48 08 22.69	LSE	sdO	12.45	-0.240	...	...
714 LSE	153	13 53 08.216 -46 43 42.28	LSE	sdO	11.35	-0.26	...	...
715 PG	1350+372	13 52 59.006 +36 55 37.52	PG	sdB	14.36 $y$	-0.237	PG 13508+3710	...
716 PB	890	13 53 34.640 +39 04 17.72	PG	sdB	14.25 $y$	-0.146	...	...
717 PG	1351+139	13 54 01.841 +13 43 50.35	PG	sdB	15.73 P	...	PG 13516+1358	...
718 PG	1352-022	13 55 04.662 -02 30 21.84	PG	sdB	12.12	-0.24	PG 13524-0215	...
719 Feige	88	13 55 04.790 +11 42 12.13	Feige	sd	15.67	-0.14	...	...
720 PB	4148	13 55 34.709 +16 00 17.00	PG	sd	15.76 P	...	...	...
721 PB	4150	13 55 39.208 +14 54 38.46	PG	sdB	15.49 P	...	...	...
722 PG	1354+016	13 57 25.881 +01 20 10.40	U PG	sdB	16.33 P	...	PG 13548+0134	...
723 PG	1355-064	13 57 54.279 -06 37 31.85	PG	sdO(B)	13.748	-0.316	PG 13552-0622	AEA
724 PG	1355+071	13 58 24.667 +06 51 35.26	PG	sdB	14.31 $y$	-0.199	PG 13559+0706	...
725 PG	1356-047	13 58 49.384 -04 57 48.33	PG	sdB-O	15.64 P	...	PG 13562-0443	...
726 TON	179	13 58 59.786 +23 59 26.10	TON	sdO(A)	15.15 P	...	...	...
727 PG	1356+354	13 58 56.040 +35 10 21.27	PG	sdB	14.61 P	...	PG 13567+3524	...
728 PG	1357+501	13 59 17.760 +49 54 04.29	PG	sdB	15.94 P	...	PG 13573+5008	...
729 LB	705	14 00 03.001 +23 44 58.89	PG	sdO(C)	16.07 P	...	...	...
730 TON	180	14 01 17.204 +27 38 41.97	PG	sdB	16.03 P	...	...	...
731 PG	1359+077	14 02 03.847 +07 25 39.19	PG	sdB	15.72 P	...	PG 13595+0740	...
732 Balloon	082700002	14 02 01.458 +28 25 39.23	ML	bin?	16.4 $y$	...	BBL082700002	Galaxy <sup>f</sup>
733 PG	1359+003	14 02 32.826 +00 05 56.47	U PG	sdB	16.78	-0.3	PG 13599+0020	...
734 PB	1207	14 02 09.162 +38 37 14.91	PG	non-sd	12.195	-0.178	...	AEA

Continued on Next Page...

Table A.1 – Continued

No.	ID <sup>1</sup>	Coordinates <sup>2</sup> (J2000)	Chart Source <sup>3</sup>	Type	$V / y^4$	$B - V^4$	KHD ID <sup>5</sup>	Notes <sup>6</sup>
735 PB 1229		14 02 52.363 +39 13 46.88	PG	sdB	15.76 ;	-0.31	...	...
736 PG 1400+224		14 03 17.256 +22 10 18.92	PG	sdB	15.68 P	...	PG 14009+2224	...
737 PG 1401+289		14 03 17.157 +28 39 29.51	PG	sdO He	14.87 P	...	PG 14010+2853	...
738 PG 1401+377		14 03 31.997 +37 27 38.79	PG	sdB	16.30 ;	-0.27	PG 14014+3742	...
739 PG 1402+065		14 04 32.149 +06 19 16.13	PGWD	sd	15.65	-0.16	PG 14020+0633	...
740 TON 181		14 04 29.934 +24 50 19.54	TON	sd	14.73	+0.10	...	...
741 PG 1403+019		14 05 45.276 +01 44 19.09	PGWD	sd	15.90	...	PG 14032+0158	...
742 Feige 89		14 06 05.390 +06 47 45.48	Feige	sd	14.67	-0.24	...	...
743 PG 1403-110		14 06 34.696 -11 17 02.20	PG	sdB	15.87 P	...	PG 14037-1101	...
744 TON 183		14 05 59.831 +31 24 36.60	TON	sdB	13.53 <i>y</i>	-0.250	...	...
745 TON 185		14 07 47.856 +23 54 24.24	TON	sdB	15.84 P	...	...	...
746 Feige 91		14 08 32.231 +59 40 25.06	Feige	sdB	13.50 <i>y</i>	-0.275	...	...
747 PB 1516		14 09 16.134 +38 28 32.54	PG	sdB	15.77 P	...	...	...
748 LB 721		14 10 20.683 +00 18 54.79	RFG	sdB	15.66 <i>y</i>	-0.26	...	...
749 PG 1407-013		14 10 25.922 -01 30 16.59	PG	sdB	13.750	-0.259	PG 14078-0116	LAN
750 KUV 14081+3239		14 10 16.233 +32 24 46.20	PG	sdB	14.61 P	...	...	...
751 SA 58-327		14 10 23.490 +28 50 05.35	PB	sdBp	13.00 P	...	...	...
752 PG 1408+098		14 10 55.831 +09 32 55.40	PG	sdB-O	13.93	-0.29	PG 14084+0947	...
753 PG 1409+604		14 11 01.808 +60 14 11.64	PG	sdB-O	14.45 <i>y</i>	+0.137	PG 14095+6028	...
754 PG 1409-103		14 12 28.183 -10 32 59.90	PG	sdO(A)	14.20	-0.27	PG 14097-1019	...
755 PG 1409-091		14 12 36.897 -09 21 54.23	PG	sdB	14.48 <i>y</i>	+0.038	PG 14099-0907	...
756 PG 1411+590		14 13 12.527 +58 46 10.00	PG	sdB	15.68 P	...	PG 14116+5900	...
757 PG 1411-061		14 14 19.475 -06 18 39.04	PG	sdB	14.56	+0.08	PG 14116-0604	...
758 PB 3547		14 14 23.704 +29 41 05.83	PG	sdB	15.87 P	...	...	...
759 PG 1412+612		14 14 20.951 +61 01 07.79	PG	sdO(C)	14.865	-0.313	PG 14129+6115	WMG
760 PB 1811		14 15 03.364 +41 49 27.28	PG	sdB	14.71 P	...	...	...
761 PG 1413+114		14 15 49.087 +11 12 13.17	PG	sdO(D)	16.07	-0.36	PG 14133+1126	...
762 PG 1415-043		14 17 36.399 -04 34 29.05	PG	sdB-O	13.78 <i>y</i>	-0.249	PG 14150-0420	...
763 PG 1415+492		14 17 02.759 +48 57 28.54	PG	sdO(D)	14.44 P	...	PG 14152+4911	...
764 PG 1415+079		14 17 42.521 +07 42 50.55	PG	sdO(A)	15.70	-0.08	PG 14152+0756	...
765 PG 1416+110		14 18 42.345 +10 49 07.76	PG	sdB	15.98 P	...	PG 14162+1102	...
766 TON 194		14 20 07.411 +25 29 18.65	PG	sdB	13.78 <i>y</i>	-0.233	...	...
767 PG 1418+178		14 21 04.807 +17 36 28.74	PG	sdB	15.95 P	...	PG 14187+1750	...
768 PG 1419+081		14 21 38.178 +07 53 19.64	PG	sd	15.10	-0.16	PG 14191+0807	...
769 PG 1419+062		14 22 18.794 +06 00 38.81	PGWD	sd	16.23 <i>y</i>	+0.22	PG 14198+0614	...
770 [CW83] 1419-09		14 22 40.325 -09 17 21.74	pl	sdOB	12.09 <i>y</i>	-0.275	UVO 1419-09	...

Continued on Next Page...

Table A.1 – Continued

No.	ID <sup>1</sup>	Coordinates <sup>2</sup> (J2000)	Chart <sup>3</sup> Source	Type	$V / y^4$	$B - V^4$	KHD ID <sup>5</sup>	Notes <sup>6</sup>
771PG 1420+162		14 23 00.271 +15 57 24.79	PG	sdB	15.98 P	...	PG 14206+1610	...
772PG 1420+518		14 22 41.918 +51 35 37.88	PG	sdB	15.75 P	...	PG 14209+5149	...
773PG 1421+150		14 23 30.692 +14 48 31.83	PG	sdB	15.32	-0.15	PG 14211+1502	...
774PG 1421-121		14 24 08.775 -12 20 20.31	PG	sdB	15.39 P	...	PG 14213-1206	...
775PG 1421+345		14 23 35.575 +34 14 19.48	PG	sdB+ K3	14.78	+0.14	PG 14215+3427	...
776PG 1422+035		14 24 59.599 +03 19 43.45	U PGWD	sd	16.46 y	...	PG 14224+0333	Ström. from PG <sup>f</sup>
777PG 1423-013		14 25 51.297 -01 33 17.25	U PG	sdB	16.79	-0.23	PG 14232-0119	...
778PG 1423-035		14 25 57.793 -03 41 40.04	PG	sd	15.41 P	...	PG 14233-0328	...
779TON 199		14 26 52.539 +32 57 33.53	TON	sdB	14.27 y	-0.194	...	E <sup>*f</sup>
780PG 1425+019		14 27 41.023 +01 42 55.67	U PG	sdB	15.61 P	...	PG 14251+1056	...
781PG 1425+590		14 27 00.078 +58 47 00.60	PG	sdO(C)	16.039	-0.323	PG 14254+5900	WMG
782PG 1425+219		14 27 56.600 +21 37 57.27	PG	sdB	15.71 P	...	PG 14256+2151	...
783PG 1426+047		14 28 34.079 +04 27 34.20	U PG	sdB	16.18 P	...	PG 14260+0440	...
784Feige 95		14 28 29.584 +21 06 01.81	Feige	sdB	13.20	-0.22	...	...
785PG 1426-067		14 28 51.295 -06 57 03.49	PG	sdB	14.50	-0.20	PG 14262-0643	...
786PG 1427+195		14 29 27.757 +19 21 36.60	PG	sdO(C)	14.110	-0.292	PG 14271+1934	WMG
787TON 203		14 29 59.261 +28 03 33.62	TON	sdB	15.80 y	-0.15	...	...
788PG 1428+513		14 30 06.247 +51 03 14.84	U PG	sdO(B)	16.25 P	...	PG 14283+5116	...
789PG 1429+406		14 31 11.125 +40 22 09.08	PG	sd	12.86 y	+0.457	PG 14291+4035	...
790HD 127493		14 32 21.493 -22 39 25.55	HIP	sdO	10.03 y	-0.261	...	...
791BPS CS 22874-14		14 32 24.171 -25 12 59.54	CS	sdB	14.95	-0.34	CSHK 22874-14	...
792PG 1430+066		14 32 46.796 +06 21 58.02	PG	sdB	15.91 P	...	PG 14302+0635	...
793LBQS 1430+0132		14 32 58.058 +01 18 57.94	U LBQS	sdB	17.6 J	...	...	...
794PG 1430+427		14 32 33.893 +42 30 19.29	PG	non-sd	14.47	-0.09	...	...
795PG 1430-082		14 33 36.845 -08 28 22.79	U PG	sdO(C)	15.36 P	...	PG 14309-0815	...
796PG 1431+081		14 33 47.629 +07 54 17.13	U PG	sdO(A)	16.29 P	...	PG 14313+0807	...
797BPS CS 22871-19		14 34 29.846 -19 21 28.52	CS	sdO He	13.25	-0.28	CSHK 22871-19	...
798PG 1431-079		14 34 38.651 -08 10 14.48	U PG	sdO(B)	15.75 P	...	PG 14319-0757	...
799PG 1432+091		14 34 58.493 +08 54 25.92	U PG	HBB	16.13 P	...	PG 14325+0907	...
800PG 1432+004		14 35 19.837 +00 13 51.10	PG	sdB	12.76 y	-0.188	PG 14327+0026	...
801PG 1432+108		14 35 14.371 +10 36 31.00	U PG	sdB-O	15.81 P	...	PG 14328+1049	...
802HD 128220		14 35 15.781 +19 12 54.42	HIP	sdO+ G	8.54	+0.21	...	s.bin
803TON 208		14 35 06.342 +28 47 50.98	TON	sdB-O	16.22 y	-0.25	...	...
804PG 1432+158		14 35 18.917 +15 40 14.46	PG	sdB	13.90 y	-0.225	PG 14329+1553	...
805TON 209		14 35 20.239 +23 45 30.57	PG	sdB	12.45	-0.21	...	...

Continued on Next Page...

Table A.1 – Continued

No.	ID <sup>1</sup>	Coordinates <sup>2</sup> (J2000)	Chart Source <sup>3</sup>	Type	$V / y^4$	$B - V^4$	KHD ID <sup>5</sup>	Notes <sup>6</sup>	
806BPS	CS 22874-1	14 36 13.456 -27 40 39.90	CS	sdB	14.8	B	CSHK 22874-1	...	
807LBQS	1433-0226	14 36 09.264 -02 39 29.11	U LBQS	sdO	18.0	J	...	...	
808LBQS	1434+0151	14 36 32.892 +01 38 12.87	U LBQS	sdB	18.0	J	...	...	
809PG	1434+386	14 36 51.437 +38 25 15.51	PG	sdB-O	15.41	-0.34	PG 14348+3838	...	
810LBQS	1434+0024	14 37 29.817 +00 11 23.65	U LBQS	sdB	18.1	J	...	...	
811PG	1435+098	14 38 22.081 +09 36 30.33	PG	sdO(B)	16.22	P	PG 14359+0949	...	
812PG	1437+727	14 37 31.879 +72 28 51.74	PG	sdO(D)	13.63	P	PG 14371+7241	...	
813LBQS	1437+0234	14 40 24.728 +02 21 18.88	U LBQS	sdBp	17.3	J	...	...	
814TON	780	14 40 14.081 +23 07 34.92	TON	sdB	14.94	y	-0.234	...	
815PG	1438-078	14 40 41.896 -08 00 20.00	PG	sdO(A)	14.58	+0.29	PG 14380-0747	...	
816PG	1438-029	14 40 52.824 -03 08 52.67	PG	sdB	13.82	P	...	...	
817PG	1438+056	14 40 36.187 +05 24 26.06	U PG	sdB	15.97	P	PG 14381+0537	...	
818LBQS	1438+0123	14 41 08.395 +01 10 20.33	U LBQS	sdB	16.8	J	...	...	
819PG	1438+018	14 41 17.328 +01 37 27.84	PG	sdB	15.00	-0.25	PG 14387+0150	...	
820LBQS	1439+0007	14 41 37.470 -00 05 27.49	U LBQS	sdB	18.5	J	...	...	
821LBQS	1439-0014	14 42 08.925 -00 27 35.43	U LBQS	sdOB	17.9	J	...	...	
822PG	1439-013	14 42 27.474 -01 32 45.97	PG	sdB	13.912	-0.293	PG 14398-0120	AEA	
823PG	1440+174	14 42 32.014 +17 10 41.06	PG	sdB	15.39	P	PG 14402+1723	...	
824PG	1441+407	14 43 21.362 +40 28 35.00	U PG	sdO(D)	15.47	P	PG 14414+4041	...	
825BPS	CS 22874-104	14 44 51.593 -26 12 59.81	CS	sdB	15.1	B	CSHK 22874-104	...	
826PG	1442+346	14 44 10.182 +34 21 13.12	PG	sdO(C)	15.13	y	-0.263	PG 14421+3433	...
827PG	1442+144	14 45 10.319 +14 13 45.22	U PG	sdB	15.97	P	PG 14427+1426	...	
828PG	1442+342	14 44 58.756 +34 03 09.28	PG	sd	14.60	-0.28	PG 14429+3415	...	
829LBQS	1443-0215	14 45 37.773 -02 28 24.86	U LBQS	sdBp	18.5	J	...	...	
830PG	1443+176	14 45 30.253 +17 27 52.95	U PG	sd	16.72	-0.32	PG 14432+1740	...	
831BPS	CS 22871-84	14 47 01.912 -18 03 44.32	CS	sdB	14.3	B	CSHK 22871-84	...	
832PG	1444+487	14 46 01.036 +48 30 57.66	PG	sdB	15.85	P	PG 14442+4843	...	
833LBQS	1444-0249	14 47 07.323 -03 02 28.87	U LBQS	sdB	17.9	J	...	...	
834PG	1444+076	14 47 08.269 +07 23 49.43	PG	sdO(B)	14.655	-0.304	PG 14446+0736	WMG	
835PG	1444+236	14 47 08.162 +23 21 38.54	PG	sd	13.14	y	-0.146	PG 14448+2334	em <sup>f</sup>
836PG	1446+084	14 48 37.442 +08 12 22.85	PG	sdB	16.12	P	PG 14461+0824	...	
837PG	1446+088	14 48 43.763 +08 35 22.36	U PG	sdB	15.73	P	PG 14462+0847	...	
838BPS	CS 22874-121	14 49 12.248 -24 52 21.30	CS	sdB	15.2	B	CSHK 22874-121	...	
839PG	1447+176	14 49 24.445 +17 26 06.43	U PG	sdB	17.04	-0.24	PG 14470+1738	...	
840PG	1447+459	14 48 57.110 +45 45 34.42	PG	sdO(A)	15.32	-0.29	PG 14471+4558	...	

Continued on Next Page...



Table A.1 – Continued

No.	ID <sup>1</sup>	Coordinates <sup>2</sup> (J2000)	Chart <sup>3</sup> Source	Type	$V / y^4$	$B - V^4$	KHD ID <sup>5</sup>	Notes <sup>6</sup>
841	PG 1447+249	14 49 33.672 +24 43 36.41	PG	sdB	15.42	P	LB 731	...
842	PG 1448-052	14 51 13.121 -05 23 16.80	PG	sdB-O	14.60	y	-0.227 PG 14485-0510	...
843	PG 1448+485	14 50 29.386 +48 18 00.03	PG	sdB	15.84	P	PG 14487+4830	...
844	PG 1449+653	14 50 36.070 +65 05 52.05	PG	sdB	13.611		-0.035 PG 14496+6517	AEA
845	PG 1449+530	14 51 17.462 +52 50 20.51	PG	sdO:	15.13	P	PG 14497+5302	...
846	PG 1449+582	14 51 14.676 +58 05 36.33	PG	sdB	15.43	P	PG 14499+5817	...
847	PG 1451+528	14 52 42.181 +52 37 03.19	PG	sdB	16.23	P	PG 14511+5249	...
848	PG 1451+397	14 53 22.733 +39 29 47.51	U PG	sdB	15.70	P	PG 14514+3941	...
849	PG 1451+472	14 53 13.795 +47 02 43.42	PG	???	13.12	y	+0.397 PG 14514+4715	v.cool
850	PG 1452+198	14 54 39.817 +19 37 00.83	PG	sdB	12.48	y	-0.232 PG 14523+1949	...
851	PG 1452+475	14 54 26.652 +47 20 04.27	PG	sdB	15.74	P	PG 14527+4732	...
852	PG 1453-080	14 56 00.284 -08 15 48.81	PG	sdB	14.27	y	-0.083 PG 14533-0803	...
853	PG 1453-113	14 56 41.538 -11 28 42.96	PG	sdO(B)	15.42	P	PG 14539-1116	...
854	PG 1454+494	14 56 06.825 +49 11 16.58	U PG	sd	16.39	P	PG 14544+4923	...
855	PG 1454+502	14 56 06.459 +50 01 55.07	U PG	sd	16.83		-0.34 PG 14544+5014	...
856	PG 1454+358	14 56 34.337 +35 36 49.28	U PG	sdO	16.72		-0.32 PG 14545+3548	...
857	PG 1455-069	14 57 57.441 -07 05 04.97	U PG	sdO(B)	15.76	P	PG 14553-0653	...
858	PG 1455+501	14 56 57.723 +49 53 10.77	PG	sdB	15.37	:	PG 14553+5005	...
859	PG 1455+369	14 57 26.259 +36 43 40.66	U PG	sdB-O	16.07	P	PG 14554+3655	...
860	PG 1457+192	14 59 28.519 +19 03 49.97	PG	sdB-O	13.99	P	PG 14571+1915	...
861	PG 1457+198	14 59 52.920 +19 37 44.15	PG	sdB-O	15.91		-0.16 PG 14575+1949	...
862	PG 1458+423	15 00 24.543 +42 05 44.84	PG	sdB	13.79		-0.24 PG 14585+4217	...
863	PG 1459+416	15 01 09.001 +41 21 35.52	PG	sd	13.60		-0.15 PG 14592+4133	...
864	PG 1459-048	15 02 06.425 -04 59 38.05	PG	sd	14.08	y	+0.121 PG 14594-0447	...
865	Name SM Star	15 02 53.155 -41 59 16.67	U SM	sdOB	16.74		S-M Star	...
866	PG 1500+053	15 02 49.821 +05 06 49.12	PG	sdB	15.65	P	PG 15003+0518	...
867	PG 1501+426	15 03 46.766 +42 21 24.75	PG	sdB	14.53		-0.23 PG 15019+4233	...
868	PG 1502+129	15 04 36.707 +12 48 12.58	PG	sdO(B)	15.46	P	PG 15022+1259	...
869	PG 1502+061	15 04 49.543 +05 54 39.66	PG	sdB	15.58	P	PG 15023+0606	...
870	PG 1502-103	15 05 22.697 -10 31 26.05	PG	sdB+ K0	15.51	:	+0.04 PG 15027-1019	...
871	PG 1502+113	15 05 13.535 +11 08 36.96	PG	sdB	15.33	:	-0.25 PG 15028+1120	...
872	TON 787	15 06 16.325 +29 16 40.14	U TON	sdB	15.97	P	...	...
873	PG 1505+074	15 08 21.050 +07 13 14.85	PG	sdB	12.44	y	-0.285 UVO 1505+07	g
874	PG 1506+757	15 05 26.083 +75 31 09.68	U PG	sdB-O	16.04		-0.24 PG 15061+7543	...
875	PG 1506+102	15 08 37.014 +10 03 14.16	PG	sdO(A)	15.26		-0.24 PG 15062+1014	...
876	PG 1506-052	15 09 19.078 -05 20 54.73	PG	sdOB	13.97	y	-0.218 PG 15066-0509	...

Continued on Next Page...

Table A.1 – Continued

No.	ID <sup>1</sup>	Coordinates <sup>2</sup> (J2000)	Chart Source <sup>3</sup>	Type	$V / y^4$	$B - V^4$	KHD ID <sup>5</sup>	Notes <sup>6</sup>
877 PG	1507-015	15 10 30.694 -01 43 46.30	PG	sdO(B)	15.98 P	...	PG 15079-0132	...
878 PG	1508+443	15 10 00.376 +44 08 04.08	PG	sdO(B)	14.972	-0.285	PG 15082+4419	WMG
879 PG	1508+177	15 11 07.066 +17 32 15.24	PG	sdB+ K1	16.28	+0.05	PG 15088+1743	...
880 PG	1508+257	15 10 33.443 +25 30 02.97	TON	sdB	16.17	-0.21	PG 15083+2541	...
881 PG	1508-101	15 11 10.513 -10 14 27.07	PG	sdB	15.16 P	...	PG 15084-1003	...
882 PG	1509-083	15 12 23.995 -08 27 40.11	PG	sdB	14.608	-0.145	PG 15097-0816	AEA
883 TON	224	15 13 21.331 +26 22 53.63	TON	sdB	15.85 P	...	...	...
884 PG	1511+367	15 13 22.456 +36 28 23.00	PG	...	12.11 y	-0.151	...	...
885 PG	1511+447	15 12 58.806 +44 32 21.21	PG	sdO(A)	15.60 P	...	PG 15112+4443	...
886 PG	1511+624	15 12 26.282 +62 10 04.65	PG	sd + K5	14.527	-0.022	PG 15114+6221	AEA
887 PG	1511-110	15 14 16.978 -11 14 12.60	PG	sdO(C)	14.965	-0.190	PG 15115-1102	WMG
888 PG	1511-048	15 14 12.961 -04 59 33.33	PG	sdB	15.64 :	-0.32	PG 15115-0448	...
889 PG	1512-035	15 14 50.048 -03 42 49.69	PG	sdO(B)	15.89 P	...	PG 15122-0331	...
890 TON	788	15 14 32.465 +24 10 40.75	TON	sdB	13.20	-0.18	...	...
891 PG	1513-045	15 16 19.124 -04 43 57.39	PG	sdB	16.21	-0.17	PG 15136-0432	...
892 PG	1514+455	15 15 50.258 +45 18 37.92	PG	sdB	15.15 P	...	PG 15141+4529	...
893 LB	9555	15 16 40.233 +22 57 12.74	PG	sdB	15.51 :	-0.09	...	...
894 PG	1514+422	15 16 17.063 +41 59 05.22	U PG	sdB	15.93 P	...	PG 15144+4209	...
895 PG	1514+034	15 17 14.265 +03 10 27.91	ML	sdB+ K2	13.997	-0.009	PG 15147+0321	LAN
896 Balloon	082800003	15 16 16.25 +56 53 01.25	D ...	sdB+ K1	11.4 y	...	BBL082800003	...
897 LB	9575	15 17 33.393 +22 59 08.48	U PG	sdB	16.13 P	...	...	...
898 PG	1515+044	15 18 08.477 +04 10 43.75	PG	sdB+ K4	15.46	-0.03	PG 15156+0421	...
899 PG	1516+205	15 18 38.803 +20 19 47.22	PG	sdB	15.16 P	...	PG 15164+2030	...
900 TON	228	15 19 13.317 +26 17 20.76	TON	sdB+ K3	15.95	-0.12	...	...
901 PG	1518-098	15 20 59.293 -09 58 56.46	PG	sdO He	13.76 y	-0.207	PG 15182-0948	...
902 LB	810	15 20 45.967 +29 48 26.62	PG	sdO(A)	15.90	-0.42	...	...
903 PG	1519-071	15 21 53.177 -07 19 22.50	PG	sdB	15.60 P	...	PG 15192-0708	...
904 PG	1519+640	15 20 31.372 +63 52 08.24	PG	sdB	12.433	-0.245	PG 15196+6402	AEA
905 Balloon	081400004	15 22 42.609 +03 23 27.62	ML	bin?	16.5 y	...	BBL081400004	...
906 BPS	CS 22890-74	15 24 03.033 +01 34 21.66	CS	sdB	17.2	+0.53	CSHK 22890-74	...
907 PG	1521+357	15 23 32.905 +35 32 37.92	U PG	sdO(A)	16.58 P	...	PG 15215+3543	...
908 PG	1522-013	15 24 38.116 -01 28 30.71	PG	sdB	15.35	-0.06	PG 15220-0117	...
909 TON	231	15 24 06.014 +30 28 47.27	TON	sdB	15.62	...	...	...
910 PG	1522-104	15 24 56.014 -10 32 50.02	PG	sd	15.62 P	...	PG 15222-1022	...
911 PG	1524+439	15 25 53.453 +43 41 27.82	PG	sdB+ K3	15.57	+0.03	PG 15242+4351	...
912 PG	1524+611	15 25 13.396 +60 53 22.62	PG	sdB-O	12.80 y	+0.063	PG 15244+6105	...

Continued on Next Page...

Table A.1 – Continued

No.	ID <sup>1</sup>	Coordinates <sup>2</sup> (J2000)	Chart <sup>3</sup> Source	Type	$V / y^4$	$B - V^4$	KHD ID <sup>5</sup>	Notes <sup>6</sup>
913PG	1525-009	15 27 44.945 -01 06 26.59	PG	sdB	14.839	-0.073	PG 15251-0056	AEA
914PG	1525+103	15 27 44.135 +10 07 22.49	PG	sd	15.83 P	...	PG 15253+1017	...
915PG	1525-071	15 28 12.003 -07 16 39.10	PG	sdO	15.053	-0.198	PG 15255-0706	LAN
916PG	1525+024	15 28 21.098 +02 14 42.43	PG	sdB	15.40	-0.23	PG 15258+0225	...
917PG	1525+107	15 28 20.266 +10 30 31.87	PG	sdB-O	15.98	-0.24	PG 15259+1040	...
918PG	1526+131	15 28 33.925 +13 00 55.23	PG	sdB	14.306	-0.067	PG 15262+1311	AEA
919PG	1526+440	15 28 02.545 +43 50 16.61	PG	sdO(D)	15.64	-0.25	PG 15263+4400	...
920PG	1527-054	15 30 14.261 -05 33 55.73	PG	sdB	15.90 P	...	PG 15275-0523	...
921PG	1528+062	15 30 49.933 +06 00 56.15	PG	sdO(B)	14.753	-0.235	PG 15283+0611	AEA
922PG	1528+029	15 30 56.333 +02 42 22.74	PG	sdO(C)	15.462	-0.284	PG 15284+0252	WMG
923PG	1528+025	15 30 59.222 +02 18 22.29	U PG	sdB-O	15.66 P	...	PG 15284+0228	...
924PG	1528+104	15 31 10.388 +10 15 01.09	PG	sdB	13.57 $y$	-0.191	PG 15287+1025	...
925PG	1530+431	15 32 03.198 +42 57 44.86	PG	sdB	15.31	+0.01	PG 15303+4307	...
926PG	1530+459	15 32 17.200 +45 46 20.58	PG	sdO(A)	16.08 P	...	PG 15306+4556	...
927PG	1530+057	15 33 10.736 +05 32 26.85	PG	sdB	14.211	+0.151	PG 15307+0542	LAN
928TON	239	15 33 16.581 +27 30 30.42	TON	sdO(A)	16.27 P	...	...	...
929PG	1531+447	15 33 16.138 +44 35 13.56	PGWD	sdB	15.62 $y$	-0.26	PG 15315+4445	...
930PG	1532+522	15 33 29.892 +52 06 49.71	PG	sdB	14.12	-0.29	PG 15320+5216	...
931PG	1532-072	15 35 07.214 -07 24 33.89	U PG	sdO(B)	15.65 P	...	PG 15324-0712	...
932PG	1532-056	15 35 22.636 -05 43 32.98	PG	sdB	16.27	-0.11	PG 15327-0533	...
933PG	1533+467	15 34 42.610 +46 31 47.84	PG	sdB	10.84 $y$	-0.165	PG 15331+4641	...
934TON	242	15 35 50.106 +31 51 46.86	TON	sdB	16.02 ;	-0.19	...	...
935PG	1534+389	15 36 22.341 +38 46 02.95	U PG	sd	16.98	-0.32	PG 15345+3855	...
936PG	1534-018	15 37 33.821 -02 00 22.03	PG	He-sdO	15.023	-0.204	PG 15349-0150	WMG
937PG	1536+278	15 38 07.341 +27 41 43.49	PG	sd	13.83	+0.27	PG 15360+2751	...
938PG	1536+097 #1	15 38 42.847 +09 34 42.19	PG	sd	15.87	+0.00	PG 15363+0944	$k$ (not in SIMBAD)
939PG	1536+690	15 36 48.789 +68 52 07.61	PG	sdO He	14.670	-0.323	PG 15366+6902	WMG
940PG	1536+097 #2	15 39 24.431 +09 33 28.31	PG	sdB	15.02 P	...	PG 15369+0943	$k$ (in SIMBAD)
941TON	243	15 39 38.207 +27 06 06.43	U TON	sdB	15.90 P	...	...	...
942PG	1537-046	15 40 33.335 -04 48 12.11	PG	sdO(C)	15.004	-0.188	PG 15379-0438	WMG
943PG	1538+002	15 40 50.570 +00 05 18.18	PG	sdO(A)	15.28 P	...	PG 15382+0014	...
944PG	1538+269	15 40 23.451 +26 48 29.76	TON	sdB	13.85	-0.19	...	#945 (TON 245)
946PG	1538+611	15 39 43.144 +60 54 59.45	U PG	sdB	15.48 P	...	PG 15387+6104	N*
947PG	1538+401	15 40 39.020 +39 55 48.89	PG	sdB	13.13	-0.25	PG 15387+4004	...

Continued on Next Page...

Table A.1 – Continued

No.	ID <sup>1</sup>	Coordinates <sup>2</sup> (J2000)	Chart Source <sup>3</sup>	Type	$V / y^4$	$B - V^4$	KHD ID <sup>5</sup>	Notes <sup>6</sup>
948 PG	1539+442	15 40 43.122+43 59 50.49 U	PG	sdO(C)	16.12 P	...	PG 15390+4409	...
949 PG	1539+292	15 41 24.950+29 01 30.45	PG	sdB+K3	14.64	+0.08	PG 15394+2911	...
950 PG	1539+043	15 42 13.569+04 08 36.34	PG	sdO(C)	15.912	-0.271	PG 15397+0418	WMG
951 PG	1540+044	15 43 07.442+04 17 08.68	PG	sd	15.84 P	...	PG 15406+0426	...
952 PG	1543+454	15 44 56.763+45 15 22.05	PG	sdO(A)	15.78 P	...	PG 15433+4524	...
953 PG	1543-124	15 46 20.081-12 32 28.86	PG	sdB	16.54	-0.14	PG 15435-1223	...
954 GD	351	15 44 38.090+62 43 24.72	GD	sdOB	14.82	-0.22	...	...
955 PG	1544+277	15 46 06.023+27 33 19.87 U	PG	sdB	16.39 :	-0.24	PG 15440+2742	...
956 TON	803	15 46 09.004+25 07 40.81	TON	sdO	14.170	-0.271	...	WMG
957 PG	1544+601	15 45 09.615+59 55 05.18	PG	sdB	14.74 P	...	PG 15441+6004	...
958 PG	1544+107	15 46 38.257+10 30 12.40	PG	sdB	14.428	-0.158	PG 15442+1039	AEA
959 PG	1544+488	15 46 11.692+48 38 37.30	PGWD	sdB He	12.80	...	PG 15446+4847	...
960 PG	1545+035	15 48 24.251+03 22 50.92	PG	sdO(B)	14.338	-0.233	PG 15458+0332	WMG
961 PG	1546+045	15 48 37.175+04 21 26.85	PG	sdB	15.54	-0.17	PG 15461+0430	...
962 PG	1547+476	15 48 43.317+47 29 35.85	PGWD	sd	15.55 y	-0.12	PG 15471+4738	...
963 PG	1547+632	15 48 11.743+63 03 08.22	PG	sdB	15.10 P	...	PG 15474+6312	...
964 PG	1548+166	15 50 48.297+16 26 25.41	PG	sdB	14.940	-0.256	PG 15485+1635	AEA
965 PG	1549+006	15 51 44.873+00 29 48.93	PG	sdB	15.27 y	-0.097	PG 15491+0038	...
966 PG	1549+476	15 51 03.608+47 27 28.93	PGWD	sdB	15.89 P	...	PG 15495+4736	...
967 BD	+33°2642	15 51 59.882+32 56 54.37	HIP	...	10.84	-0.17	...	PN <sup>f</sup>
968 PG	1551-076	15 53 46.450-07 46 21.32	PG	sdB	15.81	-0.12	PG 15510-0737	...
969 PG	1551+255	15 53 21.636+25 24 13.62	PG	sdB	13.76 y	+0.059	PG 15512+2533	...
970 PG	1551+015	15 54 25.194+01 21 09.55	PG	sdB	15.63 P	...	PG 15519+0129	...
971 PG	1552+141	15 54 22.331+13 59 14.35	PG	sdB-O	16.15 P	...	PG 15520+1407	...
972 PG	1552+460	15 53 42.742+45 53 40.34 U	PG	sd	16.54 P	...	PG 15521+4602	...
973 PG	1552+464	15 54 26.275+46 17 08.21	PG	sdO(D)	16.01 P	...	PG 15528+4625	...
974 PG	1553-077	15 56 02.848-07 48 28.38	PG	sdO(B)	14.943	-0.158	PG 15533-0739	AEA
975 PG	1553+272	15 55 37.854+27 06 48.59	PG	sdB	13.53	-0.12	PG 15535+2715	...
976 PG	1554+408	15 55 50.385+40 38 53.79	PG	sdO(D)	15.93 P	...	PG 15540+4047	...
977 PG	1554+222	15 56 33.618+22 02 45.93	PG	sdO(B)	13.816	-0.278	PG 15543+2211	WMG
978 PG	1554+505	15 56 22.667+50 21 56.78 U	PG	sd	16.01 P	...	PG 15549+5030	...
979 PG	1555+504	15 56 42.967+50 15 37.67 U	PG	sdO(C)	16.00 P	...	PG 15552+5024	...
980 PG	1555+142	15 57 58.777+14 02 20.39	PG	sdB	15.03 P	...	PG 15556+1410	...
981 PG	1555+303	15 57 56.355+30 11 25.65	PG	sdB	14.79	-0.25	PG 15559+3020	...
982 PG	1555+489	15 57 29.987+48 50 23.43 U	PG	sdO(B)	16.22 P	...	PG 15559+4858	...

Continued on Next Page...

Table A.1 – Continued

No.	ID <sup>1</sup>	Coordinates <sup>2</sup> (J2000)	Chart <sup>3</sup> Source	Type	$V / y^4$	$B - V^4$	KHD ID <sup>5</sup>	Notes <sup>6</sup>
983 PG	1558+449	15 59 55.581 +44 49 15.49 U	PG	sd	16.70	-0.12	PG 15583+4457	...
984 PG	1558-007	16 01 14.001 -00 51 41.42	PG	sdB	13.541	-0.064	PG 15586-0043	AEA
985 PG	1559+048	16 01 31.273 +04 40 27.05	PG	sdO(A)	14.48	-0.19	PG 15590+0448	...
986 PG	1559+222	16 01 13.814 +22 05 46.24	PG	sdO(D)	14.52 P	...	PG 15590+2214	...
987 PG	1559+076	16 02 09.063 +07 25 10.94	PG	sdO	15.03 ;	-0.11	PG 15597+0733	...
988 PG	1559+533	16 01 12.124 +53 11 51.76	PG	sdB	14.34	-0.32	PG 15599+5320	...
989 PG	1600+171	16 03 04.113 +16 59 54.43 U	PG	sdO(D)	16.30 P	...	K/P 16008+1708	...
990 PG	1601+145	16 04 05.519 +14 24 47.30	PG	sdB+K3	14.424	+0.028	PG 16018+1432	AEA
991 PG	1602+013	16 04 37.368 +01 10 08.34	PG	sdO(B)	15.022	-0.012	PG 16020+0118	WMG
992 PG	1602+145	16 04 28.815 +14 50 48.19	PG	sd	15.89 P	...	PG 16021+1458	...
993 PG	1604+504	16 05 34.213 +50 18 51.99	PG	sdB-O	15.73 P	...	PG 16042+5026	...
994 PG	1605+072	16 08 03.679 +07 04 28.73	PG	sdB	13.01	-0.23	PG 16056+0712	...
995 PG	1605+123	16 08 18.337 +12 12 02.57	PG	sdB	15.28 P	...	PG 16059+1219	...
996 PG	1606+627	16 06 28.535 +62 32 57.68	PG	sd	15.89 P	...	PG 16060+6239	...
997 PG	1606+387	16 07 59.301 +38 37 46.90 U	PG	sd	16.10 P	...	PG 16062+3845	...
998 PG	1607+227	16 09 32.427 +22 37 49.95 U	PG	sdO(B)	15.84 P	...	PG 16073+2245	...
999 PG	1607+174	16 09 54.931 +17 14 57.27	PG	sdO(A)	12.23 y	-0.192	PG 16076+1722	...
1000 PG	1608-029	16 10 37.696 -03 00 39.57	PG	sdO(B)	15.25 P	...	PG 16080-0252	...
1001 PG	1608+373	16 10 23.427 +37 13 16.80 U	PG	sdO(C)	16.25 P	...	PG 16085+3721	...
1002 PG	1608+481	16 10 19.488 +47 57 15.80 U	PG	sd	15.94 P	...	PG 16088+4804	...
1003 PG	1608+443	16 10 35.222 +44 10 39.90	PG	sd	14.97	-0.20	PG 16089+4418	...
1004 PG	1609+013	16 11 57.426 +01 11 53.19	PG	sdB	15.41 P	...	PG 16094+0119	...
1005 KUV	16096+1932	16 11 49.341 +19 23 50.73	PG	sdB	15.96	-0.25	...	...
1006 PG	1610+529	16 11 21.339 +52 46 05.68	PG	sdB-O	12.91	-0.27	PG 16101+5253	...
1007 PG	1610+043	16 12 45.142 +04 12 41.76 U	PG	sdO(B)	15.77 P	...	PG 16102+0420	...
1008 PG	1610+273	16 12 21.173 +27 09 45.16 U	PG	sd:	16.22 P	...	PG 16102+2717	...
1009 LB	9514	16 12 47.013 +23 48 40.46	PG	sdB-O	13.01 y	-0.063	...	...
1010 PG	1610+519	16 12 00.559 +51 49 43.17	PG	sdOB	13.726	-0.178	PG 16107+5157	AEA
1011 PG	1610+115	16 13 19.595 +11 20 15.80	PG	sdB	15.16 P	...	PG 16109+1127	...
1012 PG	1611+090	16 13 27.596 +08 53 54.32	PG	sdB	14.66 P	...	PG 16110+0901	...
1013 PG	1611+041	16 14 17.429 +03 59 51.03	PG	sdO(B)	15.28 P	...	PG 16117+0407	...
1014 PG	1612+437	16 13 50.892 +43 32 33.06	PG	sd	16.28 P	...	PG 16122+4340	...
1015 PG	1612+112	16 15 12.206 +11 02 39.75 U	PG	sdO(C)	16.34 P	...	PG 16128+1110	...
1016 PG	1612+735	16 12 06.247 +73 27 57.36	PG	sdB+?	14.474	+0.129	PG 16129+7335	AEA
1017 PG	1613+426	16 14 46.928 +42 27 36.01	PG	sdO(A)	14.40	-0.26	K/P 16131+4235	...

Continued on Next Page...

Table A.1 – Continued

No.	ID <sup>1</sup>	Coordinates <sup>2</sup> (J2000)	Chart Source <sup>3</sup>	Type	$V / y^4$	$B - V^4$	KHD ID <sup>5</sup>	Notes <sup>6</sup>
1018 PG	1613+467	16 15 02.842 +46 34 12.49	PG	sdB	14.58	-0.27	PG 16135+4641	...
1019 LB	926	16 13 09.140 +72 46 16.46	PG	sdO(B)	15.02 P	...	...	...
1020 PG	1614+378	16 15 55.236 +37 41 06.00	U PG	sdO(C)	16.30 P	...	K/P 16141+3748	...
1021 PG	1614+146	16 16 30.552 +14 26 55.62	PG	sdB	14.72 P	...	PG 16142+1434	...
1022 KUV	16160+4120	16 17 40.145 +41 12 52.37	U PG	sdO(D)	16.41 P	...	...	...
1023 PG	1616+144	16 18 23.099 +14 16 12.93	PG	sdB	13.48	-0.23	PG 16160+1423	...
1024 LB	933	16 19 35.658 -01 06 41.85	PG	sdB	15.29	-0.17	...	...
1025 PG	1617+076	16 19 45.177 +07 31 56.91	U PG	sdO(B)	15.94 P	...	PG 16173+0739	...
1026 PG	1617+309	16 19 23.224 +30 50 02.19	PG	sd	15.87	-0.42	PG 16174+3057	...
1027 PG	1618+562	16 19 26.589 +56 05 58.59	PG	sdOB	12.55 $y$	+0.166	PG 16181+5615	NE* <sup>f</sup> (v.close)
1028 PG	1618+216	16 21 09.011 +21 29 19.80	PG	sdB	16.07	-0.18	PG 16189+2136	...
1029 PG	1619+522	16 20 38.760 +52 06 08.74	PG	sdB	13.36	-0.28	PG 16193+5213	...
1030 PG	1620+017	16 23 07.331 +01 35 01.58	PG	sdB	15.58	-0.22	PG 16205+0141	...
1031 LS	IV -12°	16 23 43.989 -12 12 33.63	pre	sdO	11.14	-0.09	...	...
1032 TON	257	16 23 29.792 +24 45 41.72	TON	sdO	15.9	-0.48	...	...
1033 PG	1621+126	16 23 44.853 +12 29 13.18	PG	sdB	15.95 ;	-0.20	PG 16214+1236	...
1034 PG	1621+476	16 22 56.678 +47 30 50.83	PG	sdB	15.71 P	...	PG 16215+4737	...
1035 PG	1622+194	16 24 23.649 +19 16 02.06	PG	sdO(B)	15.61 P	...	PG 16221+1922	...
1036 KUV	16229+4106	16 24 31.893 +40 59 13.26	PG	sdB-O	14.43 $y$	-0.145	...	...
1037 PG	1623+178	16 25 15.113 +17 42 40.18	PG	sd:	16.01	-0.14	PG 16230+1749	...
1038 PG	1623+386	16 25 24.296 +38 30 18.92	PG	sd	15.84 ;	+0.02	PG 16236+3837	N* <sup>f</sup>
1039 PG	1624+014	16 26 41.307 +01 19 35.53	PG	sdB	15.43 P	...	PG 16241+0126	...
1040 PG	1624+085	16 26 54.198 +08 25 35.06	PG	sdO He	15.13 P	...	PG 16244+0832	...
1041 KUV	16245+3814	16 26 16.709 +38 07 10.23	PG	sdO(C)	15.678	-0.321	...	WMG
1042 PG	1625-034	16 28 36.158 -03 32 38.21	PG	sdO(B)	15.61	-0.13	PG 16259-0326	...
1043 PG	1626+471	16 27 46.715 +46 58 47.65	PG	sdB-O	13.75	-0.21	PG 16263+4705	...
1044 PG	1627+006	16 29 35.910 +00 31 49.12	PG	sdB	14.68 P	...	PG 16270+0038	...
1045 PG	1627+017	16 29 35.306 +01 38 18.77	PG	sdB	12.899	-0.195	PG 16270+0144	AEA
1046 PG	1627+025	16 29 50.703 +02 23 33.41	PG	sdB	15.99 P	...	PG 16273+0229	...
1047 PG	1627+112	16 29 52.880 +11 05 02.43	PG	sdB	14.38 $y$	-0.195	PG 16275+1111	...
1048 PG	1628+553	16 29 12.173 +55 15 18.94	U PG	sdO(C)	15.55 P	...	PG 16281+5521	...
1049 PG	1628+530	16 29 35.760 +52 55 53.24	PG	sdB-O	15.80	-0.20	PG 16283+5302	...
1050 PG	1628+181	16 30 45.447 +18 01 20.29	PG	sdB	15.25 P	...	PG 16285+1807	...
1051 PG	1629+081	16 32 01.287 +07 59 38.74	PG	sdB-O	12.764	-0.159	PG 16296+0805	AEA
1052 PG	1629+466	16 31 17.717 +46 31 00.27	PG	sdO(D)	14.04 P	...	PG 16298+4637	...

Continued on Next Page...

Table A.1 – Continued

No.	ID <sup>1</sup>	Coordinates <sup>2</sup> (J2000)	Chart <sup>3</sup> Source	Type	$V / y^4$	$B - V^4$	KHD ID <sup>5</sup>	Notes <sup>6</sup>
1053PG 1629+179		16 32 12.277 +17 53 19.41	U PG	sdB	16.16	-0.29	PG 16299+1759	...
1054PG 1631+001		16 33 52.031 +00 02 26.07	PG	sdB	15.65	...	PG 16313+0008	...
1055 TON 817		16 33 49.327 +26 32 58.69	TON	sdB+ G	15.51	-0.170	...	...
1056HD 149382		16 34 23.342 -04 00 52.12	HIP	sdOB	8.92	-0.27	...	...
1057PG 1632+001		16 34 38.785 +00 00 59.27	PG	sdB	15.86	-0.19	PG 16320+0007	...
1058PG 1632+053		16 34 49.201 +05 14 16.19	PG	sdB	15.45	...	PG 16323+0520	...
1059PG 1632+088		16 34 47.042 +08 40 00.10	PG	sdBpe	13.37	-0.05	PG 16323+0846	...
1060PG 1632+588		16 34 01.536 +58 36 44.48	PG	sdO(B)	15.95	...	PG 16329+5846	...
1061PG 1633+099		16 35 24.029 +09 47 49.90	PG	sdB	14.397	-0.192	PG 16330+0953	LAN
1062BPS CS 22878-21		16 35 45.722 +11 24 58.11	CS	sdB	15.30	-0.02	CSHK 22878-21	...
1063PG 1633+696		16 33 14.103 +69 29 36.84	PG	sdB	16.46	...	PG 16334+6935	...
1064PG 1634+061		16 37 03.593 +05 59 05.45	PG	sdB	13.85	-0.192	PG 16346+0604	...
1065PG 1634+014		16 37 27.972 +01 18 19.04	PG	sdO(A)	16.19	-0.22	PG 16349+0124	...
1066PG 1635+533		16 36 14.230 +53 12 57.76	PG	sdB	15.66	...	PG 16350+5319	...
1067PG 1635+413		16 37 05.179 +41 15 40.08	PG	sdB-O	13.963	-0.262	PG 16354+4121	AEA
1068PG 1636+216		16 38 26.768 +21 32 56.61	PG	sdB	15.08	-0.34	...	...
1069PG 1636+104		16 39 02.063 +10 19 04.58	PG	bin	14.039	+0.193	...	AEA
1070PG 1636+428		16 38 07.712 +42 44 57.12	U PG	sdB	16.20	...	PG 16365+4250	...
1071PG 1636+085		16 39 04.591 +08 23 00.97	PG	sdB	16.33	-0.12	PG 16366+0828	...
1072KUV 16378+3438		16 39 36.042 +34 32 30.41	PG	sdB	15.29	...	...	...
1073PG 1638+147		16 40 34.270 +14 38 00.33	PG	sdO(C)	14.917	-0.263	PG 16382+1444	WMG
1074PG 1638+128		16 40 45.953 +12 41 13.31	U PG	sdB	16.14	...	PG 16384+1246	...
1075PG 1638+675		16 38 43.707 +67 28 08.49	PG	sdO(C)	16.104	-0.296	PG 16386+6733	WMG
1076 Balloon 083500007		16 41 19.342 +34 50 13.20	ML	bin?	15.5	...	BBL083500007	...
1077PG 1639+173		16 41 34.643 +17 12 27.20	PG	sdO(B)	15.45	...	PG 16393+1718	...
1078PG 1640+645		16 40 50.697 +64 24 45.02	PG	sdOB	15.17	...	PG 16404+6430	...
1079KUV 16416+3307		16 43 26.092 +33 01 13.57	U PG	sdB	15.79	...	...	...
1080PG 1642+038		16 44 45.581 +03 42 18.80	PG	sdO(C)	15.375	-0.239	PG 16422+0347	WMG
1081PG 1642+707		16 42 19.941 +70 37 50.79	PG	sd	16.01	...	PG 16427+7043	...
1082PG 1643+209		16 45 25.276 +20 51 32.58	PG	sdB	14.82	...	PG 16432+2056	...
1083PG 1643+063		16 46 14.513 +06 23 01.44	PG	sdB-O	14.69	...	PG 16437+0618	...
1084PG 1644+403		16 46 09.134 +40 17 25.51	PG	sdB	14.24	-0.245	PG 16444+4022	...
1085 TON 261		16 46 34.462 +26 37 51.81	TON	sdO	16.20	-0.28	...	...
1086PG 1644+311		16 46 53.425 +31 03 45.55	PG	sdB	14.30	-0.095	PG 16449+3109	...
1087PG 1645+610		16 45 40.063 +60 57 10.86	PG	sdB	14.409	-0.146	PG 16450+6102	AEA
1088PG 1646+607		16 46 44.315 +60 37 09.17	U PG	sdO He	16.07	...	PG 16460+6042	...

Continued on Next Page...

Table A.1 – Continued

No.	ID <sup>1</sup>	Coordinates <sup>2</sup> (J2000)	Chart Source <sup>3</sup>	Type	$V / y^4$	$B - V^4$	KHD ID <sup>5</sup>	Notes <sup>6</sup>
1089PG 1646+042		16 49 13.126+04 11 48.26	PG	sdB	15.74 ;	-0.26	PG 16467+0416	...
1090 TON 263		16 48 58.749+24 58 02.06	TON	sdB	16.12 P	...	...	...
1091PG 1646+354		16 48 47.010+35 20 43.39	PG	sdB	16.13 P	...	PG 16469+3525	...
1092 TON 264		16 49 08.959+25 10 06.25	TON	sdB+ ?	14.074	-0.083	...	AEA
1093PG 1647+056		16 50 18.465+05 32 55.98	PG	sdB	14.733	-0.175	PG 16478+0537	AEA
1094PG 1648+315		16 50 22.057+31 27 49.60	PG	sdO(D)	16.04 P	...	PG 16484+3132	...
1095 Balloon 083600004		16 49 54.548+48 26 52.61	ML	bin?	16.9 y	...	BBL083600004	...
1096PG 1648+080		16 51 10.074+08 03 32.72	PG	sd	13.94 y	+0.263	PG 16487+0803	...
1097PG 1648+536		16 49 59.855+53 31 31.84	PG	sdB	14.06 y	-0.199	PG 16488+5336	...
1098 KUV 16491+3539		16 50 54.394+35 33 42.19	PG	sdOB	15.11	-0.25	...	...
1099PG 1649+522		16 50 39.557+52 07 34.16	PG	sdB	16.09 P	...	PG 16494+5212	...
1100 LSE 259		16 53 55.731-56 02 00.21	LSE	sdO	12.54 y	-0.112	...	crowded field <sup>f</sup>
1101PG 1650+706		16 50 19.421+70 30 52.21	PG	sdO(B)	14.96 P	...	PG 16507+7035	...
1102PG 1651+086		16 53 48.665+08 36 27.85	PG	sdO(B)	15.11 P	...	PG 16514+0834	...
1103LB 966		16 54 04.261+30 37 01.72	PG	sdB	15.42 P	...	...	...
1104PG 1652+159		16 54 48.364+15 52 58.80	PG	sdO(C)	15.591	-0.234	PG 16525+1557	WMG
1105PG 1652+517		16 54 12.550+51 39 00.28	PG	sdB	16.19	-0.30	PG 16529+5143	...
1106PG 1653+131		16 55 42.820+13 01 48.52	PG	sdB	14.421	-0.212	PG 16533+1306	AEA
1107PG 1653+115		16 55 54.129+11 24 00.80	PG	sdB	14.69 y	-0.116	PG 16535+1128	...
1108LS IV-08°03		16 56 29.621-08 34 38.75	pre	sdB	11.51 y	+0.227	...	em <sup>f</sup>
1109PG 1653+544		16 54 54.161+54 20 27.67	PG	sdB-O	15.55 P	...	PG 16538+5425	...
1110PG 1653+633		16 54 22.281+63 15 34.80	PG	sdOB	15.99 P	...	PG 16539+6320	...
1111PG 1654+322		16 55 52.978+32 08 25.45	PG	sdO(C)	15.415	-0.298	PG 16540+3213	WMG
1112PG 1655+106		16 58 07.933+10 30 42.96	PG	sdO(B)	15.71 P	...	PG 16557+1035	...
1113PG 1656+322		16 57 54.021+32 04 54.80	PG	sd	14.65 P	...	PG 16560+3209	...
1114PG 1656+253		16 58 05.089+25 15 26.82	PG	sdB	15.72 P	...	PG 16560+2519	...
1115PG 1656+600		16 56 50.163+59 55 41.84	PG	sdB	15.90 P	...	PG 16561+6000	...
1116PG 1656+213		16 58 21.110+21 10 33.65	PG	sdB+ ?	14.88	-0.20	PG 16562+2115	...
1117LB 974		16 58 16.540+27 01 32.12	PG	sdB	16.19 P	...	...	...
1118PG 1656+318		16 58 17.682+31 41 37.08	PG	sdB-O	14.24 y	-0.233	PG 16564+3146	...
1119PG 1656+356		16 58 24.075+35 30 26.94	PG	sdB	15.78 P	...	PG 16566+3534	...
1120PG 1656+552		16 57 51.585+55 11 33.07	PG	sdB	15.37 P	...	PG 16568+5516	...
1121PG 1657+291		16 59 01.553+29 02 34.18	PG	sdB	16.14	-0.13	PG 16570+2907	...
1122PG 1657+416		16 58 41.845+41 31 15.62	PG	sdB	15.87 P	...	PG 16570+4135	...
1123PG 1657+078		16 59 32.222+07 43 31.46	PG	sdB	15.015	-0.149	PG 16571+0747	LAN

Continued on Next Page...



Table A.1 – Continued

No.	ID <sup>1</sup>	Coordinates <sup>2</sup> (J2000)	Chart <sup>3</sup> Source	Type	$V / y^4$	$B - V^4$	KHD ID <sup>5</sup>	Notes <sup>6</sup>
1124PG	1657+656	16 57 23.095 +65 31 28.57	PG	sdB-O	15.95 P	...	PG 16572+6536	...
1125PG	1658+273	17 00 14.137 +27 12 36.79	PG	sdO(D)	15.73 P	...	PG 16582+2716	...
1126PG	1658+337	17 00 40.653 +33 37 48.18	PG	sdB	15.73 P	...	PG 16588+3342	...
1127LB	983	17 01 30.799 +11 02 53.77	PG	sdB-O	15.17 P	...	...	...
1128LB	984	17 02 06.141 +12 16 07.66	PG	sdB	15.91 P	...	...	...
1129PG	1700+198	17 02 14.006 +19 42 55.06	PG	sdO(B)	15.10 P	...	PG 17000+1947	...
1130PG	1700+247	17 02 37.685 +24 35 22.69	PG	sd	16.05 P	...	PG 17005+2439	...
1131LB	988	17 02 41.560 +31 25 18.79	PG	sd	16.04 P	...	...	...
1132PG	1700+486	17 02 11.783 +48 30 23.15	PG	sdB	14.80 P	...	PG 17008+4834	...
1133PG	1701+359	17 03 21.473 +35 48 49.11	PG	sdB	13.226	-0.160	PG 17015+3552	AEA
1134PG	1702+099	17 04 36.518 +09 47 58.78	PG	sdB	15.55 P	...	PG 17022+0952	...
1135PG	1703+355	17 05 15.231 +35 28 18.52	PG	sdO(C)	15.625	-0.291	PG 17034+3532	WMG
1136PG	1703+074	17 06 23.234 +07 21 52.75	PG	sdB	16.09 P	...	PG 17039+0725	...
1137	TON 266	17 06 12.467 +25 42 31.92	TON	sdB	14.9	+0.05	...	...
1138PG	1704+222	17 06 46.171 +22 05 52.09	PG	non-sd	12.73 y	-0.094	PG 17046+2209	...
1139PG	1704+466	17 06 10.649 +46 31 43.43	PG	sdO(C)	16.043	-0.241	PG 17047+4634	WMG
1140PG	1704+441	17 06 26.946 +44 02 55.30	PG	sdB	15.89 P	...	PG 17049+4406	...
1141PG	1705+398	17 06 43.621 +39 43 56.51	PG	sdB	16.01 P	...	PG 17050+3947	...
1142PG	1705+504	17 07 07.344 +50 23 46.26	PG	sdB	16.27 P	...	PG 17058+5027	...
1143PG	1706+357	17 08 12.075 +35 39 01.19	PG	sdB-O	15.53 P	...	PG 17064+3542	...
1144LB	999	17 08 22.680 +30 01 36.90	PG	sdB-O	15.95	-0.20	...	...
1145PG	1707+657	17 07 14.221 +65 40 25.42	PG	sdB	16.13 P	...	PG 17071+6544	...
1146PG	1707+214	17 09 32.621 +21 22 15.38	PG	sd	15.40 P	...	PG 17074+2125	...
1147PG	1708+614	17 08 40.636 +61 17 46.60	PG	sdO(C)	15.059	-0.297	PG 17081+6121	WMG
1148PG	1708+409	17 09 59.185 +40 54 50.24	PG	sdB	15.09 P	...	PG 17083+4058	...
1149PG	1708+602	17 09 15.889 +60 10 10.85	PG	sdO	13.750	-0.326	PG 17085+6013	WMG
1150PG	1710+566	17 11 20.471 +56 35 33.11	PG	sdB	15.99 P	...	PG 17104+5639	...
1151PG	1710+278	17 12 52.387 +27 45 13.50	PG	sdB	15.27 P	...	PG 17108+2748	...
1152PG	1710+490	17 12 18.748 +48 58 35.77	PG	sdB	12.90 y	-0.238	PG 17109+4902	...
1153PG	1711+564	17 12 37.314 +56 25 08.68	PG	sdB	16.12 P	...	PG 17117+5628	...
1154PG	1712+228	17 14 28.066 +22 47 26.02	PG	sdB	14.67 P	...	PG 17123+2250	...
1155PG	1713+248	17 15 38.475 +24 47 22.78	PG	sdB-O	15.95 P	...	PG 17135+2450	...
1156PG	1715+273	17 17 03.171 +27 16 37.48	PG	sdO(D)	16.21 P	...	PG 17150+2719	...
1157PG	1715+457	17 17 16.155 +45 36 23.63	PG	sdB	16.12 P	...	PG 17158+4539	...
1158PG	1716+426	17 18 03.860 +42 34 12.74	PG	sdB	13.97 y	-0.233	PG 17165+4237	...
1159PG	1716+367	17 18 19.879 +36 39 15.71	PG	sdB	15.25 P	...	PG 17165+3642	...

Continued on Next Page...

Table A.1 – Continued

No.	ID <sup>1</sup>	Coordinates <sup>2</sup> (J2000)	Chart Source <sup>3</sup>	Type	$V / y^4$	$B - V^4$	KHD ID <sup>5</sup>	Notes <sup>6</sup>
1160PG 1717+258		17 19 12.287 +25 44 31.25	PG	sd	15.24 P	...	PG 17171+2547	...
1161PG 1717+607		17 17 58.474 +60 39 21.16	PG	sdB-O	14.44 y	-0.240	PG 17173+6042	...
1162SC 1717-363		17 20 57.545 -36 29 54.54	U pre	sdB?	16.28	+0.43	...	(not in SIMBAD)
1163PG 1717+474		17 19 17.850 +47 22 21.01	PG	sdB	15.79 P	...	PG 17179+4725	...
1164PG 1718+519		17 19 45.344 +51 52 10.65	PG	sdB-O	13.733	+0.113	PG 17185+5155	AEA
1165SC 1721-336		17 24 34.949 -33 41 10.73	pre	sdB	15.63	+0.05	SC 1721-334	(not in SIMBAD)
1166PG 1722+286		17 24 11.958 +28 35 26.89	PG	sdB	13.39 y	-0.266	PG 17222+2837	...
1167PG 1722+317		17 24 11.830 +31 38 47.11	PG	sdO(B)	15.80 P	...	PG 17223+3141	...
1168PG 1722+353		17 24 35.468 +35 34 17.76	PG	sdB	14.71 P	...	PG 17227+3517	...
1169LB 331		17 23 38.527 +60 14 43.97	PG	sdB	15.84 P	...	...	...
1170PG 1724+523		17 25 16.448 +52 14 25.75	U PG	sdO(B)	15.76 P	...	PG 17241+5216	...
1171LB 333		17 25 06.298 +58 57 34.96	PG	sdB	14.81 P	...	...	...
1172PG 1724+278		17 26 24.110 +27 44 19.26	PG	sdB	15.94 P	...	PG 17244+2746	...
1173PG 1725+373		17 26 45.290 +37 13 30.70	PG	sdO(A)	15.29 P	...	PG 17250+3715	...
1174PG 1725+285		17 27 21.136 +28 25 20.98	PG	sdB	15.89 P	...	PG 17253+2827	...
1175PG 1725+245		17 27 33.227 +24 26 33.97	U PG	sdO(A)	16.19 P	...	PG 17254+2429	...
1176PG 1725+252		17 27 57.377 +25 08 35.68	PG	sdB	13.063	-0.205	PG 17259+2511	AEA
1177PG 1729+272		17 31 18.268 +27 08 40.79	PG	sdB	15.60 P	...	PG 17293+2710	...
1178PG 1729+500		17 30 48.371 +49 59 22.82	U PG	sdB	16.23 P	...	PG 17295+5001	...
1179GD 362		17 31 34.333 +37 05 20.92	GD	sd	16.15 P	...	...	...
1180PG 1733+326		17 35 03.187 +32 36 22.18	PG	sdB	16.28 P	...	PG 17331+3238	...
1181[CW83] 1735+22		17 37 26.431 +22 08 57.77	Drill	sdB	11.80 B	...	UVO 1735+22	...
1182BD+29°3070		17 38 21.203 +29 08 47.37	HIP	sdOB+	10.42	+0.18	...	...
			F					
1183NGC 6397 162		17 40 52.18 -53 40 32.43	D ...	sdOp	13.23 P	...	ROB 162 (NGC 6397)	...
1184PG 1738+505		17 39 28.433 +50 29 25.17	PG	sd	13.26	-0.08	PG 17382+5030	...
1185PG 1739+489		17 40 21.972 +48 53 58.11	PG	HBB	12.96 P	...	PG 17391+4855	...
1186PG 1743+477		17 44 26.401 +47 41 46.82	PG	sdB	13.79 y	-0.208	PG 17431+4742	...
1187BD+39°3226		17 46 31.913 +39 19 09.07	HIP	sdOp	10.21	-0.29	...	...
1188[CW83] 1758+36		18 00 18.867 +36 28 56.36	pl	sdB	11.36	-0.25	UVO 1758+36	...
1189KUV 18004+6836		18 00 09.616 +68 35 52.22	KUV	sdO	14.60 P	...	...	...
1190LSE 234		18 13 15.834 -64 55 16.85	LSE	sdO	12.63 y	-0.259	...	...
1191KUV 18169+6643		18 16 51.361 +66 44 12.82	U KUV	sdOB	16.3	...	...	...
1192KUV 18189+6501		18 19 04.220 +65 02 07.03	U KUV	sdB	16.0	...	...	...
1193KUV 18312+6431		18 31 29.67 +64 33 46.77	D ...	sdB	17.0	...	...	...

Continued on Next Page...

Table A.1 – Continued

No.	ID <sup>1</sup>	Coordinates <sup>2</sup> (J2000)	Chart Source <sup>3</sup>	Type	$V / y^4$	$B - V^4$	KHD ID <sup>5</sup>	Notes <sup>6</sup>
1194BD+48°2721		18 34 09.192+48 27 39.81	SIM	sdB	10.70	-0.20	...	...
1195HD 171858		18 37 56.678-23 11 35.12	TYC	sdB	9.86 $y$	-0.223	...	...
1196BPS CS 22959-140		18 55 24.903-63 05 05.66	CS	sdO	15.0 B	...	CSHK 22959-140	...
1197BPS CS 22959-145		19 02 17.534-63 12 08.25	CS	sdB	16.4 B	...	CSHK 22959-145	...
1198KPD 1856+2301		18 58 22.021+23 05 46.77	KPD	sdO	15.52	+0.13	KPD 18562+2301	...
1199LSE 263		19 02 11.746-51 30 09.47	LSE	sdO	11.75 $y$	-0.264	...	...
1200KPD 1901+1607		19 03 51.308+16 12 05.10	KPD	sdB	14.248	-0.004	KPD 19016+1607	AEA
1201JL 9		19 08 20.772-72 30 34.33	JL	sdO	13.37	-0.27	...	...
1202KPD 1903+2540		19 05 36.036+25 45 53.21	KPD	sdO	14.71	+0.01	KPD 19035+2540	...
1203KPD 1905+1144		19 08 17.652+11 49 19.54	KPD	sdB	14.563	+0.170	KPD 19059+1144	AEA
1204Cl* NGC 6752 CL 3507 19 10 23.00		-59 52 30.20 O Caloi		sdB	17.55	-0.22	#3507 (NGC 6752)	...
1205Cl* NGC 6752 CL 3118 19 10 37.88		-60 08 52.20 O Caloi		sdB	17.79	-0.25	#3-118 (NGC 6752)	...
1206Cl* NGC 6752 CL 2128 19 11 08.38		-59 52 23.03 O Caloi		sdOB	16.00 P	...	#2128 (NGC 6752)	...
1207Cl* NGC 6752 CL 3781 19 11 29.31		-60 02 57.60 O Caloi		sdB	16.96 P	...	#3781 (NGC 6752)	...
1208Cl* NGC 6752 CL 3675 19 11 41.61		-59 56 36.73 O Caloi		sdB	17.02 P	...	#3675 (NGC 6752)	...
1209BPS CS 22947-99		19 11 13.988-48 49 32.46	CS	sdB	14.03	...	CSHK 22947-99	...
1210BPS CS 22947-115		19 15 22.772-50 19 17.39	CS	sdB	15.0 B	...	CSHK 22947-115	...
1211BPS CS 22896-12		19 22 26.281-55 52 04.81	CS	sdB	15.0 B	...	CSHK 22896-12	...
1212BPS CS 22891-139		19 23 36.981-57 52 49.22	CS	sdB	16.0 B	...	CSHK 22891-139	...
1213BPS CS 22947-196		19 23 46.190-47 47 16.50	CS	sdB	13.1 B	...	CSHK 22947-196	...
1214BPS CS 22896-69		19 25 25.629-55 25 49.83	CS	sdB	14.6 B	...	CSHK 22896-69	...
1215BPS CS 22896-45		19 26 21.232-53 43 30.14	CS	sdB	15.4 B	...	CSHK 22896-45	...
1216KPD 1924+2932		19 26 41.774+29 39 34.41	KPD	sdB	13.843	-0.172	KPD 19247+2932	AEA
1217BPS CS 22891-188		19 32 38.765-60 45 37.57	CS	sdB	15.9 B	...	CSHK 22891-188	...
1218BPS CS 22947-299		19 32 40.056-49 27 05.01	CS	sdB	14.52	...	CSHK 22947-299	...
1219KPD 1930+2752		19 32 14.807+27 58 35.47	KPD	sdB	13.842	-0.085	KPD 19302+2752	AEA
1220BPS CS 22891-227		19 35 49.621-58 53 52.16	CS	sdO He	15.6 B	...	CSHK 22891-227	...
1221KPD 1931+2911		19 33 49.183+29 17 47.44	KPD	sdO	15.36	-0.04	KPD 19318+2911	...
1222JL 25		19 39 38.959-76 01 17.25	JL	sdOB	13.28	-0.19	...	...
1223HD 185510		19 39 38.818-06 03 49.46	HIP	sdB+	8.341	+1.080	...	variable *, TYC
			K0III-IV					
1224BPS CS 22896-128		19 41 04.429-52 46 57.29	CS	sdO He	16.2 B	...	CSHK 22896-128	...
1225KPD 1938+4220		19 39 39.895+42 28 01.95	KPD	sdO	15.61	-0.17	KPD 19380+4220	...
1226LS II+18°9		19 43 31.202+18 24 34.66	LSE	sdO	12.13	-0.32	...	...
1227BPS CS 22896-190		19 45 49.992-53 54 45.35	CS	sdB	15.1 B	...	CSHK 22896-190	...

Continued on Next Page...

Table A.1 – Continued

No.	ID <sup>1</sup>	Coordinates <sup>2</sup> (J2000)	Chart Source <sup>3</sup>	Type	$V / y^4$	$B - V^4$	KHD ID <sup>5</sup>	Notes <sup>6</sup>
1228BPS	CS 22896–175	19 47 26.776 –55 31 06.67	CS	sdB	15.47	–0.08	CSHK 22896–175	...
1229KPD	KPD 1943+4058	19 45 25.463 +41 05 33.91	KPD	sdB	14.866	–0.147	KPD 19436+4058	AEA
1230BPS	CS 22896–183	19 47 49.466 –54 33 43.70	CS	sdB	14.4	...	CSHK 22896–183	...
1231BPS	CS 22896–194	19 48 06.070 –53 23 26.81	CS	sdB	15.89	–0.06	CSHK 22896–194	...
1232BPS	CS 22873–30	19 48 20.932 –57 51 53.35	CS	sdB	14.36	–0.30	CSHK 22873–30	...
1233BPS	CS 22896–171	19 48 43.261 –55 55 38.37	CS	sdB	14.04	–0.23	CSHK 22896–171	...
1234BPS	CS 22964–20	19 48 33.868 –39 41 42.38	CS	sdO	15.27	–0.20	CSHK 22964–20	...
1235KPD	KPD 1946+4340	19 47 42.885 +43 47 30.67	KPD	sdB	14.284	–0.201	KPD 19461+4340	AEA
1236BPS	CS 22873–56	19 51 29.574 –59 40 21.44	CS	sdB	14.10	–0.04	CSHK 22873–56	...
1237HD	188112	19 54 31.417 –28 20 20.72	HIP	sdB	10.21	–0.206	...	...
1238LSE	21	19 55 38.219 –23 13 42.18	LSE	sdO	11.78	–0.25	...	...
1239BPS	CS 22964–112	19 56 42.986 –40 27 56.48	CS	sdB	15.40	–0.28	CSHK 22964–112	...
1240JL	36	20 01 52.295 –71 57 25.72	JL	sdB	12.98	–0.136	...	...
1241BPS	CS 22964–216	20 05 47.579 –39 18 15.76	CS	sdB	15.76	–0.27	CSHK 22964–216	...
1242LS	II+22°21	20 04 57.516 +22 20 39.79	LSN	sdO	12.58	–0.35	...	...
1243KPD	KPD 2007+4527	20 08 57.711 +45 36 05.44	KPD	sdB	15.08	+0.11	KPD 20073+4527	...
1244BPS	CS 22943–19	20 12 20.877 –45 50 39.61	CS	sdB	15.5	...	CSHK 22943–19	...
1245BPS	CS 22885–43	20 18 15.377 –38 34 00.27	CS	sdB He	15.6	...	CSHK 22885–43	...
1246BPS	CS 22950–10	20 19 21.612 –15 40 28.36	CS	sdB	13.6	...	CSHK 22950–10	...
1247BPS	CS 22950–48	20 20 27.710 –13 08 37.46	CS	He-sdO	13.9	...	CSHK 22950–48	...
1248BPS	CS 22950–1	20 20 32.680 –16 38 01.77	CS	sdB	15.8	...	CSHK 22950–1	...
1249KPD	KPD 2018+2058	20 21 07.315 +21 08 09.23	KPD	sdO	16.15	–0.23	KPD 20189+2058	...
1250BPS	CS 22950–61	20 21 58.603 –14 41 57.95	CS	sdB	15.1	...	CSHK 22950–61	...
1251BPS	CS 22943–127	20 22 49.056 –43 30 11.61	CS	sdO	13.6	...	CSHK 22943–127	...
1252BPS	CS 22955–28	20 22 36.269 –24 47 36.89	CS	sdB	14.05	...	CSHK 22955–28	...
1253BPS	CS 22955–16	20 23 41.810 –26 17 05.71	CS	sdB	14.1	...	CSHK 22955–16	...
1254KPD	KPD 2022+2033	20 25 10.805 +20 43 54.26	KPD	sdB	13.67	–0.05	KPD 20229+2033	...
1255BPS	CS 22955–79	20 26 10.193 –25 53 28.37	CS	sdB	16.0	...	CSHK 22955–79	...
1256KPD	KPD 2024+5303	20 25 34.562 +53 12 44.81	KPD	sdB	14.562	+0.026	KPD 20242+5303	AEA
1257BPS	CS 22955–89	20 27 43.264 –27 00 39.06	CS	sdB	15.4	...	CSHK 22955–89	...
1258KPD	KPD 2025+5428	20 27 17.496 +54 39 03.98	KPD	sdB	15.63	–0.05	KPD 20259+5428	...
1259KPD	KPD 2026+2205	20 28 18.230 +22 16 06.87	KPD	sdO	15.20	...	KPD 20261+2205	...
1260BPS	CS 22940–9	20 30 20.162 –59 50 39.47	CS	sdB He	14.07	–0.29	CSHK 22940–9	...
1261KPD	KPD 2026+2316	20 28 45.658 +23 27 36.80	KPD	sdB	16.18	–0.04	KPD 20267+2316	...
1262BPS	CS 22943–148	20 30 31.768 –43 58 08.68	CS	sdB	15.1	...	CSHK 22943–148	...
1263LS	IV+00°21	20 31 18.283 +01 05 25.71	pre	sdB	12.44	–0.249	...	...

Continued on Next Page...

Table A.1 – Continued

No.	ID <sup>1</sup>	Coordinates <sup>2</sup> (J2000)	Chart Source <sup>3</sup>	Type	$V / y^4$	$B - V^4$	KHD ID <sup>5</sup>	Notes <sup>6</sup>
1264BPS	CS 22943-198	20 32 21.369 -44 05 36.79	CS	sdB	15.7	B ...	CSHK 22943-198	...
1265BPS	CS 22943-177	20 35 49.675 -46 37 45.43	CS	sdB	14.9	B ...	CSHK 22943-177	...
1266BPS	CS 22880-18	20 36 41.303 -19 15 00.02	CS	sdB	15.60	-0.26	CSHK 22880-18	...
1267BPS	CS 22880-24	20 37 43.222 -18 18 26.58	CS	sdB	14.57	-0.35	CSHK 22880-24	...
1268BPS	CS 22955-176	20 40 03.504 -24 01 32.37	CS	sdB	15.18	...	CSHK 22955-176	...
1269LS	IV+10 <sup>9</sup>	20 43 02.479 +10 34 20.94	LSE	sdO	11.99	-0.27	...	...
1270KPD	KPD 2040+3955	20 42 33.919 +40 05 41.67	KPD	sdB	14.451	-0.029	KPD 20407+3955	AEA
1271BPS	CS 22880-52	20 43 56.565 -20 48 10.00	CS	sdB	15.23	-0.07	CSHK 22880-52	...
1272KUV	20417+7604	20 40 46.854 +76 14 39.70	KUV	sdO	13.00	P ...	...	...
1273KUV	20432+7457	20 42 37.309 +75 08 02.43	KUV	sd?	15.50	P ...	...	Seyfert 1 <sup>e</sup>
1274KPD	2045+3436	20 47 07.415 +34 47 01.83	KPD	sdB	15.51	+0.00	KPD 20451+3436	...
1275KPD	2045+5136	20 46 38.175 +51 47 35.71	KPD	sdB	15.06	+0.19	KPD 20452+5136	...
1276BPS	CS 22880-78	20 49 08.907 -20 30 05.37	CS	sdB	15.30	-0.07	CSHK 22880-78	...
1277KPD	2048+3515	20 50 03.483 +35 27 25.46	KPD	sdO	14.08	-0.23	KPD 20480+3515	...
1278BPS	CS 22879-82	20 51 59.976 -40 42 46.59	CS	sdB	15.20	-0.35	CSHK 22879-82	...
1279PG	2050+001	20 52 40.921 +00 16 29.41	U PG	sdB	16.07	P ...	PG 20501+0005	...
1280KPD	2051+3544	20 53 18.726 +35 55 51.69	KPD	sdB	15.93	-0.28	KPD 20514+3544	...
1281PG	2052+027	20 55 08.096 +02 52 05.00	PG	sdO(B)	15.64	P ...	PG 20526+0240	...
1282PG	2052-003	20 55 32.185 -00 04 53.61	PG	sdB	15.98	P ...	PG 20529-0016	...
1283KPD	2053+5632	20 54 23.199 +56 43 52.17	KPD	sdB	14.35	+0.27	KPD 20531+5632	...
1284BPS	CS 22879-149	20 57 15.243 -38 11 51.17	U CS	sdB	14.28	-0.23	CSHK 22879-149	...
1285LS	IV-14 <sup>116</sup>	20 57 38.871 -14 25 43.79	pre	sdOB	13.03	$y$ -0.273	...	...
1286KPD	2055+3111	20 57 26.913 +31 22 52.50	KPD:	sdO	14.12	-0.24	KPD 20553+3111	...
1287PG	2059+013	21 02 19.308 +01 32 15.66	PG	sdB	15.011	-0.181	PG 20597+0120	AEA
1288PG	2102+037	21 05 07.073 +03 54 47.04	U PG	sdO	15.67	+0.17	PG 21026+0342	$V, B - V$ from PG <sup>f</sup>
1289KPD	2104+3407	21 06 15.622 +34 19 14.68	KPD	sdO	15.95	-0.14	KPD 21042+3407	...
1290BPS	CS 22937-33	21 07 31.674 -40 05 47.78	CS	sdB	12.3	B ...	CSHK 22937-33	...
1291BPS	CS 30492-40	21 07 35.345 -38 06 42.36	CS	sdB	14.7	B ...	CSHK 30492-40	...
1292BPS	CS 22937-36	21 10 54.682 -40 35 07.04	CS	sdB	15.5	B ...	CSHK 22937-36	...
1293BPS	CS 22937-22	21 11 43.620 -38 15 07.71	CS	sdB	15.2	B ...	CSHK 22937-22	...
1294BPS	CS 30492-42	21 11 43.623 -38 15 07.59	U CS	sdB	15.2	B ...	CSHK 30492-42	$B_{pg}$ from USNO <sup>f</sup>
1295KPD	2109+4401	21 11 47.655 +44 13 50.71	KPD	sdB	13.38	-0.21	KPD 21099+4401	...
1296LB	1113	21 13 18.391 +00 17 39.04	U PG	sdO(B)	16.03	P ...	...	...
1297PG	2110+127	21 13 21.061 +12 57 09.36	PG	sdB	12.927	+0.149	PG 21109+1244	AEA
1298PG	2111+023	21 13 42.330 +02 33 09.50	PG	HBB	13.25	$y$ -0.102	PG 21111+0220	...

Continued on Next Page...

Table A.1 – Continued

No.	ID <sup>1</sup>	Coordinates <sup>2</sup> (J2000)	Chart Source <sup>3</sup>	Type	$V / y^4$	$B - V^4$	KHD ID <sup>5</sup>	Notes <sup>6</sup>
1299BPS	CS 29501–54	21 16 02.572–37 14 16.87	CS	sdB	13.8 B	...	CSHK 29501–54	...
1300BPS	CS 30492–125	21 17 12.385–41 22 11.46	CS	sdB	14.4 B	...	CSHK 30492–125	...
1301BPS	CS 29506–15	21 18 06.649–18 37 05.23	CS	sdB	14.1 B	...	CSHK 29506–15	...
1302PG	2115+145	21 18 03.273+14 40 54.09	PG	sdB	15.16 P	...	PG 21156+1428	...
1303BPS	CS 22937–84	21 19 29.521–40 31 07.07	CS	sdB	14.80	–0.07	CSHK 22937–84	...
1304PG	2116+008	21 19 21.398+00 57 50.94	PG	sdO(B)	15.41 P	...	PG 21168+0045	...
1305BPS	CS 22937–82	21 21 39.420–40 13 35.98	CS	sdB	14.6 B	...	CSHK 22937–82	...
1306PG	2118+126	21 21 02.283+12 50 49.88	PG	sdB	13.579	+0.148	PG 21186+1238	AEA
1307KPD	2118+3841	21 20 42.023+38 53 53.18	KPD	sdB	13.87	–0.22	KPD 21187+3841	...
1308PG	2120+062	21 22 31.718+06 21 56.12	PG	sd	14.40 y	–0.105	PG 21200+0609	...
1309BPS	CS 29506–31	21 23 56.138–19 00 53.73	CS	sdB	15.2 B	...	CSHK 29506–31	...
1310PG	2122+081	21 25 25.469+08 19 12.27 U	PG	sdB	16.06 P	...	PG 21229+0806	...
1311PHL	4	21 26 21.07 +01 00 01.85 D	...	sdOB	14.34 y	–0.335	...	...
1312PG	2124+071	21 26 58.491+07 20 44.67	PG	sd	14.23 y	+0.080	PG 21245+0707	...
1313BPS	CS 29506–51	21 27 43.123–22 11 48.76	CS	sdB	14.5 B	...	CSHK 29506–51	...
1314PG	2125+098	21 27 47.114+10 00 50.15 U	PG	sdB	16.13 P	...	PG 21253+0947	...
1315PHL	17	21 30 35.98 –03 02 46.72 D	...	sdOB	13.97 y	–0.076	...	...
1316PG	2128+096	21 30 42.507+09 50 20.90	PG	sdO(A)	14.74 y	–0.204	PG 21282+0936	...
1317PG	2128+089	21 31 05.169+09 07 53.26	PG	sdO(A)	16.27 P	...	PG 21286+0854	...
1318PG	2128+112	21 31 12.268+11 29 36.77 U	PG	sdB	15.73 P	...	...	...
1319PG	2128+146	21 31 18.796+14 49 23.05	PG	sd	13.21 y	–0.107	PG 21289+1436	...
1320PHL	25	21 31 55.923–17 19 31.41	Heber <sup>d</sup>	sdB	12.17 y	–0.226	...	<i>i</i>
1321PG	2129+151	21 31 40.843+15 16 49.62	PG	sdO(B)	14.23 y	–0.189	PG 21293+1503	...
1322BPS	CS 29495–21	21 32 55.465–23 59 22.17	CS	sdB	13.5 B	...	CSHK 29495–21	<i>d</i>
1323PG	2130+067	21 32 49.834+06 57 57.02	PG	sd	15.97 P	...	PG 21303+0644	...
1324JL	82	21 36 01.287–72 48 27.23	JL	sdB	12.39 y	–0.217	...	...
1325PG	2131+164	21 34 02.630+16 34 24.43	PG	sdB	14.98 P	...	PG 21316+1621	...
1326PG	2132+095	21 34 34.425+09 40 49.01	PG	sdB	15.34 P	...	PG 21321+0927	...
1327PG	2132+126	21 34 55.715+12 49 22.04	PG	sd	14.907 y	–0.036	PG 21325+1235	MEA
1328PHL	44	21 35 13.39 –13 32 34.69 D	...	sdB	13.24 y	–0.215	...	...
1329Balloon	092200002	21 37 18.41 +13 27 31.11 D	...	sdB+ K3	10.43 y	...	BBL092200002	...
1330PG	2135+045	21 38 00.829+04 42 11.69	PG	sdB	14.657	–0.073	PG 21355+0428	AEA
1331BPS	CS 22948–17	21 38 44.200–37 36 15.03	CS	sdB	13.4 B	...	CSHK 22948–17	...
1332HD	205805	21 39 10.609–46 05 51.50	HIP	sdB	10.21 y	–0.235	...	...
1333PG	2138+049	21 41 05.006+05 13 37.32	PG	sdB	14.546	–0.080	PG 21384+0457	AEA

Continued on Next Page...

Table A.1 – Continued

No.	ID <sup>1</sup>	Coordinates <sup>2</sup> (J2000)	Chart Source <sup>3</sup>	Type	$V / y^4$	$B - V^4$	KHD ID <sup>5</sup>	Notes <sup>6</sup>
1334BPS	CS 22897–112	21 43 19.979–65 49 51.71	CS	sdB	14.8	B ...	CSHK 22897–112	...
1335BPS	CS 22956–6	21 43 19.785–65 49 51.55	U CS	sdB	14.8	B ...	CSHK 22956–6	$B_{pg}$ from USNO <sup>f</sup>
1336PHL	117	21 43 58.923–23 29 12.99	CS	sdOB	13.84	$y$ –0.247	...	$d, \#1337$
1338BPS	CS 22951–31	21 44 54.115–42 50 48.01	CS	sdB	13.7	B ...	(CSHK 29495–21 #2)	(BPS CS 29495–63)
1339BPS	CS 22956–32	21 45 35.664–62 37 39.07	CS	sdB	14.7	B ...	CSHK 22951–31	...
1340BPS	CS 22951–62	21 50 42.772–43 40 28.43	CS	sdB	14.0	B ...	CSHK 22956–32	...
1341JL	87	21 48 37.731–76 20 44.55	JL	sdB pec	12.00	–0.10	CSHK 22951–62	...
1342KPD	2145+4216	21 47 24.258+42 31 34.27	KPD	sdO	15.33	–0.01	KPD 21453+4216	...
1343BPS	CS 22944–66	21 47 52.463–12 35 44.22	CS	He-sdO	14.4	B ...	CSHK 22944–66	...
1344PG	2146+087	21 49 04.797+08 55 20.70	PG	sdB	14.257	–0.036	PG 21464+0839	MEA
1345PHL	178	21 51 11.68–21 05 55.18	D ...	sdO He	13.09	$y$ –0.284	...	AEA
1346PG	2148+095	21 51 16.884+09 46 59.61	PG	sdB	13.021	–0.024	PG 21486+0930	AEA
1347BD	+28° 4211	21 51 11.024+28 51 50.41	HIP	sdO7p	10.53	–0.34	...	em <sup>f</sup>
1348PG	2151+100	21 53 57.307+10 17 34.95	PG	sd	12.75	$y$ –0.173	PG 21513+1001	W* <sup>f</sup> (close)
1349PHL	197	21 54 13.63–06 12 47.93	D ...	sdB	13.56	$y$ –0.255	...	...
1350PG	2151+089	21 54 18.645+09 11 42.90	PG	sd	16.31	P ...	PG 21517+0855	...
1351BPS	CS 22881–7	21 58 01.960–41 28 49.74	CS	sdB	15.21	–0.31	CSHK 22881–7	...
1352PG	2155+175	21 57 49.116+17 42 51.76	PG	sd	16.00	P ...	PG 21555+1728	...
1353PB	7032	21 58 04.754–04 40 39.43	PB	sdBpe	13.22	$y$ –0.201	...	...
1354BD	+25° 4655	21 59 41.975+26 25 57.39	HIP	sdO	9.69	–0.26	...	...
1355BD	–3° 5357	22 00 36.422–02 44 26.85	HIP	sdOB+	9.31	+0.86	...	e.bin
1356PG	2158+082	22 01 02.278+08 30 47.80	PG	G8III	12.66	P ...	PG 21584+0814	...
1357PG	2159+051	22 01 58.631+05 24 28.28	PG	sdO He	12.98	$y$ –0.081	PG 21593+0507	...
1358BPS	CS 22881–31	22 02 28.559–41 14 32.05	CS	sdB	15.81	–0.35	CSHK 22881–31	...
1359PG	2201+145	22 04 03.791+14 46 38.55	U PG	sdO(B)	15.30	P ...	PG 22016+1432	...
1360PG	2201+059	22 04 16.111+06 16 20.17	PG	sd	15.57	P ...	PG 22016+0559	...
1361PG	2204+034	22 07 16.501+03 42 19.77	PG	sdB	14.29	–0.23	PG 22047+0327	...
1362PG	2204+127	22 07 11.101+12 57 55.98	PG	sdO(B)	15.76	P ...	PG 22047+1243	...
1363BPS	CS 22960–18	22 08 25.034–43 12 01.60	CS	sdB	13.5	B ...	CSHK 22960–18	...
1364PG	2205+023	22 08 00.631+02 33 43.53	PG	sdB	14.136	–0.210	PG 22054+0219	AEA
1365PB	5096	22 10 45.455+01 41 35.50	PG	sdB	15.75	–0.12	...	...
1366PG	2208+056	22 10 46.459+05 50 14.53	PG	sdO	15.78	P ...	PG 22082+0535	...

Continued on Next Page...

Table A.1 – Continued

No.	ID <sup>1</sup>	Coordinates <sup>2</sup> (J2000)	Chart Source <sup>3</sup>	Type	$V / y^4$	$B - V^4$	KHD ID <sup>5</sup>	Notes <sup>6</sup>
1367BPS CS 22956–90	22 14 57.536–63 41 45.36	CS	He-sdB	13.9 B	...	...	CSHK 22956–90	...
1368PB 5110	22 14 37.875+02 57 17.48	PG	sdB-O	15.606	–0.062	...	...	MEA
1369PG 2212+173	22 15 23.794+17 31 32.18	PG	sdB	15.13 P	...	...	PG 22129+1716	...
1370BPS CS 22956–94	22 16 56.029–64 31 50.16	CS	He-sdB	12.5 B	...	...	CSHK 22956–94	...
1371BPS CS 22892–51	22 16 04.479–17 19 47.34	CS	sdO He	14.66	–0.36	...	CSHK 22892–51	...
1373BPS CS 22886–32	22 16 27.136–11 30 36.19	CS	sdB	13.79	–0.14	...	CSHK 22886–32	#1372
							(CSHK 29512–44)	(BPS CS 29512–44)
1374PB 5121	22 16 28.375–00 21 13.55	PG	sdO(B)	14.115	–0.221	...	...	AEA
1375BPS CS 29512–38	22 16 41.238–12 48 22.70	CS	sdB	15.5 B	...	...	CSHK 29512–38	...
1376PG 2214+184	22 17 04.581+18 37 53.59	PG	sd	14.24 y	–0.081	...	PG 22146+1822	...
1377PG 2215+120	22 17 28.377+12 16 43.84	U PG	sdB	15.88 P	...	...	PG 22150+1201	...
1378PG 2215+151	22 17 48.222+15 20 57.42	PG	sdO He	14.548	–0.254	...	PG 22153+1505	WMG
1379KPD 2215+5037	22 17 20.736+50 52 59.00	KPD	sdB	13.664	–0.093	...	KPD 22154+5037	AEA
1380BPS CS 22875–2	22 19 01.787–41 23 31.63	CS	sdO He	13.89	–0.33	...	CSHK 22875–2	...
1381BPS CS 29512–55	22 19 58.381–08 38 19.89	CS	sdB	14.7 B	...	...	CSHK 29512–55	...
1382PG 2217+059	22 20 28.117+06 07 23.07	U PG	sdO(B)	16.20 P	...	...	PG 22179+0552	...
1383PG 2218+051	22 21 22.563+05 24 58.45	PG	sdO(A)	15.30 P	...	...	PG 22188+0509	...
1384PHL 232	22 21 24.825+02 16 18.50	PG	sdB-O	14.171	–0.155	...	...	AEA
1385BPS CS 22960–63	22 22 08.749–42 23 41.82	U Beers	sdB	16.1 B	...	...	CSHK 22960–63	$B_{pg}$ from USNO <sup>f</sup>
1386PG 2219+093	22 21 59.166+09 37 25.70	PG	B	11.919	–0.134	...	PG 22195+0922	WMG
1387BPS CS 22960–71	22 22 41.156–43 51 08.82	CS	sdB	15.1 B	...	...	CSHK 22960–71	...
1388PHL 240	22 22 38.689+00 51 25.57	U PG	sdB	15.70 P	...	...	...	...
1389KPD 2220+5126	22 22 59.089+51 41 21.81	U KPD	sdB	15.14	–0.17	...	KPD 22209+5126	...
1390PG 2223+143	22 35 31.546+14 33 58.05	PG	sdB	14.08 y	–0.214	...	PG 22230+1418	...
1391BPS CS 22886–65	22 25 52.307–09 59 56.47	U CS	sdB	15.6 B	...	...	CSHK 22886–65	$B_{pg}$ from USNO <sup>f</sup>
1392PG 2223+171	22 25 54.404+17 23 10.65	PG	sdB-O	14.76 P	...	...	PG 22234+1707	...
1393PG 2226+094	22 28 58.467+09 37 22.58	PGWD	sdB	14.065	+0.060	...	PG 22264+0921	AEA
1394PG 2228+120	22 31 03.629+12 17 08.71	PG	sdB	15.26 P	...	...	PG 22285+1201	...
1395LBQS 2228–0017	22 31 20.964–00 02 13.62	U LBQS	sdO	18.0 J	...	...	...	...
1396PG 2229+099	22 32 08.725+10 14 25.18	PG	non-sd	13.270	–0.080	...	PG 22296+0958	...
1397KPD 2230+4937	22 32 26.491+49 53 22.15	KPD	sdB	15.710	–0.070	...	KPD 22303+4937	...
1398LBQS 2230+0125	22 32 57.117+01 41 14.74	LBQS	sdB	18.1 J	...	...	...	...
1399PG 2230+120	22 33 14.906+12 19 33.83	PG	sdB	16.24 P	...	...	PG 22307+1204	...
1400LBQS 2232+0005	22 34 37.989+00 21 12.15	U LBQS	sdB	18.0 J	...	...	...	...
1401PHL 334	22 36 16.633–31 42 13.06	TONS	sdB	13.17 y	–0.288	...	...	...

Continued on Next Page...



Table A.1 – Continued

No.	ID <sup>1</sup>	Coordinates <sup>2</sup> (J2000)	Chart <sup>3</sup> Source	Type	$V / y^4$	$B - V^4$	KHD ID <sup>5</sup>	Notes <sup>6</sup>
1402	PG 2234+160	22 36 32.623 +16 16 01.40	PG	sdB	15.22	P	PG 22340+1600	...
1403	JL 111	22 38 22.592 -76 52 43.01	JL	sdB	14.13		...	...
1404	PG 2235+082	22 37 35.443 +08 28 48.49	PGWD	sd	15.42	y	PG 22350+0813	...
1405	LBQS 2236-0201	22 39 10.338 -01 45 35.97	U LBQS	sdBp	16.7	J	...	...
1406	PG 2236+122	22 39 06.117 +12 30 35.13	PG	sdO(A)	16.24	P	PG 22366+1214	...
1407	PG 2236+134	22 39 13.455 +13 38 10.63	PG	sdB	14.99	y	PG 22367+1322	...
1408	KPD 2237+4924	22 39 36.131 +49 40 36.45	U KPD	sdB	14.92		KPD 22375+4924	...
1409	PHL 367	22 40 14.234 +02 06 31.29	PG	sd	15.50	P	...	...
1410	PG 2239+043	22 38 33.387 +04 51 25.22	PG	sdB	15.81	P	PG 22396+0419	...
1411	LBQS 2240-0259	22 42 49.935 -02 43 55.75	U LBQS	sdB	17.8	J	...	...
1412	PHL 382	22 43 06.018 -14 50 37.37	plaus <sup>e</sup>	sdB	11.35	y	...	...
1413	PG 2240+105	22 43 29.238 +10 46 53.54	PG	sdB	15.03		PG 22409+1030	...
1414	LBQS 2242+0050	22 44 51.803 +01 06 31.53	U LBQS	sdBp	18.2	J	...	...
1415	LBQS 2243-0114	22 46 26.442 -00 59 08.35	U LBQS	sdOB	18.2	J	...	...
1416	PG 2244+152	22 46 55.192 +15 30 59.90	PG	sdO	15.44	P	PG 22444+1515	...
1417	GS 259-8	22 47 59.48 +37 53 51.63	D ...	sdO	12.50	P?	...	...
1418	PG 2246+103	22 48 50.268 +10 32 43.39	PG	sdO	14.83	P	PG 22463+1016	...
1419	LBQS 2246+0101	22 49 01.549 +01 17 23.24	U LBQS	sdOB	18.5	J	...	...
1420	PG 2246+019	22 49 27.064 +02 14 32.36	PGWD	sdB-O	15.84	y	PG 22468+0158	...
1421	HD 216135	22 50 28.224 -13 18 44.32	Feige	sdB	10.1		...	...
1422	BPS CS 22938-44	22 52 19.719 -63 15 54.87	CS	sdB He	15.2	B	CSHK 22938-44	...
1423	LB 1153	22 52 18.396 +22 18 05.13	U PG	sdO	15.72	P	...	...
1424	Balloon 090900007	22 53 18.413 +21 53 54.41	ML	sdB+G2	13.30	y	BBL090900007	...
1425	JL 117	22 54 38.016 -72 23 09.71	JL	sdO	14.39		...	...
1426	PG 2251+080	22 54 23.357 +08 17 56.23	PG	sdB	15.65	P	PG 22518+0801	...
1427	PB 7352	22 55 43.186 -06 59 39.81	PB	sd/hb	12.31	y	...	...
1428	KPD 2253+4922	22 55 45.837 +49 38 16.73	KPD	sdB	15.56		KPD 22535+4922	...
1429	PG 2254+067	22 56 38.347 +06 56 51.21	PGWD	sdB	15.18	P	PG 22541+0640	...
1430	KPD 2254+5444	22 57 02.651 +55 00 13.40	KPD	sdB	14.377		KPD 22549+5444	AEA
1431	PG 2255+266	22 57 46.083 +26 57 00.74	U PG	sdO(A)	15.90	P	PG 22554+2638	...
1432	PB 7409	22 58 20.918 -07 54 04.31	PB	sdB	14.00	y	...	...
1433	BPS CS 22938-33	23 00 55.845 -65 45 35.43	CS	sdB	15.3	B	CSHK 22938-33	...
1434	KPD 2257+4928	22 59 59.468 +49 45 09.46	KPD	sdB	15.02		KPD 22577+4928	...
1435	KUV 22585+1533	23 00 57.755 +15 48 40.68	PG	sdO He	15.03	P	...	...
1436	JL 119	23 02 36.390 -71 13 00.63	JL	sdOB	13.48		...	...
1437	LB 1516	23 02 04.82 -47 59 51.17	D ...	sdB	12.97		...	...

Continued on Next Page...

Table A.1 – Continued

No.	ID <sup>1</sup>	Coordinates <sup>2</sup> (J2000)	Chart Source <sup>3</sup>	Type	$V / y^4$	$B - V^4$	KHD ID <sup>5</sup>	Notes <sup>6</sup>
1438 KUV	22593+1322	23 01 45.829 +13 38 37.42	PG	sdB	14.55 $y$	-0.165	...	...
1439 KPD	2259+5149	23 02 00.339 +52 05 21.90	KPD	sdO	13.85	-0.03	KPD 22597+5149	...
1440 PG	2300+158	23 03 21.015 +16 04 42.11	U PG	sdB	15.88 P	...	PG 23008+1548	...
1441 BPS	CS 30493-9	23 04 01.329 -35 47 17.32	CS	sdB	15.0 B	...	CSHK 30493-9	...
1442 BPS	CS 22893-38	23 04 07.532 -08 56 27.41	CS	sdB	16.18	-0.10	CSHK 22893-38	...
1443 PG	2301+259	23 04 17.233 +26 12 02.62	PG	non-sd	13.22 $y$	-0.093	PG 23017+2555	...
1444 PG	2303+115	23 05 38.995 +11 45 36.74	PGWD	sdB	14.42 $y$	-0.16	PG 23031+1129	...
1445 PHL	401	23 06 22.345 +02 09 05.88	PG	sdB	16.05 P	...	...	...
1446 PHL	402	23 06 38.180 +01 35 10.08	RFG	sdO	16.00	-0.44	...	...
1447 PG	2304+193	23 07 14.577 +19 32 19.64	U PG	sdO(C)	15.58 P	...	PG 23047+1916	...
1448 BPS	CS 22893-20	23 08 30.349 -11 38 47.28	CS	sdB He	15.1 B	...	CSHK 22893-20	...
1449 PHL	408	23 08 55.468 +02 54 27.06	U PG	sdB	16.15 P	...	...	...
1450 BPS	CS 22888-17	23 10 11.143 -32 42 04.16	CS	sdB	14.3 B	...	CSHK 22888-17 (CSHK 30493-27) CSHK 22938-73	#1451 (BPS CS 30493-27)
1452 BPS	CS 22938-73	23 10 53.809 -63 03 25.25	CS	sdO He	14.1 B	...	...	...
1453 KUV	23089+0942	23 11 23.768 +09 58 45.06	KUV	sdO	15.40 P	...	...	...
1454 Feige	108	23 16 12.418 -01 50 35.05	Feige	sdB	12.942	-0.235	...	AEA
1455 Feige	109	23 17 26.878 +07 52 04.94	Feige	sdB	13.747	-0.175	...	AEA
1456 PHL	443	23 17 35.515 -09 02 19.62	GD1107	sdO He	14.10 $y$	-0.265	...	...
1457 BD	-7°5977	23 17 46.784 -06 28 31.05	TYC	sdOB	10.52 $y$	+0.592	...	...
1458 PB	5324	23 18 19.024 +09 11 48.48	PGWD	sdB	14.485	-0.265	...	AEA
1459 PHL	457	23 19 24.428 -08 52 37.91	GD	sdB	12.95 $y$	-0.256	...	...
1460 PHL	460	23 19 36.622 -22 19 03.88	CS <sup>f</sup>	sdB	12.24 $y$	-0.153	...	...
1461 PB	5333	23 19 55.346 +04 52 34.52	PG	sdOB	12.856	-0.256	...	AEA, SE* <sup>f</sup> , em <sup>f</sup>
1462 Feige	110	23 19 58.405 -05 09 56.19	Feige	sdO	12.5	-0.32	...	...
1463 BPS	CS 22949-25	23 20 55.277 -05 51 22.92	Beers	sdB	15.22	...	CSHK 22949-25	...
1464 PG	2318+239	23 21 05.800 +24 10 39.01	PG	sd	13.66 $y$	-0.138	K/P 23186+2354	...
1465 KPD	2319+5014	23 21 18.826 +50 31 37.49	KPD	sdB	14.70	-0.13	KPD 23190+5014	...
1466 Balloon	083738002	23 21 46.35 +25 16 27.43	D ...	sdB+ K3	13.3 $y$	...	BBL083738002	...
1467 PB	5358	23 23 13.881 +08 56 42.68	PG	sdOB	14.61	+0.14	...	...
1468 LB	1181	23 23 50.817 +14 31 08.60	RFG	sdB	14.66 $y$	-0.22	...	...
1469 Balloon	093100003	23 24 03.63 +00 39 29.07	D ...	bin?	15.7 $y$	...	BBL093100003	...
1470 PG	2321+214	23 24 27.461 +21 38 51.25	PG	sdO(D)	12.89 P	...	PG 23219+2122	...
1471 KPD	2322+4933	23 24 32.730 +49 50 55.11	KPD	sdO	13.70	-0.15	KPD 23221+4933	...
1472 PG	2323+121	23 25 59.015 +12 21 24.01	PGWD	sdB	14.96 P	...	PG 23234+1204	...

Continued on Next Page...

Table A.1 – Continued

No.	ID <sup>1</sup>	Coordinates <sup>2</sup> (J2000)	Chart <sup>3</sup> Source	Type	$V / y^4$	$B - V^4$	KHD ID <sup>5</sup>	Notes <sup>6</sup>
1473PB 5376		23 26 06.584 +05 16 15.58	PG	sdB	14.67 P	...	...	...
1474BPS CS 22949–42		23 27 08.809 –04 24 36.60	Beers	sdB	13.86	...	CSHK 22949–42	...
1475PHL 540		23 29 09.854 –10 06 06.04	GD1309	sdO	13.38 y	–0.298	...	...
1476PG 2326+297		23 29 14.707 +29 56 50.01	PG	sd	14.87 P	...	PG 23267+2940	...
1477KPD 2326+5102		23 29 14.376 +51 18 57.47 U	KPD	sdO	14.68	+0.01	KPD 23268+5102	...
1478BPS CS 22945–23		23 30 43.338 –65 40 52.97	CS	sdB	15.4 B	...	CSHK 22945–23	...
1479BPS CS 29496–9		23 31 49.941 –28 52 52.98	CS	sdB	13.8 B	...	CSHK 29496–9	...
1480PG 2329+232		23 32 10.565 +23 30 40.29	PG	sdB	14.88 P	...	PG 23296+2313	...
1481PB 5443		23 33 44.472 +05 46 39.87	PG	sd	15.182	–0.066	...	LAN
1482TON S 103		23 34 01.957 –28 51 38.07	TONS,CS	sdOp	14.7	–0.23	...	#1483
							(CSHK 29496–10)	(BPS CS 29496–10)
1484PB 5446		23 33 58.193 +04 03 55.43	PG	sdB	14.942	–0.144	...	AEA
1485PB 5447		23 34 08.171 +07 46 48.63	PG	sdB	15.74 P	...	...	...
1486PB 5450		23 34 34.625 –01 19 37.03	PB	sdB	13.06 y	–0.211	...	...
1487BPS CS 22894–18		23 35 41.473 +00 02 19.01	CS	sdO He	15.5 B	...	CSHK 22894–18	...
1488PG 2335+107		23 37 43.788 +10 56 27.00	PGWD	sdB	15.55 y	–0.19	PG 23351+1039	...
1489PG 2335+133		23 37 51.357 +13 35 48.26	PG	sdB	16.00 P	...	PG 23352+1318	...
1490PG 2336+264		23 38 43.329 +26 40 00.49	PG	sd	14.63 P	...	PG 23362+2623	...
1491PG 2337+266		23 39 49.848 +26 51 02.19	PG	sdB	16.10 P	...	PG 23373+2634	...
1492PB 5495		23 40 04.753 +07 17 09.63	PGWD	sdB	13.47 y	–0.10	...	...
1493PG 2337+300		23 40 04.289 +30 17 47.47	PG	sd	13.91 y	+0.016	PG 23375+3001	em <sup>f</sup>
1494BPS CS 29496–17		23 40 15.365 –29 27 59.76	CS	sdB	14.0 B	...	CSHK 29496–17	...
1495PG 2339+199		23 41 56.741 +20 12 22.20	PG	sdB He	15.78 P	...	PG 23394+1955	...
1496PG 2341+184		23 44 08.451 +18 42 50.34	PG	sdB	15.89 P	...	PG 23416+1826	...
1497CD –35 15910		23 44 22.009 –34 27 00.33	HIP	sdB	10.96 y	–0.264	CD –3515910	...
1498PG 2343+267		23 45 51.403 +27 01 34.97 U	PG	sdO(C)	16.29 P	...	PG 23433+2644	...
1499BPS CS 29496–27		23 46 17.771 –29 27 50.16	CS	sdB	14.5 B	...	CSHK 29496–27	...
1500PG 2345+318		23 48 07.505 +32 04 47.99	PG	sdB	14.160	–0.193	PG 23455+3148	AEA
1501PG 2345+241		23 48 22.294 +24 23 06.65	PG	non-sd	12.430	–0.153	PG 23458+2406	AEA
1502PG 2346+149		23 48 53.558 +15 12 15.21	PG	sdB	15.69 P	...	PG 23463+1455	...
1503PG 2348+269		23 50 49.428 +27 08 00.25	PG	sdB	15.54 P	...	PG 23482+2651	...
1504PB 5562		23 51 53.236 +00 28 17.64	PGWD	sdB	13.262	–0.210	...	AEA
1505KPD 2349+5009		23 52 07.553 +50 26 46.16	KPD	sdO	15.30 P	...	KPD 23496+5009	...
1506LBQS 2349–0058		23 52 15.539 –00 41 18.05 U	LBQS	sdO	18.1 J	...	...	...
1507CD –30 19716		23 52 36.099 –30 10 09.37	HIP	sdO	12.09 y	–0.284	CD –3019716	...

Continued on Next Page...

Table A.1 – Continued

No.	ID <sup>1</sup>	Coordinates <sup>2</sup> (J2000)	Chart Source <sup>3</sup>	Type	$V / y^4$	$B - V^4$	KHD ID <sup>5</sup>	Notes <sup>6</sup>
1508 PG	2350+099	23 53 02.315 +10 11 21.51	U PG	sd	15.96	-0.09	PG 23505+0954	...
1509 BPS	CS 29517-17	23 53 12.357 -17 08 59.86	CS	sdB	14.0	B	CSHK 29517-17	...
1510 BPS	CS 29517-35	23 59 56.335 -16 09 15.49	CS	sdB	13.4	B	CSHK 29517-35	...
1511 BPS	CS 22876-2	23 53 36.375 -36 30 19.18	CS	sdB	14.8	B	CSHK 22876-2	...
1512 PG	2352+180	23 55 17.334 +18 20 15.28	PG	sdO He	13.359	-0.281	PG 23527+1803	WMG
1513 PG	2352+259	23 55 32.903 +26 12 01.19	PG	sdB	14.99	P	PG 23529+2555	...
1514 BPS	CS 22957-10	23 57 01.306 -02 50 27.74	CS	He-sdO	14.5	B	CSHK 22957-10	...
1515 PG	2354+298	23 57 16.709 +30 04 14.14	PG	sd	15.33	P	PG 23547+2947	...
1516 PG	2355+242	23 57 45.423 +24 26 22.91	U PG	sdO(B)	15.74	P	PG 23552+2409	...
1517 PG	2355+082	23 58 10.097 +08 31 28.38	PG	sd	15.45	P	PG 23555+0814	...
1518 LBQS	2356-0224	23 58 41.42 -02 08 08.91	O LBQS <sup>g</sup>	sdOB	18.7	J	...	...
1519 CD	-27 16503	23 59 07.149 -26 38 39.92	SB	sdO?	13.49	y	CD -2716503	...
1520 SB	933	23 59 09.860 -40 33 19.82	SB	sdO	14.24	y	...	...
1521 PG	2356+167	23 59 25.318 +16 56 41.70	PG	sdB-O	14.21	y	PG 23568+1640	...
1522 PG	2357+174	00 00 15.749 +17 38 53.13	U PG	sdB	16.14	P	PG 23577+1722	...
1523 LBQS	2357-0023	00 00 22.837 -00 06 35.75	U LBQS	sdB	18.4	J	...	...
1524 PG	2358+107	00 01 06.728 +11 00 36.30	PGWD	sdB	13.62	y	PG 23585+1043	...
1525 BPS	CS 22957-23	00 01 32.239 -05 19 17.82	CS	sdB	13.7	B	CSHK 22957-23	...
1526 BPS	CS 22876-28	00 01 37.624 -35 39 53.35	CS	sdB	14.3	B	CSHK 22876-28	...
1527 PG	2359+197	00 02 08.473 +19 59 13.24	PG	sd	15.44	P	PG 23595+1942	...

## Appendix B

### 2MASS All-Sky Data Release Photometry

Table B.1 contains a listing of all hot subdwarfs from the KHD<sup>1</sup> catalog (ordered by KHD sequence number) that were found in the 2MASS All-Sky Data Release. Table notes are as follows:

1. The sequence numbers in the first column are assigned by us, they are not intended to be used as a new designator in the literature, but are useful in navigating the KHD catalog and cross-referencing this table with Table A.1.
2. The identifiers listed in the first column are consistent with SIMBAD nomenclature.
3. P, B, J = photographic magnitude is listed;  $y$  = Strömgren  $y$  magnitude given instead of Johnson  $V$ , and the value of  $B-V$  listed was converted from Strömgren photometry; v = magnitude variable; colon (:) = magnitude or color is uncertain.
4. The reported 2MASS errors are  $1\sigma$ . If no error is listed, then the star was not detected in that band and the quoted magnitude is a 95% confidence upper limit.
5. The parameter  $Q$  is defined as:  $Q = 0.752(J-H) + (J-K_S)$  (See §3.6.2 on page 28, and Appendix G on page 262).
6.  $a$  = #87, Heber et al. (2002) report that this pair is resolved into three components with HST: the sdO is the NW star of the “pair,” while the SE “companion” star resolves into two components separated from the sdO by  $3''.37$  and  $4''.48$ ;  
 $b$  = #284, variable double M (KHD);  
 $c$  = #293, Ulla et al. (2001) report two close companions (“B” located  $\leq 2''.4$  E, and “C” located  $\sim 3''.5$  NW);  
 $d$  = #1337 and 1322 were listed with the same name (CSHK 29495–21) by KHD when in fact they are two different objects: #1322 is named correctly, while #1337 is not — #1337 should read CSHK 29495–63 in KHD;  
 $e$  = #1273 is listed as a Seyfert 1 galaxy in SIMBAD;  
 $f$  = our note, not from KHD (“CSPN” = central star of a planetary nebula, “elon?” = images of the object look slightly elongated, “em” = emission, “Gal” = images show a galaxy, “hpm” = high proper motion, “neb in field” = nebula emission in the field of the subdwarf, “PN” = object is a planetary nebula, “Sey” = object is actually a Seyfert 1 AGN);  
 COM = previously reported composite;

---

<sup>1</sup>Kilkenny, Heber, & Drilling (1988) as updated and expanded in an electronic version by Kilkenny, c. 1992, kindly made available by D. Kilkenny.

SGL = previously reported single;

AEA =  $V$  and  $B-V$  from Allard et al. (1994);

LAN =  $V$  and  $B-V$  from Landolt (1992);

MEA = #1327, Strömgren *uvby* from Mooney et al. (2000);

TYC =  $V$  and  $B-V$  for #234 and #1223 are converted from Tycho magnitudes:  $V_T = 10.194$ ,  $(B_T - V_T) = +0.111$  and  $V_T = 8.455$ ,  $(B_T - V_T) = +1.271$  respectively (ESA 1997);

WMG =  $V$  and  $B-V$  from Williams et al. (2001).

Table B.1: Visual and 2MASS Photometry for All Subwarfs.

No. <sup>1</sup>	ID <sup>2</sup>	Type	$V / y^3$	$B - V^3$	$J^4$	$H^4$	$K_S^4$	$J - K_S$	$J - H$	$Q^5$	Notes <sup>6</sup>							
			mag	$\sigma$	mag	$\sigma$	mag	$\sigma$	mag	$\sigma$								
1 SB 7		sdB	12.67	y	-0.161	12.688	0.043	12.619	0.053	12.596	0.038	+0.092	0.057	+0.069	0.068	+0.144	0.077	COM
2 TON S 135		sdB	13.302		-0.235	13.868	0.042	14.017	0.066	14.061	0.059	-0.193	0.072	-0.149	0.078	-0.305	0.093	AEA
6 TON S 137		sdO	13.87	y	-0.273	14.535	0.045	14.731	0.069	14.759	0.116	-0.224	0.124	-0.196	0.082	-0.371	0.138	...
8 BPCS 22876-35		sdB	15.4	B	...	14.777	0.055	14.540	0.066	14.367	0.083	+0.410	0.100	+0.237	0.086	+0.588	0.119	...
10 TON S 140		sdOB	13.97	y	-0.253	14.538	0.049	14.675	0.065	14.842	0.107	-0.304	0.118	-0.137	0.081	-0.407	0.133	...
12 PHL 678		sdB	13.032		-0.076	13.288	0.033	13.326	0.040	13.384	0.044	-0.096	0.055	-0.038	0.052	-0.125	0.067	SGL, AEA
14 PHL 687		sdB	14.390		-0.291	15.033	0.052	15.095	0.106	15.321	0.156	-0.288	0.164	-0.062	0.118	-0.335	0.186	AEA
16 PG 0006+120		sdB	14.69	y	-0.127	15.022	0.055	15.198	0.140	15.193	0.159	-0.171	0.168	-0.176	0.150	-0.303	0.202	...
19 TON S 144		sdO	12.8		-0.15	12.818	0.040	12.566	0.048	12.545	0.036	+0.273	0.054	+0.252	0.062	+0.463	0.071	...
18 PB 5775		sd	15.63	P	...	16.678	0.154	16.745	...	17.391	...	...	...	...	...	...	...	...
20 JL 163		sdB;	12.88		-0.17	13.581	0.039	13.761	0.051	13.828	0.056	-0.247	0.068	-0.180	0.064	-0.382	0.083	...
21 PHL 717		sdB	14.51	y	-0.209	14.746	0.041	14.505	0.065	14.356	0.072	+0.390	0.083	+0.241	0.077	+0.571	0.101	...
22 PHL 2726		B	13.16	y	-0.125	13.355	0.039	13.431	0.048	13.474	0.046	-0.119	0.060	-0.076	0.062	-0.176	0.076	SGL
23 JL 166		sdOB	15.23		-0.23	15.426	0.098	15.348	0.080	14.964	0.119	+0.462	0.154	+0.078	0.127	+0.521	0.181	...
25 BPCS 30339-8		sdB	14.7	B	...	15.151	0.064	15.425	0.146	14.992	...	...	...	-0.274	0.159	...	...	...
26 PG 0011+221		sd	13.55	y	-0.229	14.013	0.033	14.194	0.051	14.151	0.080	-0.138	0.087	-0.181	0.061	-0.274	0.098	...
27 PG 0011+283		sd	12.76	y	-0.228	13.161	0.028	13.281	0.035	13.339	0.044	-0.178	0.052	-0.120	0.045	-0.268	0.062	...
28 BPCS 30339-3		sdB	15.2	B	...	15.913	0.085	16.274	0.245	16.275	...	...	...	-0.361	0.259	...	...	...
29 PHL 766		sd	15.55	P	...	16.279	0.104	16.126	0.205	16.170	...	...	...	+0.153	0.230	...	...	...
31 LBQS 0015+0216		sdOB	17.6	J	...	16.980	0.160	16.780	0.248	15.843	...	...	...	+0.200	0.295	...	...	...
33 PG 0016+285		sdB	15.89	P	...	16.406	0.108	16.226	0.182	15.834	0.282	+0.572	0.302	+0.180	0.212	+0.707	0.341	...
35 TON S 154		sdO	14.48	y	-0.356	15.167	0.050	15.580	0.117	15.306	0.142	-0.139	0.151	-0.413	0.127	-0.450	0.179	...
36 PG 0020+240		sdB	15.60	P	...	15.143	0.047	14.766	0.065	14.689	0.114	+0.454	0.123	+0.377	0.080	+0.738	0.137	...
37 PB 5943		sdB	15.62		-0.18	16.151	0.108	15.930	...	16.396	...	...	...	...	...	...	...	...
38 PG 0023+298		sdO(A)	15.44	P	...	14.341	0.037	13.954	0.045	13.838	0.047	+0.503	0.060	+0.387	0.058	+0.794	0.074	CV?
39 PG 0023+299		sdB	15.72	P	...	16.376	0.124	16.231	...	15.425	...	...	...	...	...	...	...	...
40 LB 7736		sdOB	13.98	y	-0.262	14.249	0.039	14.029	0.049	14.085	0.071	+0.164	0.081	+0.220	0.063	+0.329	0.094	...
41 LBQS 0024-0042		sdB	17.6	J	...	16.846	0.147	16.612	0.231	15.803	...	...	...	+0.234	0.274	...	...	...
42 BPCS 30339-49		sdB	15.5	B	...	14.287	0.045	13.996	0.057	13.843	0.053	+0.444	0.070	+0.291	0.073	+0.663	0.089	...
43 PHL 809		sdB	15.64	P	...	15.648	0.072	15.942	0.153	15.725	0.200	-0.077	0.213	-0.294	0.169	-0.298	0.248	...
44 PB 8240		sdB/DA	13.50	P	...	14.590	0.046	14.749	0.076	15.067	0.150	-0.477	0.157	-0.159	0.089	-0.597	0.171	...
46 KPD 0025+5402		sdB	13.89		-0.15	14.259	0.037	14.361	0.056	14.448	0.078	-0.189	0.086	-0.102	0.067	-0.266	0.100	...
48 PB 5984		sd	14.72	P	...	15.588	0.066	15.718	0.114	15.581	0.170	+0.007	0.182	-0.130	0.132	-0.091	0.207	...
50 PG 0027+222		sdB	14.77	P	...	15.611	0.064	15.948	0.146	15.693	0.264	-0.082	0.272	-0.337	0.159	-0.335	0.297	...
51 CD -48 106		sdB	12.36		-0.26	12.991	0.038	13.079	0.040	13.159	0.046	-0.168	0.060	-0.088	0.055	-0.234	0.073	...

Continued on Next Page...

Table B.1 – Continued

No. <sup>1</sup>	ID <sup>2</sup>	Type	$V / y^3$	$B - V^3$	$J^4$	$H^4$	$K_S^4$	$J - K_S$	$J - H$	$Q^5$	Notes <sup>6</sup>
					mag	$\sigma$	mag	$\sigma$	mag	$\sigma$	
53 TON S 163		sdOB	14.22 $y$	-0.266	14.581 0.045	14.624 0.076	14.572 0.111	+0.009 0.120	-0.043 0.088	-0.023 0.137	...
54 PG 0032+247		sdB	14.080	-0.280	14.634 0.038	14.786 0.090	14.927 0.120	-0.293 0.126	-0.152 0.098	-0.407 0.146	SGL, AEA
55 KPD 0033+5229		sdO	16.00	-0.11	16.421 0.125	15.787 ...	15.951 ...	...	...	...	...
56 PG 0033+266		sdB	14.279	-0.231	14.836 0.047	14.922 0.080	14.910 0.105	-0.074 0.115	-0.086 0.093	-0.139 0.135	AEA
57 LB 1566		sdO	13.07	-0.29	13.780 0.042	13.895 0.064	14.104 0.077	-0.324 0.088	-0.115 0.077	-0.410 0.105	...
58 PG 0038+199		sdO(C)	14.544	-0.352	15.279 0.060	15.371 0.102	15.558 ...	...	-0.092 0.118	...	WMG
59 PB 6107		sdB	12.881	-0.038	12.530 0.041	12.335 0.053	12.290 0.039	+0.240 0.057	+0.195 0.067	+0.387 0.076	AEA
60 PG 0039+103		sdB-O	15.16 $y$	-0.20	15.595 0.065	15.721 0.112	17.059 ...	...	-0.126 0.129	...	...
61 PG 0039+134		sdO He	13.683	-0.186	14.171 0.043	14.201 0.055	14.255 0.071	-0.084 0.083	-0.030 0.070	-0.107 0.098	SGL, AEA
62 CD -38 222		sdB	10.48 $y$	-0.284	10.769 0.039	10.732 0.050	10.702 0.037	+0.067 0.054	+0.037 0.063	+0.095 0.072	...
63 PHL 818		sdB	15.69 P	...	16.747 0.156	15.910 ...	15.955 ...	...	...	...	...
64 PG 0042+211		sdO(A)	15.13 P	...	16.753 0.146	16.577 0.261	16.957 ...	...	+0.176 0.299	...	...
65 PB 6148		pec	12.00 P	...	11.232 0.033	11.026 0.041	10.949 0.037	+0.283 0.050	+0.206 0.053	+0.438 0.064	...
66 HD 4539		F+sd?	10.272	-0.240	10.816 0.040	10.939 0.045	11.027 0.035	-0.211 0.053	-0.123 0.060	-0.303 0.070	AEA
69 PG 0046+207		sdB	14.559	-0.221	15.091 0.049	15.153 0.081	15.189 0.191	-0.098 0.197	-0.062 0.095	-0.145 0.210	AEA
70 PHL 860		sdO(B)	15.91 $y$	-0.30	16.555 0.126	16.652 0.258	15.716 ...	...	-0.097 0.287	...	...
71 BD-11° 162		sdO+?	11.23	-0.10	10.868 0.039	10.704 0.041	10.620 0.036	+0.248 0.053	+0.164 0.057	+0.371 0.068	COM
72 PG 0050+222		sd	15.89 P	...	14.833 0.040	14.655 0.053	14.434 0.085	+0.399 0.094	+0.178 0.066	+0.533 0.106	...
73 PG 0050+201		sd	16.18 P	...	16.638 0.131	16.898 ...	17.022 ...	...	...	...	...
75 PB 6208		sd	16.08 P	...	15.863 0.090	15.302 0.104	15.779 0.248	+0.084 0.264	+0.561 0.138	+0.506 0.284	...
76 PG 0053+239		sd	15.85 P	...	15.739 0.069	15.523 0.107	15.596 0.210	+0.143 0.221	+0.216 0.127	+0.305 0.241	...
77 BPCS 22942-17		sdB	15.94	-0.02	16.245 0.106	16.073 0.187	15.974 0.283	+0.271 0.302	+0.172 0.215	+0.400 0.343	...
78 KPD 0054+5406		sdB	14.12	-0.07	14.300 0.048	14.236 0.054	14.394 0.072	-0.094 0.087	+0.064 0.072	-0.046 0.102	...
79 PG 0055+016		sdB-O	15.21 P	...	15.835 0.070	15.955 0.152	16.097 ...	...	-0.120 0.167	...	...
80 SB 395		sdB	12.55 $y$	-0.174	12.827 0.038	12.872 0.036	12.959 0.039	-0.132 0.054	-0.045 0.052	-0.166 0.067	SGL
81 PHL 932		sdB	12.076	-0.273	12.696 0.039	12.818 0.043	12.865 0.042	-0.169 0.057	-0.122 0.058	-0.261 0.072	SGL, AEA
82 TON S 183		sdB	12.65 $y$	-0.252	13.232 0.041	13.361 0.054	13.431 0.051	-0.199 0.065	-0.129 0.068	-0.296 0.083	...
83 BPCS 22942-30		sdB	15.7 B	...	16.065 0.088	15.866 0.141	16.127 ...	...	+0.199 0.166	...	...
84 Feige 11		sdB	12.06	-0.26	12.649 0.039	12.756 0.042	12.884 0.038	-0.235 0.054	-0.107 0.057	-0.315 0.069	...
85 PG 0102+261		sdB-O	14.50 $y$	-0.091	14.582 0.037	14.619 0.070	14.550 0.087	+0.032 0.095	-0.037 0.079	+0.004 0.112	...
86 TON S 191		sdB	13.54 $y$	-0.257	14.274 0.040	14.316 0.055	14.638 0.106	-0.364 0.113	-0.042 0.068	-0.396 0.124	...
87 PG 0105+276		sdO(B)	14.448	-0.087	14.323 0.051	13.837 0.053	13.747 0.055	+0.576 0.075	+0.486 0.074	+0.941 0.093	$a$ , AEA
88 KPD 0106+5227		sdB	15.46	+0.15	15.477 0.062	15.474 0.114	15.115 ...	...	+0.003 0.130	...	...
89 CD -33 417		sdB	12.30 $y$	-0.255	12.813 0.034	13.002 0.041	13.077 0.045	-0.264 0.056	-0.189 0.053	-0.406 0.069	...
90 CD -27 372		sdB	12.59 $y$	-0.138	12.878 0.039	12.927 0.052	13.016 0.045	-0.138 0.060	-0.049 0.065	-0.175 0.077	...

Continued on Next Page...



Table B.1 – Continued

No. <sup>1</sup>	ID <sup>2</sup>	Type	$V / y^3$	$B - V^3$	$J^4$		$H^4$		$K_S^4$		$J - K_S$		$J - H$		$Q^5$		Notes <sup>6</sup>
					mag	$\sigma$	mag	$\sigma$	mag	$\sigma$	mag	$\sigma$	mag	$\sigma$	mag	$\sigma$	
91 PB 8555		sd+F?	13.00 P	...	11.556	0.046	11.268	0.042	11.188	0.041	+0.368	0.062	+0.288	0.062	+0.585	0.078	...
92 PG 0108+195		sd	14.61	-0.27	15.306	0.047	15.499	0.093	15.470	0.177	-0.164	0.183	-0.193	0.104	-0.309	0.199	...
94 TON S 201		sdO	13.17 y	-0.245	13.732	0.038	13.870	0.047	13.901	0.058	-0.169	0.069	-0.138	0.060	-0.273	0.082	...
95 PG 0110+262		sdB-O	12.903	+0.074	12.410	0.033	12.207	0.033	12.215	0.029	+0.195	0.044	+0.203	0.047	+0.348	0.056	COM, AEA
96 PG 0111+177		sdB	15.85 P	...	16.202	0.122	14.280	...	13.998	...	...	...	...	...	...	...	...
97 PG 0112+142		sdB	14.70 P	...	15.903	0.098	15.630	0.188	15.410	0.217	+0.493	0.238	+0.273	0.212	+0.698	0.286	...
98 JL 236		sdB	13.45 :	-0.28 :	13.959	0.042	14.149	0.066	14.160	0.085	-0.201	0.095	-0.190	0.078	-0.344	0.112	...
99 PG 0113+259		sdO(B)	14.50 y	-0.218	14.978	0.047	15.060	0.078	15.445	0.196	-0.467	0.202	-0.082	0.091	-0.529	0.213	...
101 PG 0116+242		sd	11.88 y	+0.361	10.654	0.031	10.399	0.031	10.347	0.027	+0.307	0.041	+0.255	0.044	+0.499	0.053	COM
102 PB 8783		sdB?hb	12.50 P	...	11.840	0.040	11.720	0.051	11.662	0.034	+0.178	0.052	+0.120	0.065	+0.268	0.071	...
104 PG 0122+214		sd	12.84 y	-0.215	13.204	0.027	13.197	0.033	13.255	0.035	-0.051	0.044	+0.007	0.043	-0.046	0.055	...
105 BPS CS 29504-11		sdB	15.6 B	...	16.105	0.096	16.815	...	15.586	...	...	...	...	...	...	...	...
106 PG 0123+159		sd	14.34 y	-0.159	14.839	0.053	15.051	0.095	14.868	0.101	-0.029	0.114	-0.212	0.109	-0.188	0.140	...
107 BPS CS 22953-35		sdB	12.8 B	...	14.516	0.043	14.799	0.069	14.802	0.143	-0.286	0.149	-0.283	0.081	-0.499	0.161	...
108 PG 0132+151		sd	15.13 P	...	15.408	0.062	15.529	0.136	15.479	0.245	-0.071	0.253	-0.121	0.149	-0.162	0.277	...
109 PG 0133+114		sdB	12.31 y	-0.183	12.779	0.042	12.924	0.051	13.040	0.046	-0.261	0.062	-0.145	0.066	-0.370	0.079	...
110 PG 0135+242		sdO(D)	15.05	...	14.686	0.048	14.455	0.068	14.303	0.082	+0.383	0.095	+0.231	0.083	+0.557	0.114	...
112 BPS CS 29504-37		sdB	15.7 B	...	15.953	0.076	15.699	0.123	15.387	0.193	+0.566	0.207	+0.254	0.145	+0.757	0.234	...
113 SB 705		sdO	13.03 y	-0.298	13.771	0.044	13.845	0.045	13.987	0.060	-0.216	0.074	-0.074	0.063	-0.272	0.088	...
114 PG 0142+183		sdB	15.45 P	...	15.642	0.070	15.547	0.097	15.809	0.233	-0.167	0.243	+0.095	0.120	-0.096	0.259	...
115 PG 0142+148		sdB	13.694	-0.226	14.271	0.034	14.395	0.050	14.345	0.065	-0.074	0.073	-0.124	0.060	-0.167	0.086	SGL, AEA
116 CD -24 731		sdB	11.720	-0.292	12.404	0.038	12.583	0.043	12.662	0.041	-0.258	0.056	-0.179	0.057	-0.393	0.071	SGL, AEA
117 LB 3229		sdO He	13.55	-0.25	14.253	0.047	14.379	0.052	14.518	0.080	-0.265	0.093	-0.126	0.070	-0.360	0.107	...
118 PHL 1164		sdO	12.79 y	-0.248	13.358	0.036	13.455	0.042	13.568	0.058	-0.210	0.068	-0.097	0.055	-0.283	0.080	...
119 BPS CS 29504-46		sdO	14.8 B	...	15.996	0.076	16.056	0.170	17.059	...	...	...	-0.060	0.186	...	...	...
120 PHL 3802		sdB	12.35 y	-0.059	11.997	0.038	11.739	0.042	11.767	0.042	+0.230	0.057	+0.258	0.057	+0.424	0.071	COM
122 PHL 1212		sdB	12.8 B	...	14.071	0.028	14.161	0.033	14.297	0.070	-0.226	0.075	-0.090	0.043	-0.294	0.082	...
123 PG 0154+204		sdB-O	15.24 P	...	15.991	0.087	16.003	0.189	16.481	...	...	...	-0.012	0.208	...	...	...
124 PG 0154+182		sdB-O	15.27 P	...	15.295	0.054	14.938	0.082	14.867	0.106	+0.428	0.119	+0.357	0.098	+0.696	0.140	...
125 BD+37° 442		sdO	9.98	-0.28	10.553	0.026	10.681	0.035	10.748	0.033	-0.195	0.042	-0.128	0.044	-0.291	0.053	...
126 PG 0200+131		sdB	15.12 P	...	13.793	0.036	13.559	0.041	13.605	0.064	+0.188	0.073	+0.234	0.055	+0.364	0.084	...
127 PG 0205+134		sdO(B)	14.721	+0.006	12.799	0.030	12.198	0.039	11.961	0.031	+0.838	0.043	+0.601	0.049	+1.290	0.057	COM, AEA
128 PG 0206+225		sdB	14.071	-0.158	14.454	0.035	14.549	0.053	14.684	0.086	-0.230	0.093	-0.095	0.064	-0.301	0.105	SGL, AEA
129 PB 6710		sdB	14.77 P	...	16.104	0.083	15.742	0.160	16.233	0.403	-0.129	0.411	+0.362	0.180	+0.143	0.433	...
130 Feige 19		sdO He	13.709	-0.290	14.401	0.044	14.566	0.057	14.710	0.100	-0.309	0.109	-0.165	0.072	-0.433	0.122	WMG
131 PB 6727		sdB	14.020	-0.246	14.639	0.043	14.537	0.066	14.609	0.093	+0.030	0.102	+0.102	0.079	+0.107	0.118	SGL, AEA

Continued on Next Page...

Table B.1 – Continued

No. <sup>1</sup>	ID <sup>2</sup>	Type	$V / y^3$	$B - V^3$	$J^4$	$H^4$	$K_S^4$	$J - K_S$	$J - H$	$Q^5$	Notes <sup>6</sup>
					mag	$\sigma$	mag	$\sigma$	mag	$\sigma$	
132PB 6740		sdBp?	15.39 P	...	14.808	0.044	14.852	0.076	14.990	0.134	-0.182 0.141 -0.044 0.088 -0.215 0.156 ...
133JL 286		sdB	14.31	-0.22	14.730	0.046	14.792	0.061	14.881	0.121	-0.151 0.129 -0.062 0.076 -0.198 0.141 ...
134LB 3241		sdOB	12.81 $y$	-0.293	13.451	0.041	13.599	0.045	13.753	0.058	-0.302 0.071 -0.148 0.061 -0.413 0.085 ...
135PG 0212+230		sdB-O	15.36 P	...	16.070	0.083	16.266	0.197	16.026	...	-0.196 0.214 ...
136PG 0212+148		sdB	14.452	-0.175	14.895	0.037	14.792	0.069	14.934	0.111	-0.039 0.117 -0.103 0.078 +0.038 0.131 SGL, AEA
137PG 0212+143		sdB	14.541	-0.179	14.953	0.049	15.214	0.091	15.050	0.173	-0.097 0.180 -0.261 0.103 -0.293 0.196 SGL, AEA
138PG 0215+183		sdB	13.423	-0.112	13.678	0.033	13.705	0.041	13.764	0.050	-0.086 0.060 -0.027 0.053 -0.106 0.072 SGL, AEA
139PHL 1256		sdO(C)	14.599	-0.324	15.283	0.057	15.472	0.121	15.490	0.179	-0.207 0.188 -0.189 0.134 -0.349 0.213 WMG
140PG 0216+246		sdO(D)	15.86 P	...	16.921	0.148	16.914	...	15.744	...	...
142PG 0217+155		sdO(B)	15.099	-0.205	15.607	0.077	15.665	0.142	14.786	...	-0.058 0.162 ... AEA
143PG 0219+241		sdB	16.07 P	...	16.586	0.119	16.555	0.241	17.240	...	+0.031 0.269 ...
144PG 0220+132		sdB	14.775	-0.165	15.160	0.063	15.086	0.096	14.836	...	+0.074 0.115 ... AEA
145PG 0221+217		sdB	15.62 P	...	16.232	0.100	16.075	0.184	15.776	...	+0.157 0.209 ...
146PG 0226+151		sdO(C)	16.143	-0.262	16.662	0.162	16.750	...	17.131	...	...
147PG 0229+064		B	11.919	-0.147	12.264	0.035	12.348	0.037	12.406	0.035	-0.142 0.049 -0.084 0.051 -0.205 0.062 AEA
148PG 0231+051		sdO:	16.105	-0.329	16.716	0.144	16.807	0.251	16.790	...	-0.091 0.289 ... LAN
150PG 0232+095		sd	12.61 $y$	+0.383	11.167	0.031	10.790	0.036	10.655	0.032	+0.512 0.045 +0.377 0.048 +0.796 0.058 ...
151Feige 26		sdO	14.10 $y$	-0.348	14.795	0.044	14.848	0.072	14.916	0.103	-0.121 0.112 -0.053 0.084 -0.161 0.129 ...
153BPS CS 22954-6		sdB	15.0 B	...	16.343	0.089	17.520	...	15.868	...	...
154PG 0240+046		sdO(B)	14.14 $y$	-0.213	14.755	0.044	14.936	0.069	14.844	0.104	-0.089 0.113 -0.181 0.082 -0.225 0.129 ...
155PG 0242+132		sdB	13.205	-0.145	13.523	0.028	13.649	0.040	13.629	0.049	-0.106 0.056 -0.126 0.049 -0.201 0.067 SGL, AEA
156PG 0245+182		sdO(D)	15.79 P	...	16.690	0.133	16.566	0.309	17.194	...	+0.124 0.336 ...
157PB 9286		sdB	12.50 P	...	13.597	0.037	13.719	0.044	13.818	0.067	-0.221 0.077 -0.122 0.057 -0.313 0.088 ...
158CPD -56 464		sdB	12.01 $y$	-0.255	12.604	0.039	12.726	0.051	12.880	0.041	-0.276 0.057 -0.122 0.064 -0.368 0.075 ...
159PG 0250+189		sdB	14.112	-0.060	14.124	0.036	14.058	0.048	13.972	0.060	+0.152 0.070 +0.066 0.060 +0.202 0.083 SGL, AEA
160CPD -71 172		sdOB+	12.05	-0.327	10.137	0.041	9.994	0.053	9.956	0.036	+0.181 0.055 +0.143 0.067 +0.289 0.075 ...
F3-4IV											
161PB 6958		sdB	15.81 P	...	16.475	0.126	16.213	...	16.145	...	...
162BPS CS 22963-36		sdB	13.84	...	14.270	0.043	14.431	0.057	14.389	0.069	-0.119 0.081 -0.161 0.071 -0.240 0.097 SGL
163PG 0302+028		DA 2	15.05 $y$	-0.591	15.541	0.059	15.944	0.121	15.848	0.221	-0.307 0.229 -0.403 0.135 -0.610 0.250 ...
164PG 0305+152		sd	14.51 $y$	-0.127	14.859	0.047	14.822	0.069	14.949	0.136	-0.090 0.144 +0.037 0.083 -0.062 0.157 ...
165PG 0306+141		sd	15.47 P	...	13.557	0.033	13.222	0.041	13.110	0.036	+0.447 0.049 +0.335 0.053 +0.699 0.063 ...
166BPS CS 22968-19		He-sdB	13.9 B	...	14.598	0.053	14.753	0.084	14.820	0.122	-0.222 0.133 -0.155 0.099 -0.339 0.152 ...
167PG 0310+149		sdO	15.477	-0.023	15.315	0.069	15.290	0.102	15.086	0.148	+0.229 0.163 +0.025 0.123 +0.248 0.187 WMG
168KPD 0311+4801		sdB	14.32	-0.17	14.818	0.044	14.908	0.078	15.160	0.143	-0.342 0.150 -0.090 0.090 -0.410 0.165 ...
169PG 0313+005		sd	16.01 P	...	14.762	0.055	14.577	0.069	14.336	0.099	+0.426 0.113 +0.185 0.088 +0.565 0.131 ...

Continued on Next Page...

Table B.1 – Continued

No. <sup>1</sup>	ID <sup>2</sup>	Type	$V / y^3$	$B - V^3$	$J^4$	$H^4$	$K_S^4$	$J - K_S$	$J - H$	$Q^5$	Notes <sup>6</sup>							
			mag	$\sigma$	mag	$\sigma$	mag	$\sigma$	mag	$\sigma$								
170 PG 0314+146		sdO(B)	12.53	$y$	-0.104	12.840	0.037	12.914	0.040	13.029	0.042	-0.189	0.056	-0.074	0.054	-0.245	0.069	...
171 PG 0314+180		sd	14.31	$y$	-0.201	14.717	0.037	14.664	0.058	14.989	0.100	-0.272	0.107	+0.053	0.069	-0.232	0.119	...
172 PG 0314+103		sdB	13.30	$y$	+0.412	12.251	0.041	11.943	0.044	11.834	0.037	+0.417	0.055	+0.308	0.060	+0.649	0.071	...
174 KPD 0319+4553		sdO	13.68		+0.17	13.653	0.034	13.613	0.043	13.637	0.049	+0.016	0.060	+0.040	0.055	+0.046	0.073	...
175 PG 0319+054		sdB	15.04		-0.05	15.148	0.061	15.402	0.143	15.316	0.215	-0.168	0.223	-0.254	0.155	-0.359	0.252	...
176 PG 0322+114		sdB	15.26	P	...	14.782	0.053	14.692	0.075	14.605	0.077	+0.177	0.093	+0.090	0.092	+0.245	0.116	...
177 PG 0322+078		sd	16.01	P	...	15.689	0.081	15.808	0.167	15.926	...	...	...	-0.119	0.186	...	...	CV?
178 PHL 1534		sdB?	14.7	B	...	15.204	0.042	15.254	0.092	15.566	0.170	-0.362	0.175	-0.050	0.101	-0.400	0.191	...
179 BPS CS 22185-3		sdB	15.10		-0.28	15.806	0.088	15.628	0.149	16.373	...	...	...	+0.178	0.173	...	...	...
181 LS I+63° 198		sdO	12.0	B	...	13.019	0.033	13.143	0.039	13.160	0.041	-0.141	0.053	-0.124	0.051	-0.234	0.065	...
182 BPS CS 22190-34		sdB	13.64		-0.25	14.163	0.041	14.274	0.070	14.316	0.074	-0.153	0.085	-0.111	0.081	-0.236	0.105	SGL
183 BPS CS 22190-3		sdB He	14.90		-0.27	15.438	0.065	15.559	0.121	15.594	0.211	-0.156	0.221	-0.121	0.137	-0.247	0.244	SGL
184 PG 0342+026		HBB	10.957		-0.140	11.289	0.037	11.392	0.036	11.478	0.037	-0.189	0.052	-0.103	0.052	-0.266	0.065	AEA
185 KUV 03439-0048		sdO	14.91		-0.29	15.483	0.058	15.722	0.128	15.930	0.283	-0.447	0.289	-0.239	0.141	-0.627	0.308	...
186 PG 0349+094		sdB	15.69	P	...	15.839	0.088	15.895	0.220	15.594	0.189	+0.245	0.208	-0.056	0.237	+0.203	0.274	...
187 HDE 283048		sd+F?	10.30	P	...	9.329	0.034	9.083	0.040	9.020	0.034	+0.309	0.048	+0.246	0.052	+0.494	0.062	...
188 BPS CS 22190-4		sdB	14.0	B	...	15.163	0.050	15.193	0.087	15.382	0.205	-0.219	0.211	-0.030	0.100	-0.242	0.224	...
189 HZ 3		sdO6	12.86		-0.14	13.237	0.034	13.362	0.047	13.445	0.042	-0.208	0.054	-0.125	0.058	-0.302	0.069	...
190 BPS CS 22169-1		sdB	12.87		-0.27	13.456	0.039	13.551	0.052	13.550	0.051	-0.094	0.064	-0.095	0.065	-0.165	0.081	SGL
192 KPD 0402+4232		sdB	15.49		+0.04	15.517	0.083	15.279	0.093	15.890	0.216	-0.373	0.231	+0.238	0.125	-0.194	0.249	...
193 RL 92		sdB	14.03	:	+0.15	13.465	0.045	13.255	0.037	13.172	0.044	+0.293	0.063	+0.210	0.058	+0.451	0.077	...
194 TONS 401		sdB p?	12.28	$y$	-0.134	12.440	0.021	12.526	0.027	12.545	0.027	-0.105	0.034	-0.086	0.034	-0.170	0.043	...
195 BPS CS 22182-8		sdB	12.2	B	...	13.629	0.041	13.737	0.063	13.845	0.058	-0.216	0.071	-0.108	0.075	-0.297	0.091	...
198 BPS CS 22173-33		sdB	13.61		-0.27	14.280	0.041	14.338	0.079	14.476	0.100	-0.196	0.108	-0.058	0.089	-0.240	0.127	...
199 KUV 04110+1434		sdB	13.91		+0.23	12.756	0.027	12.704	0.031	12.662	0.036	+0.094	0.045	+0.052	0.041	+0.133	0.055	...
200 BD-13° 842		sd	11.99	$y$	-0.312	12.539	0.061	12.647	0.082	12.577	0.073	-0.038	0.095	-0.108	0.102	-0.119	0.122	CSPN <sup>f</sup>
201 KPD 0422+5421		sdB	14.66		+0.20	14.425	0.035	14.421	0.054	14.301	0.066	+0.124	0.075	+0.004	0.064	+0.127	0.089	...
202 KUV 04233+1502		sdO	14.72		-0.15	14.045	0.034	14.012	0.053	13.979	0.057	+0.066	0.066	+0.033	0.063	+0.091	0.081	...
203 KUV 04237+1649		sdOB	13.90		+0.33	12.791	0.030	12.505	0.044	12.419	0.035	+0.372	0.046	+0.286	0.053	+0.587	0.061	...
204 BPS CS 22182-37		sdO He	14.10		-0.31	14.811	0.047	14.850	0.081	15.039	0.159	-0.228	0.166	-0.039	0.094	-0.257	0.180	SGL
205 RL 105		sdB	14.60	:	+0.04	14.579	0.049	14.611	0.060	14.696	0.077	-0.117	0.091	-0.032	0.077	-0.141	0.108	...
208 KUV 04402+1455		sdO	13.97		+0.21	13.427	0.033	13.401	0.044	13.357	0.039	+0.070	0.051	+0.026	0.055	+0.090	0.066	...
209 KUV 04421+1416		sdB	15.08		+0.18	14.574	0.039	14.677	0.055	14.458	0.081	+0.116	0.090	-0.103	0.067	+0.039	0.103	...
210 KUV 04456+1502		sdO	15.80	P	...	15.491	0.063	15.279	0.091	15.347	0.194	+0.144	0.204	+0.212	0.111	+0.303	0.220	...
211 HZ 1		sdOp	12.62		-0.06	12.746	0.032	12.848	0.039	12.865	0.035	-0.119	0.047	-0.102	0.050	-0.196	0.060	SGL
212 LB 1766		sdB He	12.34	$y$	-0.269	13.062	0.027	13.181	0.031	13.248	0.038	-0.186	0.047	-0.119	0.041	-0.275	0.056	...

Continued on Next Page...

Table B.1 – Continued

No. <sup>1</sup>	ID <sup>2</sup>	Type	$V / y^3$	$B - V^3$	$J^4$	$H^4$	$K_S^4$	$J - K_S$	$J - H$	$Q^5$	Notes <sup>6</sup>
					mag	$\sigma$	mag	$\sigma$	mag	$\sigma$	
213 KUV 05053+1628		sdOB	15.50 P	...	15.767 0.071	15.864 0.175	15.470 0.169	+0.297 0.183	-0.097 0.189	+0.224 0.232	...
214 KUV 05072+1249		sdB	16.2	...	15.903 0.084	15.690 0.146	15.937 ...	...	+0.213 0.168	...	...
215 RL 114		sdOB	15.59	-0.07	15.764 0.086	15.757 0.192	15.407 0.179	+0.357 0.199	+0.007 0.210	+0.362 0.254	...
216 KUV 05109+1739		sdOB	13.50 P	...	14.167 0.030	14.070 0.050	14.133 0.051	+0.034 0.059	+0.097 0.058	+0.107 0.073	...
217 [CW83]0512-08		sdO	11.32 $y$	-0.258	11.840 0.024	11.970 0.021	12.096 0.024	-0.256 0.034	-0.130 0.032	-0.354 0.042	...
218 HD 269696		sdOB+	11.13	-0.270	11.795 0.040	11.965 0.040	12.046 0.039	-0.251 0.056	-0.170 0.057	-0.379 0.071	e.bin
		degen									
219 CPD -64 481		sdB	11.31 $y$	-0.258	11.878 0.041	11.994 0.039	12.074 0.041	-0.196 0.058	-0.116 0.057	-0.283 0.072	...
220 KPD 0549+1642		sdB	15.28	-0.07	15.239 0.044	15.188 0.082	15.296 0.181	-0.057 0.186	+0.051 0.093	-0.019 0.199	...
221 KPD 0549+1948		sdO	14.87	-0.16	15.259 0.043	15.480 0.092	15.404 0.152	-0.145 0.158	-0.221 0.102	-0.311 0.176	...
222 KPD 0550+1922		sdB	14.55	-0.13	14.923 0.035	15.042 0.064	15.057 0.116	-0.134 0.121	-0.119 0.073	-0.223 0.133	...
223 CD -61 1208		sdB	11.19 $y$	-0.193	11.601 0.042	11.680 0.051	11.750 0.037	-0.149 0.056	-0.079 0.066	-0.208 0.075	...
224 KPD 0552+1903		sdO	14.68	+0.11	14.446 0.035	14.441 0.054	14.627 0.081	-0.181 0.088	+0.005 0.064	-0.177 0.100	...
225 KPD 0553+1755		sdO	15.13	+0.07	15.076 0.047	15.069 0.097	14.938 ...	...	+0.007 0.108	...	...
226 HS 0600+6602		sdB	16.4	...	16.616 0.145	16.404 ...	15.719 ...	...	...	...	...
227 LS V+22° 38		sdO	12.00 B	...	8.354 0.015	8.051 0.067	7.785 0.019	+0.569 0.024	+0.303 0.069	+0.797 0.057	neb in field <sup>f</sup>
228 RL 54		sdB	14.69	-0.11	15.158 0.058	15.091 0.105	15.195 0.116	-0.037 0.130	+0.067 0.120	+0.013 0.158	...
229 HD 45166		B8V+	9.90	...	9.812 0.037	9.751 0.037	9.570 0.034	+0.242 0.050	+0.061 0.052	+0.288 0.063	...
		sdO?									
230 KPD 0629-0016		sdB	14.92	-0.01	15.019 0.054	15.192 0.090	14.707 ...	...	-0.173 0.105	...	...
231 KPD 0640+1412		sdB	14.85	+0.04	14.896 0.046	14.862 0.077	14.996 0.125	-0.100 0.133	+0.034 0.090	-0.074 0.149	...
232 HD 49798		sdO	8.27	-0.28	8.862 0.019	9.005 0.035	9.072 0.035	-0.210 0.040	-0.143 0.040	-0.318 0.050	s.bin
233 HD 51155		sdB	9.53 $y$	-0.133	9.750 0.023	9.852 0.024	9.822 0.022	-0.072 0.032	-0.102 0.033	-0.149 0.040	...
234 BD+34° 1543		sd	10.184	+0.094	9.485 0.039	9.326 0.029	9.207 0.032	+0.278 0.050	+0.159 0.049	+0.398 0.062	COM, TYC
236 [CW83]0711+22		sdOp	11.70 P	...	12.352 0.024	12.482 0.024	12.636 ...	...	-0.130 0.034	...	...
238 KPD 0716+0258		sdB	14.892	-0.164	15.277 0.061	15.226 0.098	15.442 0.202	-0.165 0.211	+0.051 0.115	-0.127 0.228	AEA
239 KPD 0720-0003		sdO	15.78	-0.28	16.340 0.121	16.124 0.220	16.096 ...	...	+0.216 0.251	...	...
240 KPD 0721-0026		sdB	13.83	-0.17	14.109 0.042	14.219 0.058	14.188 0.073	-0.079 0.084	-0.110 0.072	-0.162 0.100	...
241 KPD 0732+0057		sdB	15.35	-0.23	15.757 0.075	16.083 0.201	15.870 ...	...	-0.326 0.215	...	...
242 CD -31 4800		sdO8	10.52	-0.31	11.246 0.038	11.376 0.042	11.480 0.036	-0.234 0.052	-0.130 0.057	-0.332 0.067	...
243 LSS 630		sdO	13.30 B	...	14.226 0.042	14.259 0.050	14.557 0.108	-0.033 0.116	-0.033 0.065	-0.356 0.126	...
244 PG 0749+658		sdB-O	12.121	-0.106	11.769 0.040	11.460 0.040	11.404 0.035	+0.365 0.053	+0.309 0.057	+0.597 0.068	AEA
246 PG 0752+770		sdB	16.11	-0.15	16.435 0.131	15.783 0.183	15.045 ...	...	+0.652 0.225	...	...
247 KUV 07571+4233		sdB	14.97	+0.57	14.027 0.041	13.700 0.040	13.598 0.041	+0.429 0.058	+0.327 0.057	+0.675 0.072	...
248 KUV 07592+3931		sdB	15.26	-0.29	15.872 0.082	16.049 0.203	15.746 ...	...	-0.177 0.219	...	...
249 KUV 07596+4123		sdO	15.380	-0.26	15.612 0.071	15.685 0.170	15.301 0.162	+0.311 0.177	-0.073 0.184	+0.256 0.225	...

Continued on Next Page...

Table B.1 – Continued

No. <sup>1</sup>	ID <sup>2</sup>	Type	$V / y^3$	$B-V^3$		$J^4$		$H^4$		$K_S^4$		$J-K_S$		$J-H$		$Q^5$		Notes <sup>6</sup>
				mag	$\sigma$	mag	$\sigma$	mag	$\sigma$	mag	$\sigma$	mag	$\sigma$	mag	$\sigma$	mag	$\sigma$	
250 BD-3°2179		sdO	10.33	-0.29		10.954	0.042	11.126	0.051	11.176	0.035	-0.222	0.055	-0.172	0.066	-0.351	0.074	...
251 TON 299		sdB	15.2	-0.30		16.021	0.100	16.119	0.212	15.721	...	...	...	-0.098	0.234	...	...	...
252 BD+75°325		sdO	9.60	-0.334		10.261	0.026	10.425	0.033	10.549	0.029	-0.288	0.039	-0.164	0.042	-0.411	0.050	...
253 PG 0806+516		sdB	15.21	-0.19	$y$	15.939	0.095	15.734	0.190	16.046	...	...	...	+0.205	0.212	...	...	...
254 PG 0806+682		sdB	15.69	...	P	16.209	0.099	16.440	0.271	15.971	...	...	...	-0.231	0.289	...	...	...
255 LSS 982		sdO	12.60	B	...	12.930	0.041	13.147	0.052	13.214	0.045	-0.284	0.061	-0.217	0.066	-0.447	0.079	...
256 PG 0812+478		sd	15.42	P	...	14.587	0.033	14.165	0.043	13.882	0.048	+0.705	0.058	+0.422	0.054	+1.022	0.071	...
257 PG 0812+482		sdB	15.45	P	...	15.588	0.071	15.563	0.130	15.404	...	...	...	+0.025	0.148	...	...	...
258 TON 313		sdB	15.64	P	...	16.280	0.104	16.105	0.211	15.909	...	...	...	+0.175	0.235	...	...	...
260 TON 317		sd	15.94	P	...	14.760	0.053	14.557	0.070	14.519	0.071	+0.241	0.089	+0.203	0.088	+0.394	0.111	...
261 PG 0822+645		sdB	15.59	-0.37		16.207	0.097	16.098	0.210	15.618	...	...	...	+0.109	0.231	...	...	...
262 PG 0823+546		sdO(C)	14.255	-0.282		14.657	0.036	14.546	0.063	14.898	0.138	-0.241	0.143	+0.111	0.073	-0.158	0.153	WMG
263 PG 0823+465		sdB	14.54	-0.18		15.067	0.049	15.064	0.071	15.152	0.118	-0.085	0.128	+0.003	0.086	-0.083	0.143	...
264 PG 0823+499		non-sd	12.01	-0.142	$y$	12.308	0.031	12.417	0.038	12.444	0.033	-0.136	0.045	-0.109	0.049	-0.218	0.058	...
265 PG 0824+288		dC+DA	14.73	P	...	12.423	0.032	11.802	0.035	11.650	0.035	+0.773	0.047	+0.621	0.047	+1.240	0.059	blended dbl.
266 [CW83] 0825+15		sdO	11.70	P	...	12.425	0.021	12.586	0.026	12.652	0.029	-0.227	0.036	-0.161	0.033	-0.348	0.044	...
267 PG 0826+480		sdB	16.08	-0.20		16.737	0.145	16.477	0.222	16.854	...	...	...	+0.260	0.265	...	...	...
268 [CW83] 0832-01		sdOp	11.46	-0.288	$y$	12.094	0.027	12.271	0.025	12.359	0.027	-0.265	0.038	-0.177	0.037	-0.398	0.047	...
269 PG 0832+675		B1V	14.146	-0.208		14.587	0.043	14.751	0.075	14.650	0.095	-0.063	0.104	-0.164	0.086	-0.186	0.122	AEA
270 PG 0833+699		sdO(A)	13.492	-0.186		13.902	0.032	13.979	0.051	14.291	0.076	-0.389	0.082	-0.077	0.060	-0.447	0.094	AEA
272 PG 0836+619		sdO	14.407	-0.175		14.916	0.047	14.922	0.089	15.006	0.106	-0.090	0.116	-0.006	0.101	-0.095	0.139	WMG
273 PG 0837+401		sdB	14.90	P	...	16.164	0.095	15.825	0.152	15.616	...	...	...	+0.339	0.179	...	...	...
274 PG 0838+164		sdB	14.90	P	...	16.279	0.109	15.758	...	15.380	...	...	...	...	...	...	...	...
275 PG 0838+132		sdO He	13.655	-0.286		14.303	0.045	14.457	0.059	14.482	0.075	-0.179	0.087	-0.154	0.074	-0.295	0.103	WMG
276 KUV 08388+4029		sdB	16.40	...		14.989	0.055	14.237	0.057	13.313	0.043	+1.676	0.070	+0.752	0.079	+2.242	0.092	Sey <sup>f</sup>
277 PG 0839+399		sdB	14.29	-0.27		14.885	0.050	15.080	0.074	15.012	0.114	-0.127	0.124	-0.195	0.089	-0.274	0.141	...
278 TON 943		sdB	14.92	-0.19		15.324	0.066	15.369	0.123	14.943	...	...	...	-0.045	0.140	...	...	...
279 TON 202		sdB	14.65	P	...	14.188	0.032	13.864	0.039	13.833	0.052	+0.355	0.061	+0.324	0.050	+0.599	0.072	...
280 TON 345		sdO	15.79	P	...	16.235	0.115	15.958	...	16.484	...	...	...	...	...	...	...	...
281 TON 346		sdB-O	15.47	P	...	16.159	0.077	16.140	0.153	16.075	...	...	...	+0.019	0.171	...	...	...
282 TON 349		sdO(B)	15.34	-0.28		15.964	0.082	15.906	0.165	15.618	0.194	+0.346	0.211	+0.058	0.184	+0.390	0.252	...
283 CD -34 5246		sdO	12.90	B	...	13.144	0.037	13.285	0.042	13.386	0.052	-0.242	0.064	-0.141	0.056	-0.348	0.077	...
285 PG 0848+416		sdB+K1	16.13	+0.04		15.632	0.076	15.395	0.102	15.667	0.186	-0.035	0.201	+0.237	0.127	+0.143	0.223	COM
286 TON 357		sdB	14.25	-0.27		14.315	0.031	14.195	0.044	14.199	0.064	+0.116	0.071	+0.120	0.054	+0.206	0.082	...
287 PG 0848+186		non-sd	13.25	$y$	-0.171	13.677	0.031	13.791	0.049	13.819	0.048	-0.142	0.057	-0.114	0.058	-0.228	0.072	...

Continued on Next Page...

Table B.1 – Continued

No. <sup>1</sup>	ID <sup>2</sup>	Type	$V / y^3$	$B - V^3$	$J^4$ mag $\sigma$	$H^4$ mag $\sigma$	$K_S^4$ mag $\sigma$	$J - K_S$ mag $\sigma$	$J - H$ mag $\sigma$	$Q^5$ mag $\sigma$	Notes <sup>6</sup>
288 TON 358		sdO(A)	14.53	-0.23	15.177 0.058	15.318 0.100	15.255 0.130	-0.078 0.142	-0.141 0.116	-0.184 0.167	...
289 PG 0850+170		sdB	13.98	$y$	14.546 0.033	14.547 0.055	14.671 0.086	-0.125 0.092	-0.001 0.064	-0.126 0.104	SGL
290 LB 8827		sdO(A)	16.38	:	16.780 0.146	17.080 ...	15.882 ...	...	...	...	...
291 HD 76431		BO/sd?	9.22	$y$	9.846 0.038	10.003 0.037	10.105 0.037	-0.259 0.053	-0.157 0.053	-0.377 0.066	...
292 PG 0854+385		sdB	15.71	-0.29	16.210 0.099	16.393 0.229	15.813 0.208	+0.397 0.230	-0.183 0.249	+0.259 0.297	...
293 PG 0856+121		sdB	13.47	-0.19	13.953 0.036	14.048 0.063	14.195 0.074	-0.242 0.082	-0.095 0.073	-0.313 0.099	c, SGL
294 PG 0900+400		sdB+K3	12.87	+0.23	11.912 0.031	11.561 0.038	11.458 0.034	+0.454 0.046	+0.351 0.049	+0.718 0.059	COM
296 PG 0901+309		sdB-O	14.84	P	15.763 0.067	15.862 0.145	15.813 ...	...	-0.099 0.160	...	...
298 PG 0902+057		sdO(D)	14.06	P	14.742 0.045	14.789 0.059	15.116 0.164	-0.374 0.170	-0.047 0.074	-0.409 0.179	...
299 PG 0902+124		sdB	14.96	P	15.248 0.055	15.158 0.095	15.589 0.164	-0.341 0.173	+0.090 0.110	-0.273 0.192	...
300 PG 0903-032		sdB	15.56	P	16.078 0.087	15.999 0.141	16.205 ...	...	+0.079 0.166	...	...
301 [CW83] 0904-02		sdOp	12.00	P	12.639 0.028	12.799 0.030	12.884 0.036	-0.245 0.046	-0.160 0.041	-0.365 0.055	...
302 PG 0904+735		sdB	15.13	P	15.565 0.068	15.470 0.111	15.594 0.193	-0.029 0.205	+0.095 0.130	+0.042 0.227	...
304 PG 0906+190		sd	16.32	P	15.425 0.052	15.264 0.093	15.258 0.140	+0.167 0.149	+0.161 0.107	+0.288 0.169	...
305 PG 0906+597		sdB	15.37	$y$	16.171 0.101	16.031 0.219	15.416 ...	...	+0.140 0.241	...	...
306 PG 0907+123		sdB	13.94	$y$	14.474 0.041	14.666 0.071	14.571 0.079	-0.097 0.089	-0.192 0.082	-0.241 0.108	SGL
309 PG 0909+169		sd	16.28	P	14.343 0.037	14.139 0.055	14.052 0.058	+0.291 0.069	+0.204 0.066	+0.444 0.085	...
310 PG 0909+164		sdB	13.85	$y$	14.485 0.038	14.685 0.067	14.606 0.084	-0.121 0.092	-0.200 0.077	-0.271 0.109	SGL
311 PG 0909+275		sdO(A)	10.74	P	12.860 0.022	12.962 0.024	13.140 0.032	-0.280 0.039	-0.102 0.033	-0.357 0.046	...
312 PG 0911+042		sdB	15.48	-0.17	16.000 0.091	15.793 0.174	15.238 ...	...	+0.207 0.196	...	...
313 PG 0910+621		sdB	15.54	P	15.481 0.063	15.378 0.103	15.413 0.169	+0.068 0.180	+0.103 0.121	+0.145 0.202	...
314 PG 0911+456		sdB-O	14.92	P	15.317 0.053	15.654 0.141	15.427 0.220	-0.110 0.226	-0.337 0.151	-0.363 0.253	...
315 CBS 98		sdB-O	16.00	B	16.414 0.175	16.318 0.274	15.917 ...	...	+0.096 0.325	...	...
316 PG 0912+189		sd	16.05	P	16.417 0.099	16.184 0.154	17.564 ...	...	+0.233 0.183	...	...
320 PG 0914+001		sdB	14.583	$y$	14.606 0.052	14.744 0.075	14.700 0.122	-0.094 0.133	-0.138 0.091	-0.198 0.150	MEA
321 PG 0914-037		sdO(D)	16.37	P	15.981 0.099	15.907 0.217	16.363 ...	...	+0.074 0.239	...	...
322 PG 0914+120		sdB	16.420	...	15.838 0.096	15.843 0.174	15.440 0.232	+0.398 0.251	-0.005 0.199	+0.394 0.292	CV?
323 LSS 1274		sdO	12.40	B	13.340 0.040	13.516 0.061	13.524 0.045	-0.184 0.060	-0.176 0.073	-0.316 0.081	...
325 CD -45 5058		sdO	11.33	-0.31	12.029 0.038	12.151 0.040	12.296 0.038	-0.267 0.054	-0.122 0.055	-0.359 0.068	...
326 HD 80836		sdB	9.62	$y$	9.609 0.039	9.611 0.040	9.625 0.037	-0.016 0.054	-0.002 0.056	-0.018 0.068	...
327 PG 0918+029		sdB	13.327	-0.271	13.949 0.040	14.157 0.054	14.219 0.065	-0.270 0.076	-0.208 0.067	-0.426 0.091	LAN
328 TON 13		sdB	12.645	-0.276	13.303 0.029	13.420 0.041	13.570 0.046	-0.267 0.054	-0.117 0.050	-0.355 0.066	SGL, AEA
329 TON 14		sdO(A)	14.80	$y$	15.412 0.056	15.613 0.126	15.445 ...	...	-0.201 0.138	...	...
330 PG 0920+029		sdB	14.40	$y$	15.063 0.056	15.243 0.087	14.877 0.160	+0.186 0.170	-0.180 0.103	+0.051 0.187	...
331 TON 1055		sd	14.69	P	15.103 0.050	15.155 0.091	14.903 0.102	+0.200 0.114	-0.052 0.104	+0.161 0.138	...
332 BD+37° 1977		sdO	10.00	-0.31	10.837 0.036	10.990 0.039	11.037 0.028	-0.200 0.046	-0.153 0.053	-0.315 0.061	...

Continued on Next Page...

Table B.1 – Continued

No. <sup>1</sup>	ID <sup>2</sup>	Type	$V / y^3$	$B - V^3$	$J^4$	$H^4$	$K_S^4$	$J - K_S$	$J - H$	$Q^5$	Notes <sup>6</sup>							
					mag	$\sigma$	mag	$\sigma$	mag	$\sigma$								
333 CBS 7		sdO(B)	14.60	$y$	-0.232	15.302	0.052	15.630	0.129	15.332	0.156	-0.030	0.164	-0.328	0.139	-0.277	0.194	...
334 PG 0921+161		sd	14.58	$y$	-0.246	15.253	0.049	15.131	0.096	15.409	0.175	-0.156	0.182	+0.122	0.108	-0.064	0.199	...
335 PG 0922+259		sdB+K4	16.41		-0.10	15.053	0.047	14.822	0.064	14.843	0.115	+0.210	0.124	+0.231	0.079	+0.384	0.137	COM
336 TON 1059		sdB	14.94		-0.26	15.583	0.063	15.722	0.132	15.546	0.194	+0.037	0.204	-0.139	0.146	-0.068	0.232	...
337 PG 0924+565		sd	16.05	P	...	16.634	0.125	15.975	...	16.347	...	...	...	...	...	...	...	...
338 PG 0926+065		sdB	15.34	P	...	14.624	0.048	14.745	0.085	14.778	0.117	-0.154	0.126	-0.121	0.098	-0.245	0.146	...
339 PG 0926+526		sdB	16.09	P	...	16.952	0.156	16.466	...	16.195	0.288	+0.757	0.328	...	...	...	...	...
340 TON 427		sdB	15.08	:	-0.31	15.431	0.050	15.583	0.113	15.739	...	...	...	-0.152	0.124	...	...	...
341 BD+48°1777		sdOp	10.76		-0.32	11.404	0.038	11.509	0.044	11.586	0.033	-0.182	0.050	-0.105	0.058	-0.261	0.066	...
342 PG 0928+031		sdB	15.06	P	...	15.538	0.067	15.520	0.113	15.376	0.197	+0.162	0.208	+0.018	0.131	+0.176	0.230	...
343 PG 0930+085		sdB	15.97	P	...	16.781	0.192	16.580	0.257	15.936	0.326	+0.845	0.378	+0.201	0.321	+0.996	0.449	...
345 TON 438		sdB	15.00	B	...	16.399	0.126	16.469	...	16.677	...	...	...	...	...	...	...	...
346 LB 10889		sd	16.13	P	...	16.023	0.071	15.763	0.130	15.557	0.146	+0.466	0.162	+0.260	0.148	+0.662	0.197	...
347 PG 0932+166		sd	15.68		-0.11	14.340	0.036	13.897	0.045	13.895	0.057	+0.445	0.067	+0.443	0.058	+0.778	0.080	...
348 PG 0933+004		sdB	14.39	$y$	-0.252	14.905	0.059	15.054	0.094	15.163	0.172	-0.258	0.182	-0.149	0.111	-0.370	0.200	...
349 PG 0933+383		sdB	15.47	$y$	-0.14	15.981	0.083	15.778	0.125	16.371	...	...	...	+0.203	0.150	...	...	...
350 PG 0934+145		HBB	13.51	$y$	-0.136	13.788	0.040	13.781	0.052	13.944	0.055	-0.156	0.068	+0.007	0.066	-0.151	0.084	...
352 PG 0934+186		sdB	13.14	$y$	-0.265	13.759	0.034	13.972	0.048	13.927	0.051	-0.168	0.061	-0.213	0.059	-0.328	0.075	SGL
353 GD 299		sdO	12.071		-0.269	12.303	0.039	12.155	0.046	12.142	0.040	+0.161	0.056	+0.148	0.060	+0.272	0.072	WMG
354 PG 0935+084		sdB	15.35	P	...	14.654	0.043	14.533	0.068	14.392	0.068	+0.262	0.080	+0.121	0.080	+0.353	0.100	...
355 PG 0935+038		sdB	14.97	$y$	-0.295	14.967	0.059	14.860	0.072	14.838	0.149	+0.129	0.160	+0.107	0.093	+0.209	0.175	...
356 PG 0936+037		sdB	15.98	P	...	15.944	0.093	16.296	0.195	16.041	...	...	...	-0.352	0.216	...	...	...
357 PG 0940+171		sdB	16.13	P	...	16.097	0.092	15.826	0.172	15.708	...	...	...	+0.271	0.195	...	...	...
358 PG 0941+280		sdB	12.46	P	...	13.799	0.035	13.899	0.053	13.997	0.078	-0.198	0.085	-0.100	0.064	-0.273	0.098	...
360 PG 0942+461		sd	14.93	P	...	13.534	0.050	13.249	0.046	13.173	0.046	+0.361	0.068	+0.285	0.068	+0.575	0.085	...
361 PG 0942+029		sdB	14.004		-0.294	14.662	0.047	14.652	0.080	15.032	0.174	-0.370	0.180	+0.010	0.093	-0.362	0.193	LAN
362 PG 0943+043		sd	15.87	P	...	16.264	0.116	16.010	...	15.745	...	...	...	...	...	...	...	...
363 GD 104		sdB	15.91	$y$	-0.340	16.405	0.115	16.524	0.227	15.696	...	...	...	-0.119	0.254	...	...	...
365 LSS 1349		sdO	13.80	B	...	13.315	0.042	13.331	0.047	13.286	0.050	+0.029	0.065	-0.016	0.063	+0.017	0.080	...
368 PG 0947+639		sdB	14.78	P	...	15.198	0.056	15.349	0.148	15.470	...	...	...	-0.151	0.158	...	...	...
369 PG 0948+533		sd	15.33	P	...	16.220	0.104	16.153	0.254	15.500	...	...	...	+0.067	0.274	...	...	...
370 PG 0948+187		sdB	16.25	:	-0.28	16.302	0.081	15.873	0.128	15.675	0.183	+0.627	0.200	+0.429	0.151	+0.950	0.230	...
371 PG 0948+041		sdB-O	15.77	P	...	15.972	0.095	15.766	0.145	15.573	...	...	...	+0.206	0.173	...	...	...
372 PG 0948+632		sdB	14.95	P	...	15.420	0.075	15.609	0.150	15.769	0.259	-0.349	0.270	-0.189	0.168	-0.491	0.298	...
373 PG 0949+101		sdO(B)	14.86	P	...	14.099	0.042	13.790	0.044	13.768	0.056	+0.331	0.070	+0.309	0.061	+0.563	0.084	...
374 PG 0950+158		sdO(D)	15.86	P	...	16.319	0.098	16.464	0.251	15.768	...	...	...	-0.145	0.269	...	...	...

Continued on Next Page...

Table B.1 – Continued

No. <sup>1</sup>	ID <sup>2</sup>	Type	$V / y^3$	$B - V^3$	$J^4$	$H^4$	$K_S^4$	$J - K_S$	$J - H$	$Q^5$	Notes <sup>6</sup>
					mag	$\sigma$	mag	$\sigma$	mag	$\sigma$	
375 PG 0950+120		sdO(A)	15.15 :	-0.27	15.730	0.089	15.936	0.188	15.252	...	...
376 GD 300		sdO	12.651	-0.333	13.353	0.046	13.499	0.047	13.603	0.044	-0.250 0.064
377 PG 0953+024		sdO(C)	14.994	-0.292	15.839	0.074	15.565	0.119	15.302	...	-0.146 0.066
378 PG 0954+049		sd	12.90 $y$	-0.064	12.994	0.042	13.026	0.049	13.011	0.043	-0.274 0.140
379 TON 468		sdO(A)	15.49 P	...	15.968	0.086	16.136	0.205	16.252	...	-0.032 0.065
380 CBS 115		sdB	12.00 B	...	13.421	0.024	13.561	0.029	13.734	0.050	-0.168 0.222
381 PG 0956-117		sdB	15.32 P	...	16.204	0.096	15.858	...	15.153	...	-0.140 0.038
382 TON 1137		sdO(B)	15.15 P	...	15.904	0.087	16.347	...	15.734	0.226	+0.170 0.242
383 PG 0957+037		sd	15.65 P	...	15.838	0.088	15.769	0.117	15.447	0.211	+0.069 0.146
384 PG 0958-116		sdB	15.33 P	...	15.903	0.080	16.146	0.167	16.959	...	+0.443 0.254
385 PG 0958-119		sdO(B)	14.09 $y$	-0.228	14.656	0.047	14.748	0.081	15.082	0.179	-0.243 0.185
386 GD 108		sdB	13.60	-0.21	14.098	0.046	14.139	0.047	14.256	0.092	-0.092 0.094
388 PG 0959-085		sdO(D)	16.12 P	...	16.754	0.152	16.337	0.184	15.675	...	-0.041 0.066
391 KUV 10003+3732		sdB	15.46 P	...	14.358	0.032	14.007	0.040	13.892	0.056	+0.417 0.239
393 KUV 10009+4049		sdO	13.299	-0.325	13.978	0.027	14.244	0.045	14.330	0.083	+0.351 0.051
394 CBS 19		sdB	16.00 B	...	11.341	0.026	11.138	0.034	11.087	0.027	-0.266 0.052
395 LB 567		sd	16.01 P	...	16.433	0.129	16.354	0.237	15.695	...	-0.552 0.095
396 PG 1006-145		sdB	15.84 P	...	15.564	0.073	15.505	0.146	15.215	...	+0.407 0.049
398 PG 1008+689		...	12.87 $y$	-0.109	13.040	0.031	13.111	0.039	13.145	0.037	+0.079 0.270
399 PG 1008+756		sdB	15.94 P	...	15.379	0.054	15.360	0.116	15.821	...	+0.039 0.163
401 PG 1009+069		sdO(B)	16.41 P	...	16.268	0.122	16.073	0.216	16.784	...	-0.071 0.050
403 PG 1011+649		sdO(B)	14.90	-0.26	15.589	0.062	15.523	0.119	15.886	0.210	+0.019 0.128
404 PG 1012+007		sdB	14.90 $y$	-0.18	15.519	0.068	15.572	0.157	15.675	...	+0.195 0.248
405 PG 1017-113		sdB	16.17 P	...	16.820	0.148	16.309	0.194	15.669	...	-0.053 0.171
406 PG 1017+430		sdOB	15.28 P	...	16.020	0.081	16.119	0.208	15.878	0.241	+0.511 0.244
407 PG 1017-086		sdB	14.43 $y$	-0.225	14.866	0.051	15.036	0.081	15.095	0.135	-0.099 0.223
408 PG 1018-047		sdB	13.32 $y$	-0.200	13.298	0.041	12.980	0.053	12.928	0.043	+0.068 0.304
409 PG 1020+694		sdO(B)	14.63 $y$	-0.249	15.262	0.056	15.267	0.101	15.305	...	-0.170 0.096
410 LB 10383		sdB	15.19	-0.07	15.339	0.048	15.191	0.085	15.227	0.116	-0.357 0.161
411 PG 1021-029		sdB-O	15.43 P	...	16.095	0.097	16.115	0.196	15.775	...	+0.318 0.067
412 PG 1022+459		sdB	15.76 P	...	16.216	0.103	16.552	...	15.662	0.231	-0.005 0.115
414 CD -24 9052		sdO	11.77 $y$	-0.287	12.433	0.038	12.566	0.040	12.667	0.043	+0.148 0.098
415 PG 1024+238		sd	15.71 P	...	13.518	0.028	13.224	0.032	13.193	0.035	-0.020 0.219
416 TON 516		sdB	15.99 P	...	14.649	0.034	14.507	0.039	14.513	0.062	...
417 PG 1026-037		sdB-O	15.94 :	-0.24	16.574	0.140	16.526	0.233	16.781	...	+0.142 0.052
419 PG 1027-077		sdB	16.19 :	-0.20	16.645	0.111	16.581	0.194	16.096	...	+0.048 0.272
											+0.064 0.224

Continued on Next Page...



Table B.1 – Continued

No. <sup>1</sup>	ID <sup>2</sup>	Type	$V / y^3$	$B - V^3$	$J^4$	$H^4$	$K_S^4$	$J - K_S$	$J - H$	$Q^5$	Notes <sup>6</sup>
					mag $\sigma$	mag $\sigma$	mag $\sigma$	mag $\sigma$	mag $\sigma$	mag $\sigma$	
422 PG 1030+665		sdO(B)	15.48 P	...	16.084 0.089 16.553 ...	15.950 0.319 +0.134 0.331	...	...	...	...	...
423 PG 1032+406		sdB	11.52 $y$	-0.283	12.166 0.023 12.275 0.024	12.384 0.028 -0.218 0.036	-0.109 0.033	-0.300 0.044	...	...	...
424 PG 1032+007		sd	16.42 P	...	16.453 0.150 15.873 ...	16.262 ...	...	...	...	...	...
426 PG 1033+201		sdB	15.671	-0.170	15.457 0.048 15.158 0.073	15.126 0.128 +0.331 0.137	-0.299 0.087	+0.556 0.152 COM, AEA	...	...	...
427 CBS 129		sdB	13.00 B	...	11.601 0.040 11.666 0.042	11.728 0.038 -0.127 0.055	-0.065 0.058	-0.176 0.070	...	...	...
428 Feige 34		sdO	11.183	-0.354	11.643 0.038 11.563 0.043	11.540 0.033 +0.103 0.050	+0.080 0.057	+0.163 0.066 COM, WMG	...	...	...
429 LB 10694		sdB	15.42 P	...	13.676 0.032 13.416 0.041	13.322 0.038 +0.354 0.050	+0.260 0.052	+0.550 0.063	...	...	...
430 PG 1038+143		sdO(B)	14.82 P	...	15.653 0.056 15.877 0.159	15.895 0.252 -0.242 0.258	-0.224 0.169	-0.410 0.288	...	...	...
431 PG 1038+139		sdB-O	15.71 P	...	15.880 0.075 15.945 0.185	15.783 0.231 +0.097 0.243	-0.065 0.200	+0.048 0.286	...	...	...
433 TON 1273		sdB	13.15 $y$	-0.285	13.785 0.035 13.903 0.035	14.014 0.048 -0.229 0.059	-0.118 0.049	-0.318 0.070	...	...	...
435 TON 1281		sdB	13.439	+0.094	12.763 0.032 12.511 0.039	12.459 0.032 +0.304 0.045	+0.252 0.050	+0.494 0.059 COM, AEA	...	...	...
436 PG 1043+760		sdB	13.77 $y$	-0.219	14.278 0.036 14.359 0.056	14.593 0.108 -0.315 0.114	-0.081 0.067	-0.376 0.125	...	...	...
437 TON 1285		sdB	15.81 P	...	16.717 0.114 16.583 ...	16.561 ...	...	...	...	...	...
439 PG 1045+096		sd	15.89 P	...	16.018 0.095 15.370 0.088	15.265 0.188 +0.753 0.211	+0.648 0.129	+1.240 0.232 elon? <sup>f</sup>	...	...	...
440 PG 1046+189		sdB	15.29 P	...	14.756 0.034 14.584 0.055	14.431 0.068 +0.325 0.076	-0.172 0.065	+0.454 0.090	...	...	...
441 PG 1047+003		sdB	13.474	-0.290	14.152 0.045 14.214 0.065	14.319 0.080 -0.167 0.092	-0.062 0.079	-0.214 0.110 LAN	...	...	...
442 PG 1047-046		sdB	14.68 :	-0.18	15.527 0.067 15.637 0.127	15.501 0.201 +0.026 0.212	-0.110 0.144	-0.057 0.238	...	...	...
443 PG 1047-066		sdO(B)	14.77	-0.35	15.344 0.054 15.484 0.101	15.288 ...	...	-0.140 0.115	...	...	...
444 PG 1049+013		sdB	14.397	-0.132	15.217 0.113 15.240 0.167	14.843 ...	...	-0.023 0.202	...	...	AEA
445 PG 1050-065		sd	14.21 $y$	-0.245	14.775 0.050 14.934 0.080	14.853 0.129 -0.078 0.138	-0.159 0.094	-0.198 0.155	...	...	...
446 PG 1051+501		sdB	14.59	-0.32	14.096 0.062 14.181 0.084	14.432 0.069 -0.336 0.093	-0.085 0.104	-0.400 0.122	...	...	...
447 PG 1052-081		sd	15.39 $y$	-0.05	16.507 0.135 16.066 0.159	15.396 ...	...	+0.441 0.209	...	...	...
448 CBS 32		sdB	15.13 :	-0.020	14.268 0.031 14.175 0.042	14.108 0.055 +0.160 0.063	+0.093 0.052	+0.230 0.074	...	...	...
450 PG 1100-008		sdB	16.10 P	...	16.179 0.094 15.722 0.174	15.560 ...	...	+0.457 0.198	...	...	...
451 PG 1100-141		sd	15.58 $y$	-0.22	16.197 0.106 16.045 0.190	15.538 ...	...	+0.152 0.218	...	...	...
452 LB 1938		sd	13.64	-0.16	13.803 0.033 13.914 0.050	14.014 0.057 -0.211 0.066	-0.111 0.060	-0.294 0.080	...	...	...
453 LB 1941		sdB	14.88	+0.13	14.304 0.034 14.175 0.055	13.991 0.054 +0.313 0.064	+0.129 0.065	+0.410 0.081	...	...	...
454 PG 1101+113		sdO(A)	15.17	-0.28	15.987 0.098 16.115 0.227	16.757 ...	...	-0.128 0.247	...	...	...
455 Feige 36		sdB	12.70	-0.23	13.187 0.037 13.257 0.046	13.184 0.036 +0.003 0.052	-0.070 0.059	-0.050 0.068	...	...	...
457 PG 1102+499		sdO(B)	14.32 $y$	-0.295	15.049 0.045 15.272 0.104	15.213 0.141 -0.164 0.148	-0.223 0.113	-0.332 0.171	...	...	...
459 PG 1104+022		sdB+K2	11.82	+0.04	15.161 0.055 15.295 0.119	14.876 ...	...	-0.134 0.131	...	...	...
460 PG 1104+243		sd+K3	11.295	+0.073	10.768 0.043 10.520 0.036	10.510 0.039 +0.258 0.058	+0.248 0.056	+0.444 0.072 COM, AEA	...	...	...
461 TON 54		sdB	15.77 :	-0.29	16.476 0.121 16.222 0.222	15.751 ...	...	+0.254 0.253	...	...	...
462 TON 56		sdB	16.13 :	-0.90	16.147 0.104 15.629 ...	15.413 ...	...	...	...	...	...
464 G 56-17		sdB	16.08	+0.31	15.630 0.061 15.362 0.090	15.238 0.186 +0.392 0.196	+0.268 0.109	+0.594 0.212 hpm <sup>f</sup>	...	...	...

Continued on Next Page...

Table B.1 – Continued

No. <sup>1</sup>	ID <sup>2</sup>	Type	$V / y^3$	$B - V^3$	$J^4$	$H^4$	$K_S^4$	$J - K_S$	$J - H$	$Q^5$	Notes <sup>6</sup>
					mag	$\sigma$	mag	$\sigma$	mag	$\sigma$	
465 LB 254		sdB	15.32 P	...	14.364 0.033	14.173 0.054	14.036 0.063	+0.328 0.071	+0.191 0.063	+0.472 0.085	...
467 TON 59		sdB	15.06 P	...	15.904 0.070	15.981 0.125	15.340 0.144	+0.564 0.160	-0.077 0.143	+0.506 0.193	...
468 CBS 36		sdB	17.00 B	...	16.362 0.111	15.496 0.115	15.521 0.240	+0.841 0.264	+0.866 0.160	+1.492 0.290	...
469 PG 1108-018		sdO(A)	16.61	-0.27	16.434 0.108	16.467 0.199	15.785 ...	...	-0.033 0.226	...	...
470 PG 1109-070		sdB+K2	14.16 :	+0.07	13.960 0.044	13.741 0.052	13.611 0.062	+0.349 0.076	+0.219 0.068	+0.514 0.092	COM
471 PG 1109-016		sdB	15.36 P	...	15.313 0.053	15.291 0.091	15.237 0.176	+0.076 0.184	+0.022 0.105	+0.093 0.200	...
473 TON 62		sdB	14.09 y	-0.219	14.626 0.040	14.674 0.067	15.031 0.142	-0.405 0.148	-0.048 0.078	-0.441 0.159	...
474 PG 1110+045		sdO(A)	15.12 P	...	14.308 0.043	13.994 0.062	13.804 0.068	+0.504 0.080	+0.314 0.075	+0.740 0.098	...
475 PG 1111-077		sdB-O	13.666	-0.202	14.154 0.052	14.355 0.058	14.386 0.102	-0.232 0.114	-0.201 0.078	-0.383 0.128	SGL, AEA
476 PG 1111+339		sd	13.01	+0.23	11.272 0.026	10.786 0.027	10.697 0.024	+0.575 0.035	+0.486 0.037	+0.940 0.045	...
477 TON 1371		sdB	15.21 P	...	15.302 0.057	15.015 0.079	15.076 0.113	+0.226 0.127	+0.287 0.097	+0.442 0.146	...
478 Feige 38		sdB	13.00	-0.23	13.567 0.045	13.654 0.057	13.788 0.061	-0.221 0.076	-0.087 0.073	-0.286 0.094	...
479 PG 1115-065		sdB-O	15.03	-0.26	15.623 0.084	15.580 0.131	16.109 ...	...	+0.043 0.156	...	...
480 TON 577		sdB	15.41 P	...	16.373 0.136	16.311 ...	17.203 ...	...	...	...	...
481 TON 1384		sd	13.20 y	-0.216	13.726 0.029	13.894 0.041	13.902 0.044	-0.176 0.053	-0.168 0.050	-0.302 0.065	...
482 TON 63		sdB	14.34 y	-0.249	14.945 0.042	14.635 ...	14.477 ...	...	...	...	...
483 TON 64		sdB	15.86	-0.22	15.259 0.050	15.415 0.107	15.280 0.147	-0.021 0.155	-0.156 0.118	-0.138 0.179	SGL
485 PG 1118+061		sdB	14.28	-0.15	14.534 0.053	14.414 0.061	14.166 0.084	+0.368 0.099	+0.120 0.081	+0.458 0.116	...
486 PG 1119+377		sdB	15.72 P	...	16.787 0.152	17.116 ...	16.407 ...	...	...	...	...
487 LB 256		sdB	15.60 P	...	16.027 0.086	16.207 ...	16.615 ...	...	...	...	...
489 PG 1124+123		sd	15.71	-0.22	16.158 0.115	16.047 0.194	15.157 ...	...	+0.111 0.226	...	...
492 TON 67		sdB	14.72 P	...	15.929 0.075	16.363 0.223	15.745 0.203	+0.184 0.216	-0.434 0.235	-0.142 0.279	...
494 PG 1127+019		sdO(D)	13.01 P	...	14.498 0.043	14.751 0.077	14.688 0.114	-0.190 0.122	-0.253 0.088	-0.380 0.139	...
496 PG 1128+199		sdB	15.15 P	...	16.089 0.082	16.451 0.227	15.950 0.240	+0.139 0.254	-0.362 0.241	-0.133 0.312	...
497 CBS 141		sdB	16.00 B	...	16.355 0.110	16.236 0.240	16.565 ...	...	+0.119 0.264	...	...
498 PG 1129-081		sdB-O	16.06 P	...	14.618 0.040	14.219 0.047	14.248 0.084	+0.370 0.093	+0.399 0.062	+0.670 0.104	...
499 PG 1130-063		sdB	16.09	-0.33	16.684 0.145	17.720 ...	16.782 ...	...	...	...	...
500 PG 1130+054		sdB	14.92	-0.19	15.325 0.072	15.663 0.142	15.566 0.254	-0.241 0.264	-0.338 0.159	-0.495 0.290	...
501 LB 239		sdB	15.26	-0.21	15.321 0.051	15.164 0.086	15.492 0.165	-0.171 0.173	+0.157 0.100	-0.053 0.189	...
503 LB 2045		sdB	15.71 P	...	14.890 0.043	14.720 0.077	14.607 0.099	+0.283 0.108	+0.170 0.088	+0.411 0.127	...
504 PG 1133+103		sdB-O	15.42 P	...	15.784 0.082	16.175 0.197	15.972 ...	...	-0.391 0.213	...	...
506 PG 1134+463		sdO(B)	15.107	-0.325	15.951 0.086	16.086 0.203	15.953 0.250	-0.002 0.264	-0.135 0.220	-0.104 0.312	WMG
508 Feige 46		sdO	13.260	-0.297	13.968 0.040	14.106 0.053	14.260 0.059	-0.292 0.071	-0.138 0.066	-0.396 0.087	WMG
509 PG 1135-116		sdO(B)	15.70 P	...	16.690 0.150	16.876 ...	16.310 ...	...	...	...	...
510 PG 1136-003		sdB	14.52 y	-0.276	15.161 0.055	15.137 0.089	15.267 0.173	-0.106 0.182	+0.024 0.105	-0.088 0.198	...
511 PG 1137+470		sdB	15.46 P	...	16.164 0.093	15.816 0.143	15.858 ...	...	+0.348 0.171	...	...

Continued on Next Page...

Table B.1 – Continued

No. <sup>1</sup>	ID <sup>2</sup>	Type	$V / y^3$	$B - V^3$	$J^4$		$H^4$		$K_S^4$		$J - K_S$		$J - H$		$Q^5$		Notes <sup>6</sup>
					mag	$\sigma$	mag	$\sigma$	mag	$\sigma$	mag	$\sigma$	mag	$\sigma$	mag	$\sigma$	
513 KUV 11386+4229		sdB-O	15.90	-0.22	15.892	0.078	15.565	0.135	15.056	...	...	...	+0.327	0.156	...	...	...
514 PG 1138-101		sdB	14.54	$y$	-0.252		15.103	0.057	15.150	0.097	14.842	0.147	+0.261	0.158	-0.047	0.113	+0.226 0.179 ...
515 PG 1140-050		sdB-O	15.33	...	-0.15		15.165	0.055	15.125	0.077	14.766	0.114	+0.399	0.127	+0.040	0.093	+0.429 0.145 ...
516 LBQS 1140+0026		sdB	18.3	J	...		15.550	0.079	15.061	0.095	15.117	0.161	+0.433	0.179	+0.489	0.124	+0.801 0.202 ...
518 PG 1141-116		sd	14.77	P	...		13.621	0.041	13.454	0.044	13.404	0.051	+0.217	0.065	+0.167	0.060	+0.343 0.079 ...
519 PG 1141+000		sdB	15.97	-0.22	16.636	0.118	17.886	...	15.739	...	...	...	...	...	...	...	...
520 PG 1142-037		sdB-O	15.88	-0.21	16.437	0.114	16.527	0.212	15.307	...	...	...	-0.090	0.241	...	...	...
521 PG 1144+005		sdO(B)	15.04	P	...		15.979	0.101	16.133	0.233	15.975	...	-0.154	0.254	...	...	...
522 Feige 48		sd	13.48	-0.25	13.983	0.041	14.137	0.057	14.243	0.070	-0.260	0.081	-0.154	0.070	-0.376	0.097	...
524 PG 1145-135		sd	14.27	$y$	-0.187		14.774	0.050	14.947	0.081	14.819	0.125	-0.045	0.135	-0.173	0.095	-0.175 0.153 ...
527 CBS 146		sdB	16.00	B	...		16.319	0.102	15.981	...	15.571	...	...	...	...	...	...
528 KUV 11495+3925		sdB	15.35	+0.03	15.268	0.055	15.252	0.083	15.358	0.142	-0.090	0.152	+0.016	0.100	-0.078	0.170	...
529 PG 1150-105		sdB	15.06	$y$	-0.267		15.584	0.058	15.678	0.112	15.571	0.275	+0.013	0.281	-0.094	0.126	-0.058 0.297 ...
531 PG 1152-119		sdB	16.08	P	...		16.515	0.145	16.149	0.180	15.993	...	+0.366	0.231	...	...	...
533 BD+10°2357		sdO+A	8.70	...	...		8.542	0.017	8.479	0.041	8.461	0.034	+0.081	0.038	+0.063	0.044	+0.128 0.050 ...
534 TON 1462		sdB	14.91	P	...		15.611	0.062	15.694	0.112	15.478	0.170	+0.133	0.181	-0.083	0.128	+0.071 0.205 ...
536 PG 1154-031		sdB-O	16.29	P	...		16.433	0.097	16.388	0.202	15.476	...	...	...	+0.045	0.224	...
537 PG 1154-070		sd	14.33	$y$	-0.08		14.465	0.048	14.117	0.067	14.207	0.093	+0.258	0.105	+0.348	0.082	+0.520 0.122 ...
539 PG 1155+741		sdB	15.39	-0.15	15.040	0.057	14.687	0.059	14.481	0.082	+0.559	0.100	+0.353	0.082	+0.824	0.117	...
540 PG 1200+094		sdB-O	14.96	P	...		14.206	0.046	14.036	0.050	14.079	0.083	+0.127	0.095	+0.170	0.068	+0.255 0.108 ...
541 TON 74		sdB-O	15.31	P	...		15.127	0.045	14.819	0.060	14.723	0.093	+0.404	0.103	+0.308	0.075	+0.636 0.117 ...
542 LB 2197		sdB	13.61	-0.38	14.359	0.038	14.595	0.076	14.580	0.121	-0.221	0.127	-0.236	0.085	-0.398	0.142	...
543 HZ 17		sdB	15.50	-0.22	16.322	0.116	15.790	0.154	15.820	...	...	...	+0.532	0.193	...	...	...
544 PG 1203+093		sdB	15.26	P	...		15.608	0.077	15.737	0.147	16.755	...	-0.129	0.166	...	...	...
545 PG 1203-108		sdO(C)	15.56	P	...		16.350	0.118	15.999	0.182	15.573	0.246	+0.777	0.273	+0.351	0.217	+1.041 0.318 ...
547 LB 2211		sdB	14.92	P	...		15.576	0.063	15.691	0.141	15.737	0.219	-0.161	0.228	-0.115	0.154	-0.247 0.256 ...
550 HZ 18		sdB	15.15	-0.17	16.178	0.091	16.268	0.202	17.309	...	...	...	-0.090	0.222	...	...	...
551 PB 3854		sdB+?	13.75	-0.11	13.466	0.028	13.186	0.035	13.079	0.034	+0.387	0.044	+0.280	0.045	+0.598	0.056	COM
553 PG 1208+224		non-sd	15.10	$y$	-0.199		15.034	0.049	15.139	0.091	15.051	0.110	-0.017	0.120	-0.105	0.103	-0.096 0.143 ...
555 PG 1210+141		sd	14.71	$y$	-0.227		15.316	0.054	15.437	0.108	15.604	0.194	-0.288	0.201	-0.121	0.121	-0.379 0.221 ...
556 HZ 20		sdBp+?	15.02	+0.01	14.476	0.044	14.206	0.056	14.168	0.061	+0.308	0.075	+0.270	0.071	+0.511	0.092	...
557 CBS 158		sdB	14.00	B	...		12.129	0.040	11.919	0.037	11.910	0.040	+0.219	0.057	+0.210	0.054	+0.377 0.070 ...
558 HZ 22		sdB-O	13.11	$y$	-0.238		13.828	0.030	13.945	0.039	14.008	0.062	-0.180	0.069	-0.117	0.049	-0.268 0.078 s.bin
560 PG 1214+031		sd	13.94	$y$	-0.242		14.328	0.033	14.682	0.079	14.643	0.096	-0.315	0.102	-0.354	0.086	-0.581 0.121 ...
565 LBQS 1218+1606		sdB	18.7	J	...		15.956	0.099	15.350	0.124	15.300	0.149	+0.656	0.179	+0.606	0.159	+1.112 0.215 ...
566 PG 1219+533		sd	13.23	$y$	-0.299		13.925	0.033	14.008	0.054	14.118	0.074	-0.193	0.081	-0.083	0.063	-0.255 0.094 ...

Continued on Next Page...

Table B.1 – Continued

No. <sup>1</sup>	ID <sup>2</sup>	Type	$V / y^3$	$B - V^3$	$J^4$			$H^4$			$K_S^4$			$J - K_S$			$J - H$			$Q^5$			Notes <sup>6</sup>
					mag	$\sigma$	mag	$\sigma$	mag	$\sigma$	mag	$\sigma$	mag	$\sigma$	mag	$\sigma$	mag	$\sigma$	mag	$\sigma$	mag	$\sigma$	
568 PG 1220-056		sdO(C)	14.754	-0.318	15.414	0.064	15.489	0.108	15.365	0.228	+0.049	0.237	-0.075	0.126	-0.007	0.255	WMG						
572 PG 1223+059		non-sd	15.99	P	16.479	0.150	16.284	...	15.077	...	...	...	...	...	...	...	...	...	...	...	...	...	
574 PG 1224+672		non-sd	11.86	$y$	-0.213		12.421	0.029	12.569	0.038	12.665	0.034	-0.244	0.045	-0.148	0.048	-0.355	0.058	...	...	...	...	
576 PG 1225-122		sdB	14.604	-0.205	15.102	0.058	15.134	0.081	16.366	...	...	...	...	...	-0.032	0.100	...	...	...	...	...	...	AEA
579 PG 1230+226		sd	15.19	P	...		13.593	0.040	13.343	0.039	13.339	0.044	+0.254	0.059	+0.250	0.056	+0.442	0.072	...	...	...	...	
580 PG 1230+052		sdB	13.26	-0.20	-0.20		13.804	0.039	13.926	0.062	14.032	0.066	-0.228	0.077	-0.122	0.073	-0.320	0.095	...	...	...	...	
581 PG 1230+067		sdO(B)	13.20	$y$	-0.248		13.841	0.042	13.944	0.066	14.007	0.069	-0.166	0.081	-0.103	0.078	-0.243	0.100	...	...	...	...	
583 LB 2392		sd	13.98	-0.04	13.706	0.034	13.566	0.047	13.471	0.044	+0.235	0.056	+0.140	0.058	+0.340	0.071	COM						
584 LBQS 1232+1046		sdB	16.6	J	...		15.956	0.104	15.777	0.194	15.537	0.236	+0.419	0.258	+0.179	0.220	+0.554	0.306	...	...	...	...	
585 PG 1232-136		sdO(A)	13.24	-0.13	13.758	0.042	13.897	0.052	13.886	0.072	-0.128	0.083	-0.139	0.067	-0.233	0.097	SGL						
586 PG 1232+228		sd	15.62	P	...		14.899	0.052	14.743	0.083	14.568	0.084	+0.331	0.099	+0.156	0.098	+0.448	0.123	...	...	...	...	
587 Feige 65		sdB	12.0	-0.23	-0.23		12.597	0.025	12.716	0.027	12.804	0.029	-0.207	0.038	-0.119	0.037	-0.296	0.047	SGL				
588 PG 1234+481		DA	14.545	-0.350	14.977	0.049	14.955	0.076	14.937	0.107	+0.040	0.118	+0.022	0.090	+0.057	0.136	AEA						
589 TON 90		sdB	14.73	$y$	-0.24		15.448	0.055	15.682	0.135	15.595	0.165	-0.147	0.174	-0.234	0.146	-0.323	0.206	...	...	...	...	
591 BD+25°2534		sdB	10.5	-0.27	11.157	0.036	11.270	0.038	11.367	0.034	-0.210	0.050	-0.113	0.052	-0.295	0.063	...	...	...	...	...	...	
592 CS 1235		sdB	16.22	+0.14	15.646	0.083	14.938	...	14.115	...	...	...	...	...	...	...	...	...	...	...	...	...	
593 PG 1236+479		sdB	15.60	-0.21	16.219	0.108	16.089	0.223	15.720	...	...	...	+0.130	0.248	...	...	...	...	...	...	...	...	
594 TON 97		sdB	14.65	$y$	-0.235		15.273	0.051	15.473	0.122	15.503	0.156	-0.230	0.164	-0.200	0.132	-0.380	0.192	...	...	...	...	
595 PG 1237-141		sdB	15.72	P	...		16.664	0.169	17.028	...	16.283	...	...	...	...	...	...	...	...	...	...	...	
597 TON 101		sd	14.95	-0.18	15.189	0.064	15.107	0.098	15.457	0.166	-0.268	0.178	+0.082	0.117	-0.206	0.199	...	...	...	...	...	...	
598 TON 102		sdO He	13.54	-0.25	14.304	0.045	14.407	0.058	14.458	0.079	-0.154	0.091	-0.103	0.073	-0.231	0.106	SGL						
599 CS 1238		sdO	16.34	+0.06	13.532	...	13.194	0.052	12.997	0.047	...	...	...	...	...	...	...	...	...	...	...	...	
600 BD+18°2647		sdO	11.846	-0.337	12.504	0.039	12.697	0.040	12.747	0.042	-0.243	0.057	-0.193	0.056	-0.388	0.071	WMG						
602 TON 108		sdB	15.50	-0.25	16.179	0.122	16.183	0.262	16.157	...	...	...	-0.004	0.289	...	...	...	...	...	...	...	...	
603 TON 109		sdO(B)	15.733	-0.296	16.299	0.124	16.491	0.290	16.623	...	...	...	-0.192	0.315	...	...	...	...	...	...	...	...	
604 CS 1240		sdB	16.12	+0.17	15.343	0.067	15.295	...	14.604	...	...	...	...	...	...	...	...	...	...	...	...	...	
605 PG 1241-084		sdB	10.58	-0.219	10.974	0.040	11.093	0.049	11.122	0.037	-0.148	0.054	-0.119	0.063	-0.237	0.072	...	...	...	...	...	...	
607 PG 1241-101		sdB	15.57	P	...		15.468	0.070	15.318	0.097	15.225	0.204	+0.243	0.216	+0.150	0.120	+0.356	0.234	...	...	...	...	
612 TON 640		sdB	15.32	-0.34	15.917	0.083	16.290	0.214	15.039	...	...	...	-0.373	0.230	...	...	...	...	...	...	...	...	
615 PG 1244+113		sdB	14.17	-0.23	14.758	0.044	14.998	0.083	14.950	0.145	-0.192	0.152	-0.240	0.094	-0.372	0.168	...	...	...	...	...	...	
616 CS 1244		sdO	14.57	-0.16	14.181	0.051	14.293	0.083	14.205	0.092	-0.024	0.105	-0.112	0.097	-0.108	0.128	...	...	...	...	...	...	
618 PG 1245-042		sd	13.61	-0.128	13.876	0.043	13.886	0.049	13.976	0.067	-0.100	0.080	-0.010	0.065	-0.108	0.094	...	...	...	...	...	...	
620 CS 1246		sdB	14.59	+0.28	14.013	0.052	14.032	0.074	14.091	0.086	-0.078	0.100	-0.019	0.090	-0.092	0.121	...	...	...	...	...	...	
621 PG 1246-122		sdO	14.55	-0.16	15.115	0.045	15.328	0.097	15.348	0.199	-0.233	0.204	-0.213	0.107	-0.393	0.219	...	...	...	...	...	...	
622 PG 1247-115		sd	15.21	P	...		16.062	0.086	15.912	0.168	15.967	...	...	...	+0.150	0.189	...	...	...	...	...	...	
623 G 60-38B		sdO(B)	14.55	-0.02	14.811	0.052	14.174	0.061	13.899	0.065	+0.912	0.083	+0.637	0.080	+1.391	0.103	...	...	...	...	...	...	

Continued on Next Page...

Table B.1 – Continued

No. <sup>1</sup>	ID <sup>2</sup>	Type	$V / y^3$	$B - V^3$	$J^4$	$H^4$	$K_S^4$	$J - K_S$	$J - H$	$Q^5$	Notes <sup>6</sup>							
			mag	$\sigma$	mag	$\sigma$	mag	$\sigma$	mag	$\sigma$								
624 PB 4288		sdO(B)	15.94 P	...	16.660	0.153	17.490	...	16.856	...	...							
625 PG 1249+761		sdO He	15.423	-0.323	15.979	0.105	15.741	0.175	15.590	...	...							
626 GD 150		sdB	14.63	-0.27	15.219	0.047	15.236	0.086	15.396	0.139	-0.177	0.147	-0.017	0.098	-0.190	0.164	...	WMG
627 PG 1249+028		sdB	15.61 P	...	16.159	0.088	17.589	...	15.652	...	...	...	...	...	...	...	...	...
628 HZ 35		sdB	15.85	-0.32	16.387	0.143	17.546	...	16.588	...	...	...	...	...	...	...	...	...
629 PG 1251+019		sdO(B)	15.571	-0.328	16.315	0.132	15.892	...	15.400	...	...	...	...	...	...	...	...	WMG
630 TON 139		sdB	12.76	+0.07	12.215	0.031	12.042	0.036	11.998	0.028	+0.217	0.042	+0.173	0.048	+0.347	0.055	...	...
631 TON 140		sdB	15.43 P	...	16.507	0.113	16.361	...	16.049	...	...	...	...	...	...	...	...	...
633 PG 1255+546		sdO(A)	13.53 $y$	-0.250	14.184	0.047	14.379	0.059	14.418	0.072	-0.234	0.086	-0.195	0.075	-0.381	0.103	...	...
634 HZ 38		sdO	14.46	-0.28	14.889	0.056	15.116	0.075	15.133	0.120	-0.244	0.132	-0.227	0.094	-0.415	0.150	...	...
635 HZ 47		non-sd	15.51 :	-0.22	15.693	0.074	16.205	0.197	15.556	0.175	+0.137	0.190	-0.512	0.210	-0.248	0.247	...	...
636 PG 1257+171		sdB	14.319	-0.265	14.837	0.038	14.976	0.074	15.163	0.122	-0.326	0.128	-0.139	0.083	-0.431	0.142	AEA	...
638 PG 1257-026		sdB	13.96 $y$	+0.151	13.530	0.038	13.319	0.043	13.263	0.040	+0.267	0.055	+0.211	0.057	+0.426	0.070	...	...
639 PG 1257+010		sdB-0	15.79 :	-0.06	15.409	0.069	15.007	0.089	15.008	0.161	+0.401	0.175	+0.402	0.113	+0.703	0.195	...	...
640 HD 113001		sdO+F	10.58	-0.25	9.024	0.027	8.863	0.029	8.830	0.028	+0.194	0.039	+0.161	0.040	+0.315	0.049	COM	...
641 PG 1258+012		sdO(B)	15.89 P	...	16.398	0.160	16.157	0.219	16.382	...	...	...	+0.241	0.271	...	...	...	...
642 PG 1258-030		HBB	13.10 $y$	-0.109	13.325	0.041	13.362	0.041	13.454	0.052	-0.129	0.066	-0.037	0.058	-0.157	0.079	...	...
643 LB 27		sdO	15.97	-0.25	14.830	0.039	14.991	0.070	15.053	0.131	-0.223	0.137	-0.161	0.080	-0.344	0.150	...	...
644 TON 143		sdO He	15.658	-0.309	16.215	0.086	16.103	0.165	16.172	0.274	+0.043	0.287	+0.112	0.186	+0.127	0.319	WMG	...
646 HZ 39		sdB	15.40	-0.24	16.174	0.092	16.207	0.215	16.540	...	...	...	-0.033	0.234	...	...	...	...
647 CS 1303		sd/DA	15.99	+0.72	15.589	0.094	15.377	0.118	13.907	...	...	...	+0.212	0.151	...	...	...	...
649 PG 1303+097		sdB	14.50 $y$	-0.254	15.069	0.058	15.155	0.092	15.584	...	...	...	-0.086	0.109	...	...	...	...
650 PG 1303-114		sdB	13.96 $y$	-0.263	14.311	0.042	14.465	0.057	14.572	0.106	-0.261	0.114	-0.154	0.071	-0.377	0.126	SGL	...
651 PG 1304+491		sdB-O	13.78 $y$	-0.253	14.414	0.038	14.498	0.062	14.616	0.098	-0.202	0.105	-0.084	0.073	-0.265	0.118	...	...
654 PG 1310+179		sdB-O	15.38	-0.20	15.178	0.050	14.888	0.085	14.800	0.109	+0.378	0.120	+0.290	0.099	+0.596	0.141	...	...
656 LB 249		sdB-O	15.98	-0.21	16.536	0.136	16.207	...	16.659	...	...	...	...	...	...	...	...	...
657 HZ 40		sdB	14.81	-0.23	15.185	0.041	15.456	0.105	15.624	0.165	-0.439	0.170	-0.271	0.113	-0.643	0.190	...	...
658 PG 1313+165		sdB-O	15.93	-0.23	16.711	0.153	16.314	0.267	16.767	...	...	...	+0.397	0.308	...	...	...	...
659 Feige 75		sdB	14.57 $y$	-0.218	15.136	0.054	15.130	0.094	15.362	0.174	-0.226	0.182	+0.006	0.108	-0.221	0.199	...	...
660 PG 1314+442		sdO(A)	15.16 P	...	15.066	0.053	14.767	0.091	14.759	0.102	+0.307	0.115	+0.299	0.105	+0.532	0.139	...	...
661 PG 1314+003		sdO(C)	16.063	-0.357	16.792	0.159	16.390	...	16.357	...	...	...	...	...	...	...	WMG	...
662 PG 1315-077		HBB	12.25 $y$	-0.145	12.550	0.039	12.629	0.049	12.706	0.039	-0.156	0.055	-0.079	0.063	-0.215	0.073	...	...
663 PG 1315-123		sdB	15.39	+0.01	14.539	0.041	14.290	0.056	14.151	0.083	+0.388	0.093	+0.249	0.069	+0.575	0.106	COM, CV?	...
665 PG 1316-125		sd	15.15	-0.11	15.660	0.069	15.936	0.159	14.892	...	...	...	-0.276	0.173	...	...	...	...
666 PB 146		sdO(B)	14.77 P	...	15.607	0.071	16.016	0.203	15.806	0.245	-0.199	0.255	-0.409	0.215	-0.507	0.302	...	...
667 PG 1316+212		sdO	14.72 P	...	15.880	0.084	16.353	0.263	15.991	...	...	...	-0.473	0.276	...	...	...	...

Continued on Next Page...

Table B.1 – Continued

No. <sup>1</sup>	ID <sup>2</sup>	Type	$V / y^3$	$B - V^3$	$J^4$ mag $\sigma$	$H^4$ mag $\sigma$	$K_S^4$ mag $\sigma$	$J - K_S$ mag $\sigma$	$J - H$ mag $\sigma$	$Q^5$ mag $\sigma$	Notes <sup>6</sup>
668	Feige 80	sdO+?	11.350	-0.095	11.177 0.023	11.055 0.025	11.049 0.024	+0.128 0.033	+0.122 0.034	+0.220 0.042	WMG
669	PG 1318+062	sdO(C)	14.771	-0.289	15.369 0.059	15.503 0.106	15.369 ...	...	-0.134 0.121	...	WMG
671	TON 158	sdB-O	16.18	-0.25	16.608 0.142	16.903 ...	17.437 ...	...	...	...	...
673	HZ 44	sdO	11.712	-0.311	12.386 0.027	12.569 0.032	12.672 0.034	-0.286 0.043	-0.183 0.042	-0.424 0.053	SGL, WMG
674	TON 708	sdB	15.09	-0.26	15.915 0.067	16.104 0.198	15.901 0.231	+0.014 0.241	-0.189 0.209	-0.128 0.288	...
675	PG 1323+391	sdB	16.30	P	15.696 0.061	15.411 0.105	15.141 0.125	+0.555 0.139	+0.285 0.121	+0.769 0.166	...
676	PG 1323-085	B?	13.481	-0.140	13.766 0.040	13.773 0.059	13.795 0.070	-0.029 0.081	-0.007 0.071	-0.034 0.097	LAN
677	PG 1323+125	sdO	15.37	P	15.019 0.041	14.787 0.066	14.734 0.087	+0.285 0.096	+0.232 0.078	+0.459 0.113	...
678	PG 1323+042	sdO(A)	15.26	-0.04	14.927 0.050	14.545 0.062	14.529 0.108	+0.398 0.119	+0.382 0.080	+0.685 0.133	...
679	PG 1325+101	sdB-O	13.76	-0.31	14.622 0.049	14.764 0.071	14.866 0.147	-0.244 0.155	-0.142 0.086	-0.351 0.168	...
680	PG 1325+054	sdO He	14.409	-0.300	15.141 0.060	15.249 0.107	15.231 0.181	-0.090 0.191	-0.108 0.123	-0.171 0.212	WMG
681	PG 1326-132	sd	15.85	-0.31	16.337 0.121	16.115 0.209	16.064 ...	...	+0.222 0.241	...	...
683	PG 1327-119	sdB	15.72	P	16.213 0.122	16.196 0.207	15.721 ...	...	+0.017 0.240	...	...
684	PG 1327+546	sdB	15.17	P	13.886 0.030	13.630 0.040	13.615 0.042	+0.271 0.052	+0.256 0.050	+0.464 0.064	...
685	PG 1328+000	sdB	16.17	-0.27	16.668 0.124	16.790 ...	16.934 ...	...	...	...	...
687	Feige 81	sdB	13.48	-0.225	14.035 0.036	14.183 0.046	14.235 0.069	-0.200 0.078	-0.148 0.058	-0.311 0.089	SGL
688	PG 1330-074	sdB-O	14.89	P	14.255 0.045	13.990 0.056	14.126 0.071	+0.129 0.084	+0.265 0.072	+0.328 0.100	...
689	LB 270	sdB	15.01	P	15.337 0.063	15.204 0.080	15.222 0.140	+0.115 0.154	+0.133 0.102	+0.215 0.172	...
690	PG 1332-091	sd	15.88	P	16.777 0.161	16.521 ...	16.428 ...	...	...	...	...
691	Feige 84	sdB 3	11.84	-0.17	12.225 0.026	12.311 0.029	12.327 0.028	-0.102 0.038	-0.086 0.039	-0.167 0.048	...
692	TON 165	sdB	15.5	-0.43	16.135 0.090	15.970 0.178	16.691 ...	...	+0.165 0.199	...	...
693	PG 1334+629	sdB	15.41	P	14.204 0.048	13.795 0.048	13.728 0.052	+0.476 0.071	+0.409 0.068	+0.784 0.087	...
694	PG 1334+117	sdB-O	16.37	-0.19	16.013 0.087	15.775 0.133	15.484 ...	...	+0.238 0.159	...	...
695	PG 1336-018	sdB	13.45	y	14.594 0.047	14.646 0.060	14.635 0.099	-0.041 0.110	-0.052 0.076	-0.080 0.124	...
696	PG 1338+481	sdB	13.605	-0.244	14.166 0.041	14.318 0.057	14.279 0.067	-0.113 0.079	-0.152 0.070	-0.227 0.095	SGL, AEA
697	Feige 87	sdB	11.693	-0.095	11.484 0.033	11.359 0.039	11.312 0.034	+0.172 0.047	+0.125 0.051	+0.266 0.061	AEA
698	PG 1339+052	sdO	15.76	P	16.569 0.142	16.477 ...	16.931 ...	...	...	...	...
700	PG 1340+607	sdB	13.14	y	13.634 0.044	13.614 0.047	13.697 0.056	-0.063 0.071	+0.020 0.064	-0.048 0.086	...
701	PG 1343-101	sdB-O	13.76	y	14.317 0.056	14.393 0.088	14.413 0.112	-0.096 0.125	-0.076 0.104	-0.153 0.147	...
702	PG 1343+578	...	13.78	y	13.543 0.034	13.323 0.044	13.346 0.041	+0.197 0.053	+0.220 0.056	+0.362 0.068	...
703	TON 168	sdB	14.68	P	15.469 0.061	15.497 0.125	15.521 0.177	-0.052 0.187	-0.028 0.139	-0.073 0.214	...
704	PG 1344+114	sdB	14.76	P	15.430 0.070	15.457 0.127	16.191 ...	...	-0.027 0.145	...	...
706	PG 1347+086	sd	11.86	y	10.924 0.040	10.659 0.042	10.595 0.037	+0.329 0.054	+0.265 0.058	+0.528 0.069	...
707	PG 1348+745	sdB	15.75	P	16.563 0.156	16.182 ...	15.439 ...	...	...	...	...
708	PG 1348+083	sdB	15.65	P	15.219 0.053	15.080 0.087	15.286 0.180	-0.067 0.188	+0.139 0.102	+0.038 0.203	...
710	PG 1348+369	sdO(B)	13.525	-0.328	13.991 0.029	13.894 0.036	13.800 0.043	+0.191 0.052	+0.097 0.046	+0.264 0.062	WMG

Continued on Next Page...

Table B.1 – Continued

No. <sup>1</sup>	ID <sup>2</sup>	Type	$V / y^3$	$B - V^3$	$J^4$	$H^4$	$K_S^4$	$J - K_S$	$J - H$	$Q^5$	Notes <sup>6</sup>
					mag $\sigma$	mag $\sigma$	mag $\sigma$	mag $\sigma$	mag $\sigma$	mag $\sigma$	
711 PG 1349-012		sdB	15.40 P	...	16.192 0.115	16.363 0.201	15.338 ...	...	-0.171 0.232	...	...
712 PG 1349+659		sdO(A)	15.72 P	...	16.597 0.119	16.761 ...	16.021 0.255	+0.576 0.281	...	...	...
713 LSE 44		sdO	12.45	-0.240	13.006 0.039	13.136 0.053	13.208 0.046	-0.202 0.060	-0.130 0.066	-0.300 0.078	...
714 LSE 153		sdO	11.35	-0.26	11.923 0.040	12.057 0.050	12.132 0.034	-0.209 0.052	-0.134 0.064	-0.310 0.071	...
715 PG 1350+372		sdB	14.36 $y$	-0.237	14.923 0.036	14.877 0.061	15.039 0.107	-0.116 0.113	+0.046 0.071	-0.081 0.125	...
716 PB 890		sdB	14.25 $y$	-0.146	14.565 0.033	14.799 0.057	14.764 0.086	-0.199 0.092	-0.234 0.066	-0.375 0.105	...
717 PG 1351+139		sdB	15.73 P	...	15.791 0.070	15.435 0.112	15.006 0.140	+0.785 0.157	+0.356 0.132	+1.053 0.186	...
718 PG 1352-022		sdB	12.12	-0.24	12.759 0.039	12.937 0.054	13.029 0.043	-0.270 0.058	-0.178 0.067	-0.404 0.077	...
719 Feige 88		sd	15.67	-0.14	16.013 0.104	15.860 0.191	15.933 ...	...	+0.153 0.217	...	...
720 PB 4148		sd	15.76 P	...	16.256 0.124	16.085 ...	15.789 ...	...	...	...	...
721 PB 4150		sdB	15.49 P	...	15.972 0.093	15.814 0.170	15.336 0.165	+0.636 0.189	+0.158 0.194	+0.755 0.239	...
723 PG 1355-064		sdO(B)	13.748	-0.316	14.426 0.045	14.570 0.064	14.574 0.099	-0.148 0.109	-0.144 0.078	-0.256 0.124	AEA
724 PG 1355+071		sdB	14.31 $y$	-0.199	14.974 0.056	14.991 0.079	14.932 0.143	+0.042 0.154	-0.017 0.097	+0.029 0.170	...
725 PG 1356-047		sdB-O	15.64 P	...	15.754 0.075	15.547 0.116	15.349 0.185	+0.405 0.200	+0.207 0.138	+0.561 0.225	...
726 TON 179		sdO(A)	15.15 P	...	15.433 0.057	15.281 0.106	14.989 0.153	+0.444 0.163	+0.152 0.120	+0.558 0.186	...
727 PG 1356+354		sdB	14.61 P	...	15.501 0.055	15.576 0.111	15.574 0.194	-0.073 0.202	-0.075 0.124	-0.129 0.222	...
728 PG 1357+501		sdB	15.94 P	...	15.986 0.069	15.812 0.121	15.322 ...	...	+0.174 0.139	...	...
729 LB 705		sdO(C)	16.07 P	...	15.172 0.054	15.304 0.120	15.022 0.115	+0.150 0.127	-0.132 0.132	+0.051 0.161	...
730 TON 180		sdB	16.03 P	...	15.560 0.063	15.348 0.100	15.026 ...	...	+0.212 0.118	...	...
731 PG 1359+077		sdB	15.72 P	...	15.657 0.069	15.418 0.106	15.461 0.223	+0.196 0.233	+0.239 0.126	+0.376 0.252	...
732 Balloon 082700002		bin?	16.4	+0.60	16.462 0.132	15.633 0.133	15.104 0.165	+1.358 0.211	+0.829 0.187	+1.981 0.254	Gal <sup>f</sup>
734 PB 1207		non-sd	12.195	-0.178	12.593 0.026	12.756 0.030	12.732 0.029	-0.139 0.039	-0.163 0.040	-0.262 0.049	AEA
735 PB 1229		sdB	15.76 :	-0.31	16.400 0.102	15.827 ...	15.896 0.246	+0.504 0.266	...	...	...
736 PG 1400+224		sdB	15.68 P	...	15.125 0.049	14.733 0.075	14.603 0.074	+0.522 0.089	+0.392 0.090	+0.817 0.112	...
737 PG 1401+289		sdO He	14.87 P	...	15.539 0.059	15.739 0.143	15.509 ...	...	-0.200 0.155	...	...
738 PG 1401+377		sdB	16.30 :	-0.27	16.298 0.099	17.090 ...	15.808 0.221	+0.490 0.242	...	...	...
739 PG 1402+065		sd	15.65	-0.16	16.181 0.092	15.992 0.169	16.445 ...	...	+0.189 0.192	...	...
740 TON 181		sd	14.73	+0.10	14.244 0.032	14.164 0.048	14.027 0.067	+0.217 0.074	+0.080 0.058	+0.277 0.086	...
741 PG 1403+019		sd	15.90	...	16.306 0.112	16.395 ...	16.939 ...	...	...	...	...
742 Feige 89		sd	14.67	-0.24	14.773 0.053	14.837 0.072	14.980 0.141	-0.207 0.151	-0.064 0.089	-0.255 0.165	...
743 PG 1403-110		sdB	15.87 P	...	16.654 0.137	16.584 ...	15.788 ...	...	...	...	...
744 TON 183		sdB	13.53 $y$	-0.250	14.179 0.039	14.376 0.056	14.636 0.084	-0.457 0.093	-0.197 0.068	-0.605 0.106	SGL
745 TON 185		sdB	15.84 P	...	15.515 0.061	15.151 0.087	15.094 0.109	+0.421 0.125	+0.364 0.106	+0.695 0.148	...
746 Feige 91		sdB	13.50 $y$	-0.275	14.084 0.035	14.320 0.053	14.407 0.086	-0.323 0.093	-0.236 0.064	-0.500 0.105	...
747 PB 1516		sdB	15.77 P	...	15.704 0.070	15.445 0.116	15.422 ...	...	+0.259 0.136	...	...
748 LB 721		sdB	15.66 $y$	-0.26	16.390 0.149	16.209 ...	15.769 ...	...	...	...	...

Continued on Next Page...

Table B.1 – Continued

No. <sup>1</sup>	ID <sup>2</sup>	Type	$V / y^3$	$B - V^3$	$J^4$	$H^4$	$K_S^4$	$J - K_S$	$J - H$	$Q^5$	Notes <sup>6</sup>			
			mag	$\sigma$	mag	$\sigma$	mag	$\sigma$	mag	$\sigma$				
749 PG 1407-013		sdB	13.750	-0.259	14.368	0.040	14.407	0.056	14.397	0.084	-0.029 0.093	-0.039 0.069	-0.058 0.106	LAN
750 KUV 14081+3239		sdB	14.61 P	...	15.559	0.059	15.878	0.167	15.779	0.214	-0.220 0.222	-0.319 0.177	-0.460 0.259	...
751 SA 58-327		sdBp	13.00 P	...	14.024	0.044	14.114	0.050	14.151	0.067	-0.127 0.080	-0.090 0.067	-0.195 0.095	...
752 PG 1408+098		sdB-O	13.93	-0.29	14.694	0.052	14.819	0.078	15.210	0.174	-0.516 0.182	-0.125 0.094	-0.610 0.195	...
753 PG 1409+604		sdB-O	14.45 $y$	+0.137	13.778	0.034	13.554	0.047	13.478	0.040	+0.300 0.052	+0.224 0.058	+0.468 0.068	...
754 PG 1409-103		sdO(A)	14.20	-0.27	14.863	0.047	15.101	0.097	14.822	0.130	+0.041 0.138	-0.238 0.108	-0.138 0.160	...
755 PG 1409-091		sdB	14.48 $y$	+0.038	14.028	0.043	13.743	0.050	13.925	0.064	+0.103 0.077	+0.285 0.066	+0.317 0.092	...
756 PG 1411+590		sdB	15.68 P	...	15.942	0.079	15.587	0.139	15.465	0.182	+0.477 0.198	+0.355 0.160	+0.744 0.232	...
757 PG 1411-061		sdB	14.56	+0.08	15.157	0.059	15.124	0.097	15.094	0.165	+0.063 0.175	+0.033 0.114	+0.088 0.195	...
759 PG 1412+612		sdO(C)	14.865	-0.313	15.510	0.054	15.479	0.098	15.461	0.158	+0.049 0.167	+0.031 0.112	+0.072 0.187	WMG
760 PB 1811		sdB	14.71 P	...	15.369	0.047	15.369	0.096	15.652	0.242	-0.283 0.247	+0.000 0.107	-0.283 0.260	...
761 PG 1413+114		sdO(D)	16.07	-0.36	16.609	0.141	16.701	0.319	15.514	...	...	-0.092 0.349	...	...
762 PG 1415-043		sdB-O	13.78 $y$	-0.249	14.377	0.045	14.518	0.070	14.709	0.112	-0.332 0.121	-0.141 0.083	-0.438 0.136	...
763 PG 1415+492		sdO(D)	14.44 P	...	14.966	0.048	15.031	0.072	15.243	0.118	-0.277 0.127	-0.065 0.087	-0.326 0.143	...
764 PG 1415+079		sdO(A)	15.70	-0.08	15.782	0.070	15.701	0.121	15.938	...	...	+0.081 0.140	...	...
766 TON 194		sdB	13.78 $y$	-0.233	14.296	0.030	14.421	0.052	14.443	0.073	-0.147 0.079	-0.125 0.060	-0.241 0.091	SGL
767 PG 1418+178		sdB	15.95 P	...	15.904	0.083	15.459	0.116	15.710	0.207	+0.194 0.223	+0.445 0.143	+0.529 0.248	...
768 PG 1419+081		sd	15.10	-0.16	14.844	0.054	14.557	0.069	14.585	0.101	+0.259 0.115	+0.287 0.088	+0.475 0.133	...
769 PG 1419+062		sd	16.23 $y$	+0.22	16.235	0.121	16.487	0.245	15.871	...	...	-0.252 0.273	...	...
770 [CW83] 1419-09		sdOB	12.09 $y$	-0.275	12.692	0.023	12.835	0.025	12.957	0.030	-0.265 0.038	-0.143 0.034	-0.373 0.046	...
771 PG 1420+162		sdB	15.98 P	...	14.431	0.046	14.207	0.050	14.119	0.067	+0.312 0.081	-0.224 0.068	+0.480 0.096	...
772 PG 1420+518		sdB	15.75 P	...	14.376	0.038	13.764	0.046	13.705	0.059	+0.671 0.070	+0.612 0.060	+1.131 0.083	...
773 PG 1421+150		sdB	15.32	-0.15	15.279	0.048	15.177	0.082	15.170	0.130	+0.109 0.139	+0.102 0.095	+0.186 0.156	...
774 PG 1421-121		sdB	15.39 P	...	15.891	0.080	15.872	0.171	16.274	...	...	+0.019 0.189	...	...
775 PG 1421+345		sdB+K3	14.78	+0.14	14.000	0.037	13.688	0.047	13.690	0.043	+0.310 0.057	+0.312 0.060	+0.545 0.073	COM
778 PG 1423-035		sd	15.41 P	...	16.122	0.087	16.303	0.208	15.970	...	...	-0.181 0.225	...	...
779 TON 199		sdB	14.27 $y$	-0.194	14.772	0.035	14.876	0.078	14.924	0.119	-0.152 0.124	-0.104 0.085	-0.230 0.140	...
781 PG 1425+590		sdO(C)	16.039	-0.323	16.698	0.141	17.074	...	17.047	...	...	...	...	WMG
782 PG 1425+219		sdB	15.71 P	...	15.500	0.056	15.303	0.094	15.421	0.220	+0.079 0.227	+0.197 0.109	+0.227 0.241	...
784 Feige 95		sdB	13.20	-0.22	13.834	0.030	14.033	0.051	13.999	0.075	-0.165 0.081	-0.199 0.059	-0.315 0.092	...
785 PG 1426-067		sdB	14.50	-0.20	14.715	0.046	14.386	0.054	14.377	0.086	+0.338 0.098	+0.329 0.071	+0.585 0.112	...
786 PG 1427+195		sdO(C)	14.110	-0.292	14.876	0.043	15.180	0.088	15.321	0.201	-0.445 0.206	-0.304 0.098	-0.674 0.219	WMG
787 TON 203		sdB	15.80 $y$	-0.15	15.846	0.069	15.616	0.115	15.516	0.205	+0.330 0.216	+0.230 0.134	+0.503 0.238	...
789 PG 1429+406		sd	12.86 $y$	+0.457	11.941	0.033	11.688	0.032	11.664	0.028	+0.277 0.043	+0.253 0.046	+0.467 0.055	...
790 HD 127493		sdO	10.03 $y$	-0.261	10.641	0.037	10.816	0.039	10.907	0.036	-0.266 0.052	-0.175 0.054	-0.398 0.066	...
791 BPS CS 22874-14		sdB	14.95	-0.34	15.473	0.069	15.334	0.119	15.902	0.340	-0.429 0.347	+0.139 0.138	-0.324 0.362	...

Continued on Next Page...



Table B.1 – Continued

No. <sup>1</sup>	ID <sup>2</sup>	Type	$V / y^3$	$B - V^3$	$J^4$		$H^4$		$K_S^4$		$J - K_S$		$J - H$		$Q^5$		Notes <sup>6</sup>
					mag	$\sigma$	mag	$\sigma$	mag	$\sigma$	mag	$\sigma$	mag	$\sigma$	mag	$\sigma$	
792 PG 1430+066		sdB	15.91 P	...	16.321	0.122	16.220	0.229	16.895...	...	...	...	+0.101	0.259	...	...	...
794 PG 1430+427		non-sd	14.47	-0.09	14.563	0.033	14.585	0.065	14.572	0.093	-0.009	0.099	-0.022	0.073	-0.026	0.113	...
797 BPS CS 22871-19		sdO He	13.25	-0.28	13.773	0.037	13.848	0.053	13.933	0.067	-0.160	0.077	-0.075	0.065	-0.216	0.091	SGL
800 PG 1432+004		sdB	12.76 y	-0.188	13.244	0.043	13.316	0.053	13.436	0.052	-0.192	0.067	-0.072	0.068	-0.246	0.084	...
802 HD 128220		sdO+G	8.54	+0.21	7.425	0.011	7.078	0.005	7.021	0.017	+0.404	0.020	+0.347	0.012	+0.665	0.022	s.bin
803 TON 208		sdB-O	16.22 y	-0.25	15.997	0.076	15.682	0.126	15.448	0.170	+0.549	0.186	+0.315	0.147	+0.786	0.216	...
804 PG 1432+158		sdB	13.90 y	-0.225	14.445	0.032	14.530	0.054	14.650	0.075	-0.205	0.082	-0.085	0.063	-0.269	0.095	SGL
805 TON 209		sdB	12.45	-0.21	13.105	0.027	13.242	0.034	13.383	0.040	-0.278	0.048	-0.137	0.043	-0.381	0.058	...
806 BPS CS 22874-1		sdB	14.8 B	...	16.235	0.104	16.214	0.210	17.024...	...	...	...	+0.021	0.234	...	...	...
809 PG 1434+386		sdB-O	15.41	-0.34	15.800	0.067	15.876	0.136	15.494...	...	...	...	-0.076	0.152	...	...	...
811 PG 1435+098		sdO(B)	16.22 P	...	15.134	0.054	14.936	0.068	14.747	0.103	+0.387	0.116	+0.198	0.087	+0.536	0.133	...
812 PG 1437+727		sdO(D)	13.63 P	...	15.793	0.081	15.843	0.179	16.093...	...	...	...	-0.050	0.196	...	...	...
814 TON 780		sdB	14.94 y	-0.234	15.490	0.060	15.515	0.106	15.923	0.198	-0.433	0.207	-0.025	0.122	-0.452	0.226	...
815 PG 1438-078		sdO(A)	14.58	+0.29	13.544	0.044	13.158	0.053	13.122	0.044	+0.422	0.062	+0.386	0.069	+0.712	0.081	...
816 PG 1438-029		sdB	13.82 P	...	14.168	0.043	14.240	0.070	14.201	0.072	-0.033	0.084	-0.072	0.082	-0.087	0.104	...
819 PG 1438+018		sdB	15.00	-0.25	14.768	0.049	14.827	0.074	14.766	0.112	+0.002	0.122	-0.059	0.089	-0.042	0.139	...
822 PG 1439-013		sdB	13.912	-0.293	14.506	0.047	14.692	0.061	14.782	0.118	-0.276	0.127	-0.186	0.077	-0.416	0.140	SGL, AEA
823 PG 1440+174		sdB	15.39 P	...	15.094	0.042	14.883	0.068	14.783	0.102	+0.311	0.110	+0.211	0.080	+0.470	0.125	...
825 BPS CS 22874-104		sdB	15.1 B	...	15.398	0.058	15.483	0.110	15.661	0.224	-0.263	0.231	-0.085	0.124	-0.327	0.249	...
826 PG 1442+346		sdO(C)	15.13 y	-0.263	16.559	0.136	16.291...	...	17.125...	...	...	...	...	...	...	...	...
828 PG 1442+342		sd	14.60	-0.28	15.196	0.048	15.317	0.105	15.810	0.307	-0.614	0.311	-0.121	0.115	-0.705	0.323	...
831 BPS CS 22871-84		sdB	14.3 B	...	14.686	0.048	14.814	0.071	14.808	0.123	-0.122	0.132	-0.128	0.086	-0.218	0.147	...
832 PG 1444+487		sdB	15.85 P	...	15.521	0.058	15.464	0.101	15.052	0.159	+0.469	0.169	+0.057	0.116	+0.512	0.190	...
834 PG 1444+076		sdO(B)	14.655	-0.304	15.384	0.062	15.503	0.139	15.182...	...	...	...	-0.119	0.152	...	...	WMG
835 PG 1444+236		sd	13.14 y	-0.146	13.269	0.026	13.214	0.035	13.079	0.039	+0.190	0.047	+0.055	0.044	+0.231	0.057	em <sup>f</sup>
836 PG 1446+084		sdB	16.12 P	...	16.206	0.110	15.877	0.196	14.909...	...	...	...	+0.329	0.225	...	...	...
838 BPS CS 22874-121		sdB	15.2 B	...	15.843	0.075	15.760	0.125	15.919...	...	...	...	+0.083	0.146	...	...	...
840 PG 1447+459		sdO(A)	15.32	-0.29	14.733	0.039	14.387	0.053	14.127	0.068	+0.606	0.078	+0.346	0.066	+0.866	0.092	...
841 PG 1447+249		sdB	15.42 P	...	16.371	0.123	16.622...	...	15.700	0.315	+0.671	0.338	...	...	...	...	...
842 PG 1448-052		sdB-O	14.60 y	-0.227	15.199	0.062	15.234	0.102	15.105	0.181	+0.094	0.191	-0.035	0.119	+0.068	0.211	...
843 PG 1448+485		sdB	15.84 P	...	16.545	0.128	16.799...	...	14.982...	...	...	...	...	...	...	...	...
844 PG 1449+653		sdB	13.611	-0.035	13.283	0.046	13.058	0.044	13.068	0.042	+0.215	0.062	+0.225	0.064	+0.384	0.078	AEA
845 PG 1449+530		sdO:	15.13 P	...	16.018	0.084	16.499...	...	15.591...	...	...	...	...	...	...	...	...
846 PG 1449+582		sdB	15.43 P	...	16.204	0.094	16.372	0.205	15.709...	...	...	...	-0.168	0.226	...	...	...
847 PG 1451+528		sdB	16.23 P	...	16.661	0.155	16.324...	...	16.095...	...	...	...	...	...	...	...	...

Continued on Next Page...

Table B.1 – Continued

No. <sup>1</sup>	ID <sup>2</sup>	Type	$V / y^3$	$B - V^3$	$J^4$	$H^4$	$K_S^4$	$J - K_S$	$J - H$	$Q^5$	Notes <sup>6</sup>
					mag $\sigma$	mag $\sigma$	mag $\sigma$	mag $\sigma$	mag $\sigma$	mag $\sigma$	
849 PG	1451+472	???	13.12 $y$	+0.397	12.158 0.043	12.013 0.039	11.861 0.039	+0.297 0.058	+0.145 0.058	+0.406 0.073 v.cool	
850 PG	1452+198	sdB	12.48 $y$	-0.232	13.055 0.023	13.179 0.025	13.276 0.033	-0.221 0.040	-0.124 0.034	-0.314 0.047	...
851 PG	1452+475	sdB	15.74 P	...	16.781 0.148	15.859 ...	15.741 ...	...	...	...	...
852 PG	1453-080	sdB	14.27 $y$	-0.083	14.471 0.043	14.422 0.064	14.454 0.078	+0.017 0.089	+0.049 0.077	+0.054 0.106	...
853 PG	1453-113	sdO(B)	15.42 P	...	15.103 0.054	15.083 0.088	15.037 0.139	+0.066 0.149	+0.020 0.103	+0.081 0.168	...
858 PG	1455+501	sdB	15.37 :	-0.11	14.933 0.051	14.759 0.065	14.561 0.084	+0.372 0.098	+0.174 0.083	+0.503 0.116	...
860 PG	1457+192	sdB-O	13.99 P	...	14.921 0.048	14.998 0.081	15.381 0.203	-0.460 0.209	-0.077 0.094	-0.518 0.221	...
861 PG	1457+198	sdB-O	15.91	-0.16	16.418 0.117	16.423 0.232	16.641 ...	...	-0.005 0.260	...	...
862 PG	1458+423	sdB	13.79	-0.24	14.455 0.040	14.545 0.061	14.865 0.102	-0.410 0.110	-0.090 0.073	-0.478 0.123	...
863 PG	1459+416	sd	13.60	-0.15	13.689 0.033	13.798 0.044	13.750 0.048	-0.061 0.058	-0.109 0.055	-0.143 0.071	...
864 PG	1459-048	sd	14.08 $y$	+0.121	12.819 0.041	12.578 0.051	12.540 0.043	+0.279 0.059	+0.241 0.065	+0.460 0.077	...
866 PG	1500+053	sdB	15.65 P	...	16.031 0.118	16.273 0.234	14.861 ...	...	-0.242 0.262	...	...
867 PG	1501+426	sdB	14.53	-0.23	15.280 0.063	15.195 0.104	15.454 0.175	-0.174 0.186	+0.085 0.122	-0.110 0.207	...
868 PG	1502+129	sdO(B)	15.46 P	...	16.097 0.094	16.204 0.218	15.897 ...	...	-0.107 0.237	...	...
869 PG	1502+061	sdB	15.58 P	...	15.656 0.070	15.946 0.134	15.408 ...	...	-0.290 0.151	...	...
870 PG	1502-103	sdB+K0	15.51 :	+0.04	14.970 0.055	14.767 0.075	14.850 0.122	+0.120 0.134	+0.203 0.093	+0.273 0.151	...
871 PG	1502+113	sdB	15.33 :	-0.25	16.078 0.097	16.001 0.231	15.419 0.218	+0.659 0.239	-0.077 0.251	+0.717 0.305	...
873 PG	1505+074	sdB	12.44 $y$	-0.285	13.058 0.040	13.208 0.051	13.304 0.048	-0.246 0.062	-0.150 0.065	-0.359 0.079	...
875 PG	1506+102	sdO(A)	15.26	-0.24	15.833 0.062	15.846 0.132	15.931 ...	...	-0.013 0.146	...	...
876 PG	1506-052	sdOB	13.97 $y$	-0.218	14.423 0.045	14.541 0.073	14.660 0.111	-0.237 0.120	-0.118 0.086	-0.326 0.136	...
877 PG	1507-015	sdO(B)	15.98 P	...	16.772 0.176	17.175 ...	16.420 ...	...	...	...	...
878 PG	1508+443	sdO(B)	14.972	-0.285	15.683 0.079	15.828 0.185	15.200 ...	...	-0.145 0.201	...	WMG
879 PG	1508+177	sdB+K1	16.28	+0.05	15.797 0.064	15.562 0.109	15.527 0.160	+0.270 0.172	+0.235 0.126	+0.447 0.196	...
881 PG	1508-101	sdB	15.16 P	...	14.861 0.050	14.626 0.059	14.583 0.101	+0.278 0.113	+0.235 0.077	+0.455 0.127	...
882 PG	1509-083	sdB	14.608	-0.145	15.030 0.058	15.183 0.091	15.227 ...	...	-0.153 0.108	...	AEA
884 PG	1511+367	...	12.11 $y$	-0.151	12.414 0.026	12.490 0.026	12.541 0.027	-0.127 0.037	-0.076 0.037	-0.184 0.046	...
885 PG	1511+447	sdO(A)	15.60 P	...	16.314 0.129	15.991 ...	16.974 ...	...	...	...	...
886 PG	1511+624	sd+K5	14.527	-0.022	14.107 0.041	13.807 0.044	13.845 0.056	+0.262 0.069	+0.300 0.060	+0.488 0.082 COM, AEA	...
887 PG	1511-110	sdO(C)	14.965	-0.190	15.599 0.079	15.650 0.111	15.312 ...	...	-0.051 0.136	...	WMG
888 PG	1511-048	sdB	15.64 :	-0.32	16.012 0.088	16.158 0.155	16.851 ...	...	-0.146 0.178	...	...
889 PG	1512-035	sdO(B)	15.89 P	...	16.757 0.156	16.069 ...	16.738 ...	...	...	...	...
890 TON	788	sdB	13.20	-0.18	13.696 0.032	13.957 0.048	14.004 0.073	-0.308 0.080	-0.261 0.058	-0.504 0.091	...
891 PG	1513-045	sdB	16.21	-0.17	16.088 0.089	15.842 0.133	15.944 ...	...	+0.246 0.160	...	...
892 PG	1514+455	sdB	15.15 P	...	15.400 0.064	15.622 0.155	16.662 ...	...	-0.222 0.168	...	...
893 LB	9555	sdB	15.51 :	-0.09	14.772 0.039	14.392 0.057	14.381 0.082	+0.391 0.091	+0.380 0.069	+0.677 0.105	...
895 PG	1514+034	sdB+K2	13.997	-0.009	13.579 0.039	13.328 0.045	13.270 0.041	+0.309 0.057	+0.251 0.060	+0.498 0.073 LAN	...

Continued on Next Page...

Table B.1 – Continued

No. <sup>1</sup>	ID <sup>2</sup>	Type	$V / y^3$	$B - V^3$	$J^4$		$H^4$		$K_S^4$		$J - K_S$		$J - H$		$Q^5$		Notes <sup>6</sup>
					mag	$\sigma$	mag	$\sigma$	mag	$\sigma$	mag	$\sigma$	mag	$\sigma$	mag	$\sigma$	
898 PG 1515+044		sdB+K4	15.46	-0.03	14.907	0.047	14.616	0.063	14.596	0.107	+0.311	0.117	+0.291	0.079	+0.530	0.131	...
899 PG 1516+205		sdB	15.16	P	14.019	0.031	13.750	0.033	13.680	0.045	+0.339	0.055	+0.269	0.045	+0.541	0.065	...
900 TON 228		sdB+K3	15.95	-0.12	15.601	0.062	15.272	0.102	15.437	0.143	+0.164	0.156	+0.329	0.119	+0.411	0.180	...
901 PG 1518-098		sdO He	13.76	y	14.175	0.040	14.309	0.067	14.456	0.085	-0.281	0.094	-0.134	0.078	-0.382	0.111	...
902 LB 810		sdO(A)	15.90	-0.42	16.393	0.098	16.783	...	16.225	...	...	...	...	...	...	...	...
903 PG 1519-071		sdB	15.60	P	16.374	0.120	16.175	0.200	15.737	...	...	...	+0.199	0.233	...	...	...
904 PG 1519+640		sdB	12.433	-0.245	13.007	0.028	13.185	0.041	13.164	0.044	-0.157	0.052	-0.178	0.050	-0.291	0.064	SGL, AEA
905 Balloon 081400004		bin?	16.5	+0.51	14.832	0.043	14.464	0.061	14.456	0.079	+0.376	0.090	+0.368	0.075	+0.653	0.106	...
906 BPS CS 22890-74		sdB	17.2	+0.53	13.497	0.040	13.376	0.052	13.305	0.047	+0.192	0.062	+0.121	0.066	+0.283	0.079	...
908 PG 1522-013		sdB	15.35	-0.06	15.386	0.053	15.368	0.108	15.344	0.202	+0.042	0.209	+0.018	0.120	+0.056	0.228	...
909 TON 231		sdB	15.62	...	15.720	0.086	15.597	0.133	15.067	0.122	+0.653	0.149	+0.123	0.158	+0.745	0.191	...
910 PG 1522-104		sd	15.62	P	14.907	0.051	14.668	0.066	14.579	0.090	+0.328	0.103	+0.239	0.083	+0.508	0.120	...
911 PG 1524+439		sdB+K3	15.57	+0.03	14.455	0.037	14.072	0.051	14.007	0.050	+0.448	0.062	+0.383	0.063	+0.736	0.078	COM
912 PG 1524+611		sdB-O	12.80	y	12.283	0.026	12.091	0.034	12.070	0.032	+0.213	0.041	+0.192	0.043	+0.357	0.052	...
913 PG 1525-009		sdB	14.839	-0.073	14.980	0.054	15.007	0.096	15.233	0.191	-0.253	0.198	-0.027	0.110	-0.273	0.215	AEA
914 PG 1525+103		sd	15.83	P	13.879	0.038	13.342	0.041	13.141	0.045	+0.738	0.059	+0.537	0.056	+1.142	0.072	...
915 PG 1525-071		sdO	15.053	-0.198	14.995	0.049	14.605	0.072	14.495	0.095	+0.500	0.107	+0.390	0.087	+0.793	0.125	LAN
916 PG 1525+024		sdB	15.40	-0.23	15.876	0.072	15.640	0.116	15.656	0.233	+0.220	0.244	+0.236	0.137	+0.397	0.265	...
917 PG 1525+107		sdB-O	15.98	-0.24	16.819	0.150	16.175	...	15.144	...	...	...	...	...	...	...	...
918 PG 1526+131		sdB	14.306	-0.067	14.001	0.032	13.653	0.048	13.593	0.044	+0.408	0.054	+0.348	0.058	+0.670	0.069	COM, AEA
919 PG 1526+440		sdO(D)	15.64	-0.25	15.663	0.059	15.523	0.098	15.197	0.160	+0.466	0.171	+0.140	0.114	+0.571	0.191	...
920 PG 1527-054		sdB	15.90	P	16.258	0.138	16.183	0.228	14.914	...	...	...	+0.075	0.267	...	...	...
921 PG 1528+062		sdO(B)	14.753	-0.235	15.255	0.063	15.306	0.091	15.324	0.159	-0.069	0.171	-0.051	0.111	-0.107	0.190	AEA
922 PG 1528+029		sdO(C)	15.462	-0.284	16.084	0.090	16.016	0.168	16.524	...	...	...	+0.068	0.191	...	...	WMG
924 PG 1528+104		sdB	13.57	y	14.195	0.042	14.268	0.048	14.245	0.085	-0.050	0.095	-0.073	0.064	-0.105	0.106	...
925 PG 1530+431		sdB	15.31	+0.01	14.934	0.037	14.655	0.052	14.586	0.095	+0.348	0.102	+0.279	0.064	+0.558	0.113	...
926 PG 1530+459		sdO(A)	16.08	P	16.218	0.091	15.730	0.119	14.817	...	...	...	+0.488	0.150	...	...	...
927 PG 1530+057		sdB	14.211	+0.151	13.490	0.039	13.270	0.057	13.277	0.044	+0.213	0.059	+0.220	0.069	+0.378	0.079	LAN
928 TON 239		sdO(A)	16.27	P	16.266	0.137	15.739	...	14.944	...	...	...	...	...	...	...	...
929 PG 1531+447		sdB	15.62	y	16.127	0.092	16.022	0.161	15.065	...	...	...	+0.105	0.185	...	...	...
930 PG 1532+522		sdB	14.12	-0.29	14.690	0.041	14.871	0.082	14.841	0.107	-0.151	0.115	-0.181	0.092	-0.287	0.134	...
932 PG 1532-056		sdB	16.27	-0.11	16.150	0.095	15.541	0.108	15.572	0.249	+0.578	0.267	+0.609	0.144	+1.036	0.288	...
933 PG 1533+467		sdB	10.84	y	11.193	0.026	11.296	0.027	11.342	0.022	-0.149	0.034	-0.103	0.037	-0.226	0.044	...
934 TON 242		sdB	16.02	-0.19	15.878	0.069	15.603	0.114	15.594	0.174	+0.284	0.187	+0.275	0.133	+0.491	0.212	...
936 PG 1534-018		He-sdO	15.023	-0.204	15.397	0.063	15.319	0.097	15.725	0.271	-0.328	0.278	+0.078	0.116	-0.269	0.291	WMG
937 PG 1536+278		sd	13.83	+0.27	13.112	0.043	12.894	0.037	12.867	0.038	+0.245	0.057	+0.218	0.057	+0.409	0.071	...

Continued on Next Page...

Table B.1 – Continued

No. <sup>1</sup>	ID <sup>2</sup>	Type	$V / y^3$	$B - V^3$	$J^4$			$H^4$			$K_S^4$			$J - K_S$			$J - H$			$Q^5$			Notes <sup>6</sup>
					mag	$\sigma$	mag	$\sigma$	mag	$\sigma$	mag	$\sigma$	mag	$\sigma$	mag	$\sigma$	mag	$\sigma$	mag	$\sigma$	mag	$\sigma$	
938 PG	1536+097 #1	sd	15.87	+0.00	15.268	0.056	15.020	0.094	14.611	0.122	+0.657	0.134	+0.248	0.109	+0.843	0.157	...	...	...	...	...	...	...
939 PG	1536+690	sdO He	14.670	-0.323	15.373	0.060	15.396	0.116	15.090	...	...	...	-0.023	0.131	...	...	...	...	...	...	...	...	WMG
940 PG	1536+097 #2	sdB	15.02 P	...	14.536	0.045	14.347	0.051	14.605	0.140	-0.069	0.147	+0.189	0.068	+0.073	0.156	...	...	...	...	...	...	...
942 PG	1537-046	sdO(C)	15.004	-0.188	15.526	0.068	15.756	0.134	15.396	0.187	+0.130	0.199	-0.230	0.150	-0.043	0.229	WMG	...	...	...	...	...	...
943 PG	1538+002	sdO(A)	15.28 P	...	15.691	0.089	15.411	0.100	15.447	0.187	+0.244	0.207	+0.280	0.134	+0.455	0.230	...	...	...	...	...	...	...
944 PG	1538+269	sdB	13.85	-0.19	14.370	0.046	14.495	0.063	14.516	0.084	-0.146	0.096	-0.125	0.078	-0.240	0.113	...	...	...	...	...	...	...
947 PG	1538+401	sdB	13.13	-0.25	13.882	0.044	14.002	0.044	14.020	0.055	-0.138	0.070	-0.120	0.062	-0.228	0.084	...	...	...	...	...	...	...
949 PG	1539+292	sdB+K3	14.64	+0.08	14.186	0.034	13.995	0.055	13.954	0.071	+0.232	0.079	+0.191	0.065	+0.376	0.093	...	...	...	...	...	...	...
950 PG	1539+043	sdO(C)	15.912	-0.271	16.502	0.115	16.511	0.219	16.053	...	...	...	-0.009	0.247	...	...	...	...	...	...	...	...	WMG
951 PG	1540+044	sd	15.84 P	...	16.812	0.154	16.605	...	16.246	...	...	...	...	...	...	...	...	...	...	...	...	...	...
952 PG	1543+454	sdO(A)	15.78 P	...	16.851	0.149	17.178	...	16.896	...	...	...	...	...	...	...	...	...	...	...	...	...	...
953 PG	1543-124	sdB	16.54	-0.14	16.816	0.137	16.601	...	16.250	...	...	...	...	...	...	...	...	...	...	...	...	...	...
954 GD	351	sdOB	14.82	-0.22	15.583	0.064	15.575	0.121	15.683	0.221	-0.100	0.230	+0.008	0.137	-0.094	0.252	...	...	...	...	...	...	...
956 TON	803	sdO	14.170	-0.271	14.800	0.050	14.977	0.083	14.841	0.105	-0.041	0.116	-0.177	0.097	-0.174	0.137	WMG	...	...	...	...	...	...
957 PG	1544+601	sdB	14.74 P	...	15.081	0.049	15.206	0.083	15.226	0.152	-0.145	0.160	-0.125	0.096	-0.239	0.176	...	...	...	...	...	...	...
958 PG	1544+107	sdB	14.428	-0.158	14.771	0.042	14.856	0.076	14.998	0.115	-0.227	0.122	-0.085	0.087	-0.291	0.138	AEA	...	...	...	...	...	...
959 PG	1544+488	sdB He	12.80	...	13.460	0.029	13.561	0.041	13.666	0.050	-0.206	0.058	-0.101	0.050	-0.282	0.069	...	...	...	...	...	...	...
960 PG	1545+035	sdO(B)	14.338	-0.233	14.915	0.052	14.993	0.070	14.894	0.137	+0.021	0.147	-0.078	0.087	-0.038	0.161	WMG	...	...	...	...	...	...
961 PG	1546+045	sdB	15.54	-0.17	15.865	0.076	15.875	0.120	17.172	...	...	...	-0.010	0.142	...	...	...	...	...	...	...	...	...
962 PG	1547+476	sd	15.55 y	-0.12	16.343	0.121	16.168	0.233	16.041	0.257	+0.302	0.284	+0.175	0.263	+0.434	0.346	...	...	...	...	...	...	...
963 PG	1547+632	sdB	15.10 P	...	15.558	0.060	15.399	0.116	15.074	0.160	+0.484	0.171	+0.159	0.131	+0.604	0.197	...	...	...	...	...	...	...
964 PG	1548+166	sdB	14.940	-0.256	15.449	0.062	15.438	0.104	15.921	0.224	-0.472	0.232	+0.011	0.121	-0.464	0.249	SGL, AEA	...	...	...	...	...	...
965 PG	1549+006	sdB	15.27 y	-0.097	15.566	0.083	15.671	0.136	15.530	...	...	...	-0.105	0.159	...	...	...	...	...	...	...	...	...
966 PG	1549+476	sdB	15.89 P	...	16.337	0.113	15.942	0.194	16.057	...	...	...	+0.395	0.225	...	...	...	...	...	...	...	...	...
967 BD	+33° 2642	...	10.84	-0.17	11.090	0.027	11.137	0.031	11.199	0.026	-0.109	0.037	-0.047	0.041	-0.144	0.048	PN <sup>f</sup>	...	...	...	...	...	...
968 PG	1551-076	sdB	15.81	-0.12	15.813	0.073	15.986	0.171	15.728	0.252	+0.085	0.262	-0.173	0.186	-0.045	0.297	...	...	...	...	...	...	...
969 PG	1551+255	sdB	13.76 y	+0.059	13.196	0.030	12.930	0.043	12.905	0.039	+0.291	0.049	+0.266	0.052	+0.491	0.063	...	...	...	...	...	...	...
970 PG	1551+015	sdB	15.63 P	...	14.817	0.050	14.607	0.063	14.486	0.093	+0.331	0.106	+0.210	0.080	+0.489	0.122	...	...	...	...	...	...	...
971 PG	1552+141	sdB-O	16.15 P	...	16.354	0.112	16.318	0.228	15.395	...	...	...	+0.036	0.254	...	...	...	...	...	...	...	...	...
973 PG	1552+464	sdO(D)	16.01 P	...	16.426	0.140	16.473	...	17.168	...	...	...	...	...	...	...	...	...	...	...	...	...	...
974 PG	1553-077	sdO(B)	14.943	-0.158	15.201	0.053	15.396	0.105	15.364	0.174	-0.163	0.182	-0.195	0.118	-0.310	0.202	AEA	...	...	...	...	...	...
975 PG	1553+272	sdB	13.53	-0.12	13.991	0.036	14.033	0.049	14.062	0.075	-0.071	0.083	-0.042	0.061	-0.103	0.095	...	...	...	...	...	...	...
976 PG	1554+408	sdO(D)	15.93 P	...	16.757	0.161	16.378	...	15.978	...	...	...	...	...	...	...	...	...	...	...	...	...	...
977 PG	1554+222	sdO(B)	13.816	-0.278	14.488	0.040	14.515	0.058	14.588	0.116	-0.100	0.123	-0.027	0.070	-0.120	0.134	WMG	...	...	...	...	...	...
980 PG	1555+142	sdB	15.03 P	...	15.792	0.072	15.847	0.158	16.134	...	...	...	-0.055	0.174	...	...	...	...	...	...	...	...	...

Continued on Next Page...

Table B.1 – Continued

No. <sup>1</sup>	ID <sup>2</sup>	Type	$V / y^3$	$B - V^3$	$J^4$		$H^4$		$K_S^4$		$J - K_S$		$J - H$		$Q^5$		Notes <sup>6</sup>
					mag	$\sigma$	mag	$\sigma$	mag	$\sigma$	mag	$\sigma$	mag	$\sigma$	mag	$\sigma$	
981 PG	1555+303	sdB	14.79	-0.25	15.447	0.055	15.439	0.102	15.638	0.183	-0.191	0.191	+0.008	0.116	-0.185	0.210	...
984 PG	1558-007	sdB	13.541	-0.064	13.508	0.064	12.725	...	12.573	...	...	...	...	...	...	...	AEA
985 PG	1559+048	sdO(A)	14.48	-0.19	14.958	0.052	15.075	0.070	15.218	0.156	-0.260	0.164	-0.127	0.087	-0.356	0.177	...
986 PG	1559+222	sdO(D)	14.52	P	...	...	15.398	0.058	15.482	0.115	15.555	0.220	-0.157	0.228	-0.084	0.129	-0.220 0.248
987 PG	1559+076	sdO	15.03	...	...	...	14.138	0.044	13.842	0.051	13.837	0.060	+0.301	0.074	+0.296	0.067	+0.524 0.090
988 PG	1559+533	sdB	14.34	-0.32	14.955	0.042	15.086	0.083	15.103	0.157	-0.148	0.163	-0.131	0.093	-0.247	0.177	...
990 PG	1601+145	sdB+K3	14.424	+0.028	13.903	0.031	13.598	0.038	13.593	0.057	+0.310	0.065	+0.305	0.049	+0.539	0.075	COM, AEA
991 PG	1602+013	sdO(B)	15.022	-0.012	14.616	0.042	14.281	0.055	14.189	0.077	+0.427	0.088	+0.335	0.069	+0.679	0.102	WMG
992 PG	1602+145	sd	15.89	P	...	...	16.096	0.079	15.826	0.157	16.024	...	+0.270	0.176	...	...	...
993 PG	1604+504	sdB-O	15.73	P	...	...	13.566	0.032	13.663	0.039	13.888	0.058	-0.322	0.066	-0.097	0.050	-0.395 0.076
994 PG	1605+072	sdB	13.01	-0.23	13.406	0.043	13.485	0.050	13.564	0.051	-0.158	0.067	-0.079	0.066	-0.217	0.083	...
995 PG	1605+123	sdB	15.28	P	...	...	15.724	0.067	15.586	0.103	15.642	0.185	+0.082	0.197	+0.138	0.123	+0.186 0.218
996 PG	1606+627	sd	15.89	P	...	...	14.976	0.047	14.800	0.082	14.667	0.118	+0.309	0.127	+0.176	0.095	+0.441 0.146
999 PG	1607+174	sdO(A)	12.23	y	-0.192	...	12.770	0.030	12.914	0.038	12.984	0.035	-0.214	0.046	-0.144	0.048	-0.322 0.058
1000 PG	1608-029	sdO(B)	15.25	P	...	...	16.009	0.121	16.336	...	...	...	...	...	...	...	...
1003 PG	1608+443	sd	14.97	-0.20	15.293	0.059	15.262	0.127	15.361	...	...	...	+0.031	0.140	...	...	...
1004 PG	1609+013	sdB	15.41	P	...	...	14.055	0.045	13.653	0.047	13.552	0.059	+0.503	0.074	+0.402	0.065	+0.805 0.089
1005 KUV	16096+1932	sdB	15.96	-0.25	16.504	0.148	16.478	...	17.044	...	...	...	...	...	...	...	...
1006 PG	1610+529	sdB-O	12.91	-0.27	13.371	0.031	13.530	0.039	13.637	0.050	-0.266	0.059	-0.159	0.050	-0.386	0.070	...
1009 LB	9514	sdB-O	13.01	y	-0.063	...	13.210	0.048	13.297	0.045	13.314	0.048	-0.104	0.068	-0.087	0.066	-0.169 0.084
1010 PG	1610+519	sdOB	13.726	-0.178	13.596	0.037	13.273	0.042	13.237	0.040	+0.359	0.054	+0.323	0.056	+0.602	0.068	COM, AEA
1011 PG	1610+115	sdB	15.16	P	...	...	15.298	0.059	15.200	0.104	15.336	0.173	-0.038	0.183	+0.098	0.120	+0.036 0.204
1012 PG	1611+090	sdB	14.66	P	...	...	15.297	0.060	15.294	0.114	15.386	0.176	-0.089	0.186	+0.003	0.129	-0.087 0.210
1013 PG	1611+041	sdO(B)	15.28	P	...	...	16.380	0.134	15.823	...	...	...	...	...	...	...	...
1014 PG	1612+437	sd	16.28	P	...	...	16.453	0.133	16.031	0.198	16.078	...	+0.422	0.239	...	...	...
1016 PG	1612+735	sdB+?	14.474	+0.129	13.926	0.031	13.661	0.051	13.732	0.048	+0.194	0.057	+0.265	0.060	+0.393	0.073	AEA
1017 PG	1613+426	sdO(A)	14.40	-0.26	15.082	0.047	15.242	0.106	15.351	0.205	-0.269	0.210	-0.160	0.116	-0.389	0.227	...
1018 PG	1613+467	sdB	14.58	-0.27	15.217	0.050	15.363	0.118	15.445	0.238	-0.228	0.243	-0.146	0.128	-0.338	0.261	...
1019 LB	926	sdO(B)	15.02	P	...	...	15.530	0.068	15.687	0.156	15.679	0.228	-0.149	0.238	-0.157	0.170	-0.267 0.270
1021 PG	1614+146	sdB	14.72	P	...	...	14.490	0.042	14.463	0.056	14.651	0.088	-0.161	0.098	+0.027	0.070	-0.141 0.111
1023 PG	1616+144	sdB	13.48	-0.23	14.055	0.040	14.075	0.054	14.176	0.064	-0.121	0.075	-0.020	0.067	-0.136	0.090	...
1024 LB	933	sdB	15.29	-0.17	15.601	0.066	15.662	0.157	15.365	...	...	...	-0.061	0.170	...	...	...
1026 PG	1617+309	sd	15.87	-0.42	16.425	0.110	16.329	...	17.316	...	...	...	...	...	...	...	...
1027 PG	1618+562	sdOB	12.55	y	+0.166	...	11.719	...	11.568	...	...	...	...	...	...	...	...
1028 PG	1618+216	sdB	16.07	-0.18	16.403	0.120	16.731	...	15.936	...	...	...	...	...	...	...	...
1029 PG	1619+522	sdB	13.36	-0.28	13.883	0.033	13.969	0.050	14.036	0.067	-0.153	0.075	-0.086	0.060	-0.218	0.088	SGL

Continued on Next Page...

Table B.1 – Continued

No. <sup>1</sup>	ID <sup>2</sup>	Type	$V / y^3$	$B - V^3$	$J^4$	$H^4$	$K_S^4$	$J - K_S$	$J - H$	$Q^5$	Notes <sup>6</sup>
					mag	$\sigma$	mag	$\sigma$	mag	$\sigma$	
1030 PG 1620+017		sdB	15.58	-0.22	16.026	0.091	16.097	0.187	15.919	...	...
1031 LS IV -12°1		sdO	11.14	-0.09	11.295	0.042	11.361	0.050	11.444	0.035	-0.199 0.074
1032 TON 257		sdO	15.9	-0.48	16.253	0.087	16.492	0.238	16.628	...	...
1033 PG 1621+126		sdB	15.95 ;	-0.20	16.184	0.095	15.922	0.166	16.271	...	...
1034 PG 1621+476		sdB	15.71 P	...	16.732	0.137	17.002	...	15.600	...	...
1035 PG 1622+194		sdO(B)	15.61 P	...	15.372	0.064	15.216	0.101	15.079	0.142	+0.156 0.120 +0.410 0.180
1036 KUV 16229+4106		sdB-O	14.43 $y$	-0.145	14.643	0.035	14.591	0.055	14.274	0.071	+0.369 0.079 +0.052 0.065 +0.408 0.093
1037 PG 1623+178		sd:	16.01	-0.14	15.829	0.075	15.716	0.133	15.309	0.151	+0.520 0.169 +0.113 0.153 +0.605 0.204
1038 PG 1623+386		sd	15.84 ;	+0.02	15.873	0.072	15.385	0.094	15.325	0.162	+0.548 0.177 +0.488 0.118 +0.915 0.198
1039 PG 1624+014		sdB	15.43 P	...	16.225	0.103	16.261	0.201	15.482	...	...
1040 PG 1624+085		sdO He	15.13 P	...	15.570	0.067	15.752	0.150	15.606	0.227	-0.036 0.237 -0.182 0.164 -0.173 0.267
1041 KUV 16245+3814		sdO(C)	15.678	-0.321	16.463	0.117	16.314	...	17.138	...	WMG
1042 PG 1625-034		sdO(B)	15.61	-0.13	15.763	0.075	15.881	0.162	15.788	0.270	-0.025 0.280 -0.118 0.179 -0.114 0.311
1043 PG 1626+471		sdB-O	13.75	-0.21	14.371	0.039	14.563	0.064	14.512	0.100	-0.141 0.107 -0.192 0.075 -0.285 0.121
1044 PG 1627+006		sdB	14.68 P	...	15.362	0.056	15.426	0.098	15.367	0.152	-0.005 0.162 -0.064 0.113 -0.053 0.183
1045 PG 1627+017		sdB	12.899	-0.195	13.369	0.039	13.476	0.045	13.544	0.050	-0.175 0.063 -0.107 0.060 -0.255 0.077 AEA
1046 PG 1627+025		sdB	15.99 P	...	16.785	0.144	16.557	...	16.613	...	...
1047 PG 1627+112		sdB	14.38 $y$	-0.195	14.805	0.048	15.012	0.107	15.069	0.136	-0.264 0.144 -0.207 0.117 -0.420 0.169
1049 PG 1628+530		sdB-O	15.80	-0.20	15.981	0.077	16.233	0.175	16.081	...	...
1050 PG 1628+181		sdB	15.25 P	...	15.859	0.084	16.136	0.196	15.744	0.244	+0.115 0.258 -0.277 0.213 -0.093 0.304
1051 PG 1629+081		sdB-O	12.764	-0.159	12.836	0.045	12.611	0.062	12.597	0.043	+0.239 0.062 +0.225 0.077 +0.408 0.085 AEA
1052 PG 1629+466		sdO(D)	14.04 P	...	14.552	0.045	14.593	0.061	14.782	0.088	-0.230 0.099 -0.041 0.076 -0.261 0.114
1054 PG 1631+001		sdB	15.65 P	...	13.617	0.040	13.184	0.043	13.072	0.041	+0.545 0.057 +0.433 0.059 +0.871 0.072
1055 TON 817		sdB+G	15.51 $y$	-0.170	15.983	0.094	16.160	0.253	15.596	0.184	+0.387 0.207 -0.177 0.270 +0.254 0.290
1056 HD 149382		sdOB	8.92	-0.27	9.463	0.040	9.461	0.045	9.418	0.037	+0.045 0.054 +0.002 0.060 +0.047 0.070
1057 PG 1632+001		sdB	15.86	-0.19	16.264	0.115	15.729	0.130	16.048	...	...
1058 PG 1632+053		sdB	15.45 P	...	14.973	0.051	14.748	0.067	14.746	0.086	+0.227 0.100 +0.225 0.084 +0.396 0.118
1059 PG 1632+088		sdBpe	13.37	-0.05	13.329	0.042	13.378	0.056	13.406	0.048	-0.077 0.064 -0.049 0.070 -0.114 0.083
1060 PG 1632+588		sdO(B)	15.95 P	...	16.129	0.100	15.659	0.163	15.427	0.216	+0.702 0.238 +0.470 0.191 +1.055 0.278
1061 PG 1633+099		sdB	14.397	-0.192	14.817	0.045	15.005	0.076	14.928	0.126	-0.111 0.134 -0.188 0.088 -0.252 0.149 LAN
1062 BPS CS 22878-21		sdB	15.30	-0.02	14.951	0.051	14.759	0.070	14.658	0.102	+0.293 0.114 +0.192 0.087 +0.437 0.131
1063 PG 1633+696		sdB	16.46 P	...	15.872	0.080	15.570	0.145	15.589	...	...
1064 PG 1634+061		sdB	13.85 $y$	-0.192	14.324	0.041	14.502	0.058	14.436	0.077	-0.112 0.087 -0.178 0.071 -0.246 0.102
1065 PG 1634+014		sdO(A)	16.19 ;	-0.22	16.707	0.142	16.231	...	16.064	...	...
1066 PG 1635+533		sdB	15.66 P	...	16.148	0.109	15.913	0.171	15.686	...	...
1067 PG 1635+413		sdB-O	13.963	-0.262	14.570	0.041	14.694	0.067	14.547	0.094	+0.023 0.103 -0.124 0.079 -0.070 0.119 SGL, AEA

Continued on Next Page...

Table B.1 – Continued

No. <sup>1</sup>	ID <sup>2</sup>	Type	$V / y^3$	$B - V^3$	$J^4$		$H^4$		$K_S^4$		$J - K_S$		$J - H$		$Q^5$		Notes <sup>6</sup>
					mag	$\sigma$	mag	$\sigma$	mag	$\sigma$	mag	$\sigma$	mag	$\sigma$	mag	$\sigma$	
1068 PG 1636+216		sdB	15.08	-0.34	15.495	0.062	15.817	0.185	15.724	0.288	-0.229	0.295	-0.322	0.195	-0.471	0.329	...
1069 PG 1636+104		bin	14.039	+0.193	13.333	0.041	13.082	0.052	13.053	0.046	+0.280	0.062	+0.251	0.066	+0.469	0.079	AEA
1071 PG 1636+085		sdB	16.33	-0.12	15.687	0.064	15.376	0.097	15.626	0.207	+0.061	0.217	+0.311	0.116	+0.295	0.234	...
1072 KUV 16378+3438		sdB	15.29	P	15.129	0.046	15.071	0.077	15.098	0.139	+0.031	0.146	+0.058	0.090	+0.075	0.161	...
1073 PG 1638+147		sdO(C)	14.917	-0.263	15.426	0.057	15.589	0.112	15.579	...	...	...	-0.163	0.126	...	...	WMG
1075 PG 1638+675		sdO(C)	16.104	-0.296	16.588	0.149	16.876	...	15.590	...	...	...	...	...	...	...	WMG
1076 Balloon 083500007		bin?	15.5	$y$	13.711	0.031	13.285	0.036	13.227	0.043	+0.484	0.053	+0.426	0.048	+0.804	0.064	BBL
1077 PG 1639+173		sdO(B)	15.45	P	16.262	0.124	16.071	0.194	15.533	...	...	...	+0.191	0.230	...	...	...
1078 PG 1640+645		sdOB	15.17	P	15.474	0.065	15.832	0.165	15.476	0.219	-0.002	0.228	-0.358	0.177	-0.271	0.264	...
1080 PG 1642+038		sdO(C)	15.375	-0.239	15.832	0.079	16.178	0.201	15.454	...	...	...	-0.346	0.216	...	...	WMG
1081 PG 1642+707		sd	16.01	P	14.371	0.039	14.032	0.049	13.955	0.064	+0.416	0.075	+0.339	0.063	+0.671	0.089	...
1082 PG 1643+209		sdB	14.82	P	16.396	0.128	16.460	0.276	15.759	...	...	...	-0.064	0.304	...	...	...
1083 PG 1643+063		sdB-O	14.69	P	15.457	0.063	15.357	0.099	15.444	0.213	+0.013	0.222	+0.100	0.117	+0.088	0.239	...
1084 PG 1644+403		sdB	14.24	$y$	14.733	0.037	14.824	0.067	14.802	0.103	-0.069	0.109	-0.091	0.077	-0.137	0.123	...
1085 TON 261		sdO	16.20	-0.28	16.521	0.159	15.774	...	15.422	...	...	...	...	...	...	...	...
1086 PG 1644+311		sdB	14.30	$y$	14.572	0.040	14.484	0.061	14.774	0.150	-0.202	0.155	+0.088	0.073	-0.136	0.164	...
1087 PG 1645+610		sdB	14.409	-0.146	14.489	0.044	14.290	0.056	14.210	0.071	+0.279	0.084	+0.199	0.071	+0.429	0.100	AEA
1089 PG 1646+042		sdB	15.74	-0.26	15.922	0.085	16.182	0.189	16.204	0.332	-0.282	0.343	-0.260	0.207	-0.478	0.377	...
1090 TON 263		sdB	16.12	P	16.305	0.109	16.156	0.199	17.016	...	...	...	+0.149	0.227	...	...	...
1092 TON 264		sdB+?	14.074	-0.083	13.451	0.029	13.033	0.036	12.932	0.041	+0.519	0.050	+0.418	0.046	+0.833	0.061	AEA
1093 PG 1647+056		sdB	14.733	-0.175	15.302	0.062	15.014	0.097	15.322	0.192	-0.020	0.202	+0.288	0.115	+0.197	0.220	AEA
1094 PG 1648+315		sdO(D)	16.04	P	15.219	0.057	14.747	0.067	14.663	0.079	+0.556	0.097	+0.472	0.088	+0.911	0.117	...
1095 Balloon 083600004		bin?	16.9	+0.74	15.228	0.044	14.757	0.062	14.664	0.099	+0.564	0.108	+0.471	0.076	+0.918	0.122	BBL
1096 PG 1648+080		sd	13.94	$y$	12.808	0.041	12.545	0.042	12.397	0.036	+0.411	0.055	+0.263	0.059	+0.609	0.071	...
1097 PG 1648+536		sdB	14.06	$y$	14.553	0.038	14.587	0.058	14.790	0.112	-0.237	0.118	-0.034	0.069	-0.263	0.129	...
1098 KUV 16491+3539		sdOB	15.11	-0.25	15.731	0.080	15.788	0.140	15.548	...	...	...	-0.057	0.161	...	...	...
1099 PG 1649+522		sdB	16.09	P	16.893	0.142	16.280	...	15.927	...	...	...	...	...	...	...	...
1100 LSE 259		sdO	12.54	$y$	13.972	0.049	13.331	0.058	13.144	0.055	+0.828	0.074	+0.641	0.076	+1.310	0.094	crowded field
1101 PG 1650+706		sdO(B)	14.96	P	15.548	0.062	15.812	0.141	15.501	0.216	+0.047	0.225	-0.264	0.154	-0.152	0.253	...
1102 PG 1651+086		sdO(B)	15.11	P	15.139	0.056	14.900	0.085	14.850	0.129	+0.289	0.141	+0.239	0.102	+0.469	0.161	...
1103 LB 966		sdB	15.42	P	15.950	0.103	16.834	...	15.444	...	...	...	...	...	...	...	...
1104 PG 1652+159		sdO(C)	15.591	-0.234	16.088	0.093	16.170	0.205	15.286	...	...	...	-0.082	0.225	...	...	WMG
1106 PG 1653+131		sdB	14.421	-0.212	14.882	0.042	15.141	0.084	15.255	0.212	-0.373	0.216	-0.259	0.094	-0.568	0.227	AEA
1107 PG 1653+115		sdB	14.69	$y$	14.805	0.050	14.600	0.074	14.810	0.126	-0.005	0.136	+0.205	0.089	+0.149	0.152	...
1108 LS IV -08°03		sdB	11.51	$y$	10.638	0.039	10.463	0.041	10.288	0.034	+0.350	0.052	+0.175	0.057	+0.482	0.067	em <sup>f</sup>

Continued on Next Page...

Table B.1 – Continued

No. <sup>1</sup>	ID <sup>2</sup>	Type	$V$	$y$	$B-V$ <sup>3</sup>	$J^4$ mag	$H^4$ mag	$K_S^4$ mag	$J-K_S$ mag	$J-H$ mag	$Q^5$ mag	Notes <sup>6</sup>
1109 PG 1653+544		sdB-O	15.55	P	...	15.815	0.081	15.775	0.191	17.131	...	...
1111 PG 1654+322		sdO(C)	15.415	-0.298	...	16.105	0.091	16.245	0.209	15.960	0.237	+0.145 0.254 -0.140 0.228 +0.040 0.306 WMG
1112 PG 1655+106		sdO(B)	15.71	P	...	16.442	0.135	16.251	0.234	15.232	...	...
1113 PG 1656+322		sd	14.65	P	...	14.514	0.038	14.192	0.048	14.235	0.057	+0.279 0.069 +0.322 0.061 +0.521 0.083
1115 PG 1656+600		sdB	15.90	P	...	16.490	0.150	16.553	...	16.339	...	...
1116 PG 1656+213		sdB+?	14.88	-0.20	...	14.933	0.049	14.974	0.077	15.102	0.116	-0.169 0.126 -0.041 0.091 -0.200 0.143
1117 LB 974		sdB	16.19	P	...	15.785	0.075	15.519	0.128	15.271	0.215	+0.514 0.228 +0.266 0.148 +0.714 0.254
1118 PG 1656+318		sdB-O	14.24	$y$ -0.233	...	14.939	0.046	14.940	0.068	15.234	0.130	-0.295 0.138 -0.001 0.082 -0.296 0.151
1119 PG 1656+356		sdB	15.78	P	...	16.525	0.133	16.800	...	16.095	...	...
1120 PG 1656+552		sdB	15.37	P	...	16.219	0.099	16.140	0.220	16.082	...	...
1121 PG 1657+291		sdB	16.14	-0.13	...	16.819	0.151	16.353	...	17.035	...	...
1122 PG 1657+416		sdB	15.87	P	...	15.802	0.077	15.645	0.136	15.169	0.130	+0.633 0.151 +0.157 0.156 +0.751 0.191
1123 PG 1657+078		sdB	15.015	-0.149	...	15.448	0.065	15.513	0.140	15.427	0.188	+0.021 0.199 -0.065 0.154 -0.028 0.230 LAN
1124 PG 1657+656		sdB-O	15.95	P	...	15.994	0.101	15.601	0.144	15.493	...	...
1125 PG 1658+273		sdO(D)	15.73	P	...	16.662	0.144	16.363	0.230	15.865	...	...
1126 PG 1658+337		sdB	15.73	P	...	16.387	0.144	16.160	...	15.359	...	...
1127 LB 983		sdB-O	15.17	P	...	15.828	0.079	15.728	0.143	15.582	...	...
1128 LB 984		sdB	15.91	P	...	16.629	0.156	16.825	...	17.010	...	...
1129 PG 1700+198		sdO(B)	15.10	P	...	16.374	0.132	16.737	0.303	15.560	...	...
1130 PG 1700+247		sd	16.05	P	...	16.559	0.133	15.751	...	16.145	...	...
1132 PG 1700+486		sdB	14.80	P	...	14.830	0.036	14.985	0.080	14.918	0.119	-0.088 0.124 -0.155 0.088 -0.205 0.141
1133 PG 1701+359		sdB	13.226	-0.160	...	13.133	0.032	12.963	0.041	12.912	0.035	+0.221 0.047 +0.170 0.052 +0.349 0.061 COM, AEA
1134 PG 1702+099		sdB	15.55	P	...	16.068	0.109	16.710	...	15.910	...	...
1135 PG 1703+355		sdO(C)	15.625	-0.291	...	16.258	0.081	16.150	0.179	15.663	...	...
1137 TON 266		sdB	14.9	+0.05	...	14.258	0.037	14.008	0.043	13.997	0.059	+0.261 0.070 +0.250 0.057 +0.449 0.082
1138 PG 1704+222		non-sd	12.73	$y$ -0.094	...	12.906	0.029	12.989	0.039	13.016	0.036	-0.110 0.046 -0.083 0.049 -0.172 0.059
1139 PG 1704+466		sdO(C)	16.043	-0.241	...	16.661	0.144	16.510	0.285	15.679	...	...
1140 PG 1704+441		sdB	15.89	P	...	15.441	0.058	15.274	0.115	15.046	0.140	+0.395 0.152 +0.167 0.129 +0.521 0.180
1141 PG 1705+398		sdB	16.01	P	...	16.296	0.110	16.237	0.254	15.557	0.205	+0.739 0.233 +0.059 0.277 +0.783

Continued on Next Page...



Table B.1 – Continued

No. <sup>1</sup>	ID <sup>2</sup>	Type	$V / y^3$	$B - V^3$	$J^4$		$H^4$		$K_S^4$		$J - K_S$		$J - H$		$Q^5$		Notes <sup>6</sup>
					mag	$\sigma$	mag	$\sigma$	mag	$\sigma$	mag	$\sigma$	mag	$\sigma$	mag	$\sigma$	
1151 PG	1710+278	sdB	15.27 P	...	15.913	0.071	15.812	0.127	15.871	0.269	+0.042	0.278	+0.101	0.145	+0.118	0.299	...
1152 PG	1710+490	sdB	12.90 $y$	-0.238	13.419	0.040	13.613	0.044	13.612	0.040	-0.193	0.057	-0.194	0.059	-0.339	0.072	SGL
1153 PG	1711+564	sdB	16.12 P	...	16.124	0.093	15.899	0.146	15.625	...	...	...	+0.225	0.173	...	...	...
1154 PG	1712+228	sdB	14.67 P	...	15.386	0.052	15.473	0.091	15.115	0.126	+0.271	0.136	-0.087	0.105	+0.206	0.157	...
1157 PG	1715+457	sdB	16.12 P	...	16.142	0.097	15.676	0.143	15.721	0.222	+0.421	0.242	+0.466	0.173	+0.771	0.275	...
1158 PG	1716+426	sdB	13.97 $y$	-0.233	14.518	0.042	14.677	0.077	15.033	0.118	-0.515	0.125	-0.159	0.088	-0.635	0.141	...
1159 PG	1716+367	sdB	15.25 P	...	15.914	0.081	15.885	0.180	16.403	...	...	...	+0.029	0.197	...	...	...
1160 PG	1717+258	sd	15.24 P	...	13.589	0.031	13.346	0.041	13.261	0.037	+0.328	0.048	+0.243	0.051	+0.511	0.061	...
1161 PG	1717+607	sdB-O	14.44 $y$	-0.240	14.994	0.047	15.139	0.106	15.318	0.172	-0.324	0.178	-0.145	0.116	-0.433	0.198	...
1163 PG	1717+474	sdB	15.79 P	...	16.245	0.108	16.254	...	17.252	...	...	...	...	...	...	...	...
1164 PG	1718+519	sdB-O	13.733	+0.113	13.003	0.026	12.716	0.033	12.663	0.028	+0.340	0.038	+0.287	0.042	+0.556	0.049	COM, AEA
1165 SC	1721-336	sdB	15.63	+0.05	15.569	0.112	14.223	...	13.753	...	...	...	...	...	...	...	...
1166 PG	1722+286	sdB	13.39 $y$	-0.266	14.003	0.032	14.150	0.057	14.193	0.068	-0.190	0.075	-0.147	0.065	-0.301	0.090	...
1167 PG	1722+317	sdO(B)	15.80 P	...	16.503	0.120	16.234	...	15.942	...	...	...	...	...	...	...	...
1168 PG	1722+353	sdB	14.71 P	...	15.535	0.057	15.844	0.147	15.418	0.195	+0.117	0.203	-0.309	0.158	-0.115	0.235	...
1169 LB	331	sdB	15.84 P	...	15.071	0.045	14.897	0.076	14.990	0.156	+0.081	0.162	+0.174	0.088	+0.212	0.175	...
1171 LB	333	sdB	14.81 P	...	15.166	0.055	15.445	0.126	15.383	0.176	-0.217	0.184	-0.279	0.137	-0.427	0.211	...
1172 PG	1724+278	sdB	15.94 P	...	16.467	0.107	15.916	...	16.540	...	...	...	...	...	...	...	...
1173 PG	1725+373	sdO(A)	15.29 P	...	15.247	0.046	14.928	0.066	15.062	0.124	+0.185	0.132	+0.319	0.080	+0.425	0.145	...
1174 PG	1725+285	sdB	15.89 P	...	16.365	0.127	17.532	...	15.919	...	...	...	...	...	...	...	...
1176 PG	1725+252	sdB	13.063	-0.205	13.496	0.042	13.641	0.044	13.662	0.045	-0.166	0.062	-0.145	0.061	-0.275	0.077	AEA
1177 PG	1729+272	sdB	15.60 P	...	16.268	0.114	16.363	0.220	17.236	...	...	...	-0.095	0.248	...	...	...
1179 GD	362	sd	16.15 P	...	16.162	0.094	16.070	...	15.604	...	...	...	...	...	...	...	...
1180 PG	1733+326	sdB	16.28 P	...	15.677	0.060	15.614	0.131	15.979	...	...	...	+0.063	0.144	...	...	...
1181 [CW83]	1735+22	sdB	11.80 B	...	12.509	0.026	12.650	0.030	12.703	0.033	-0.194	0.042	-0.141	0.040	-0.300	0.052	...
1182 BD+29°3070		sdOB+F10.42	+0.18	+0.18	9.773	0.027	9.621	0.036	9.546	0.029	+0.227	0.040	+0.152	0.045	+0.341	0.052	...
1184 PG	1738+505	sd	13.26	-0.08	13.668	0.045	13.835	0.050	13.915	0.054	-0.247	0.070	-0.167	0.067	-0.373	0.086	...
1185 PG	1739+489	HBB	12.96 P	...	13.717	0.047	13.873	0.056	13.966	0.064	-0.249	0.079	-0.156	0.073	-0.366	0.096	...
1186 PG	1743+477	sdB	13.79 $y$	-0.208	14.313	0.039	14.526	0.067	14.429	0.082	-0.116	0.091	-0.213	0.078	-0.276	0.108	...
1187 BD+39°3226		sdOp	10.21	-0.29	10.873	0.032	11.023	0.031	11.097	0.027	-0.224	0.042	-0.150	0.045	-0.337	0.054	...
1188 [CW83]	1758+36	sdB	11.36	-0.25	11.956	0.020	12.121	0.019	12.226	0.021	-0.270	0.029	-0.165	0.028	-0.394	0.036	...
1189 KUV	18004+6836	sdO	14.60 P	...	15.501	0.063	15.930	0.177	15.443	...	...	...	-0.429	0.188	...	...	...
1190 LSE	234	sdO	12.63 $y$	-0.259	13.286	0.044	13.495	0.059	13.656	0.050	-0.370	0.067	-0.209	0.074	-0.527	0.087	...
1194 BD+48°2721		sdB	10.70	-0.20	11.107	0.030	11.215	0.033	11.277	0.022	-0.170	0.037	-0.108	0.045	-0.251	0.050	...
1195 HD	171858	sdB	9.86 $y$	-0.223	10.321	0.037	10.432	0.035	10.562	0.035	-0.241	0.051	-0.111	0.051	-0.324	0.064	...

Continued on Next Page...

Table B.1 – Continued

No. <sup>1</sup>	ID <sup>2</sup>	Type	$V / y^3$	$B - V^3$	$J^4$	$H^4$	$K_S^4$	$J - K_S$	$J - H$	$Q^5$	Notes <sup>6</sup>
					mag	$\sigma$	mag	$\sigma$	mag	$\sigma$	
1196	BPS CS 22959–140	sdO	15.0	B ...	15.268	0.064	15.403	0.152	15.230	0.140	+0.038 0.154 –0.135 0.165 –0.064 0.198 ...
1197	BPS CS 22959–145	sdB	16.4	B ...	15.672	0.067	15.841	0.165	15.436	0.177	+0.236 0.189 –0.169 0.178 +0.109 0.232 ...
1198	KPD 1856+2301	sdO	15.52	+0.13	15.468	0.069	15.343	0.111	15.213	0.135	+0.255 0.152 +0.125 0.131 +0.349 0.181 ...
1199	LSE 263	sdO	11.75	$y$ –0.264	12.103	0.036	12.063	0.036	12.158	0.036	–0.055 0.051 +0.040 0.051 –0.025 0.064 ...
1200	KPD 1901+1607	sdB	14.248	–0.004	14.228	0.037	14.107	0.049	14.344	0.082	–0.116 0.090 +0.121 0.061 –0.025 0.101 SGL, AEA
1201	JL 9	sdO	13.37	–0.27	13.951	0.043	14.082	0.064	14.255	0.075	–0.304 0.086 –0.131 0.077 –0.403 0.104 ...
1202	KPD 1903+2540	sdO	14.71	+0.01	14.241	0.050	13.971	0.042	13.957	0.056	+0.284 0.075 +0.270 0.065 +0.487 0.090 ...
1203	KPD 1905+1144	sdB	14.563	+0.170	14.435	0.067	14.508	0.066	14.059	...	–0.073 0.094 ... AEA
1209	BPS CS 22947–99	sdB	14.03	...	14.520	0.054	14.590	0.085	14.753	0.113	–0.233 0.125 –0.070 0.101 –0.286 0.146 ...
1210	BPS CS 22947–115	sdB	15.0	B ...	15.649	0.069	15.940	...	15.255	...	...
1211	BPS CS 22896–12	sdB	15.0	B ...	16.219	0.107	15.730	0.166	15.800	0.229	+0.419 0.253 +0.489 0.197 +0.787 0.293 ...
1212	BPS CS 22891–139	sdB	16.0	B ...	16.036	0.132	16.722	...	16.330	...	...
1213	BPS CS 22947–196	sdB	13.1	B ...	13.906	0.039	14.004	0.050	14.086	0.070	–0.180 0.080 –0.098 0.063 –0.254 0.093 ...
1214	BPS CS 22896–69	sdB	14.6	B ...	16.016	0.096	16.130	0.236	16.136	...	–0.114 0.255 ...
1215	BPS CS 22896–45	sdB	15.4	B ...	16.359	0.116	15.768	...	15.301	...	...
1216	KPD 1924+2932	sdB	13.843	–0.172	14.098	0.031	14.163	0.055	14.199	0.069	–0.101 0.076 –0.065 0.063 –0.150 0.090 SGL, AEA
1217	BPS CS 22891–188	sdB	15.9	B ...	14.931	0.055	14.526	0.063	14.392	0.084	+0.539 0.100 +0.405 0.084 +0.844 0.118 ...
1218	BPS CS 22947–299	sdB	14.52	...	15.009	0.053	15.087	0.102	14.854	0.135	+0.155 0.145 –0.078 0.115 +0.096 0.169 ...
1219	KPD 1930+2752	sdB	13.842	–0.085	13.983	0.045	13.968	0.051	14.038	0.063	–0.055 0.077 +0.015 0.068 –0.044 0.092 AEA
1220	BPS CS 22891–227	sdO He	15.6	B ...	15.686	0.078	15.768	0.145	15.742	0.244	–0.056 0.256 –0.082 0.165 –0.118 0.284 ...
1221	KPD 1931+2911	sdO	15.36	–0.04	15.613	0.070	15.732	0.188	16.276	...	–0.119 0.201 ...
1222	JL 25	sdOB	13.28	–0.19	13.256	0.042	13.023	0.059	12.866	0.044	+0.390 0.061 +0.233 0.072 +0.565 0.082 ...
1223	HD 185510	sdB+	8.341	+1.080	6.153	0.019	5.511	0.027	5.328	0.015	+0.825 0.024 +0.642 0.033 +1.308 0.035 var *, TYC
K0III-IV											
1224	BPS CS 22896–128	sdO He	16.2	B ...	16.209	0.136	16.885	...	15.953	...	...
1225	KPD 1938+4220	sdO	15.61	–0.17	16.049	0.088	15.907	...	16.494	...	...
1226	LS II+18°9	sdO	12.13	–0.32	12.770	0.035	12.906	0.037	13.049	0.036	–0.279 0.050 –0.136 0.051 –0.381 0.063 ...
1227	BPS CS 22896–190	sdB	15.1	B ...	15.369	0.055	15.482	0.142	15.520	0.199	–0.151 0.206 –0.113 0.152 –0.236 0.236 ...
1228	BPS CS 22896–175	sdB	15.47	–0.08	15.622	0.070	15.914	0.152	15.389	0.142	+0.233 0.158 –0.292 0.167 +0.013 0.202 ...
1229	KPD 1943+4058	sdB	14.866	–0.147	15.356	0.048	15.593	0.138	15.495	...	–0.237 0.146 ... AEA
1230	BPS CS 22896–183	sdB	14.4	B ...	15.099	0.048	15.213	0.092	15.334	0.142	–0.235 0.150 –0.114 0.104 –0.321 0.169 ...
1231	BPS CS 22896–194	sdB	15.89	–0.06	15.952	0.078	15.790	0.144	15.727	0.235	+0.225 0.248 +0.162 0.164 +0.347 0.277 ...
1232	BPS CS 22873–30	sdB	14.36	–0.30	14.839	0.051	14.812	0.090	15.140	0.142	–0.301 0.151 +0.027 0.103 –0.281 0.170 ...
1233	BPS CS 22896–171	sdB	14.04	–0.23	14.173	0.040	14.050	0.057	14.062	0.072	+0.111 0.082 +0.123 0.070 +0.203 0.097 ...
1234	BPS CS 22964–20	sdO	15.27	–0.20	15.605	0.071	15.319	0.140	15.255	0.184	+0.350 0.197 +0.286 0.157 +0.565 0.230 ...
1235	KPD 1946+4340	sdB	14.284	–0.201	14.683	0.032	14.836	0.061	14.727	0.103	–0.044 0.108 –0.153 0.069 –0.159 0.120 SGL, AEA

Continued on Next Page...

Table B.1 – Continued

No. <sup>1</sup>	ID <sup>2</sup>	Type	$V / y^3$	$B - V^3$	$J^4$		$H^4$		$K_S^4$		$J - K_S$		$J - H$		$Q^5$		Notes <sup>6</sup>
					mag	$\sigma$	mag	$\sigma$	mag	$\sigma$	mag	$\sigma$	mag	$\sigma$	mag	$\sigma$	
1236	BPS CS 22873–56	sdB	14.10	–0.04	14.046	0.047	14.055	0.061	14.008	0.060	+0.038	0.076	–0.009	0.077	+0.031	0.096	...
1237	HD 188112	sdB	10.21	$y$	–0.206												...
1238	LSE 21	sdO	11.78	–0.25	12.112	0.040	12.123	0.051	12.841	0.035	–0.174	0.055	–0.110	0.066	–0.257	0.074	...
1239	BPS CS 22964–112	sdB	15.40	–0.28	15.918	0.073	15.974	0.161	16.528	...	–0.028	0.056	–0.011	0.065	–0.036	0.074	...
1240	JL 36	sdB	12.98	$y$	–0.136						...	...	–0.056	0.177	...	...	...
1241	BPS CS 22964–216	sdB	15.76	–0.27	16.298	0.131	16.254	0.278	15.727	...	–0.190	0.069	–0.099	0.056	–0.264	0.081	...
1242	LS II+22° 21	sdO	12.58	–0.35	13.310	0.040	13.470	0.040	13.579	0.053	–0.269	0.066	–0.160	0.057	–0.389	0.079	...
1243	KPD 2007+4527	sdB	15.08	+0.11	14.383	0.034	14.094	0.054	13.969	0.061	+0.414	0.070	+0.289	0.064	+0.631	0.085	...
1244	BPS CS 22943–19	sdB	15.5	B	...						...	...	...	...	...	...	...
1245	BPS CS 22885–43	sdB He	15.6	B	...						...	...	...	...	...	...	...
1246	BPS CS 22950–10	sdB	13.6	B	...						...	...	...	...	...	...	...
1247	BPS CS 22950–48	He-sdO	13.9	B	...						...	...	...	...	...	...	...
1248	BPS CS 22950–1	sdB	15.8	B	...						...	...	...	...	...	...	...
1249	KPD 2018+2058	sdO	16.15	–0.23	16.629	0.146	17.355	...	16.030	...	...	...	...	...	...	...	...
1250	BPS CS 22950–61	sdB	15.1	B	...						...	...	–0.417	0.221	...	...	...
1251	BPS CS 22943–127	sdO	13.6	B	...						...	...	–0.067	0.079	–0.231	0.105	...
1252	BPS CS 22955–28	sdB	14.05	...	14.827	0.049	14.895	0.073	15.117	0.115	–0.290	0.125	–0.068	0.088	–0.341	0.141	SGL
1253	BPS CS 22955–16	sdB	14.1	B	...						...	...	–0.157	0.102	–0.416	0.175	...
1254	KPD 2022+2033	sdB	13.67	–0.05	13.813	0.032	13.858	0.049	13.993	0.057	–0.180	0.065	–0.045	0.059	–0.214	0.079	...
1255	BPS CS 22955–79	sdB	16.0	B	...						...	...	...	...	...	...	...
1256	KPD 2024+5303	sdB	14.562	+0.026	14.239	...	14.914	0.090	14.143	...	...	...	...	...	...	...	AEA
1257	BPS CS 22955–89	sdB	15.4	B	...						...	...	–0.087	0.225	...	...	...
1258	KPD 2025+5428	sdB	15.63	–0.05	15.953	0.090	15.417	...	15.490	...	...	...	...	...	...	...	...
1259	KPD 2026+2205	sdO	15.20	P	...						...	...	–0.099	0.123	...	...	...
1260	BPS CS 22940–9	sdB He	14.07	–0.29	14.611	0.054	14.698	0.075	14.674	0.132	–0.063	0.143	–0.087	0.092	–0.128	0.159	...
1261	KPD 2026+2316	sdB	16.18	–0.04	16.511	0.139	16.006	...	15.444	...	...	...	...	...	...	...	...
1262	BPS CS 22943–148	sdB	15.1	B	...						...	...	...	...	...	...	...
1263	LS IV+00° 21	sdB	12.44	$y$	–0.249						+0.467	0.087	+0.233	0.087	+0.642	0.109	...
1264	BPS CS 22943–198	sdB	15.7	B	...						–0.216	0.064	–0.115	0.055	–0.302	0.076	...
1265	BPS CS 22943–177	sdB	14.9	B	...						...	...	+0.014	0.272	...	...	...
1266	BPS CS 22880–18	sdB	15.60	–0.26	16.327	0.092	16.264	0.190	16.640	...	...	...	...	...	...	...	...
1267	BPS CS 22880–24	sdB	14.57	–0.35	15.360	0.050	15.350	0.104	15.391	0.157	–0.031	0.165	+0.010	0.115	–0.023	0.186	SGL
1268	BPS CS 22955–176	sdB	15.18	...	15.388	0.064	15.392	0.134	15.166	0.192	+0.222	0.202	–0.004	0.148	+0.219	0.231	...
1269	LS IV+10° 9	sdO	11.99	–0.27	12.632	0.041	12.813	0.050	12.916	0.044	–0.284	0.060	–0.181	0.065	–0.420	0.077	...
1270	KPD 2040+3955	sdB	14.451	–0.029	14.560	0.049	14.560	0.070	14.584	0.092	–0.024	0.104	+0.000	0.085	–0.024	0.122	SGL, AEA
1271	BPS CS 22880–52	sdB	15.23	–0.07	14.808	0.048	14.539	0.069	14.559	0.086	+0.249	0.098	+0.269	0.084	+0.451	0.117	...

Continued on Next Page...

Table B.1 – Continued

No. <sup>1</sup>	ID <sup>2</sup>	Type	$V / y^3$	$B - V^3$	$J^4$	$H^4$	$K_S^4$	$J - K_S$	$J - H$	$Q^5$	Notes <sup>6</sup>
					mag	$\sigma$	mag	$\sigma$	mag	$\sigma$	
1272 KUV 20417+7604	sdO	13.00	P	...	13.065	0.038	13.144	0.038	13.212	0.038	-0.147 0.054 -0.079 0.054 -0.206 0.068 ...
1273 KUV 20432+7457	sd?	15.50	P	...	12.503	0.043	11.667	0.042	10.514	0.034	+1.989 0.055 +0.836 0.060 +2.618 0.071 Sey <sup>e</sup>
1274 KPD 2045+3436	sdB	15.51	+0.00	+0.00	15.703	0.071	15.684	0.123	15.641	0.224	+0.062 0.235 +0.019 0.142 +0.076 0.258 ...
1275 KPD 2045+5136	sdB	15.06	+0.19	+0.19	15.255	0.056	15.293	0.096	15.849	...	...
1276 BPS CS 22880-78	sdB	15.30	-0.07	-0.07	14.538	0.050	14.084	0.059	13.997	0.057	+0.541 0.076 +0.454 0.077 +0.882 0.096 ...
1277 KPD 2048+3515	sdO	14.08	-0.23	-0.23	14.632	0.041	14.767	0.064	14.733	0.118	-0.135 0.076 -0.203 0.137 ...
1278 BPS CS 22879-82	sdB	15.20	-0.35	-0.35	15.764	0.077	15.787	0.153	15.908	...	...
1280 KPD 2051+3544	sdB	15.93	-0.28	-0.28	15.912	0.075	16.267	0.195	16.872	...	...
1281 PG 2052+027	sdO(B)	15.64	P	...	16.633	0.129	16.398	...	17.150	...	...
1282 PG 2052-003	sdB	15.98	P	...	15.762	0.077	15.920	0.194	15.516	...	...
1283 KPD 2053+5632	sdB	14.35	+0.27	+0.27	13.907	0.060	13.841	0.067	13.936	0.085	-0.029 0.104 +0.066 0.090 +0.021 0.124 ...
1285 LS IV -14° 116	sdOB	13.03	y	-0.273	13.638	0.044	13.799	0.055	13.898	0.058	-0.260 0.073 -0.161 0.070 -0.381 0.090 ...
1286 KPD 2055+3111	sdO	14.12	-0.24	-0.24	14.681	0.045	14.745	0.078	14.966	0.135	-0.285 0.142 -0.064 0.090 -0.333 0.157 ...
1287 PG 2059+013	sdB	15.011	-0.181	-0.181	15.584	0.056	15.428	0.084	15.437	0.162	+0.147 0.171 +0.156 0.101 +0.264 0.187 AEA
1289 KPD 2104+3407	sdO	15.95	-0.14	-0.14	16.357	0.097	16.403	0.243	15.985	...	...
1290 BPS CS 22937-33	sdB	12.3	B	...	13.696	0.039	13.838	0.058	13.968	0.056	-0.272 0.068 -0.142 0.070 -0.379 0.086 ...
1291 BPS CS 30492-40	sdB	14.7	B	...	15.500	0.056	15.531	0.111	15.441	0.186	+0.059 0.194 -0.031 0.124 +0.036 0.215 ...
1292 BPS CS 22937-36	sdB	15.5	B	...	15.194	0.060	14.926	0.088	14.863	0.106	+0.331 0.122 +0.268 0.107 +0.533 0.146 ...
1293 BPS CS 22937-22	sdB	15.2	B	...	15.955	0.077	16.146	0.195	17.059	...	...
1295 KPD 2109+4401	sdB	13.38	-0.21	-0.21	13.882	0.034	13.982	0.046	14.026	0.076	-0.144 0.083 -0.100 0.057 -0.219 0.093 ...
1297 PG 2110+127	sdB	12.927	+0.149	+0.149	12.293	0.031	12.070	0.036	12.016	0.029	+0.277 0.042 +0.223 0.048 +0.445 0.055 AEA
1298 PG 2111+023	HBB	13.25	y	-0.102	13.423	0.039	13.545	0.044	13.615	0.056	-0.192 0.068 -0.122 0.059 -0.284 0.081 ...
1299 BPS CS 29501-54	sdB	13.8	B	...	14.455	0.044	14.607	0.071	14.597	0.092	-0.142 0.102 -0.152 0.084 -0.256 0.120 ...
1300 BPS CS 30492-125	sdB	14.4	B	...	15.179	0.051	15.467	0.111	15.615	0.202	-0.436 0.208 -0.288 0.122 -0.653 0.227 ...
1301 BPS CS 29506-15	sdB	14.1	B	...	15.499	0.070	15.701	0.167	15.318	...	...
1302 PG 2115+145	sdB	15.16	P	...	15.578	0.072	15.763	0.168	15.589	0.240	-0.011 0.251 -0.185 0.183 -0.150 0.286 ...
1303 BPS CS 22937-84	sdB	14.80	-0.07	-0.07	14.953	0.047	15.009	0.078	15.090	0.119	-0.137 0.128 -0.056 0.091 -0.179 0.145 ...
1304 PG 2116+008	sdO(B)	15.41	P	...	16.327	0.101	16.525	0.270	15.889	0.266	+0.438 0.285 -0.198 0.288 +0.289 0.358 ...
1305 BPS CS 22937-82	sdB	14.6	B	...	15.290	0.061	15.389	0.102	15.544	0.186	-0.254 0.196 -0.099 0.119 -0.328 0.215 ...
1306 PG 2118+126	sdB	13.579	+0.148	+0.148	13.025	0.030	12.816	0.039	12.790	0.033	+0.235 0.045 +0.209 0.049 +0.392 0.058 COM, AEA
1307 KPD 2118+3841	sdB	13.87	-0.22	-0.22	14.314	0.048	14.383	0.051	14.475	0.094	-0.161 0.106 -0.069 0.070 -0.213 0.118 ...
1308 PG 2120+062	sd	14.40	y	-0.105	14.112	0.044	13.840	0.045	13.772	0.059	+0.340 0.074 +0.272 0.063 +0.545 0.088 ...
1309 BPS CS 29506-31	sdB	15.2	B	...	16.453	0.120	16.394	0.238	17.156	...	...
1312 PG 2124+071	sd	14.23	y	+0.080	13.474	0.039	13.261	0.040	13.194	0.052	+0.280 0.065 +0.213 0.056 +0.440 0.077 ...
1313 BPS CS 29506-51	sdB	14.5	B	...	15.700	0.081	15.763	0.147	15.765	0.248	-0.065 0.261 -0.063 0.168 -0.112 0.290 ...
1316 PG 2128+096	sdO(A)	14.74	y	-0.204	15.294	0.060	15.361	0.152	15.276	0.179	+0.018 0.189 -0.067 0.163 -0.032 0.225 ...

Continued on Next Page...

Table B.1 – Continued

No. <sup>1</sup>	ID <sup>2</sup>	Type	$V / y^3$	$B - V^3$	$J^4$	$H^4$	$K_S^4$	$J - K_S$	$J - H$	$Q^5$	Notes <sup>6</sup>
					mag	$\sigma$	mag	$\sigma$	mag	$\sigma$	
1317 PG 2128+089		sdO(A)	16.27 P	...	16.022 0.122	16.131 0.233	16.991 ...	...	-0.109 0.263	...	...
1319 PG 2128+146		sd	13.21 $y$	-0.107	13.327 0.031	13.392 0.041	13.443 0.043	-0.116 0.053	-0.065 0.051	-0.165 0.065	SGL
1320 PHL 25		sdB	12.17 $y$	-0.226	12.449 0.026	12.572 0.024	12.616 0.029	-0.167 0.039	-0.123 0.035	-0.259 0.047	...
1321 PG 2129+151		sdO(B)	14.23 $y$	-0.189	14.697 0.038	14.932 0.065	14.742 0.117	-0.045 0.123	-0.235 0.075	-0.222 0.135	...
1322 BPS CS 29495-21		sdB	13.5 B	...	13.112 0.041	12.882 0.039	12.815 0.040	+0.297 0.057	+0.230 0.057	+0.470 0.071	$d$
1323 PG 2130+067		sd	15.97 P	...	16.373 0.120	16.593 0.369	15.498 ...	...	-0.220 0.388	...	...
1324 JL 82		sdB	12.39 $y$	-0.217	12.857 0.042	12.960 0.037	13.052 0.046	-0.195 0.062	-0.103 0.056	-0.272 0.075	...
1325 PG 2131+164		sdB	14.98 P	...	14.918 0.040	15.034 0.077	15.055 0.143	-0.137 0.148	-0.116 0.087	-0.224 0.162	...
1326 PG 2132+095		sdB	15.34 P	...	16.247 0.090	16.085 0.204	15.722 0.244	+0.525 0.260	+0.162 0.223	+0.647 0.309	...
1327 PG 2132+126		sd	14.907 $y$	-0.036	14.987 0.042	15.113 0.077	15.145 0.133	-0.158 0.139	-0.126 0.088	-0.253 0.154	MEA
1330 PG 2135+045		sdB	14.657	-0.073	14.487 0.046	14.370 0.072	14.310 0.073	+0.177 0.086	+0.117 0.085	+0.265 0.107	AEA
1331 BPS CS 22948-17		sdB	13.4 B	...	14.598 0.044	14.650 0.058	14.679 0.087	-0.081 0.097	-0.052 0.073	-0.120 0.111	...
1332 HD 205805		sdB	10.21 $y$	-0.235	10.693 0.039	10.878 0.051	10.934 0.033	-0.241 0.051	-0.185 0.064	-0.380 0.070	...
1333 PG 2138+049		sdB	14.546	-0.080	14.878 0.053	15.000 0.096	15.204 0.175	-0.326 0.183	-0.122 0.110	-0.418 0.201	AEA
1334 BPS CS 22897-112		sdB	14.8 B	...	16.459 0.150	15.892 ...	16.096 0.345	+0.363 0.376	...	...	...
1336 PHL 117		sdOB	13.84 $y$	-0.247	14.527 0.051	14.633 0.064	14.679 0.105	-0.152 0.117	-0.106 0.082	-0.232 0.132	...
1338 BPS CS 22951-31		sdB	13.7 B	...	14.528 0.049	14.649 0.067	14.707 0.085	-0.179 0.098	-0.121 0.083	-0.270 0.116	...
1339 BPS CS 22956-32		sdB	14.7 B	...	15.128 0.059	14.935 0.084	14.765 0.107	+0.363 0.122	+0.193 0.103	+0.508 0.145	...
1340 BPS CS 22951-62		sdB	14.0 B	...	13.667 0.043	13.408 0.054	13.422 0.049	+0.245 0.065	+0.259 0.069	+0.440 0.083	...
1341 JL 87		sdB pec	12.00	-0.10	12.308 0.039	12.388 0.053	12.410 0.039	-0.102 0.055	-0.080 0.066	-0.162 0.074	...
1342 KPD 2145+4216		sdO	15.33	-0.01	15.460 0.068	15.786 0.144	15.319 0.190	+0.141 0.202	-0.326 0.159	-0.104 0.235	...
1343 BPS CS 22944-66		He-sdO	14.4 B	...	15.095 0.063	15.232 0.114	15.260 0.174	-0.165 0.185	-0.137 0.130	-0.268 0.209	...
1344 PG 2146+087		sdB	14.257	-0.036	14.407 0.044	14.433 0.063	14.640 0.103	-0.233 0.112	-0.026 0.077	-0.253 0.126	MEA
1346 PG 2148+095		sdB	13.021	-0.024	12.665 0.037	12.582 0.039	12.554 0.041	+0.111 0.055	+0.083 0.054	+0.173 0.068	AEA
1347 BD+28° 4211		sdO7p	10.53	-0.34	11.275 0.038	11.438 0.046	11.556 0.034	-0.281 0.051	-0.163 0.060	-0.404 0.068	$em^f$
1348 PG 2151+100		sd	12.75 $y$	-0.173	12.835 0.041	12.605 0.044	12.606 0.045	+0.229 0.061	+0.230 0.060	+0.402 0.076	...
1350 PG 2151+089		sd	16.31 P	...	16.605 0.148	15.997 0.224	15.646 ...	...	+0.608 0.268	...	...
1351 BPS CS 22881-7		sdB	15.21	-0.31	15.545 0.066	15.324 0.113	15.428 0.176	+0.117 0.188	+0.221 0.131	+0.283 0.212	...
1352 PG 2155+175		sd	16.00 P	...	16.525 0.136	15.645 ...	15.284 ...	...	...	...	...
1353 PB 7032		sdBpe	13.22 $y$	-0.201	13.609 0.039	13.617 0.057	13.625 0.050	-0.016 0.063	-0.008 0.069	-0.022 0.082	...
1354 BD+25° 4655		sdO	9.69	-0.26	10.370 0.040	10.516 0.040	10.632 0.038	-0.262 0.055	-0.146 0.057	-0.372 0.070	...
1355 BD-3° 5357		sdOB+	9.31	+0.86	7.351 0.015	6.782 0.023	6.615 0.009	+0.736 0.017	+0.569 0.027	+1.164 0.026	COM, e.bin
		G8III									
1356 PG 2158+082		sdO He	12.66 P	...	13.407 0.037	13.307 0.055	13.300 0.048	+0.107 0.061	+0.100 0.066	+0.182 0.079	...
1357 PG 2159+051		sd	12.98 $y$	-0.081	13.049 0.041	13.132 0.051	13.156 0.039	-0.107 0.057	-0.083 0.065	-0.169 0.075	...

Continued on Next Page...

Table B.1 – Continued

No. <sup>1</sup>	ID <sup>2</sup>	Type	$V / y^3$	$B - V^3$	$J^4$	$H^4$	$K_S^4$	$J - K_S$	$J - H$	$Q^5$	Notes <sup>6</sup>
					mag	$\sigma$	mag	$\sigma$	mag	$\sigma$	
1358BPCS 22881-31	sdB	15.81	-0.35	16.626 0.142 16.448 0.255 16.960 ...	...	...	...	...	+0.178 0.292	...	...
1360 PG 2201+059	sd	15.57 P	...	16.203 0.097 16.464 0.240 15.696 0.208 +0.507 0.230	...	...	...	...	-0.261 0.259	+0.311 0.301	...
1361 PG 2204+034	sdB	14.29	-0.23	14.849 0.051 15.042 0.101 15.175 0.168 -0.326 0.176	...	...	...	...	-0.193 0.113	-0.471 0.195	...
1362 PG 2204+127	sdO(B)	15.76 P	...	16.212 0.116 15.636 ...	15.815	...	...	...	...	...	...
1363 BPCS 22960-18	sdB	13.5 B	...	14.479 0.045 14.491 0.069 14.511 0.084 -0.032 0.095	...	...	...	...	-0.041 0.113	...	...
1364 PG 2205+023	sdB	14.136	-0.210	14.607 0.044 14.703 0.081 14.783 0.104 -0.176 0.113	...	...	...	...	-0.096 0.092	-0.248 0.132	AEA
1365 PB 5096	sdB	15.75	-0.12	16.524 0.134 16.425 0.259 15.558 ...	...	...	...	...	+0.099 0.292	...	...
1366 PG 2208+056	sdO	15.78 P	...	16.530 0.141 15.920 ...	15.563	...	...	...	...	...	...
1367 BPCS 22956-90	He-sdB	13.9 B	...	15.144 0.054 15.118 0.088 15.321 0.154 -0.177 0.163	...	...	...	...	-0.026 0.103	-0.157 0.180	...
1368 PB 5110	sdB-O	15.606	-0.062	15.897 0.074 15.913 0.192 15.684 0.214 +0.213 0.226	...	...	...	...	-0.016 0.206	+0.201 0.274	MEA
1369 PG 2212+173	sdB	15.13 P	...	15.704 0.071 16.159 0.173 15.467 0.233 +0.237 0.244	...	...	...	...	-0.455 0.187	-0.105 0.282	...
1370 BPCS 22956-94	He-sdB	12.5 B	...	12.629 0.041 12.189 0.056 12.107 0.038 +0.522 0.056	...	...	...	...	-0.440 0.069	+0.853 0.076	...
1371 BPCS 22892-51	sdO He	14.66	-0.36	15.411 0.058 15.449 0.138 15.677 0.246 -0.266 0.253	...	...	...	...	-0.038 0.150	-0.295 0.277	...
1373 BPCS 22886-32	sdB	13.79	-0.14	14.153 0.043 14.174 0.067 14.238 0.082 -0.085 0.093	...	...	...	...	-0.021 0.080	-0.101 0.111	...
1374 PB 5121	sdO(B)	14.115	-0.221	14.681 0.048 14.768 0.071 14.670 0.097 +0.011 0.108	...	...	...	...	-0.087 0.086	-0.054 0.126	SGL, AEA
1375 BPCS 229512-38	sdB	15.5 B	...	15.776 0.074 15.635 0.143 15.347 ...	...	...	...	...	+0.141 0.161	...	...
1376 PG 2214+184	sd	14.24 y	-0.081	14.528 0.049 14.668 0.075 14.527 0.086 +0.001 0.099	...	...	...	...	-0.140 0.090	-0.104 0.120	...
1378 PG 2215+151	sdO He	14.548	-0.254	15.174 0.052 15.290 0.095 16.779 ...	...	...	...	...	-0.116 0.108	...	WMG
1379 KPD 2215+5037	sdB	13.664	-0.093	14.218 0.053 14.313 0.050 14.329 0.077 -0.111 0.093	...	...	...	...	-0.095 0.073	-0.182 0.108	AEA
1380 BPCS 22875-2	sdO He	13.89	-0.33	14.665 0.047 14.828 0.081 15.012 0.109 -0.347 0.119	...	...	...	...	-0.163 0.094	-0.470 0.138	SGL
1381 BPCS 229512-55	sdB	14.7 B	...	15.204 0.050 15.234 0.114 15.363 0.225 -0.159 0.230	...	...	...	...	-0.030 0.124	-0.182 0.248	...
1383 PG 2218+051	sdO(A)	15.30 P	...	15.794 0.072 15.968 0.200 16.015 ...	...	...	...	...	-0.174 0.213	...	...
1384 PHL 232	sdB-O	14.171	-0.155	14.616 0.048 14.792 0.076 14.818 0.108 -0.202 0.118	...	...	...	...	-0.176 0.090	-0.334 0.136	AEA
1386 PG 2219+093	B	11.919	-0.134	12.215 0.034 12.278 0.037 12.315 0.038 -0.100 0.051	...	...	...	...	-0.063 0.050	-0.147 0.063	WMG
1387 BPCS 22960-71	sdB	15.1 B	...	15.653 0.069 15.605 0.109 16.146 ...	...	...	...	...	+0.048 0.129	...	...
1390 PG 2223+143	sdB	14.08 y	-0.214	14.643 0.035 14.752 0.057 14.922 0.151 -0.279 0.155	...	...	...	...	-0.109 0.067	-0.361 0.163	...
1392 PG 2223+171	sdB-O	14.76 P	...	14.353 0.034 14.034 0.045 14.059 0.069 +0.294 0.077	...	...	...	...	+0.319 0.056	+0.534 0.088	...
1393 PG 2226+094	sdB	14.065	+0.060	13.349 0.041 12.928 0.048 12.879 0.041 +0.470 0.058	...	...	...	...	+0.421 0.063	+0.787 0.075	AEA
1394 PG 2228+120	sdB	15.26 P	...	16.256 0.091 16.292 0.207 15.788 ...	...	...	...	...	-0.036 0.226	...	...
1396 PG 2229+099	non-sd	13.270	-0.080	13.467 0.041 13.569 0.058 13.693 0.058 -0.226 0.071	...	...	...	...	-0.102 0.071	-0.303 0.089	...
1397 KPD 2230+4937	sdB	15.710	-0.070	16.207 0.112 16.008 ...	16.873	...	...	...	...	...	...
1398 LBQS 2230+0125	sdB	18.1 J	...	16.528 0.109 15.974 0.133 15.550 0.180 +0.978 0.210	...	...	...	...	+0.554 0.172	+1.395 0.247	...
1399 PG 2230+120	sdB	16.24 P	...	16.094 0.090 15.848 0.149 16.894 ...	...	...	...	...	+0.246 0.174	...	...
1401 PHL 334	sdB	13.17 y	-0.288	13.834 0.043 14.021 0.066 14.059 0.062 -0.225 0.075	...	...	...	...	-0.187 0.079	-0.366 0.096	...
1402 PG 2234+160	sdB	15.22 P	...	16.007 0.085 16.225 0.195 15.774 ...	...	...	...	...	-0.218 0.213	...	...
1403 JL 111	sdB	14.13	-0.037	13.900 0.040 13.592 0.038 13.536 0.055 +0.364 0.068	...	...	...	...	+0.308 0.055	+0.596 0.080	...

Continued on Next Page...

Table B.1 – Continued

No. <sup>1</sup>	ID <sup>2</sup>	Type	$V / y^3$	$B - V^3$	$J^4$	$H^4$	$K_S^4$	$J - K_S$	$J - H$	$Q^5$	Notes <sup>6</sup>
					mag $\sigma$	mag $\sigma$	mag $\sigma$	mag $\sigma$	mag $\sigma$	mag $\sigma$	
1404 PG 2235+082		sd	15.42 $y$	-0.27	16.156 0.102	16.010 0.250	16.320 ...	...	+0.146 0.270	...	...
1406 PG 2236+122		sdO(A)	16.24 $P$	...	16.681 0.154	16.561 0.276	16.260 ...	...	+0.120 0.316	...	...
1407 PG 2236+134		sdB	14.99 $y$	-0.216	15.505 0.062	15.611 0.120	15.533 0.248	-0.028 0.256	-0.106 0.135	-0.108 0.275	...
1409 PHL 367		sd	15.50 $P$	...	16.228 0.102	16.208 0.228	16.506 ...	...	+0.020 0.250	...	...
1410 PG 2239+043		sdB	15.81 $P$	...	13.842 0.040	13.525 0.052	13.462 0.047	+0.380 0.062	+0.317 0.066	+0.618 0.079	...
1412 PHL 382		sdB	11.35 $y$	-0.161	11.644 0.022	11.675 0.021	11.705 0.021	-0.061 0.030	-0.031 0.030	-0.084 0.038	...
1413 PG 2240+105		sdB	15.03	-0.24	15.733 0.074	15.870 0.196	15.482 0.176	+0.251 0.191	-0.137 0.210	+0.148 0.248	...
1416 PG 2244+152		sdO	15.44 $P$	...	16.160 0.097	16.514 0.293	16.250 ...	...	-0.354 0.309	...	...
1418 PG 2246+103		sdO	14.83 $P$	...	15.686 0.078	15.948 0.193	15.229 ...	...	-0.262 0.208	...	...
1420 PG 2246+019		sdB-O	15.84 $y$	-0.20	16.220 0.095	16.919 ...	15.188 ...	...	...	...	...
1421 HD 216135		sdB	10.1	-0.13	10.366 0.038	10.441 0.049	10.479 0.037	-0.113 0.053	-0.075 0.062	-0.169 0.071	...
1422 BPS CS 22938-44		sdB He	15.2 $B$	...	16.057 0.083	16.785 ...	16.749 ...	...	...	...	...
1424 Balloon 090900007		sdB+G2	13.30	+0.23	12.372 0.028	12.180 0.029	12.158 0.034	+0.214 0.044	+0.192 0.040	+0.358 0.053	...
1425 JL 117		sdO	14.39	-0.36	15.240 0.059	15.426 0.134	15.327 0.184	-0.087 0.193	-0.186 0.146	-0.227 0.222	...
1426 PG 2251+080		sdB	15.65 $P$	...	16.107 0.095	16.180 0.186	15.612 0.240	+0.495 0.258	-0.073 0.209	+0.440 0.302	...
1427 PB 7352		sd/hb	12.31 $y$	-0.217	12.819 0.043	12.915 0.037	13.032 0.044	-0.213 0.062	-0.096 0.057	-0.285 0.075	...
1428 KPD 2253+4922		sdB	15.56	-0.06	15.805 0.079	15.683 0.152	15.681 0.239	+0.124 0.252	+0.122 0.171	+0.216 0.283	...
1429 PG 2254+067		sdB	15.18 $P$	...	15.661 0.064	15.837 0.169	15.671 0.250	-0.010 0.258	-0.176 0.181	-0.142 0.292	...
1430 KPD 2254+5444		sdB	14.377	+0.034	14.435 0.071	14.391 0.060	13.662 ...	...	+0.044 0.093	...	AEA
1432 PB 7409		sdB	14.00 $y$	-0.266	14.560 0.043	14.701 0.078	14.780 0.117	-0.220 0.125	-0.141 0.089	-0.326 0.142	...
1433 BPS CS 22938-33		sdB	15.3 $B$	...	16.021 0.097	15.654 ...	15.641 ...	...	...	...	...
1434 KPD 2257+4928		sdB	15.02	-0.04	15.266 0.057	15.257 0.103	15.454 0.176	-0.188 0.185	+0.009 0.118	-0.181 0.205	...
1435 KUV 22585+1533		sdO He	15.03 $P$	...	15.941 0.079	16.536 0.245	17.003 ...	...	-0.595 0.257	...	...
1436 JL 119		sdOB	13.48	-0.27	14.194 0.042	14.210 0.062	14.314 0.085	-0.120 0.095	-0.016 0.075	-0.132 0.110	...
1438 KUV 22593+1322		sdB	14.55 $y$	-0.165	14.916 0.044	14.865 0.062	14.891 0.126	+0.025 0.133	+0.051 0.076	+0.063 0.145	...
1439 KPD 2259+5149		sdO	13.85	-0.03	14.035 0.029	14.122 0.053	14.114 0.059	-0.079 0.066	-0.087 0.060	-0.144 0.080	...
1441 BPS CS 30493-9		sdB	15.0 $B$	...	15.247 0.072	15.373 0.123	15.417 0.188	-0.170 0.201	-0.126 0.143	-0.265 0.228	...
1442 BPS CS 22893-38		sdB	16.18	-0.10	16.368 0.115	17.367 ...	16.573 ...	...	...	...	...
1443 PG 2301+259		non-sd	13.22 $y$	-0.093	13.399 0.034	13.518 0.047	13.526 0.043	-0.127 0.055	-0.119 0.058	-0.216 0.070	...
1444 PG 2303+115		sdB	14.42 $y$	-0.16	14.276 0.046	13.955 0.059	13.841 0.061	+0.435 0.076	+0.321 0.075	+0.676 0.095	...
1445 PHL 401		sdB	16.05 $P$	...	16.250 0.120	15.717 0.158	15.867 ...	...	+0.533 0.198	...	...
1446 PHL 402		sdO	16.00	-0.44	16.652 0.147	16.267 0.234	16.409 ...	...	+0.385 0.276	...	...
1448 BPS CS 22893-20		sdB He	15.1 $B$	...	16.303 0.097	16.072 0.179	15.629 ...	...	+0.231 0.204	...	...
1450 BPS CS 22888-17		sdB	14.3 $B$	...	15.568 0.066	15.646 0.121	15.667 0.194	-0.099 0.205	-0.078 0.138	-0.158 0.230	...
1452 BPS CS 22938-73		sdO He	14.1 $B$	...	15.001 0.058	15.045 0.103	15.305 0.198	-0.304 0.206	-0.044 0.118	-0.337 0.224	...
1453 KUV 23089+0942		sdO	15.40 $P$	...	15.545 0.068	15.261 0.095	15.223 0.161	+0.322 0.175	+0.284 0.117	+0.536 0.196	...

Continued on Next Page...

Table B.1 – Continued

No. <sup>1</sup>	ID <sup>2</sup>	Type	$V / y^3$	$B - V^3$	$J^4$	$H^4$	$K_S^4$	$J - K_S$	$J - H$	$Q^5$	Notes <sup>6</sup>
					mag $\sigma$	mag $\sigma$	mag $\sigma$	mag $\sigma$	mag $\sigma$	mag $\sigma$	
1454 Feige 108		sdB	12.942	-0.235	13.529 0.039	13.704 0.056	13.776 0.061	-0.247 0.072	-0.175 0.068	-0.379 0.088	SGL, AEA
1455 Feige 109		sdB	13.747	-0.175	14.135 0.043	14.277 0.060	14.360 0.085	-0.225 0.095	-0.142 0.074	-0.332 0.110	AEA
1456 PHL 443		sdO He	14.10 $y$	-0.265	14.829 0.035	15.036 0.069	14.969 0.125	-0.140 0.130	-0.207 0.077	-0.296 0.142	...
1457 BD-7°5977		sdOB	10.52 $y$	+0.592	9.006 0.021	8.520 0.043	8.406 0.032	+0.600 0.038	+0.486 0.048	+0.965 0.052	COM
1458 PB 5324		sdB	14.485	-0.265	15.128 0.056	15.152 0.093	15.459 0.203	-0.331 0.211	-0.024 0.109	-0.349 0.226	AEA
1459 PHL 457		sdB	12.95 $y$	-0.256	13.499 0.043	13.595 0.049	13.674 0.052	-0.175 0.067	-0.096 0.065	-0.247 0.083	...
1460 PHL 460		sdB	12.24 $y$	-0.153	12.499 0.021	12.555 0.021	12.587 0.026	-0.088 0.033	-0.056 0.030	-0.130 0.040	...
1461 PB 5333		sdOB	12.856	-0.256	12.896 0.037	12.647 0.037	12.624 0.041	+0.272 0.055	+0.249 0.052	+0.459 0.067	AEA, em <sup>f</sup>
1462 Feige 110		sdO	12.5	-0.32	12.548 0.043	12.663 0.038	12.796 0.044	-0.248 0.062	-0.115 0.057	-0.334 0.075	...
1463 BPS CS 22949-25		sdB	15.22	...	15.844 0.077	16.001 0.176	16.013	...	-0.157 0.192	...	...
1464 PG 2318+239		sd	13.66 $y$	-0.138	13.874 0.032	13.964 0.046	14.034 0.058	-0.160 0.066	-0.090 0.056	-0.228 0.078	SGL
1465 KPD 2319+5014		sdB	14.70	-0.13	14.817 0.053	14.697 0.076	14.867 0.102	-0.050 0.115	+0.120 0.093	+0.040 0.135	...
1467 PB 5358		sdOB	14.61	+0.14	14.235 0.042	14.013 0.054	13.941 0.068	+0.294 0.080	+0.222 0.068	+0.461 0.095	...
1468 LB 1181		sdB	14.66 $y$	-0.22	15.244 0.045	15.431 0.100	15.483 0.247	-0.239 0.251	-0.187 0.110	-0.380 0.264	...
1470 PG 2321+214		sdO(D)	12.89 P	...	14.289 0.034	14.430 0.048	14.434 0.078	-0.145 0.085	-0.141 0.059	-0.251 0.096	...
1471 KPD 2322+4933		sdO	13.70	-0.15	13.984 0.033	14.076 0.052	14.125 0.061	-0.141 0.069	-0.092 0.062	-0.210 0.083	...
1472 PG 2323+121		sdB	14.96 P	...	15.416 0.058	15.634 0.136	14.778	...	-0.218 0.148	...	...
1473 PB 5376		sdB	14.67 P	...	15.886 0.062	16.083 0.159	15.901 0.249	-0.015 0.257	-0.197 0.171	-0.163 0.287	...
1474 BPS CS 22949-42		sdB	13.86	...	14.317 0.039	14.501 0.059	14.381 0.079	-0.064 0.088	-0.184 0.071	-0.202 0.103	...
1475 PHL 540		sdO	13.38 $y$	-0.298	14.027 0.034	14.168 0.046	14.154 0.060	-0.127 0.069	-0.141 0.057	-0.233 0.081	...
1476 PG 2326+297		sd	14.87 P	...	15.278 0.052	15.260 0.084	15.500 0.187	-0.222 0.194	+0.018 0.099	-0.208 0.208	...
1478 BPS CS 22945-23		sdB	15.4 B	...	15.574 0.061	15.306 0.116	15.344 0.181	+0.230 0.191	+0.268 0.131	+0.432 0.215	...
1479 BPS CS 29496-9		sdB	13.8 B	...	14.533 0.041	14.599 0.070	14.680 0.095	-0.147 0.103	-0.066 0.081	-0.197 0.120	...
1480 PG 2329+232		sdB	14.88 P	...	16.539 0.133	15.957	15.815	...	...	...	...
1481 PB 5443		sd	15.182	-0.066	15.313 0.054	15.286 0.116	15.382 0.146	-0.069 0.156	+0.027 0.128	-0.049 0.183	LAN
1482 TON S 103		sdOp	14.7	-0.23	15.410 0.076	15.490 0.145	15.138	...	-0.080 0.164	...	...
1484 PB 5446		sdB	14.942	-0.144	15.321 0.062	15.611 0.149	15.306 0.150	+0.015 0.162	-0.290 0.161	-0.203 0.202	AEA
1485 PB 5447		sdB	15.74 P	...	16.568 0.157	16.637 0.348	15.580	...	-0.069 0.382	...	...
1486 PB 5450		sdB	13.06 $y$	-0.211	13.498 0.041	13.585 0.043	13.538 0.052	-0.040 0.066	-0.087 0.059	-0.105 0.080	...
1487 BPS CS 22894-18		sdO He	15.5 B	...	16.654 0.131	16.215 0.197	16.408	...	+0.439 0.237	...	...
1488 PG 2335+107		sdB	15.55 $y$	-0.19	16.019 0.093	16.191 0.213	15.616	...	-0.172 0.232	...	...
1489 PG 2335+133		sdB	16.00 P	...	16.728 0.163	17.032	16.624	...	...	...	...
1490 PG 2336+264		sd	14.63 P	...	14.362 0.038	14.064 0.050	14.105 0.072	+0.257 0.081	+0.298 0.063	+0.481 0.094	...
1491 PG 2337+266		sdB	16.10 P	...	16.549 0.142	17.638	15.509	...	...	...	...
1492 PB 5495		sdB	13.47 $y$	-0.10	13.735 0.041	13.802 0.044	13.933 0.060	-0.198 0.073	-0.067 0.060	-0.248 0.086	...

Continued on Next Page...



Table B.1 – Continued

No. <sup>1</sup>	ID <sup>2</sup>	Type	$V / y^3$	$B - V^3$	$J^4$		$H^4$		$K_S^4$		$J - K_S$		$J - H$		$Q^5$		Notes <sup>6</sup>
					mag	$\sigma$	mag	$\sigma$	mag	$\sigma$	mag	$\sigma$	mag	$\sigma$	mag	$\sigma$	
1493 PG 2337+300		sd	13.91 $y$	+0.016	13.775	0.046	13.687	0.047	13.647	0.059	+0.128	0.075	+0.088	0.066	+0.194	0.090	em <sup>f</sup>
1494 BPS CS 29496-17		sdB	14.0 B	...	15.183	0.064	15.145	0.116	15.098	0.166	+0.085	0.178	+0.038	0.132	+0.114	0.204	...
1495 PG 2339+199		sdB He	15.78 P	...	16.702	0.136	16.317	0.239	16.126	...	...	...	+0.385	0.275	...	...	...
1496 PG 2341+184		sdB	15.89 P	...	15.851	0.071	15.919	0.144	15.659	0.232	+0.192	0.243	-0.068	0.161	+0.141	0.271	...
1497 CD -35 15910		sdB	10.96 $y$	-0.264	11.581	0.039	11.684	0.050	11.771	0.037	-0.190	0.054	-0.103	0.063	-0.267	0.072	...
1499 BPS CS 29496-27		sdB	14.5 B	...	15.645	0.069	15.852	0.188	15.294	...	...	...	-0.207	0.200	...	...	...
1500 PG 2345+318		sdB	14.160	-0.193	14.690	0.052	14.833	0.075	14.805	0.105	-0.115	0.117	-0.143	0.091	-0.223	0.136	AEA
1501 PG 2345+241		non-sd	12.430	-0.153	12.762	0.029	12.834	0.036	12.896	0.034	-0.134	0.045	-0.072	0.046	-0.188	0.057	AEA
1502 PG 2346+149		sdB	15.69 P	...	16.005	0.077	15.666	0.107	15.676	0.215	+0.329	0.228	+0.339	0.132	+0.584	0.249	...
1503 PG 2348+269		sdB	15.54 P	...	16.534	0.124	16.194	0.233	15.983	...	...	...	+0.340	0.264	...	...	...
1504 PB 5562		sdB	13.262	-0.210	13.745	0.043	13.887	0.056	13.922	0.061	-0.177	0.075	-0.142	0.071	-0.284	0.092	AEA
1505 KPD 2349+5009		sdO	15.30 P	...	15.093	0.060	14.682	...	14.762	...	...	...	...	...	...	...	...
1507 CD -30 19716		sdO	12.09 $y$	-0.284	12.866	0.040	12.987	0.052	13.071	0.041	-0.205	0.057	-0.121	0.066	-0.296	0.076	...
1509 BPS CS 29517-17		sdB	14.0 B	...	14.041	0.040	13.788	0.039	13.882	0.055	+0.159	0.068	+0.253	0.056	+0.349	0.080	...
1510 BPS CS 29517-35		sdB	13.4 B	...	14.832	0.051	14.814	0.072	14.999	0.121	-0.167	0.131	+0.018	0.088	-0.153	0.147	...
1511 BPS CS 22876-2		sdB	14.8 B	...	15.490	0.069	15.792	0.187	15.643	0.216	-0.153	0.227	-0.302	0.199	-0.380	0.272	...
1512 PG 2352+180		sdO He	13.359	-0.281	13.966	0.038	14.116	0.056	14.184	0.068	-0.218	0.078	-0.150	0.068	-0.331	0.093	WMG
1513 PG 2352+259		sdB	14.99 P	...	15.040	0.049	15.075	0.090	15.033	0.124	+0.007	0.133	-0.035	0.102	-0.019	0.154	...
1514 BPS CS 22957-10		He-sdO	14.5 B	...	15.636	0.065	15.750	0.135	16.530	...	...	...	-0.114	0.150	...	...	...
1515 PG 2354+298		sd	15.33 P	...	16.249	0.100	15.984	...	15.493	...	...	...	...	...	...	...	...
1517 PG 2355+082		sd	15.45 P	...	13.542	0.036	13.224	0.047	13.202	0.046	+0.340	0.058	+0.318	0.059	+0.579	0.073	...
1519 CD -27 16503		sdO?	13.49 $y$	-0.173	13.474	0.039	13.356	0.057	13.343	0.051	+0.131	0.064	+0.118	0.069	+0.220	0.082	COM
1520 SB 933		sdO	14.24 $y$	-0.298	14.970	0.059	15.067	0.105	14.969	0.137	+0.001	0.149	-0.097	0.120	-0.072	0.174	...
1521 PG 2356+167		sdB-O	14.21 $y$	-0.154	14.583	0.040	14.703	0.074	14.782	0.104	-0.199	0.111	-0.120	0.084	-0.289	0.128	...
1524 PG 2358+107		sdB	13.62 $y$	-0.140	14.063	0.040	14.191	0.050	14.218	0.063	-0.155	0.075	-0.128	0.064	-0.251	0.089	...
1525 BPS CS 22957-23		sdB	13.7 B	...	12.740	0.040	12.337	0.051	12.306	0.036	+0.434	0.054	+0.403	0.065	+0.737	0.073	...
1526 BPS CS 22876-28		sdB	14.3 B	...	15.065	0.049	15.126	0.107	15.263	0.202	-0.198	0.208	-0.061	0.118	-0.244	0.226	...
1527 PG 2359+197		sd	15.44 P	...	16.234	0.097	16.227	0.215	17.160	...	...	...	+0.007	0.236	...	...	...

## Appendix C

### Tricks with Magnitudes and Colors

#### C.1 Converting Bessel & Brett *JHK* to 2MASS *JHK<sub>S</sub>*

The conversions between various filter systems and the 2MASS filters are given in Carpenter (2001). The relevant conversions for my purposes are the ones which convert to 2MASS *J*, *H*, and *K<sub>S</sub>* from Bessell & Brett (1988) *J*, *H*, and *K*. They are given as:

$$\begin{aligned}
 K_{S,2MASS} &= K_{BB} & -0.039 & +0.001(J-K)_{BB} \\
 & & (\pm 0.007) & (\pm 0.005) \\
 (J-H)_{2MASS} &= 0.990(J-H)_{BB} & -0.049 & \\
 & & (\pm 0.012) & (\pm 0.007) \\
 (J-K_S)_{2MASS} &= 0.983(J-K)_{BB} & -0.018 & \\
 & & (\pm 0.008) & (\pm 0.007) \\
 (H-K_S)_{2MASS} &= 0.971(H-K)_{BB} & +0.034 & \\
 & & (\pm 0.022) & (\pm 0.006)
 \end{aligned}$$

The colors for the main sequence from Bessell & Brett (1988) and Johnson (1966) are given in Table C.1, and those same colors converted to the 2MASS filter system are given in Table C.2.

#### C.2 Determining Extinction Vectors

##### C.2.1 Extinction Vectors

This section will describe how to calculate extinction vectors for color-color plots.

The color excess relations are:

$$E(U-B) = A_U - A_B \quad (C.1)$$

$$E(B-V) = A_B - A_V \quad (C.2)$$

$$E(V-K) = A_V - A_K \quad (C.3)$$

$$E(J-K) = A_J - A_K \quad (C.4)$$

$$E(J-H) = A_J - A_H \quad (C.5)$$

From Cardelli, Clayton, & Mathis (1989) we have the values of  $A(\lambda)/A(V)$  given in Table C.3. So if  $A_V = 1$ , then:

$$\begin{aligned} A_U &= 1.569 \\ A_B &= 1.337 \\ A_J^1 &= 0.282 \\ A_H^1 &= 0.190 \\ A_K^1 &= 0.114 \end{aligned}$$

So plugging these values into Equations C.1–C.4 we get color excesses of:

$$\begin{aligned} E(U-B) &= 0.232 \\ E(B-V) &= 0.337 \\ E(V-K) &= 0.886 \\ E(J-K) &= 0.168 \\ E(J-H) &= 0.092 \end{aligned}$$

These values are plotted as a reddening vector in a color-color diagram (with  $A_V = 1$ ).

Note, converting  $E(J-K)$ ,  $E(J-H)$ , and  $E(V-K)$  into 2MASS filters results in the following values:

$$\begin{aligned} E(V-K_S) &= 0.886 \\ E(J-K_S) &= 0.165 \\ E(J-H) &= 0.091 \end{aligned}$$

### C.2.2 Reddening Correction

Here is how to correct colors based on a value of  $E(B-V)$  taken from Schlegel et al. (1998). Using the values from Table C.3 for 2MASS filters, we can say:

$$A_B = 1.337A_V \tag{C.6}$$

$$A_V = 1.000A_V \tag{C.7}$$

$$A_J = 0.279A_V \tag{C.8}$$

$$A_H = 0.188A_V \tag{C.9}$$

$$A_{K_S} = 0.114A_V \tag{C.10}$$

---

<sup>1</sup>These values are not for 2MASS filters, the corresponding 2MASS values for  $A_x$  are given in Table C.3.

combining those values with

$$\begin{aligned}
 R(V) &= \frac{A_V}{E(B-V)} \\
 R(V) &= 2.97 \\
 A_V &= 2.97 E(B-V)
 \end{aligned} \tag{C.11}$$

Equation C.11 from Cardelli, Clayton, & Mathis (1989), and equations C.2–C.5, then the excesses for  $V-K_S$  based on  $E(B-V)$  becomes:

$$\begin{aligned}
 E(V-K_S) &= A_V - 0.114A_V \\
 E(V-K_S) &= 0.886A_V \\
 E(V-K_S) &= 0.886 [2.97 E(B-V)] \\
 E(V-K_S) &= 2.6314 E(B-V)
 \end{aligned} \tag{C.12}$$

and likewise, the other colors become:

$$E(J-K_S) = 0.4901 E(B-V) \tag{C.13}$$

$$E(J-H) = 0.2703 E(B-V) \tag{C.14}$$

Now using Equations C.12–C.14 the reddening corrected colors (for Johnson  $BV$  and 2MASS  $JHK_S$  filters) become:

$$\begin{aligned}
 (B-V) &= (B-V)_{\text{obs}} - E(B-V) \\
 (V-K_S) &= (V-K_S)_{\text{obs}} - 2.6314 E(B-V) \\
 (J-K_S) &= (J-K_S)_{\text{obs}} - 0.4901 E(B-V) \\
 (J-H) &= (J-H)_{\text{obs}} - 0.2703 E(B-V)
 \end{aligned}$$

## C.3 Creating Composite Colors and Magnitudes

### C.3.1 Combining Two Colors

In this section I will describe that mathematics involved with calculating a composite color from two stars with given colors and flux ratios.

First start with the definition of a magnitude:

$$m_2 - m_1 = 2.5 \log \left( \frac{F_1}{F_2} \right)$$

This can be rearranged to become:

$$\log F_1 - \log F_2 = \frac{m_2 - m_1}{2.5}$$

So, for two stars that I want to blend together, I know  $J$  and  $K_S$  for both of them which gives the following four equations:

$$\log F_{K_S1} - \log F_{J1} = \frac{(J - K_S)_1}{2.5} \equiv \log C_1 \quad (\text{C.15})$$

$$\log F_{K_S2} - \log F_{J2} = \frac{(J - K_S)_2}{2.5} \equiv \log C_2 \quad (\text{C.16})$$

$$\log F_{K_S2} - \log F_{K_S1} = \frac{K_{S1} - K_{S2}}{2.5} \equiv \log \kappa \quad (\text{C.17})$$

$$\log F_{J2} - \log F_{J1} = \frac{J_1 - J_2}{2.5} \equiv \log j \quad (\text{C.18})$$

I am using the shorthand notation for the right hand side of the equations as indicated. These four equations can be rewritten to give the following:

$$\begin{aligned} \log F_{K_S1} &= \log C_1 + \log F_{J1} \\ \log F_{K_S2} &= \log C_2 + \log F_{J2} \\ \log F_{K_S2} &= \log \kappa + \log F_{K_S1} \\ \log F_{J2} &= \log j + \log F_{J1} \end{aligned}$$

Therefore, so a blended flux ratio would look something like the following:

$$\begin{aligned} \log F_{K_S\text{blend}} - \log F_{J\text{blend}} &= \log (F_{K_S1} + F_{K_S2}) - \log (F_{J1} + F_{J2}) \\ &= \log (C_1 F_{J1} + C_2 F_{J2}) - \log (F_{J1} + F_{J2}) \\ &= \log (C_1 F_{J1} + j C_2 F_{J1}) - \log (F_{J1} + j F_{J1}) \\ &= \log (C_1 + j C_2) - \log (1 + j) \end{aligned}$$

where  $j$  is the ratio of light fractions contributed at  $J$ . However, I want the fractions contributed at  $V$ :

$$\log F_{V2} - \log F_{V1} = \log \nu$$

I know the  $V - J$  colors for the two stars:

$$\left. \begin{aligned} \frac{F_{J1}}{F_{V1}} &= 10^{(V-J)_1/2.5} \equiv T_1 \implies \log F_{J1} = \log T_1 + \log F_{V1} \\ \frac{F_{J2}}{F_{V2}} &= 10^{(V-J)_2/2.5} \equiv T_2 \implies \log F_{J2} = \log T_2 + \log F_{V2} \end{aligned} \right\} \Rightarrow \log j$$

$$\log j \equiv \log F_{J2} - \log F_{J1} = \log (T_2 F_{V2}) - \log (T_1 F_{V1}) = \log T_2 - \log T_1 + \log \nu$$

So, I eventually arrive at:

$$\frac{F_{K_S\text{blend}}}{F_{J\text{blend}}} = \frac{C_1 + \frac{\nu C_2 T_2}{T_1}}{1 + \nu \frac{T_2}{T_1}} = \frac{C_1 T_1 + \nu C_2 T_2}{T_1 + \nu T_2}$$

or...

$$\log F_{K_S\text{blend}} - \log F_{J\text{blend}} = \log (C_1 T_1 + \nu C_2 T_2) - \log (T_1 + \nu T_2)$$

where:

$$\begin{aligned}
\log C_1 &\equiv \log F_{K_S1} - \log F_{J1} = \frac{(J - K_S)_1}{2.5} \\
\log C_2 &\equiv \log F_{K_S2} - \log F_{J2} = \frac{(J - K_S)_2}{2.5} \\
\log T_1 &\equiv \log F_{J1} - \log F_{V1} = \frac{(V - J)_1}{2.5} \\
\log T_2 &\equiv \log F_{J2} - \log F_{V2} = \frac{(V - J)_2}{2.5} \\
\log \nu &\equiv \log F_{V2} - \log F_{V1}
\end{aligned}$$

Similarly, I can get the following for the blended flux ratios of  $V-K_S$  and  $B-K_S$ :

$$\log F_{K_S\text{blend}} - \log F_{V\text{blend}} = \log (C_1 + \nu C_2) - \log (1 + \nu)$$

where:

$$\begin{aligned}
\log C_1 &\equiv \log F_{K_S1} - \log F_{V1} = \frac{(V - K_S)_1}{2.5} \\
\log C_2 &\equiv \log F_{K_S2} - \log F_{V2} = \frac{(V - K_S)_2}{2.5} \\
\log \nu &\equiv \log F_{V2} - \log F_{V1}
\end{aligned}$$

and...

$$\log F_{K_S\text{blend}} - \log F_{B\text{blend}} = \log (C_1 T_1 + \nu C_2 T_2) - \log (T_1 + \nu T_2)$$

where:

$$\begin{aligned}
\log C_1 &\equiv \log F_{K_S1} - \log F_{B1} = \frac{(B - K_S)_1}{2.5} \\
\log C_2 &\equiv \log F_{K_S2} - \log F_{B2} = \frac{(B - K_S)_2}{2.5} \\
\log T_1 &\equiv \log F_{B1} - \log F_{V1} = \frac{(V - B)_1}{2.5} \\
\log T_2 &\equiv \log F_{B2} - \log F_{V2} = \frac{(V - B)_2}{2.5} \\
\log \nu &\equiv \log F_{V2} - \log F_{V1}
\end{aligned}$$

So, the complete equations for blended colors become:

$$(J-K_S)_{\text{blend}} = 2.5 \log \left( 10^{[(J-K_S)_1 + (V-J)_1]/2.5} + \nu 10^{[(J-K_S)_2 + (V-J)_2]/2.5} \right) - 2.5 \log \left( 10^{(V-J)_1/2.5} + \nu 10^{(V-J)_2/2.5} \right) \quad (\text{C.19})$$

$$(H-K_S)_{\text{blend}} = 2.5 \log \left( 10^{[(H-K_S)_1 + (V-H)_1]/2.5} + \nu 10^{[(H-K_S)_2 + (V-H)_2]/2.5} \right) - 2.5 \log \left( 10^{(V-H)_1/2.5} + \nu 10^{(V-H)_2/2.5} \right) \quad (\text{C.20})$$

$$(V-K_S)_{\text{blend}} = 2.5 \log \left( 10^{(V-K_S)_1/2.5} + \nu 10^{(V-K_S)_2/2.5} \right) - 2.5 \log (1 + \nu) \quad (\text{C.21})$$

$$(B-K_S)_{\text{blend}} = 2.5 \log \left( 10^{[(B-K_S)_1 + (V-B)_1]/2.5} + \nu 10^{[(B-K_S)_2 + (V-B)_2]/2.5} \right) - 2.5 \log \left( 10^{(V-B)_1/2.5} + \nu 10^{(V-B)_2/2.5} \right) \quad (\text{C.22})$$

In all cases  $\nu = \frac{F_{V2}}{F_{V1}}$ , where (in the case of a hot subdwarf composite)  $F_{V2}$  is the flux at  $V$  due to the late-type companion, and  $F_{V1}$  is the flux at  $V$  due to the hot subdwarf. All other colors can be calculated as combinations of these colors [i.e.,  $B-V = (B-K_S) - (V-K_S)$ ].

### C.3.2 Combining Two Magnitudes

The previous section dealt with determining the composite color of two blended stars with a given flux ratio. In this section I will discuss how to determine the magnitude of the blended object in a single band given the magnitude of one of the stars in that band and the flux ratio of the two stars. Begin with:

$$\log F_{\text{rat}} = \frac{m_1 - m_2}{2.5} \quad (\text{C.23})$$

where  $m_1$  and the flux ratio,  $F_{\text{rat}} (= \frac{F_2}{F_1}$ , the flux ratio in the band of interest), are known. In the case of a hot subdwarf composite,  $F_2$  is the companion, and  $F_1$  is the hot subdwarf. Then:

$$m_{\text{comp}} = m_{\text{sd}} - 2.5 \log (F_{\text{rat}})$$

Now, to find the value of  $m_{\text{tot}}$ , I'll play a little "trick" by including a third object,  $m_{\text{o}}$ . Then I can also write the following:

$$\begin{aligned} m_{\text{o}} - m_{\text{sd}} &= 2.5 \log \left( \frac{F_{\text{sd}}}{F_{\text{o}}} \right) \\ m_{\text{o}} - m_{\text{comp}} &= 2.5 \log \left( \frac{F_{\text{comp}}}{F_{\text{o}}} \right) \end{aligned}$$

Which leads to:

$$F_{\text{tot}} = F_{\text{sd}} + F_{\text{comp}} = F_{\text{o}} \left( 10^{(m_{\text{o}} - m_{\text{sd}})/2.5} + 10^{(m_{\text{o}} - m_{\text{comp}})/2.5} \right)$$

Then converting the fluxes back to magnitudes:

$$m_{\text{tot}} = m_{\circ} - 2.5 \log \left( \frac{F_{\text{tot}}}{F_{\circ}} \right) = m_{\circ} - 2.5 \log \left( 10^{(m_{\circ}-m_{\text{sd}})/2.5} + 10^{(m_{\circ}-m_{\text{comp}})/2.5} \right)$$

Now I can be really clever and choose  $m_{\circ} = 0$ , so I get the following:

$$m_{\text{tot}} = -2.5 \log \left[ 10^{-m_{\text{sd}}/2.5} + 10^{(\{2.5 \log F_{\text{rat}}\} - m_{\text{sd}})/2.5} \right] \quad (\text{C.24})$$

where again,  $F_{\text{rat}} = \frac{F_{\text{comp}}}{F_{\text{sd}}}$  in the band of interest (i.e., for magnitudes in  $V$ :  $F_{\text{rat}} \equiv \nu = \frac{F_{V,\text{comp}}}{F_{V,\text{sd}}}$ ).

So, in the case of making the loci of composite sdB+late type star in the  $(K_S, J-K_S)$  color-magnitude diagram (for example, see §3.4), the values of  $J-K_S$  would be calculated as described in §C.3.1 (and shown in Equ. C.19). However, the corresponding values of  $K_S$ , involve a little more work, since we have assumed the faintest sdB has  $K_S = 15.75$  and some percent contribution from the companion at  $V$  ( $F_{\text{rat}} \equiv \nu = \frac{F_{V,\text{comp}}}{F_{V,\text{sd}}}$ ). Thus, in order to use Equ. C.24 to find the total  $K_S$  magnitude, I need the flux ratio from the companion at  $K_S$ :  $F_{\text{rat}} \equiv \kappa = \frac{F_{K_S,\text{comp}}}{F_{K_S,\text{sd}}}$  (not at  $V$ :  $F_{\text{rat}} \equiv \nu = \frac{F_{V,\text{comp}}}{F_{V,\text{sd}}}$ ). So I need to convert the flux ratio at  $V$  ( $\nu$ ) to the corresponding flux ratio at  $K_S$  ( $\kappa$ ) using the following relation:

$$\log \kappa = \log \nu + \frac{(V-K_S)_{\text{comp}}}{2.5} - \frac{(V-K_S)_{\text{sd}}}{2.5} \quad (\text{C.25})$$

Then I simply set  $F_{\text{rat}} = \kappa$  in Equ. C.24 to find the  $K_S$  magnitude of the blended stars.



Table C.1. Colors for Main Sequence Stars.

Type	$M_V$	$U-B^1$	$B-V^1$	$V-K^2$	$B-K^3$	$J-K^2$	$J-H^2$
B3 <sup>4</sup>	...	-0.71	-0.20	-0.60	-0.80	-0.15	...
B5 <sup>4</sup>	...	-0.56	-0.16	-0.46	-0.62	-0.11	...
B8	...	-0.23	-0.16	-0.35	-0.51	-0.09	-0.05
A0	0.7	+0.00	+0.00	+0.00	+0.00	+0.00	+0.00
A5	2.0	+0.11	+0.14	+0.38	+0.52	+0.08	+0.06
F0	3.1	+0.06	+0.31	+0.70	+1.01	+0.16	+0.13
F5	3.4	+0.00	+0.43	+1.10	+1.53	+0.27	+0.23
G0	4.4	+0.11	+0.59	+1.41	+2.00	+0.36	+0.31
G6	5.3	+0.20	+0.66	+1.64	+2.30	+0.43	+0.37
K0	5.9	+0.47	+0.82	+1.96	+2.78	+0.53	+0.45
K5	7.3	+1.03	+1.15	+2.85	+4.00	+0.72	+0.61
M0	9.0	+1.26	+1.41	+3.65	+5.06	+0.86	+0.69

<sup>1</sup>Johnson (1966).

<sup>2</sup>Bessell & Brett (1988).

<sup>3</sup>Calculated based on Johnson (1966) and Bessell & Brett (1988).

<sup>4</sup> $V-K$  and  $J-K$  for this spectral type taken from Johnson (1966) and converted to the Bessell & Brett (1988) system using:  $(J-K)_{\text{BB}} = 0.01 + 0.99(J-K)_{\text{J}}$  and  $(V-K)_{\text{BB}} = 0.01 + 0.993(V-K)_{\text{J}}$  — the converted BB color is given.

Table C.2. Colors for Main Sequence Stars Transformed into 2MASS Filters.

Type	$M_V$	$U-B^1$	$B-V^1$	$V-K_S^2$	$B-K_S^3$	$J-K_S^2$	$J-H^2$
B3	...	-0.71	-0.20	-0.639	-0.839	-0.196	...
B5	...	-0.56	-0.16	-0.499	-0.659	-0.157	...
B8	...	-0.23	-0.16	-0.311	-0.471	-0.106	-0.099
A0	0.7	+0.00	+0.00	+0.039	+0.039	-0.018	-0.049
A5	2.0	+0.11	+0.14	+0.419	+0.559	+0.061	+0.014
F0	3.1	+0.06	+0.31	+0.739	+1.049	+0.139	+0.080
F5	3.4	+0.00	+0.43	+1.139	+1.569	+0.247	+0.179
G0	4.4	+0.11	+0.59	+1.449	+2.039	+0.336	+0.253
G6	5.3	+0.20	+0.66	+1.679	+2.339	+0.405	+0.317
K0	5.9	+0.47	+0.82	+1.998	+2.818	+0.503	+0.397
K5	7.3	+1.03	+1.15	+2.888	+4.038	+0.690	+0.555
M0	9.0	+1.26	+1.41	+3.688	+5.098	+0.827	+0.639

<sup>1</sup>Johnson (1966).<sup>2</sup>Bessell & Brett (1988) converted to 2MASS.<sup>3</sup>Calculated based on Johnson (1966) and Bessell & Brett (1988) then converted into 2MASS filters.

Table C.3. Extinction Values for Various Filters.

Filter	$\lambda$ ( $\mu\text{m}$ )	$A(\lambda)/A(V)$
$U$	0.360	1.569
$B$	0.441	1.337
$V$	0.550	1.000
$J$	1.25	0.282
$H$	1.59	0.190
$K$	2.17	0.114
$J_{2\text{MASS}}^1$	1.235	0.279
$H_{2\text{MASS}}^1$	1.662	0.188
$K_{S,2\text{MASS}}^1$	2.159	0.114

<sup>1</sup>Converted to 2MASS filters following Appendix C.1

## Appendix D

### Confidence Intervals for a Binomial Distribution

In this section I will describe how to calculate the confidence intervals (CI) for binomial percentages (for example, errors on the fractions of hot subdwarfs that are single and/or composite in 2MASS, see §3.6).

The equation to calculate the CI is:

$$\hat{\pi} \pm z_{\alpha/2} \sqrt{\frac{\hat{\pi}(1 - \hat{\pi})}{n}} \quad (\text{D.1})$$

where:  $z_{\alpha/2}$  is a value that depends on the CI you desire and can be looked up in a statistics book (i.e., for a 95% CI,  $z_{\alpha/2} = 1.96$ ),  $\hat{\pi}$  is the fraction corresponding to one category (i.e., fraction of sdBs that are “single”), and  $n$  is the total number of “trials” (i.e., the number of subdwarfs).

For example, from the 2MASS All-Sky Survey (see Chapter 3 and in particular Table 3.4) there are a total of 826 hot subdwarfs with 2MASS  $J-K_S$  color, 485 (or 59%) appear “single”, and 341 (or 41%) appear “composite”. The 95% CI on these percentages is from equation D.1:

$$\begin{aligned} 0.59 \pm 1.96 \sqrt{\frac{0.59(1 - 0.59)}{826}} &\implies 0.59 \pm 0.03 \\ 0.41 \pm 1.96 \sqrt{\frac{0.41(1 - 0.41)}{826}} &\implies 0.41 \pm 0.03 \end{aligned}$$

(obviously they should come out to be exactly the same error, which they did). Thus, the fractions of single vs. composite hot subdwarfs with 95% CI on the numbers is:  $59 \pm 3\%$  single, and  $41 \pm 3\%$  composite.

Similarly, for all cases based on the 2MASS All Sky Survey:

Type	Total #	Single	Composite
All	826	$59 \pm 3\%$	$41 \pm 3\%$
sdB	636	$56 \pm 4\%$	$44 \pm 4\%$
sdO	190	$69 \pm 7\%$	$31 \pm 7\%$

## Appendix E

### HIP Standard $M_V$ Calculation

This appendix describes the process of calculating  $M_V$  based on  $V$  and Hipparcos parallax measurements (given in Table E.1) for the HIP Standard stars in my observing program (see also Chapter 4.4 on pg. 49). Tycho-1  $B_T$  and  $V_T$  magnitudes for these stars were converted to Johnson  $B_J$  and  $V_J$  magnitudes using:

$$\begin{aligned} V_J &= V_T - 0.090 \times (B_T - V_T) \\ (B - V)_J &= 0.850 \times (B_T - V_T) \end{aligned}$$

This conversion is valid over  $-0.2 < (B_T - V_T) < 1.8$ , and generally gives errors  $< 0.015$  in  $V_J$  and  $< 0.05$  in  $(B - V)_J$  (ESA 1997). Both original Tycho and converted Johnson magnitudes are reported in Table E.1.

The value of  $M_V$  depends on both the parallax ( $\pi$ ) and the observed magnitude ( $V$ ) as:

$$\begin{aligned} M_V &= V - 5 \log \left( \frac{D}{10 \text{pc}} \right) \\ M_V &= V - 5 \log \left( \frac{100}{\pi} \right) \end{aligned} \tag{E.1}$$

(where  $D[\text{pc}] = [0.001\pi]^{-1} = 10^3/\pi$  and  $\pi$  is the parallax in milliarcseconds, or “mas”) and since each of those measurements ( $V$  and  $\pi$ ) contains an error, it is necessary to propagate their errors to the final value of  $M_V$ .

The general formula for error propagation is:

$$\sigma_y^2 = \sum_i \left( \frac{df}{dx_i} \right)^2 \sigma_i^2 \tag{E.2}$$

where  $y = f(x_i)$ , and  $\sigma_i$  are the errors on  $x_i$ .

So combining Equation E.1 and E.2 the error on  $M_V$  would become:

$$\sigma_{M_V}^2 = \left( \frac{dM_V}{dV} \right)^2 \sigma_V^2 + \left( \frac{dM_V}{d\pi} \right)^2 \sigma_\pi^2 \tag{E.3}$$

The two parts of this equation work out to:

$$\frac{dM_V}{dV} = 1 \quad (\text{E.4})$$

$$\begin{aligned} \frac{dM_V}{d\pi} &= \frac{d}{d\pi} \left[ -5 \frac{\ln \frac{100}{\pi}}{\ln 10} \right] \\ &= \frac{5}{\pi \ln 10} \end{aligned} \quad (\text{E.5})$$

Combining Equations E.4 and E.5 with Equation E.3 results in the combined error on  $M_V$  of:

$$\sigma_{M_V}^2 = \sigma_V^2 + \left( \frac{5}{\pi \ln 10} \right)^2 \sigma_\pi^2 \quad (\text{E.6})$$

(where  $\pi$  and  $\sigma_\pi$  are measured in milliarcseconds).

Table E.1: HIP data for Standards.

HIP	HD	RA (J1991.1)	Dec	$\pi$ (mas)	$\sigma_\pi$	$B_T$ mag $\sigma$	$V_T$ mag $\sigma$	$V_J^a$ mag $\sigma$	$M_{V,J}$ mag $\sigma$	$(B-V)_J^a$ mag $\sigma$
954	745	00 11 47.55 +09 08 24.0	24.0	7.81	0.96	8.582 0.013	7.560 0.009	7.468 0.0099	+1.931 0.2671	+0.87 0.016
1078	...	00 13 24.36 +19 04 17.9	28.30 1.48	28.30	1.48	11.478 0.076	10.003 0.031	9.870 0.0345	+7.129 0.1187	+1.25 0.082
1169	1031	00 14 36.56 +01 17 48.7	11.81 0.82	11.81	0.82	7.571 0.007	7.081 0.007	7.037 0.0077	+2.398 0.1510	+0.42 0.010
1427	1352	00 17 49.85 +16 19 51.9	21.66 0.87	21.66	0.87	7.775 0.008	7.259 0.008	7.213 0.0087	+3.891 0.0877	+0.44 0.011
1495	1449	00 18 39.63 +22 52 46.7	8.99 0.84	8.99	0.84	8.242 0.013	7.244 0.008	7.154 0.0088	+1.923 0.2031	+0.85 0.015
1499	1461	00 18 41.62 -08 03 09.5	42.67 0.85	42.67	0.85	7.305 0.006	6.540 0.006	6.472 0.0066	+4.623 0.0438	+0.65 0.008
1532	...	00 19 05.58 -09 57 50.8	48.17 1.73	48.17	1.73	11.599 0.100	10.041 0.038	9.901 0.0424	+8.315 0.0888	+1.32 0.107
1691	1689	00 21 13.11 -03 18 43.1	12.60 0.96	12.60	0.96	7.960 0.011	7.424 0.009	7.376 0.0099	+2.878 0.1657	+0.46 0.014
2050	2173	00 25 58.65 +21 01 27.4	6.11 0.88	6.11	0.88	8.668 0.013	7.595 0.009	7.498 0.0099	+1.429 0.3129	+0.91 0.016
2498	2816	00 31 41.51 +12 54 50.0	12.27 0.88	12.27	0.88	8.415 0.011	7.372 0.007	7.278 0.0077	+2.722 0.1559	+0.89 0.013
2512	2827	00 31 51.06 +18 06 20.0	10.47 0.81	10.47	0.81	7.845 0.007	7.273 0.007	7.222 0.0077	+2.321 0.1682	+0.49 0.010
3093	3651	00 39 22.09 +21 15 04.9	90.03 0.72	90.03	0.72	...	...	5.880 ...	+5.652 0.0200	+0.85 0.009
3203	3821	00 40 47.48 -07 13 56.6	38.65 1.10	38.65	1.10	7.788 0.011	7.040 0.009	6.969 0.0099	+4.905 0.0626	+0.64 0.014
3765	4628	00 48 22.53 +05 17 00.2	134.04 0.86	134.04	0.86	6.875 0.010	5.845 0.003	5.752 0.0033	+6.388 0.0143	+0.88 0.007
3979	4915	00 51 10.69 -05 02 20.4	45.27 0.97	45.27	0.97	7.805 0.014	7.060 0.010	6.989 0.0110	+5.268 0.0478	+0.64 0.017
4087	5036	00 52 28.14 +21 24 36.3	10.73 0.99	10.73	0.99	7.855 0.010	7.336 0.010	7.289 0.0109	+2.442 0.2006	+0.44 0.014
4893	6133	01 02 50.29 +26 17 57.6	14.49 0.94	14.49	0.94	7.672 0.007	7.257 0.007	7.220 0.0077	+3.025 0.1411	+0.35 0.010
5291	6720	01 07 42.98 -19 18 43.3	14.15 1.45	14.15	1.45	8.867 0.017	7.997 0.013	7.919 0.0143	+3.672 0.2230	+0.74 0.021
5315	6734	01 07 59.58 +01 59 38.7	21.53 0.83	21.53	0.83	7.521 0.010	6.548 0.005	6.460 0.0055	+3.126 0.0839	+0.83 0.009
5741	7377	01 13 44.88 -08 18 56.9	29.30 1.17	29.30	1.17	10.498 0.048	9.279 0.029	9.169 0.0319	+6.504 0.0924	+1.04 0.056
5806	7449	01 14 29.42 -05 02 49.4	25.96 0.77	25.96	0.77	8.202 0.008	7.568 0.008	7.511 0.0087	+4.582 0.0650	+0.54 0.011
6308	8117	01 21 03.60 +25 09 31.1	19.48 0.99	19.48	0.99	8.431 0.012	7.925 0.013	7.879 0.0142	+4.327 0.1113	+0.43 0.018
6442	8331	01 22 43.51 +10 22 11.2	18.97 0.92	18.97	0.92	8.289 0.013	7.544 0.011	7.477 0.0120	+3.867 0.1060	+0.63 0.017
6558	...	01 24 16.37 +12 54 27.9	29.60 1.43	29.60	1.43	10.828 0.058	9.574 0.031	9.461 0.0342	+6.818 0.1103	+1.07 0.066
6917	8997	01 29 04.61 +21 43 25.0	43.16 0.93	43.16	0.93	8.943 0.020	7.828 0.012	7.728 0.0132	+5.903 0.0486	+0.95 0.022
7117	9307	01 31 42.65 +10 53 21.8	7.48 1.02	7.48	1.02	8.285 0.012	7.135 0.008	7.032 0.0088	+1.401 0.2962	+0.98 0.014
7549	9958	01 37 16.16 -00 21 00.5	11.31 0.93	11.31	0.93	7.898 0.008	7.150 0.007	7.083 0.0077	+2.350 0.1787	+0.64 0.011
7564	9939	01 37 25.23 +25 10 05.8	23.80 0.86	23.80	0.86	8.149 0.010	7.095 0.007	7.000 0.0077	+3.883 0.0788	+0.90 0.013
8524	11170	01 49 55.99 +07 13 25.3	10.97 1.01	10.97	1.01	8.147 0.011	7.466 0.010	7.405 0.0109	+2.606 0.2002	+0.58 0.015
8872	11616	01 54 11.94 +09 57 02.9	12.53 1.19	12.53	1.19	8.584 0.015	7.875 0.012	7.811 0.0131	+3.301 0.2066	+0.60 0.019
9035	11833	01 56 22.43 +08 30 34.7	11.47 1.34	11.47	1.34	8.633 0.021	7.998 0.019	7.941 0.0208	+3.239 0.2545	+0.54 0.028
9911	13043	02 07 34.42 -00 36 59.7	27.04 0.86	27.04	0.86	7.646 0.006	6.950 0.006	6.883 0.0066	+4.043 0.0694	+0.60 0.008
10781	14290	02 18 46.03 +07 42 20.9	12.43 1.17	12.43	1.17	8.471 0.014	8.023 0.014	7.983 0.0153	+3.455 0.2050	+0.38 0.020
10915	14516	02 20 30.80 -06 22 43.9	15.30 1.22	15.30	1.22	8.463 0.014	7.963 0.014	7.918 0.0153	+3.841 0.1738	+0.43 0.020
12114	16160	02 36 03.83 +06 53 00.1	138.72 1.04	138.72	1.04	...	...	5.790 ...	+6.501 0.0191	+0.92 0.019
12350	16548	02 39 00.65 -08 55 39.9	18.88 0.99	18.88	0.99	7.842 0.008	7.060 0.008	6.984 0.0087	+3.364 0.1142	+0.67 0.011

Continued on Next Page...

Table E.1 – Continued

HIP	HD	RA (J1991.1)	Dec	$\pi$ (mas)	$B_T$ mag $\sigma$	$V_T$ mag $\sigma$	$V_J^a$ mag $\sigma$	$M_{V,J}$ mag $\sigma$	$(B-V)_J^a$ mag $\sigma$
12493	...	02 40 42.71	+01 11 53.2	44.84 1.46	11.197 0.056	9.693 0.025	9.558 0.0277	+7.816 0.0759	+1.28 0.061
12926	17190	02 46 15.05	+25 39 00.9	38.95 1.13	8.920 0.020	7.962 0.012	7.876 0.0131	+5.828 0.0643	+0.81 0.019
13026	17397	02 47 26.98	+01 03 33.4	18.83 1.44	8.555 0.018	7.976 0.016	7.924 0.0175	+4.298 0.1670	+0.49 0.024
13081	17382	02 48 08.97	+27 04 08.2	44.71 1.15	8.613 0.010	7.652 0.010	7.566 0.0110	+5.818 0.0569	+0.82 0.017
13345	...	02 51 44.43	-08 16 09.5	33.01 1.97	11.437 0.069	9.967 0.030	9.835 0.0333	+7.428 0.1338	+1.25 0.075
15457	20630	03 19 21.54	+03 22 11.9	109.18 0.78	5.678 0.004	4.920 0.003	4.854 0.0033	+5.045 0.0159	+0.64 0.005
15776	21019	03 23 17.70	-07 47 36.8	27.09 0.83	7.081 0.007	6.300 0.005	6.228 0.0055	+3.392 0.0668	+0.67 0.009
16537	22049	03 32 56.42	-09 27 29.9	310.75 0.85	4.859 0.004	3.830 0.003	3.734 0.0033	+6.196 0.0068	+0.88 0.005
17027	22713	03 39 01.13	-05 37 32.5	28.44 0.77	7.122 0.006	6.070 0.005	5.971 0.0055	+3.241 0.0590	+0.90 0.008
19431	26337	04 09 40.87	-07 53 35.2	17.80 0.97	7.869 0.011	7.130 0.008	7.058 0.0088	+3.310 0.1187	+0.63 0.014
20373	27642	04 21 46.30	+02 23 25.6	16.12 1.03	7.591 0.009	6.990 0.009	6.932 0.0098	+2.968 0.1391	+0.51 0.013
22319	30508	04 48 27.65	+02 42 54.5	21.03 0.86	7.572 0.008	6.610 0.005	6.523 0.0055	+3.138 0.0890	+0.82 0.009
22336	30562	04 48 36.20	-05 40 24.4	37.73 0.89	6.548 0.005	5.840 0.004	5.775 0.0044	+3.659 0.0514	+0.60 0.006
22919	31412	04 55 55.80	+04 40 15.1	29.85 0.90	7.691 0.009	7.090 0.007	7.035 0.0077	+4.253 0.0708	+0.51 0.011
23105	31738	04 58 17.08	+00 27 14.4	27.78 1.04	8.090 0.012	7.300 0.009	7.223 0.0099	+4.598 0.0763	+0.68 0.015
24130	33555	05 10 57.97	-02 15 13.5	20.66 0.84	7.498 0.008	6.350 0.005	6.247 0.0055	+2.822 0.0885	+0.98 0.009
27058	38277	05 44 17.56	-10 00 59.0	25.43 0.76	7.865 0.007	7.190 0.006	7.133 0.0066	+4.159 0.0652	+0.57 0.009
27253	38529	05 46 34.96	+01 10 06.7	23.57 0.92	6.894 0.007	6.020 0.005	5.938 0.0055	+2.800 0.0849	+0.75 0.009
27435	38858	05 48 34.90	-04 05 38.7	64.25 1.19	...	6.390 0.006	6.965 0.0065	+6.004 0.0407	+0.64 0.002
31083	46090	06 31 21.55	+02 54 40.6	35.72 0.88	7.998 0.009	7.220 0.009	7.146 0.0098	+4.910 0.0544	+0.66 0.013
32984	50281	06 52 18.37	-05 10 25.3	114.94 0.86	7.969 0.009	6.710 0.005	6.592 0.0055	+6.895 0.0172	+1.07 0.010
61946	110463	12 41 44.40	+55 43 28.9	43.06 0.82	9.519 0.015	8.380 0.010	8.281 0.0110	+6.451 0.0428	+0.97 0.018
65420	116568	13 24 33.14	-05 09 50.1	33.23 1.33	6.249 0.004	5.810 0.004	5.773 0.0044	+3.380 0.0870	+0.37 0.006
68619	122603	14 02 47.73	+03 32 44.7	16.44 1.02	8.254 0.009	7.620 0.007	7.557 0.0077	+3.637 0.1349	+0.54 0.011
69881	125184	14 18 00.57	-07 32 30.5	30.47 1.00	...	...	6.470 ...	+3.889 0.0720	+0.72 0.004
70755	126868	14 28 12.22	-02 13 40.6	24.15 1.00	5.681 0.004	4.910 0.003	4.844 0.0033	+1.758 0.0900	+0.65 0.005
70782	126961	14 28 31.25	+02 47 19.3	24.65 1.00	7.662 0.009	7.070 0.006	7.020 0.0066	+3.979 0.0883	+0.50 0.011
72659	131156	14 51 23.28	+19 06 02.3	149.26 0.76	5.485 0.005	4.610 0.004	4.533 0.0044	+5.403 0.0119	+0.74 0.006
79119	145328	16 08 58.33	+36 29 24.4	28.84 0.54	6.037 0.004	4.850 0.002	4.740 0.0022	+2.040 0.0407	+1.01 0.004
80021	147266	16 20 04.29	+21 07 57.9	9.46 0.70	7.235 0.004	6.140 0.002	6.044 0.0022	+0.923 0.1607	+0.93 0.004
80214	147767	16 22 29.22	+33 42 12.1	5.98 0.58	7.421 0.006	5.579 0.003	5.413 0.0033	-0.703 0.2106	+1.57 0.007
81693	150680	16 41 17.48	+31 36 06.8	92.63 0.60	3.647 0.003	2.920 0.003	2.853 0.0033	+2.687 0.0144	+0.62 0.004
95962	183658	19 30 52.80	-06 30 50.7	29.18 1.00	8.061 0.009	7.340 0.007	7.275 0.0077	+4.601 0.0748	+0.61 0.011
96100	185144	19 32 20.59	+69 39 55.4	173.41 0.46	5.681 0.006	4.760 0.007	4.673 0.0076	+5.868 0.0095	+0.79 0.009
96901	186427	19 41 52.10	+50 31 04.5	46.70 0.52	7.029 0.006	6.290 0.004	6.219 0.0044	+4.566 0.0246	+0.63 0.007
97255	186704	19 45 57.30	+04 14 54.6	33.05 0.99	7.755 0.010	7.090 0.011	7.031 0.0120	+4.627 0.0661	+0.56 0.015

Continued on Next Page...

Table E.1 – Continued

HIP	HD	RA	Dec (J1991.1)	$\pi$ (mas)	$\sigma_\pi$	$B_T$ mag $\sigma$	$V_T$ mag $\sigma$	$V_J^a$ mag $\sigma$	$M_{V,J}$ mag $\sigma$	$(B-V)_J^a$ mag $\sigma$
97635	188056	19 50 37.73	+52 59 17.4	16.96	0.45	6.721 0.004	5.166 0.003	5.026 0.0033	+1.173 0.0577	+1.32 0.005
98416	189340	19 59 47.49	-09 57 26.2	40.75	1.35	6.582 0.008	5.930 0.006	5.869 0.0066	+3.920 0.0722	+0.56 0.010
99894	192699	20 16 06.03	+04 34 51.3	14.84	0.91	7.528 0.007	6.540 0.005	6.449 0.0055	+2.306 0.1333	+0.84 0.009
100501	194193	20 22 45.29	+41 01 34.1	3.81	0.54	8.056 0.008	6.131 0.004	5.958 0.0044	-1.138 0.3078	+1.64 0.009
101622	196203	20 35 47.09	-00 00 04.1	9.84	1.01	7.701 0.008	6.160 0.007	7.106 0.0077	+2.071 0.2230	+0.46 0.011
101955	196795	20 39 37.20	+04 58 18.7	53.82	2.21	9.539 0.021	8.090 0.012	7.955 0.0132	+6.610 0.0901	+1.24 0.024
104202	200964	21 06 39.79	+03 48 10.8	14.63	1.03	7.596 0.009	6.590 0.007	6.497 0.0077	+2.324 0.1531	+0.86 0.011
104214	201091	21 06 50.84	+38 44 29.4	287.13	1.51	...	...	5.203 ...	+7.493 0.0152	+1.07 0.015
104217	201092	21 06 52.19	+38 44 03.9	285.42	0.72	7.764 0.012	6.210 0.009	6.068 0.0099	+8.345 0.0113	+1.32 0.015
107857	207687	21 51 05.60	-10 02 17.0	12.46	1.00	8.492 0.012	7.590 0.009	7.510 0.0099	+2.988 0.1746	+0.77 0.015
108782	209290	22 02 10.54	+01 24 03.3	96.98	1.48	11.009 0.068	9.420 0.031	9.277 0.0343	+9.210 0.0477	+1.35 0.075
109378	210277	22 09 29.82	-07 32 51.2	46.97	0.79	7.489 0.006	6.630 0.005	6.547 0.0055	+4.906 0.0369	+0.73 0.008
109820	211022	22 14 37.20	-15 06 05.4	11.14	1.06	7.718 0.008	7.272 0.010	7.232 0.0109	+2.466 0.2069	+0.38 0.013
110205	211786	22 19 25.06	+12 27 36.1	23.88	0.98	8.792 0.015	8.066 0.013	8.001 0.0142	+4.891 0.0902	+0.62 0.020
111312	213612	22 33 01.49	-17 30 05.0	14.28	0.98	8.625 0.013	7.648 0.009	7.560 0.0099	+3.334 0.1494	+0.83 0.016
111571	214100	22 36 09.65	-00 50 24.5	57.04	1.77	...	...	9.980 ...	+8.761 0.0681	+1.41 0.028
114854	219452	23 15 52.57	-13 11 02.0	14.17	0.96	7.747 0.008	7.329 0.007	7.291 0.0077	+3.048 0.1473	+0.36 0.011
114906	219516	23 16 28.07	-10 12 41.2	13.56	1.33	8.593 0.015	8.046 0.014	7.997 0.0153	+3.658 0.2135	+0.46 0.021
115004	...	23 17 32.23	+09 41 36.8	26.96	1.40	11.149 0.071	9.868 0.039	9.753 0.0430	+6.906 0.1207	+1.09 0.081
116384	...	23 35 00.08	+01 36 19.2	51.80	1.74	11.474 0.125	9.759 0.046	9.605 0.0514	+8.176 0.0892	+1.46 0.133
116600	222111	23 37 49.09	+03 22 13.1	14.58	1.06	7.836 0.013	7.339 0.013	7.294 0.0142	+3.113 0.1585	+0.42 0.018
117112	222878	23 44 32.50	-03 10 31.3	12.13	1.03	7.950 0.008	7.328 0.008	7.272 0.0087	+2.691 0.1846	+0.53 0.011
117980	224173	23 55 48.72	-13 57 59.9	17.00	1.18	7.869 0.010	7.360 0.010	7.314 0.0109	+3.466 0.1511	+0.43 0.014
1481-722-2	131156B	14 51 23.00	+19 06 08.0	144.90	6.40	8.313 0.022	6.950 0.015	6.823 0.0165	+7.628 0.0973	+1.16 0.027

<sup>a</sup>Johnson magnitudes and colors converted from Tycho magnitudes and colors (see text).



## Appendix F

### Calculating Chi Squared Values and Errors

#### F.1 Chi Square Goodness-of-Fit Test

Say I am trying to fit a distribution with some function (i.e., fitting a Gaussian to a histogram, such as in §3.6.1, or finding the best model to describe an observed composite hot subdwarf, such as in §6.3). The “best fit” can be called the fit with the minimum value of Chi Square ( $\chi^2$ ). The equation for  $\chi^2$  is as follows:

$$\chi^2 = \sum_{k=0}^n \frac{(O_k - E_k)^2}{\sigma_k^2}$$

where  $n$  is the number of points,  $O_k$  are the observed values at each point,  $E_k$  are the model (or “expected”) values at each point, and  $\sigma_k$  is the error in each observed value at each point.

The “reduced  $\chi^2$ ” ( $\chi_R^2$ ) is:

$$\chi_R^2 = \chi^2/d$$

where  $d$  is the number of degrees of freedom (DOF, basically the number of points minus the number of fit parameters).

#### F.2 Confidence Intervals for a Gaussian Fit Based on Chi Squared

To calculate the 95% confidence interval (CI) on each fit parameter: set all parameters to their “best fit” values, then increase (decrease) one parameter until the value of  $\chi^2$  increases by  $1.96^2$  ( $\chi_{95\%CI}^2 = \chi_{\text{best}}^2 + 1.96^2$ ). The amount the parameter was changed from its best fit value is the positive (negative) error for that parameter. Repeat for each fitting parameter to find the positive and negative errors on each fit parameter. This technique was used to determine the errors on the Gaussian fits to the  $J-K_S$  distribution discussed in §3.6.1.

## Appendix G

### Defining a “ $Q$ ” Parameter for $(J-H, J-K_S)$ Color-Color Space

In the color-color space made up of  $(J-H, J-K_S)$ , there are two distinct clusters of sdB stars (Figure 3.9 left panel, on page 39). I am going to define a parameter, “ $Q$ ”, that will define a point’s position along the line of the Pop I main sequence in the  $(J-H, J-K_S)$  color-color space. I discussed the use of the “ $Q$ ” parameter in §3.6.2 (pg. 28).

#### G.1 Finding the Least-Squares Linear Fit

To define the  $Q$  parameter, I found the linear least-squares fit to the sdBs that had  $\sigma(J-K_S)$  and  $\sigma(J-H) \leq 0.1$ , using the `sm` macro `lsq2` (which calculates the least-squares fit taking into account errors in both  $x$  and  $y$ ). The macro `lsq2` takes as input arrays containing the  $x_i$  values,  $y_i$  values, and an error on both  $x$  and  $y$  in the form of  $\frac{\sigma_y^2}{\sigma_x^2} \equiv \lambda$ . I used the average value of all of the errors for those point included in the fit ( $\langle J-H \rangle = 0.0609$  and  $\langle J-K_S \rangle = 0.0665$ ) as the input value of  $\lambda$ :

$$\lambda = \frac{\langle J-K_S \rangle^2}{\langle J-H \rangle^2} = \frac{0.0665^2}{0.0609^2} = 1.192$$

This macro outputs the values of the coefficients for the best fit line,  $y = a + bx$ . The macro determines  $n$  (the number of points in the array), and the median values of  $x$  and  $y$ :

$$m_x = \frac{1}{n} \sum_{i=0}^n x_i$$

$$m_y = \frac{1}{n} \sum_{i=0}^n y_i$$

It then defines quantities related to the variance in  $x$  and  $y$  ( $\sigma_{xx}$  and  $\sigma_{yy}$ ) and the covariance of  $x$  and  $y$  ( $\sigma_{xy}$ ):

$$\begin{aligned}\sigma_{xx} &= \sum_{i=0}^n (x_i - m_x)^2 \\ \sigma_{yy} &= \sum_{i=0}^n (y_i - m_y)^2 \\ \sigma_{xy} &= \sum_{i=0}^n (x_i - m_x)(y_i - m_y)\end{aligned}$$

Then, the coefficients of the linear fit ( $y = a + bx$ ) are defined as:

$$\begin{aligned}b &= \sigma_{yy} - \lambda\sigma_{xx} + \frac{\sqrt{(\sigma_{yy} - \lambda\sigma_{xx})^2 + 4\lambda\sigma_{xy}^2}}{2\sigma_{xy}} \\ a &= m_y - bm_x\end{aligned}$$

The resulting coefficients of the linear fit (taking  $x = J - H$  and  $y = J - K_S$ ) are  $a = -0.0197$  and  $b = 1.329$ .

## G.2 Defining the Color Parameter $Q$

Now, say I choose two points:

$$(x, y) = \begin{matrix} (x_o, y_o) \\ (x_o + \Delta x, y_o + \Delta y) \end{matrix} = (x_o + \Delta x, y_o + \gamma\Delta x)$$

where  $\gamma = \frac{dy}{dx} = b$ . Then I can define a parameter,  $Q_{\parallel}$ , that is the equal for both points, and is along the line of the least-squares fit:

$$Q_{\parallel} = Ax + By \tag{G.1}$$

$$Ax_o + Bx_o = A(x_o + \Delta x) + B(y_o + \gamma\Delta x) \tag{G.2}$$

Solving for  $A$ :

$$A = -B\gamma \tag{G.3}$$

Substituting Equation G.3 back into Equation G.1 results in:

$$Q_{\parallel} = -B\gamma x + By \tag{G.4}$$

However, the constant  $B$  in Equation G.4 is just a scaling constant, so it can be set equal to one, leaving:

$$Q_{\parallel} = -\gamma x + y \tag{G.5}$$

substituting color values in:

$$Q_{\parallel} = -b(J-H) + (J-K_S) \quad (\text{G.6})$$

$$Q_{\parallel} = -1.329(J-H) + (J-K_S) \quad (\text{G.7})$$

for lines that run parallel to the fit line. However, I want to use  $Q_{\perp}$  which is perpendicular to the fit line (hereafter just  $Q$ ). To get  $Q$  I need to replace  $\gamma$  with  $-\frac{1}{\gamma}$  (where  $\gamma = b$ ) in Equ. G.5 (this is basically swapping the slope of the fit line with the slope of a line perpendicular to the fit) to get:

$$Q = \frac{1}{\gamma}x + y \quad (\text{G.8})$$

substituting color values in:

$$Q = \frac{1}{b}(J-H) + (J-K_S) \quad (\text{G.9})$$

$$Q = \frac{1}{1.329}(J-H) + (J-K_S) \quad (\text{G.10})$$

$$Q = 0.752(J-H) + (J-K_S) \quad (\text{G.11})$$

Defined in this manner, lines of constant  $Q$  run perpendicular to the fit through the data (and thus roughly perpendicular to the main sequence, see Figure 3.10 on page 40). Thus binning the data points in  $Q$  (along the least-squares fit line) will show the greatest separation between composite and single sdBs using only a single parameter (see Figure 3.11 on page 41).

## Appendix H

### All About Equivalent Widths

#### H.1 Basics of Calculating Equivalent Widths

This section describes the basic concepts and equations for calculation of the equivalent width (EW) of a line in a spectrum.

##### H.1.1 EW and Poisson Error

True EW is defined (Gray 1992) as:

$$W_t = \int_{-\infty}^{\infty} \frac{F_c - F_\nu}{F_c} d\nu \quad (\text{H.1})$$

where  $F_c$  is the flux at the continuum and  $F_\nu$  is the actual flux from the object. This definition also implies that there is only a single line in the spectrum and that the integration can be carried out over the full spectrum to account completely for the line wings. However, for an observed spectrum we do not measure  $F_\nu$ , instead we measure  $D_\nu = I(\lambda) * F_\nu$ , where  $I(\nu)$  (the instrumental profile) is not narrow compared to the spectral features. Thus the measured profile is

$$\frac{D_c - D_\nu}{D_c} = \frac{I(\lambda) * (F_c - F_\nu)}{D_c} \quad (\text{H.2})$$

and the measured EW is

$$W_m = \int_{-\Delta}^{\Delta} \frac{D_c - D_\nu}{D_c} d\nu = \int_{-\Delta}^{\Delta} \frac{I(\lambda) * (F_c - F_\nu)}{D_c} d\nu$$

where  $2\Delta$  is the spectral range over which the profile can be traced.

The contribution to the total EW and Poisson error at each point  $i$  in a spectrum can be computed as:

$$W_i = \frac{C_i - F_i}{C_i} \Delta\lambda \quad (\text{H.3})$$

$$\sigma_{W_i} = \frac{\sigma_i}{C_i} \Delta\lambda \quad (\text{H.4})$$

where  $F_i$  is the flux at a given pixel,  $C_i$  is the continuum at the pixel,  $\Delta\lambda$  is the wavelength covered by the pixel, and  $\sigma_i$  is the value of the error spectrum for the pixel.

Thus the total observed EW and Poisson error for a line would be:

$$W = \sum_{i=1}^n \frac{C_i - F_i}{C_i} \Delta\lambda \quad (\text{H.5})$$

$$\sigma_W^2(F) = \sum_{i=1}^n \left( \frac{\sigma_i}{C_i} \Delta\lambda \right)^2 \quad (\text{H.6})$$

where  $i = 1$  is the pixel of the starting wavelength to sum over,  $i = n$  is the pixel of the final wavelength to sum over, so the total amount of wavelength space used to compute the total EW would be  $\lambda_{\text{tot}} = n\Delta\lambda$ .

### H.1.2 Continuum Fitting Errors

The errors in the local continuum fit for a given line were calculated following the technique described in Sembach & Savage (1992) for Legendre polynomials. This technique estimates the continuum in the region of an absorption line by fitting selected regions on either side of the line with a low order (order  $\leq 5$ ) polynomial. The general equation for a Legendre polynomial is:

$$P(x) = \sum_{k=0}^K a_k P_k(x) \quad (\text{H.7})$$

where  $K$  is the order of the polynomial. The coefficients,  $a_k$ , are determined by the continuum to the selected regions, and the functions,  $P_k(x)$ , are:

$$P_k(x) = \begin{cases} 1 & \text{for } k = 0 \\ x & \text{for } k = 1 \\ [(2k-1)xP_{k-1}(x) - (k-1)P_{k-2}(x)]/k & \text{for } k \geq 2 \end{cases} \quad (\text{H.8})$$

When defined over the range  $-1 \leq x \leq 1$ , Legendre polynomials are orthogonal. Thus it is desirable to normalize the fitting region to the range  $-1 \leq x \leq 1$ .

From Sembach & Savage (1992), the continuum fitting error is given by:

$$\sigma_{W_\lambda}(C) = x_s \frac{\lambda_0}{c} \sigma \sum_{i=1}^n \left[ \sum_{h=0}^K \sigma_{a_h}^2 P_h(x_i) P_k(x_i) \right]^{1/2} \left[ \frac{F(x_i)}{P^2(x_i)} \right] dx_i \quad (\text{H.9})$$

where  $x_i = v_i/x_s$  ( $v_i$  is the velocity offset from line center:  $v_i = c \frac{\lambda_i - \lambda_{\text{line}}}{\lambda_{\text{line}}}$ ),  $x_s$  is the normalization constant [so  $-1 \leq x \leq 1$ ,  $x_s = \max(|v|)$ ],  $c$  is the speed of light,  $\lambda_0$  is the wavelength of the line,  $F(x_i)$  is the flux at each point,  $P(x_i)$  is the Legendre polynomial fit to the continuum (Equ. H.7), and  $\sigma$  is the standard deviation of the data points about the continuum in the fitting regions.

The total error ( $\sigma_W$ ) on a measured EW is a combination of the continuum fitting error [ $\sigma_W(C)$ ] and the Poisson error [ $\sigma_W(F)$ ]:

$$\sigma_W = \left[ \sigma_W^2(F) + \sigma_W^2(C) \right]^{1/2} \quad (\text{H.10})$$

## H.2 Diluting Equivalent Widths by Combining Two Spectra

### H.2.1 Introduction

In this section I will describe the process of diluting equivalent widths (EWs) measured in the spectrum of a late-type star by combining it with the spectrum of an early type-star (i.e., a hot subdwarf star). This is graphically represented in Figures H.1 and H.2. The properties used to set the flux scale of these models are given in Tables H.1 and H.2. I plan to use these spectral energy distributions (SEDs) to appropriately dilute the EWs measured from my KPNO HIP standard star spectra to see how they are affected by varying the temperature of the late-type star, and by varying the temperature of the hot subdwarf.

### H.2.2 Hot Subdwarf Gravity Effects

Using Kurucz (1998, hereafter referred to as just “Kurucz”) flux SEDs as proxies for hot subdwarfs introduces a small amount of error due to the surface gravity of the models. The highest gravity Kurucz model has  $\log g = 5.0$ , while, as I described in §1.1.2, sdB stars typically have surface gravities in the range of  $4.5 < \log g < 6.65$ . Thus, using only  $\log g = 5.0$  models as a hot subdwarf proxy will introduce some uncertainty. To estimate the magnitude of the effect, for the three temperature models used (20kK, 26kK, and 32kK), I compared the three lowest gravity SEDs ( $\log g = 4.0, 4.5$ , and  $5.0$ ). A comparison of these three gravities for the three different temperatures is shown in Figures H.3 and H.4. The effect is not very large (few percent), but is slightly greater for higher temperature models and at longer wavelengths:

$$\begin{aligned} \left( \frac{F_{\log g=4.5} - F_{\log g=5.0}}{F_{\log g=5.0}} \right)_{T_{\text{eff}}=20\text{kK}} &\approx 0.001 \text{ to } 0.02 \\ \left( \frac{F_{4.5} - F_{5.0}}{F_{5.0}} \right)_{26\text{kK}} &\approx 0.01 \text{ to } 0.02 \\ \left( \frac{F_{4.5} - F_{5.0}}{F_{5.0}} \right)_{32\text{kK}} &\approx 0.02 \text{ to } 0.03 \end{aligned}$$

The ranges given are the differences for the flux values at Mg I b (minimum value) and Ca II triplet (maximum value). The error from this effect is smaller than other error sources, so I will continue to use  $\log g = 5.0$  models as proxies for sdBs.

A similar comparison to the Kurucz models was done using Hubeny (1998) (hereafter “Hubeny”) LTE models with  $\log g = 5.0, 5.5$ , and  $6.0$ , and  $T_{\text{eff}} = 20, 26$ , and  $32$  kK (see Figure H.5). Unfortunately the Hubeny models have only about a dozen points covering the visual ( $\sim 4000\text{--}10000$  Å), so the wavelength resolution is much less than

the Kurucz models. However, in this case, the exact opposite effect was seen from the Kurucz models, the difference was slightly greater at *lower* temperatures and *shorter* wavelengths (the magnitude of the effect is still of the order of a few percent):

$$\begin{aligned} \left| \frac{F_{\log g=6.0} - F_{\log g=5.0}}{F_{\log g=5.0}} \right|_{T_{\text{eff}}=20\text{kK}} &\approx 0.078 \text{ to } 0.096 \\ \left| \frac{F_{6.0} - F_{5.0}}{F_{5.0}} \right|_{26\text{kK}} &\approx 0.038 \text{ to } 0.038 \\ \left| \frac{F_{6.0} - F_{5.0}}{F_{5.0}} \right|_{32\text{kK}} &\approx 0.003 \text{ to } 0.010 \end{aligned}$$

The ranges given are the differences for the flux values at Ca II triplet (minimum value), and Na I D for 20 and 26kK or Mg I b for 32kK (maximum value). However, since again the effect is only on the order of a few (10 at most) percent (and opposite that seen in the Kurucz models), and since the wavelength/frequency resolution of the Hubeny models is significantly worse than the Kurucz models, I will continue to use  $\log g = 5.0$  Kurucz models as proxies for hot subdwarfs.

Another point of interest can be seen in Figures H.3 and H.4. Since sdB stars are horizontal branch stars, they all have roughly the same total luminosity. This manifests itself by causing sdB stars of different temperatures to have different radii; in particular the cooler the sdB star, the larger its radius (see Table H.2). This has the effect of causing cooler sdB stars to be *brighter* than hotter ones in the visible and near-IR. So, a cooler sdB star will dilute the lines from its late-type companion more than a hotter sdB. In Figure H.6, the SEDs have been extended into the UV to demonstrate that the models all converge to the same flux, indicating that they in fact all have the same luminosity.

### H.2.3 Calculating a Diluted EW

From Appendix H.1, I defined the EW per pixel as:

$$W_i = \frac{C_i - F_i}{C_i} \Delta\lambda \quad (\text{H.11})$$

where  $F_i$  is the flux at a given pixel,  $C_i$  is the local continuum at the pixel, and  $\Delta\lambda$  is the wavelength covered by the pixel. (Please note that when I refer to the “continuum” in this section, and §H.2.4, I am referring to the “local continuum” in the vicinity of the line of interest, as opposed to a “global continuum” defined at extremely high resolution or without spectral lines.) Thus the total observed EW for a line would be:

$$W_{\text{tot}} = \sum_{i=1}^n \frac{C_i - F_i}{C_i} \Delta\lambda \quad (\text{H.12})$$

where  $i = 1$  is the pixel of the starting wavelength to sum over,  $i = n$  is the pixel of the final wavelength to sum over, so the total amount of wavelength space used to compute the total EW would be  $\lambda_{\text{tot}} = n\Delta\lambda$ .



The EW in a pixel of a diluted line from Equ. H.11 is:

$$W_{d,i} = \frac{C_{d,i} - F_{d,i}}{C_{d,i}} \Delta\lambda \quad (\text{H.13})$$

However, in the diluted spectrum,  $F_d = F_1 + F_2$  and  $C_d = C_1 + C_2$ . If star #2 is a hot subdwarf, then effectively  $F_2 = C_2$  (a hot subdwarf can be thought of as a continuum light source), so  $F_d = F_1 + C_2$ . If star #1 contributes a fraction  $D$  to the combined light in the local continuum, then  $C_1 = D C_d$ . Then substituting these into Eqn. H.13 for a given pixel, the diluted EW becomes:

$$W_{d,i} = \frac{C_{1,i} + C_{2,i} - (F_{1,i} + C_{2,i})}{\frac{C_{1,i}}{D}} \Delta\lambda \quad (\text{H.14})$$

$$W_{d,i} = D \frac{C_{1,i} - F_{1,i}}{C_{1,i}} \Delta\lambda \quad (\text{H.15})$$

Thus the diluted EW per pixel is:

$$W_{d,i} = D W_{u,i} \quad (\text{H.16})$$

Where  $D$  (the dilution) is the fraction of the total composite light contributed by the late-type star, and  $W_{u,i}$  is the undiluted EW. Thus, when a star with a feature that has an intrinsic (undiluted) EW of  $W_u$  is diluted to some amount  $D$ , then the resulting diluted EW becomes:

$$W_d = D W_u \quad (\text{H.17})$$

where the subscript “u” refers to the undiluted values, and “d” to the diluted values, and again “ $D$ ” refers to the fraction of the combined light contributed by the star with the intrinsic spectral feature (the late-type star in the specific case of a sd+late-type composite).

For example, if a line with  $W_u = 0.2 \text{ \AA}$ , is diluted so that its originating star contributes only 75% of the light at that wavelength, then  $W_d = 0.75 \times 0.2 \text{ \AA} = 0.15 \text{ \AA}$ .

#### H.2.4 Predicting Diluted EWs using Stellar Flux Distributions

In this section I will describe the steps to use a Kurucz flux distribution to determine the dilution at various locations in the spectrum assuming the dilution is known at one wavelength.

From the Kurucz files I can get the flux values at the local continuum around the lines of interest (Ca II triplet, Na I D, and Mg I b — see Table H.3). Assuming a temperature for both the companion and the subdwarf, and setting the dilution at Ca II,

then the dilutions at Mg I and Na I can be determined using these values:

$$D_{c, \text{Ca}} = \frac{F_{c, \text{Ca}}}{F_{c, \text{Ca}} + F_{\text{sd}, \text{Ca}}} \quad (\text{H.18})$$

$$D_{c, \text{Na}} = \frac{R_{c, \text{Na}/\text{Ca}} F_{c, \text{Ca}}}{R_{c, \text{Na}/\text{Ca}} F_{c, \text{Ca}} + R_{\text{sd}, \text{Na}/\text{Ca}} F_{\text{sd}, \text{Ca}}} \quad (\text{H.19})$$

$$D_{c, \text{Mg}} = \frac{R_{c, \text{Mg}/\text{Ca}} F_{c, \text{Ca}}}{R_{c, \text{Mg}/\text{Ca}} F_{c, \text{Ca}} + R_{\text{sd}, \text{Mg}/\text{Ca}} F_{\text{sd}, \text{Ca}}} \quad (\text{H.20})$$

where  $R_{\text{sd}, \text{Na}/\text{Ca}} \equiv \frac{F_{\text{sd}, \text{Na}}}{F_{\text{sd}, \text{Ca}}}$ ,  $R_{\text{sd}, \text{Mg}/\text{Ca}} \equiv \frac{F_{\text{sd}, \text{Mg}}}{F_{\text{sd}, \text{Ca}}}$ ,  $R_{c, \text{Na}/\text{Ca}} \equiv \frac{F_{c, \text{Na}}}{F_{c, \text{Ca}}}$ ,  $R_{c, \text{Mg}/\text{Ca}} \equiv \frac{F_{c, \text{Mg}}}{F_{c, \text{Ca}}}$ . However,  $F_{\text{sd}, \text{Ca}} = F_{c, \text{Ca}}(\frac{1}{D_{c, \text{Ca}}} - 1)$ , so Equations H.19 and H.20 become:

$$D_{c, \text{Na}} = \frac{D_{c, \text{Ca}}}{D_{c, \text{Ca}} + \frac{R_{\text{sd}, \text{Na}/\text{Ca}}}{R_{c, \text{Na}/\text{Ca}}}(1 - D_{c, \text{Ca}})} \quad (\text{H.21})$$

$$D_{c, \text{Mg}} = \frac{D_{c, \text{Ca}}}{D_{c, \text{Ca}} + \frac{R_{\text{sd}, \text{Mg}/\text{Ca}}}{R_{c, \text{Mg}/\text{Ca}}}(1 - D_{c, \text{Ca}})} \quad (\text{H.22})$$

Now, to make a composite of a 20,000 K sdB with a 5000 K late-type star from Fig. H.1, where the late-type star contributes  $\frac{1}{3}$  of the light at the Ca II triplet (so  $D_{c, \text{Ca}} = 0.333$ ). The corresponding dilutions at Na I and Mg I using Equations H.21 and H.22, and the flux ratio values from Table H.3 are:

$$\begin{aligned} D_{c, \text{Na}} &= 0.162 \\ D_{c, \text{Mg}} &= 0.093 \end{aligned}$$

The fact that the fraction of light contributed by the companion decreases toward shorter wavelengths is expected and can be pictured by comparing the shapes of the flux distributions for a 5000 K star with the 20,000 K star in Figs. H.1 and/or H.2.

Now, the diluted EW for combinations of sdB, late-type companions, and Ca II dilutions ( $D_{c, \text{Ca}}$ ) can be computed using Equations H.17, H.21, and H.22.

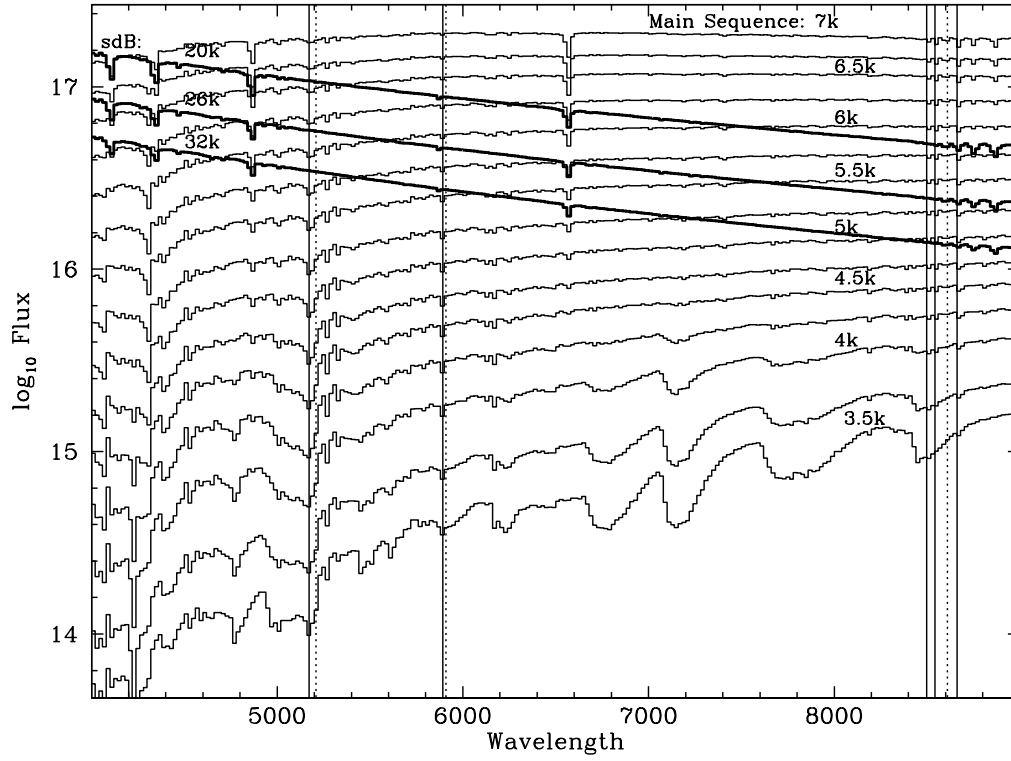


Fig. H.1 Relative spectral flux distributions (from Kurucz) for main sequence stars and several hot subdwarfs of varying temperatures. Assuming the parameters for the main sequence given in Table H.1, and for the hot subdwarfs given in Table H.2. The solid vertical lines mark the approximate wavelengths of MgI b, NaI D, and CaII triplet (from left to right). The dotted vertical lines mark the location for the flux values reported in Table H.3.

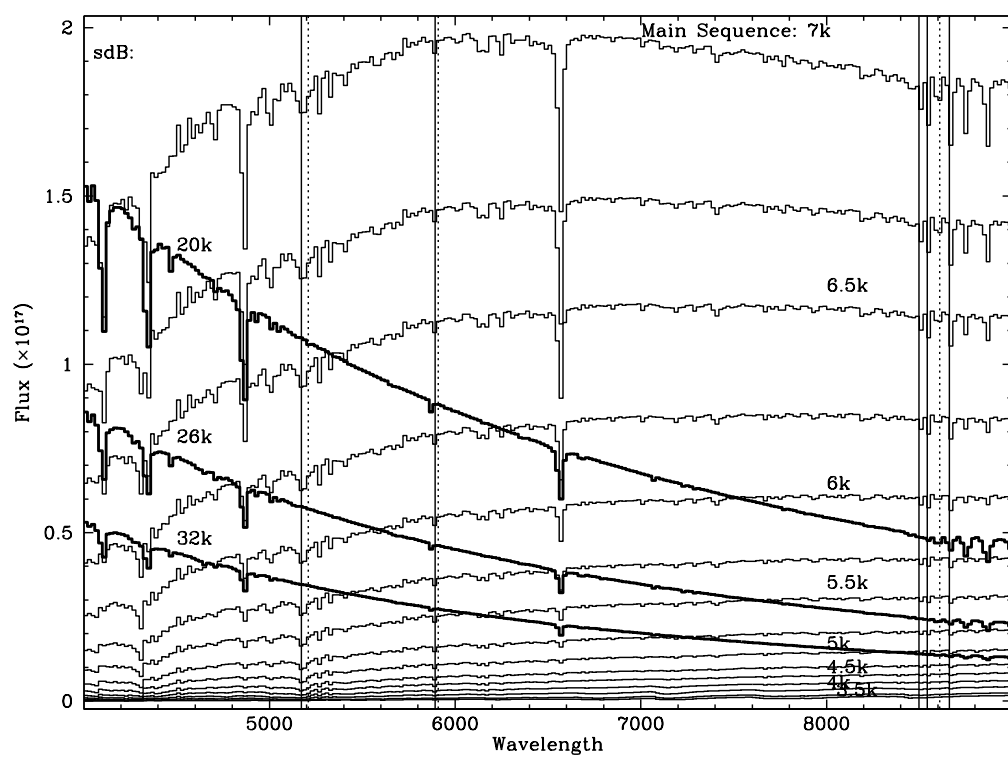


Fig. H.2 Same as Figure H.1 except flux is plotted on a linear scale.

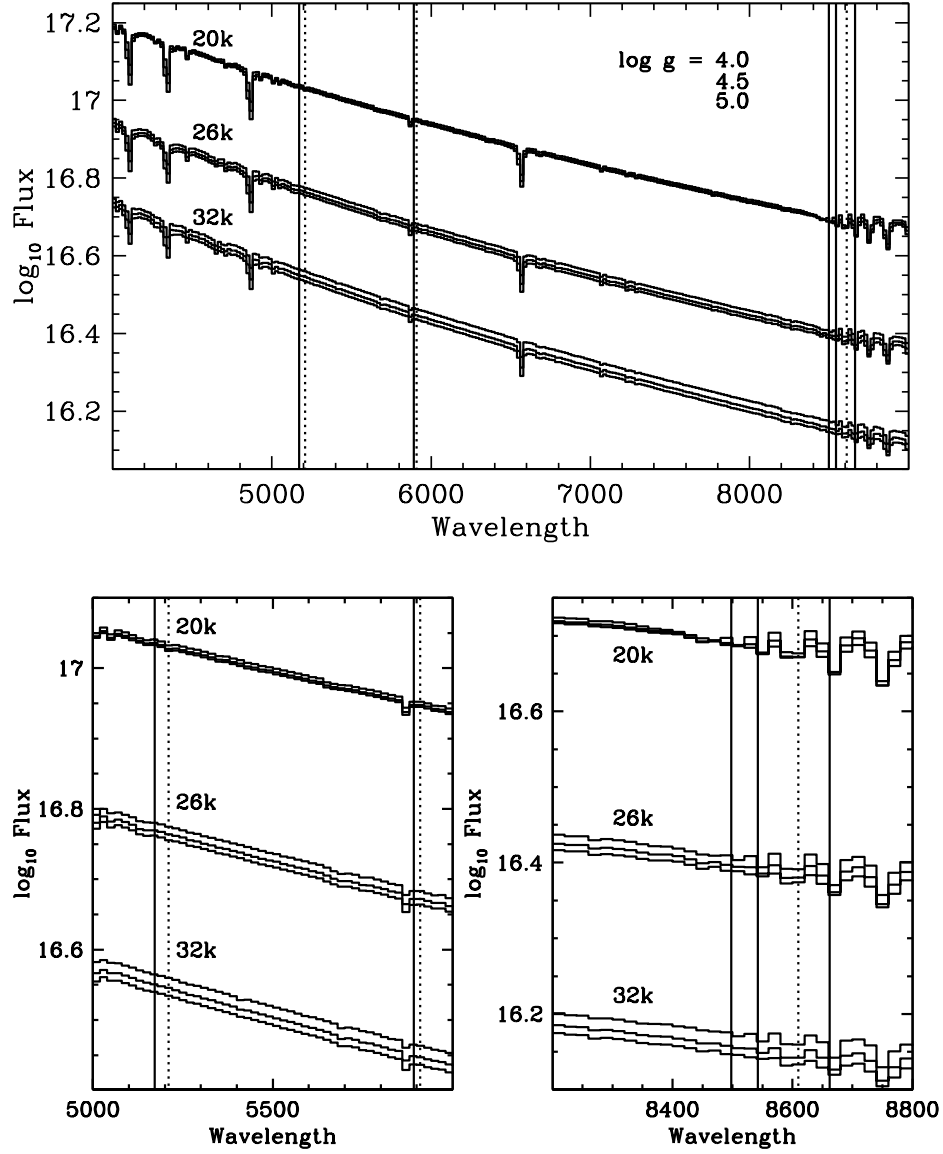


Fig. H.3 Relative spectral flux distributions (from Kurucz) for three different temperature hot subdwarfs (groups from top to bottom: 20kK, 26kK, and 32kK) and three different gravities for each temperature (from top to bottom in each temperature group:  $\log g = 4.0, 4.5, 5.0$ ). Assuming the parameters for the hot subdwarfs given in Table H.2. The solid vertical lines mark the approximate wavelengths of Mg I b, Na I D, and Ca II triplet (from left to right). The dotted vertical lines mark the location for the flux values reported in Table H.3. Bottom two panels show the details around Mg I b and Na I D (left), and around Ca II (right).

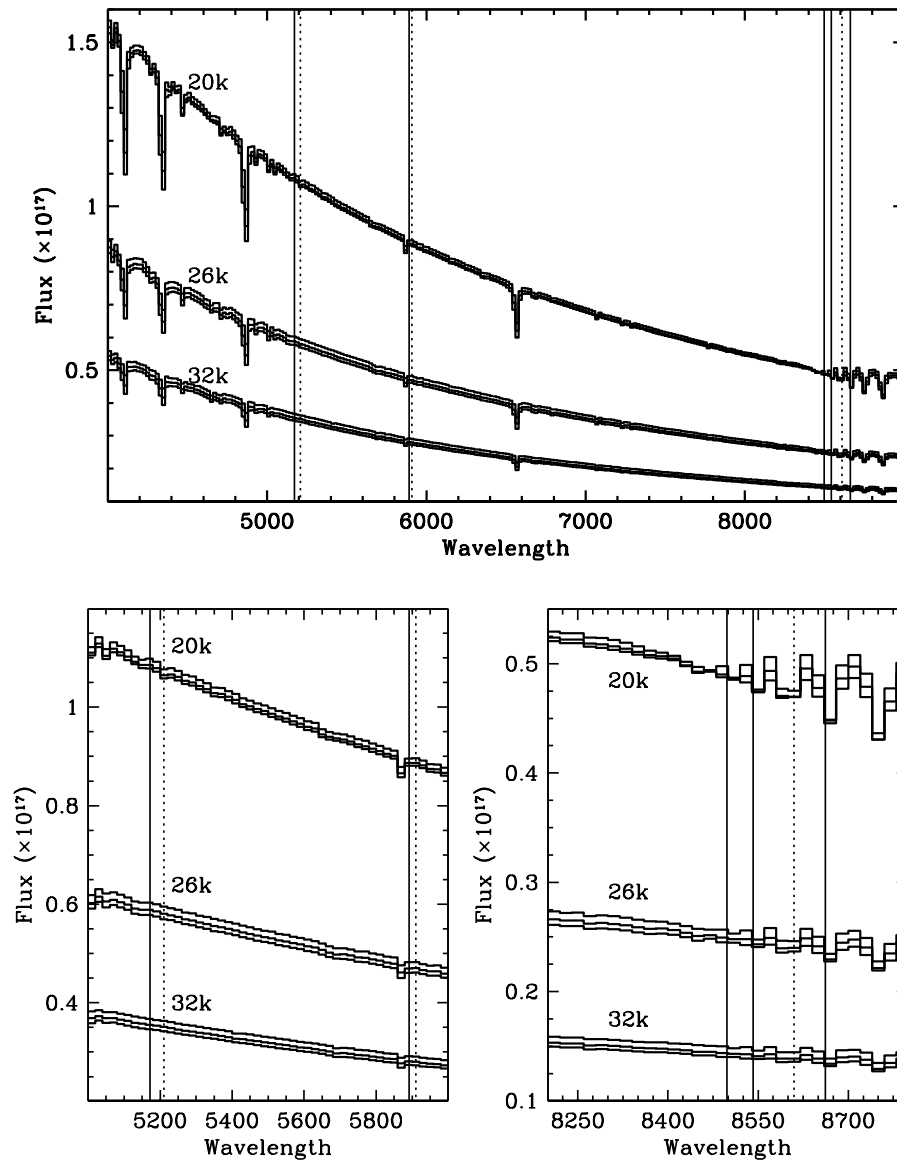


Fig. H.4 Same as Figure H.3 except flux is plotted on a linear scale.

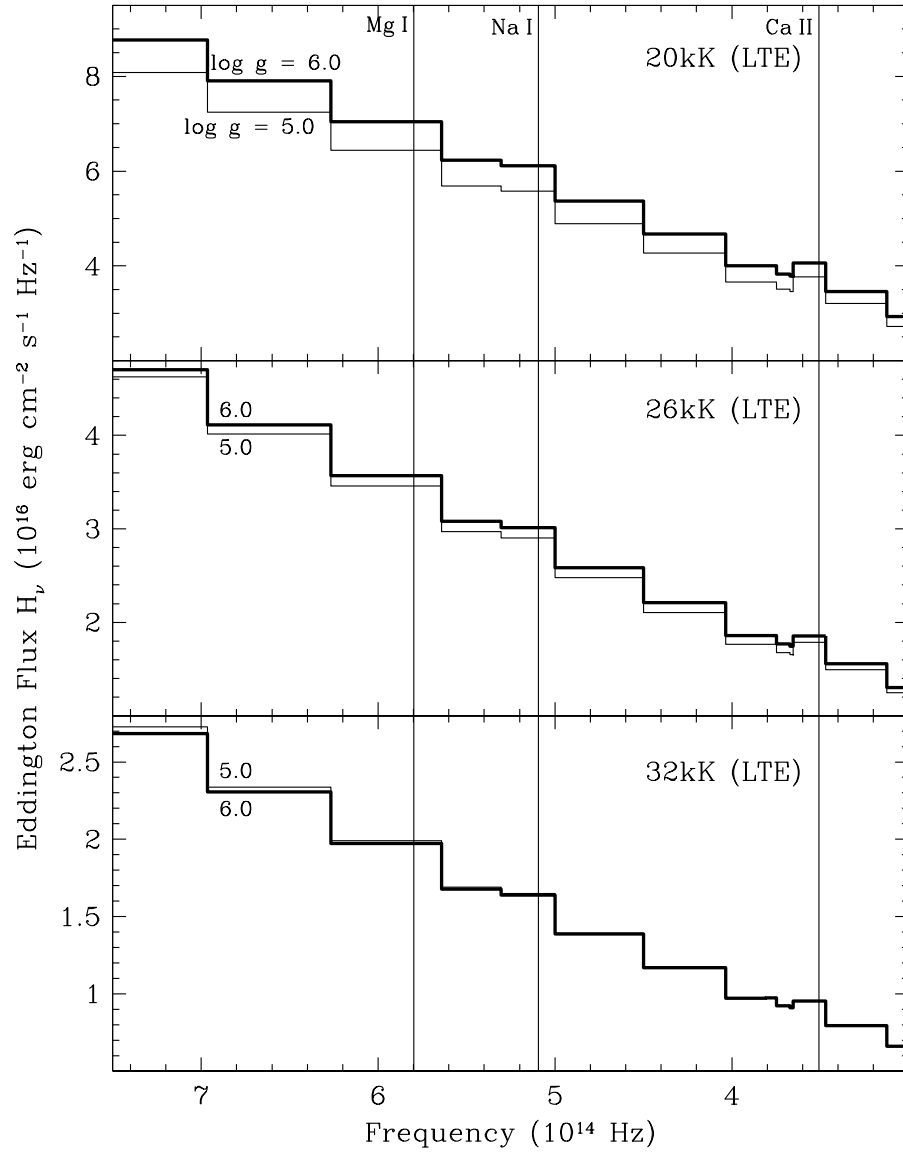


Fig. H.5 Relative spectral flux distributions (from Hubeny) for three different temperature hot subdwarfs (panels from top to bottom: 20kK, 26kK, and 32kK) and two different gravities for each temperature (thin line  $\log g = 5.0$ , thick line  $\log g = 6.0$ ). Eddington fluxes have been adjusted assuming the parameters for the hot subdwarfs given in Table H.2. The vertical lines mark the approximate frequencies of Mg I b, Na I D, and Ca II triplet (from left to right).

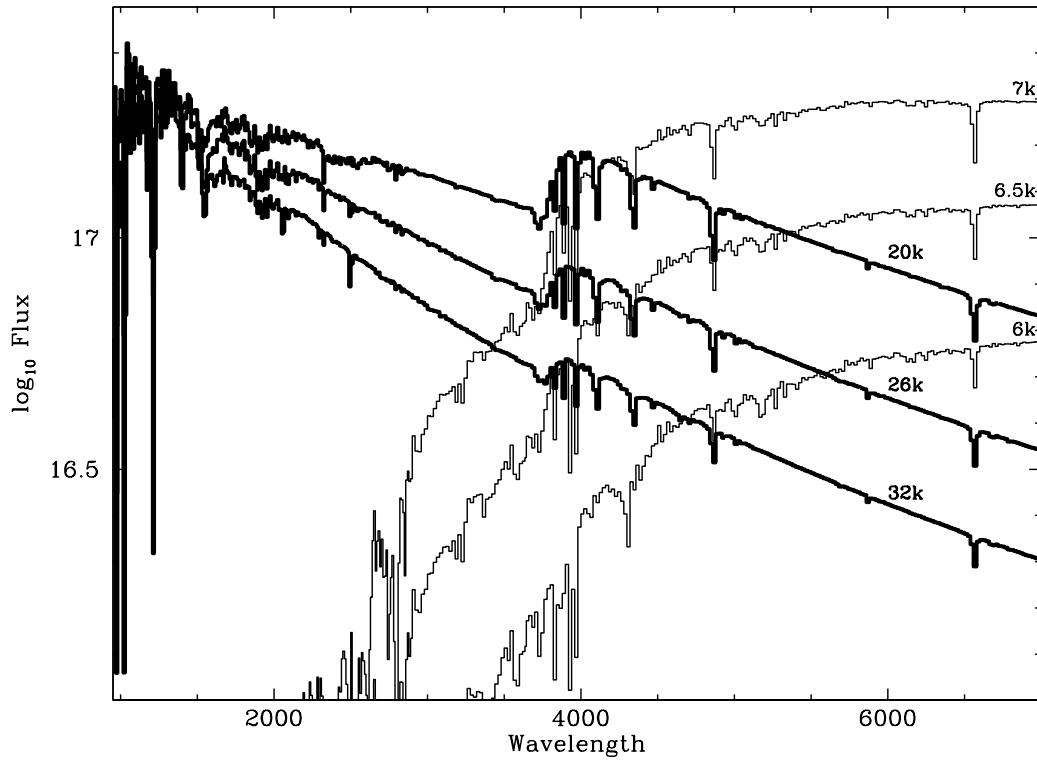


Fig. H.6 Proxy SEDs from Kurucz extended out to the UV for hot subdwarfs ( $T_{\text{eff}} = 20\text{kK}$ ,  $26\text{kK}$ , and  $32\text{kK}$ , thick lines) and main sequence stars ( $T_{\text{eff}} = 7\text{kK}$ ,  $6.5\text{kK}$ , and  $6\text{kK}$ , thin lines). Note that the hot subdwarfs all converge to the same UV flux, demonstrating that they are indeed horizontal branch stars.



Table H.1. Adopted Properties of Main Sequence Stars.

Approx. Spectral Type	$T_{\text{eff}}$ (K)	Radius <sup>a</sup> ( $R_{\odot}$ )	$B-V$ <sup>b</sup>
M2	3500	0.50	1.447
M1	3750	0.52	1.430
M0	4000	0.61	1.360
K7	4250	0.65	1.252
K5	4500	0.68	1.129
K4	4750	0.70	1.022
K2	5000	0.75	0.933
K0	5250	0.81	0.851
G7	5500	0.91	0.769
G3	5750	0.99	0.688
F9	6000	1.11	0.612
F6	6250	1.23	0.541
F4	6500	1.36	0.477
F2	6750	1.44	0.420
A9	7000	1.56	0.371

<sup>a</sup>Gray (1992).<sup>b</sup> $B-V$  color based on Kurucz  $\log g = 5.0$ , solar metallicity models.

Table H.2. Adopted Properties for Hot Subdwarf Stars.

$T_{\text{eff}}$ (K)	Radius <sup>a</sup> ( $R_{\odot}$ )	$B-V$ <sup>b</sup>	$\log L_{\text{sd}}$ <sup>a</sup>	$BC_B$ <sup>b</sup>	$BC_V$ <sup>b</sup>	$BC_J$ <sup>b</sup>	$BC_H$ <sup>b</sup>	$BC_{K_S}$ <sup>b</sup>
20000	0.3454	-0.196	1.262	-1.750	-1.933	-2.413	-2.493	-2.562
26000	0.2016	-0.242	1.193	-2.355	-2.588	-3.193	-3.297	-3.389
32000	0.1274	-0.279	1.169	-2.781	-3.053	-3.748	-3.868	-3.977

<sup>a</sup>Caloi (1972), for the ZAEHB.<sup>b</sup> $B-V$  color and BC based on Kurucz models.

Table H.3. Flux Values from the Kurucz Files.

$T_{\text{eff}}$ (K)	$\log g$	Model $B-V^{\text{a}}$	Flux at ...			Flux Ratios	
			Ca II Triplet <sup>b</sup>	Na I D <sup>b</sup>	Mg I b <sup>b</sup>	$R_{\text{Na/Ca}}^{\text{c}}$	$R_{\text{Mg/Ca}}^{\text{d}}$
Hot Subdwarfs							
20000	5.0	−0.196	8.1210 $E-5$	1.5242 $E-4$	1.8313 $E-4$	1.87686	2.25502
26000	5.0	−0.242	1.2025 $E-4$	2.3452 $E-4$	2.8934 $E-4$	1.95027	2.40615
32000	5.0	−0.279	1.7280 $E-4$	3.4716 $E-4$	4.3561 $E-4$	2.00903	2.52089
Main Sequence							
3500	4.5	+1.447	9.5757 $E-7$	3.1620 $E-7$	1.1152 $E-7$	0.33021	0.11646
3750	4.5	+1.430	1.5005 $E-6$	6.0910 $E-7$	2.2000 $E-7$	0.40593	0.14662
4000	4.5	+1.360	2.0861 $E-6$	9.9720 $E-7$	3.7125 $E-7$	0.47802	0.17796
4250	4.5	+1.252	2.7609 $E-6$	1.5278 $E-6$	6.1590 $E-7$	0.55337	0.22308
4500	4.5	+1.129	3.5563 $E-6$	2.1987 $E-6$	1.0310 $E-6$	0.61825	0.28991
4750	4.5	+1.022	4.4483 $E-6$	3.0025 $E-6$	1.6622 $E-6$	0.67498	0.37367
5000	4.5	+0.933	5.4273 $E-6$	3.9521 $E-6$	2.5228 $E-6$	0.72819	0.46484
5250	4.5	+0.851	6.4931 $E-6$	5.0462 $E-6$	3.5678 $E-6$	0.77716	0.54948
5500	4.5	+0.769	7.6304 $E-6$	6.2816 $E-6$	4.7476 $E-6$	0.82323	0.62220
5750	4.5	+0.688	8.8198 $E-6$	7.6517 $E-6$	6.0552 $E-6$	0.86756	0.68655
6000	4.5	+0.612	1.0050 $E-5$	9.1578 $E-6$	7.5084 $E-6$	0.91122	0.74710
6250	4.5	+0.541	1.1304 $E-5$	1.0801 $E-5$	9.1264 $E-6$	0.95550	0.80736
6500	4.5	+0.477	1.2576 $E-5$	1.2583 $E-5$	1.0935 $E-5$	1.00056	0.86951
6750	4.5	+0.420	1.3851 $E-5$	1.4518 $E-5$	1.2951 $E-5$	1.05032	0.93502
7000	4.5	+0.371	1.5136 $E-5$	1.6644 $E-5$	1.5230 $E-5$	1.09963	1.00621
Subgiants							
3500	2.5	+1.370	6.3438 $E-7$	1.8021 $E-7$	7.3774 $E-8$	0.28407	0.11629
3750	3.5	+1.392	1.2902 $E-6$	5.2146 $E-7$	1.8935 $E-7$	0.40417	0.14676
4000	3.5	+1.346	1.9913 $E-6$	9.7330 $E-7$	3.7368 $E-7$	0.48878	0.18766
4250	3.5	+1.241	2.7379 $E-6$	1.5220 $E-6$	6.7735 $E-7$	0.55590	0.24740
4500	3.5	+1.128	3.5449 $E-6$	2.1867 $E-6$	1.1548 $E-6$	0.61686	0.32576
4750	3.5	+1.033	4.4386 $E-6$	2.9909 $E-6$	1.8403 $E-6$	0.67384	0.41461
5000	4.0	+0.934	5.4229 $E-6$	3.9442 $E-6$	2.6267 $E-6$	0.72732	0.48437
5250	4.0	+0.850	6.4903 $E-6$	5.0394 $E-6$	3.6488 $E-6$	0.77645	0.56219
5500	4.0	+0.767	7.6252 $E-6$	6.2764 $E-6$	4.8005 $E-6$	0.82311	0.62956
5750	4.0	+0.685	8.8117 $E-6$	7.6519 $E-6$	6.0949 $E-6$	0.86838	0.69168
6000	4.0	+0.609	1.0030 $E-5$	9.1711 $E-6$	7.5486 $E-6$	0.91437	0.75260
6250	4.0	+0.539	1.1272 $E-5$	1.0835 $E-5$	9.1808 $E-6$	0.96123	0.81448
6500	4.0	+0.475	1.2520 $E-5$	1.2655 $E-5$	1.1023 $E-5$	1.01078	0.88043
6750	4.0	+0.418	1.3770 $E-5$	1.4641 $E-5$	1.3102 $E-5$	1.06325	0.95149
7000	4.0	+0.368	1.5022 $E-5$	1.6822 $E-5$	1.5454 $E-5$	1.11982	1.02876

<sup>a</sup> Adopted  $B-V$ , based on synthetic colors corresponding to the models.

<sup>b</sup> Ca II Triplet = 8610 Å; Na I D = 5910 Å; Mg I b = 5210 Å. The tabulated flux is the Eddington flux ( $H_{\nu}$ ) in units of  $\text{erg cm}^{-2} \text{s}^{-1} \text{Hz}^{-1} \text{Sr}^{-1}$

<sup>c</sup>  $R_{\text{Na/Ca}} = F_{\text{Na}}/F_{\text{Ca}}$ .

<sup>d</sup>  $R_{\text{Mg/Ca}} = F_{\text{Mg}}/F_{\text{Ca}}$ .

## Appendix I

### Calculating Cubic Spline Approximations

#### I.1 Formalism of the Cubic Spline<sup>1</sup>

This is a basic description of the steps to calculate a spline fit through some number ( $N$ ) of points which have x-coordinates that I will call  $x_i$ , and y-coordinates that I will call  $f(x_i)$ .

The cubic spline polynomial is written as:

$$S_i(x) = a_i + b_i(x - x_i) + c_i(x - x_i)^2 + d_i(x - x_i)^3 \quad (\text{I.1})$$

The conditions that need to be satisfied for a cubic spline are as follows:

1.  $S(x)$  is a cubic polynomial, denoted  $S_i(x)$  in the subinterval  $[x_i, x_{i+1}]$  for each  $i = 0, 1, \dots, N-2$ . This condition leads to the form of Equ. I.1.
2.  $S_i(x_i) = f(x_i)$  for each  $i = 0, 1, \dots, N-1$  [or in other words,  $S_i$  goes through the points  $f(x_i)$ ]. This implies:  $S_i(x_i) = a_i = f(x_i)$ .
3.  $S_{i+1}(x_{i+1}) = S_i(x_{i+1})$  for each  $i = 0, 1, \dots, N-2$ , the values are the same. Which implies:

$$S_{i+1}(x_{i+1}) = a_{i+1} = a_i + b_i(x_{i+1} - x_i) + c_i(x_{i+1} - x_i)^2 + d_i(x_{i+1} - x_i)^3 \quad (\text{I.2})$$

defining  $h_i = x_{i+1} - x_i$ , then Equ. I.2 becomes:

$$S_{i+1}(x_{i+1}) = a_{i+1} = a_i + b_i h_i + c_i h_i^2 + d_i h_i^3 \quad (\text{I.3})$$

4.  $S'_{i+1}(x_{i+1}) = S'_i(x_{i+1})$  for each  $i = 0, 1, \dots, N-2$ , the derivatives are the same. This implies:

$$S'_{i+1}(x_{i+1}) = b_{i+1} = b_i + 2c_i h_i + 3d_i h_i^2 \quad (\text{I.4})$$

5.  $S''_{i+1}(x_{i+1}) = S''_i(x_{i+1})$  for each  $i = 0, 1, \dots, N-2$ , the second derivatives are the same. Which implies:

$$S''_{i+1}(x_{i+1}) = c_{i+1} = c_i + 3d_i h_i$$

---

<sup>1</sup>Based on *Computational Physics* (PHYS 527) notes, instructor Jorge Pullin, Penn State, Fall Semester, 2000.

which leads to:

$$d_i = \frac{c_{i+1} - c_i}{3h_i} \quad (\text{I.5})$$

6. One of the following boundary conditions are satisfied:

- (a)  $S''(x_0) = S''(x_N) = 0$  (free or “natural” boundary — I have opted to use this one).
- (b)  $S'(x_0) = f'(x_0)$  and  $S'(x_N) = f'(x_N)$  (“clamped” boundary).

By combining Equ. I.3, I.4, and I.5, it is possible to solve for the individual coefficients of Equ. I.1 (namely  $b_i$ ,  $c_i$ , and  $d_i$ , since  $a_i$  and  $h_i$  are already known).

## I.2 Algorithm for Coefficient Calculation

Here is an outline of a procedure to compute the values of  $b_i$ ,  $c_i$ , and  $d_i$  (for  $i = 0, 1, \dots, n-1$ ):

1. Define the variable  $\alpha_i = 3 \frac{a_{i+1} - a_i}{h_i} - 3 \frac{a_i - a_{i-1}}{h_{i-1}}$ .
2. Define the variables  $L_i$ ,  $\mu_i$ , and  $Z_i$ , and set the values of  $L_0 = \mu_0 = Z_0 = 0$ .
3. Then for the values of  $i = 1$  to  $i < n-1$  set:

$$\begin{aligned} L_i &= 2(x_{i+1} - x_{i-1}) - h_{i-1}\mu_{i-1} \\ \mu_i &= \frac{h_i}{L_i} \\ Z_i &= \frac{\alpha_i - h_{i-1}Z_{i-1}}{L_i} \end{aligned}$$

4. Then set the values of  $c_{n-1} = 0$ ,  $L_{n-1} = 1$ , and  $Z_{n-1} = 0$ .
5. Then calculate the coefficients of Equ. I.1 starting with  $j = n-2$  and decreasing to  $j = 0$ :

$$c_j = Z_j - \mu_j c_{j+1} \quad (\text{I.6})$$

$$b_j = \frac{a_{j+1}a_j}{h_j} - \frac{h_j}{3}(c_{j+1} + 2c_j) \quad (\text{I.7})$$

$$d_j = \frac{c_{j+1} - c_j}{3h_j} \quad (\text{I.8})$$

6. Equ. I.6, I.7, and I.8 are the coefficients for Equ. I.1, along with condition #2 which states  $a_i = f(x_i)$ . Thus it is possible to solve Equ. I.1 at any location between  $x_0$  and  $x_{N-1}$  to make a continuous, smooth, fit through  $N$  sparse points.

## Appendix J

### Second Order Lagrange Polynomial Interpolation

This is a brief description of calculating a second order Lagrange polynomial to interpolate between points. The general Lagrange equation for any order is:

$$\begin{aligned} P(x) &= f(x_0)L_{n,0}(x) + \cdots + f(x_n)L_{n,n}(x) \\ P(x) &= \sum_{k=0}^n f(x_k)L_{n,k}(x) \end{aligned} \quad (\text{J.1})$$

where the coefficients  $L_{n,k}(x)$  are defined as:

$$\begin{aligned} L_{n,k}(x) &= \frac{(x-x_0)(x-x_1) \cdots (x-x_{k-1})(x-x_{k+1}) \cdots (x-x_n)}{(x_k-x_0)(x_k-x_1) \cdots (x_k-x_{k-1})(x_k-x_{k+1}) \cdots (x_k-x_n)} \\ L_{n,k}(x) &= \prod_{\substack{i=0 \\ i \neq k}}^n \frac{x-x_i}{x_k-x_i} \end{aligned} \quad (\text{J.2})$$

For second order ( $n = 2$ ) the coefficients  $L_{2,k}(x)$  from Equ. J.2 become:

$$L_{2,0}(x) = \frac{(x-x_1)(x-x_2)}{(x_0-x_1)(x_0-x_2)} \quad (\text{J.3})$$

$$L_{2,1}(x) = \frac{(x-x_0)(x-x_2)}{(x_1-x_0)(x_1-x_2)} \quad (\text{J.4})$$

$$L_{2,2}(x) = \frac{(x-x_0)(x-x_1)}{(x_2-x_0)(x_2-x_1)} \quad (\text{J.5})$$

Then a second order Lagrange polynomial from Equ. J.1 becomes:

$$\begin{aligned} P(x) &= \sum_{k=0}^2 f(x_k)L_{2,k}(x) \\ P(x) &= f(x_0)L_{2,0}(x) + f(x_1)L_{2,1}(x) + f(x_2)L_{2,2}(x) \end{aligned} \quad (\text{J.6})$$

So combining Equ. J.6 with Equ. J.3–J.5 results in a final second order Lagrange equation of:

$$\begin{aligned} P(x) &= f(x_0) \frac{(x-x_1)(x-x_2)}{(x_0-x_1)(x_0-x_2)} + f(x_1) \frac{(x-x_0)(x-x_2)}{(x_1-x_0)(x_1-x_2)} \\ &\quad + f(x_2) \frac{(x-x_0)(x-x_1)}{(x_2-x_0)(x_2-x_1)} \end{aligned} \quad (\text{J.7})$$

## Appendix K

### Measurements of Equivalent Widths for Program Stars

In this section I will present tables containing the measurements of EW for the HIP standard stars, followed by the hot subdwarfs. Table K.1 lists the EWs measured for the HIP standards, and Table K.3 for the hot subdwarfs, from the blue<sup>1</sup> spectrograph setting:  $H\beta$ , Mg I b, Na I D, and  $H\alpha$ . Table K.2 lists the EWs measured for the HIP standards, and Table K.4 for the hot subdwarfs, from the red<sup>1</sup> spectrograph setting:  $H\alpha$  and CaT. (Note that the EW for *each* member of the CaT is reported separately in Tables K.2 and K.4, while the sum of the EWs of all three lines, and the quadrature sum of the errors, were used in the analysis discussed in Chapter 5.)

Notes for all tables are as follows:

- a. EW of the line measured in Å; negative values imply emission; null values imply either (1) that the line was not covered in the spectrum, or (2) that the deviation of the normalized flux at the nominal line center was less than  $\pm 0.01$  from the continuum.
- b. Poisson error  $[\sigma_W(F)]$  for the measurement, see §H.1.1.
- c. Continuum fitting error  $[\sigma_W(C)]$  for the measurement, see §H.1.2.
- d. Combined EW for all three lines in the Mg I b triplet.
- e. Combined EW for both lines in the Na I D doublet.
- f. Identification number from KHD.
- g. EW of the Paschen-14 8598 Å line, this line was measured to determine if the CaT lines were being contaminated by Paschen lines.
- h. UT Dates for the hot subdwarf observations are given as two digit year, two digit month, and two digit day (YYMMDD).
- i. Residual fringing affecting the CaT, additional error corresponding to the approximate size in EW of the fringes has been added to  $\sigma_W(C)$  to account for this systematic effect (in all cases the first decimal place in  $\sigma_W(C)$  is equal to the additional error added — for an error given as “0.Nnnn”, the formal error was “0.0nnn” and the amount added to account for the systematic effect is “0.N”). See also §4.6.5.1.

---

<sup>1</sup>Settings described in §4.2.1.

Table K.1: EW Measurements for HIP Standard Stars from the  
Blue Spectrograph Setting.

HIP#	HD#	UT Date	H $\beta$			Mg I b <sup>d</sup>			Na I D <sup>e</sup>			H $\alpha$		
			EW <sup>a</sup>	$\sigma_F$ <sup>b</sup>	$\sigma_C$ <sup>c</sup>	EW <sup>a</sup>	$\sigma_F$ <sup>b</sup>	$\sigma_C$ <sup>c</sup>	EW <sup>a</sup>	$\sigma_F$ <sup>b</sup>	$\sigma_C$ <sup>c</sup>	EW <sup>a</sup>	$\sigma_F$ <sup>b</sup>	$\sigma_C$ <sup>c</sup>
954	745	Sep 18 2003	2.8921	0.0218	0.0172	5.0438	0.0266	0.0323	1.9082	0.0249	0.0185	1.7564	0.0228	0.0132
1078	...	Sep 18 2003	1.3529	0.0719	0.0611	11.2795	0.0779	0.0861	9.0262	0.0548	0.0348	1.0300	0.0522	0.0306
1169	1031	Sep 18 2003	5.3529	0.0162	0.0121	2.4710	0.0223	0.0280	1.0093	0.0228	0.0171	4.2739	0.0206	0.0113
1427	1352	Sep 18 2003	4.7657	0.0185	0.0145	2.5788	0.0240	0.0302	0.8759	0.0228	0.0172	4.0369	0.0192	0.0106
1495	1449	Sep 18 2003	2.4831	0.0164	0.0131	4.2308	0.0195	0.0240	1.5968	0.0173	0.0128	1.7252	0.0152	0.0089
1499	1461	Oct 15 2002	3.8643	0.0120	0.0093	4.7373	0.0146	0.0178	2.1850	0.0134	0.0099	3.0557	0.0144	0.0081
1532	...	Sep 18 2003	0.2541	0.0819	0.0722	9.3760	0.0808	0.0924	8.9250	0.0499	0.0319	0.7567	0.0451	0.0266
1691	1689	Sep 18 2003	4.3402	0.0193	0.0148	2.2467	0.0243	0.0306	0.8324	0.0225	0.0168	3.6110	0.0192	0.0107
2050	2173	Sep 18 2003	2.9583	0.0197	0.0162	4.0696	0.0237	0.0293	1.9575	0.0208	0.0152	1.7926	0.0183	0.0106
2498	2816	Sep 18 2003	2.8619	0.0184	0.0152	5.7974	0.0211	0.0255	2.3112	0.0184	0.0135	1.7475	0.0163	0.0095
2512	2827	Sep 18 2003	4.2955	0.0159	0.0126	2.4339	0.0205	0.0258	0.8759	0.0196	0.0146	3.5044	0.0170	0.0095
3093	3651	Sep 18 2003	3.0645	0.0160	0.0131	7.9032	0.0183	0.0215	3.3552	0.0165	0.0118	1.9892	0.0149	0.0086
3203	3821	Oct 15 2002	3.4518	0.0176	0.0137	4.1997	0.0226	0.0265	1.6735	0.0234	0.0174	3.0471	0.0262	0.0148
3765	4628	Oct 15 2002	2.3236	0.0145	0.0116	9.0211	0.0163	0.0179	3.7920	0.0143	0.0103	1.7828	0.0150	0.0086
3979	4915	Oct 15 2002	3.2433	0.0185	0.0145	4.7552	0.0214	0.0262	1.7989	0.0186	0.0139	2.7712	0.0193	0.0109
4087	5036	Sep 18 2003	5.1177	0.0174	0.0131	2.5790	0.0232	0.0291	1.0401	0.0225	0.0169	4.1053	0.0197	0.0108
4893	6133	Sep 18 2003	5.6195	0.0147	0.0109	1.8042	0.0200	0.0242	0.6788	0.0196	0.0148	4.6327	0.0170	0.0093
5291	6720	Sep 18 2003	2.9449	0.0298	0.0237	5.9213	0.0330	0.0397	2.1009	0.0281	0.0207	2.1970	0.0241	0.0139
5315	6734	Oct 16 2002	2.3599	0.0175	0.0145	5.5116	0.0203	0.0243	1.9173	0.0183	0.0133	1.8102	0.0185	0.0107
5741	7337	Sep 18 2003	1.8107	0.0349	0.0283	10.5153	0.0376	0.0406	6.2973	0.0297	0.0203	1.2230	0.0282	0.0166
5806	7449	Sep 18 2003	3.8987	0.0197	0.0159	3.5352	0.0238	0.0296	1.2003	0.0217	0.0161	3.3647	0.0188	0.0104
6308	8117	Sep 18 2003	4.1959	0.0246	0.0196	2.6542	0.0321	0.0403	0.8199	0.0315	0.0237	3.6449	0.0267	0.0148
6442	8331	Sep 17 2003	3.4159	0.0278	0.0226	3.8508	0.0342	0.0422	1.5028	0.0321	0.0238	2.7152	0.0283	0.0161
6558	...	Sep 17 2003	1.8104	0.0700	0.0588	10.5620	0.0766	0.0818	5.8008	0.0630	0.0432	1.4958	0.0587	0.0342
6917	8997	Sep 17 2003	2.4995	0.0294	0.0234	8.7912	0.0328	0.0379	5.1915	0.0272	0.0190	1.6249	0.0249	0.0145
7117	9307	Sep 18 2003	2.6374	0.0178	0.0148	4.6085	0.0207	0.0254	1.5907	0.0180	0.0134	1.6723	0.0152	0.0089
7549	9958	Sep 18 2003	4.1800	0.0170	0.0137	3.6556	0.0210	0.0258	1.5686	0.0184	0.0136	2.9014	0.0159	0.0090
7564	9939	Sep 18 2003	2.8458	0.0182	0.0150	7.4219	0.0213	0.0252	2.9768	0.0188	0.0135	1.7586	0.0164	0.0095
8524	11170	Sep 17 2003	4.5357	0.0268	0.0212	3.1762	0.0346	0.0430	1.4053	0.0329	0.0244	3.4888	0.0288	0.0161
8872	11616	Sep 17 2003	3.8557	0.0277	0.0214	3.4887	0.0343	0.0426	1.4631	0.0318	0.0237	3.1645	0.0277	0.0156
9035	11833	Sep 17 2003	4.3962	0.0315	0.0249	3.7271	0.0401	0.0497	1.6358	0.0381	0.0281	3.4782	0.0336	0.0187
9911	13043	Oct 15 2002	3.8988	0.0190	0.0152	3.9070	0.0223	0.0278	1.6465	0.0193	0.0143	3.2671	0.0197	0.0110
10781	14290	Sep 18 2003	5.5022	0.0240	0.0186	2.0423	0.0316	0.0400	0.6930	0.0298	0.0224	4.5128	0.0252	0.0137
10915	14516	Sep 18 2003	4.5336	0.0238	0.0189	2.3383	0.0309	0.0390	0.8611	0.0302	0.0227	3.9299	0.0267	0.0148

Continued on Next Page...

Table K.1 – Continued

HIP #	HD #	UT Date	H $\beta$			Mg I b <sup>d</sup>			Na I D <sup>e</sup>			H $\alpha$		
			EW <sup>a</sup>	$\sigma_F$ <sup>b</sup>	$\sigma_C$ <sup>c</sup>	EW <sup>a</sup>	$\sigma_F$ <sup>b</sup>	$\sigma_C$ <sup>c</sup>	EW <sup>a</sup>	$\sigma_F$ <sup>b</sup>	$\sigma_C$ <sup>c</sup>	EW <sup>a</sup>	$\sigma_F$ <sup>b</sup>	$\sigma_C$ <sup>c</sup>
12114	16160	Sep 18 2003	1.9682	0.0114	0.0095	10.9440	0.0123	0.0137	5.2177	0.0104	0.0072	1.4856	0.0096	0.0056
12350	16548	Oct 15 2002	3.6172	0.0261	0.0212	4.1910	0.0295	0.0363	1.7871	0.0240	0.0178	2.8377	0.0241	0.0137
12493	...	Sep 17 2003	0.2236	0.1020	0.0857	11.0060	0.1097	0.1142	8.7149	0.0744	0.0476	1.0456	0.0693	0.0408
12926	17190	Sep 17 2003	2.6831	0.0384	0.0319	7.6477	0.0429	0.0503	3.0816	0.0378	0.0275	1.9912	0.0337	0.0194
13026	17397	Sep 18 2003	3.9733	0.0233	0.0180	2.9022	0.0292	0.0350	1.0950	0.0277	0.0208	3.3875	0.0241	0.0136
13081	17382	Sep 17 2003	3.0639	0.0372	0.0291	7.1843	0.0441	0.0519	2.9545	0.0414	0.0301	2.0049	0.0380	0.0219
13345	...	Sep 18 2003	1.4326	0.0665	0.0568	10.6458	0.0684	0.0764	7.7637	0.0469	0.0308	0.8014	0.0441	0.0260
15457	20630	Oct 15 2002	3.5144	0.0111	0.0086	4.9065	0.0136	0.0157	1.9799	0.0126	0.0092	2.8601	0.0127	0.0070
15776	21019	Oct 15 2002	2.6604	0.0149	0.0119	3.6556	0.0171	0.0203	1.4919	0.0149	0.0111	2.4669	0.0153	0.0087
16537	22049	Oct 15 2002	2.6371	0.0116	0.0092	8.4124	0.0132	0.0147	3.6349	0.0128	0.0089	1.9737	0.0140	0.0080
17027	22713	Oct 15 2002	2.7686	0.0256	0.0204	6.0652	0.0279	0.0322	2.7079	0.0222	0.0162	1.9298	0.0230	0.0133
19431	26337	Oct 15 2002	3.0576	0.0272	0.0214	3.4928	0.0331	0.0393	1.6083	0.0300	0.0224	1.8724	0.0311	0.0180
20373	27642	Oct 16 2002	4.3242	0.0433	0.0329	2.8783	0.0570	0.0713	1.3101	0.0559	0.0414	3.5229	0.0567	0.0315
22319	30508	Oct 15 2002	2.7540	0.0173	0.0137	4.7703	0.0203	0.0237	1.8855	0.0175	0.0128	2.0861	0.0176	0.0097
22336	30562	Oct 15 2002	4.0413	0.0127	0.0097	3.5847	0.0156	0.0196	1.6728	0.0141	0.0106	3.2180	0.0148	0.0082
22919	31412	Oct 15 2002	4.3126	0.0160	0.0123	3.3034	0.0197	0.0235	1.3673	0.0174	0.0130	3.6512	0.0177	0.0097
23105	31738	Oct 15 2002	3.3377	0.0171	0.0134	4.7847	0.0205	0.0251	2.1698	0.0184	0.0136	1.9781	0.0190	0.0110
24130	33555	Oct 15 2002	2.5395	0.0140	0.0111	6.3478	0.0160	0.0184	2.6651	0.0136	0.0099	1.6777	0.0141	0.0081
27058	38277	Oct 15 2002	3.6749	0.0102	0.0079	3.7648	0.0121	0.0144	1.4475	0.0107	0.0080	3.1518	0.0114	0.0063
27253	38529	Oct 15 2002	3.7238	0.0136	0.0106	4.3168	0.0163	0.0193	2.2149	0.0139	0.0102	2.5673	0.0146	0.0079
27435	38858	Oct 15 2002	3.3834	0.0134	0.0105	4.3663	0.0158	0.0186	1.5929	0.0140	0.0105	2.9670	0.0150	0.0080
31083	46090	Oct 16 2002	3.2663	0.0289	0.0226	3.0002	0.0367	0.0438	1.1290	0.0361	0.0274	2.9113	0.0412	0.0234
32984	50281	Oct 16 2002	1.9963	0.0261	0.0216	10.5348	0.0286	0.0322	6.2036	0.0240	0.0164	1.3512	0.0309	0.0181
61946	110463	Jul 01 2002	2.5123	0.0271	0.0216	9.2340	0.0299	0.0343	4.4998	0.0244	0.0173	1.5809	0.0260	0.0151
65420	116568	Jun 12 2003	5.1726	0.0248	0.0186	1.9265	0.0322	0.0390	0.7166	0.0291	0.0220	4.4956	0.0284	0.0155
68619	122603	Jun 13 2003	4.2365	0.0326	0.0259	3.1351	0.0421	0.0524	1.2163	0.0408	0.0303	3.4251	0.0432	0.0241
69881	125184	Jun 13 2003	4.0152	0.0260	0.0195	4.5940	0.0292	0.0358	1.8591	0.0237	0.0176	2.7325	0.0232	0.0132
70755	126868	Jul 01 2002	3.3771	0.0232	0.0183	3.2138	0.0278	0.0347	1.5007	0.0238	0.0177	2.6159	0.0238	0.0136
70782	126961	Jun 14 2003	4.7314	0.0249	0.0183	3.2181	0.0306	0.0381	1.1163	0.0279	0.0209	3.8222	0.0283	0.0157
72659A	131156A	Jul 01 2002	3.0366	0.0222	0.0175	5.4220	0.0260	0.0301	2.0866	0.0231	0.0170	2.5041	0.0242	0.0139
72659B	131156B	Jul 01 2002	1.1042	0.0140	0.0115	9.7202	0.0150	0.0163	8.2269	0.0101	0.0065	0.9668	0.0110	0.0065
79199	145328	Jul 01 2002	2.6859	0.0189	0.0149	5.5785	0.0212	0.0257	2.6582	0.0172	0.0125	1.6349	0.0182	0.0106
80021	147266	Jul 01 2002	2.9913	0.0269	0.0213	4.2260	0.0309	0.0380	2.2166	0.0251	0.0184	1.9658	0.0253	0.0147
80214	147767	Jul 01 2002	2.6488	0.0160	0.0134	8.3234	0.0169	0.0196	5.3486	0.0119	0.0082	1.6067	0.0119	0.0069
81693	150680	Jul 02 2002	3.9215	0.0193	0.0155	3.3208	0.0236	0.0289	1.6181	0.0204	0.0150	3.0775	0.0209	0.0117
95962	183658	Oct 16 2002	3.5661	0.0163	0.0119	3.9553	0.0196	0.0251	1.7984	0.0186	0.0140	3.0814	0.0214	0.0122

Continued on Next Page...



Table K.1 – Continued

HIP #	HD #	UT Date	H $\beta$			Mg I b <sup>d</sup>			Na I D <sup>e</sup>			H $\alpha$		
			EW <sup>a</sup>	$\sigma_F$ <sup>b</sup>	$\sigma_C$ <sup>c</sup>	EW <sup>a</sup>	$\sigma_F$ <sup>b</sup>	$\sigma_C$ <sup>c</sup>	EW <sup>a</sup>	$\sigma_F$ <sup>b</sup>	$\sigma_C$ <sup>c</sup>	EW <sup>a</sup>	$\sigma_F$ <sup>b</sup>	$\sigma_C$ <sup>c</sup>
96100	185144	Jul 01 2002	2.7546	0.0226	0.0179	6.8173	0.0258	0.0292	2.7342	0.0233	0.0170	2.2748	0.0259	0.0149
96901	186427	Jul 01 2002	3.7455	0.0217	0.0175	4.4102	0.0262	0.0321	1.8539	0.0228	0.0168	3.0816	0.0235	0.0133
97255	186704	Oct 16 2002	3.7454	0.0197	0.0152	3.8701	0.0235	0.0278	1.4730	0.0207	0.0155	3.1569	0.0214	0.0121
97635	188056	Jul 01 2002	2.9328	0.0198	0.0163	7.7019	0.0227	0.0266	6.1734	0.0170	0.0115	1.4389	0.0191	0.0112
98416	189340	Oct 15 2002	3.8935	0.0225	0.0173	3.5787	0.0277	0.0327	1.7725	0.0255	0.0192	3.4188	0.0285	0.0161
99894	192699	Oct 15 2002	2.5088	0.0488	0.0388	4.4705	0.0557	0.0653	1.8088	0.0479	0.0355	1.8748	0.0513	0.0299
100501	194193	Jul 01 2002	2.7339	0.0282	0.0228	8.5824	0.0289	0.0334	4.9806	0.0203	0.0142	1.4464	0.0197	0.0115
101622	196203	Jun 13 2003	5.0012	0.0230	0.0173	2.3760	0.0286	0.0360	0.8190	0.0270	0.0201	3.9127	0.0277	0.0153
		Jun 14 2003	4.8202	0.0128	0.0099	2.5500	0.0165	0.0207	0.8900	0.0159	0.0119	3.9427	0.0157	0.0087
101955	196795	Jul 02 2002	1.2487	0.0427	0.0367	9.7797	0.0440	0.0501	8.8195	0.0271	0.0174	1.0258	0.0279	0.0164
104202	200964	Jun 13 2003	2.7608	0.0194	0.0154	4.6156	0.0225	0.0270	1.6862	0.0204	0.0149	1.8349	0.0214	0.0124
104214	201091	Jul 01 2002	0.8994	0.0197	0.0168	9.9008	0.0211	0.0237	7.6933	0.0142	0.0093	1.1925	0.0163	0.0094
104217	201092	Jul 01 2002	0.4252	0.0303	0.0266	8.5882	0.0316	0.0363	9.6156	0.0189	0.0118	0.9442	0.0211	0.0124
107857	207687	Oct 15 2002	2.2417	0.0935	0.0752	4.5285	0.1045	0.1275	1.5775	0.0918	0.0676	1.9827	0.1007	0.0583
		Oct 15 2002	2.2122	0.0254	0.0206	4.4824	0.0282	0.0348	1.5895	0.0247	0.0184	2.0378	0.0267	0.0154
108782	209290	Sep 17 2003	0.7695	0.0635	0.0563	7.9815	0.0615	0.0719	11.5922	0.0354	0.0215	0.6740	0.0316	0.0188
109378	210277	Jun 13 2003	3.5093	0.0177	0.0137	6.1778	0.0237	0.0283	2.6439	0.0276	0.0203	2.5964	0.0365	0.0208
		Oct 15 2002	3.8146	0.0228	0.0162	6.1920	0.0288	0.0345	2.3057	0.0326	0.0238	2.5211	0.0382	0.0218
109820	211022	Sep 18 2003	4.9762	0.0199	0.0150	1.7461	0.0253	0.0321	0.6898	0.0234	0.0177	4.1822	0.0198	0.0109
110205	211786	Sep 17 2003	3.2948	0.0231	0.0181	4.1943	0.0285	0.0335	1.4312	0.0274	0.0205	2.8410	0.0243	0.0138
111312	213612	Sep 18 2003	2.4986	0.0265	0.0212	4.8644	0.0310	0.0362	1.7591	0.0285	0.0212	1.8587	0.0257	0.0149
111571	214100	Sep 17 2003	0.9218	0.1131	0.0988	8.9982	0.1053	0.1151	11.3232	0.0600	0.0364	0.7697	0.0514	0.0305
114854	219452	Sep 17 2003	5.4712	0.0170	0.0127	1.8272	0.0223	0.0283	0.8835	0.0215	0.0163	4.6063	0.0188	0.0103
114906	219516	Sep 17 2003	4.2900	0.0234	0.0180	2.4691	0.0291	0.0366	1.1450	0.0278	0.0209	3.6780	0.0248	0.0138
115004	...	Sep 17 2003	1.6393	0.0568	0.0482	10.1078	0.0610	0.0689	7.0737	0.0451	0.0303	1.0254	0.0419	0.0247
116384	...	Sep 17 2003	0.6465	0.0531	0.0464	9.6247	0.0553	0.0631	10.1503	0.0358	0.0223	0.0037	0.0348	0.0208
116600	222111	Sep 17 2003	5.5677	0.0155	0.0119	2.5334	0.0208	0.0261	1.1472	0.0205	0.0153	4.5096	0.0182	0.0099
117112	222878	Sep 18 2003	4.6725	0.0213	0.0161	2.9863	0.0286	0.0357	1.2915	0.0295	0.0221	3.6846	0.0274	0.0153
117980	224173	Sep 18 2003	4.8254	0.0232	0.0176	2.4996	0.0289	0.0363	0.8607	0.0263	0.0198	4.0627	0.0222	0.0122

Table K.2: EW Measurements for HIP Standard Stars from the Red Spectrograph Setting.

HIP #	HD #	UT Date	H $\alpha$			Ca II 8498			Ca II 8542			Ca II 8662		
			EW <sup>a</sup>	$\sigma_F$	$\sigma_C$	EW <sup>a</sup>	$\sigma_F$	$\sigma_C$	EW <sup>a</sup>	$\sigma_F$	$\sigma_C$	EW <sup>a</sup>	$\sigma_F$	$\sigma_C$
954	745	Sep 15 2003	1.9062	0.0134	0.0076	1.2274	0.0228	0.0161	3.2479	0.0222	0.0146	2.5846	0.0237	0.0150
1078	...	Sep 13 2003	1.8020	0.0269	0.0145	1.0315	0.0419	0.0304	3.4256	0.0404	0.0264	2.5083	0.0429	0.0276
1169	1031	Sep 15 2003	4.3605	0.0125	0.0066	1.2993	0.0241	0.0174	3.0351	0.0236	0.0156	2.7466	0.0250	0.0160
1427	1352	Sep 13 2003	4.0125	0.0129	0.0070	0.8168	0.0258	0.0183	2.4831	0.0252	0.0168	2.3458	0.0264	0.0168
1495	1449	Sep 13 2003	1.7716	0.0126	0.0070	1.1149	0.0203	0.0144	2.9405	0.0199	0.0133	2.3863	0.0211	0.0134
1499	1461	Oct 12 2002	2.9114	0.0182	0.0103	1.4589	0.0364	0.0256	3.3032	0.0357	0.0234	2.7997	0.0380	0.0238
1532	...	Sep 13 2003	0.8992	0.0422	0.0248	1.0598	0.0559	0.0405	3.0094	0.0540	0.0356	1.9970	0.0567	0.0364
1691	1689	Sep 13 2003	3.6736	0.0135	0.0072	1.1261	0.0235	0.0163	2.8206	0.0229	0.0152	2.3800	0.0247	0.0154
2050	2173	Sep 15 2003	1.9199	0.0190	0.0109	1.2171	0.0335	0.0242	3.3790	0.0324	0.0212	2.8306	0.0342	0.0218
2498	2816	Sep 15 2003	1.7753	0.0147	0.0084	1.1393	0.0254	0.0184	3.1463	0.0248	0.0163	2.5972	0.0261	0.0168
2512	2827	Sep 15 2003	3.6068	0.0152	0.0083	1.2232	0.0294	0.0212	2.9477	0.0287	0.0190	2.6657	0.0302	0.0194
3093	3651	Sep 13 2003	2.0400	0.0161	0.0090	1.0523	0.0283	0.0205	3.1833	0.0273	0.0178	2.5848	0.0289	0.0186
3203	3821	Oct 12 2002	2.9916	0.0289	0.0164	1.5235	0.0608	0.0426	3.0281	0.0603	0.0401	2.6741	0.0632	0.0396
3765	4628	Oct 12 2002	1.7239	0.0128	0.0074	1.3333	0.0219	0.0156	3.1840	0.0219	0.0142	2.4866	0.0228	0.0143
3979	4915	Oct 12 2002	2.8387	0.0229	0.0130	1.3690	0.0468	0.0330	3.1441	0.0460	0.0302	2.4652	0.0487	0.0308
4087	5036	Sep 13 2003	4.1430	0.0166	0.0091	1.2517	0.0331	0.0234	3.0009	0.0326	0.0217	2.8494	0.0345	0.0217
4893	6133	Sep 15 2003	4.6131	0.0166	0.0089	0.9152	0.0330	0.0235	2.2716	0.0327	0.0219	2.2188	0.0343	0.0219
5291	6720	Sep 14 2003	2.2237	0.0245	0.0139	0.8132	0.0492	0.0342	2.9307	0.0482	0.0322	2.3486	0.0530	0.0333
5315	6734	Oct 14 2002	1.8959	0.0127	0.0073	1.2701	0.0252	0.0190	3.1110	0.0248	0.0160	2.4572	0.0262	0.0172
5741	7337	Sep 14 2003	1.2828	0.0278	0.0163	0.9811	0.0479	0.0340	3.0863	0.0467	0.0311	2.3784	0.0500	0.0318
5806	7449	Sep 14 2003	3.4135	0.0143	0.0079	1.1817	0.0281	0.0203	2.8147	0.0277	0.0183	2.3839	0.0294	0.0190
6308	8117	Sep 14 2003	3.6986	0.0183	0.0101	1.3762	0.0362	0.0261	2.6457	0.0358	0.0238	2.2000	0.0377	0.0244
6442	8331	Sep 14 2003	2.6761	0.0139	0.0079	1.3411	0.0266	0.0191	3.2007	0.0259	0.0170	2.6199	0.0273	0.0176
6558	...	Sep 14 2003	1.4781	0.0275	0.0160	1.1454	0.0474	0.0336	3.2163	0.0461	0.0306	2.5025	0.0488	0.0309
6917	8997	Sep 14 2003	1.4554	0.0229	0.0133	1.2333	0.0396	0.0286	3.2997	0.0384	0.0251	2.4579	0.0407	0.0258
7117	9307	Sep 15 2003	1.7901	0.0182	0.0103	1.2027	0.0289	0.0204	3.2875	0.0281	0.0186	2.7138	0.0295	0.0187
7549	9958	Sep 14 2003	3.1210	0.0125	0.0070	1.5045	0.0250	0.0175	3.5844	0.0243	0.0160	2.9949	0.0258	0.0162
7564	9939	Sep 15 2003	1.9193	0.0163	0.0092	1.0596	0.0282	0.0205	3.0344	0.0274	0.0181	2.4488	0.0289	0.0187
8524	11170	Sep 15 2003	3.4833	0.0158	0.0087	1.4834	0.0292	0.0208	3.6251	0.0281	0.0183	3.0541	0.0300	0.0191
8872	11616	Sep 15 2003	3.2064	0.0212	0.0117	1.1743	0.0388	0.0268	3.0695	0.0379	0.0253	2.4532	0.0406	0.0255
9035	11833	Sep 15 2003	3.4375	0.0205	0.0113	1.2434	0.0379	0.0274	3.2537	0.0370	0.0243	2.7355	0.0393	0.0252
9911	13043	Oct 14 2002	3.2722	0.0190	0.0106	1.4030	0.0405	0.0290	3.1608	0.0396	0.0257	2.7902	0.0418	0.0266
10781	14290	Sep 15 2003	4.5826	0.0196	0.0106	1.0475	0.0396	0.0280	2.5750	0.0390	0.0259	2.3967	0.0409	0.0260
10915	14516	Sep 15 2003	3.9461	0.0264	0.0147	0.9059	0.0475	0.0337	2.6034	0.0467	0.0310	1.9965	0.0501	0.0322

Continued on Next Page...

Table K.2 – Continued

HIP #	HD #	UT Date	H $\alpha$			Ca II 8498			Ca II 8542			Ca II 8662		
			EW <sup>a</sup>	$\sigma_F$	$\sigma_C$	EW <sup>a</sup>	$\sigma_F$	$\sigma_C$	EW <sup>a</sup>	$\sigma_F$	$\sigma_C$	EW <sup>a</sup>	$\sigma_F$	$\sigma_C$
12114	16160	Sep 13 2003	1.5390	0.0165	0.0095	0.8847	0.0273	0.0194	2.9999	0.0265	0.0175	2.3278	0.0280	0.0177
12350	16548	Oct 14 2002	2.8363	0.0176	0.0100	1.4926	0.0438	0.0308	3.4415	0.0431	0.0281	2.9408	0.0457	0.0285
12493	...	Sep 13 2003	1.0632	0.0387	0.0222	0.9518	0.0557	0.0387	3.0298	0.0541	0.0365	2.1238	0.0574	0.0362
12926	17190	Sep 15 2003	2.0821	0.0214	0.0122	1.2667	0.0364	0.0257	3.1046	0.0357	0.0234	2.3093	0.0381	0.0243
13026	17397	Sep 14 2003	3.5152	0.0179	0.0100	1.0649	0.0364	0.0253	2.3909	0.0360	0.0247	2.1014	0.0380	0.0239
13081	17382	Sep 13 2003	1.9417	0.0146	0.0080	0.8256	0.0251	0.0183	2.9372	0.0244	0.0161	2.5844	0.0257	0.0163
13345	...	Sep 14 2003	1.1355	0.0294	0.0173	0.8957	0.0485	0.0345	3.2357	0.0468	0.0311	2.3194	0.0501	0.0319
15457	20630	Oct 12 2002	4.8050	0.0172	0.0081	1.5029	0.0145	0.0098	3.1606	0.0144	0.0091	2.6671	0.0152	0.0094
15776	21019	Oct 12 2002	2.3737	0.0110	0.0063	1.2911	0.0223	0.0157	2.7830	0.0223	0.0147	2.1997	0.0233	0.0147
16537	22049	Oct 12 2002	1.8617	0.0112	0.0064	0.7808	0.0178	0.0144	3.0492	0.0178	0.0124	2.3076	0.0196	0.0125
17027	22713	Oct 12 2002	1.8237	0.0118	0.0068	1.4750	0.0237	0.0164	3.2799	0.0233	0.0150	2.6823	0.0240	0.0148
19431	26337	Oct 12 2002	1.5902	0.0277	0.0161	0.8018	0.0641	0.0456	2.3104	0.0636	0.0424	1.9560	0.0670	0.0428
22319	30508	Oct 12 2002	2.0152	0.0205	0.0118	1.5872	0.0387	0.0268	3.3737	0.0380	0.0248	2.8261	0.0396	0.0247
22336	30562	Oct 14 2002	3.3377	0.0231	0.0128	1.2645	0.0338	0.0233	3.3949	0.0326	0.0215	2.7167	0.0342	0.0213
22919	31412	Oct 12 2002	3.6278	0.0283	0.0158	1.7108	0.0576	0.0403	3.3223	0.0568	0.0376	2.7752	0.0600	0.0375
23105	31738	Oct 14 2002	1.9347	0.0152	0.0088	0.8158	0.0295	0.0209	2.4852	0.0289	0.0193	2.0121	0.0307	0.0197
24130	33555	Oct 14 2002	1.6065	0.0198	0.0115	1.4562	0.0381	0.0268	3.3673	0.0374	0.0247	2.7292	0.0390	0.0247
27058	38277	Oct 14 2002	3.2189	0.0180	0.0101	1.1076	0.0413	0.0292	2.8604	0.0408	0.0273	2.4165	0.0434	0.0276
27253	38529	Oct 12 2002	2.5549	0.0172	0.0099	1.7573	0.0338	0.0235	3.6896	0.0333	0.0213	3.0706	0.0351	0.0215
27435	38858	Oct 12 2002	2.9430	0.0166	0.0094	1.4520	0.0333	0.0232	3.1634	0.0334	0.0213	2.5783	0.0355	0.0218
31083	46090	Oct 14 2002	2.8388	0.0178	0.0101	1.5369	0.0389	0.0273	3.3840	0.0382	0.0253	2.6546	0.0407	0.0257
32984	50281	Oct 12 2002	1.3435	0.0209	0.0122	1.2887	0.0379	0.0271	3.5473	0.0368	0.0237	2.7125	0.0388	0.0247
61946	110463	Jun 29 2002	1.5568	0.0133	0.0077	0.8949	0.0224	0.0159	3.0489	0.0217	0.0143	2.5061	0.0230	0.0146
65420	116568	Jun 09 2003	4.6328	0.0079	0.0037	0.7212	0.0136	0.0095	2.0960	0.0134	0.0091	2.1650	0.0141	0.0089
68619	122603	Jun 09 2003	3.3889	0.0158	0.0087	0.9971	0.0324	0.0230	2.6045	0.0320	0.0216	2.5756	0.0334	0.0211
69881	125184	Jun 09 2003	2.7795	0.0151	0.0083	0.8740	0.0283	0.0199	3.0574	0.0273	0.0178	2.7826	0.0283	0.0179
79199	145328	Jun 30 2002	1.6313	0.0108	0.0061	0.9984	0.0185	0.0136	2.9332	0.0178	0.0120	2.6551	0.0197	0.0121
80021	147266	Jun 30 2002	1.9934	0.0121	0.0068	1.1779	0.0197	0.0139	3.3003	0.0192	0.0124	2.9218	0.0201	0.0127
80214	147767	Jun 30 2002	1.5755	0.0123	0.0069	1.1833	0.0174	0.0124	4.0644	0.0164	0.0106	3.3154	0.0186	0.0113
81693	150680	Jun 30 2002	2.9145	0.0088	0.0045	1.1129	0.0141	0.0101	3.1617	0.0132	0.0088	2.7579	0.0156	0.0095
96100	185144	Jun 29 2002	2.2845	0.0144	0.0081	0.9947	0.0311	0.0220	2.6910	0.0306	0.0203	2.4717	0.0325	0.0206
96901	180427	Jun 29 2002	2.9506	0.0133	0.0073	1.0733	0.0234	0.0168	3.0078	0.0227	0.0150	2.6148	0.0241	0.0156
97635	188056	Jun 29 2002	1.3536	0.0120	0.0069	0.9691	0.0180	0.0133	3.6021	0.0173	0.0113	3.3306	0.0186	0.0115
98416	189340	Oct 12 2002	3.1886	0.0153	0.0086	0.7645	0.0368	0.0256	2.6936	0.0363	0.0247	2.3393	0.0395	0.0248
99894	192699	Oct 12 2002	1.8457	0.0182	0.0105	0.9953	0.0335	0.0233	2.8938	0.0327	0.0219	2.4010	0.0346	0.0217
100501	194193	Jun 30 2002	1.4947	0.0146	0.0082	1.2588	0.0201	0.0142	4.0937	0.0188	0.0119	3.4905	0.0199	0.0126

Continued on Next Page...

Table K.2 – Continued

HIP #	HD #	UT Date	H $\alpha$			Ca II 8498			Ca II 8542			Ca II 8662		
			EW <sup>a</sup>	$\sigma_F$	$\sigma_C$	EW <sup>a</sup>	$\sigma_F$	$\sigma_C$	EW <sup>a</sup>	$\sigma_F$	$\sigma_C$	EW <sup>a</sup>	$\sigma_F$	$\sigma_C$
101622	196203	Jun 09 2003	4.2753	0.1170	0.0627	1.4300	0.3200	0.2257	2.1626	0.3211	0.2076	2.6139	0.3391	0.2109
101955	196795	Jun 29 2002	1.0867	0.0178	0.0104	0.8210	0.0257	0.0192	2.8788	0.0246	0.0162	2.1941	0.0263	0.0174
104202	200964	Jun 10 2003	1.7130	0.0237	0.0137	0.9111	0.0417	0.0311	2.8425	0.0406	0.0262	2.4397	0.0426	0.0278
104214	201091	Jun 30 2002	1.1680	0.0147	0.0086	0.8608	0.0233	0.0175	3.0333	0.0227	0.0146	2.3663	0.0244	0.0158
104217	201092	Jun 30 2002	0.8941	0.0253	0.0148	0.7050	0.0338	0.0252	2.7508	0.0326	0.0214	2.0122	0.0346	0.0230
107857	207687	Oct 14 2002	2.0191	0.0348	0.0200	0.8186	0.0714	0.0506	2.5361	0.0707	0.0475	1.9421	0.0772	0.0495
108782	209290	Sep 13 2003	0.5941	0.0178	0.0104	0.5961	0.0236	0.0169	2.4282	0.0229	0.0155	1.6424	0.0241	0.0156
109378	210277	Jun 10 2003	2.5923	0.0208	0.0118	1.2040	0.0383	0.0270	3.1892	0.0374	0.0245	2.6969	0.0393	0.0248
		Oct 14 2002	2.5075	0.0313	0.0178	1.0445	0.0718	0.0520	2.7317	0.0708	0.0468	2.5256	0.0742	0.0476
109820	211022	Sep 13 2003	4.1646	0.0127	0.0067	1.3250	0.0239	0.0176	2.4272	0.0237	0.0161	2.3366	0.0248	0.0160
110205	211786	Sep 14 2003	2.9334	0.0150	0.0084	1.0600	0.0281	0.0195	2.7612	0.0275	0.0185	2.1940	0.0293	0.0187
111312	213612	Sep 13 2003	1.9206	0.0145	0.0083	1.2054	0.0242	0.0169	3.0367	0.0232	0.0155	2.2753	0.0244	0.0154
111571	214100	Sep 13 2003	0.7047	0.0270	0.0160	0.7267	0.0356	0.0255	2.5056	0.0347	0.0234	1.7284	0.0365	0.0235
114854	219452	Sep 13 2003	4.5675	0.0145	0.0071	0.8853	0.0257	0.0179	2.3727	0.0254	0.0172	2.1988	0.0279	0.0171
114906	219516	Sep 13 2003	3.5804	0.0173	0.0092	0.9807	0.0305	0.0216	2.5689	0.0303	0.0202	2.1585	0.0322	0.0204
115004	...	Sep 14 2003	1.0923	0.0337	0.0198	0.8169	0.0553	0.0393	3.0054	0.0537	0.0358	2.1994	0.0571	0.0365
116384	...	Sep 14 2003	−0.0295	0.0263	0.0156	0.6468	0.0377	0.0270	2.7198	0.0366	0.0242	1.9702	0.0388	0.0249
116600	222111	Sep 14 2003	4.5040	0.0124	0.0066	1.1335	0.0267	0.0189	2.8980	0.0267	0.0176	2.7249	0.0285	0.0179
117112	222878	Sep 14 2003	3.6780	0.0137	0.0075	1.3451	0.0270	0.0190	3.3849	0.0264	0.0175	2.8722	0.0281	0.0177
117980	224173	Sep 15 2003	4.1972	0.0184	0.0099	1.3117	0.0349	0.0251	2.8586	0.0343	0.0226	2.4046	0.0358	0.0230

Table K.3: EW Measurements for Hot Subdwarfs from the Blue Spectrograph Setting.

ID <sup>f</sup>	Name	UT <sup>h</sup> Date	H $\beta$ EW <sup>a</sup> $\sigma_F$ $\sigma_C$	Mg I b <sup>d</sup> EW <sup>a</sup> $\sigma_F$ $\sigma_C$	He I 5785 EW <sup>a</sup> $\sigma_F$ $\sigma_C$	Na I D <sup>e</sup> EW <sup>a</sup> $\sigma_F$ $\sigma_C$	H $\alpha$ EW <sup>a</sup> $\sigma_F$ $\sigma_C$
<b>Composite-Colored Hot Subdwarfs (<math>J-K_S \gtrsim +0.05</math>)</b>							
1	SB 7	021015	3.7928 0.1015 0.0779	0.3939 0.1323 0.1706	0.1766 0.1254 0.0958	0.9052 0.1483 0.1060	4.0554 0.1774 0.0957
59	PB 6107	021016	3.7772 0.0291 0.0225	0.5502 0.0384 0.0496	0.1307 0.0357 0.0270	0.6075 0.0402 0.0304	3.7758 0.0477 0.0265
65	PB 6148	030918	5.0112 0.0262 0.0204	1.6432 0.0364 0.0463	0.2348 0.0341 0.0273	0.9757 0.0381 0.0283	3.6573 0.0352 0.0195
71	BD-11 <sup>o</sup> 162	030918	4.6944 0.0211 0.0166	2.3107 0.0273 0.0343	...	1.0560 0.0260 0.0193	4.0537 0.0222 0.0122
87A	PG 0105+276A	021015	3.2875 0.0472 0.0367	1.2403 0.0635 0.0809	...	1.0705 0.0693 0.0512	3.2722 0.0792 0.0442
91A	PB 8555A	021016	2.2846 0.0670 0.0557	0.0671 0.0908 0.1162	0.2570 0.0866 0.0659	0.5641 0.1005 0.0728	2.5864 0.1136 0.0640
95	PG 0110+262	021015	3.6254 0.0612 0.0472	1.8192 0.0824 0.1044	0.4086 0.0821 0.0625	1.4041 0.0949 0.0679	3.1030 0.1188 0.0663
101	PG 0116+242	021015	4.9889 0.0689 0.0512	1.2631 0.0950 0.1191	0.4899 0.0859 0.0653	1.4058 0.0980 0.0705	4.0000 0.1003 0.0545
102	PB 8783	021016	3.9933 0.0323 0.0259	0.5059 0.0417 0.0530	0.0679 0.0341 0.0257	0.6737 0.0382 0.0284	3.7260 0.0355 0.0196
120	PHL 3802	021015	5.1737 0.0513 0.0383	1.0845 0.0669 0.0828	0.0385 0.0583 0.0453	1.2033 0.0658 0.0481	4.9719 0.0706 0.0378
150	PG 0232+095	021016	3.9601 0.0470 0.0361	1.0615 0.0575 0.0708	0.3693 0.0492 0.0368	0.8093 0.0559 0.0410	3.3379 0.0614 0.0345
172	PG 0314+103	030917	4.1994 0.0244 0.0195	3.1825 0.0312 0.0390	0.5557 0.0262 0.0209	2.6992 0.0286 0.0207	2.3504 0.0261 0.0149
187A	HDE 283048A	030917	5.2216 0.0481 0.0371	0.8403 0.0637 0.0820	0.3559 0.0542 0.0418	1.6639 0.0600 0.0440	3.5773 0.0550 0.0294
199	KUV 04110+1434	030919	2.7420 0.0168 0.0140	1.1261 0.0216 0.0276	0.8116 0.0185 0.0140	1.4395 0.0207 0.0153	2.7391 0.0187 0.0106
203	KUV 04237+1649	030918	6.6595 0.0458 0.0328	0.1523 0.0637 0.0739	0.0545 0.0543 0.0424	1.1338 0.0603 0.0446	4.8432 0.0514 0.0277
234	BD+34 <sup>o</sup> 1543	030919	4.9046 0.0415 0.0335	1.3023 0.0544 0.0683	0.2601 0.0459 0.0346	1.3248 0.0509 0.0376	3.5054 0.0442 0.0244
294	PG 0900+400	021016	4.0193 0.0185 0.0141	2.0227 0.0241 0.0305	0.3064 0.0206 0.0158	0.9930 0.0230 0.0173	3.4417 0.0245 0.0137
460	PG 1104+243	020311	...	...	0.2364 0.0464 0.0349	0.9614 0.0515 0.0386	3.4498 0.0469 0.0264
476	PG 111+339	020311	2.1146 0.1151 0.0957	1.4211 0.1449 0.1850	0.8841 0.1279 0.0945	1.4241 0.1548 0.1171	1.5767 0.1576 0.0906
533	BD+10 <sup>o</sup> 2357	020312	...	...	1.0275 0.0890 0.0657	1.7187 0.0992 0.0730	1.3205 0.0949 0.0557
551	PB 3854	020312	...	...	0.7788 0.1116 0.0828	1.4634 0.1241 0.0918	1.7317 0.1158 0.0673
583	LB 2392	020617	...	...	0.2987 0.0423 0.0322	0.8440 0.0471 0.0350	3.6013 0.0431 0.0240
630	TON 139	030612	6.2165 0.0186 0.0133	0.8434 0.0259 0.0317	0.3738 0.0960 0.0731	1.1052 0.1067 0.0783	1.9392 0.0968 0.0546
638	PG 1257-026	030612	3.4689 0.0218 0.0170	4.0669 0.0264 0.0312	...	0.5700 0.0262 0.0198	5.4114 0.0272 0.0145
697	Feige 87	030612	4.8131 0.0267 0.0197	1.2290 0.0353 0.0451	...	1.6497 0.0234 0.0174	2.7771 0.0241 0.0137
702	PG 1343+578	030612	4.9898 0.0451 0.0335	1.2099 0.0580 0.0714	0.0189 0.1590 0.1231	0.2032 0.1784 0.1334	3.4082 0.1683 0.0934
706	PG 1347+086	030612	4.9230 0.0171 0.0122	0.9666 0.0229 0.0281	0.1731 0.0308 0.0240	0.6761 0.0344 0.0260	3.8593 0.0357 0.0198
789	PG 1429+406	020701	5.3497 0.0488 0.0371	0.4195 0.0678 0.0848	0.1015 0.0492 0.0390	0.5766 0.0550 0.0415	4.0329 0.0551 0.0304
		030614	3.8206 0.0198 0.0148	0.5438 0.0240 0.0309	0.2860 0.0212 0.0159	0.6129 0.0237 0.0180	3.7106 0.0262 0.0146
		030612	4.3957 0.0266 0.0208	2.7916 0.0337 0.0423	0.1614 0.0614 0.0484	0.5597 0.0697 0.0511	4.2845 0.0756 0.0406
					...	0.2785 0.0213 0.0162	3.6118 0.0210 0.0117
					-0.0088 0.0282 0.0222	0.9192 0.0313 0.0233	3.8689 0.0298 0.0165

Continued on Next Page...

Table K.3 – Continued

ID <sup>f</sup>	Name	UT Date <sup>h</sup>	H $\beta$ EW <sup>a</sup> $\sigma_F$ $\sigma_C$	Mg I b <sup>d</sup> EW <sup>a</sup> $\sigma_F$ $\sigma_C$	He I 5785 EW <sup>a</sup> $\sigma_F$ $\sigma_C$	Na I D <sup>e</sup> EW <sup>a</sup> $\sigma_F$ $\sigma_C$	H $\alpha$ EW <sup>a</sup> $\sigma_F$ $\sigma_C$
835	PG 1444+236	030613	-5.1952 0.0426 0.0412	-2.1681 0.0505 0.0646	-0.1440 0.0473 0.0364	-0.7435 0.0537 0.0449	-100.7836 0.1251 0.1679
		030614	-5.2958 0.0320 0.0306	-2.1907 0.0371 0.0473	-0.1337 0.0344 0.0268	-0.6632 0.0390 0.0326	-100.4549 0.0950 0.1306
		030614	-5.3976 0.0353 0.0346	-2.2293 0.0411 0.0526	-0.1468 0.0372 0.0291	...	-100.6778 0.1014 0.1389
844	PG 1449+653	030612	4.2936 0.0310 0.0239	1.0682 0.0417 0.0525	0.1559 0.0373 0.0295	0.6028 0.0417 0.0310	3.5210 0.0431 0.0238
849	PG 1451+472	030612	3.7288 0.0306 0.0247	0.4371 0.0390 0.0504	...	0.3707 0.0352 0.0264	3.6621 0.0338 0.0187
850	PG 1452+198	030613	5.4829 0.0198 0.0152	...	0.4454 0.0272 0.0210	0.1492 0.0308 0.0267	4.4292 0.0332 0.0180
895	PG 1514+034	030613	4.2622 0.0414 0.0323	1.2741 0.0550 0.0708	0.3104 0.0510 0.0394	0.6548 0.0572 0.0429	3.4479 0.0615 0.0341
912	PG 1524+611	020702	4.1169 0.0631 0.0481	1.4800 0.0826 0.1050	0.4358 0.0724 0.0549	1.0866 0.0831 0.0607	3.7775 0.0889 0.0484
937	PG 1536+278	030612	4.6923 0.0453 0.0348	1.5978 0.0584 0.0733	0.2137 0.0477 0.0388	0.9572 0.0532 0.0395	4.0640 0.0505 0.0276
969	PG 1551+255	030917	5.4047 0.0454 0.0350	1.8080 0.0625 0.0793	...	1.5027 0.0632 0.0463	3.6043 0.0576 0.0319
1010	PG 1610+519	020701	3.5610 0.0623 0.0483	0.6509 0.0837 0.1043	0.3885 0.0776 0.0591	1.4310 0.0877 0.0634	3.1479 0.1031 0.0573
		030918	3.4774 0.0424 0.0343	0.6455 0.0581 0.0716	0.2917 0.0571 0.0448	1.3434 0.0639 0.0470	2.9938 0.0642 0.0358
1051	PG 1629+081	030612	3.7464 0.0272 0.0213	...	0.1728 0.0332 0.0254	0.7388 0.0371 0.0277	3.5495 0.0397 0.0221
1092	TON 264	030919	4.3727 0.0377 0.0287	0.8779 0.0520 0.0668	0.5750 0.0480 0.0360	1.5073 0.0535 0.0399	2.4648 0.0509 0.0289
1096	PG 1648+080	030613	4.2254 0.0477 0.0363	2.1709 0.0609 0.0741	0.4327 0.0502 0.0389	1.5865 0.0555 0.0412	3.3230 0.0543 0.0304
		030917	4.0892 0.0466 0.0356	2.2883 0.0607 0.0731	0.3520 0.0549 0.0420	1.6467 0.0611 0.0451	3.2199 0.0568 0.0318
1108	LS IV -08 <sup>o</sup> 03	030613	2.3156 0.0182 0.0151	0.3265 0.0226 0.0293	0.4928 0.0193 0.0147	1.1500 0.0215 0.0160	-1.5733 0.0253 0.0158
		030613	2.4311 0.0206 0.0161	0.2434 0.0238 0.0296	...	1.2083 0.0211 0.0156	-1.5583 0.0236 0.0146
		030917	2.2861 0.0316 0.0265	...	1.0894 0.0329 0.0240	1.3099 0.0371 0.0277	-1.0592 0.0375 0.0229
1133	PG 1701+359	030919	2.7067 0.0415 0.0310	0.2091 0.0528 0.0654	...	1.2358 0.0510 0.0381	-0.7153 0.0481 0.0294
		030612	4.5928 0.0327 0.0252	0.9354 0.0463 0.0585	0.1755 0.0437 0.0335	0.6390 0.0489 0.0365	3.4798 0.0493 0.0272
		030613	4.5989 0.0263 0.0203	0.8126 0.0368 0.0466	0.0392 0.0343 0.0276	0.6199 0.0383 0.0287	3.5181 0.0417 0.0231
		030917	4.5899 0.0347 0.0268	0.7787 0.0492 0.0622	0.2817 0.0475 0.0358	0.7825 0.0535 0.0426	3.5467 0.0502 0.0277
1164	PG 1718+519	020701	4.3541 0.0453 0.0352	1.8253 0.0606 0.0756	...	1.2887 0.0614 0.0448	3.3834 0.0692 0.0383
		030917	4.3677 0.0481 0.0381	1.9282 0.0643 0.0816	0.1377 0.0587 0.0454	1.0587 0.0656 0.0485	3.2738 0.0590 0.0329
1182	BD+29 <sup>o</sup> 3070	030612	5.3687 0.0154 0.0112	2.1672 0.0196 0.0244	0.2075 0.0172 0.0135	1.1333 0.0191 0.0142	4.1311 0.0197 0.0108
		030919	5.2942 0.0154 0.0120	2.0573 0.0211 0.0267	0.1682 0.0190 0.0149	1.1382 0.0210 0.0157	4.0381 0.0189 0.0104
1223	HD 185510	030612	2.8729 0.0192 0.0147	5.4078 0.0193 0.0235	0.3463 0.0138 0.0110	2.6942 0.0149 0.0108	0.7000 0.0152 0.0090
		030919	2.7120 0.0211 0.0169	5.3085 0.0237 0.0288	0.3301 0.0176 0.0141	2.6506 0.0191 0.0140	1.3356 0.0166 0.0097
1297	PG 2110+127	030613	4.6374 0.0271 0.0200	2.0458 0.0350 0.0443	...	1.5974 0.0330 0.0243	3.6090 0.0341 0.0189
		030917	4.4651 0.0268 0.0204	1.9208 0.0365 0.0442	0.2336 0.0334 0.0257	1.6590 0.0369 0.0274	3.5635 0.0343 0.0192
1304	PG 2116+008	030919	2.8346 0.0893 0.0729	0.2017 0.1243 0.1608	1.1104 0.1286 0.0960	1.4043 0.1483 0.1069	2.5879 0.1552 0.0865
1306	PG 2118+126	020701	4.4995 0.0432 0.0339	2.0533 0.0577 0.0731	0.7112 0.0508 0.0364	1.2988 0.0569 0.0419	3.7105 0.0585 0.0323
		030613	4.3646 0.0509 0.0402	1.8167 0.0655 0.0834	0.1956 0.0556 0.0432	1.6712 0.0614 0.0451	3.8770 0.0676 0.0371
		030917	4.3960 0.0369 0.0280	1.9295 0.0501 0.0633	...	1.6279 0.0510 0.0378	3.7932 0.0473 0.0263
1322	BPS CS 29495-21	030917	3.4368 0.0479 0.0390	1.3483 0.0596 0.0760	0.3079 0.0520 0.0385	1.1495 0.0581 0.0429	3.2399 0.0532 0.0297
1346	PG 2148+095	030612	4.2306 0.0225 0.0167	0.6461 0.0291 0.0346	...	0.8653 0.0285 0.0213	3.6632 0.0303 0.0167
		030917	4.1758 0.0333 0.0262	0.6841 0.0445 0.0554	0.1912 0.0405 0.0327	0.9453 0.0453 0.0337	3.7004 0.0410 0.0226

Continued on Next Page...

Table K.3 – Continued

ID <sup>f</sup>	Name	UT <sup>h</sup> Date	H $\beta$ EW <sup>a</sup> $\sigma_F$ <sup>b</sup>	H $\beta$ $\sigma_C$ <sup>c</sup>	Mg I b <sup>d</sup> EW <sup>a</sup> $\sigma_F$ <sup>b</sup>	Mg I b <sup>d</sup> $\sigma_C$ <sup>c</sup>	He I 5785 EW <sup>a</sup> $\sigma_F$ <sup>b</sup>	He I 5785 $\sigma_C$ <sup>c</sup>	Na I D <sup>e</sup> EW <sup>a</sup> $\sigma_F$ <sup>b</sup>	Na I D <sup>e</sup> $\sigma_C$ <sup>c</sup>	H $\alpha$ EW <sup>a</sup> $\sigma_F$ <sup>b</sup>	H $\alpha$ $\sigma_C$ <sup>c</sup>
1348A	PG 2151+100	020701 030919	4.5089 0.0311 0.0246 4.5240 0.0264 0.0201	...	0.1931 0.0372 0.0473	...	0.0432 0.0387 0.0312 0.1318 0.0357 0.0273	...	0.9699 0.0430 0.0321 0.8381 0.0399 0.0297	...	3.6965 0.0488 0.0270 3.4808 0.0380 0.0211	...
1355	BD-3° 5357	020701	2.4206 0.0175 0.0146	...	5.1999 0.0194 0.0236	...	0.3752 0.0140 0.0110	...	3.9771 0.0145 0.0103	...	-0.6480 0.0160 0.0098	...
1356	PG 2158+082	030919	2.0876 0.0286 0.0231	...	...	...	0.2797 0.0369 0.0285	...	1.0475 0.0413 0.0310	...	2.1703 0.0411 0.0235	...
1424	Balloon 090900007	030917	5.1043 0.0353 0.0275	...	1.4057 0.0456 0.0572	...	0.1289 0.0394 0.0312	...	1.2111 0.0438 0.0325	...	4.2241 0.0382 0.0209	...
1457	BD-7° 5977	021015	3.1346 0.0322 0.0264	...	3.7786 0.0372 0.0461	...	0.1768 0.0280 0.0225	...	2.0281 0.0306 0.0226	...	2.0554 0.0319 0.0185	...
1461A	PB 5333A	021015	3.7887 0.0383 0.0307	...	0.1485 0.0525 0.0669	...	...	...	1.2130 0.0554 0.0411	...	2.9705 0.0631 0.0357	...
1493	PG 2337+300	030917	-0.9206 0.0494 0.0441	...	-0.1380 0.0611 0.0745	...	0.5537 0.0559 0.0430	...	0.8714 0.0632 0.0469	...	-8.5868 0.0718 0.0502	...
...	...	030919	-0.5690 0.0283 0.0252	...	-0.2176 0.0353 0.0444	...	1.0910 0.0319 0.0230	...	0.9079 0.0362 0.0269	...	-4.6311 0.0389 0.0253	...
1519	CD-27 16503	030918	3.5578 0.0488 0.0396	...	0.5818 0.0633 0.0816	...	0.0465 0.0579 0.0449	...	0.3104 0.0653 0.0523	...	3.3099 0.0593 0.0331	...
1525	BPS CS 22957-23	021015	3.7337 0.0932 0.0715	...	2.0554 0.1178 0.1487	...	0.8727 0.1003 0.0753	...	1.9536 0.1163 0.0814	...	2.3717 0.1232 0.0697	...
<b>Single-Colored Hot Subdwarfs (<math>J-K_S \lesssim +0.05</math>)</b>												
50A	PG 0027+222A	021014	5.0287 0.0988 0.0755	...	0.1513 0.1454 0.1870	...	0.3993 0.1548 0.1140	...	0.3631 0.1828 0.1292	...	4.6759 0.1925 0.1003	...
130A	Feige 19A	021015	2.7132 0.0653 0.0516	...	-0.0545 0.0864 0.1087	...	1.7732 0.0809 0.0580	...	1.4570 0.0969 0.0710	...	2.7298 0.1102 0.0618	...
157A	PB 9286A	030918	5.4910 0.0267 0.0202	...	...	...	0.1667 0.0375 0.0291	...	0.0972 0.0405 0.0324	...	4.2967 0.0403 0.0220	...
...	...	030919	5.4733 0.0295 0.0212	...	...	...	0.3031 0.0401 0.0298	...	0.3859 0.0452 0.0390	...	4.4124 0.0429 0.0235	...
216	KUV 05109+1739	021016	5.2805 0.1925 0.1420	...	0.6762 0.2765 0.3564	...	0.8553 0.3143 0.2225	...	0.2702 0.4194 0.2893	...	3.6357 0.3961 0.2071	...
550A	HZ 18A	030613	4.7284 0.1053 0.0757	...	0.1534 0.1463 0.1889	...	0.6643 0.1457 0.1098	...	0.5835 0.1659 0.1243	...	3.9649 0.1910 0.1028	...
700A	PG 1340+607A	020701	5.7297 0.0244 0.0178	...	-0.0837 0.0356 0.0444	...	0.3346 0.0339 0.0259	...	0.2026 0.0383 0.0297	...	4.5664 0.0421 0.0228	...
1152	PG 1710+490	030614	5.6790 0.0360 0.0275	...	...	...	0.4046 0.0521 0.0397	...	0.4599 0.0596 0.0443	...	4.6261 0.0683 0.0370	...
1158	PG 1716+426	030612	5.4088 0.0198 0.0142	...	...	...	0.2931 0.0263 0.0204	...	0.1591 0.0298 0.0225	...	4.3690 0.0340 0.0185	...
1181	[CW83]1735+22	030614	5.5465 0.0417 0.0304	...	...	...	0.1947 0.0568 0.0429	...	0.2318 0.0639 0.0509	...	4.5974 0.0652 0.0353	...
...	...	030613	3.8801 0.0214 0.0166	...	...	...	0.0638 0.0275 0.0217	...	0.4855 0.0308 0.0232	...	3.5415 0.0332 0.0184	...
1187	BD+39° 3226	030917	2.5263 0.0254 0.0198	...	...	...	1.2839 0.0296 0.0234	...	0.3311 0.0342 0.0266	...	2.4795 0.0334 0.0188	...
1188	[CW83]1758+36	020702	5.1393 0.0209 0.0163	...	...	...	0.7302 0.0274 0.0208	...	0.8153 0.0312 0.0232	...	4.3118 0.0356 0.0193	...
1194	BD+48° 2721	020701	5.9080 0.0179 0.0133	...	-0.1358 0.0255 0.0329	...	0.2925 0.0233 0.0184	...	0.4256 0.0262 0.0211	...	4.4860 0.0290 0.0157	...
1195	HD 171858	030918	5.8772 0.0184 0.0136	...	...	...	0.3396 0.0255 0.0204	...	0.4600 0.0287 0.0216	...	4.4868 0.0271 0.0146	...
1263	LS IV+00° 21	030917	5.3814 0.0280 0.0203	...	...	...	0.3345 0.0335 0.0249	...	0.5158 0.0377 0.0286	...	4.3819 0.0335 0.0184	...
...	...	030614	4.6976 0.0225 0.0168	...	...	...	0.5490 0.0277 0.0213	...	0.4610 0.0313 0.0235	...	3.8940 0.0334 0.0184	...
...	...	030918	4.4790 0.0199 0.0157	...	...	...	0.6335 0.0285 0.0217	...	0.5203 0.0324 0.0304	...	3.9217 0.0320 0.0176	...
1347	BD+28° 4211	030612	2.8831 0.0406 0.0320	...	0.1430 0.0564 0.0697	...	...	...	0.2201 0.0621 0.0469	...	2.6621 0.0712 0.0401	...
...	...	030613	2.9521 0.0208 0.0164	...	...	...	...	...	0.1037 0.0316 0.0256	...	2.5959 0.0352 0.0199	...
...	...	030614	3.1894 0.0122 0.0084	...	...	...	...	...	0.1883 0.0158 0.0120	...	2.5018 0.0171 0.0097	...
...	...	030917	2.9711 0.0179 0.0141	...	...	...	...	...	0.3171 0.0280 0.0211	...	2.5209 0.0278 0.0158	...
...	...	030918	2.9173 0.0180 0.0142	...	...	...	...	...	0.2515 0.0286 0.0218	...	2.5684 0.0288 0.0163	...
...	...	030919	2.9739 0.0161 0.0127	...	...	...	...	...	0.2640 0.0256 0.0193	...	2.5385 0.0254 0.0144	...

Continued on Next Page...

Table K.3 – Continued

ID# <sup>f</sup>	Name	UT Date <sup>h</sup>	H $\beta$ EW <sup>a</sup> $\sigma_F$ <sup>b</sup> $\sigma_C$ <sup>c</sup>	Mg I b <sup>d</sup> EW <sup>a</sup> $\sigma_F$ <sup>b</sup> $\sigma_C$ <sup>c</sup>	He I 5785 EW <sup>a</sup> $\sigma_F$ <sup>b</sup> $\sigma_C$ <sup>c</sup>	Na I D <sup>e</sup> EW <sup>a</sup> $\sigma_F$ <sup>b</sup> $\sigma_C$ <sup>c</sup>	H $\alpha$ EW <sup>a</sup> $\sigma_F$ <sup>b</sup> $\sigma_C$ <sup>c</sup>
1357	PG 2159+051	021015	5.4251 0.0342 0.0253	0.2805 0.0484 0.0616	0.0659 0.0457 0.0349	1.0704 0.0504 0.0377	4.4217 0.0572 0.0312
1459	PHL 457	021016	5.5562 0.0325 0.0239	... ..	0.2737 0.0410 0.0309	0.4224 0.0464 0.0392	4.4099 0.0529 0.0289
<b>Visual Double and Nearby Companions of Hot Subdwarfs</b>							
50B	PG 0027+222B	021014	3.4617 0.0705 0.0530	2.6733 0.0883 0.1061	0.2698 0.0726 0.0557	1.3593 0.0823 0.0594	3.0303 0.0760 0.0427
87B	PG 0105+276B	021016	2.6494 0.2786 0.2289	6.8920 0.3315 0.3789	0.3068 0.2746 0.2026	2.3954 0.3226 0.2111	2.8264 0.2814 0.1571
91B	PB 8555B	021015	3.3255 0.0745 0.0608	3.8491 0.0785 0.0970	0.1048 0.0550 0.0420	1.6928 0.0614 0.0444	3.0797 0.0572 0.0320
130B	Feige 19B	021015	0.7870 0.1834 0.1586	10.3095 0.1837 0.2001	2.6672 0.1038 0.0743	10.7422 0.1135 0.0615	1.0447 0.1102 0.0647
157B	PB 9286B	030918	4.2458 0.0804 0.0637	1.8891 0.1018 0.1290	... ..	0.7594 0.0974 0.0722	3.7689 0.0835 0.0459
		030919	4.1911 0.0950 0.0754	1.6895 0.1153 0.1417	-0.0336 0.0909 0.0715	0.9701 0.1015 0.0749	3.7075 0.0853 0.0467
187B	HDE 283048B	030919	4.2340 0.0528 0.0421	3.1994 0.0648 0.0794	0.2347 0.0521 0.0397	2.2204 0.0571 0.0414	3.4989 0.0486 0.0269
550B	HZ 18B	030613	3.1023 0.2055 0.1488	0.3899 0.2463 0.3000	0.0117 0.1977 0.1597	0.3683 0.2239 0.2249	3.5010 0.2082 0.1154
700B	PG 1340+607B	020701	2.5511 0.0759 0.0629	6.2882 0.0857 0.1014	0.9133 0.0647 0.0473	2.3871 0.0714 0.0515	2.1899 0.0705 0.0404
		030614	2.4341 0.1293 0.1064	6.2452 0.1408 0.1667	0.8695 0.1084 0.0774	2.3960 0.1216 0.0829	2.1295 0.1235 0.0699
1461B	PB 5333B	021015	4.0123 0.2638 0.1978	3.6375 0.3083 0.3639	-0.3739 0.2515 0.2001	1.4644 0.3080 0.2040	3.2075 0.2803 0.1541

Table K.4: EW Measurements for Hot Subdwarfs from the Red Spectrograph Setting.

ID# <sup>f</sup>	Name	UT Date <sup>h</sup>	H $\alpha$ EW <sup>a</sup> $\sigma_F$ <sup>b</sup> $\sigma_C$ <sup>c</sup>	Ca II 8498 EW <sup>a</sup> $\sigma_F$ <sup>b</sup> $\sigma_C$ <sup>c</sup>	Ca II 8542 EW <sup>a</sup> $\sigma_F$ <sup>b</sup> $\sigma_C$ <sup>c</sup>	Ca II 8662 EW <sup>a</sup> $\sigma_F$ <sup>b</sup> $\sigma_C$ <sup>c</sup>	P-14 8598 <sup>g</sup> EW <sup>a</sup> $\sigma_F$ <sup>b</sup> $\sigma_C$ <sup>c</sup>
<b>Composite-Colored Hot Subdwarfs (<math>J-K_S \gtrsim +0.05</math>)</b>							
1	SB 7	021014	3.7379 0.0472 0.0258	0.2424 0.1709 0.1208	0.9152 0.1735 0.1177	1.1534 0.2026 0.1267	0.2490 0.1808 0.1329
59	PB 6107	030913	3.6550 0.0256 0.0142	0.5852 0.0578 0.0421	1.6197 0.0575 0.0390	1.4532 0.0613 0.0402	... ..
65	PB 6148	030915	4.0334 0.0224 0.0123	0.9695 0.0425 0.0308	2.2414 0.0421 0.0281	2.0376 0.0444 0.0287	0.2218 0.0448 0.0322
71	BD-11 <sup>o</sup> 162	021012	3.1124 0.0258 0.0146	0.6930 0.0675 0.0478	1.4823 0.0677 0.0458	1.3688 0.0725 0.0466	... ..
87A	PG 0105+276	021108	... ..	-0.0367 1.3441 0.8724	... ..	-0.5602 1.5507 1.0264	-0.8996 1.3707 1.0061
91A	PB 8555A	021012	2.7377 0.0554 0.0313	0.3643 0.1732 0.1245	1.5084 0.1718 0.1157	1.8334 0.1965 0.1246	0.2694 0.1788 0.1306
95	PG 0110+262	021012	3.8587 0.0416 0.0229	0.6843 0.0964 0.0669	1.6990 0.0963 0.0656	1.8072 0.1049 0.0662	0.0434 0.1013 0.0740
101	PG 0116+242	021012	3.7705 0.0227 0.0125	0.6307 0.0491 0.0367	0.8382 0.0498 0.0335	1.0012 0.0527 0.0353	-0.0118 0.0519 0.0376
102	PB 8783	021014	4.7095 0.0322 0.0174	0.7893 0.0995 0.0702	1.2546 0.1010 0.0695	1.8423 0.1095 0.0702	0.3381 0.1046 0.0758
120	PHL 3802	021014	3.2367 0.0297 0.0166	0.1600 0.0882 0.0617	0.9842 0.0895 0.0627	0.7905 0.1025 0.0657	-0.0669 0.0945 0.0689
150	PG 0232+095	030913	2.1316 0.0226 0.0130	0.5543 0.0420 0.0307	2.0694 0.0414 0.0273	1.7422 0.0431 0.0281	0.2264 0.0435 0.0314

Continued on Next Page...



Table K.4 – Continued

ID# <sup>f</sup>	Name	UT Date <sup>h</sup>	H $\alpha$ EW <sup>a</sup> $\sigma_F$ <sup>b</sup> $\sigma_C$ <sup>c</sup>	Ca II 8498 EW <sup>a</sup> $\sigma_F$ <sup>b</sup> $\sigma_C$ <sup>c</sup>	Ca II 8542 EW <sup>a</sup> $\sigma_F$ <sup>b</sup> $\sigma_C$ <sup>c</sup>	Ca II 8662 EW <sup>a</sup> $\sigma_F$ <sup>b</sup> $\sigma_C$ <sup>c</sup>	P-14 8598 <sup>g</sup> EW <sup>a</sup> $\sigma_F$ <sup>b</sup> $\sigma_C$ <sup>c</sup>
172	PG 0314+103	030913	3.6277 0.0315 0.0175	0.3806 0.0594 0.0424	1.1886 0.0592 0.0404	1.2113 0.0622 0.0404	-0.1703 0.0620 0.0450
187A	HDE 283048A	030913	2.5946 0.0198 0.0107	0.6078 0.0387 0.0283	1.6352 0.0384 0.0257	1.8871 0.0397 0.0258	0.1333 0.0402 0.0290
199	KUV 04110+1434	030914	4.9364 0.0367 0.0197	1.0218 0.0773 0.0534	1.5140 0.0769 0.0520	3.1867 0.0768 0.0460	1.8215 0.0775 0.0537
203	KUV 04237+1649	030914	3.4692 0.0392 0.0217	0.6308 0.0764 0.0556	1.5317 0.0760 0.0514	1.1851 0.0809 0.0538	...
234	BD+34 <sup>o</sup> 1543	020309	...	0.6196 0.0723 0.0505	1.9476 0.0717 0.0496	1.6301 0.0762 0.0486	0.1313 0.0760 0.0546
294	PG 0900+400	020310	...	0.7140 0.1085 0.0755	1.9787 0.1076 0.0732	1.5272 0.1153 0.0736	0.2277 0.1140 0.0816
460	PG 1104+243	020309	...	-0.1186 0.3908 0.2790	1.4180 0.3771 0.2560	2.0113 0.4252 0.2581	0.3528 0.3872 0.2823
476	PG 1111+339	020616	...	0.4792 0.1573 0.1123	1.6825 0.1566 0.1057	1.4091 0.1696 0.1110	0.2498 0.1651 0.1186
533	BD+10 <sup>o</sup> 2357	030611	5.2881 0.0157 0.0083	0.5160 <sup>i</sup> 0.0365 0.5261	1.1819 <sup>i</sup> 0.0367 0.5255	2.0597 <sup>i</sup> 0.0380 0.5242	1.0162 <sup>i</sup> 0.0376 0.5265
551	PB 3854	030611	2.7781 0.0139 0.0080	1.1328 <sup>i</sup> 0.0258 0.3181	3.1190 <sup>i</sup> 0.0248 0.3165	2.0642 <sup>i</sup> 0.0268 0.3169	0.1850 <sup>i</sup> 0.0270 0.3195
583	LB 2392	020310	...	-0.6387 1.1681 0.8197	-0.2839 1.1872 0.8251	-0.0972 1.3820 0.8921	1.7675 1.1693 0.8251
630	TON 139	030611	3.6921 0.0288 0.0160	0.4585 <sup>i</sup> 0.0650 0.4455	1.6653 <sup>i</sup> 0.0644 0.4441	1.8018 <sup>i</sup> 0.0675 0.4426	0.0672 <sup>i</sup> 0.0673 0.4487
638	PG 1257-026	030611	3.8011 0.0494 0.0272	0.0909 0.1247 0.0872	1.2198 0.1234 0.0849	1.6581 0.1346 0.0840	0.2222 0.1283 0.0931
697	Feige 87	030610	3.6242 0.0302 0.0168	0.2711 0.0724 0.0509	0.8745 0.0730 0.0515	1.0497 0.0772 0.0495	-0.0294 0.0755 0.0557
702	PG 1343+578	020629	4.0736 0.0668 0.0361	...	1.1908 0.1551 0.1021	2.0751 0.1658 0.1065	...
706	PG 1347+086	030609	3.6898 0.0231 0.0128	0.0264 0.0482 0.0348	0.3948 0.0485 0.0338	0.9802 0.0504 0.0328	0.4474 0.0493 0.0352
789	PG 1429+406	030610	3.6961 0.0440 0.0243	0.7243 0.0971 0.0703	1.9941 0.0959 0.0632	2.5736 0.1005 0.0633	-0.1681 0.1007 0.0736
835	PG 1444+236	030610	-101.459 0.1180 0.1450	-8.3472 0.1380 0.1139	-10.4166 0.1505 0.1306	-8.1662 0.1535 0.1198	-9.2096 0.1495 0.1325
844	PG 1449+653	030610	3.5221 0.0460 0.0253	0.3506 0.1253 0.0959	1.4229 0.1240 0.0811	0.5527 0.1429 0.0924	...
849	PG 1451+472	030611	3.6038 0.0314 0.0174	0.1918 <sup>i</sup> 0.0679 0.7511	0.0998 <sup>i</sup> 0.0687 0.7474	0.9083 <sup>i</sup> 0.0712 0.7467	-0.4007 <sup>i</sup> 0.0700 0.7519
850	PG 1452+198	030611	4.4081 0.0301 0.0163	-0.1930 <sup>i</sup> 0.0830 0.7615	-0.7041 <sup>i</sup> 0.0855 0.7607	0.4479 <sup>i</sup> 0.0890 0.7575	-0.4637 <sup>i</sup> 0.0865 0.7636
895	PG 1514+034	030610	3.4582 0.0485 0.0268	0.2583 0.1143 0.0851	1.0382 0.1138 0.0764	1.3927 0.1256 0.0806	-0.1136 0.1178 0.0869
912	PG 1524+611	020630	3.6606 0.0434 0.0240	0.7577 0.1045 0.0754	1.1596 0.1052 0.0717	1.3309 0.1123 0.0732	-0.3925 0.1102 0.0811
937	PG 1536+278	030611	3.9590 0.0521 0.0284	0.7301 <sup>i</sup> 0.1086 0.7803	1.5896 <sup>i</sup> 0.1077 0.7714	2.1330 <sup>i</sup> 0.1146 0.7733	...
969	PG 1551+255	030610	3.5849 0.0543 0.0299	0.4105 0.1238 0.0893	1.0346 0.1233 0.0826	1.4560 0.1347 0.0861	-0.5312 0.1277 0.0950
		030915	3.4900 0.0477 0.0263	0.9327 0.0998 0.0717	1.6599 0.0997 0.0670	1.3502 0.1073 0.0700	...
		030916	3.9087 0.0513 0.0280	0.0672 0.1513 0.1085	1.0742 0.1489 0.0987	0.8271 0.1648 0.1061	0.0687 0.1531 0.1114
1010	PG 1610+519	020629	2.9950 0.0764 0.0428	0.4374 0.1924 0.1356	1.0757 0.1908 0.1277	0.2580 0.2087 0.1372	-0.6515 0.2014 0.1489
		030916	3.0383 0.0451 0.0250	-0.1251 0.1259 0.0887	0.4492 0.1246 0.0839	0.8598 0.1417 0.0904	0.3310 0.1272 0.0934
1027A	PG 1618+562A	020630	3.8117 0.0285 0.0157	0.8052 0.0553 0.0411	1.7814 0.0550 0.0366	1.5712 0.0610 0.0386	...
1051	PG 1629+081	030611	3.1175 0.0411 0.0231	-0.3032 <sup>i</sup> 0.1038 0.6750	...	0.8472 <sup>i</sup> 0.1114 0.6738	-0.4300 <sup>i</sup> 0.1059 0.6784
1092	TON 264	030915	2.6593 0.0446 0.0254	0.0483 0.0953 0.0682	0.9960 0.0944 0.0644	0.7254 0.1023 0.0676	-0.2557 0.0982 0.0717
1096	PG 1648+080	030610	3.2351 0.0461 0.0258	0.5697 <sup>i</sup> 0.0978 0.7676	1.6546 <sup>i</sup> 0.0965 0.7655	2.1880 <sup>i</sup> 0.1022 0.7628	-0.2403 <sup>i</sup> 0.1002 0.7734
		030914	3.2953 0.0575 0.0322	1.1355 0.1173 0.0796	2.5674 0.1144 0.0754	1.8484 0.1231 0.0769	-0.0568 0.1223 0.0885

Continued on Next Page...

Table K.4 – Continued

ID# <sup>f</sup>	Name	UT Date <sup>h</sup>	H $\alpha$ EW <sup>a</sup> $\sigma_F$ $\sigma_C$	Ca II 8498 EW <sup>a</sup> $\sigma_F$ $\sigma_C$	Ca II 8542 EW <sup>a</sup> $\sigma_F$ $\sigma_C$	Ca II 8662 EW <sup>a</sup> $\sigma_F$ $\sigma_C$	P-14 8598 <sup>g</sup> EW <sup>a</sup> $\sigma_F$ $\sigma_C$
1108	LS IV-08°03	030609	-1.3030 0.0544 0.0335	-0.7146 0.1151 0.0834	-0.4954 0.1153 0.0791	-0.1960 0.1275 0.0837	0.2173 0.1159 0.0847
		030611	-1.7554 0.0376 0.0233	-0.6433 0.0745 0.0559	-0.7164 0.0761 0.0535	-0.1795 0.0790 0.0534	...
		030914	-1.0883 0.0646 0.0393	0.5780 0.1100 0.0805	0.2004 0.1117 0.0804	0.0853 0.1167 0.0720	-0.4182 0.1170 0.0848
1133	PG 1701+359	030915	-0.9940 0.0261 0.0159	-0.1708 0.0473 0.0336	-0.1228 0.0480 0.0341	-0.2657 0.0501 0.0331	-0.2041 0.0491 0.0356
		030609	3.5446 0.0640 0.0349	0.2826 0.1738 0.1205	0.9486 0.1707 0.1106	0.9452 0.2041 0.1272	0.7692 0.1744 0.1282
		030610	3.5328 0.0458 0.0252	0.3800 0.1108 0.0822	0.5586 0.1110 0.0743	0.0748 0.1194 0.0795	-0.5570 0.1140 0.0845
		030913	3.4278 0.0343 0.0182	0.2676 0.0773 0.0532	0.8909 0.0775 0.0519	0.9216 0.0831 0.0565	-0.2458 0.0811 0.0590
1164	PG 1718+519	020629	3.4591 0.0562 0.0309	0.7152 0.1114 0.0825	1.7764 0.1105 0.0732	1.8326 0.1183 0.0774	0.0894 0.1162 0.0838
		030913	3.2020 0.0421 0.0226	0.6825 0.0860 0.0643	1.8716 0.0852 0.0570	1.8502 0.0904 0.0593	0.1157 0.0899 0.0651
1182	BD+29°3070	030610	4.0529 0.0151 0.0083	0.7090 <sup>i</sup> 0.0321 0.0241	2.0170 <sup>i</sup> 0.0318 0.0212	2.3855 <sup>i</sup> 0.0328 0.0214	...
		030913	4.6384 0.0155 0.0079	0.9257 0.0319 0.0232	2.4078 0.0315 0.0208	2.2349 0.0331 0.0214	...
1223	HD 185510	030609	1.3682 0.0114 0.0067	0.2605 0.0190 0.0140	2.0227 0.0185 0.0123	1.8567 0.0192 0.0125	...
		030610	1.0682 0.0154 0.0091	0.2593 0.0272 0.0201	1.8764 0.0270 0.0181	1.7990 0.0275 0.0179	...
		030913	1.5760 0.0158 0.0085	0.5943 0.0238 0.0170	2.4254 0.0233 0.0156	1.9205 0.0247 0.0158	0.1098 0.0249 0.0179
1297	PG 2110+127	030610	1.5631 0.0114 0.0065	1.0362 <sup>i</sup> 0.0199 0.0143	2.9794 <sup>i</sup> 0.0192 0.0126	3.0303 <sup>i</sup> 0.0198 0.0124	-0.1752 <sup>i</sup> 0.0205 0.0148
		030913	3.4260 0.0263 0.0141	0.8019 0.0544 0.0378	2.1641 0.0537 0.0364	2.0048 0.0572 0.0361	0.1143 0.0570 0.0411
1304	PG 2116+008	030915	2.3116 0.1152 0.0649	0.4858 0.3566 0.2349	-0.1105 0.3547 0.2384	1.3081 0.4185 0.2609	-0.2840 0.3604 0.2736
1306	PG 2118+126	020629	3.8566 0.0453 0.0248	1.0106 0.0880 0.0659	2.2202 0.1066 0.0603	2.1955 0.0944 0.0606	1.4515 0.0889 0.0660
		030611	3.6232 0.0496 0.0274	0.4590 <sup>i</sup> 0.1254 0.0306	1.7814 <sup>i</sup> 0.1231 0.0311	1.7904 <sup>i</sup> 0.1331 0.0348	...
		030916	3.7065 0.0394 0.0219	0.6805 0.0893 0.0625	2.0804 0.0874 0.0578	2.3291 0.0961 0.0605	0.1827 0.0915 0.0669
1322	BPS CS 29495-21	021012	3.2112 0.0624 0.0347	0.4218 0.1787 0.1236	1.7754 0.1767 0.1174	1.0410 0.2181 0.1369	0.3296 0.1854 0.1375
		030913	3.2277 0.0484 0.0266	0.5729 0.1037 0.0745	1.5843 0.1028 0.0680	1.4119 0.1156 0.0745	-0.0414 0.1085 0.0795
1346	PG 2148+095	030611	3.5467 0.0349 0.0192	0.4233 <sup>i</sup> 0.0779 0.0592	1.0198 <sup>i</sup> 0.0783 0.0516	1.5700 <sup>i</sup> 0.0834 0.0564	...
		030914	3.6664 0.0322 0.0179	0.8417 0.0695 0.0524	1.5866 0.0695 0.0453	1.2452 0.0738 0.0499	-0.0826 0.0735 0.0530
1348	PG 2151+100	020629	3.5902 0.0402 0.0221	0.0842 0.0913 0.0675	0.2724 0.0925 0.0650	0.4400 0.0998 0.0661	-0.2911 0.0966 0.0714
		030914	3.4955 0.0269 0.0150	0.1849 0.0647 0.0464	0.6161 0.0651 0.0444	0.3544 0.0698 0.0468	-0.2857 0.0681 0.0494
1355	BD-3°5357	020630	-1.4219 0.0131 0.0080	-0.2615 0.0217 0.0158	1.3394 0.0213 0.0142	1.2318 0.0221 0.0150	0.1639 0.0220 0.0159
1356	PG 2158+082	030914	2.2589 0.0324 0.0183	...	0.3925 0.0777 0.0526	0.4562 0.0833 0.0565	-0.3009 0.0810 0.0588
1424	Balloon 090900007	030913	4.1696 0.0253 0.0139	0.9253 0.0533 0.0385	2.0423 0.0529 0.0354	2.1711 0.0559 0.0355	...
		030915	4.2425 0.0241 0.0132	0.7623 0.0509 0.0368	1.9681 0.0500 0.0336	1.9904 0.0528 0.0342	0.3040 0.0527 0.0379
1457	BD-7°5977	021012	1.8831 0.0192 0.0111	1.1468 0.0391 0.0276	3.0214 0.0383 0.0252	2.6080 0.0404 0.0255	0.2236 0.0413 0.0296
1461A	PB 5333A	021012	2.7884 0.1439 0.0784	0.5103 0.4178 0.2744	2.0591 0.3967 0.2485	1.9147 0.5414 0.3190	...
		030916	2.7254 0.0350 0.0198	-0.3156 0.0883 0.0667	...	0.2565 0.0960 0.0639	-0.3479 0.0914 0.0670
		030914	-7.0517 0.0490 0.0333	-0.8468 0.0963 0.0706	-1.5862 0.0998 0.0731	-1.7329 0.1069 0.0736	-1.3296 0.1020 0.0758
		030915	-5.1403 0.0478 0.0314	-1.1369 0.1006 0.0737	-1.7482 0.1030 0.0728	-1.8311 0.1116 0.0769	-1.3952 0.1050 0.0787
		030916	-5.9778 0.0482 0.0319	-1.0330 0.1025 0.0768	-1.5582 0.1052 0.0768	-1.3364 0.1130 0.0769	-0.7705 0.1059 0.0780

Continued on Next Page...

Table K.4 – Continued

ID# <sup>f</sup>	Name	UT Date <sup>h</sup>	H $\alpha$ EW <sup>a</sup> $\sigma_F$ $\sigma_C$	Ca II 8498 EW <sup>a</sup> $\sigma_F$ $\sigma_C$	Ca II 8542 EW <sup>a</sup> $\sigma_F$ $\sigma_C$	Ca II 8662 EW <sup>a</sup> $\sigma_F$ $\sigma_C$	P-14 8598 <sup>g</sup> EW <sup>a</sup> $\sigma_F$ $\sigma_C$
Single-Colored Hot Subdwarfs ( $J-K_S \lesssim +0.05$ )							
1519	CD -27 16503	030913	3.3066 0.0579 0.0323	0.6176 0.1302 0.0950	1.1469 0.1289 0.0856	0.9924 0.1452 0.0937	0.0879 0.1335 0.0983
1525	BPS CS 22957-23	021012	1.9439 0.0678 0.0389	0.5235 0.1811 0.1251	1.0666 0.1793 0.1197	1.4133 0.1993 0.1287	-0.0685 0.1820 0.1353
50A	PG 0027+222A	021014	4.5939 0.1183 0.0623	-0.5615 0.4462 0.3181	-1.2107 0.4587 0.3324	-0.5065 0.5561 0.3548	0.0510 0.4616 0.3574
130A	Feige 19	021014	2.8126 0.0716 0.0402	...	0.3553 0.2623 0.1802	-0.0322 0.3318 0.2128	0.2380 0.2751 0.2105
157A	PB 9286A	030916	4.5150 0.0627 0.0337	-0.3498 0.1923 0.1396	-0.1771 0.1955 0.1356	0.1425 0.2148 0.1418	0.2025 0.2002 0.1444
700A	PG 1340+607A	020629	4.4007 0.0612 0.0331	0.7318 0.1589 0.1105	0.1496 0.1616 0.1116	0.1366 0.1773 0.1165	-0.3241 0.1664 0.1232
1152	PG 1710+490	030611	4.2634 0.0334 0.0181	-0.1833 0.0932 0.0729	-0.3966 0.0948 0.0659	-0.0307 0.1028 0.0660	0.1042 0.0959 0.0700
1181	[CW83]1735+22	030611	3.5072 0.0361 0.0203	-0.1575 0.0997 0.0737	-0.4195 0.1023 0.0714	-0.1620 0.1096 0.0720	-0.0172 0.1042 0.0754
1187	BD+39°3226	030916	2.4679 0.0150 0.0085	-0.0341 0.0372 0.0276	-0.1863 0.0384 0.0274	0.1193 0.0405 0.0274	...
1188	[CW83]1758+36	020630	4.2413 0.0193 0.0107	...	-0.2048 0.0509 0.0368	0.2562 0.0543 0.0361	-0.1714 0.0523 0.0379
1194	BD+48 2721	020629	4.4468 0.0134 0.0072	-0.0150 0.0312 0.0221	...	1.0101 0.0328 0.0218	...
		020630	4.4660 0.0147 0.0079	...	-0.1248 0.0377 0.0272	1.1238 0.0384 0.0251	0.2332 0.0381 0.0273
		030914	4.4066 0.0237 0.0127	0.1754 0.0660 0.0488	0.1298 0.0681 0.0469	1.2126 0.0701 0.0462	...
1195	HD 171858	030914	4.3906 0.0245 0.0135	0.3012 0.0480 0.0354	0.3623 0.0488 0.0339	0.2357 0.0511 0.0349	-0.1901 0.0504 0.0364
1263	LS IV+00°21	030916	3.9309 0.0238 0.0131	...	-0.0675 0.0643 0.0450	0.1152 0.0694 0.0460	-0.0685 0.0659 0.0478
1347	BD+28°4211	030610	2.5585 0.0491 0.0277	-0.6061 0.1459 0.1098	-0.5647 0.1493 0.1062	0.3657 0.1564 0.1045	-0.6675 0.1528 0.1145
		030611	2.4843 0.0187 0.0106	-0.1838 0.0500 0.0363	-0.4475 0.0514 0.0364	0.1909 0.0538 0.0367	-0.1669 0.0523 0.0377
		030914	2.6103 0.0244 0.0138	0.0239 0.0646 0.0466	...	0.0161 0.0701 0.0475	-0.1591 0.0681 0.0491
		030916	2.5338 0.0149 0.0084	-0.0994 0.0382 0.0276	-0.2099 0.0390 0.0262	...	-0.1260 0.0400 0.0292
1357	PG 2159+051	020629	4.1873 0.0694 0.0375	0.7365 0.1561 0.1164	1.1069 0.1552 0.1079	3.3657 0.1618 0.0999	2.2140 0.1597 0.1079
		021012	4.3078 0.0356 0.0195	0.6874 0.1023 0.0720	1.3201 0.1021 0.0690	3.2994 0.1067 0.0638	2.0021 0.1026 0.0714
1459	PHL 457	021014	4.4921 0.0421 0.0229	0.0225 0.1384 0.1006	-0.4617 0.1434 0.1036	...	-0.2156 0.1473 0.1087
Visual Double and Nearby Companions of Hot Subdwarfs							
50B	PG 0027+222B	021014	3.2328 0.0605 0.0339	1.1840 0.1382 0.0959	2.4124 0.1368 0.0909	1.8335 0.1527 0.0939	-0.2201 0.1460 0.1079
87B	PG 0105+276B	021108	...	...	2.7990 0.7910 0.4866	0.7972 0.9185 0.5836	-0.6628 0.8279 0.6069
91B	PB 8555B	021012	2.8045 0.0296 0.0168	0.9361 0.0653 0.0460	2.3808 0.0647 0.0430	2.3598 0.0708 0.0448	0.0751 0.0691 0.0501
157B	PB 9286B	030916	3.5912 0.0852 0.0467	0.7526 0.1826 0.1347	1.8815 0.1811 0.1192	1.9584 0.1991 0.1282	0.3545 0.1891 0.1373
187B	HDE 283048B	030913	3.6137 0.0757 0.0419	0.7270 0.1506 0.1118	2.5321 0.1471 0.0956	2.1718 0.1555 0.1010	0.2298 0.1555 0.1113
700B	PG 1340+607B	020629	2.1085 0.0667 0.0378	0.8594 0.1139 0.0817	2.8030 0.1104 0.0711	1.9341 0.1205 0.0773	...
1027B	PG 1618+562B	020630	3.6902 0.0680 0.0367	0.3657 0.1719 0.1237	1.4399 0.1708 0.1127	1.5450 0.1920 0.1224	0.3280 0.1771 0.1286
1461B	PB 5333B	021012	2.6252 0.0494 0.0282	0.1331 0.1506 0.1092	0.3025 0.1518 0.1045	0.3438 0.1693 0.1108	-0.1803 0.1561 0.1151
		030916	3.2882 0.1101 0.0605	0.7265 0.2090 0.1456	2.0160 0.2022 0.1311	1.8869 0.2353 0.1459	0.2668 0.2098 0.1553

## Appendix L

### Summary of Acronyms and Abbreviations

This is an alphabetically ordered summary of the acronyms and abbreviations as they have been used throughout this document along with the first page the acronym or abbreviation appears on. The entry format is: “**Acronym** — Description or meaning, page #”.

**2IDR** — Second Incremental Data Release (from 2MASS), 49

**2MASS** — *Two Micron All Sky Survey*, 17

**A** — Hot subdwarf member of a visual double (NOTE: the designation as the “A” component does **not** imply the hot subdwarf is the brighter member of the visual double), 53

**AGB** — Asymptotic Giant Branch, 2

**AGN** — Active Galactic Nuclei, 17

**ASDR** — All-Sky Data Release (from 2MASS), 19

**ATOG** — Automated Telescope Offset Guider, 47

**B** — Companion to a hot subdwarf in a visual double (NOTE: the designation as the “B” component does **not** imply that this star is the fainter member of the visual double), 53

**BC** — Bolometric Correction, 102

**BD** — Brown Dwarf, 8

$\chi^2$  — Chi Squared, 261

$\chi^2_{\text{R}}$  — Reduced Chi Squared, 261

**CaT** — Ca II IR Triplet, 47

**CCD** — Charged Coupled Device, 47

**CE** — Common Envelope, 6

**CI** — Confidence Interval, 255

**CMD** — Color-Magnitude Diagram, 50

**COM** — “Composite” (known composite hot subdwarfs flagged in Table B.1), 21

**CV** — Cataclysmic Variable, 18

- DA** — Class of white dwarfs dominated by hydrogen lines only, 1
- DIB** — Diffuse Interstellar Band, 51
- dM** — M-dwarf, M-type main sequence star, 8
- DOF** — Degrees of Freedom, 261
- DSS** — Digitized Sky Survey, 20
- $\eta_{\text{R}}$  — Mass-Loss Efficiency Parameter, 11
- EC** — Edinburgh-Cape survey (Stobie et al. 1997), 7
- EHB** — Extended (or Extreme) Horizontal Branch, 2
- EW** — Equivalent Width, 51
- FWHM** — Full Width at Half Maximum, 48
- GoldCam** — Gold Camera, the CCD spectrometer on the Gold Spectrograph at the Kitt Peak 2.1-meter telescope, 46
- HB** — Horizontal Branch, 2
- HBB** — Horizontal Branch Blue, 1
- HET** — Hobby-Eberly Telescope, 17
- HIP** — Hipparcos Catalog (Perryman et al. 1997), 17
- HR** — Hertzsprung-Russell (as in the Hertzsprung-Russell Diagram), 2
- HS** — Hamburg Quasar Survey (or Hamburg-Schmidt Survey) (Hagen et al. 1995), 3
- IBHB** — Intermediate Blue Horizontal Branch, 11
- ICRS** — International Celestial Reference System, 17
- IR** — Infrared, 19
- IRAF** — Image Reduction and Analysis Facility, 50
- K** — Kelvin, 1
- KHD** — Kilkenny, Heber, & Drilling (1988) as updated and expanded in an electronic version by Kilkenny, c.1992, kindly made available by D. Kilkenny, 16
- kK** — Kilo-Kelvin (1000 Kelvin), 90
- KPNO** — Kitt Peak National Observatory, 46
- Kurucz** — Kurucz (1998), 101
- LCS** — Large Cassegrain Spectrograph, 47

**loess** — The *lowess* function contained in the statistical program *R*, 98

**log g** — Surface Gravity, 1

**lowess** — Locally-weighted scatterplot smoother, 98

**LTE** — Local Thermodynamic Equilibrium, 18

**mas** — Milliarcseconds, 256

**MLS** — Magnitude Limited Sample, 25

$\pi$  — Parallax, 256

**NLTE** — Non-local thermodynamic equilibrium, 18

**NOAO** — National Optical Astronomy Observatories, 50

**NSVS** — Northern Sky Variability Survey, 55

**PG** — Palomar-Green survey (Green et al. 1986), 7

**RGB** — Red Giant Branch, 10

**RLOF** — Roche Lobe Overflow, 6

**RV** — Radial Velocity, 4

$\sigma_{\mathbf{W}}$  — Total error on an EW, 267

$\sigma_{\mathbf{W}}(\mathbf{C})$  — Continuum fitting error on an EW, 267

$\sigma_{\mathbf{W}}(\mathbf{F})$  — Poisson error on an EW, 267

**sd** — Subdwarf (specifically a hot subdwarf), 1

**sdB** — Subdwarf B, 1

**sdBV** — Variable subdwarf B star (generally used to refer to the short period systems officially called V361 Hya, but also known unofficially as EC 14026 stars after the class prototype), 5

**sdO** — Subdwarf O, 1

**sdOB** — Subdwarf OB, 1

**SED** — Spectral Energy Distribution, 101

**SGL** — “Single” (known single hot subdwarfs flagged in Table B.1), 21

**SIMBAD** — Set of Identifications, Measurements and Bibliography for Astronomical Data, <http://simbad.u-strasbg.fr/Simbad>, 17

**S/N** — Signal-to-noise, 20

**STIS** — *Space Telescope Imaging Spectrograph*, 4

**TAEHB** — Terminal-Age Extended Horizontal Branch, 123

**T<sub>eff</sub>** — Effective Temperature, 1

**TYC** — Tycho catalog, 17

**USNO** — U.S. Naval Observatory, 16

**UT** — Universal Time, 85

**UV** — Ultraviolet, 1

**UVX** — Ultraviolet Excess, 4

**VLS** — Volume Limited Sample, 26

**WD** — White Dwarf, 1

**ZAEHB** — Zero-Age Extended Horizontal Branch, 10

**ZAHB** — Zero-Age Horizontal Branch, 11

## Bibliography

- Ahmad, A., Jeffery, C. S., & Fullerton, A. W. 2004, *A&A*, 418, 275
- Allard, F., Wesemael, F., Fontaine, G., Bergeron, P., & Lamontagne, R. 1994, *AJ*, 107, 1565
- Altmann, M., de Boer, K. S., & Edelmann, H. 2001, *Astronomische Nachrichten*, 322, 397
- Altmann, M., Edelmann, H., & de Boer, K. S. 2004, *A&A*, 414, 181
- Arkhipova, V. P., Ikonnikova, N. P., Komissarova, G. V., & Esipov, V. F. 2002, *Astronomy Letters*, 28, 778
- Armandroff, T. E. 1989, *AJ*, 97, 375
- Aznar Cuadrado, R. & Jeffery, C. S. 2001, *A&A*, 368, 994
- . 2002, *A&A*, 385, 131
- Baschek, B. & Norris, J. 1970, *ApJS*, 19, 327
- . 1975, *ApJ*, 199, 694
- Baschek, B., Scholz, M., Kudritzki, R. P., & Simon, K. P. 1982, *A&A*, 108, 387
- Beers, T. C., Doinidis, S. P., Griffin, K. E., Preston, G. W., & Shectman, S. A. 1992, *AJ*, 103, 267
- Berg, C., Wegner, G., Foltz, C. B., Chaffee, F. H., & Hewett, P. C. 1992, *ApJS*, 78, 409
- Berger, J. & Fringant, A. M. 1977, *A&AS*, 28, 123
- Berger, J. & Fringant, A.-M. 1980, *A&AS*, 39, 39
- . 1984, *A&AS*, 58, 565
- Bessell, M. S. & Brett, J. M. 1988, *PASP*, 100, 1134
- Billères, M., Fontaine, G., Brassard, P., & Liebert, J. 2002, *ApJ*, 578, 515
- Bixler, J. V., Bowyer, S., & Laget, M. 1991, *A&A*, 250, 370
- Boffin, H. M. J., Cerf, N., & Paulus, G. 1993, *A&A*, 271, 125
- Brassard, P., Fontaine, G., Billères, M., Charpinet, S., Liebert, J., & Saffer, R. A. 2001, *ApJ*, 563, 1013
- Brown, T. M., Bowers, C. W., Kimble, R. A., Sweigart, A. V., & Ferguson, H. C. 2000, *ApJ*, 532, 308



- Buonanno, R., Corsi, C. E., Buzzoni, A., Cacciari, C., Ferraro, F. R., & Fusi Pecci, F. 1994, *A&A*, 290, 69
- Caloi, V. 1972, *A&A*, 20, 357
- Cardelli, J. A., Clayton, G. C., & Mathis, J. S. 1989, *ApJ*, 345, 245
- Carnochan, D. J. & Wilson, R. 1983, *MNRAS*, 202, 317
- Carpenter, J. M. 2001, *AJ*, 121, 2851
- Cassisi, S., Schlattl, H., Salaris, M., & Weiss, A. 2003, *ApJL*, 582, L43
- Castellani, M. & Castellani, V. 1993, *ApJ*, 407, 649
- Chavira, E. 1958, *Boletin de los Observatorios Tonantzintla y Tacubaya*, 2, part no. 17, 15
- . 1959, *Boletin de los Observatorios Tonantzintla y Tacubaya*, 2, part no. 18, 3
- Cleveland, W. S. 1985, *The Elements of Graphing Data* (Wadsworth Advanced Book Program, Monterey, California)
- Colin, J., de Boer, K. S., Dauphole, B., Ducourant, C., Dulou, M. R., Geffert, M., Le Campion, J.-F., Moehler, S., Odenkirchen, M., Schmidt, J. H. K., & Theissen, A. 1994, *A&A*, 287, 38
- D’Cruz, N. L., Dorman, B., Rood, R. T., & O’Connell, R. W. 1996, *ApJ*, 466, 359
- de Boer, K. S., Aguilar Sanchez, Y., Altmann, M., Geffert, M., Odenkirchen, M., Schmidt, J. H. K., & Colin, J. 1997a, *A&A*, 327, 577
- de Boer, K. S., Drilling, J., Jeffery, C. S., & Sion, E. M. 1997b, in *The Third Conference on Faint Blue Stars*, ed. A. G. D. Philip, J. Liebert, R. Saffer, & D. S. Hayes (L. Davis Press), 515
- Demers, S., Wesemael, F., Irwin, M. J., Fontaine, G., Lamontagne, R., Kepler, S. O., & Holberg, J. B. 1990, *ApJ*, 351, 271
- Dorman, B., O’Connell, R. W., & Rood, R. T. 1995, *ApJ*, 442, 105
- Dorman, B., Rood, R. T., & O’Connell, R. W. 1993, *ApJ*, 419, 596
- Downes, R. A. 1986, *ApJS*, 61, 569
- Drechsel, H., Heber, U., Napiwotzki, R., Østensen, R., Solheim, J.-E., Johannessen, F., Schuh, S. L., Deetjen, J., & Zola, S. 2001, *A&A*, 379, 893
- Dreizler, S., Heber, U., Werner, K., Moehler, S., & de Boer, K. S. 1990, *A&A*, 235, 234
- Drilling, J. S. & Bergeron, L. E. 1995, *PASP*, 107, 846

- Drilling, J. S., Moehler, S., Jeffery, C. S., Heber, U., & Napiwotzki, R. 2000, in *The Kth Reunion*, ed. A. G. D. Philip (L. Davis Press, Schenectady NY), 49
- Drilling, J. S., Moehler, S., Jeffery, C. S., Heber, U., & Napiwotzki, R. 2003, in *The Garrison Festschrift*, ed. R. O. Gray, C. J. Corbally, & A. G. D. Philip (L. Davis Press, Schenectady NY), 27–38
- Duquennoy, A. & Mayor, M. 1991, *A&A*, 248, 485
- Dworetsky, M. M., Lanning, H. H., Etzel, P. B., & Patenaude, D. J. 1977, *Informational Bulletin on Variable Stars*, 1284, 1
- Edelmann, H., Heber, U., Hagen, H.-J., Lemke, M., Dreizler, S., Napiwotzki, R., & Engels, D. 2003, *A&A*, 400, 939
- Edelmann, H., Heber, U., & Napiwotzki, R. 2001, *Astronomische Nachrichten*, 322, 401
- ESA. 1997, *VizieR Online Data Catalog*, 1239
- Etzel, P. B., Lanning, H. H., Patenaude, D. J., & Dworetsky, M. M. 1977, *PASP*, 89, 616
- Falter, S., Heber, U., Dreizler, S., Schuh, S. L., Cordes, O., & Edelmann, H. 2003, *A&A*, 401, 289
- Feige, J. 1958, *ApJ*, 128, 267
- Fekel, F. X. & Simon, T. 1985, *AJ*, 90, 812
- Ferguson, D. H., Green, R. F., & Liebert, J. 1984, *ApJ*, 287, 320
- Giclas, H. L., Burnham, R., & Thomas, N. G. 1961, *Lowell Observatory Bulletin*, 5, 61
- . 1965, *Lowell Observatory Bulletin*, 6, 155
- Gray, D. F. 1992, *The Observation and Analysis of Stellar Photospheres* (Cambridge; New York: Cambridge University Press, 1992. 2nd ed.)
- Green, E. M., Fontaine, G., Reed, M. D., Callera, K., Seitzzahl, I. R., White, B. A., Hyde, E. A., Østensen, R., Cordes, O., Brassard, P., Falter, S., Jeffery, E. J., Dreizler, S., Schuh, S. L., Giovanni, M., Edelmann, H., Rigby, J., & Bronowska, A. 2003, *ApJL*, 583, L31
- Green, E. M., For, B., Hyde, E. A., Seitzzahl, I. R., Callera, K., White, B. A., Young, C. N., Huff, C. S., Mills, J., & Steinfadt, J. D. R. 2004, *Astrophysics and Space Science*, 291, 267
- Green, R. F., Schmidt, M., & Liebert, J. 1986, *ApJS*, 61, 305
- Greenstein, J. L. 1952, *PASP*, 64, 256
- Greenstein, J. L. & Sargent, A. I. 1974, *ApJS*, 28, 157

- Greggio, L. & Renzini, A. 1990, *ApJ*, 364, 35
- Hagen, H.-J., Groote, D., Engels, D., & Reimers, D. 1995, *A&AS*, 111, 195
- Han, Z., Podsiadlowski, P., Maxted, P. F. L., & Marsh, T. R. 2003, *MNRAS*, 341, 669
- Han, Z., Podsiadlowski, P., Maxted, P. F. L., Marsh, T. R., & Ivanova, N. 2002, *MNRAS*, 336, 449
- Hartman, J. D., Kaluzny, J., Szentgyorgyi, A., & Stanek, K. Z. 2005, *AJ*, 129, 1596
- Heber, U. 1986, *A&A*, 155, 33
- Heber, U., Drechsel, H., Østensen, R., Karl, C., Napiwotzki, R., Altmann, M., Cordes, O., Solheim, J.-E., Voss, B., Koester, D., & Folkes, S. 2004, *A&A*, 420, 251
- Heber, U., Hunger, K., Jonas, G., & Kudritzki, R. P. 1984, *A&A*, 130, 119
- Heber, U., Moehler, S., Napiwotzki, R., Thejll, P., & Green, E. M. 2002, *A&A*, 383, 938
- Herbig, G. H. 1975, *ApJ*, 196, 129
- . 1992, *Revista Mexicana de Astronomia y Astrofisica*, 24, 187
- Hewett, P. C., Foltz, C. B., & Chaffee, F. H. 1995, *AJ*, 109, 1498
- Høg, E., Fabricius, C., Makarov, V. V., Urban, S., Corbin, T., Wycoff, G., Bastian, U., Schwekendiek, P., & Wicenec, A. 2000, *A&A*, 355, L27
- Høg, E., Kuzmin, A., Bastian, U., Fabricius, C., Kuimov, K., Lindegren, L., Makarov, V. V., & Roeser, S. 1998, *A&A*, 335, L65
- Hubeny, I. 1998, *Comput. Phys. Commun.*, 52, 103
- Humason, M. L. & Zwicky, F. 1947, *ApJ*, 105, 85
- Iben, I. J. 1990, *ApJ*, 353, 215
- Iriarte, B. & Chavira, E. 1957, *Boletin de los Observatorios Tonantzintla y Tacubaya*, 2, part no. 16, 3
- Jaidee, S. & Lyngå, G. 1974, *Arkiv for Astronomi*, 5, 345
- Jeffery, C. S. & Aznar Cuadrado, R. 2001, *A&A*, 378, 936
- Jeffery, C. S., Drilling, J. S., Harrison, P. M., Heber, U., & Moehler, S. 1997, *A&AS*, 125, 501
- Jeffery, C. S. & Pollacco, D. L. 1998, *MNRAS*, 298, 179
- Johnson, H. L. 1966, *Annual Review of Astronomy and Astrophysics*, 4, 193
- Kilkenny, D., Heber, U., & Drilling, J. S. 1988, *South African Astronomical Observatory Circular*, 12, 1

- Kilkenny, D., Koen, C., O'Donoghue, D., & Stobie, R. S. 1997, MNRAS, 285, 640
- Kilkenny, D., O'Donoghue, D., Koen, C., Lynas-Gray, A. E., & van Wyk, F. 1998, MNRAS, 296, 329
- Koen, C., Kilkenny, D., O'Donoghue, D., van Wyk, F., & Stobie, R. S. 1997, MNRAS, 285, 645
- Koen, C. & Orosz, J. 1997, Informational Bulletin on Variable Stars, 4539, 1
- Kurucz, R. 1998, *Solar abundance model atmospheres for 0,1,2,4,8 km/s.* (Cambridge, Mass.: Smithsonian Astrophysical Observatory), <http://kurucz.harvard.edu/>
- Landolt, A. U. 1992, AJ, 104, 340
- Liebert, J., Saffer, R. A., & Green, E. M. 1994, AJ, 107, 1408
- Lisker, T., Heber, U., Napiwotzki, R., Christlieb, N., Reimers, D., & Homeier, D. 2004, *Astrophysics and Space Science*, 291, 351
- Marilli, E., Frasca, A., Bellina Terra, M., & Catalano, S. 1995, A&A, 295, 393
- Massey, P. & Gronwall, C. 1990, ApJ, 358, 344
- Maxted, P. F. L., Heber, U., Marsh, T. R., & North, R. C. 2001, MNRAS, 326, 1391
- Maxted, P. F. L., Marsh, T. R., Heber, U., Morales-Rueda, L., North, R. C., & Lawson, W. A. 2002, MNRAS, 333, 231
- Mengel, J. G., Norris, J., & Gross, P. G. 1976, ApJ, 204, 488
- Menzies, J. W. & Marang, F. 1986, in IAU Symp. 118: Instrumentation and Research Programmes for Small Telescopes (D. Reidel Publishing Company, Dordrecht, Holland, U.S.A. and Canada by Kluwer Academic Publishers), 305
- Mitchell, K. J. 1998, ApJ, 494, 256
- Moehler, S. 2001, PASP, 113, 1162
- Moehler, S., Heber, U., & de Boer, K. S. 1990a, A&A, 239, 265
- Moehler, S., Richtler, T., de Boer, K. S., Dettmar, R. J., & Heber, U. 1990b, A&AS, 86, 53
- Monet, D. B. A., Canzian, B., Dahn, C., Guetter, H., Harris, H., Henden, A., Levine, S., Luginbuhl, C., Monet, A. K. B., Rhodes, A., Riepe, B., Sell, S., Stone, R., Vrba, F., & Walker, R. 1998, The USNO-A2.0 Catalogue (U.S. Naval Observatory Flagstaff Station [USNOFS] and Universities Space Research Association stationed at USNOFS)
- Mooney, C. J., Rolleston, W. R. J., Keenan, F. P., Pinfield, D. J., Pollacco, D. L., Dufton, P. L., & Katsiyannis, A. C. 2000, A&A, 357, 553

- Morales-Rueda, L., Maxted, P. F. L., & Marsh, T. R. 2004, *Astrophysics and Space Science*, 291, 299
- Morales-Rueda, L., Maxted, P. F. L., Marsh, T. R., North, R. C., & Heber, U. 2003, *MNRAS*, 338, 752
- Murdin, P. 1990, *Wood's Anomalies in the INT Spectrograph*, Tech. Rep. 76, ING La Palma
- Napiwotzki, R. 1993, *Acta Astronomica*, 43, 343
- . 1999, *A&A*, 350, 101
- Newell, E. B. 1973, *ApJS*, 26, 37
- Noguchi, T., Maehara, H., & Kondo, M. 1980, *Annals of the Tokyo Astronomical Observatory*, 18, 55
- O'Connell, R. W. 1999, *Annual Review of Astronomy and Astrophysics*, 37, 603
- O'Donoghue, D., Koen, C., Kilkenney, D., Stobie, R. S., & Lynas-Gray, A. E. 1999, in *ASP Conf. Ser. 169: 11th European Workshop on White Dwarfs*, 149
- Orosz, J., Wade, R. A., & Harlow, J. J. B. 1997, *AJ*, 114, 317
- Østensen, R., Heber, U., Silvotti, R., Solheim, J.-E., Dreizler, S., & Edelmann, H. 2001, *A&A*, 378, 466
- Paczyński, B. 1980, *Acta Astronomica*, 30, 113
- Perryman, M. A. C., Lindegren, L., Kovalevsky, J., Hoeg, E., Bastian, U., Bernacca, P. L., Crézé, M., Donati, F., Grenon, M., van Leeuwen, F., van der Marel, H., Mignard, F., Murray, C. A., Le Poole, R. S., Schrijver, H., Turon, C., Arenou, F., Froeschlé, M., & Petersen, C. S. 1997, *A&A*, 323, L49
- Pesch, P. & Sanduleak, N. 1983, *ApJS*, 51, 171
- Rauch, T. 2000, *A&A*, 356, 665
- Reed, M. D., Green, E. M., Callera, K., Seitzzahl, I. R., White, B. A., Hyde, E. A., Giovanni, M. K., Østensen, R., Bronowska, A., Jeffery, E. J., Cordes, O., Falter, S., Edelmann, H., Dreizler, S., & Schuh, S. L. 2004, *ApJ*, 607, 445
- Reed, M. D. & Stiening, R. 2004, *PASP*, 116, 506
- Reid, N. & Wegner, G. 1988, *ApJ*, 335, 953
- Reid, N. & Wegner, G. 1989, in *IAU Colloq. 114: White Dwarfs*, 396–400
- Rubin, V. C. & Losee, J. M. 1971, *AJ*, 76, 1099
- Rubin, V. C., Westpfahl, D., & Tuve, M. 1974, *AJ*, 79, 1406

- Saffer, R. A., Bergeron, P., Koester, D., & Liebert, J. 1994, *ApJ*, 432, 351
- Saffer, R. A., Green, E. M., & Bowers, T. 2001, in *ASP Conf. Ser. 226: 12th European Workshop on White Dwarfs*, 408
- Saffer, R. A., Livio, M., & Yungelson, L. R. 1998, *ApJ*, 502, 394
- Sandage, A., Lubin, L. M., & Vandenberg, D. A. 2003, *PASP*, 115, 1187
- Sandage, A. R. 1953, *AJ*, 58, 61
- Schlegel, D. J., Finkbeiner, D. P., & Davis, M. 1998, *ApJ*, 500, 525
- Schweizer, F. & Middleditch, J. 1980, *ApJ*, 241, 1039
- Sembach, K. R. & Savage, B. D. 1992, *ApJS*, 83, 147
- Silvotti, R., Solheim, J.-E., Gonzalez Perez, J. M., Heber, U., Dreizler, S., Edelmann, H., Østensen, R., & Kotak, R. 2000, *A&A*, 359, 1068
- Slettebak, A. & Brundage, R. K. 1971, *AJ*, 76, 338
- Stark, M. A. & Wade, R. A. 2003, *AJ*, 126, 1455
- Stark, M. A., Wade, R. A., & Berriman, G. B. 2004, *Astrophysics and Space Science*, 291, 333
- Stephenson, C. B. & Sanduleak, N. 1971, *Publications of the Warner & Swasey Observatory*, 1, 1
- Stobie, R. S., Kilkenny, D., O'Donoghue, D., Chen, A., Koen, C., Morgan, D. H., Barrow, J., Buckley, D. A. H., Cannon, R. D., Cass, C. J. P., Cranston, M. R., Drinkwater, M., Hartley, M., Hawkins, M. R. S., Hughes, S., Humphries, C. M., MacGillivray, H. T., McKenzie, P. B., Parker, Q. A., Read, M., Russell, K. S., Savage, A., Thomson, E. B., Tritton, S. B., Waldron, J. D., Warner, B., & Watson, F. G. 1997, *MNRAS*, 287, 848
- Stock, J., Nassau, J. J., & Stephenson, C. B. 1960, *Hamburger Sternw. Warner & Swasey Obs.*, 2
- Sweigart, A. V., Mengel, J. G., & Demarque, P. 1974, *A&A*, 30, 13
- Theissen, A., Moehler, S., Heber, U., & de Boer, K. S. 1993, *A&A*, 273, 524
- Theissen, A., Moehler, S., Heber, U., Schmidt, J. H. K., & de Boer, K. S. 1995, *A&A*, 298, 577
- Theissen, A., Moehler, S., Schmidt, J. H., & Heber, U. 1992, in *Lecture Notes in Physics Vol. 401: The Atmospheres of Early-Type Stars*, ed. U. Heber & C. S. Jeffery (Springer-Verlag, Berlin Heidelberg New York), 264
- Thejll, P., Bauer, F., Saffer, R., Liebert, J., Kunze, D., & Shipman, H. L. 1994, *ApJ*, 433, 819

- Thejll, P., Flynn, C., Williamson, R., & Saffer, R. 1997, *A&A*, 317, 689
- Thejll, P., Ulla, A., & MacDonald, J. 1995, *A&A*, 303, 773
- Turner, D. G. 1990, *PASP*, 102, 1331
- Ulla, A. & Thejll, P. 1998, *A&AS*, 132, 1
- Ulla, A., Zapatero Osorio, M. R., Pérez Hernández, F., & MacDonald, J. 2001, *A&A*, 369, 986
- Villeneuve, B., Wesemael, F., Fontaine, G., Carignan, C., & Green, R. F. 1995, *ApJ*, 446, 646
- Viton, M., Deleuil, M., Tobin, W., Prevot, L., & Bouchet, P. 1991, *A&A*, 242, 175
- Voges, W., Aschenbach, B., Boller, T., Bräuninger, H., Briel, U., Burkert, W., Dennerl, K., Englhauser, J., Gruber, R., Haberl, F., Hartner, G., Hasinger, G., Kürster, M., Pfeffermann, E., Pietsch, W., Predehl, P., Rosso, C., Schmitt, J. H. M. M., Trümper, J., & Zimmermann, H. U. 1999, *A&A*, 349, 389
- Wade, R. A. & Stark, M. A. 2004, *Astrophysics and Space Science*, 291, 337
- Wesemael, F., Fontaine, G., Bergeron, P., Lamontagne, R., & Green, R. F. 1992, *AJ*, 104, 203
- White, N. E., Giommi, P., & Angelini, L. 2000, *VizieR Online Data Catalog*, 9031
- Williams, T., McGraw, J. T., & Grashuis, R. 2001, *PASP*, 113, 490
- Woźniak, P. R., Vestrand, W. T., Akerlof, C. W., Balsano, R., Bloch, J., Casperson, D., Fletcher, S., Gisler, G., Kehoe, R., Kinemuchi, K., Lee, B. C., Marshall, S., McGowan, K. E., McKay, T. A., Rykoff, E. S., Smith, D. A., Szymanski, J., & Wren, J. 2004, *AJ*, 127, 2436
- Wood, R. W. 1935, *Physical Review*, 48, 928
- Yi, S., Afshari, E., Demarque, P., & Oemler, A. J. 1995, *ApJL*, 453, L69

# Vita

## Michele A. Stark

### Education

***The Pennsylvania State University*** State College, Pennsylvania 1999–2005  
Ph.D. in Astronomy & Astrophysics, expected in August 2005  
Area of Specialization: Stellar Astronomy, Hot Subdwarf Stars  
***Michigan State University*** East Lansing, Michigan 1995–1999  
B.S. in Astrophysics, *summa cum laude* with distinction in the major

### Awards and Honors

NASA Graduate Student Research Program Fellowship 2002–2005  
Pennsylvania Space Grant Consortium Fellowship 2001–2003  
Zaccheus Daniel Foundation for Astronomical Science Grant 2001, 2002, 2004  
Sigma Xi Grants-in-Aid of Research 2001  
Braddock Fellowship, The Pennsylvania State University 1999–2001  
Michelson Interferometry Summer School 2000  
Teaching Assistant of the Year, Dept. of Astronomy & Astrophysics, Penn State 2000

### Research Experience

***Doctoral Research*** The Pennsylvania State University 2000–2005  
Thesis Advisor: Prof. Richard A. Wade  
Variety of aspects of hot subdwarfs, including: composite-spectrum, visual doubles, rejects from the PG catalog.  
***Graduate Research*** The Pennsylvania State University 2000  
Research Advisor: Prof. Michael Eracleous  
Assisted with characterizing the Hobby-Eberly Telescope Marcario Low-Resolution Spectrograph.  
***Undergraduate Research*** Michigan State University 1997–1999  
Research Advisor: Prof. Horace A. Smith  
Variable Stars in the Small Magallanic Cloud. XX Leo eclipsing variable star observing project.  
***Undergraduate Research*** National Optical Astronomy Observatories 1998  
Research Advisor: Dr. Buell T. Jannuzi  
Galaxy redshifts for quasar absorption line association using WIYN-Hydra observations.

### Teaching Experience

***Teaching Assistant*** The Pennsylvania State University 1999–2002  
Taught introductory astronomy laboratories for non-science majors, and assisted with a course and associated lab for astronomy majors. Helped design new labs for inclusion in the ASTRO 11 lab manual.  
***Head Teaching Assistant*** The Pennsylvania State University 2001–2002  
Supervised and coordinated the teaching assistants for introductory astronomy laboratories for non-science majors. Editor for the 2003–2004 ASTRO 11 lab manual.